frontiers | Research Topics

Women in avian physiology: 2022

Edited by
Sandra G. Velleman and Francesca Soglia

Published in
Frontiers in Physiology

ISSN 1664-8714
ISBN 978-2-83250-965-4
DOI 10.3389/978-2-83250-965-4

About Frontiers

Frontiers is more than just an open access publisher of scholarly articles: it is a pioneering approach to the world of academia, radically improving the way scholarly research is managed. The grand vision of Frontiers is a world where all people have an equal opportunity to seek, share and generate knowledge. Frontiers provides immediate and permanent online open access to all its publications, but this alone is not enough to realize our grand goals.

Frontiers journal series

The Frontiers journal series is a multi-tier and interdisciplinary set of open-access, online journals, promising a paradigm shift from the current review, selection and dissemination processes in academic publishing. All Frontiers journals are driven by researchers for researchers; therefore, they constitute a service to the scholarly community. At the same time, the *Frontiers journal series* operates on a revolutionary invention, the tiered publishing system, initially addressing specific communities of scholars, and gradually climbing up to broader public understanding, thus serving the interests of the lay society, too.

Dedication to quality

Each Frontiers article is a landmark of the highest quality, thanks to genuinely collaborative interactions between authors and review editors, who include some of the world's best academicians. Research must be certified by peers before entering a stream of knowledge that may eventually reach the public - and shape society; therefore, Frontiers only applies the most rigorous and unbiased reviews. Frontiers revolutionizes research publishing by freely delivering the most outstanding research, evaluated with no bias from both the academic and social point of view. By applying the most advanced information technologies, Frontiers is catapulting scholarly publishing into a new generation.

What are Frontiers Research Topics?

Frontiers Research Topics are very popular trademarks of the *Frontiers journals series*: they are collections of at least ten articles, all centered on a particular subject. With their unique mix of varied contributions from Original Research to Review Articles, Frontiers Research Topics unify the most influential researchers, the latest key findings and historical advances in a hot research area.

Find out more on how to host your own Frontiers Research Topic or contribute to one as an author by contacting the Frontiers editorial office: frontiersin.org/about/contact

Women in avian physiology: 2022

Topic editors

Sandra G. Velleman — The Ohio State University, United States

Francesca Soglia — University of Bologna, Italy

Citation

Velleman, S. G., Soglia, F., eds. (2022). *Women in avian physiology: 2022*. Lausanne: Frontiers Media SA. doi: 10.3389/978-2-83250-965-4

Table of contents

frontiers | Frontiers in Physiology

TYPE Editorial
PUBLISHED 21 November 2022
DOI 10.3389/fphys.2022.1086815

OPEN ACCESS

EDITED AND REVIEWED BY
Colin Guy Scanes,
University of Arkansas,
United States

*CORRESPONDENCE
Sandra G. Velleman,
velleman.1@osu.edu

SPECIALTY SECTION
This article was submitted
to Avian Physiology,
a section of the journal
Frontiers in Physiology

RECEIVED 01 November 2022
ACCEPTED 07 November 2022
PUBLISHED 21 November 2022

CITATION
Velleman SG and Soglia F (2022),
Editorial: Women in Avian Physiology:
2022.
Front. Physiol. 13:1086815.
doi: 10.3389/fphys.2022.1086815

Editorial: Women in Avian Physiology: 2022

Sandra G. Velleman[1]* and Francesca Soglia[2]

[1]Department of Animal Sciences, The Ohio State University, Columbus, OH, United States,
[2]Department of Agricultural and Food Sciences, University of Bologna, Bologna, Italy

KEYWORDS

avian, genetic selection, muscle physiology, neurobiology, pathology, reproduction

Editorial on the Research Topic
Women in Avian Physiology: 2022

The Women in Avian Physiology Research Topic is part of an inclusive Frontiers series across all sections focused on Women in Physiology. The purpose of the series is to showcase physiological research of women and to highlight their achievements. Submissions were welcomed covering all areas of Avian Physiology. Submissions were encouraged from early career researchers and/or where the lead/last author were females. A total of 12 submissions were accepted for publication in this Research Topic covering the areas of: 1. Skeletal Muscle Physiology and Meat Quality; 2. Female Reproduction; 3. Pathobiology; 4. Genetic Selection; and 5. Neurobiology.

Skeletal muscle physiology and meat quality

Three contributions addressed skeletal muscle physiology and/or meat quality by Swanson et al., Bordini et al., and Xu et al. Swanson et al. reviewed phenotypic plasticity to environmental variation focusing on metabolic rates and skeletal muscle physiology in wild birds. The ultrastructural plasticity of skeletal muscle with regard to thermal variation and increased workload was reviewed and correlated with myostatin, Insulin-like growth factor-1, and satellite cell proliferation. Xu et al. examined the effects of temperature and selection for growth on the proliferation, differentiation, adipogenic potential of turkey myogenic satellite cells through frizzled-7-mediated Wnt planar cell polarity (Wnt/PCP) pathway. It was found that thermal stress altered frizzled-7 regulation of the Wnt/PCP pathway in a growth-dependent manner affecting the growth potential of the breast muscle and protein to fat ratio. Bordini et al. contributed an original Research Topic studying molecular pathways and key genes associated with White Striping and Wooden Breast in chickens. Using Weighted Gene Co-expression Network Analysis to identify clusters of co-expressed genes associated with White Striping and Wooden Breast, they found that endoplasmic reticulum stress may underly the inflammatory condition in affected breast muscles and Collagen type IV may have significant role in the events leading to White Striping and Wooden Breast.

Female reproduction

Hanlon et al. provided a comprehensive review on the roles of 17β-estradiol in non-gonadal tissues and its impact on reproduction in both laying and broiler breeder hens. Estradiol-17β are involved in reproduction, liver metabolism, and medullary bone formation. Thus, this hormone may regulate all aspects of egg formation and hence the timing of estradiol-17β is critical to reproduction which has been altered by genetic selection for intense growth. Mehlhorn et al. investigated how hen line, age and housing affect estradiol-17β on egg laying performance. High performance hen lines had higher estradiol-17ß concentrations compared to low performing hens. Regardless of line, maximal estradiol-17ß concentration was measured at their 49th to their 51st week of age. Furthermore, cages hens had highest estradiol-17β levels compared to floor housed hens. We could show that laying performance is strongly linked with estradiol -17ß concentration. This concentration changes during laying period and is also influenced by the housing system.

Pathobiology

Use of an oral-killed chitosan nanoparticle *Salmonella* vaccine (as an alternative to conventional *Salmonella* poultry vaccines) was shown to decrease *Salmonella* enterica serovar enteritidis load in immunized broiler chickens by Acevedo-Villanueva et al. Shanmugasundaram et al. contributed an original Research Topic demonstrating that subclinical doses of combined fumonisins and deoxynivalenol (mycotoxins contaminating poultry diets) predispose *Clostridum perfringens* inoculated broilers to necrotic enteritis, an economically important disease negatively impacting digestion and absorption of nutrients in broilers.

Genetic selection

Two contributions addressed the effects of genetic selection. Bernardi et al. reported on chemerin as a possible genetic selection tool for embryo survivability pending larger scale testing. Research on how the somatotrophic axis has changed with commercial growth selection and its relationship to increased growth was reported by Vaccaro et al. They found the expression of insulin-like growth factors 1 and 2 was greater in the modern commercial chicken and maybe linked with increased breast muscle growth and overall muscle accretion. In broilers divergently selected for ultimate pH, it was found by Beauclercq et al. that there is an association between serum lipid profile, ultimate pH and meat quality. Furthermore, since ultimate pH can be obtained on live birds, it may be a useful marker in genetic selection.

Neurobiology

Loveland et al. contributed a perspective paper on how inversion variants can affect neural circuitry. This review covered how behavior polymorphisms can evolve from genetic inversions, especially when inversions are associated with sets of genes involved with hormonal regulation. Primary focus was on the three-morph system of the ruff (*Calidris pugnax*), two alternative morphs (Satellites and Faeders) each with distinct behaviors and low circulating testosterone that is genetically determined by an inverted region on an autosomal chromosome. Franco et al. examined the bird sense of sight and found that broilers raised under blue light were more hyperopic than those raised with white light. The blue light reared broilers had better spatial vision and higher success in selecting the right feeder.

Author contributions

The contributions are all original to the Research Topic. All authors contributed to the article and approved the submitted version.

Conflict of interest

The authors declare that the research was conducted in the absence of any commercial or financial relationships that could be construed as a potential conflict of interest.

Publisher's note

frontiers in Physiology

ORIGINAL RESEARCH
published: 10 March 2022
doi: 10.3389/fphys.2022.855266

Light Color and the Commercial Broiler: Effect on Ocular Health and Visual Acuity

*Bruna Remonato Franco[1], Marina L. Leis[2], Melody Wong[3], Tory Shynkaruk[1], Trever Crowe[4], Bryan Fancher[5], Nick French[5], Scot Gillingham[5] and Karen Schwean-Lardner[1]**

[1] Department of Animal and Poultry Science, University of Saskatchewan, Saskatoon, SK, Canada, [2] Department of Small Animal Clinical Sciences, Western College of Veterinary Medicine, University of Saskatchewan, Saskatoon, SK, Canada, [3] Department of Ophthalmology, Saskatoon City Hospital, University of Saskatchewan, Saskatoon, SK, Canada, [4] Department of Mechanical Engineering, University of Saskatchewan, Saskatoon, SK, Canada, [5] Aviagen™ Inc., Cummings Research Park, Huntsville, AL, United States

Light is a critical management factor for broiler production, and the wavelength spectrum, one of its components, can affect bird physiology, behavior and production. Among all the senses, sight is important to birds, and their visual system possess several adaptations that allow them to perceive light differently from humans. Therefore, it is critical to consider whether the exposure to monochromatic light colors influences broiler visual ability, which could affect behavioral expression. The present study examined the effects of various light colors on the visual systems of broiler chickens. Ross 708 males were raised from 0 to 35 days under three wavelength programs [blue (dominant wavelengths near 455 nm), green (dominant wavelengths near 510 nm) or white]. Broilers were given a complete ophthalmic examination, including chromatic pupillary light reflex testing, rebound tonometry, anterior segment biomicroscopy and indirect ophthalmoscopy (n = 36, day 21). To assess ocular anatomy, broilers were euthanized, eyes were weighed, and dimensions were taken (n = 108, day 16 and day 24). An autorefractor was used to assess the refractive index and the corneal curvature (n = 18, day 26). To evaluate spatial vision, broilers underwent a grating acuity test at one of three distances–50, 75, or 100 cm (n = 24, day 29). Data were analyzed as a one-way ANOVA using the MIXED procedure or Proc Par1way for non-normally distributed data. Significant differences were observed for refractive index and spatial vision. Birds raised under blue light were slightly more hyperopic, or far-sighted, than birds raised under white light (P = 0.01). As for spatial vision, birds raised under blue light took less time to approach the stimulus at distances of 50 cm (P = 0.03) and 75 cm (P = 0.0006) and had a higher success rate (choosing the right feeder, P = 0.03) at 100 cm than birds raised under white light. Improvements in spatial vision for birds exposed to blue light can partially explain the behavioral differences resulting from rearing broilers under different wavelengths.

Keywords: broiler, wavelength, light color, spatial vision, visual function

OPEN ACCESS

Edited by:
Sandra G. Velleman, The Ohio State University, United States

Reviewed by:
Colin Guy Scanes, University of Arkansas, United States
Gregoy Y. Bedecarrats, University of Guelph, Canada

****Correspondence:***
Karen Schwean-Lardner
karen.schwean@usask.ca

Specialty section:
This article was submitted to Avian Physiology, a section of the journal Frontiers in Physiology

Received: *15 January 2022*
Accepted: *16 February 2022*
Published: *10 March 2022*

Citation:
Remonato Franco B, Leis ML, Wong M, Shynkaruk T, Crowe T, Fancher B, French N, Gillingham S and Schwean-Lardner K (2022) Light Color and the Commercial Broiler: Effect on Ocular Health and Visual Acuity. Front. Physiol. 13:855266. doi: 10.3389/fphys.2022.855266

INTRODUCTION

Light is a crucial management factor for broiler production, and its components, such as photoperiod and light intensity, affect broiler growth, diurnal rhythms, behavior and welfare (Deep et al., 2010, 2012; Schwean-Lardner et al., 2012a,b, 2014). Light spectrum, another aspect of light, appears to affect poultry growth; however, the results published to date are inconsistent (Prayitno et al., 1997a; Rozenboim et al., 1999; Mohamed et al., 2017). It is well documented that behavioral responses are altered when birds are reared under specific light wavelengths (Prayitno et al., 1997a,b; Lewis and Morris, 2000; Sultana et al., 2013; Mohamed et al., 2017). Previous studies have indicated that raising broilers under long wavelengths, such as red light (630–780 nm), increased bird activity, with increased walking and wing and leg stretching (Prayitno et al., 1997b). Broilers were also more active when raised under yellow light (565–600 nm), which is also considered a long wavelength (Sultana et al., 2013). In contrast, birds raised under shorter wavelengths, such as blue light, spent more time sitting or resting (Prayitno et al., 1997a; Sultana et al., 2013). In addition to the impacts on behavioral output, light wavelength also influences fear and stress levels. Broilers raised under blue light had lower fear levels, assessed through tonic immobility, than birds raised under white light (Mohamed et al., 2014, 2017). Likewise, the heterophil: lymphocyte ratio, an indicator of chronic stress, was lower in broilers reared under blue light compared to green or white light, indicating a reduction in stress (Remonato Franco et al., under review a[1]).

These impacts on bird behavior may suggest that lighting programs with varying wavelengths may be a usable tool to improve welfare and production. However, it is important to understand the origin of the behavioral changes and whether they are related to visual ability. A bird's large eyes in relation to their body weight and brain size suggest that vision is a critical sense for poultry (Garamszegi et al., 2002; Prescott et al., 2003). Birds use visual cues for several activities, such as awareness of other birds' intentions, status recognition, determining what is safe to eat and drink, and navigation (Collins et al., 2011). When comparing the behavior of blind and sighted chickens, Collins et al. (2011) demonstrated that blind birds exhibited difficulties in expressing key behaviors, displaying increased frustration, which is associated with reduced animal welfare.

Birds have developed several adaptations to their visual system compared to mammals, despite sharing similar gross features (Bennett and Cuthill, 1994). Birds are tetrachromatic, which means they possess four types of cone photoreceptor cells compared to trichromatic animals, such as humans. The lens and aqueous humor of birds are optically clear in the ultraviolet (UV) range, giving birds a color vision expanded to UV light (Lewis and Morris, 2000; Marshall and Arikawa, 2014). They also possess a double-cone photoreceptor, of which the function is related to the perception of movement (Kram et al., 2010). The oil droplets in the cones filter light before it reaches the photopigments, providing birds with increased accuracy in color discrimination (Prescott and Wathes, 1999; Kelber, 2019). Birds also possess a different spectral sensitivity and therefore perceive color and intensity differently than humans (Prescott and Wathes, 1999; Prescott et al., 2003). This is particularly true in the blue color range, and birds see this light color much brighter than do humans (Lewis and Morris, 2000). This implies that measuring intensity in units of lux, the traditional unit used to assess illuminance under white light, may not be the correct methodology when assessing light intensity of colored lighting in poultry settings, as it is based on human spectral sensitivity rather than that of a bird. A more accurate assessment unit has been developed, known as clux (corrected lux or chicken lux), that considers birds' spectral sensitivity and how they perceive their environment (Nuboer et al., 1992; Prescott and Wathes, 1999; Lewis and Morris, 2000; Prescott et al., 2003; Kristensen et al., 2006).

Previous research has highlighted the impacts of other light components, such as long daylengths, in broiler (Schwean-Lardner et al., 2013) and turkey production (Vermette et al., 2016). These animals display increased eye weights and dimensions as daylength increases, likely through disruption of the diurnal rhythms, which also happens when light intensity is very low during broiler production (Deep et al., 2013).

Besides affecting eye shape and size, visual function may be impaired by different light components, influencing refraction, ocular health, and visual acuity (Flaxman et al., 2017). The chicken eye has been used as a model for studying human ocular diseases and conditions (Wisely et al., 2017). Results demonstrate an immoscopy was performed to assess thpact of varying wavelengths on emmetropization, with eyes exhibiting increased axial length and vitreous chamber depth when chicks were exposed to red or white light (Lin et al., 2020), and on refractive error, with long wavelengths, such as red light, leading to progressive myopia (Foulds et al., 2013). To our knowledge, no study has been conducted to understand the structural ocular changes or effects in visual function and spatial vision caused by raising broilers under different wavelengths in a simulated commercial setting.

To encompass this, in the present study, broilers reared under one of three wavelengths underwent a series of tests to assess their visual ability. These data were of a larger experiment, testing the response to wavelength treatments in production, health and behavior parameters of broilers (3 manuscripts: **Table 1**. see text foot note 1[2,3]). The objective of this study was to assess ocular health and vision in broilers raised under different wavelength treatments.

MATERIALS AND METHODS

This experiment was approved by the Animal Care Committee of the University of Saskatchewan and was conducted following

[1] Remonato Franco, B., Shynkaruk, T., Crowe, T., Fancher, B., French, N., Gillingham, S., et al. (under review a). *Light Color and the Commercial Broiler: Effect on Behavior, Fear and Stress*.

[2] Remonato Franco, B., Shynkaruk, T., Crowe, T., Fancher, B., French, N., Gillingham, S., et al. (under review b). *Does Light Color During Brooding and Rearing Impact Broiler Productivity?*

[3] Remonato Franco, B., Shynkaruk, T., Crowe, T., Fancher, B., French, N., Gillingham, S., et al. (under review c). *Light Wavelength and its Impact on Diurnal Rhythms and Broiler Health*.

TABLE 1 | Summary of experiments/trials and measurements obtained from each.

	Current manuscript		Other measures taken within specific experiment
Experiment 1	Trial 1	*Ocular health* (chromatic PLR, anterior segment biomicroscopy, indirect ophthalmoscopy, IOP) *Eye measurements* (eye weight, corneal diameter, mediolateral diameter, dorsoventral diameter and anteroposterior size)	Behavioral expression, fear and stress levels (see text foot note 1) Production variables (see text foot note 2) Health parameters (see text foot note 3)
	Trial 2	*Refraction Index* *Eye measurements* (eye weight, corneal diameter, mediolateral diameter, dorsoventral diameter and anteroposterior size)	
Experiment 2		*Spatial vision*	

the guidelines of the Canadian Council on Animal Care (1999) as specified in the Guide to the Care and Use of Experimental Animals.

The assessments of ocular health and vision were conducted as a part of a larger experiment that studied the impact of wavelength treatments on production, physiology, behavior and welfare of broilers. Tests were conducted within 2 experiments, one of which involved 2 blocked trials.

Housing

For both experiments, each lasting 35 days, broilers were raised at the Poultry Research and Teaching Unit located at the University of Saskatchewan. The facility contains nine individual environmentally controlled rooms. Each room was subdivided into 12 individual pens (2.0 m × 2.3 m). In Experiment 1 (2 repeated trials), Ross YPMx708 and Ross EPMx708 males and females were housed sex-separately within nine rooms (12 pens per room), with 62 males, or 70 females per pen, resulting in a final estimated density of 31 kg/m^2 (total of 7128 broilers housed in each of two trials). For Experiment 2, mixed-sex Ross 308 chicks were housed in two rooms, with each pen containing 42 broilers, for a total of 710 broilers.

Water, available *ad libitum*, was provided using pendulum nipple drinkers, with six nipples available per pen. Commercially prepared feed (starter diet–0.5 kg per bird, grower diet–2.0 kg per bird and the remainder as finisher diet) was provided *ad libitum* using aluminum tube feeders. Chicks were housed on the day of hatch in pens containing approximately 7.5–10 cm of wheat straw bedding. Room temperatures were set to 32.1°C at the time of placement and were reduced gradually until 21°C was reached by 25 days of age and maintained until the end of the trial. Temperature was monitored twice each day in each room *via* behavioral observations and computer output.

Lighting

Light was provided *via* light emitting diode (LED) light bulbs (11W Alice Non-Directional LED Lamps, Greengage Agritech Limited, Roslin Innovation Centre, University of Edinburgh, Easter Bush Campus, Midlothian, EH25 9RG, United Kingdom) that, for Experiment 1, emitted one of three lighting treatments: blue (dominant wavelengths near 455 nm), green (dominant wavelengths near 510 nm), and white (combination of wavelengths). Experiment 2 treatments were refined (chosen based on behavioral differences noted between broilers reared under blue light compared to white and green: see text foot note 1), and included only the blue and white lighting treatments. These were chosen based on behavioral measures taken in Experiment 1 (see text foot note 1). Measurements of light spectra were taken for each light treatment to verify the spectral distribution (Asensetek Incorporation, New Taipei City, Taiwan, **Figure 1**).

On day 0, birds received 23 h of light, which was decreased (1 h per day) until day 5, when 18 h of light was provided. Dawn and dusk periods of 15 min were provided daily, prior to lights turning on or off. Light intensity was measured in clux. For trial 1 of Experiment 1, light intensity was 9.6 ± 0.4 clux. In the second blocked trial of Experiment 1, and for Experiment 2, the first week was set at 14.3 ± 0.1 clux and the remaining weeks at 9.6 ± 0.4 clux (Galilux Light Meter, Hato Agricultural Lighting, Sittard, Netherlands).

Data Collection

Ocular Health

A summary of the data collected during the different experiments and trials is presented at **Table 1**. In the first trial of Experiment 1, twelve YPM-708 males per lighting treatment (from 2 pens per room and 2 birds from each pen) were randomly selected at 21 days (n = 36) to undergo complete ophthalmic examinations performed by a board-certified veterinary ophthalmologist. The examinations included chromatic pupillary light reflex (PLR) testing (Melan-100 unit, BioMed Vision Technologies, Ames, IA, United States), anterior segment biomicroscopy performed with a portable slit lamp (SL-17, Kowa, Tokyo Japan), and indirect ophthalmoscopy [IOP, (Heine Omega 200, Heine Instruments Canada, Kitchener, Ontario)]. Rebound tonometry (Tonovet, Tiolat, Helsinki, Finland) was used to estimate intraocular pressure (Wahl et al., 2016; Leis et al., 2017).

Eye Measurements

In Experiment 1 (trials 1 and 2), 36 birds per light treatment (YPM-708 males only, 2 pens per room, 1 bird per pen, n = 108) were euthanized by decapitation, and both eyes were immediately extracted. Adhering tissues were removed, and eye weights and dimensions were taken for both eyes using a digital scale and digital caliper. Dimensions included corneal diameter, mediolateral diameter, dorsoventral diameter and anteroposterior size (Schwean-Lardner et al., 2013; Vermette et al., 2016).

Refraction Index

In the second trial of Experiment 1, a handheld autorefractor (Nikon Retinomax K-plus 2) was used to assess the corneal curvature and the refractive index in six birds per lighting treatment at 26 days (YPM-708 males only, from 2 pens per room

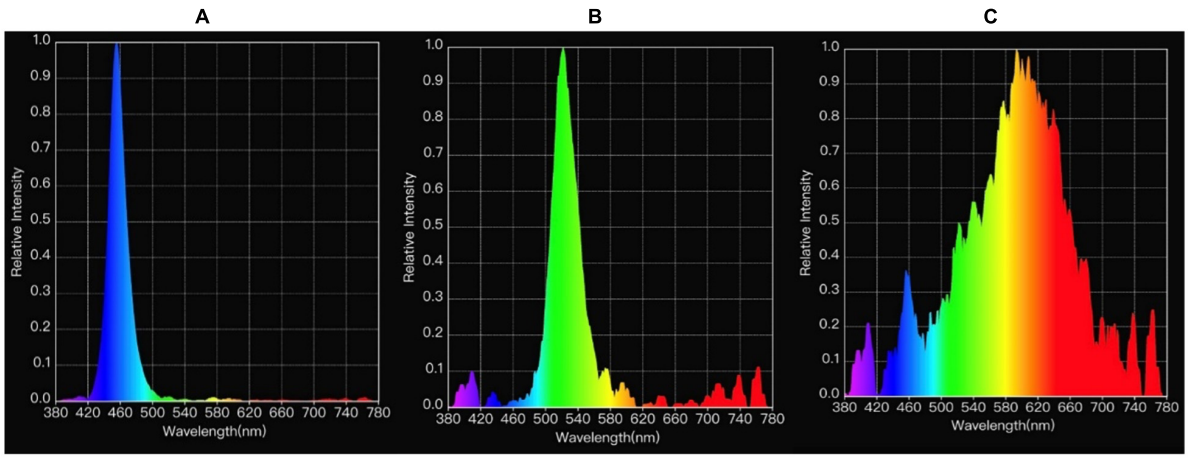

FIGURE 1 | Measurements of light spectrum, respectively, from blue **(A)**, green **(B)** and white **(C)** light treatments.

and 1 bird from each pen, n = 18). Tests were conducted and results were assessed by an ophthalmologist from Saskatoon City Hospital, University of Saskatchewan (Saskatoon, SK, Canada).

Spatial Vision Test

Based on behavioral differences noted for birds under blue compared to white and green light in Experiment 1 (see text foot note 1), a second experiment was added to determine if visual acuity could explain these behavioral changes. In Experiment 2, 12 birds per lighting treatment (blue or white, from one pen per room, males only, n = 24) underwent testing to evaluate spatial vision at 29 days, using a spatial conditional discrimination procedure (DeMello et al., 1992). For a period of 4 days before the test day, a test space was set up in the middle of a pen, and selected birds were placed individually inside the pen. Birds remained in the test space for 5 min, for acclimation with the features related to rewarding and non-rewarding feeders (Kristensen, 2004). The test pen included two feed stations: one contained previously weighed feed (rewarding) and the other without feed (non-rewarding), **Figure 2**. The feed stations were located either in front of gray or black and white square-wave grating boards [vertical stripes–2.5 mm wide, 5 mm per cycle (Hyvärinen, 2018)].

On the fifth day of spatial vision testing, the chosen birds were individually tested in the test pens. Each test pen contained both feed dispensers (rewarding and non-rewarding–the same as presented in the training period), placed in front of the gray or grating stimulus boards at the end of the pen (DeMello et al., 1992). The feed dispensers were separated by a partition, which varied in length to test birds at different distances from the stimulus boards. Feed was withdrawn from birds 1 h prior to testing. Birds were individually placed in the "choice area" at one of three different distances at a time (50, 75, and 100 cm from the feeders), where they chose between the two stimuli. The average time taken to approach a feed dispenser and whether animals chose the dispenser that contained feed (success rate) was recorded by an observer, who stayed outside of the vision area of the birds being tested (Kristensen, 2004).

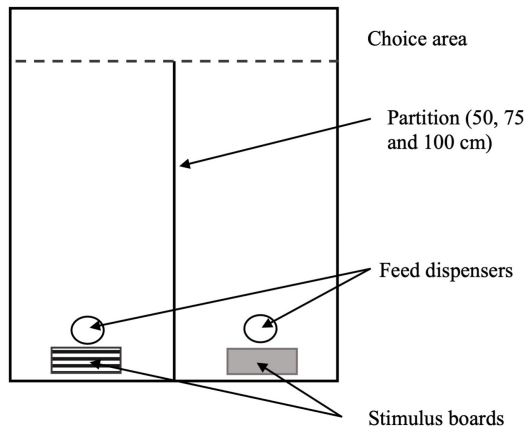

FIGURE 2 | Schematic representation of the test pens, adapted from Kristensen (2004).

Statistical Analyses

Data were statistically analyzed using SAS (SAS 9.4, Cary, NC, United States). Bird was used as the experimental unit for all tests. All data were tested for normality before analyses using the UNIVARIATE procedure. Data were analyzed as a one-way ANOVA using the MIXED procedure or PAR1WAY procedure for data not normally distributed. Tukey's range test was used to separate means when significant differences were found. Differences were considered significant when $P \leq 0.05$.

RESULTS

Ocular Health

Chromatic PLR (cPLR) testing, which indicates retina and optic nerve functions after light stimulus, did not reveal any significant differences between birds reared on various light treatments. Likewise, both anterior segment biomicroscopy and indirect ophthalmoscopy did not reveal abnormalities in any birds,

TABLE 2 | The effect of light color treatments on intraocular pressure (mmHg) of YPMx708 male broilers at 21 days of age (n = 36, Experiment 1, trial 1).

	Light treatment				
	Blue[1]	Green[2]	White[3]	*P*-value	SEM[4]
Intraocular Pressure (mmHg)	8.58	8.83	8.88	0.74	0.122

[1]*Blue light–dominant wavelengths 435–500 nm, peak at 455 nm.*
[2]*Green light–dominant wavelengths 500–565 nm, peak at 510 nm.*
[3]*White light–range of wavelengths from 380 to 780 nm.*
[4]*SEM = Standard error of the mean.*

TABLE 3 | Effect of different light color treatments on left and right eye weight and dimensions of YPMx708 male broilers at 17 days of age (n = 108, Experiment 1).

	Light treatment				
	Blue[1]	Green[2]	White[3]	*P*-value	SEM[4]
Eye wt. (g)	1.12	1.14	1.16	0.13	0.001
Eye wt./body wt. (%)	0.03	0.03	0.03	0.51	0.236
Corneal diameter (mm)	6.40	6.39	6.42	0.95	0.029
DV diameter[5] (mm)	13.94	14.06	14.19	0.22	0.073
ML diameter[6] (mm)	13.92	13.94	14.16	0.14	0.060
AP depth[7] (mm)	11.57	11.66	11.52	0.78	0.067

[1]*Blue light–dominant wavelengths 435–500 nm, peak at 455 nm.*
[2]*Green light–dominant wavelengths 500–565 nm, peak at 510 nm.*
[3]*White light–range of wavelengths from 380 to 780 nm.*
[4]*SEM = Standard error of the mean.*
[5]*Dorsoventral (DV) diameter.*
[6]*Mediolateral (ML) diameter.*
[7]*Anteriorposterior (AP) depth.*

indicating no abnormalities in the fundus of the eye. Intraocular pressure, which, if high, can lead to glaucoma, was within normal limits in all birds and did not differ with the use of blue, green or white light during the production period of broilers (P = 0.74, **Table 2**).

Eye Measurements

Raising broilers under either blue, green or white lights had no effect on eye weight (P = 0.13) or dimensions (shape) of the eye, which, if altered, could impact image forming, including the corneal diameter (P = 0.95), mediolateral diameter (P = 0.14), dorsoventral diameter (P = 0.22) or anteroposterior size (P = 0.78, **Table 3**).

Refractive Index

Testing refraction, which, if altered, can lead to impacts on visual accommodation, leading to myopia or hyperopia, revealed that birds raised under blue light had a higher sphere index (0.625) than birds raised under white light (−0.020, P = 0.01). No differences were observed for cylinder (P = 0.62) and axis indices (P = 0.91, **Table 4**).

TABLE 4 | Effect of different light color treatments on the refraction index of YPMX708 male broilers at 26 days of age (n = 18, Experiment 1, trial 2).

	Light treatment				
	Blue[1]	Green[2]	White[3]	*P*-value	SEM[4]
Sphere	0.625[a]	0.083[ab]	−0.020[b]	0.01	0.1032
Cylinder	0.604	0.458	0.667	0.62	0.0651
Axis	121.58	114.50	117.83	0.91	6.869

[a,b]*Means with common letters do not differ significantly ($P \leq 0.05$).*
[1]*Blue light–dominant wavelengths 435–500 nm, peak at 455 nm.*
[2]*Green light–dominant wavelengths 500–565 nm, peak at 510 nm.*
[3]*White light–range of wavelengths from 380 to 780 nm.*
[4]*SEM = Standard error of the mean.*

Spatial Vision

Light treatment had an impact on spatial vision. Birds raised under blue light took less time to approach the stimulus from a distance of 50 (P = 0.03) and 75 cm (P = 0.006) and had a higher success rate (choosing the right dispenser) at 100 cm (P = 0.03) than birds raised under white light (**Table 5**).

DISCUSSION AND CONCLUSION

As with light intensity and photoperiod, light wavelength can impact poultry behavior. As vision is important for birds, altering their ability to perceive their environment could potentially impact their welfare and affect behavior. Previous research has suggested that broilers raised under shorter wavelengths, including blue light, are less fearful and less stressed than broilers raised under green or white lights (see text foot note 1).

Ocular Health

In response to a light stimulus, the normal pupillary light reflex results in the sphincter muscle of the iris contracting or relaxing, resulting in dilation or constriction of the pupil. Ideal vision is usually correlated to a good pupillary response to light (Bremner, 2004). A variation of the PLR test is the cPLR, where the device used for the test emits light of a specific wavelength. This may provide information about particular ocular changes and functions of photoreceptors (Rukmini et al., 2019). Given that each photoreceptor can be stimulated by a selective wavelength, the cPLR can assess the contribution of each photoreceptor to PLR (Rukmini et al., 2019). In the current study, the cPLR, performed on birds raised under white, blue or green lights, indicates that wavelength did not affect the function of photoreceptors. In an *in vitro* study conducted with mouse-derived cells, blue light led to more severe damage to photoreceptors than white and green light (Kuse et al., 2014). The differences found between this study and the current study may have been related to the particular characteristics of each species' visual system or the light intensity used.

Anterior segment biomicroscopy was performed to screen for diseases in the anterior segment of the eye, including cataracts

TABLE 5 | The effect of light color treatments on spatial vision of YPMx708 male broiler chickens at 29 days of age (n = 24, Experiment 2).

Distance	50 cm			75 cm			100 cm			
	Light treatment									
	Blue[1]	White[2]	*P*-value	Blue[1]	White[2]	*P*-value	Blue[1]	White[2]	*P*-value	SEM[3]
Average time to approach (s)	8.6[b]	15.8[a]	0.03	5.9[b]	27.1[a]	0.006	11.7	13.2	0.42	2.27
Success rate (%)	91.7	91.7	1.00	91.7	66.7	0.11	91.7[a]	50[b]	0.03	4.69

[a,b]*Means with common letters do not differ significantly ($P \leq 0.05$).*
[1]*Blue light–dominant wavelengths 435–500 nm, peak at 455 nm.*
[2]*White light–range of wavelengths from 380 to 780 nm.*
[3]*SEM = Standard error of the mean.*

(Brown et al., 1987) and anterior uveitis (Rothova et al., 1987). Previous research has indicated that continual exposure to specific wavelengths, such as UV light regularly emitted by specific light sources such as fluorescent light bulbs, may cause cataracts (Walls et al., 2011). In humans, the development of cataracts can be caused by oxidative stress in corneal epithelial cells and may lead to apoptosis of the cornea (Ouyang et al., 2020). However, in our study, the anterior segment biomicroscopy assessment did not reveal any abnormalities in the birds tested, meaning that the use of wavelengths resulting in the blue, green or white lights emitted from LED bulbs had no impact on the anterior segment of the eye.

Indirect ophthalmoscopy was performed to assess the fundus of the eye, including the retina and pecten. Concerns in this area of the eye include damage to the photoreceptors present on the retina and impairment of retinal pigment epithelium (RPE) cells, as the normal function of both photoreceptors and RPE cells are necessary for the development of vision (Ouyang et al., 2020). The authors cited damage to these cells to be caused by blue light due to proliferation of the inflammatory response and DNA, lysosomes or mitochondria damage (Ouyang et al., 2020). Effects of shorter wavelengths, such as blue light, were cited in the literature studying mice (Nakamura et al., 2017) or cell cultures (Ozkaya et al., 2019). To our knowledge, no models using chickens were applied in research to investigate the effects of wavelength treatments resulting in blue light from LED bulbs on retinal damage. In the current study, light color did not have a clinically appreciable effect on the retina. As birds have a different spectral sensitivity than mammals, this could explain why no effects of short wavelength were found on retinal damage, even though the previously cited works reported microscopic retinal damage.

Normal intraocular pressure for broilers has been reported to be in the range of 16 mmHg (Prashar et al., 2007). In the current study, intraocular pressure remained within this range for all light treatments. In addition, no significant differences in IOP were found between birds raised under white, blue or green light. A previous study using cell cultures revealed blue light-induced necroptosis of the retinal ganglion cells' mitochondria, which can lead to glaucoma (del Olmo-Aguado et al., 2016), even though our study focused on clinical exams vs. ultrastructure. However, as previously mentioned, chickens have a different spectral sensitivity, which could result in altered outcomes when exposed to shorter wavelengths.

Eye Measurements

Normally, eye growth follows light-dark cues, with growth occurring during the photophase and decreased growth during the scotophase (Nickla, 2013; Leis et al., 2017). This can be correlated to hormones such as dopamine and melatonin (Nickla, 2013), which are released in a diurnal fashion (Nickla et al., 1998). Lack of these diurnal rhythms can directly lead to eye abnormalities, with the lack of control of eye growth resulting in adjustments to their shape or size. Turkeys and broilers exposed to longer daylength or low light intensity were found to have altered eye weights and dimensions, which could induce ocular diseases (Deep et al., 2013; Schwean-Lardner et al., 2013; Vermette et al., 2016). Buphthalmia, which is an enlargement of the eye globe, is usually related to elevated IOP and could lead to glaucoma or even blindness (Whitley et al., 1984). In some studies, eye shape appears to be altered by exposure to monochromatic light. For example, guinea pigs exposed to longer wavelengths had increased eye length (Liu et al., 2011). Depending on the species, eye growth is also related to exposure to different chromatic lights. In humans, eyes may display a longitudinal chromatic aberration, which causes wavelength defocus. In this scenario, eye growth is reduced when humans are under blue light compared to red light exposure (Rucker, 2019). Chickens, however, appear to be an exception for this pattern of response as eye growth did not differ when exposed to either UV, white or red light under low light intensities (Rohrer et al., 1992). In our study, wavelength treatments had no impact on eye shape and size when birds were exposed to blue, green or white light, suggesting that exposing broilers to these monochromatic colors had no or minor impact on physiology that could affect ocular growth.

Refractive Index for Determination of Visual Accommodation

Results obtained from this test indicate the presence of emmetropia (normal vision), myopia, hyperopia or astigmatism. Light exposure is related to effects on emmetropization. In this dynamic process, the eye undergoes adjustments, so the image falls on the retina, instead of falling in front of the retina, leading to myopic defocus (nearsightedness) or behind the retina, leading to hyperopic defocus (farsightedness) (Nickla and Schroedl, 2012). Chicks raised under high light intensity develop hyperopia, whereas chicks raised under dim light acquire myopic

refractive errors (Cohen et al., 2011). Previous work indicates that, in addition to illuminance, light wavelength appears to impact refraction. Wavelength defocus occurs due to a process called longitudinal chromatic aberration, which is a wavelength-depended refractive error, and the eye may compensate by altering growth, and therefore, exerting impacts on refraction (Liu et al., 2011; Smith et al., 2015; Rucker, 2019). As longer wavelengths (red light) are focused more posteriorly on the retina as compared to shorter wavelengths (blue light), it is expected that accommodation responds to chromaticity (Foulds et al., 2013). Therefore, exposing chicks to longer wavelengths results in myopic refraction (Foulds et al., 2013; Rucker, 2013), and in contrast, exposing chicks to shorter wavelengths results in hyperopic refraction (Foulds et al., 2013). The sphere values obtained in our study, which denote the eye's refractive error, revealed that birds raised under blue light are slightly more hyperopic, or far-sighted, than birds raised under white light, which contains a range of wavelengths from short to long in its spectrum. The farther away from zero the sphere value is, the more hyperopic/myopic the refractive error. The results obtained were significantly different but numerically similar to an emmetropic eye; therefore, it is unclear if this level of refractive error would be large enough to result in significant visual impairment.

Spatial Vision

To assess spatial vision, this study used visual acuity as an indicator *via* a "Grating Acuity Test". This visual acuity test is commonly used for young children when language skills and letter identification are limited (Teller et al., 1986). Previous studies have successfully used grating stimulus to determine chicken visual acuity (DeMello et al., 1992).

To our knowledge, spatial vision has not been assessed in broilers with respect to varying wavelength treatments. In our study, birds reared under blue light approached the feeder sooner (50 or 75 cm) and were more successful at choosing the right feeder (100 cm), indicating that overall, they had better visual acuity than birds raised under white light. Chickens have a peculiar spectral sensitivity curve as compared to humans. These animals possess a significantly greater spectral sensitivity between 380 and 486 nm, corresponding to the violet and blue colors (Prescott and Wathes, 1999). This indicates that the common misconception in the poultry industry that birds would have impaired visual acuity under shorter wavelengths, such as blue, is incorrect. Such a misconception could be related to the comparison made using the pattern of human visual acuity and not considering the specificity of the avian species.

In conclusion, in our study, no impact of light color was observed on pupil light reflex, anterior segment biomicroscopy, indirect ophthalmoscopy, intraocular pressure, eye shape or size. The exposure to constant blue light resulted in minor differences in refraction. Birds raised under blue light were slightly more far-sighted than birds raised under white light. Birds raised under blue light approached a novel object with less delay when the object was near (50 and 75 cm) and were more successful when approaching a preferred object from a farther distance (100 cm), suggesting a superior visual acuity than birds raised under white light. The minor differences observed on refraction index and eye health may indicate that vision was similar for birds reared under blue and white light, except for spatial acuity. The improved spatial vision observed may partially explain the behavioral differences perceived when broilers are raised under blue light.

DATA AVAILABILITY STATEMENT

The raw data supporting the conclusions of this article will be made available by the authors, without undue reservation.

ETHICS STATEMENT

The animal study was reviewed and approved by the Animal Care Committee of the University of Saskatchewan.

AUTHOR CONTRIBUTIONS

KS-L was the primary investigator. BR collected, analyzed and interpreted data, and drafted the manuscript. ML, MW, TS, TC, BF, NF, SG, and KS-L assisted with data collection and experimental design. All authors edited the manuscript.

FUNDING

This project was funded by Natural Sciences and Engineering Research Council of Canada and Aviagen account number RGPIN-2016-05671.

ACKNOWLEDGMENTS

We would like to acknowledge the Natural Sciences and Engineering Research Council of Canada and Aviagen for their financial support, and the University of Saskatchewan Poultry Centre staff and students for their technical assistance.

REFERENCES

Bennett, A. T. D., and Cuthill, I. C. (1994). Ultraviolet vision in birds: what is its function? *Vis. Res.* 34, 1471–1478. doi: 10.1016/0042-6989(94)90149-X

Bremner, F. D. (2004). Pupil assessment in optic nerve disorders. *Eye* 18, 1175–1181. doi: 10.1038/sj.eye.6701560

Brown, N. A. P., Bron, A. J., Ayliffe, W., Sparrow, J., and Hill, A. R. (1987). The objective assessment of cataract. *Eye* 1, 234–246. doi: 10.1038/eye.1987.43

Canadian Council on Animal Care (1999). *CCAC Guidelines on: the Care and Use of Farm Animals in Research, Teaching, and Testing*. Ottawa: Canadian Council on Animal Care.

Cohen, Y., Belkin, M., Yehezkel, O., Solomon, A. S., and Polat, U. (2011). Dependency between light intensity and refractive development under light-dark cycles. *Exp. Eye Res.* 92, 40–46. doi: 10.1016/j.exer.2010.10.012

Collins, S., Forkman, B., Kristensen, H. H., Sandøe, P., and Hocking, P. M. (2011). Investigating the importance of vision in poultry: comparing the behaviour of blind and sighted chickens. *Appl. Anim. Behav. Sci.* 133, 60–69. doi: 10.1080/17466202.2011.611619

Deep, A., Raginski, C., Schwean-Lardner, K., Fancher, B. I., and Classen, H. L. (2013). Minimum light intensity threshold to prevent negative effects on broiler production and welfare. *Br. Poult. Sci.* 54, 686–694. doi: 10.1080/00071668.2013.847526

Deep, A., Schwean-Lardner, K., Crowe, T. G., Fancher, B. I., and Classen, H. L. (2010). Effect of light intensity on broiler production, processing characteristics, and welfare. *Poult. Sci.* 89, 2326–2333. doi: 10.3382/ps.2010-00964

Deep, A., Schwean-Lardner, K., Crowe, T. G., Fancher, B. I., and Classen, H. L. (2012). Effect of light intensity on broiler behaviour and diurnal rhythms. *Appl. Anim. Behav. Sci.* 136, 50–56. doi: 10.1016/j.applanim.2011.11.002

del Olmo-Aguado, S., Núñez-Álvarez, C., and Osborne, N. N. (2016). Blue Light Action on Mitochondria Leads to Cell Death by Necroptosis. *Neurochem. Res.* 41, 2324–2335. doi: 10.1007/s11064-016-1946-5

DeMello, L. R., Foster, T. M., and Temple, W. (1992). Discriminative Performance of the Domestic Hen in a Visual Acuity Task. *J. Exp. Anal. Behav.* 58, 147–157. doi: 10.1901/jeab.1992.58-147

Flaxman, S. R., Bourne, R. R. A., Resnikoff, S., Ackland, P., Braithwaite, T., Cicinelli, M. V., et al. (2017). Global causes of blindness and distance vision impairment 1990–2020: a systematic review and meta-analysis. *Lancet Glob. Heal.* 5, e1221–e1234. doi: 10.1016/S2214-109X(17)30393-5

Foulds, W. S., Barathi, V. A., and Luu, C. D. (2013). Progressive myopia or hyperopia can be induced in chicks and reversed by manipulation of the chromaticity of ambient light. *Investig. Ophthalmol. Vis. Sci.* 54, 8004–8012. doi: 10.1167/iovs.13-12476

Garamszegi, L. Z., Møller, A. P., and Erritzøe, J. (2002). Coevolving avian eye size and brain size in relation to prey capture and nocturnality. *Proc. R. Soc. B Biol. Sci.* 269, 961–967. doi: 10.1098/rspb.2002.1967

Hyvärinen, L. (2018). *LEA Grating Acuity Test - 251300*. Available online at: https://www.leatest.com/sites/default/files/pdf/251300_GratingAcuity.pdf. (Accessed Jan 12, 2022)

Kelber, A. (2019). Bird colour vision – from cones to perception. *Curr. Opin. Behav. Sci.* 30, 34–40. doi: 10.1016/j.cobeha.2019.05.003

Kram, Y. A., Mantey, S., and Corbo, J. C. (2010). Avian cone photoreceptors tile the retina as five independent, self-organizing mosaics. *PLoS One* 5:e8992. doi: 10.1371/journal.pone.0008992

Kristensen, H. H. (2004). *The Behaviour and Welfare of Broiler Chickens in Different Light Environments*. [PhD Thesis]. Copenhagen: The Royal Veterinary and Agricultural University.

Kristensen, H. H., Perry, G. C., Prescott, N. B., Ladewig, J., Ersboll, A. K., and Wathes, C. M. (2006). Leg health and performance of broiler chickens reared in different light environments. *Br. Poult. Sci.* 47, 257–263.

Kuse, Y., Ogawa, K., Tsuruma, K., Shimazawa, M., and Hara, H. (2014). Damage of photoreceptor-derived cells in culture induced by light emitting diode-derived blue light. *Sci. Rep.* 4:5223. doi: 10.1038/srep05223

Leis, M. L., Dodd, M. M. U., Starrak, G., Vermette, C. J., Gomis, S., Bauer, B. S., et al. (2017). Effect of prolonged photoperiod on ocular tissues of domestic turkeys. *Vet. Ophthalmol.* 20, 232–241. doi: 10.1111/vop.12395

Lewis, P. D., and Morris, T. R. (2000). Poultry and coloured light. *Worlds Poult. Sci. J.* 56, 203–207. doi: 10.1079/WPS20000015

Lin, G., Taylor, C., and Rucker, F. (2020). Effect of duration, and temporal modulation, of monochromatic light on emmetropization in chicks. *Vis. Res.* 166, 12–19. doi: 10.1016/j.visres.2019.11.002

Liu, R., Qian, Y. F., He, J. C., Hu, M., Zhou, X. T., Dai, J. H., et al. (2011). Effects of different monochromatic lights on refractive development and eye growth in guinea pigs. *Exp. Eye Res.* 92, 447–453. doi: 10.1016/j.exer.2011.03.003

Marshall, J., and Arikawa, K. (2014). Unconventional colour vision. *Curr. Biol.* 24, R1150–R1154. doi: 10.1016/j.cub.2014.10.025

Mohamed, R., ElKholya, S., Shukry, M., ElKassas, S., and Saidy, N. (2017). Manipulation of Broiler Growth Performance, Physiological and Fear Responses Using Three Monochromatic LED lights. *Alexandria J. Vet. Sci.* 53:57. doi: 10.5455/ajvs.263048

Mohamed, R. A., Eltholth, M. M., and El-Saidy, N. R. (2014). Rearing broiler chickens under monochromatic blue light improve performance and reduce fear and stress during pre-slaughter handling and transportation. *Biotechnol. Anim. Husb.* 30, 457–471. doi: 10.2298/BAH1403457M

Nakamura, M., Kuse, Y., Tsuruma, K., Shimazawa, M., and Hara, H. (2017). The involvement of the oxidative stress in murine blue LED light-induced retinal damage model. *Biol. Pharm. Bull.* 40, 1219–1225. doi: 10.1248/bpb.b16-01008

Nickla, D. L. (2013). Ocular diurnal rhythms and eye growth regulation: where we are 50 years after Lauber. *Exp. Eye Res.* 114, 25–34. doi: 10.1016/j.exer.2012.12.013

Nickla, D. L., and Schroedl, F. (2012). Parasympathetic influences on emmetropization in chicks: evidence for different mechanisms in form deprivation vs negative lens-induced myopia. *Exp. Eye Res.* 102, 93–103. doi: 10.1016/j.exer.2012.07.002

Nickla, D. L., Wildsoet, C., and Wallman, J. (1998). The Circadian Rhythm in Intraocular Pressure and its Relation to Diurnal Ocular Growth Changes in Chicks. *Exp. Eye Res.* 66, 183–193. doi: 10.1006/exer.1997.0425

Nuboer, J. F. W., Coemans, M. A. J. M., and Vos, J. J. (1992). Artificial lighting in poultry houses: are photometric units appropriate for describing illumination intensities? *Br. Poult. Sci.* 33, 135–140.

Ouyang, X., Yang, J., Hong, Z., Wu, Y., Xie, Y., and Wang, G. (2020). Mechanisms of blue light-induced eye hazard and protective measures: a review. *Biomed. Pharmacother.* 130:110577. doi: 10.1016/j.biopha.2020.110577

Ozkaya, E. K., Anderson, G., Dhillon, B., and Bagnaninchi, P. O. (2019). Blue-light induced breakdown of barrier function on human retinal epithelial cells is mediated by PKC-ζ over-activation and oxidative stress. *Exp. Eye Res.* 189:107817. doi: 10.1016/j.exer.2019.107817

Prashar, A., Guggenheim, J. A., Erichsen, J. T., Hocking, P. M., and Morgan, J. E. (2007). Measurement of intraocular pressure (IOP) in chickens using a rebound tonometer: quantitative evaluation of variance due to position inaccuracies. *Exp. Eye Res.* 85, 563–571. doi: 10.1016/j.exer.2007.07.010

Prayitno, D. S., Phillips, C. J. C., and Omed, H. (1997a). The Effects of Color of Lighting on the Behavior and Production of Meat Chickens. *Poult. Sci.* 76, 452–457. doi: 10.1093/ps/76.3.452

Prayitno, D. S., Phillips, C. J. C., and Stokes, D. K. (1997b). The Effects of Color and Intensity of Light on Behavior and Leg Disorders in Broiler Chickens. *Poult. Sci.* 76, 1674–1681. doi: 10.1093/ps/76.12.1674

Prescott, N. B., and Wathes, C. M. (1999). Spectral sensitivity of the domestic fowl (Gallus g. domesticus). *Brit. Poult. Sci.* 40, 332–339. doi: 10.1080/00071669987412

Prescott, N. B., Wathes, C. M., and Jarvis, J. R. (2003). Light, vision and the welfare of poultry. *Anim. Welf.* 12, 269–288.

Rohrer, B., Schaeffel, F., and Zrenner, E. (1992). Longitudinal chromatic aberration and emmetropization: results from the chicken eye. *J. Physiol.* 449, 363–376. doi: 10.1113/jphysiol.1992.sp019090

Rothova, A., van Veenendaal, W. G., and Linssen, A. (1987). Clinical features of acute anterior uveitis. *Am. J. Ophthalmol.* 103, 137–145. doi: 10.1016/S0002-9394(14)74218-7

Rozenboim, I., Biran, I., Zehava, U., Robinzon, B., and Halevy, O. (1999). The effect of monochromatic light on broiler growth and development. *Poult. Sci.* 78, 135–138. doi: 10.1093/ps/83.5.842

Rucker, F. (2019). Monochromatic and white light and the regulation of eye growth. *Exp. Eye Res.* 184, 172–182. doi: 10.1016/j.exer.2019.04.020

Rucker, F. J. (2013). The role of luminance and chromatic cues in emmetropization. *Ophthalmic Physiol. Opt.* 33, 196–214. doi: 10.1111/opo.12050

Rukmini, A. V., Milea, D., and Gooley, J. J. (2019). Chromatic pupillometry methods for assessing photoreceptor health in retinal and optic nerve diseases. *Front. Neurol.* 10:76. doi: 10.3389/fneur.2019.00076

Schwean-Lardner, K., Fancher, B. I., and Classen, H. L. (2012a). Impact of daylength on behavioural output in commercial broilers. *Appl. Anim. Behav. Sci.* 137, 43–52. doi: 10.1016/j.applanim.2012.01.015

Schwean-Lardner, K., Fancher, I., and Classen, H. L. (2012b). Impact of daylength on the productivity of two commercial broiler strains. *Br. Poult. Sci.* 53, 7–18. doi: 10.1080/00071668.2012.659652

Schwean-Lardner, K., Fancher, B. I., Gomis, S., van Kessel, A., Dalal, S., and Classen, H. L. (2013). Effect of day length on cause of mortality, leg health, and ocular health in broilers. *Poult. Sci.* 92, 1–11. doi: 10.3382/ps.2011-01967

Schwean-Lardner, K., Fancher, B. I., Laarveld, B., and Classen, H. L. (2014). Effect of day length on flock behavioural patterns and melatonin rhythms in broilers. *Br. Poult. Sci.* 55, 21–30. doi: 10.1080/00071668.2013.860211

Smith, E. L., Hung, L. F., Arumugam, B., Holden, B. A., Neitz, M., and Neitz, J. (2015). Effects of long-wavelength lighting on refractive development in infant rhesus monkeys. *Investig. Ophthalmol. Vis. Sci.* 56, 6490–6500. doi: 10.1167/iovs.15-17025

Sultana, S., Hassan, M. R., Choe, H. S., and Ryu, K. S. (2013). The effect of monochromatic and mixed LED light colour on the behaviour and fear responses of broiler chicken. *Avian Biol. Res.* 6, 207–214. doi: 10.3184/175815513X13739879772128

Teller, D. Y., McDonald, M., Preston, K., Sebris, S. L., and Dobson, V. (1986). Assessment of visual acuity in infant and children: the acuity card procedure. *Dev. Med. Child Neurol.* 28, 779–789. doi: 10.1111/j.1469-8749.1986.tb03932.x

Vermette, C., Schwean-Lardner, K., Gomis, S., Grahn, B. H., Crowe, T. G., and Classen, H. L. (2016). The impact of graded levels of day length on Turkey health and behavior to 18 weeks of age. *Poult. Sci.* 95, 1223–1237. doi: 10.3382/ps/pew078

Wahl, C., Lim, T., and Howland, H. C. (2016). Intraocular pressure fluctuation of growing chick eyes are suppressed in constant light condition. *Exp. Eye Res.* 148, 52–54.

Walls, H. L., Walls, K. L., and Benke, G. (2011). Eye disease resulting from increased use of fluorescent lighting as a climate change mitigation strategy. *Am. J. Public Health* 101, 2222–2225. doi: 10.2105/AJPH.2011.300246

Whitley, R. D., Albert, R. A., McDaniel, G. R., Brewer, R. N., Mora, E. C., and Henderson, R. A. (1984). Photoinduced Buphthalmic Avian Eyes. 1. Continuous Fluorescent Light. *Poult. Sci.* 63, 1537–1542. doi: 10.3382/ps.0631537

Wisely, C. E., Sayed, J. A., Tamez, H., Zelinka, C., Abdel-Rahman, M. H., Fischer, A. J., et al. (2017). The chick eye in vision research: an excellent model for the study of ocular disease. *Prog. Retin. Eye Res.* 61, 72–97. doi: 10.1016/j.preteyeres.2017.06.004

Conflict of Interest: BF, SG, and NF are employees by Aviagen Inc.

The remaining authors declare that the research was conducted in the absence of any commercial or financial relationships that could be construed as a potential conflict of interest.

Publisher's Note: All claims expressed in this article are solely those of the authors and do not necessarily represent those of their affiliated organizations, or those of the publisher, the editors and the reviewers. Any product that may be evaluated in this article, or claim that may be made by its manufacturer, is not guaranteed or endorsed by the publisher.

frontiers | Frontiers in Physiology

ORIGINAL RESEARCH
published: 23 May 2022
doi: 10.3389/fphys.2022.892887

Temperature and Growth Selection Effects on Proliferation, Differentiation, and Adipogenic Potential of Turkey Myogenic Satellite Cells Through Frizzled-7-Mediated Wnt Planar Cell Polarity Pathway

Jiahui Xu[1], *Gale M. Strasburg*[2], *Kent M. Reed*[3] *and Sandra G. Velleman*[1]*

[1]Department of Animal Sciences, The Ohio State University, Wooster, OH, United States, [2]Department of Food Science and Human Nutrition, Michigan State University, East Lansing, MI, United States, [3]Department of Veterinary and Biomedical Sciences, University of Minnesota, St. Paul, MN, United States

OPEN ACCESS

Edited by:
Krystyna Pierzchala-Koziec, University of Agriculture in Krakow, Poland

Reviewed by:
Avais Daulat, Institut Paoli-Calmettes (IPC), France
Rosario Donato, University of Perugia, Italy

***Correspondence:**
Sandra G. Velleman
velleman.1@osu.edu

Specialty section:
This article was submitted to Avian Physiology, a section of the journal Frontiers in Physiology

Received: *09 March 2022*
Accepted: *19 April 2022*
Published: *23 May 2022*

Citation:
Xu J, Strasburg GM, Reed KM and Velleman SG (2022) Temperature and Growth Selection Effects on Proliferation, Differentiation, and Adipogenic Potential of Turkey Myogenic Satellite Cells Through Frizzled-7-Mediated Wnt Planar Cell Polarity Pathway. Front. Physiol. 13:892887. doi: 10.3389/fphys.2022.892887

Satellite cells (SCs) are a heterogeneous population of multipotential stem cells. During the first week after hatch, satellite cell function and fate are sensitive to temperature. Wingless-type mouse mammary tumor virus integration site family/planar cell polarity (Wnt/PCP) signaling pathway is significantly affected by thermal stress in turkey pectoralis major (p. major) muscle SCs. This pathway regulates the activity of SCs through a frizzled-7 (Fzd7) cell surface receptor and two intracellular effectors, rho-associated protein kinase (ROCK) and c-Jun. The objective of the present study was to determine the effects of thermal stress, growth selection, and the Fzd7-mediated Wnt/PCP pathway on proliferation, myogenic differentiation, lipid accumulation, and expression of myogenic and adipogenic regulatory genes. These effects were evaluated in SCs isolated from the p. major muscle of 1-week faster-growing modern commercial (NC) line of turkeys as compared to SCs of a slower-growing historic Randombred Control Line 2 (RBC2) turkey line. Heat stress (43°C) increased phosphorylation of both ROCK and c-Jun with greater increases observed in the RBC2 line. Cold stress (33°C) had an inhibitory effect on both ROCK and c-Jun phosphorylation with the NC line showing greater reductions. Knockdown of the expression of *Fzd7* decreased proliferation, differentiation, and expression of myogenic regulatory genes: *myoblast determination factor-1* and *myogenin* in both lines. Both lipid accumulation and expression of adipogenic regulatory genes: *peroxisome proliferator-activated receptor-γ*, *CCAAT/enhancer-binding protein-β*, and *neuropeptide-Y* were suppressed with the *Fzd7* knockdown. The RBC2 line was more dependent on the Fzd7-mediated Wnt/PCP pathway for proliferation, differentiation, and lipid accumulation compared to the NC line. Thus, thermal stress may affect poultry breast muscle growth potential and protein to fat ratio by altering function and fate of SCs through the Fzd7-mediated Wnt/PCP pathway in a growth-dependent manner.

Keywords: adipogenesis, growth selection, muscle, satellite cell, temperature, turkey

1 INTRODUCTION

Birds are homeotherms, and thus, maintain body temperature within a limited range (Yahav, 2015). Newly hatched poults have a poorly developed thermal regulatory system (Dunnington and Siegel, 1984; Modrey and Nichelmann, 1992), that limits their ability to cope with external thermal stress. For example, the body temperature of poults significantly changes with thermal stress (Shinder et al., 2007; Maman et al., 2019). Post-hatch thermal stress can affect muscle growth and structure by changing myofiber diameter (Piestun et al., 2017; Patael et al., 2019), capillary density (Joiner et al., 2014), and fat deposition (Zhang et al., 2012; Patael et al., 2019) particularly in the pectoralis major (p. major; breast) muscle. With intensive genetic selection for increased growth rate and breast muscle yield, modern faster-growing poultry lines produce more heat due to a greater metabolic rate (Konarzewski et al., 2000). In addition, faster-growing poultry also have a reduced ability to remove metabolic heat and byproducts like lactic acid due to decreased capillary supply in the p. major muscle (Hoving-Bolink et al., 2000; Joiner et al., 2014). Thus, faster-growing poultry lines have a lower tolerance to external heat stress (Berrong and Washburn, 1998; Chiang et al., 2008).

The number of myofibers is fixed by the time of hatch (Smith, 1963). Muscle growth after hatch occurs mainly through hypertrophy of existing myofibers mediated by the activity of adult myoblasts, satellite cells (SCs). Post-hatch myofiber hypertrophy proceeds through accretion of satellite cell (SC) nuclei to existing myofibers (Moss and Leblond, 1971; Cardasis and Cooper, 1975). During the period of SC peak mitotic activity, the first week after hatch in poultry (Mozdziak et al., 1994; Halevy et al., 2000), both proliferation and myogenic differentiation of SCs in the p. major muscle are highly responsive to environmental thermal stress (Halevy et al., 2001; Xu et al., 2021b). Thus, early-age hot and cold thermal stress has long-lasting effects on p. major muscle growth and structure (Piestun et al., 2017; Patael et al., 2019), in part, by altering the proliferation and myogenic activity of SCs.

As multipotential stem cells (Shefer et al., 2004), SCs also express adipogenic genes and produce lipid with appropriate extrinsic stimuli, including hot temperature (Harding et al., 2015; Patael et al., 2019; Xu et al., 2021a). Due to heterogeneity, SCs from the same myofiber type can contain different cell populations varying in proliferation and differentiation rate (McFarland et al., 1995), and adipogenic potential (Rossi et al., 2010). In *in vitro* studies, faster-proliferating SCs synthesize more lipid than slower-proliferating SCs (Rossi et al., 2010; Xu et al., 2021a). Selection for increased growth in turkeys has facilitated the conversion of the p. major muscle SCs to a faster-proliferating population (Velleman et al., 2000; Clark et al., 2016; Xu et al., 2021b) with increased lipid production (Velleman, 2014; Clark et al., 2017; Xu et al., 2021a). Heat stress further increases the lipid content in SCs, while it is suppressed under cold stress (Clark et al., 2017; Xu et al., 2021a). Increased lipid synthesis by SCs *in vivo* will result in increased intramuscular fat deposition (Velleman et al., 2014; Piestun et al., 2017; Patael et al., 2019), and alter protein to fat ratio in the poultry p. major muscle.

Changes in cellular function with response to thermal stress are mediated through signal transduction pathways. Results from transcriptome analysis showed that the expression of genes associated with wingless-type mouse mammary tumor virus integration site family (Wnt) signaling pathway was greatly altered by both hot and cold thermal stress in turkey p. major muscle SCs (Reed et al., 2017a). Among the most affected *Wnt* genes, *Wnt7a* expression was upregulated with heat stress, particularly in a growth-selected turkey line (Reed et al., 2017a). In mice, protein-ligand Wnt7a activates a non-canonical planar cell polarity (PCP) pathway in SCs through a cell surface receptor, frizzled-7 (Fzd7) (Le Grand et al., 2009; Von Maltzahn et al., 2012). A recent *in vitro* study by Risha et al. (2021) showed that both hot and cold thermal stress significantly altered the expression of *Wnt7a* and *Fzd7* in mouse myoblasts. Thus, in the turkey p. major muscle SCs, thermal stress may similarly function through the Wnt/PCP pathway and Fzd7 receptor.

Downstream branches of the Wnt/PCP pathway include but are not limited to: 1) ras homolog gene family member A (RhoA) (Strutt et al., 1997; Fanto et al., 2000) through its effector rho-associated protein kinase (ROCK) (Laumanns et al., 2009); and 2) ras-related C3 botulinum toxin substrate 1 (Rac1) (Eaton et al., 1996; Fanto et al., 2000) *via* its effector c-Jun (Weber et al., 2000). In mammalian skeletal muscle, the Wnt/PCP pathway promotes proliferation of SCs through the Fzd7 receptor and increases the SC pool stimulating myofiber hypertrophy resulting in increased skeletal muscle mass (Le Grand et al., 2009). The Fzd7-mediated Wnt-PCP pathway is also involved in the rearrangement of cytoskeleton protein, actin, during cell migration *via* the RhoA/ROCK signaling (Fortier et al., 2008; Kaucká et al., 2013; Asad et al., 2014; Wang et al., 2018). Migration is required for SC alignment before fusion to form multinucleated myotubes (Chazaud et al., 1998). In addition to migration, RhoA/ROCK signaling is also involved in regulating myogenic differentiation (Iwasaki et al., 2008) and adipogenic potential (Sordella et al., 2003; Bryan et al., 2005; Hosoyama et al., 2009) in mouse myoblasts. Another Wnt/PCP effector, c-Jun, is a cell proliferation activator that promotes cell cycle progression through G1 phase (Schreiber et al., 1999; Wisdom et al., 1999). In myogenic myoblasts (Daury et al., 2001) and SCs (Umansky et al., 2015; Hindi and Kumar, 2016), the primary function of c-Jun is to stimulate proliferation and inhibit myogenic differentiation. Thus, one of the objectives in the present study was to analyze the role of the Fzd7-mediated Wnt/PCP pathway in thermal stress-induced changes in the function and fate of SCs.

Although previous evidence showed the Wnt/PCP pathway is involved in proliferation (Le Grand et al., 2009), migration (Wang et al., 2018), and adipogenesis (Bryan et al., 2005) through its downstream effectors in mammalian SCs, the role of the Wnt/PCP pathway in regulating the function and fate of SCs in poultry during thermal stress has not been examined. Growth-selected turkeys display differential expression of *Wnt* genes in SCs compared to non-growth-selected turkeys (Reed et al., 2017a). With peak mitotic activity during the first week after hatch (Mozdziak et al., 1994; Halevy et al., 2000), the function and fate of turkey SCs are highly responsive to thermal stress (Xu

et al., 2021a; Xu et al., 2021b) likely through the Wnt/PCP pathway. Thus, the objective of the present study was to determine the effects of thermal stress, growth selection, and the Fzd7-mediated Wnt/PCP pathway on proliferation, myogenic differentiation, lipid accumulation, and expression of myogenic and adipogenic regulatory genes in the p. major muscle SCs isolated from 1-week turkeys. To determine how the Fzd7-mediated Wnt/PCP pathway participates in regulating SC activity, *Fzd7* expression was knocked down with small interfering RNA (siRNA) in SCs isolated from modern commercial (NC) line turkeys and Randombred Control Line 2 (RBC2) turkeys representing slower-growing turkeys of the 1960s (Nestor et al., 1969). Alterations in SC function and fate will have long-term effects on the growth, structure, and protein to fat ratio of the poultry p. major muscle.

2 MATERIALS AND METHODS

2.1 Satellite Cells

Satellite cells were previously isolated from the p. major muscle of 1-week-old RBC2 and NC turkeys following the method of Velleman et al. (2000). Only male turkeys were selected for cell isolation to avoid the confounding effect of sex (Velleman et al., 2000). All the SCs were passaged to a fourth pass and stored in liquid nitrogen until use.

2.2 Small Interfering RNA

Small interfering RNA targeting *Fzd7* (Gene bank ID: XM_010713460.1) was synthesized as a stealth siRNA duplex (Thermo Fisher Scientific, Waltham, MA, United States), and was designed using Invitrogen Block-iT siRNA designer (https://rnaidesigner.thermofisher.com/rnaiexpress/setOption.do?designOption=stealth&pid). The *Fzd7* siRNA targets the *Fzd7* open reading frame from 1522 to 1546 with the following sequence: sense strand: 5′-CCG GAC UUC ACA GUC UUC AUG AUC A-3′; anti-sense strand: 5′-UGA UCA UGA AGA CUG UGA AGU CCG G-3′. A stealth siRNA with 48% guanine and cytosine content was used as the negative control siRNA (Thermo Fisher Scientific).

To determine the knockdown efficiency of the *Fzd7* siRNA, p. major muscle SCs from each line were plated (18,000 cells per well) in 24-well gelatin-coated plates (Greiner Bio-One, Monroe, NC, United States) in 500 µl of Dulbecco's Modified Eagle's Medium (DMEM, Sigma-Aldrich, St. Louis, MO, United States) transfection medium supplemented with 10% chicken serum (Gemini Bio-Products, West Sacramento, CA, United States) and 5% horse serum (Gemini Bio-Products), and incubated at 38°C in a 95% air/5% CO_2 incubator (Thermo Fisher Scientific) for 24 h allowing for cell attachment. After 24 h, cells in each well were transfected with 20 pmol/µl of either the *Fzd7* siRNA or the negative control siRNA with 1 µl of lipofectamine 2000 (Thermo Fisher Scientific) according to the manufacturer's protocol. After 12 h of transfection, the medium was replaced with McCoy's 5A growth medium (Sigma Aldrich) containing 10% chicken serum (Gemini Bio-Products), 5% horse serum (Gemini Bio-Products), 1% antibiotics-antimycotics (Corning, Corning, NY, United States), and 0.1% gentamicin (Omega Scientific, Tarzana, CA, United States) for 72 h of proliferation with the medium changed every 24 h. At 72 h post transfection, cells were removed from the incubator and total RNA was extracted for gene expression analysis by Real-Time Quantitative PCR (RT-qPCR) as described in **Section 2.8**. The transfection experiment and RT-qPCR was independently repeated twice to confirm knockdown efficiency of the *Fzd7* siRNA.

2.3 Western Blot Analysis

The RBC2 and NC line SCs were plated in 24-well plates (15,000 cells per well) in a DMEM plating medium containing 10% chicken serum, 5% horse serum, 1% antibiotics-antimycotics, and 0.1% gentamicin. The plated cells were allowed to attach for 24 h while incubated at 38°C in a 95% air/5% CO_2 incubator. After 24 h, the plating medium was replaced with the growth medium. Satellite cells from both lines were then randomly assigned to proliferate at 33°C, 38°C, or 43°C for 72 h, with the growth medium changed every 24 h. After 72 h of proliferation, the growth medium was replaced with a DMEM differentiation medium containing 3% horse serum, 1% antibiotics-antimycotics, 0.1% gentamicin, 0.1% gelatin, and 1 mg/ml bovine serum albumin (BSA, Sigma Aldrich). The differentiation medium was changed every 24 h. At 24-h intervals during differentiation, one plate in each group was removed from incubation and rinsed with phosphate buffered saline (PBS, 171 mM NaCl, 3.35 mM KCl, 1.84 mM KH_2PO_4, and 10 mM Na_2HPO_4, pH7.08) for protein extraction.

For *Fzd7* siRNA transfection, cell culture and transfection procedures were the same as described in **Section 2.3** until 72 h of proliferation. At 72 h of proliferation, the growth medium was replaced with differentiation medium, and incubation continued with the differentiation medium changed every 24 h. At 48 h of differentiation, all plates were removed, rinsed with PBS and total protein immediately extracted.

For protein extraction, 100 µl per well of ice-cold protein extraction buffer [50 mM Tris–HCl, 1% Nonidet P-40, 0.5% sodium deoxycholate, 0.1% sodium dodecyl sulphate (SDS), 150 mM NaCl, 1 mM EDTA, 1 mM Na_3VO_4, and protease and phosphatase inhibitors (Thermo Fisher Scientific)] was added to the 24-well plates and incubated for 15 min on ice. Cells were scraped from each well, and the lysate was incubated on ice for another 15 min. A syringe with a 26 G needle was used to aspirate the cell lysate. The cell lysate was centrifuged at 10,000 rpm for 15 min at 4°C, and supernatant was collected. Protein concentration was measured using the Bradford method (Bradford, 1976) and samples were adjusted to equal concentration. A denaturation buffer containing 0.1 M tris-HCl, 10% glycerol, 1% β-mercaptoethanol, 0.1% bromophenol blue, and 1% sodium dodecyl sulfate (SDS) was added to each protein sample before boiling for 10 min. The denatured samples (30 µg/well) and a pre-stained protein molecular weight standard (Thermo Fisher Scientific) were separated using 8% sodium dodecyl sulfate-polyacrylamide gel electrophoresis (SDS-PAGE) with 40 mA of constant current in a running buffer (25 mM Tris, 200 mM glycine, and 10% SDS, pH 8.3)

according to the method of Laemmli (1970). Separated proteins were transferred from the SDS-PAGE to a polyvinylidene difluoride (PVDF) membrane at 200 mA in a transfer buffer containing 25 mM tris, 192 mM glycine, and 20% methanol for 2.5 h on ice. The PVDF membrane was blocked with a blocking buffer (5% non-fat milk, 20% Tween-20, 20 mM Tris-HCl, 500 mM NaCl, pH 7.5) for 60 min at room temperature, then, incubated overnight with a primary antibody diluted in blocking buffer at 4°C. Primary antibodies included: rabbit anti-ROCK1 (1: 1000 dilution, Abcam, Waltham, MA, United States), rabbit anti-phospho-ROCK1 at Thr455/Ser456 (1:700 dilution, Bioss Antibodies, Woburn, MA, United States), rabbit anti-c-Jun (1: 700 dilution, MyBioSource, San Diego, CA, United States), rabbit anti-phospho-c-Jun at Ser73 (1:700 dilution, Cell Signaling Technology, MA, United States), and rabbit anti-β-actin (1: 1,000 dilution, Cell Signaling Technology). After incubation with primary antibody, the PVDF membrane was gently agitated for 10 min in a washing buffer (20% Tween-20, 20 mM Tris-HCl, 500 mM NaCl, pH 7.5) for three times. The PVDF membrane was then incubated for 2 h at room temperature in a horseradish peroxidase-conjugated goat anti-rabbit secondary antibody (1:1000 dilution, Cell Signaling Technology) in the blocking buffer. After gentle agitation the PVDF membrane in washing buffer three times, a chemiluminescent substrate (Thermo Fishier Scientific) was used to visualize target protein bands on a Bio-Rad ChemiDoc XRS imaging system (Bio-Rad, Hercules, CA, United States). The membrane was re-stripped using a western blot stripping buffer (Thermal Fishier Scientific) before incubating with other primary antibodies as described above. Density of the band β-actin was used to normalize each target protein. The ratio of phosphorylated protein to total protein was calculated from normalized band densities (Zhang et al., 2008). Fold change was calculated as the ratio of each treatment group divided by the calculated ratio of the control group. The western blot analysis was independently repeated in twice per treatment. Due to reduced cellular growth at 33°C and being able to isolate sufficient protein, the following number of replicate wells were used: 12 wells per cell line at 38°C and 43°C, 24 wells per cell line at 33°C.

2.4 Proliferation Assay

Cell culture and transfection procedures were the same as described in **Section 2.2**. During the 72 h of proliferation, one plate from each treatment group was removed from incubator every 24 h and stored at −70°C until assayed.

Proliferation assay was conducted according to the method of McFarland et al. (1995). All plates were removed from −70°C and thawed at room temperature for 15 min, 200 µl of 0.05% trypsin-EDTA (Thermo Fisher Scientific) in 10 mM Tris, 2 M NaCl, and 1 mM EDTA (TNE) was added to each culture well and incubated at room temperature for 7 min. The plates were then returned to −70°C overnight. After thawing the plates for 15 min at room temperature, 1.8 ml of TNE buffer containing 0.2% (1 mg/ml) Hoechst dye (Sigma-Aldrich) was added to each well, and the plates were gently agitated for 2 h at room temperature. DNA-incorporated Hoechst dye was measured using a Fluoroskan Ascent FL plate reader (Thermo Fisher Scientific). A standard curve constructed using double-stranded calf thymus DNA (Sigma-Aldrich) to determine sample DNA concentration. The proliferation assay was repeated in two independent cultures with four replicate wells per treatment per culture.

2.5 Differentiation Assay

For transfection at the beginning of proliferation, 11, 000 cells were plated in each well of 48-well gelatin-coated plates in 500 µl of transfection medium and incubated at 38°C in a 95% air/5% CO_2 incubator. After 24 h of attachment, cells in each well were transfected with 20 pmol/µl of either *Fzd7* siRNA or negative control siRNA with 0.5 µl of Lipofectamine 2000. After 12 h of transfection at 38°C, the transfection medium was replaced with growth medium, and cells were randomly assigned to a 33°C, 38°C, or 43°C incubator for 72 h, with the growth medium changed daily. After 72 h of proliferation, the growth medium was replaced with differentiation medium for 72 h of differentiation with the media changed every day. One plate from each treatment group was removed at 24 h of intervals, rinsed with PBS, and stored at −70°C for the differentiation assay.

For transfection at the beginning of differentiation (at 0 h of differentiation), 9,000 cells were plated in each well of 48-well gelatin-coated plates in plating medium at 38°C. After 24 h of attachment, plating medium was replaced with growth medium, and cells from both lines were randomly assigned to a 33°C, 38°C, or 43°C incubator for 72 h of proliferation. The growth medium was changed every 24 h. At 72 h of proliferation, the cells were transfected with 20 pmol/µl of either the *Fzd7* siRNA or the negative control siRNA with 0.5 µl Lipofectamine 2000 per well. After 12 h of transfection, the growth medium was replaced with differentiation medium for 72 h of differentiation. Differentiation medium was changed every 24 h. One plate from each treatment group was removed every 24 h, rinsed with PBS and stored at −70°C for the differentiation assay.

Satellite cell differentiation was determined by measuring creatine kinase activity using a modified method of Yun et al. (1997). All plates were removed from −70°C and thawed at room temperature for 15 min, and 500 µl of creatine kinase buffer [20 mM glucose (Thermo Fisher Scientific), 20 mM phosphocreatine (Calbiochem, San Diego, CA, United States), 10 mM mg acetate (Thermo Fisher Scientific), 10 mM adenosine monophosphate (Sigma Aldrich), 1 mM adenosine diphosphate (Sigma Aldrich), 1 Unit (U)/ml glucose-6-phosphate dehydrogenase (Worthington Biochemical), 0.5 U/ml hexokinase (Worthington Biochemical, Lakewood, NJ, United States), 0.4 mM thio-nicotinamide adenine dinucleotide (Oriental Yeast Co., Tokyo, Japan), 1 mg/ml BSA, to 0.1 M glycylglycine (PH = 7.5)] was added to each well including the standard curve wells containing creatine phosphokinase with concentrations from 0 to 140 milliunits/well (mU/well, Sigma-Aldrich). The optical density of each well was measured at a wavelength of 405 nm using a BioTek ELx800 (BioTek, Winooski, VT, United States) plate reader. The differentiation assay was repeated in two independent cultures with five wells per treatment per culture.

TABLE 1 | Primer sequences for real-time quantitative polymerase chain reaction.

Primer	Sequence	Product size	GenBank accession number
MyoD[a]	5′-GAC GGC ATG ATG GAG TAC AG-3′ (forward) 5′-AGC TTC AGC TGG AGG CAG TA-3′ (reverse)	201 bp[h]	AY641567.1
MyoG[b]	5′-CCT TTC CCA CTC CTC TCC AAA-3′ (forward) 5′-GAC CTT GGT CGA AGA GCA ACT-3′ (reverse)	175 bp	AY560111.3
Fzd7[c]	5′-CAC CGG CTT CTC CTT TTC TTG-3′ (forward) 5′-ACA GTA AAG AGG GTG GAC GC-3′ (reverse)	207 bp	XM_010713460.1
PPARγ[d]	5′-CCA CTG CAG GAA CAG AAC AA-3′ (forward) 5′-CTC CCG TGT CAT GAA TCC TT-3′ (reverse)	249 bp	XM_010718432.1
C/EBPβ[e]	5′-GCA CAG CGA CGA GTA CAA G-3′ (forward) 5′-GTT GCG CAT TTT GGC TTT GTC-3′ (reverse)	82 bp	XM_003212165.2
NPY[f]	5′-CCC AGA GAC ACT GAT CTC AGA C-3′ (forward) 5′-AGG GTC TTC AAA CCG GGA TCT-3′ (reverse)	76 bp	XM_010712774.3
GAPDH[g]	5′-GAG GGT AGT GAA GGC TGC TG-3′ (forward) 5′-CCA CAA CAC GGT TGC TGT AT-3′ (reverse)	200 bp	U94327.1

[a]MyoD, *myogenic determination factor-1.*
[b]MyoG, *myogenin.*
[c]Fzd7, *frizzled-7.*
[d]PPARγ, *peroxisome proliferator-activated receptor gamma.*
[e]C/EBPβ, *CCAAT/enhancer-binding protein beta.*
[f]NPY, *neuropeptide Y.*
[g]GAPDH, *glyceraldehyde-3-phosphate dehydrogenase.*
[h]*bp, number of base pairs.*

2.6 Myotube Measurement

Cell culture and transfection procedures were as described in **Section 2.5**. At 48 h of differentiation, photomicrographs of SCs and myotubes in each treatment group were taken with an Olympus IX70 fluorescence microscope equipped with a QImaging Retiga Exi Fast digital camera (Qimaging, Surrey, BC, Canada) and CellSens software (Olympus America, Center Valley, PA, United States). The diameter of the myotubes was measured using Image Pro Software (Media Cybernectics, Silver Spring, MD, United States). A total of 100 measurements were taken per treatment with measurements independently repeated in two cultures with five replicate wells per treatment per culture.

2.7 Lipid Content Measurement

Cell culture and transfection procedures were the same as described in **Section 2.2** during proliferation. At 72 h of proliferation, growth medium was replaced with differentiation medium. Differentiation medium was changed every 24 h for the 72 h of differentiation. One plate from each treatment group was collected at 24 h intervals during the 72 h of proliferation and 72 h of differentiation for AdipoRed assay.

Lipids were stained with AdipoRed lipid fluorochrome (Lonza, Walkersville, MD, United States). In brief, after removing the medium, each well was rinsed twice with PBS. Another 1 ml of PBS containing 30 µl of AdipoRed was added to each well with the cultured cells and one blank well without any cells in. After incubating for 15 min at room temperature, the AdipoRed optical density (OD) of each well was measured in the Fluoroskan Ascent FL plate reader at a wavelength of 485 nm. The final OD of each well was the OD of each well minus the measured OD of the blank well. The AdipoRed assay was independently repeated in two cultures with four replicate wells per treatment per culture.

2.8 Gene Expression Analysis

Myogenic regulatory genes measured in this study include myoblast determination factor 1 (*MyoD*) and myogenin (*MyoG*) with the former a proliferation marker (Yablonka-Reuveni and Rivera, 1994) and the latter a myogenic differentiation marker (Brunetti and Goldfine, 1990; Hasty et al., 1993). Adipogenic regulatory genes examined included peroxisome proliferator activated receptor-gamma (*PPARγ*) (Rosen et al., 1999), neuropeptide-Y (*NPY*) (Baker et al., 2009), and CCAAT/enhancer-binding protein-beta (*C/EBPβ*) (Clarke et al., 1997).

Total RNA from each sample was extracted using RNAzol (Molecular Research Center, OH, United States) and the concentration of each sample was quantified by a spectrophotometer (NanoDrop™ ND-1000, Thermo Fisher Scientific). Reverse transcription was performed with Moloney Murine Leukemia Virus Reverse Transcriptase (M-MLV; Promega, WI, United States) to produce cDNA from total RNA. Real-Time Quantitative PCR (RT-qPCR) was conducted with DyNAmo Hot Start SYBR Green qPCR kit (Thermo FisherScientific). Information of all the primers is listed in **Table 1**. Primers for *C/EBPβ*, *MyoD, MyoG, NPY*, *PPARγ*, and an internal control gene glyceraldehyde-3-phosphate dehydrogenase (*GAPDH*) were previously designed, and the specificity was confirmed in this lab as reported by Clark et al. (2017), Clark et al. (2018). Primers for *Fzd7* were designed using primer-BLAST tool (https://www.ncbi.nlm.nih.gov/tools/primer-blast/), and the specificity of the *Fzd7* primers was confirmed by DNA sequencing the PCR product (Molecular and Cellular Imaging Center, The Ohio State University, Wooster, OH). The RT-qPCR reaction was performed in a DNA Engine Opticon 2 real-time machine (Bio-Rad) and included: 1) denaturation at 94°C for 15 min; 2) amplification for 35 cycles with each cycle including denaturation for 30 s at 94°C, annealing

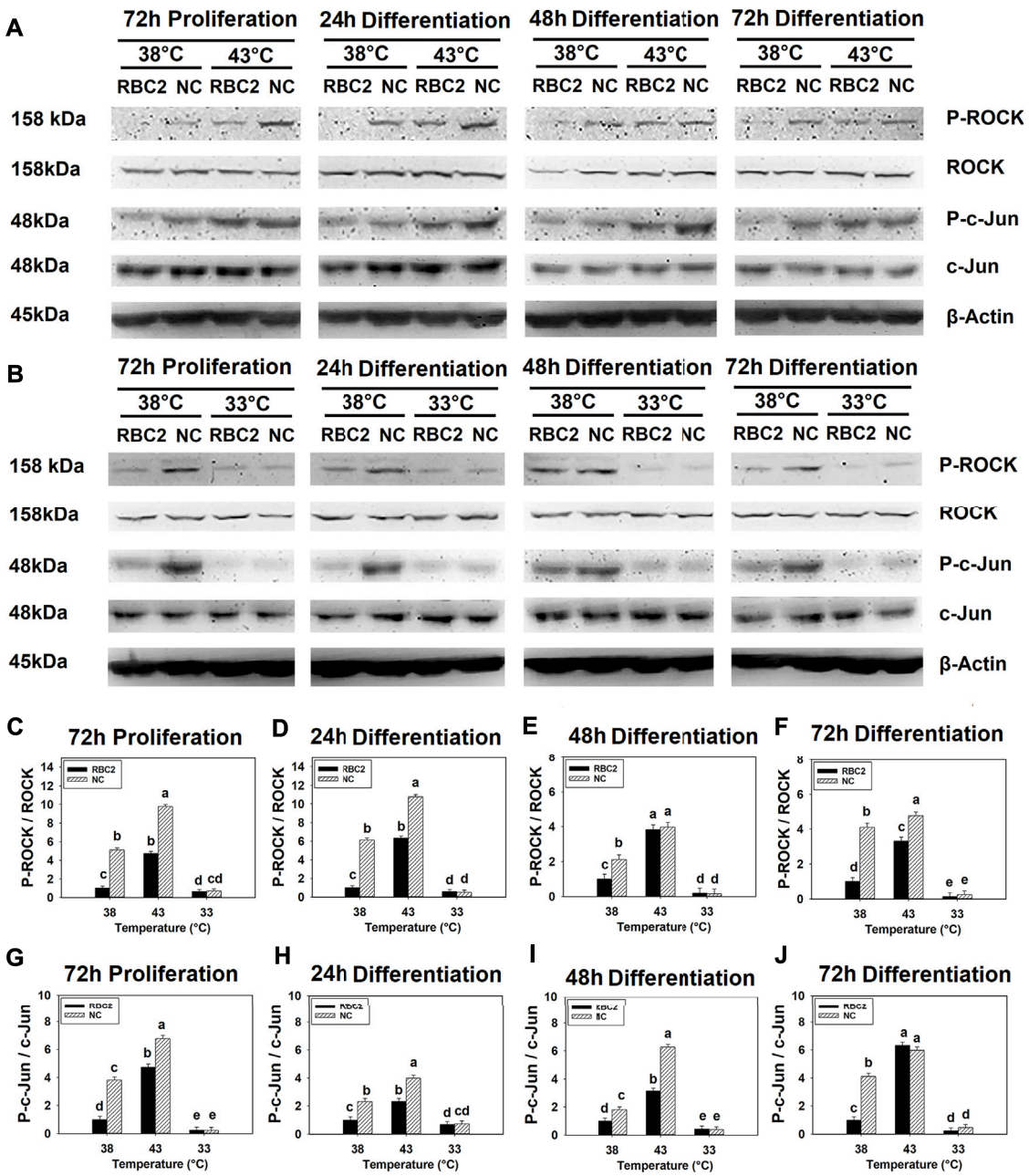

FIGURE 1 | Effect of hot and cold thermal stress on the phosphorylation of rho-associated protein kinase (ROCK) and c-Jun in satellite cells (SCs). **(A)** Western blots of unphosphorylated and phosphorylated ROCK and c-Jun, and an internal control β-actin in the Randombred Control Line 2 (RBC2) and modern commercial (NC) line SCs cultured at 38°C or 43°C and determined at 72 h of proliferation (also represents 0 h of differentiation) and 24, 48, and 72 h of differentiation. **(B)** Western blots of unphosphorylated and phosphorylated ROCK and c-Jun, and an internal control β-actin in the RBC2 and NC line SCs cultured at 38°C or 33°C and determined at 72hP, 24hD, 48hD, and 72hD. Molecular weight is on the left and protein name is on the right side of each figure, respectively. The ratio of phosphorylated to unphosphorylated ROCK band density was calculated at 72 h of proliferation **(C)**, 24 h **(D)**, 48 h **(E)**, and 72 h **(F)** of differentiation. The ratio of phosphorylated to unphosphorylated c-Jun band density was calculated at 72 h of proliferation **(G)**, 24 h **(H)**, 48 h **(I)**, and 72 h **(J)** of differentiation. Each graph bar represents a mean ratio, and each error bar represents a standard error of the mean. Mean values with different letters are significantly different ($p \leq 0.05$).

for 30 s at 55°C (*Fzd7*, *GAPDH*, *NPY*, and *PPARγ*), at 58°C (*MyoD* and *MyoG*), or at 60°C (*C/EBPβ*), and elongation for 30 s at 72°C; and 3) final elongation at 72°C for 5 min. A standard curve of each gene was generated using serial dilutions of purified PCR products (Liu et al., 2006). Arbitrary concentrations from 1 to 100,000 were assigned to each serial dilution. An arbitrary molar concentration of each amplified sample was calculated according to the threshold cycle and was normalized by *GAPDH*. The RT-qPCR for each gene was independently repeated in two cultures with twelve wells per treatment per culture.

2.9 Statistical Analysis

Data from proliferation, differentiation, and AdipoRed assays, myotube measurement, and gene expression analysis were analyzed as a mixed model at each sampling time in SAS (SAS 9.4, SAS Institute INC., NC, United States). Two fixed effects of temperature and cell line, an interaction effect between temperature and cell line, and a random effect of repeat experiment were included in the model. The statement of lsmean in the MIXED procedure was used to determine each mean value and the standard error of the mean (SEM). Differences between each mean were separated with the Pdiff option. Line effect within each treatment group and temperature effect within each cell line was determined with the SLICE option at each sampling time. For AdipoRed assay, the REG procedure was used to evaluate the linear relationship between sampling times and the OD of AdipoRed for each cell line in each treatment group. Difference in the linear response was determined with the contrast statement. $p \leq 0.05$ was considered as statistically significant.

3 RESULTS

3.1 Effects of Thermal Stress and Growth Selection on Rho-Associated Protein Kinase and c-Jun Phosphorylation

Phosphorylation of ROCK showed a significant interaction effect between temperature and cell line ($p < 0.001$) at all sampling times (**Figures 1A–F**). In the RBC2 and NC line SCs, heat stress (43°C) increased ROCK phosphorylation, while cold stress (33°C) showed a significant inhibitory effect ($p < 0.001$). At both 38°C and 43°C, ROCK phosphorylation was greater in the NC line than RBC2 line at 72 h of proliferation, and 24 and 72 h of differentiation ($p < 0.001$). During the cold stress of 33°C, line effects were not significant at any sampling times.

Similarly, a significant interaction effect ($p < 0.001$) between temperature and cell line was observed for c-Jun phosphorylation at all sampling times (**Figures 1A,B,G–J**). Phosphorylation in both lines increased at 43°C but decreased at 33°C compared to the control temperature of 38°C ($p < 0.001$). The NC line showed greater c-Jun phosphorylation at both 38°C and 43°C from 72 h of proliferation to 48 h of differentiation ($p < 0.001$). A significant line effect was not observed at 33°C at any sampling time.

3.2 Effect of Frizzled-7 Knockdown, Thermal Stress, and Growth Selection on Rho-Associated Protein Kinase and c-Jun Phosphorylation

Phosphorylation profiles of both ROCK and c-Jun during 72 h of differentiation in the absence of *Fzd7* knock down are shown in **Supplementary Figure S1**. Phosphorylation of both ROCK and c-Jun peaked at 24 h of differentiation in both lines at 38°C and 43°C (**Supplementary Figures S1A–F**). At 33°C, the NC line showed maximal phosphorylation of c-Jun at 24 h of differentiation (**Supplementary Figures S1G–I**). Thus, 24 h of differentiation was chosen as the sampling time to determine the combined effects of *Fzd7* knockdown, thermal stress, and growth selection on ROCK and c-Jun phosphorylation.

Knockdown efficiency of *Fzd7* siRNA was determined in both lines at 38°C with RT-qPCR. At 72 h post transfection, mRNA expression of *Fzd7* decreased 4.08-fold ($p < 0.001$) and 5.31-fold ($p < 0.001$) in the RBC2 and NC *Fzd7* knockdown groups compared to the control groups, respectively (**Figure 2A**). At 24 h of differentiation, a significant interaction ($p < 0.001$) among the effects of *Fzd7* knockdown, temperature, and line was observed in phosphorylation of both ROCK and c-Jun (**Figures 2B–E**). Knockdown of *Fzd7* decreased phosphorylation of ROCK ($p \leq 0.013$) and c-Jun ($p < 0.001$) in both lines at all the temperatures. However, the NC line showed greater reductions in phosphorylation of both ROCK and c-Jun compared to the RBC2 line independent of temperature.

3.3 Effect of Frizzled-7 Knockdown, Thermal Stress, and Growth Selection on Satellite Cell Proliferation

No significant interaction was observed among *Fzd7* knockdown, temperature, and line effects at any sampling time during SC proliferation (**Table 2**). A significant interaction was observed between temperature and cell line at 24 h ($p = 0.003$), 48 h ($p < 0.001$), and 72 h ($p < 0.001$). The factors of temperature and *Fzd7* knockdown significantly interacted at 72 h ($p < 0.001$). In both the RBC2 and NC control groups, heat stress (43°C) showed a positive effect on the proliferation of SCs (promote, $p < 0.001$) while cold stress (33°C) had a negative effect (suppress, $p < 0.001$) on proliferaton at 72 h. Knockdown of *Fzd7* decreased ($p < 0.001$) proliferation of both lines at 38°C (RBC2: 1.82-fold; NC: 1.70-fold) and 43°C (RBC2: 2.81-fold; NC: 1.58-fold) when measured at 72 h. At 33°C, no significant reduction in proliferation was observed in either line at any sampling time.

From 0 to 72 h of the proliferation assay, cell proliferation linearly increased as a function of sampling time in both the RBC2 and NC control groups at all the temperatures. The slope of the linear regression was always greater in the NC line compared to the RBC2 line ($p \leq 0.001$). Knockdown of *Fzd7* decreased ($p < 0.001$) the regression slope in both lines at 38°C (RBC2: 2.20-fold; NC: 1.73-fold) and 43°C (RBC2: 3.18-fold; NC: 1.66-fold).

3.4 Effect of Frizzled-7 Knockdown, Thermal Stress, and Growth Selection on Satellite Cell Differentiation

3.4.1 Knockdown of Frizzled-7 at Zero Hour of Proliferation

There was a significant interaction ($p < 0.001$) among the effects of *Fzd7* knockdown, temperature, and line at 0, 24, and 72 h of differentiation (**Table 3**). However, at 48 h, a significant

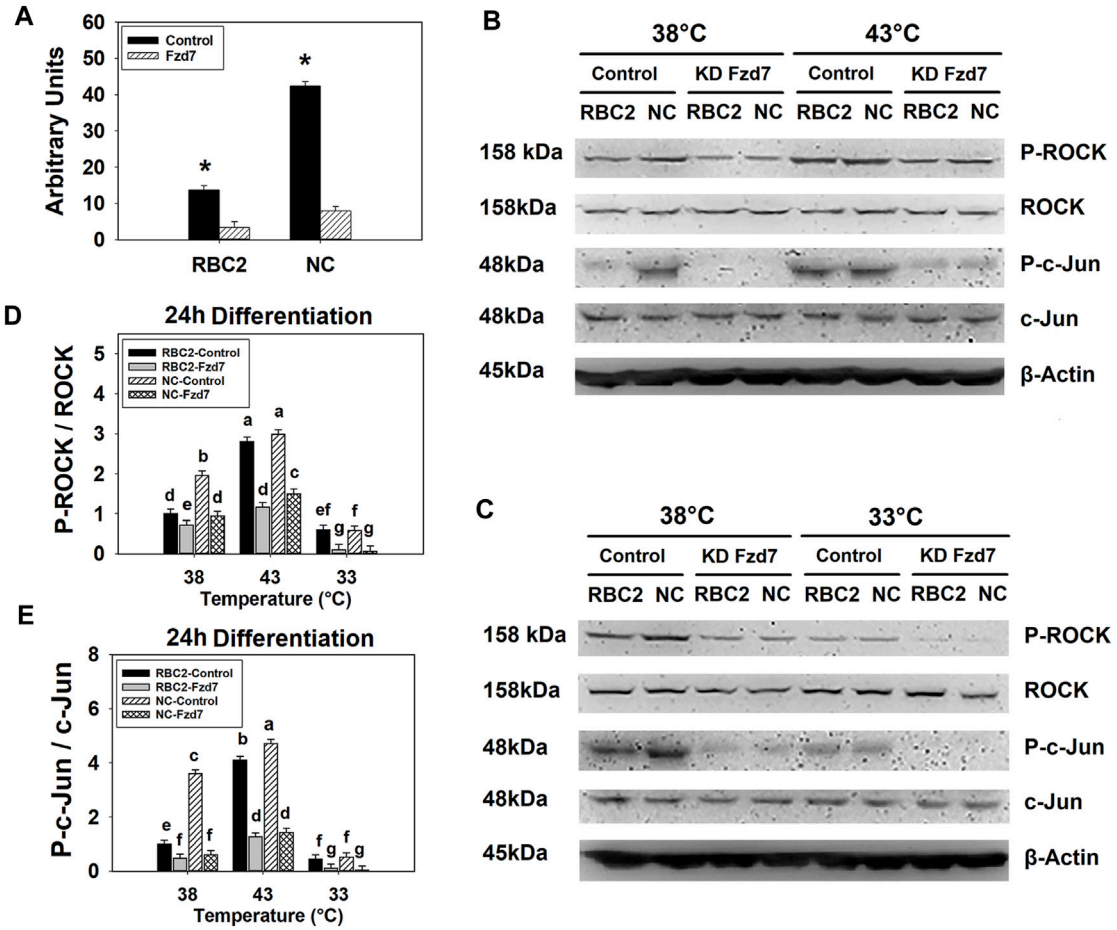

FIGURE 2 | Knockdown of frizzled-7 (*Fzd7*) with small interfering RNA (siRNA) in satellite cells (SCs). **(A)** Expression of *Fzd7* mRNA was measured at 72 h of proliferation after *Fzd7* knockdown at the beginning of proliferation in Randombred Control Line 2 (RBC2) and modern commercial (NC) line SCs. Asterisk (*) above the bars represents a significant difference between the two adjacent groups ($p \leq 0.05$). **(B)** Western blots of unphosphorylated and phosphorylated forms of rho-associated protein kinase (ROCK) and c-Jun, and an internal control β-actin in SCs from the RBC2 and NC lines cultured at 38°C and 43°C was determined at 24 h of differentiation. **(C)** Western blots of the unphosphorylated and phosphorylated forms of ROCK and c-Jun, and an internal control β-actin in SCs from the RBC2 and NC lines cultured at 38°C and 33°C was determined at 24 h of differentiation. **(D)** The ratio of phosphorylated to unphosphorylated ROCK. **(E)** The ratio of phosphorylated to unphosphorylated c-Jun. Treatment group was above of each lane, and molecular weight and protein name is on the left and right side of each figure in **(B and C)**. Control = SCs transfected with a negative control siRNA, and KD Fzd7 = SCs transfected with a siRNA targeting *Fzd7* in **(B and C)**. Each graph bar represents a mean ratio, and each error bar represents a standard error of the mean value. Mean values with different letters are significantly different ($p \leq 0.05$).

interaction ($p < 0.001$) was only observed between line and temperature and between temperature and *Fzd7* knockdown. Within each temperature, differentiation of the NC control group was greater ($p < 0.001$) than that of the RBC2 control group at 0, 24 and 48 h of differentiation. In the control groups, differentiation was greater at 43°C ($p \leq 0.002$), and less at 33°C ($p \leq 0.030$) at all sampling times compared to 38°C. Differentiation was linearly increased in both the RBC2 and NC control groups from 0 to 48 h of differentiation at 38°C and 43°C. The NC control group had a greater slope as shown by linear regression compared to the RBC2 line only at 38°C ($p = 0.003$).

Knockdown of *Fzd7* decreased ($p < 0.001$) differentiation of SCs of both lines at 38°C and 43°C with a greater reduction observed in the RBC2 line compared to the NC line at all sampling times. At 33°C, knockdown of *Fzd7* caused no significant reduction at 24, 48 and 72 h. Differentiation changed linearly with the knockdown of *Fzd7* and the slope of the regression line decreased ($p < 0.001$) in both line at 38°C (RBC2: 6.05-fold; NC: 2.87-fold) and 43°C (RBC2: 3.14-fold; NC: 1.71-fold). The linear relationship between differentiation and sampling time was absent in either line at 33°C.

Knockdown of *Fzd7* also had a significant effect on myotube diameter. A significant interaction ($p < 0.001$) was observed among the effects *Fzd7* knockdown, temperature, and line at 48 h of differentiation (**Figure 3**). Myotube diameter increased with heat stress (43°C) and decreased with cold stress (33°C) in both line control groups. Knockdown of *Fzd7* decreased ($p < 0.001$)

TABLE 2 | Effect of temperature and knockdown of frizzled-7 (*Fzd7*) on proliferation of randombred control line 2 (RBC2) and modern commercial line (NC) satellite cells[1].

Line	Temperature[2]	Knockdown[3]	Sampling time			
			0 h	24 h	48 h	72 h
RBC2	38	Control	$0.14^{a,x}$ ± 0.07	$0.20^{c,x}$ ± 0.08	$0.44^{cd,y}$ ± 0.08	$0.94^{d,z}$ ± 0.07
		Fzd7	$0.13^{a,x}$ ± 0.09	$0.15^{cd,x}$ ± 0.07	$0.20^{de,y}$ ± 0.08	$0.52^{e,z}$ ± 0.09
	43	Control	$0.10^{a,x}$ ± 0.07	$0.19^{bc,x}$ ± 0.08	$0.51^{c,y}$ ± 0.07	$1.55^{c,z}$ ± 0.06
		Fzd7	$0.11^{a,x}$ ± 0.07	$0.11^{cd,x}$ ± 0.07	$0.24^{cde,y}$ ± 0.07	$0.55^{e,z}$ ± 0.07
	33	Control	$0.13^{a,w}$ ± 0.08	$0.15^{cd,x}$ ± 0.09	$0.17^{de,y}$ ± 0.07	$0.23^{f,z}$ ± 0.08
		Fzd7	$0.13^{a,z}$ ± 0.11	$0.10^{d,z}$ ± 0.08	$0.12^{e,z}$ ± 0.08	$0.12^{f,z}$ ± 0.08
NC	38	Control	$0.13^{a,w}$ ± 0.09	$0.32^{b,x}$ ± 0.08	$0.58^{c,y}$ ± 0.08	$1.84^{b,z}$ ± 0.08
		Fzd7	$0.13^{a,x}$ ± 0.08	$0.21^{c,x}$ ± 0.08	$0.41^{cde,y}$ ± 0.08	$1.08^{d,z}$ ± 0.08
	43	Control	$0.10^{a,w}$ ± 0.07	$0.46^{a,x}$ ± 0.07	$1.41^{a,y}$ ± 0.06	$2.74^{a,z}$ ± 0.07
		Fzd7	$0.10^{a,x}$ ± 0.07	$0.27^{b,x}$ ± 0.07	$0.97^{b,y}$ ± 0.06	$1.73^{bc,z}$ ± 0.09
	33	Control	$0.13^{a,x}$ ± 0.08	$0.19^{cd,y}$ ± 0.07	$0.23^{de,y}$ ± 0.07	$0.34^{ef,z}$ ± 0.08
		Fzd7	$0.11^{a,x}$ ± 0.07	$0.15^{cd,yx}$ ± 0.09	$0.19^{de,y}$ ± 0.09	$0.32^{ef,z}$ ± 0.11
	p-value[4]	L × T	0.999	0.003	<0.001	<0.001
		L × K	0.502	0.242	0.724	0.326
		T × K	0.747	0.176	0.125	<0.001
		L × T × K	0.664	0.528	0.589	0.099

[1]Mean DNA concentration (μg/well) ± Standard error of mean (SEM).
[2]Incubation temperature (°C).
[3]Control, transfecting cells with a negative control small interfering RNA sequence; Fzd7, knockdown of Fzd7.
[4](L × T), interaction effect between line and temperature; (L × K), between line and knockdown; (T × K), between temperature and knockdown; (L × T × K), among line, temperature, and knockdown.
[a-f]Mean DNA concentration (μg/well ± SEM) within a column (sampling time) without a common letter are significantly different.
[w-z]Mean DNA concentration (μg/well ± SEM) within a row (line, temperature, and knockdown) without a common letter are significantly different.
$p \leq 0.05$ was considered as significant different.

TABLE 3 | Effect of temperature and knockdown of frizzled-7 (*Fzd7*) on differentiation of randombred control line 2 (RBC2) and modern commercial line (NC) satellite cells[1].

Line	Temperature[2]	Knockdown[3]	Sampling time			
			0 h	24 h	48 h	72 h
RBC2	38	Control	$5.40^{c,w}$ ± 1.34	$12.46^{e,x}$ ± 1.13	$49.45^{c,y}$ ± 1.34	$67.62^{b,z}$ ± 1.34
		Fzd7	$2.23^{f,y}$ ± 1.13	$1.63^{f,y}$ ± 1.34	$9.58^{e,z}$ ± 1.22	$9.24^{h,z}$ ± 1.13
	43	Control	$8.01^{b,x}$ ± 1.22	$45.97^{b,y}$ ± 1.22	$68.50^{b,z}$ ± 1.49	$72.80^{a,z}$ ± 1.22
		Fzd7	$4.36^{cde,x}$ ± 1.06	$11.89^{e,y}$ ± 1.06	$24.55^{d,z}$ ± 1.34	$21.81^{g,z}$ ± 1.13
	33	Control	$4.00^{de,z}$ ± 1.13	$2.32^{f,x}$ ± 1.22	$2.49^{f,x}$ ± 1.13	$2.7^{ij,y}$ ± 1.22
		Fzd7	$1.82^{f,z}$ ± 1.34	$1.13^{f,y}$ ± 1.34	$0.58^{f,x}$ ± 1.49	$0.60^{j,x}$ ± 1.22
NC	38	Control	$7.11^{b,w}$ ± 1.22	$34.08^{d,x}$ ± 1.22	$74.40^{b,z}$ ± 1.49	$58.54^{d,y}$ ± 1.13
		Fzd7	$4.86^{cd,x}$ ± 1.13	$10.67^{e,y}$ ± 1.22	$28.19^{d,z}$ ± 1.22	$26.55^{f,z}$ ± 1.13
	43	Control	$17.35^{a,x}$ ± 1.22	$62.19^{a,y}$ ± 1.22	$86.68^{a,z}$ ± 1.49	$63.22^{c,y}$ ± 1.34
		Fzd7	$7.99^{b,w}$ ± 1.22	$37.19^{c,x}$ ± 1.49	$49.49^{c,z}$ ± 1.22	$44.48^{e,y}$ ± 1.22
	33	Control	$4.40^{cde,z}$ ± 1.34	$3.48^{f,y}$ ± 1.22	$3.51^{f,y}$ ± 1.22	$4.68^{i,z}$ ± 1.22
		Fzd7	$3.33^{e,z}$ ± 1.13	$1.91^{f,yx}$ ± 1.34	$2.35^{f,y}$ ± 1.22	$1.86^{ij,x}$ ± 1.49
	p-value[4]	L × T	<0.001	<0.001	<0.001	0.008
		L × K	0.018	0.237	0.825	<0.001
		T × K	<0.001	<0.001	<0.001	<0.001
		L × T × K	<0.001	<0.001	0.121	<0.001

[1]Mean creatine kinase activity (Unit/well) ± Standard error of mean (SEM).
[2]Incubation temperature (°C).
[3]Control, transfecting cells with a negative control small interfering RNA sequence; Fzd7, knockdown of Fzd7.
[4](L × T), interaction effect between line and temperature; (L × K), between line and knockdown; (T × K), between temperature and knockdown; (L × T × K), among line, temperature, and knockdown.
[a-f]Mean creatine kinase activity (Unit/well ± SEM) within a column (sampling time) without a common letter are significantly different.
[w-z]Mean creatine kinase activity (Unit/well ± SEM) within a row (line, temperature, and knockdown) without a common letter are significantly different.
$p \leq 0.05$ was considered as significant different.

the myotube diameter in both lines at 38°C (RBC2: 1.16-fold; NC: 1.90-fold) and 43°C (RBC2: 1.56-fold; NC: 1.73-fold). At 33°C myotube diameter only decreased in the NC group ($p = 0.040$).

3.4.2 Knockdown of Frizzled-7 at Zero Hour of Differentiation

The interaction among *Fzd7* knockdown, temperature, and line effect was significant ($p < 0.001$) at all sampling times (**Table 4**).

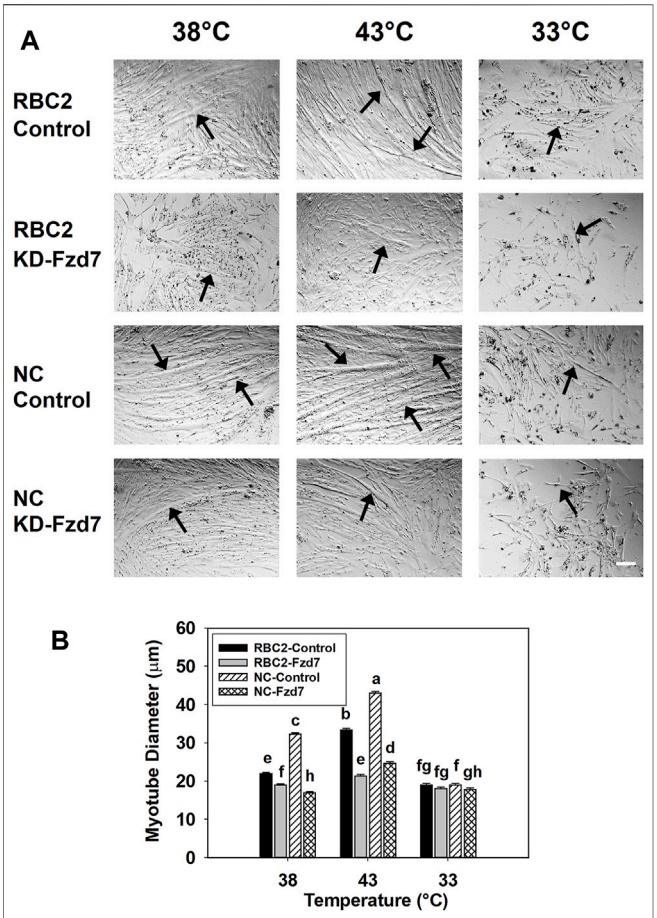

FIGURE 3 | Effect of hot and cold thermal stress and knockdown of frizzled-7 (*Fzd7*) at the beginning of proliferation on myotube diameter. **(A)** Representative photomicrographs of Randombred Control Line 2 (RBC2) and modern commercial (NC) line SCs transfected with either a negative control siRNA (Control) or a siRNA targeting *Fzd7* (KD-Fzd7) at the beginning of proliferation and followed for 72 h of proliferation and 48 h of differentiation at 38°C, 43°C, or 33°C. **(B)** Diameter of myotubes in each treatment group. Each graph bar represents a mean diameter of the myotubes, and each error bar represents a standard error of the mean. Mean values with different letters are significantly different ($p \leq 0.05$). Black arrows highlight representative myotubes. Scale bar (White) = 100 μm.

At 38°C and 43°C, differentiation was greater in the NC line ($p < 0.001$) compared to the RBC2. Heat stress increased SC differentiation in both line at 0 and 72 h ($p < 0.001$), and cold stress showed a significant inhibitory effect ($p < 0.001$) on both lines at all sampling times. At 38°C, differentiation was lower ($p < 0.001$) in the RBC2 and NC *Fzd7* knockdown groups compared to the controls at 48 h (RBC2: 1.15-fold; NC: 1.14-fold) and 72 h (RBC2: 1.15-fold; NC: 1.08-fold). Knockdown of *Fzd7* also decreased ($p < 0.001$) SC differentiation at 43°C, with 1.21 and 1.46-fold reductions observed at 72 h in the RBC2 and NC lines, respectively. At 33°C, the knockdown effect was only significant in the RBC2 line at 72 h ($p = 0.045$). From 0 to 48 h, there was a linear increase in SC differentiation in the control and *Fzd7* knockdown groups of both lines at 38°C and 43°C. Knockdown of *Fzd7* at the beginning of differentiation did not significantly change the slope of the linear regression in either line at either 38°C or 43°C. A linear increase was absent in either line at 33°C.

Effects on myotube diameter were also seen when *Fzd7* was knocked down at the beginning of differentiation (**Figure 4**). The effects *Fzd7* knockdown, temperature, and line showed a significant ($p < 0.001$) interaction at 48 h of differentiation. Heat stress increased myotube diameter ($p < 0.001$) while cold stress decreased the diameter ($p < 0.001$) in both lines. However, at 38°C myotube diameter decreased only in the NC line, with the knockdown of *Fzd7* (1.18-fold, $p < 0.001$). Both lines had reductions ($p < 0.001$) in myotube diameter with the knockdown of *Fzd7* at 43°C (RBC2: 1.15-fold; NC: 1.16-fold). No significant knockdown effect was observed in either line at 33°C.

3.5 Effect of Frizzled-7 Knockdown, Thermal Stress, and Growth Selection on the Expression of Myogenic Regulatory Genes

3.5.1 Myoblast Determination Factor 1 Expression

Interaction effects were significant ($p < 0.001$) between temperature and line, between line and knockdown, and between temperature and knockdown at 72 h of proliferation (**Figure 5A**). Expression of *MyoD* increased at 43°C ($p < 0.001$) and decreased at 33°C ($p < 0.001$) in both lines compared to the control (38°C) (**Figure 5A**). Knockdown of *Fzd7* decreased ($p < 0.001$) *MyoD* expression in both lines, with the RBC2 line showing greater reductions (fold change) compared to the NC line at 33°C and 43°C (**Figure 5A**).

A significant three-way interaction was also observed among the effects of *Fzd7* knockdown, temperature, and line at 48 h of differentiation (**Figure 5B**). Heat stress (43°C) increased ($p < 0.001$) *MyoD* expression in both lines while cold stress (33°C) had an inhibitory effect ($p < 0.001$, **Figure 5B**). Knockdown of *Fzd7* reduced *MyoD* expression in both lines at all temperatures (**Figure 5B**).

3.5.2 Myogenin Expression

A significant interaction was observed among *Fzd7* knockdown, temperature, and line effects at both 72 h of proliferation ($p < 0.001$, **Figure 5C**) and 48 h of differentiation ($p < 0.001$, **Figure 5D**). At 72 h of proliferation, heat stress (43°C) increased *MyoG* expression in both lines ($p \leq 0.004$) while cold stress (33°C) showed no significant effect in either line (**Figure 5C**). Knockdown of *Fzd7* decreased expression of *MyoG* in the RBC2 and NC groups only at 43°C (**Figure 5C**).

At 48 h of differentiation, *MyoG* expression was increased at 43°C ($p < 0.001$) and decreased at 33°C ($p < 0.001$) in both lines (**Figure 5D**). Knockdown of *Fzd7* decreased *MyoG* expression ($p < 0.001$) in both lines at both 38°C and 43°C with the NC line having a greater reduction than the RBC2 line (**Figure 5D**). At 33°C, reduced *MyoG* expression was observed only in the NC

TABLE 4 | Effect of temperature and knockdown of frizzled-7 (*Fzd7*) at the beginning of differentiation on differentiation of randombred control line 2 (RBC2) and modern commercial line (NC) satellite cells[1].

Line	Temperature[2]	Knockdown[3]	Sampling time			
			0 h	24 h	48 h	72 h
RBC2	38	Control	$7.23^{e,w} \pm 0.39$	$15.79^{f,x} \pm 0.45$	$37.12^{g,y} \pm 0.50$	$54.13^{f,z} \pm 0.50$
		Fzd7	$6.39^{ef,w} \pm 0.42$	$16.11^{f,x} \pm 0.50$	$32.29^{h,y} \pm 0.50$	$47.27^{g,z} \pm 0.50$
	43	Control	$12.47^{c,w} \pm 0.42$	$51.59^{d,x} \pm 0.50$	$72.03^{e,z} \pm 0.55$	$68.15^{d,y} \pm 0.45$
		Fzd7	$10.79^{d,w} \pm 0.42$	$43.66^{e,x} \pm 0.45$	$60.97^{f,z} \pm 0.55$	$56.37^{e,y} \pm 0.55$
	33	Control	$5.54^{fg,z} \pm 0.64$	$2.57^{h,w} \pm 0.56$	$3.40^{i,x} \pm 0.56$	$4.38^{i,y} \pm 0.64$
		Fzd7	$4.65^{g,z} \pm 0.56$	$2.16^{h,x} \pm 0.56$	$3.45^{i,y} \pm 0.79$	$2.52^{j,x} \pm 0.56$
NC	38	Control	$11.83^{c,w} \pm 0.42$	$68.78^{a,x} \pm 0.50$	$111.20^{a,z} \pm 0.55$	$83.74^{b,y} \pm 0.55$
		Fzd7	$11.58^{cd,w} \pm 0.50$	$54.4^{c,x} \pm 0.55$	$97.81^{b,z} \pm 0.50$	$77.33^{c,y} \pm 0.50$
	43	Control	$24.75^{a,w} \pm 0.45$	$57.87^{b,x} \pm 0.50$	$85.66^{c,y} \pm 0.45$	$99.01^{a,z} \pm 0.55$
		Fzd7	$17.40^{b,w} \pm 0.45$	$56.88^{b,x} \pm 0.50$	$80.07^{d,z} \pm 0.55$	$67.52^{d,y} \pm 0.55$
	33	Control	$6.44^{ef,y} \pm 0.79$	$4.70^{g,x} \pm 0.64$	$4.27^{i,x} \pm 0.64$	$8.11^{h,z} \pm 0.64$
		Fzd7	$5.83^{fg,z} \pm 0.64$	$4.43^{g,y} \pm 0.79$	$3.75^{i,y} \pm 0.79$	$6.53^{h,z} \pm 0.64$
p-value[4]		L × T	<0.001	<0.001	<0.001	<0.001
		L × K	<0.001	<0.001	0.214	<0.001
		T × K	<0.001	<0.001	<0.001	<0.001
		L × T × K	<0.001	<0.001	<0.001	<0.001

[1]Mean creatine kinase activity (Unit/well) ± Standard error of mean (SEM).
[2]Incubation temperature (°C).
[3]Control, transfecting cells with a negative control small interfering RNA sequence; Fzd7, knockdown of Fzd7.
[4](L × T), interaction effect between line and temperature; (L × K), between line and knockdown; (T × K), between temperature and knockdown; (L × T × K), among line, temperature, and knockdown.
[a-f]Mean creatine kinase activity (Unit/well ± SEM) within a column (sampling time) without a common letter are significantly different.
[w-z]Mean creatine kinase activity (Unit/well ± SEM) within a row (line, temperature, and knockdown) without a common letter are significantly different.
$p \leq 0.05$ was considered as significant different.

Fzd7 knockdown group compared to the control ($p = 0.009$, **Figure 5D**).

3.6 Effect of Frizzled-7 Knockdown, Thermal Stress, and Growth Selection on Satellite Cell Lipid Accumulation

3.6.1 Lipid Accumulation During Proliferation

During proliferation, a significant interaction ($p \leq 0.046$) for lipid accumulation was observed among *Fzd7* knockdown, temperature and line effects at all sampling times (**Table 5**). Lipid content increased ($p < 0.001$) with heat stress (43°C) and decreased ($p < 0.001$) with cold stress (33°C) in both line control groups at 48 and 72 h. At 48 and 72 h, the NC line had higher ($p \leq 0.007$) lipid levels compared to the RBC2 line regardless of temperature. With knockdown of *Fzd7*, lipid content at 24, 48, and 72 h was significantly reduced ($p \leq 0.002$) in both lines at all temperatures.

From 24 to 72 h of proliferation, lipid content in both lines linearly increased at all temperatures (**Table 5**). Within the control groups, the slope of the linear regression was larger in the NC line compared to the RBC2 line ($p \leq 0.023$). Heat stress increased the slopes of both lines while cold stress decreased the slopes ($p < 0.001$). Knockdown of *Fzd7* decreased ($p < 0.001$) the slope of both lines at all temperatures [38°C (RBC2: 5.27-fold; NC: 1.92-fold), 43°C (RBC2: 6.09-fold; NC: 6.20-fold), and 33°C (RBC2: 1.28-fold; NC: 1.23-fold)].

3.6.2 Lipid Accumulation During Differentiation

During differentiation, an interaction among the effects of *Fzd7* knockdown, temperature and line effects was significant ($p < 0.001$) at all sampling times (**Table 6**). Within the control groups, lipid content was greater at 43°C ($p < 0.001$) only in the NC line at 24 and 48 h. A significant decrease ($p < 0.001$) in lipid content was observed in both lines under cold stress (33°C) but only at 24 h of differentiation. Knocking down *Fzd7* significantly decreased ($p \leq 0.007$) lipid content at 24 and 48 h in both lines at all temperatures, except at 33°C for the NC line ($p = 0.247$).

From 24 to 72 h of differentiation, lipid content showed a linear decrease at 43°C in the control groups for both lines (**Table 6**). The slope of the linear regression ($p < 0.001$) was negative [9.13-fold and 22.75-fold in the RBC2 and NC *Fzd7* ($p < 0.001$) knockdown groups, respectively]. At 38°C and 33°C, lipid content was lower ($p < 0.001$) in both line control groups s at 48 and 72 h, compared to the 24 h.

3.7 Effect of Frizzled-7 Knockdown, Thermal Stress, and Growth Selection on the Expression of Adipogenic Regulatory Genes

3.7.1 Peroxisome Proliferator Activated Receptor-Gamma Expression

A significant interaction was observed among the effects *Fzd7* knockdown, temperature, and line at both 72 h of proliferation

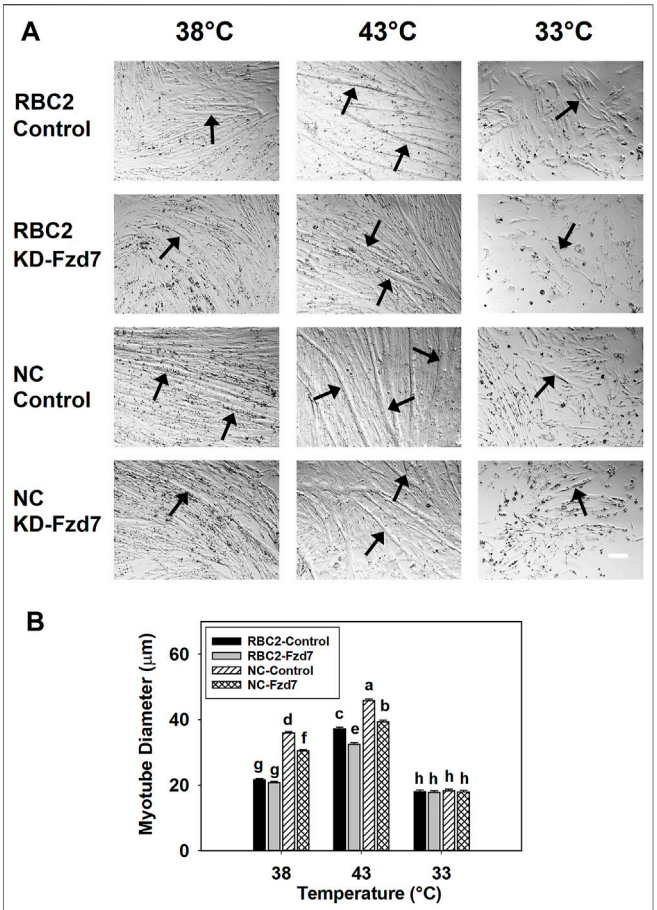

FIGURE 4 | Effect of hot and cold thermal stress and knockdown of frizzled-7 (*Fzd7*) at the beginning of differentiation on myotube diameter. **(A)** Randombred Control Line 2 (RBC2) and modern commercial (NC) line SCs proliferated normally at 38°C, 43°C, or 33°C and transfected with either a negative control siRNA (Control) or a siRNA targeting *Fzd7* (KD-Fzd7) at 72 h of proliferation, and photomicrographs were captured at 48 h of differentiation. **(B)** Diameter of myotubes in each treatment group. Each graph bar represents a mean diameter of the myotubes, and each error bar represents a standard error of the mean. Mean values with different letters are significantly different ($p \leq 0.05$). Black arrows highlight representative myotubes. Scale bar (White) = 100 μm.

($p < 0.001$, **Figure 6A**) and 48 h of differentiation ($p < 0.001$, **Figure 6B**). With heat stress (43°C), *PPARγ* expression decreased ($p < 0.001$) in both lines with a greater reduction observed in the NC line compared to the RBC2 line at 72 h of proliferation (**Figure 6A**). In contrast, expression of *PPARγ* was greatly increased with the cold stress (33°C), with the NC line showing a greater increase (**Figure 6A**). At 48 h of differentiation, *PPARγ* expression increased ($p < 0.001$) in both lines at 43°C but decreased at 33°C in the RBC2 line ($p < 0.001$) (**Figure 6B**). Knockdown of *Fzd7* downregulated ($p \leq 0.002$) expression of *PPARγ* in both lines at both sampling times, with greater reductions (fold change) in the RBC2 line compared to the NC line at both 43°C and 33°C (**Figures 6A,B**).

3.7.2 Neuropeptide-Y Expression

The effects of *Fzd7* knockdown, temperature, and line significantly interacted with each other at both sampling times ($p < 0.001$, **Figures 6C,D**). At 72 h of proliferation, heat stress (43°C) inhibited ($p < 0.001$) *NPY* expression in the RBC2 control group while cold stress (33°C) had a positive effect ($p < 0.001$, **Figure 6C**). In the NC control group, *NPY* expression showed a significant positive response to the cold stress ($p < 0.001$, **Figure 6C**). With the knockdown of *Fzd7*, *NPY* expression was downregulated ($p < 0.001$) in both lines at all temperatures during proliferation with the RBC2 line having greater reductions compared to the NC line at 38°C and 33°C (**Figure 6C**). At 48 h of differentiation, expression of *NPY* was upregulated at 43°C ($p < 0.001$) and downregulated at 33°C ($p \leq 0.013$) in both the RBC2 and NC compared to 38°C ($p < 0.001$, **Figure 6D**). Knocking down *Fzd7* inhibited *NPY* expression in both lines at 38°C and 43°C ($p < 0.001$), with the NC SCs showing greater reductions than the RBC2 SCs (**Figure 6D**).

3.7.3 CCAAT/Enhancer-Binding Protein-Beta Expression

There was a significant interaction among the *Fzd7* knockdown, temperature, and line effects during both proliferation and differentiation (**Figures 6E,F**). At 72 h of proliferation, *C/EBPβ* expression increased ($p < 0.001$) in the RBC2 control group at both 43°C and 33°C (**Figure 6E**). The NC SCs showed reduced *C/EBPβ* expression only at 43°C ($p < 0.001$) (**Figure 6E**). Knockdown of *Fzd7* suppressed expression of *C/EBPβ* at all temperatures ($p < 0.001$, **Figure 5E**). The RBC2 line had a greater reduction in C/EBPβ expression than the NC line at 43°C and 33°C (**Figure 5E**). At 48 h of differentiation, heat stress upregulated the expression of *C/EBPβ* in both the RBC2 and NC controls ($p < 0.001$), while cold stress downregulated the *C/EBPβ* only in the NC control group ($p = 0.027$, **Figure 6F**). Expression of *C/EBPβ* was significant lower ($p \leq 0.019$) in both the RBC2 and NC *Fzd7* knockdown groups, compared to the controls at all temperatures with the NC line having greater reductions than the RBC2 line (**Figure 6F**).

4 DISCUSSION

Thermal stress immediately after hatch has been shown to affect the growth and structure of the poultry p. major muscle (Piestun et al., 2017; Patael et al., 2019; Halevy, 2020), in part, through altering proliferation (Halevy et al., 2001; Xu et al., 2021b), myogenic differentiation (Halevy et al., 2001; Xu et al., 2021b), and adipogenic potential (Xu et al., 2021a) of SCs. Selection for growth further affects the function and fate of poultry p. major muscle SCs (Clark et al., 2016; Clark et al., 2017; Xu et al., 2021a; Xu et al., 2021b). As shown by transcriptome analysis, the Wnt pathway is greatly altered by thermal stress in turkey p. major muscle SCs (Reed et al., 2017a). Among the most affected *Wnt* genes, *Wnt7a*, which regulates the Wnt/PCP pathway through the Fzd7 receptor (Le Grand et al., 2009; Von Maltzahn et al., 2012), was significantly upregulated during heat stress,

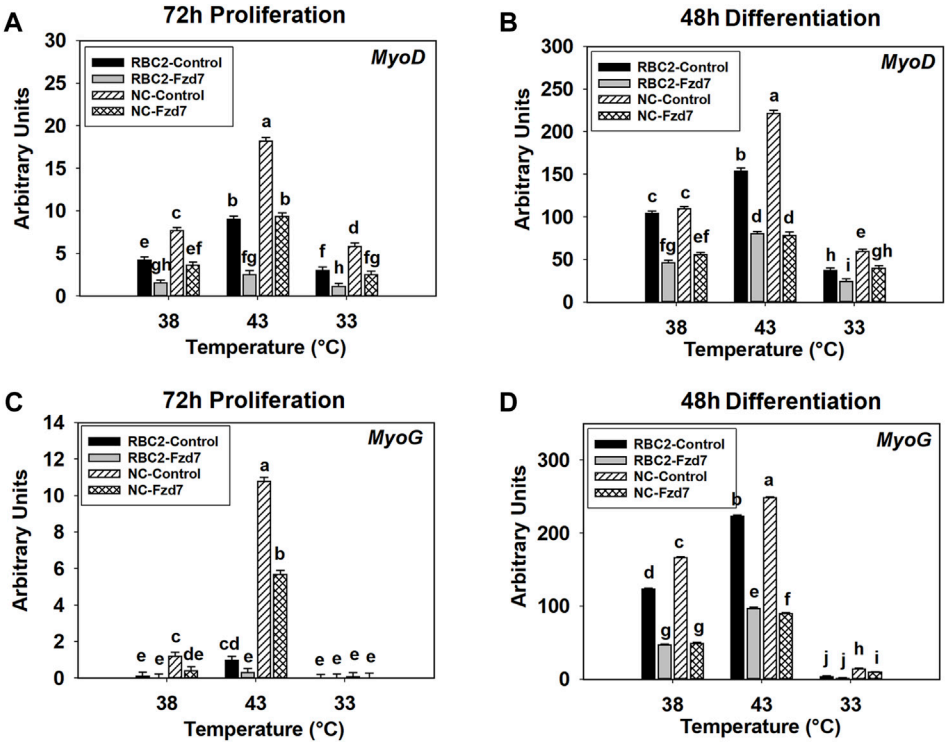

FIGURE 5 | Effect of hot and cold thermal stress and frizzled-7 (*Fzd7*) knockdown on the expression of myogenic determination factor 1 (*MyoD*) and myogenin (*MyoG*) in satellite cells (SCs). After transfection with either a negative control siRNA or a siRNA targeting *Fzd7*, both Randombred Control Line 2 (RBC2) and modern commercial (NC) line SCs proliferated at 38°C, 43°C, or 33°C. Expression of *MyoD* was determined at 72 h of proliferation **(A)** and 48 h of differentiation **(B)**. Expression of *MyoG* was determined at 72 h of proliferation **(C)** and 48 h of differentiation **(D)**. Each graph bar represents a mean arbitrary unit, and each error bar represents a standard error of the mean. Mean values with different letters are significantly different ($p \leq 0.05$).

particularly in SCs from a growth-selected turkey line (Reed et al., 2017a). In mouse myoblasts, expression of *Wnt7a* and *Fzd7* increases with elevated temperatures (Risha et al., 2021). The Wnt7a-Fzd7-initiated Wnt/PCP pathway has been shown to stimulate the proliferation of SCs, promote myofiber hypertrophy, and increase skeletal muscle mass in mammals (Le Grand et al., 2009). Furthermore, the Wnt/PCP pathway is also involved in regulating the migration (Wang et al., 2018), myogenic differentiation (Iwasaki et al., 2008), and adipogenesis (Sordella et al., 2003; Bryan et al., 2005; Hosoyama et al., 2009) in mouse myoblasts through downstream RhoA/ROCK signaling and stimulates myoblast proliferation *via* Rac1/c-Jun signaling (Umansky et al., 2015; Hindi and Kumar, 2016). A schematic illustration of how thermal stress may affect satellite cell function and fate through the Fzd7-mediated Wnt/PCP pathway is presented in **Figure 7**. Taken together, these studies suggest both thermal stress and growth selection may alter poultry breast muscle growth, structure, and protein to fat ratio through a SC-mediated Wnt/PCP-dependent mechanism.

Satellite cells comprise a heterogeneous population (Schultz, 1974; Kuang et al., 2007; Tierney and Sacco, 2016) of multipotential stem cells (Asakura et al., 2001; Shefer et al., 2004). Selection for increased breast muscle yield in the turkey (Havenstein et al., 2003) has facilitated the conversion of the SCs in the p. major muscle to a population with higher rates of proliferation and myogenic differentiation (Velleman et al., 2000; Clark et al., 2016; Xu et al., 2021b) and elevated adipogenic potential (Velleman, 2014; Xu et al., 2021a). Results from the current study support these findings as the commercial NC line SCs showed significant increases in proliferation, myogenic differentiation, myotube diameter, and lipid accumulation compared to the non-selected RBC2 line. Phosphorylation (activation) of both ROCK and c-Jun was greater in the NC line compared to the RBC2 line. The activity of ROCK is associated with myoblast migration (Wang et al., 2018), myogenic differentiation (Iwasaki et al., 2008), and adipogenesis (Hosoyama et al., 2009) while c-Jun regulates the proliferation of SCs (Hindi and Kumar, 2016). With increased Wnt/PCP pathway signal transduction as supported by increased ROCK and c-Jun activity, the commercial NC line SCs can create a larger SC pool having a higher myogenic potential for myofiber hypertrophy compared to the RBC2 line. As reported by Xu et al. (2021a), the NC line SCs also synthesize more lipid than the RBC2 line during late proliferation and early differentiation, when SCs are not fully committed to a myogenic pathway. These studies suggest growth selection may have increased the myofiber hypertrophy and fat deposition in the turkey p. major muscle through a SC-mediated Wnt/PCP-dependent mechanism.

TABLE 5 | Effect of temperature and knockdown of frizzled-7 (*Fzd7*) on lipid content during proliferation of randombred control line 2 (RBC2) and modern commercial line (NC) satellite cells[1].

Line	Temperature[2]	Knockdown[3]	Sampling time			
			0 h	24 h	48 h	72 h
RBC2	38	Control	$0.06^{c,w}$ ± 0.03	$0.09^{e,x}$ ± 0.03	$0.20^{g,y}$ ± 0.03	$1.14^{d,z}$ ± 0.03
		Fzd7	$0.05^{d,x}$ ± 0.03	$0.07^{f,y}$ ± 0.03	$0.04^{j,w}$ ± 0.03	$0.28^{ghi,z}$ ± 0.03
	43	Control	$0.06^{c,x}$ ± 0.03	$0.09^{de,x}$ ± 0.03	$0.80^{c,y}$ ± 0.03	$3.42^{b,z}$ ± 0.03
		Fzd7	$0.06^{cd,x}$ ± 0.03	$0.04^{h,x}$ ± 0.03	$0.15^{h,y}$ ± 0.03	$0.61^{f,z}$ ± 0.03
	33	Control	$0.06^{cd,x}$ ± 0.03	$0.05^{g,x}$ ± 0.03	$0.08^{i,y}$ ± 0.03	$0.16^{hi,z}$ ± 0.04
		Fzd7	$0.06^{cd,y}$ ± 0.03	$0.03^{h,x}$ ± 0.03	$0.01^{j,w}$ ± 0.03	$0.12^{i,z}$ ± 0.03
NC	38	Control	$0.11^{b,w}$ ± 0.03	$0.20^{a,x}$ ± 0.03	$0.96^{b,y}$ ± 0.03	$2.32^{c,z}$ ± 0.03
		Fzd7	$0.12^{b,x}$ ± 0.03	$0.18^{b,x}$ ± 0.03	$0.35^{e,y}$ ± 0.03	$1.32^{d,z}$ ± 0.03
	43	Control	$0.12^{ab,x}$ ± 0.02	$0.14^{c,x}$ ± 0.03	$1.42^{a,y}$ ± 0.03	$4.56^{a,z}$ ± 0.03
		Fzd7	$0.12^{a,x}$ ± 0.03	$0.10^{d,x}$ ± 0.03	$0.44^{d,y}$ ± 0.03	$0.82^{e,z}$ ± 0.03
	33	Control	$0.12^{ab,x}$ ± 0.03	$0.10^{d,x}$ ± 0.03	$0.28^{f,y}$ ± 0.03	$0.49^{fg,z}$ ± 0.03
		Fzd7	$0.12^{ab,x}$ ± 0.03	$0.07^{f,w}$ ± 0.03	$0.16^{h,y}$ ± 0.03	$0.40^{fgh,z}$ ± 0.04
p-value[4]		L × T	<0.001	<0.001	<0.001	<0.001
		L × K	<0.001	0.502	<0.001	<0.001
		T × K	<0.001	<0.001	<0.001	<0.001
		L × T × K	<0.001	0.046	<0.001	<0.001

[1]Mean of AdipoRed optical density (OD/well) ± Standard error of mean (SEM).
[2]Incubation temperature during proliferation, ˚C.
[3]Control, transfecting cells with a negative control small interfering RNA sequence; Fzd7, knockdown of Fzd7.
[4](L × T), interaction effect between line and temperature; (L × K), between line and knockdown; (T × K), between temperature and knockdown; (L × T × K), among line, temperature, and knockdown.
[a-h]Mean of AdipoRed OD (mean ± SEM) within a column (sampling time) without a common letter are significantly different.
[w-z]Mean of AdipoRed OD (mean ± SEM) within a row (line, temperature, and knockdown) without a common letter are significantly different.
p ≤ 0.05 was considered as significant different.

TABLE 6 | Effect of temperature and knockdown of frizzled-7 (*Fzd7*) on lipid content during differentiation of randombred control line 2 (RBC2) and modern commercial line (NC) satellite cells[1].

Line	Temperature[2]	Knockdown[3]	Sampling time		
			24 h	48 h	72 h
RBC2	38	Control	$1.61^{c,z}$ ± 0.05	$0.62^{c,x}$ ± 0.05	$0.74^{b,y}$ ± 0.05
		Fzd7	$0.09^{e,x}$ ± 0.05	$0.25^{e,z}$ ± 0.05	$0.18^{f,y}$ ± 0.05
	43	Control	$1.65^{c,z}$ ± 0.05	$0.44^{d,y}$ ± 0.05	$0.25^{e,x}$ ± 0.05
		Fzd7	$0.36^{d,z}$ ± 0.05	$0.19^{ef,z}$ ± 0.05	$0.21^{ef,z}$ ± 0.05
	33	Control	$0.38^{d,z}$ ± 0.05	$0.26^{e,y}$ ± 0.04	$0.18^{ef,x}$ ± 0.05
		Fzd7	$0.12^{e,z}$ ± 0.05	$0.09^{f,y}$ ± 0.05	$0.03^{g,x}$ ± 0.05
NC	38	Control	$2.33^{b,z}$ ± 0.04	$0.84^{b,x}$ ± 0.05	$0.96^{a,y}$ ± 0.05
		Fzd7	$1.50^{c,z}$ ± 0.05	$0.38^{d,x}$ ± 0.06	$0.59^{c,y}$ ± 0.05
	43	Control	$2.65^{a,z}$ ± 0.04	$1.88^{a,y}$ ± 0.05	$0.90^{a,x}$ ± 0.04
		Fzd7	$0.57^{d,z}$ ± 0.05	$0.56^{c,z}$ ± 0.05	$0.49^{d,z}$ ± 0.05
	33	Control	$0.54^{d,y}$ ± 0.05	$0.78^{b,z}$ ± 0.05	$0.77^{b,z}$ ± 0.05
		Fzd7	$0.41^{d,z}$ ± 0.05	$0.37^{d,z}$ ± 0.05	$0.15^{f,y}$ ± 0.05
p-value[4]		L × T	<0.001	<0.001	<0.001
		L × K	0.921	<0.001	<0.001
		T × K	<0.001	<0.001	<0.001
		L × T × K	<0.001	<0.001	<0.001

[1]Mean of AdipoRed optical density (OD/well) ± Standard error of mean (SEM).
[2]Incubation temperature during differentiation, ˚C.
[3]Control, transfecting cells with a negative control small interfering RNA sequence; Fzd7*, knockdown of* Fzd7*.*
[4](L × T), interaction effect between line and temperature; (L × K), between line and knockdown; (T × K), between temperature and knockdown; (L × T × K), among line, temperature, and knockdown.
[a-g]Mean of AdipoRed OD (mean ± SEM) within a column (sampling time) without a common letter are significantly different.
[x-z]Mean of AdipoRed OD (mean ± SEM) within a row (line, temperature, and knockdown) without a common letter are significantly different.
p ≤ *0.05 was considered as significant different.*

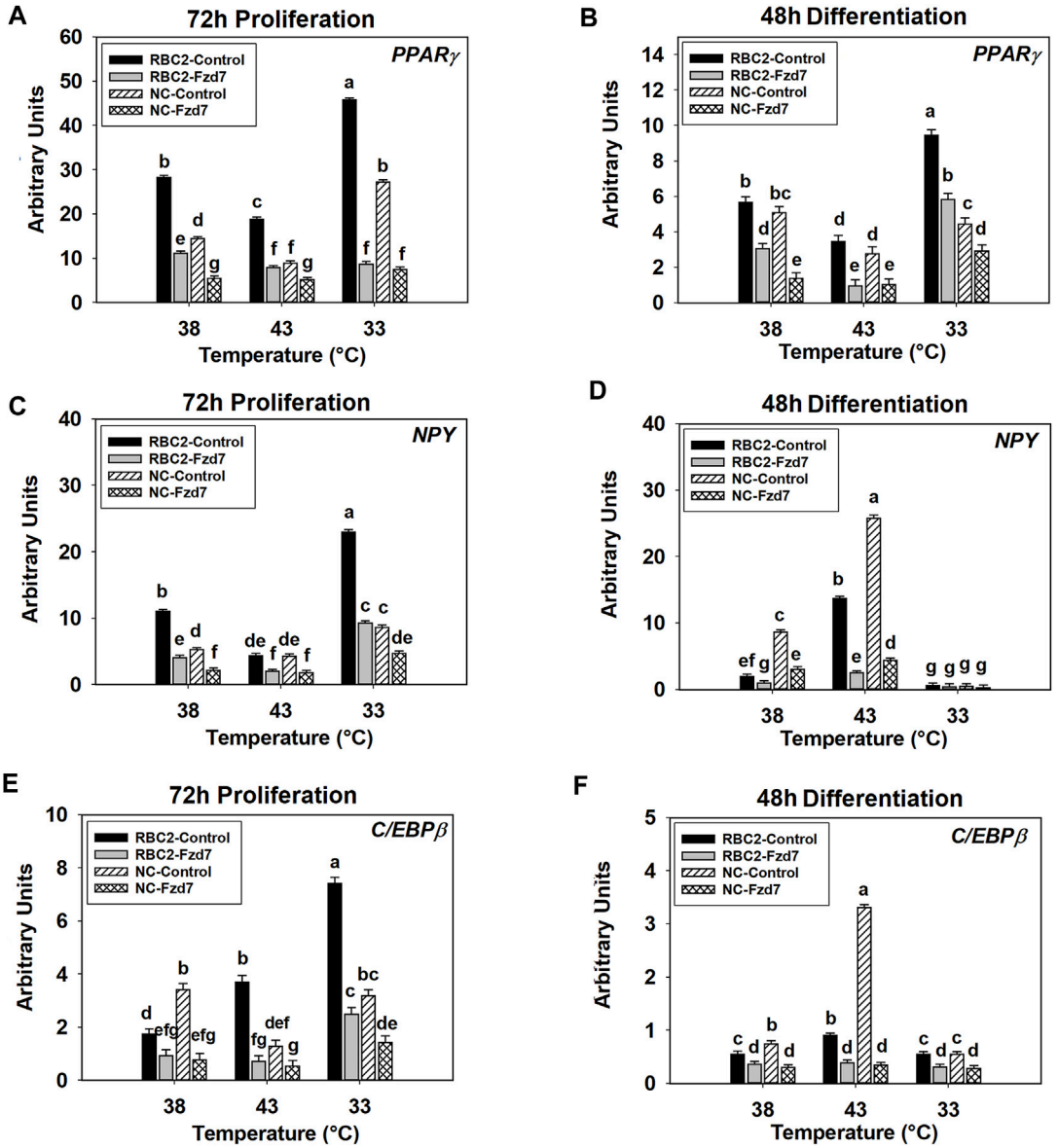

FIGURE 6 | Effect of hot and cold thermal stress and frizzled-7 (*Fzd7*) knockdown on the expression of proliferator-activated receptor gamma (*PPARγ*), neuropeptide-Y (*NPY*), and CCAAT/Enhancer-Binding Protein-Beta (*C/EBPβ*) in satellite cells (SCs). After transfection with either a negative control siRNA or a siRNA targeting *Fzd7*, both Randombred Control Line 2 (RBC2) and modern commercial (NC) line SCs proliferated at 38°C, 43°C, or 33°C. Expression of *PPARγ* was determined at 72 h of proliferation **(A)** and 48 h of differentiation **(B)**. Expression of *NPY* was determined at 72 h of proliferation **(C)** and 48 h of differentiation **(D)**. Expression of *C/EBPβ* was determined at 72 h of proliferation **(E)** and 48 h of differentiation **(F)**. Each graph bar represents a mean arbitrary unit, and each error bar represents a standard error of the mean. Mean values with different letters are significantly different ($p \leq 0.05$).

Post-hatch thermal stress appears to affect myofiber hypertrophy and fat deposition in the p. major muscle by regulating the Wnt/PCP pathway. Previous studies have reported expression of *Wnt7a* was greatly upregulated during heat stress in both mouse myoblasts (Risha et al., 2021) and turkey SCs (Reed et al., 2017a). The activity of SCs including proliferation and myogenic differentiation (Clark et al., 2016; Xu et al., 2021b) as well as the lipid synthesis (Clark et al., 2017; Xu et al., 2021a) was also increased during heat stress. In the current study, heat stress not only stimulated the activity of SCs but also promoted phosphorylation of both ROCK and c-Jun. Inhibition of the Wnt/PCP pathway through knockdown of *Fzd7* suppressed proliferation, differentiation, and adipogenesis of SCs during heat stress. These findings imply that heat stress-induces the Wnt/PCP pathway and may change the structure of turkey p. major muscle by altering the function and fate of SCs. Growth-selected faster-growing turkeys can display impaired p. major muscle morphology including decreased connective tissue spacing, reduced

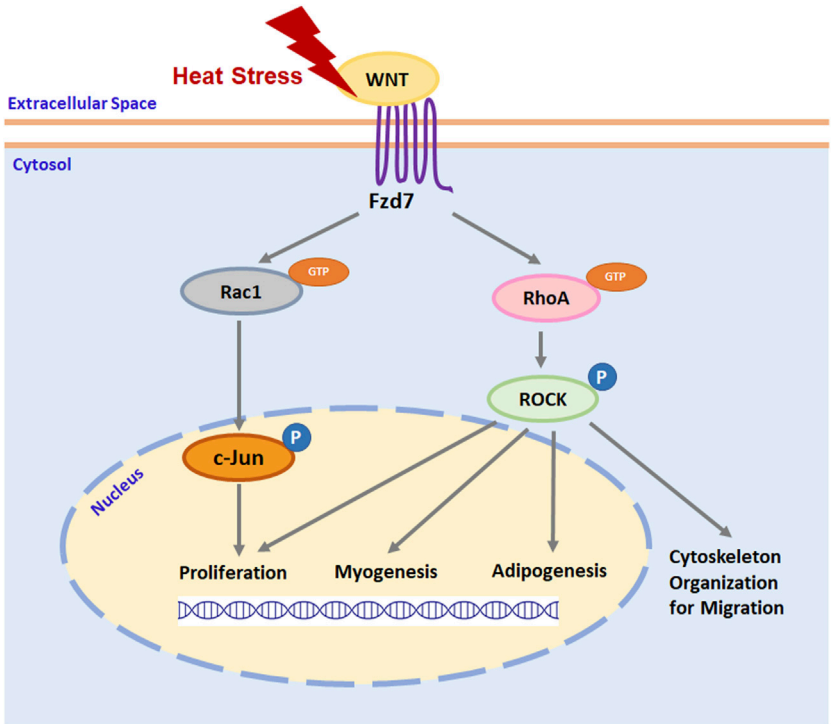

FIGURE 7 | A schematic illustration of thermal stress regulation of satellite cell function and fate through Wnt planar cell polarity pathway. Heat stress stimulates the expression of wingless-type mouse mammary tumor virus integration site family (Wnt) protein ligands. Interaction between Wnt ligand and cell surface receptor Frizzled-7 (Fzd7) stimulates the activation of ras homolog gene family member A (RhoA) and ras-related C3 botulinum toxin substrate 1 (Rac1) by binding guanosine-5′-triphosphate (GTP) to RhoA and Rac1. Activated RhoA and Rac1 will activate its downstream effector rho-associated protein kinase (ROCK) and c-Jun, respectively, by phosphorylation (P). Activated ROCK not only organizes cytoskeleton protein for cell migration but also regulates the expression of specific genes that are associated with satellite cell proliferation, myogenesis, and adipogenesis. Activated c-Jun regulates satellite cell proliferation by stimulating the expression of genes promoting cell cycle progression through the G1 phase.

capillary density, and myofiber degeneration at normal growth temperature (Velleman et al., 2003). As homeotherms, chickens and turkeys have a reduced capacity to maintain body temperature (Yahav, 2000; Yahav, 2015). Fast-growing chickens exposed to heat stress also have lower capillary density (Hadad et al., 2014; Joiner et al., 2014), increased myofiber degeneration (Joiner et al., 2014), and more fat depots (Zhang et al., 2012) in the p. major muscle compared to heat-stressed slowing-growing chickens. Thus, environmental heat stress can further affect the development of muscle structure.

Cold stress, in contrast, has inhibitory effects on the activities of turkey SCs including proliferation and myogenic differentiation (Clark et al., 2016; Xu et al., 2021b) and lipid synthesis (Xu et al., 2021a), and the SCs of growth-selected turkeys exhibit a lower tolerance to cold stress compared to non-select turkeys. Reed et al. (2017a) reported that a greater number of genes significantly changed during cold stress in SCs from a growth-selected turkey line compared to that of a non-selected line. In the present study, both the Wnt/PCP pathway, as shown by the phosphorylation of ROCK and c-Jun, and SC activity as reflected by proliferation, myogenic differentiation, and lipid accumulation were suppressed during cold stress. This is similar to the response of mouse myoblasts where cold stress downregulated the expression of *Wnt7a* and *Fzd7* (Risha et al., 2021). These findings suggest that cold stress has an inhibitory effect on turkey breast muscle growth and structure, in part, by suppressing the Fzd7-mediated Wnt/PCP pathway, and that fast-growing turkeys are more sensitive to cold stress.

With regard to SC proliferation, the mitotic activity of poultry SCs peaks during the first week after hatch (Mozdziak et al., 1994; Halevy et al., 2000). During this time, SCs are highly responsive to temperature (Halevy et al., 2001; Halevy, 2020) as evidenced by increased proliferation and expression of *MyoD* with heat stress and suppression under cold stress (Clark et al., 2016; Xu et al., 2021b). Inhibition of the Wnt/PCP pathway through knockdown of *Fzd7* significantly decreased both the rate of proliferation and *MyoD* expression in both lines at both the control (38°C) and elevated (43°C) temperatures. The effect of the knockdown was not significant under cold stress since the proliferation of SCs had already been suppressed. These results imply that the Wnt/PCP pathway through the Fzd7 receptor acts in the proliferation of turkey SCs only at higher temperatures. The SCs of the growth-selected NC line were less dependent on the Fzd7-mediated Wnt/PCP pathway in maintaining proliferation compared to the RBC2 line. It is possible that other signaling pathways which support the

proliferation of SCs have also been affected by growth selection. As reported by Xu et al. (2022a), the mechanistic target of rapamycin (mTOR) signaling pathway, which also stimulates avian SC proliferation (Vignale et al., 2015; Xu et al., 2022a), has increased activity in the NC line compared to the RBC2 line independent of temperature. With more proliferation-promotive pathways being activated, SCs from faster-growing turkeys are more likely to create a larger SC pool, and thus promoting breast muscle mass accretion through hypertrophic growth.

With the progression of myogenic differentiation, SCs in cell cultures gradually fuse to form multinucleated myotubes (McFarland et al., 1988). The activity of both ROCK and c-Jun in the turkey SCs was higher during the early stages of differentiation and gradually decreased. This can be expected as the function of ROCK and c-Jun in myogenic cells is dependent on cellular developmental stage. Both ROCK (Castellani et al., 2006) and c-Jun (Umansky et al., 2015; Hindi and Kumar, 2016) function in maintaining the proliferation of myogenic cells. During the early stages of myogenic differentiation, migration is required for the alignment of SCs before fusion to form multinucleated myotubes (Chazaud et al., 1998). The activation of ROCK regulates the migration of myogenic cells (Fortier et al., 2008; Wang et al., 2018), and therefore, is required during early differentiation. In the current study, knockdown of *Fzd7* decreased the activity of both ROCK and c-Jun. If *Fzd7* knockdown occurred at the beginning of proliferation, SC differentiation as well as myotube diameter was reduced to a greater extent compared to *Fzd7* being knocked down at the beginning of differentiation. This suggests that the Fzd7-mediated Wnt/PCP pathway affects myogenic differentiation of SCs mainly through regulating SC proliferation and migration prior to subsequent fusion to existing myofibers.

Satellite cell adipogenic potential depends on the developmental stage of the p. major muscle SCs (Xu et al., 2021a). Due to asymmetric division of SCs (Shinin et al., 2006), some daughter cells self-renew to maintain the SC pool (Kuang et al., 2007), some commit to a myogenic pathway (Kuang et al., 2007), while others spontaneously convert to an adipogenic population (Rossi et al., 2010). The lipid content in turkey SCs peaks during later proliferation and early differentiation (Xu et al., 2021a). Thus, the adipogenic potential of SCs is higher when SC fate is not fully committed to form a differentiated myotube. Furthermore, SC adipogenesis is also growth-dependent with the faster-proliferating population synthesizing more lipids than the slower-proliferating population (Rossi et al., 2010; Xu et al., 2021a). After the SCs begin differentiating, adipogenic potential will gradually decrease as reflected in the linear reduction in lipid content. Knockdown of *Fzd7* significantly decreased both lipid accumulation and the expression of *PPARγ*, *C/EBPβ*, and *NPY* during later proliferation and early differentiation. The commercial NC line SCs were less dependent on the Fzd7-mediated Wnt-PCP pathway in maintaining lipid accumulation compared to the RBC2 line. Together, these findings suggest thermal stress-induced changes in SC adipogenesis is regulated, in part, by the Fzd7-mediated Wnt/PCP pathway in a developmental time- and growth-dependent manner.

Additional pathways associated with adipogenesis may also be affected by growth selection. For example, activity of the mTOR pathway is higher in the NC line SCs compared to the RBC2 line independent of temperature (Xu et al., 2022a). The increased mTOR activity stimulates the adipogenesis in both mammalian (Yue et al., 2010) and avian (Xu et al., 2022b) SCs. Changes in SC adipogenesis *in vivo* is associated with altered intramuscular fat deposition (Piestun et al., 2017; Patael et al., 2019). Heat stress during the period of SC peak mitotic activity, the first week after hatch, may greatly increase the fat deposition in the p. major muscle of faster-growing turkeys. Increased intramuscular fat deposition may be associated with fat-related myopathies like white striping in the turkey p. major muscle (Soglia et al., 2018; Zampiga et al., 2019), and result in reduced breast meat quality.

In conclusion, the results from the current study indicate that thermal stress affects proliferation, differentiation, lipid accumulation, and expression of myogenic and adipogenic regulatory genes in turkey p. major muscle SCs through the Fzd7-mediated Wnt/PCP pathway in a growth-dependent manner. Specifically, heat stress promotes proliferation, differentiation, and lipid synthesis by stimulating the phosphorylation of both ROCK and c-Jun in both the NC and RBC2 line SCs, while cold stress showed an inhibitory effect. During cold stress, knockdown of the expression of *Fzd7* suppressed the proliferation, differentiation, and lipid accumulation in both lines of SCs. The reduction in these processes were greater in the commercial NC line compared to the non-selected RBC2 line. At normal temperature or during heat stress, the proliferation, differentiation, and adipogenesis of the NC line SCs, were overall less responsive to the knockdown of *Fzd7* compared to the non-selected RBC2 line. Furthermore, knockdown of *Fzd7* at the beginning of proliferation decreased the differentiation and myotube diameter to a greater extent in both lines compared to the knockdown of *Fzd7* at the beginning of differentiation. These results indicate that Fzd7-mediated SC myogenesis was initiated during proliferation. Hence, thermal stress during the period of SC peak mitotic activity may affect the structure and composition of turkey p. major muscle, in part, through the Fzd7-mediated Wnt/PCP pathway. During heat stress, increased SC proliferation and differentiation is associated with myofiber hypertrophy whereas intracellular lipid production will result in more intramuscular fat depots. Muscle fibers resulting from excessive hypertrophic growth will occupy the available connective tissue spacing and come in contact with each other (Velleman et al., 2003). This will result in degeneration of the muscle fibers. Furthermore, increased intramuscular fat depots may change the protein to fat ratio and affect turkey breast meat quality. Future studies will need to assess mechanisms of other signal transduction pathways in mediating SC function and fate. Target pathways include NPY- and myocyte enhancer factor 2C (MEF2C)-related signal transduction as expression of *NPY* (Reed et al., 2017b; Clark et al., 2018) and *MEF2C* (Reed et al., 2017b) are altered by thermal stress and growth selection in turkey SCs.

DATA AVAILABILITY STATEMENT

The original contributions presented in the study are included in the article/**Supplementary Material**, further inquiries can be directed to the corresponding author.

AUTHOR CONTRIBUTIONS

All co-authors have made a substantial and intellectual contribution to the work and approved the submitted article. SV conceived and designed the experiments with JX, GS, and KR. JX preformed the experiments, data collection, statistical analysis, and visualization. The manuscript was written by JX and revised by SV, GS, and KR.

FUNDING

This project was supported by the Agriculture and Food Research Initiative Competitive Grant No. 2020-67015-30827 from the United States Department of Agriculture to GS, KR, and SV.

SUPPLEMENTARY MATERIAL

The Supplementary Material for this article can be found online at: https://www.frontiersin.org/articles/10.3389/fphys.2022.892887/full#supplementary-material

REFERENCES

Asad, M., Wong, M. K., Tan, T. Z., Choolani, M., Low, J., Mori, S., et al. (2014). FZD7 Drives *In Vitro* Aggressiveness in Stem-A Subtype of Ovarian Cancer via Regulation of Non-canonical Wnt/PCP Pathway. *Cell Death Dis.* 5, e1346. doi:10.1038/cddis.2014.302

Asakura, A., Rudnicki, M. A., and Komaki, M. (2001). Muscle Satellite Cells Are Multipotential Stem Cells that Exhibit Myogenic, Osteogenic, and Adipogenic Differentiation. *Differentiation* 68, 245–253. doi:10.1046/j.1432-0436.2001.680412.x

Baker, S. B., Cohen, M., Kuo, L., Johnson, M., Al-Attar, A., and Zukowska, Z. (2009). The Role of the Neuropeptide Y2 Receptor in Liporemodeling: Neuropeptide Y-Mediated Adipogenesis and Adipose Graft Maintenance. *Plastic Reconstr. Surg.* 123, 486–492. doi:10.1097/PRS.0b013e3181954c80

Berrong, S. L., and Washburn, K. W. (1998). Effects of Genetic Variation on Total Plasma Protein, Body Weight Gains, and Body Temperature Responses to Heat Stress. *Poult. Sci.* 77, 379–385. doi:10.1093/ps/77.3.379

Bradford, M. M. (1976). A Rapid and Sensitive Method for the Quantitation of Microgram Quantities of Protein Utilizing the Principle of Protein-Dye Binding. *Anal. Biochem.* 72, 248–254. doi:10.1016/0003-2697(76)90527-3

Brunetti, A., and Goldfine, I. D. (1990). Role of Myogenin in Myoblast Differentiation and its Regulation by Fibroblast Growth Factor. *J. Biol. Chem.* 265, 5960–5963. doi:10.1016/S0021-9258(19)39275-0

Bryan, B. A., Mitchell, D. C., Zhao, L., Ma, W., Stafford, L. J., Teng, B.-B., et al. (2005). Modulation of Muscle Regeneration, Myogenesis, and Adipogenesis by the Rho Family Guanine Nucleotide Exchange Factor GEFT. *Mol. Cell Biol.* 25, 11089–11101. doi:10.1128/MCB.25.24.11089-11101.2005

Cardasis, C. A., and Cooper, G. W. (1975). An Analysis of Nuclear Numbers in Individual Muscle Fibers during Differentiation and Growth: A Satellite Cell-Muscle Fiber Growth Unit. *J. Exp. Zool.* 191, 347–357. doi:10.1002/jez.1401910305

Castellani, L., Salvati, E., Alemà, S., and Falcone, G. (2006). Fine Regulation of RhoA and Rock is Required for Skeletal Muscle Differentiation. *J. Biol. Chem.* 281, 15249–15257. doi:10.1074/jbc.M601390200

Chazaud, B., Christov, C., Gherardi, R. K., and Barlovatz-Meimon, G. (1998). *In Vitro* evaluation of Human Muscle Satellite Cell Migration Prior to Fusion into Myotubes. *J. Muscle Res. Cell. Motil.* 19, 931–936. doi:10.1023/a:1005451725719

Chiang, W., Booren, A., and Strasburg, G. (2008). The Effect of Heat Stress on Thyroid Hormone Response and Meat Quality in Turkeys of Two Genetic Lines. *Meat Sci.* 80, 615–622. doi:10.1016/j.meatsci.2008.02.012

Clark, D. L., Coy, C. S., Strasburg, G. M., Reed, K. M., and Velleman, S. G. (2016). Temperature Effect on Proliferation and Differentiation of Satellite Cells from Turkeys with Different Growth Rates. *Poult. Sci.* 95, 934–947. doi:10.3382/ps/pev437

Clark, D. L., Strasburg, G. M., Reed, K. M., and Velleman, S. G. (2017). Influence of Temperature and Growth Selection on turkey Pectoralis Major Muscle Satellite Cell Adipogenic Gene Expression and Lipid Accumulation. *Poult. Sci.* 96, 1015–1027. doi:10.3382/ps/pew374

Clark, D. L., Mccormick, J. L., and Velleman, S. G. (2018). Effect of Incubation Temperature on Neuropeptide Y and Neuropeptide Y Receptors in turkey and Chicken Satellite Cells. *Comp. Biochem. Physiol. Part A Mol. Integr. Physiol.* 219-220, 58–66. doi:10.1016/j.cbpa.2018.02.014

Clarke, S. L., Robinson, C. E., and Gimble, J. M. (1997). CAAT/Enhancer Binding Proteins Directly Modulate Transcription from the Peroxisome Proliferator-Activated Receptor γ2 Promoter. *Biochem. Biophys. Res. Commun.* 240, 99–103. doi:10.1006/bbrc.1997.7627

Daury, L., Busson, M., Tourkine, N., Casas, F., Cassar-Malek, I., Wrutniak-Cabello, C., et al. (2001). Opposing Functions of ATF2 and Fos-like Transcription Factors in C-Jun-Mediated Myogenin Expression and Terminal Differentiation of Avian Myoblasts. *Oncogene* 20, 7998–8008. doi:10.1038/sj.onc.1204967

Dunnington, E. A., and Siegel, P. B. (1984). Thermoregulation in Newly Hatched Chicks. *Poult. Sci.* 63, 1303–1313. doi:10.3382/ps.0631303

Eaton, S., Wepf, R., and Simons, K. (1996). Roles for Rac1 and Cdc42 in Planar Polarization and Hair Outgrowth in the Wing of Drosophila. *J. Cell Biol.* 135, 1277–1289. doi:10.1083/jcb.135.5.1277

Fanto, M., Weber, U., Strutt, D. I., and Mlodzik, M. (2000). Nuclear Signaling by Rac and Rho GTPases is Required in the Establishment of Epithelial Planar Polarity in the Drosophila Eye. *Curr. Biol.* 10, 979–S1. doi:10.1016/s0960-9822(00)00645-x

Fortier, M., Comunale, F., Kucharczak, J., Blangy, A., Charrasse, S., and Gauthier-Rouvière, C. (2008). RhoE Controls Myoblast Alignment Prior Fusion through RhoA and ROCK. *Cell Death Differ.* 15, 1221–1231. doi:10.1038/cdd.2008.34

Hadad, Y., Cahaner, A., and Halevy, O. (2014). Featherless and Feathered Broilers under Control versus Hot Conditions. 2. Breast Muscle Development and Growth in Pre- and Posthatch Periods. *Poult. Sci.* 93, 1076–1088. doi:10.3382/ps.2013-03592

Halevy, O., Geyra, A., Barak, M., Uni, Z., and Sklan, D. (2000). Early Posthatch Starvation Decreases Satellite Cell Proliferation and Skeletal Muscle Growth in Chicks. *J. Nutr.* 130, 858–864. doi:10.1093/jn/130.4.858

Halevy, O., Krispin, A., Leshem, Y., Mcmurtry, J. P., and Yahav, S. (2001). Early-age Heat Exposure Affects Skeletal Muscle Satellite Cell Proliferation and Differentiation in Chicks. *Am. J. Physiol. Regulatory Integr. Comp. Physiol.* 281, R302–R309. doi:10.1152/ajpregu.2001.281.1.R302

Halevy, O. (2020). Timing is Everything-The High Sensitivity of Avian Satellite Cells to Thermal Conditions during Embryonic and Posthatch Periods. *Front. Physiol.* 11, 235. doi:10.3389/fphys.2020.00235

Harding, R. L., Clark, D. L., Halevy, O., Coy, C. S., Yahav, S., and Velleman, S. G. (2015). The Effect of Temperature on Apoptosis and Adipogenesis on Skeletal Muscle Satellite Cells Derived from Different Muscle Types. *Physiol. Rep.* 3, e12539. doi:10.14814/phy2.12539

Hasty, P., Bradley, A., Morris, J. H., Edmondson, D. G., Venuti, J. M., Olson, E. N., et al. (1993). Muscle Deficiency and Neonatal Death in Mice with a Targeted Mutation in the Myogenin Gene. *Nature* 364, 501–506. doi:10.1038/364501a0

Havenstein, G., Ferket, P., and Qureshi, M. (2003). Carcass Composition and Yield of 1957 versus 2001 Broilers when Fed Representative 1957 and 2001 Broiler Diets. *Poult. Sci.* 82, 1509–1518. doi:10.1093/ps/82.10.1509

Hindi, S. M., and Kumar, A. (2016). TRAF6 Regulates Satellite Stem Cell Self-Renewal and Function during Regenerative Myogenesis. *J. Clin. Invest.* 126, 151–168. doi:10.1172/JCI81655

Hosoyama, T., Ishiguro, N., Yamanouchi, K., and Nishihara, M. (2009). Degenerative Muscle Fiber Accelerates Adipogenesis of Intramuscular Cells via RhoA Signaling Pathway. *Differentiation* 77, 350–359. doi:10.1016/j.diff.2008.11.001

Hoving-Bolink, A. H., Kranen, R. W., Klont, R. E., Gerritsen, C. L. M., and De Greef, K. H. (2000). Fibre Area and Capillary Supply in Broiler Breast Muscle in Relation to Productivity and Ascites. *Meat Sci.* 56, 397–402. doi:10.1016/s0309-1740(00)00071-1

Iwasaki, K., Hayashi, K. i., Fujioka, T., and Sobue, K. (2008). Rho/Rho-associated Kinase Signal Regulates Myogenic Differentiation via Myocardin-Related Transcription Factor-A/Smad-dependent Transcription of the Id3 Gene. *J. Biol. Chem.* 283, 21230–21241. doi:10.1074/jbc.M710525200

Joiner, K. S., Hamlin, G. A., Lien, R. J., and Bilgili, S. F. (2014). Evaluation of Capillary and Myofiber Density in the Pectoralis Major Muscles of Rapidly Growing, High-Yield Broiler Chickens during Increased Heat Stress. *Avian Dis.* 58, 377–382. doi:10.1637/10733-112513-Reg.1

Kaucká, M., Plevová, K., Pavlová, Š., Janovská, P., Mishra, A., Verner, J., et al. (2013). The Planar Cell Polarity Pathway Drives Pathogenesis of Chronic Lymphocytic Leukemia by the Regulation of B-Lymphocyte Migration. *Cancer Res.* 73, 1491–1501. doi:10.1158/0008-5472.CAN-12-1752

Konarzewski, M., Gavin, A., Mcdevitt, R., and Wallis, I. R. (2000). Metabolic and Organ Mass Responses to Selection for High Growth Rates in the Domestic Chicken (*Gallus domesticus*). *Physiol. Biochem. Zool.* 73, 237–248. doi:10.1086/316729

Kuang, S., Kuroda, K., Le Grand, F., and Rudnicki, M. A. (2007). Asymmetric Self-Renewal and Commitment of Satellite Stem Cells in Muscle. *Cell* 129, 999–1010. doi:10.1016/j.cell.2007.03.044

Laemmli, U. K. (1970). Cleavage of Structural Proteins during the Assembly of the Head of Bacteriophage T4. *Nature* 227, 680–685. doi:10.1038/227680a0

Laumanns, I. P., Fink, L., Wilhelm, J., Wolff, J.-C., Mitnacht-Kraus, R., Graef-Hoechst, S., et al. (2009). The Noncanonical WNT Pathway Is Operative in Idiopathic Pulmonary Arterial Hypertension. *Am. J. Respir. Cell Mol. Biol.* 40, 683–691. doi:10.1165/rcmb.2008-0153OC

Le Grand, F., Jones, A. E., Seale, V., Scimè, A., and Rudnicki, M. A. (2009). Wnt7a Activates the Planar Cell Polarity Pathway to Drive the Symmetric Expansion of Satellite Stem Cells. *Cell Stem Cell* 4, 535–547. doi:10.1016/j.stem.2009.03.013

Liu, C., McFarland, D. C., Nestor, K. E., and Velleman, S. G. (2006). Differential Expression of Membrane-Associated Heparan Sulfate Proteoglycans in the Skeletal Muscle of Turkeys with Different Growth Rates. *Poult. Sci.* 85, 422–428. doi:10.1093/ps/85.3.422

Maman, A. H., Özlü, S., Uçar, A., and Elibol, O. (2019). Effect of Chick Body Temperature during Post-hatch Handling on Broiler Live Performance. *Poult. Sci.* 98, 244–250. doi:10.3382/ps/pey395

McFarland, D. C., Doumit, M. E., and Minshall, R. D. (1988). The turkey Myogenic Satellite Cell: Optimization of *In Vitro* Proliferation and Differentiation. *Tissue Cell* 20, 899–908. doi:10.1016/0040-8166(88)90031-6

McFarland, D. C., Pesall, J. E., Gilkerson, K. K., and Ferrin, N. H. (1995). The Response to Growth Factors of Cultured Satellite Cells Derived from Turkeys Having Different Growth Rates. *Cytobios* 82, 229–238.

Modrey, P., and Nichelmann, M. (1992). Development of Autonomic and Behavioural Thermoregulation in Turkeys (*Meleagris gallopavo*). *J. Therm. Biol.* 17, 287–292. doi:10.1016/0306-4565(92)90035-e

Moss, F. P., and Leblond, C. P. (1971). Satellite Cells as the Source of Nuclei in Muscles of Growing Rats. *Anat. Rec.* 170, 421–435. doi:10.1002/ar.1091700405

Mozdziak, P. E., Schultz, E., and Cassens, R. G. (1994). Satellite Cell Mitotic Activity in Posthatch turkey Skeletal Muscle Growth. *Poult. Sci.* 73, 547–555. doi:10.3382/ps.0730547

Nestor, K. E., Mccartney, M. G., and Bachev, N. (1969). Relative Contributions of Genetics and Environment to turkey Improvement. *Poult. Sci.* 48, 1944–1949. doi:10.3382/ps.0481944

Patael, T., Piestun, Y., Soffer, A., Mordechay, S., Yahav, S., Velleman, S. G., et al. (2019). Early Posthatch Thermal Stress Causes Long-Term Adverse Effects on Pectoralis Muscle Development in Broilers. *Poult. Sci.* 98, 3268–3277. doi:10.3382/ps/pez123

Piestun, Y., Patael, T., Yahav, S., Velleman, S. G., and Halevy, O. (2017). Early Posthatch Thermal Stress Affects Breast Muscle Development and Satellite Cell Growth and Characteristics in Broilers. *Poult. Sci.* 96, 2877–2888. doi:10.3382/ps/pex065

Reed, K. M., Mendoza, K. M., Abrahante, J. E., Barnes, N. E., Velleman, S. G., and Strasburg, G. M. (2017a). Response of turkey Muscle Satellite Cells to Thermal Challenge. I. Transcriptome Effects in Proliferating Cells. *BMC Genomics* 18, 1–15. doi:10.1186/s12864-017-3740-4

Reed, K. M., Mendoza, K. M., Strasburg, G. M., and Velleman, S. G. (2017b). Response of Turkey Muscle Satellite Cells to Thermal Challenge. II. Transcriptome Effects in Differentiating Cells. *Front. Physiol.* 8, 948. doi:10.3389/fphys.2017.00948

Risha, M. A., Ali, A., Siengdee, P., Trakooljul, N., Haack, F., Dannenberger, D., et al. (2021). Wnt Signaling Related Transcripts and Their Relationship to Energy Metabolism in C2C12 Myoblasts under Temperature Stress. *PeerJ* 9, e11625. doi:10.7717/peerj.11625

Rosen, E. D., Sarraf, P., Troy, A. E., Bradwin, G., Moore, K., Milstone, D. S., et al. (1999). PPARγ is Required for the Differentiation of Adipose Tissue *In Vivo* and *In Vitro*. *Mol. Cell* 4, 611–617. doi:10.1016/s1097-2765(00)80211-7

Rossi, C. A., Pozzobon, M., Ditadi, A., Archacka, K., Gastaldello, A., Sanna, M., et al. (2010). Clonal Characterization of Rat Muscle Satellite Cells: Proliferation, Metabolism and Differentiation Define an Intrinsic Heterogeneity. *PLoS One* 5, e8523. doi:10.1371/journal.pone.0008523

Schreiber, M., Kolbus, A., Piu, F., Szabowski, A., Möhle-Steinlein, U., Tian, J., et al. (1999). Control of Cell Cycle Progression by C-Jun Is P53 Dependent. *Genes Dev.* 13, 607–619. doi:10.1101/gad.13.5.607

Schultz, E. (1974). A Quantitative Study of the Satellite Cell Population in Postnatal Mouse Lumbrical Muscle. *Anat. Rec.* 180, 589–595. doi:10.1002/ar.1091800405

Shefer, G., Wleklinski-Lee, M., and Yablonka-Reuveni, Z. (2004). Skeletal Muscle Satellite Cells Can Spontaneously Enter an Alternative Mesenchymal Pathway. *J. Cell Sci.* 117, 5393–5404. doi:10.1242/jcs.01419

Shinder, D., Rusal, M., Tanny, J., Druyan, S., and Yahav, S. (2007). Thermoregulatory Responses of Chicks (*Gallus domesticus*) to Low Ambient Temperatures at an Early Age. *Poult. Sci.* 86, 2200–2209. doi:10.1093/ps/86.10.2200

Shinin, V., Gayraud-Morel, B., Gomès, D., and Tajbakhsh, S. (2006). Asymmetric Division and Cosegregation of Template DNA Strands in Adult Muscle Satellite Cells. *Nat. Cell Biol.* 8, 677–682. doi:10.1038/ncb1425

Smith, J. H. (1963). Relation of Body Size to Muscle Cell Size and Number in the Chicken. *Poult. Sci.* 42, 283–290. doi:10.3382/ps.0420283

Soglia, F., Baldi, G., Laghi, L., Mudalal, S., Cavani, C., and Petracci, M. (2018). Effect of White Striping on turkey Breast Meat Quality. *Animal* 12, 2198–2204. doi:10.1017/S1751731117003469

Sordella, R., Jiang, W., Chen, G.-C., Curto, M., and Settleman, J. (2003). Modulation of Rho GTPase Signaling Regulates a Switch between Adipogenesis and Myogenesis. *Cell* 113, 147–158. doi:10.1016/s0092-8674(03)00271-x

Strutt, D. I., Weber, U., and Mlodzik, M. (1997). The Role of RhoA in Tissue Polarity and Frizzled Signalling. *Nature* 387, 292–295. doi:10.1038/387292a0

Tierney, M. T., and Sacco, A. (2016). Satellite Cell Heterogeneity in Skeletal Muscle Homeostasis. *Trends Cell Biol.* 26, 434–444. doi:10.1016/j.tcb.2016.02.004

Umansky, K. B., Gruenbaum-Cohen, Y., Tsoory, M., Feldmesser, E., Goldenberg, D., Brenner, O., et al. (2015). Runx1 Transcription Factor Is Required for Myoblasts Proliferation during Muscle Regeneration. *PLoS Genet.* 11, e1005457. doi:10.1371/journal.pgen.1005457

Velleman, S. G., Liu, X., Nestor, K. E., and McFarland, D. C. (2000). Heterogeneity in Growth and Differentiation Characteristics in Male and Female Satellite Cells Isolated from turkey Lines with Different Growth Rates. *Comp. Biochem. Physiol. Part A Mol. Integr. Physiol.* 125, 503–509. doi:10.1016/s1095-6433(00)00178-1

Velleman, S., Anderson, J., Coy, C., and Nestor, K. (2003). Effect of Selection for Growth Rate on Muscle Damage during turkey Breast Muscle Development. *Poult. Sci.* 82, 1069–1074. doi:10.1093/ps/82.7.1069

Velleman, S. G., Coy, C. S., and Emmerson, D. A. (2014). Effect of the Timing of Posthatch Feed Restrictions on the Deposition of Fat during Broiler Breast Muscle Development. *Poult. Sci.* 93, 2622–2627. doi:10.3382/ps.2014-04206

Velleman, S. G. (2014). Effect of Growth Selection on Adipogenic Gene Expression during the Development of the turkey Breast Muscle. *Int. J. Poult. Sci.* 13, 680–684. doi:10.3923/ijps.2014.680.684

Vignale, K., Greene, E. S., Caldas, J. V., England, J. A., Boonsinchai, N., Sodsee, P., et al. (2015). 25-hydroxycholecalciferol Enhances Male Broiler Breast Meat Yield through the mTOR Pathway. *J. Nutr. Sci.* 145, 855–863. doi:10.3945/jn.114.207936

Von Maltzahn, J., Bentzinger, C. F., and Rudnicki, M. A. (2012). Wnt7a-Fzd7 Signalling Directly Activates the Akt/mTOR Anabolic Growth Pathway in Skeletal Muscle. *Nat. Cell Biol.* 14, 186–191. doi:10.1038/ncb2404

Wang, W., Chen, M., Gao, Y., Song, X., Zheng, H., Zhang, K., et al. (2018). P2Y6 Regulates Cytoskeleton Reorganization and Cell Migration of C2C12 Myoblasts via ROCK Pathway. *J Cell. Biochem.* 119, 1889–1898. doi:10.1002/jcb.26350

Weber, U., Paricio, N., and Mlodzik, M. (2000). Jun Mediates Frizzled-Induced R3/R4 Cell Fate Distinction and Planar Polarity Determination in the Drosophila Eye. *Development* 127, 3619–3629. doi:10.1242/dev.127.16.3619

Wisdom, R., Johnson, R. S., and Moore, C. (1999). c-Jun Regulates Cell Cycle Progression and Apoptosis by Distinct Mechanisms. *EMBO J.* 18, 188–197. doi:10.1093/emboj/18.1.188

Xu, J., Strasburg, G. M., Reed, K. M., and Velleman, S. G. (2021a). Effect of Temperature and Selection for Growth on Intracellular Lipid Accumulation and Adipogenic Gene Expression in turkey Pectoralis Major Muscle Satellite Cells. *Front. Physiol.* 12, 667814. doi:10.3389/fphys.2021.667814

Xu, J., Strasburg, G. M., Reed, K. M., and Velleman, S. G. (2021b). Response of turkey Pectoralis Major Muscle Satellite Cells to Hot and Cold Thermal Stress: Effect of Growth Selection on Satellite Cell Proliferation and Differentiation. *Comp. Biochem. Physiol. Part A Mol. Integr. Physiol.* 252, 110823. doi:10.1016/j.cbpa.2020.110823

Xu, J., Strasburg, G. M., Reed, K. M., and Velleman, S. G. (2022a). Thermal Stress Affects Proliferation and Differentiation of turkey Satellite Cells through the mTOR/S6K Pathway in a Growth-dependent Manner. *PloS One* 17, e0262576. doi:10.1371/journal.pone.0262576

Xu, J., Strasburg, G. M., Reed, K. M., and Velleman, S. G. (2022b). Thermal Stress and Selection for Growth Affect Myogenic Satellite Cell Lipid Accumulation and Adipogenic Gene Expression through Mechanistic Target of Rapamycin Pathway. *J. Anim. Sci.* (accepted). doi:10.1093/jas/skac001

Yablonka-Reuveni, Z., and Rivera, A. J. (1994). Temporal Expression of Regulatory and Structural Muscle Proteins during Myogenesis of Satellite Cells on Isolated Adult Rat Fibers. *Dev. Biol.* 164, 588–603. doi:10.1006/dbio.1994.1226

Yahav, S. (2000). Domestic Fowl-Strategies to Confront Environmental Conditions. *Poult. Avian Biol. Rev.* 11, 81–95.

Yahav, S. (2015). "Regulation of Body Temperature," in *Sturkie's Avian Physiology* (Cambridge, MA, USA: Elsevier), 869–905. doi:10.1016/B978-0-12-407160-5.00037-3

Yue, T., Yin, J., Li, F., Li, D., and Du, M. (2010). High Glucose Induces Differentiation and Adipogenesis in Porcine Muscle Satellite Cells via mTOR. *BMB Rep.* 43, 140–145. doi:10.5483/bmbrep.2010.43.2.140

Yun, Y., McFarland, D. C., Pesall, J. E., Gilkerson, K. K., Wal, L. S. V., and Ferrin, N. H. (1997). Variation in Response to Growth Factor Stimuli in Satellite Cell Populations. *Comp. Biochem. Physiol. Part A Physiol.* 117, 463–470. doi:10.1016/s0300-9629(96)00404-5

Zampiga, M., Tavaniello, S., Soglia, F., Petracci, M., Mazzoni, M., Maiorano, G., et al. (2019). Comparison of 2 Commercial turkey Hybrids: Productivity, Occurrence of Breast Myopathies, and Meat Quality Properties. *Poult. Sci.* 98, 2305–2315. doi:10.3382/ps/pey607

Zhang, X., Nestor, K., McFarland, D., and Velleman, S. (2008). The Role of Syndecan-4 and Attached Glycosaminoglycan Chains on Myogenic Satellite Cell Growth. *Matrix Biol.* 27, 619–630. doi:10.1016/j.matbio.2008.06.002

Zhang, Z. Y., Jia, G. Q., Zuo, J. J., Zhang, Y., Lei, J., Ren, L., et al. (2012). Effects of Constant and Cyclic Heat Stress on Muscle Metabolism and Meat Quality of Broiler Breast Fillet and Thigh Meat. *Poult. Sci.* 91, 2931–2937. doi:10.3382/ps.2012-02255

Conflict of Interest: The authors declare that the research was conducted in the absence of any commercial or financial relationships that could be construed as a potential conflict of interest.

Publisher's Note: All claims expressed in this article are solely those of the authors and do not necessarily represent those of their affiliated organizations, or those of the publisher, the editors and the reviewers. Any product that may be evaluated in this article, or claim that may be made by its manufacturer, is not guaranteed or endorsed by the publisher.

frontiers | Frontiers in Physiology

ORIGINAL RESEARCH
published: 22 June 2022
doi: 10.3389/fphys.2022.935868

A Divergent Selection on Breast Meat Ultimate pH, a Key Factor for Chicken Meat Quality, is Associated With Different Circulating Lipid Profiles

Stéphane Beauclercq[1], Sandrine Mignon-Grasteau[1], Angélique Petit[1], Quentin Berger[1], Antoine Lefèvre[2], Sonia Métayer-Coustard[1], Sophie Tesseraud[1], Patrick Emond[2,3,4], Cécile Berri[1] and Elisabeth Le Bihan-Duval[1]*

[1]INRAE, Université de Tours, BOA, Tours, France, [2]Université de Tours, PST Analyse des Systèmes Biologiques, Tours, France, [3]UMR 1253, iBrain, Université de Tours, Inserm, Tours, France, [4]CHRU de Tours, Service de Médecine Nucléaire In Vitro, Tours, France

OPEN ACCESS

Edited by:
Sandra G. Velleman,
The Ohio State University,
United States

Reviewed by:
Yuwares Malila,
National Center for Genetic Engineering and Biotechnology (BIOTEC), Thailand
Servet Yalcin,
Ege University, Turkey

***Correspondence:**
Stéphane Beauclercq
stephane.beauclercq@skynet.be

Specialty section:
This article was submitted to Avian Physiology, a section of the journal Frontiers in Physiology

Received: 04 May 2022
Accepted: 30 May 2022
Published: 22 June 2022

Citation:
Beauclercq S, Mignon-Grasteau S, Petit A, Berger Q, Lefèvre A, Métayer-Coustard S, Tesseraud S, Emond P, Berri C and Le Bihan-Duval E (2022) A Divergent Selection on Breast Meat Ultimate pH, a Key Factor for Chicken Meat Quality, is Associated With Different Circulating Lipid Profiles. Front. Physiol. 13:935868. doi: 10.3389/fphys.2022.935868

Background: Chicken meat has become a major source of protein for human consumption. However, the quality of the meat is not yet under control, especially since pH values that are too low or too high are often observed. In an attempt to get a better understanding of the genetic and biochemical determinants of the ultimate pH, two genetic lines of broilers were divergently selected for low (pHu–) or high (pHu+) breast meat pHu. In this study, the serum lipidome of 17-day-old broilers from both lines was screened for pHu markers using liquid-chromatography coupled with mass spectrometry (LC-HRMS).

Results: A total of 185 lipids belonging to 4 groups (glycerolipids, glycerophospholipids, sterols, sphingolipids) were identified in the sera of 268 broilers from the pHu lines by targeted lipidomics. The glycerolipids, which are involved in energy storage, were in higher concentration in the blood of pHu– birds. The glycerophospholipids (phosphatidylcholines, phosphatidylethanolamines) with long and polyunsaturated acyl chains were more abundant in pHu+ than in pHu– while the lysophosphatidylcholines and lysophosphatidylethanolamines, known to be associated with starch, were observed in higher quantity in the serum of the pHu– line. Finally, the concentration of the sterols and the ceramides, belonging to the sphingolipids class, were higher in the pHu+ and pHu–, respectively. Furthermore, orthogonal partial least-squares analyses highlighted a set of 68 lipids explaining 77% of the differences between the two broilers lines ($R^2Y = 0.77$, $Q^2 = 0.67$). Among these lipids, a subset of 40 predictors of the pHu value was identified with a Root Mean Squared Error of Estimation of 0.18 pH unit ($R^2Y = 0.69$ and $Q^2 = 0.62$). The predictive model of the pHu value was externally validated on 68 birds with a Root Mean Squared Error of Prediction of 0.25 pH unit.

Conclusion: The sets of molecules identified will be useful for a better understanding of relationship between serum lipid profile and meat quality, and will contribute to define easily accessible pHu biomarkers on live birds that could be useful in genetic selection.

Keywords: meat quality, ultimate pH, broiler chicken, circulating lipids, targeted lipidomics

INTRODUCTION

Poultry meat is mainly consumed as cuts and processed products in most developed countries. For this reason, the technological quality of meat is a major issue for the competitiveness of the poultry meat industry as it affects the storage ability, the processing yields and the organoleptic properties of meat and further processed products (Gigaud et al., 2009; Mir et al., 2017; Baéza et al., 2021). The breast meat ultimate pH (pHu), which is closely linked to muscle glycogen stores (Le Bihan-Duval et al., 2008; Jlali et al., 2012), is one of the most important traits to describe this technological quality (Berri, 2000). The normal pHu range for chicken breast meat is between 5.7 and 6.1. Below 5.7, the meat is referred to as acid, and over 6.1 as DFD (dark, firm, and dry) (Barbut, 1997; Fletcher et al., 2000; Qiao et al., 2001). In rapid-growing chickens, the incidence of these metabolic disorders was estimated about 10 years ago at 18% for acid meat and 5% for DFD meat (Le Bihan-Duval et al., 2020). If the variations in meat pHu result from complex interactions between genetics and rearing factors, a relatively high level of heritability (0.30–0.50) was found for this meat parameter in several genetic lines (Le Bihan-Duval and Berri, 2017). It facilitated the creation of a valuable model of two broiler lines divergently selected on estimated breeding values for breast meat pHu (Alnahhas et al., 2014; Alnahhas et al., 2015). After 14 generations of selection, a deviation of 0.6 pH unit was found between the two lines (Berger et al., 2022). As the level of glycogen stored in breast muscle is also highly heritable ($h^2 = 0.43$) and has a −0.97 genetic correlation with pHu (Le Bihan-Duval et al., 2008), this selection strongly modified the glycogen contents of muscles in the divergent lines.

The chickens exhibiting low muscle pHu (pHu− line) were characterized, at 6 weeks of age, by an overexpression of most glycolysis/gluconeogenesis genes and an overabundance of carbohydrates in blood and muscle. The chickens with high meat pHu (pHu+ line) exhibited an overexpression of genes involved in muscle development and of metabolites linked to oxidative stress, muscle proteolysis, and lipid β-oxidation. That was possibly related to an over activation of oxidative energetic metabolism and protein catabolism in response to the glycogen deficiency that characterizes the muscles of the pHu+ line (Beauclercq et al., 2016, 2017). To some extent, the birds of the pHu+ line have metabolic characteristics similar to those described in chickens affected by Wooden Breast myopathy, which also exhibit low muscle glycogen content associated with downregulation of glycolysis and glycogenesis. Alterations in carbohydrate and lipid metabolisms have recently been described as being at the origin of this muscle pathophysiology (Lake and Abasht, 2020). In the case of the pHu+ genetic line, we observed a higher frequency of White Striping, another emerging myopathy, which was associated with an increase in intramuscular fat content at 6 weeks of age (Alnahhas et al., 2016). Compared to the pHu- line, an activation of certain genes involved in lipid metabolism was also reported at this age (Beauclercq et al., 2017). It seems that the divergent selection on the breast meat ultimate pH has also led to variations in lipid metabolism but apart from a lower plasma triglycerides level in the pHu+ chicks at hatch (Métayer-Coustard et al., 2021) or 7 days post-hatching after a challenging start (Bergeot et al., 2022), the circulating lipid profiles of these broilers remain unknown.

High coverage lipidomics has been mostly used in biomedical sciences to develop diagnostic or therapeutic tools based on biomarkers (Hinterwirth et al., 2014; Lu et al., 2019; Wang et al., 2020). However, it has also been used in animal sciences and food sciences to evaluate food quality, to determinate the origin or identify adulteration in fish, milks, oils, and plants (Trivedi et al., 2016; Sun et al., 2020; Kehelpannala et al., 2021). Very recently, muscle lipidome was investigated as well, notably, to differentiate pig breeds (Mi et al., 2019; Zhang et al., 2021) or to study feed efficiency in beef steers (Artegoitia et al., 2019). In poultry, LC-HRMS lipidomics has been used to access the effect of oils in the diet on muscle lipidome (Cui et al., 2020), muscle lipid composition in black-boned silky fowls (Mi et al., 2018; Dirong et al., 2021), or egg yolk composition (Meng et al., 2021; Wood et al., 2021). The blood lipidome has been considered only twice, for one study on heat stress and one on digestive efficiency markers in broilers (Beauclercq et al., 2019; Guo et al., 2021).

This innovative lipidomics study was the first attempt to characterize the serum lipid profiles of broilers selected divergently for high or low breast muscle ultimate pH. The first aim of this study was to know how far this genetic selection for pHu, which impacted the carbohydrate metabolism of birds, also affected lipidic metabolism. The second aim was to identify new potential criteria of selection for meat quality, accessible on live animals. Indeed, meat pH measurement implies sacrificing animals (at 42 days in the conditions of this selection), which means that only a costly sib-selection is feasible. Much gain would be brought by the access to lipidic markers of the pHu available from blood on live animals.

MATERIALS AND METHODS

All chemicals were bought from Merck—Sigma Aldrich (Saint-Quentin Fallavier, France) unless otherwise specified.

Birds and Sample Collection

Chickens originating from the 14th generation of two fast-growing genetic lines divergently selected for high (pHu+) or low (pHu−) ultimate pH of the *Pectoralis major* (*P. major*) muscle were reared at the PEAT experimental unit (https://doi.org/10.15454/1.5572326250887292E12), registered by the French Ministry of Agriculture under license number C-37-175-1 for animal experimentation. The 339 pHu− and 311 pHu+ broilers were fed a 3 phases diet containing a high proportion of sunflower, rapeseed, and faba bean in order to reduce the soybean meal proportion in the diet and were fed and watered *ad libitum* (Berger et al., 2022). Potential interesting feedstuffs, such as Faba bean, sunflower meal and rapeseed were included in the diet based on the results of a former project dedicated to the test of alternative feedstuffs for poultry diets (Pampouille et al., 2021). At 17 days after 6 h of fasting, blood samples for the

lipidomics analysis were collected from 134 broilers per line (males and females selected to represent all the diversity of the families within each line), i.e., just before the second diet change and at a time when metabolic differences between the two lines are already established. Indeed, significant differences were seen as early as hatching for muscle glycogen content and 5 days after hatching for ultimate pH (Métayer-Coustard et al., 2021).

After coagulation for 15 min at room temperature and centrifugation (3,000 g for 10 min), sera were aliquoted and stored at −80°C until further analysis. Animals were slaughtered at 42 days and the pHu of the *P. major* muscle was measured the next day after 24 h of chilling, using a portable pH meter (Model 506, Crison Instruments SA, Barcelona, Spain) by direct insertion of the glass electrode into the thickest part of the muscle. Samples were randomly split into a training dataset containing 100 broilers of each line (pHu+: 43 males and 57 females, pHu−: 39 males and 61 females) and an external validation dataset of 34 birds per line (pHu+: 16 males and 18 females, pHu−: 15 males and 19 females). Average pHu values of breast meat were 6.18 ± 0.13 for the pHu+ and 5.57 ± 0.09 for the pHu− in the training data set and 6.20 ± 0.13 for the pHu+ and 5.57 ± 0.08 for the pHu− in the validation data set.

Lipids Extraction and Mass Spectrometry

LC-HRMS analysis method was adapted from Beauclercq et al. (2019). Hundred microliters of serum were combined with 750 µl of a chloroform/methanol mix (1:2), vortexed for 5 s before addition of 250 µl of chloroform and 250 µl of water and vortexed for another 30 s. The resulting mixture was chilled for 20 min at −20°C and centrifuged (15,000 g, 20 min, 4°C). The lower phase was recovered, and put in glass tubes for further solvent evaporation in a SpeedVac at 35°C for around 1 hour. The residues were then reconstituted with 100 µl isopropanol/acetonitrile/water (35:60:5) for Ultra-High-Performance Liquid Chromatography (UHPLC) separation and mass spectrometry analysis. LC-HRMS analysis was performed on a UHPLC Ultimate 3000 system (Dionex, Sunnyvale, CA), coupled to a Q-Exactive mass spectrometer (Thermo Fisher Scientific) and operated in positive (ESI+) and negative (ESI−) ionization modes. Chromatography was carried out with a 1.7 µm XB—C18 (150 mm × 2.10 mm, 100 Å) UHPLC column (Kinetex, Phenomenex, Torrance, CA) heated at 55°C. The solvent system comprised mobile phase A [Isopropanol/Acetonitrile (9:1) + 0.1% (vol/vol) formic acid +10 mM ammonium formate], and mobile phase B [Acetonitrile/Water (6:4) + 0.1% (vol/vol) formic acid +10 mM ammonium formate]; the gradient operated at a flow rate of 0.26 ml/min over a run time of 24 min. The multistep gradient was programmed as follows: 0–1.5 min, 32%–45% A; 1.5–5 min, 45%–52% A; 5–8 min, 52%–58% A; 8–11 min, 58%–66% A; 11–14 min, 66%–70% A; 14–18 min, 70%–75% A; 18–21 min, 75%–97% A; 21–24 min, 97% A. The autosampler (Ultimate WPS-3000 UHPLC system, Dionex, Sunnyvale, CA) temperature was set at 4°C, and the injection volume for each sample was 5 µl. Heated ESI source parameters were a spray voltage of 3.5 kV, capillary temperature of 350°C, heater temperature of 250°C, sheath gas flow of 35 arbitrary units (AU), auxiliary gas flow of 10 AU, spare gas flow of 1 AU, and tube lens voltage of 60 V for C18. During the full-scan acquisition, which ranged from 250 to 1,600 m/*z*, the instrument operated at 35,000 resolution, with an automatic gain control target of 2×10^5 charges and a maximum injection time of 120 ms. The samples were distributed in 2 series. Quality control (QC) samples, a pool of 10 µl of all samples analyzed, were injected at the beginning of both series of analyses, every 10-sample injections, and at the end of both runs.

Data Processing and Spectral Assignment (Targeted Analysis)

The spectral data acquired in positive and negative ionization modes were processed using XCMS R package implemented in Workflow4Metabolomics tools to extract detected signals and eliminate signal redundancies (Smith et al., 2006; Guitton et al., 2017). The XCMS' parameters are provided in additional file 1, **Supplementary Table S1**. The lipids assignment was targeted to an in-house database, with a precision of 5 ppm or 10 ppm for positive or negative ionization modes, respectively. This database was based on the lipidome of several biological matrices from different animals (serum, chicken egg yolk, cells, feces) and contained 542 and 265 lipids in positive and negative ionization mode, respectively. These lipids were annotated with SimLipid software (Premier Biosoft, San Francisco, Ca) according to their retention time, exact mass and MS/MS spectra. The database contains 23 classes of lipids mainly phosphatidylcholine (PC; 279), phosphatidylethanolamine (PE; 91), diacylglycerol (DG; 80), and triglyceride (TG; 61) (additional file 1, **Supplementary Figure S1**). This annotation reached level 1 on the scale of confidence in lipid identification (Sumner et al., 2007). Lipids were annotated according the LIPID MAPS Lipid Classification System (Fahy et al., 2009). Each peak area was normalized to the total peaks area of each chromatogram. The LC-HRMS analyses were performed in 2 batches. To overcome the signal drift between the 2 batches and be able to compare samples between them, the signal was corrected using the method "LOcally WEighted Scatter-plot Smoother" (LOWESS) available in Workflow4metabolomics tool (Guitton et al., 2017). This method consists in performing a non-linear regression on the QCs, identical in both batches, for each lipid. This regression has then been applied to all samples enabling the comparison of samples from the two batches. Lipids with variability in QC samples greater than 30% were rejected as unsuitable for further investigation. If a lipid was detected both in positive and negative ionization modes, only the data in the positive ionization mode was kept for the subsequent analyses to avoid over-representation of some lipids in the chemometric analysis.

Chemometric Analysis

Orthogonal Projection to Latent Structures Discriminant Analysis and Orthogonal Projection to Latent Structures

An orthogonal projection to latent structures discriminant analysis (OPLS-DA) was performed using the SIMCA 16 Software (version 16.0.2, Umetrics, Umea°, Sweden) on the training dataset (100 pHu+, 100 pHu−). All data were scaled

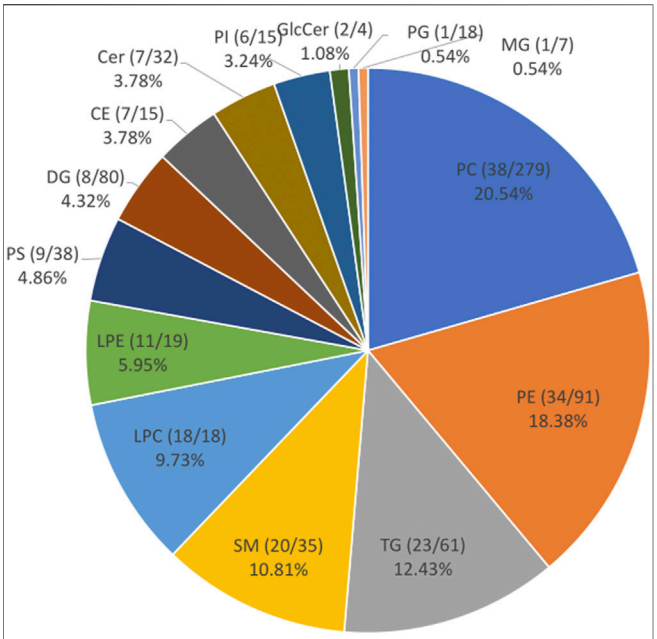

FIGURE 1 | The different classes of lipids identified in the serum of broilers from the pHu lines. The pie chart represents the proportion of each class of lipids in the lipidome of the pHu chickens identified by targeted lipidomics. The names of each lipid class is followed by: the number of lipids in each class/the number of lipids in the class in the database. PC, phosphatidylcholines; PE, phosphatidylethanolamines; PG, phosphatidylglycerols; PI, phosphatidylinositols; PS, phosphatidylserines; SM, Sphingomyelins; TG, triacylglycerols; CE, cholesterol esters; Cer, ceramides; DG, diacylglycerols; GlcCer, glucosylceramides; LPC, lysophosphatidylcholines; LPE, lysophosphatidylethanolamines; MG, monoradylglycerols.

to unit variance. OPLS-DA is a method of supervised classification that predicts the categorical factor Y (pHu+ or pHu− group) by explanatory quantitative variables X (185 lipids). The minimum number of features needed for optimal classification of the OPLS-DA models was determined by iteratively excluding the variables with low regression coefficients and wide confidence intervals derived from jackknifing combined with low variable importance in the projection (VIP) until maximum improvement of the quality of the models. The model quality was evaluated after 7-fold cross validation by cumulative R^2Y (goodness of fit) and cumulative Q^2 (goodness of prediction). The contribution of each predictor in the model was evaluated through the variable score contribution (i.e., the differences, in scaled units, for all the terms in the model, between the outlying and the normal observation, multiplied by the absolute value of the normalized weight) and the importance in the model (VIP). Furthermore, the relation between acyl chain properties (i.e., number of carbon atoms, unsaturation) and the pHu lines was studied in each lipid class by plotting the total number of carbons and unsaturation level to the VIP and contribution of each unique lipid as defined by the initial OPLS-DA model. Position jitter was introduced in the lysophosphatidylcholines (LPC), lysophosphatidylethanolamines (LPE), phosphatidylcholines (PC), phosphatidylethanolamines (PE), and sphingomyelin (SM) plots to avoid over plotting. The significance of the differences in number of carbons or unsaturation level between the acyl chains of the lipids contributing to the pHu+ and pHu− lines was tested through Welch's means equality t-test.

Subsequently, the ability of the lipidome to predict the numerical value of the breast meat pHu on live animals was investigated using OPLS modeling, which differs from OPLS-DA models by the use of a quantitative Y. The pHu values from the chickens included in the training dataset (100 pHu+, 100 pHu−) were fitted to the minimum feature of the lipidome with OPLS. The quality of the model was evaluated by its explicative (R^2Y) and predictive (Q^2) abilities, root meaned squared error of estimation (RMSEE), root meaned squared error by a 7-fold cross-validation (RMSEcv), and meaned squared error of prediction (RMSEP) for the external validation.

The OPLS-DA and OPLS models were externally validated on the validation dataset composed of 34 pHu+ and 34 pHu− chickens randomly selected.

The biochemical information about the lipids retained in the OPLS-DA and OPLS models that was used to develop the discussion was partly extracted from the HMDB database (Wishart et al., 2018), Reactome (Jassal et al., 2020), and KEGG (Kanehisa and Goto, 2000).

RESULTS

Comparative Lipidic Profiles of the pHu Lines

Generation of Lipid Profiles

The targeted lipidomics approach chosen for this study permitted the identification of 185 unique lipids (**Figure 1**) from a database of 731 unique lipids (**Supplementary Figure S1**). The lipids identified in the sera belong to 14 classes, themselves classified into 4 categories (i.e., glycerolipids, glycerophospholipids, sterols, and sphingolipids). The most represented in our analysis were phosphatidylcholines (PC, 20.54%), phosphatidylethanolamines (PE, 18.38%), triglycerides (TG, 12.43%), sphingomyelins (SM, 10.81%), and lysophosphatidylcholines (LPC, 9.73%).

Variation of Lipid Profiles Between the Two pHu Lines

An initial OPLS-DA (M1a) model was fitted to the 185 lipids identified in the sera of the 100 pHu+ and 100 pHu− that compose the training dataset to identify which lipids and acyl chain properties distinguish pHu lines. This model was composed of 1 predictive and 3 orthogonal components and had discriminant [$R^2Y_{(cum)}$] and predictive [$Q^2_{(cum)}$] abilities of 0.74 and 0.56, respectively, to separate pHu+ and pHu− lines (**Supplementary Table S2**). The total number of carbons and unsaturation in the acyl chains of the lipids were plotted and overlaid with the values of the VIPs and the contributions extracted from the OPLS-DA model. Lipids belonging to the LPC, LPE, TG, DG, and Cer classes contributed exclusively or almost exclusively to the pHu-line, Cer containing 36 or 38 carbons in their acyl chain contributing the most (**Supplementary Figure S2**). The CE and PI were the only two classes of lipids contributing entirely to the pHu+, CE with at least 4 unsaturation contributing the most

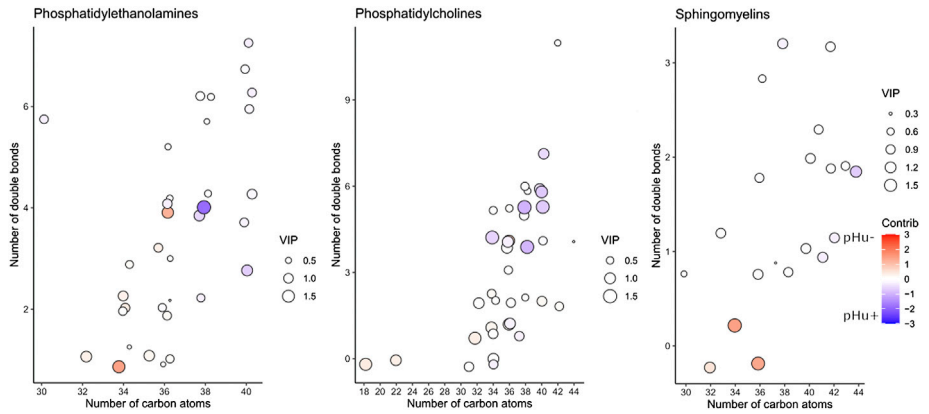

FIGURE 2 | Relation between lipids, acyl chain properties, and the pHu lines. The total number of carbons and unsaturation in the acyl chains of the lipids were plotted with the VIPs and the contributions extracted from the initial OPLS-DA model including the 185 lipids (**Supplementary Table S2**) identified by targeted lipidomics in the serum of broilers from the pHu lines (training dataset; n = 100 for each line). The importance of the lipids (VIP) in the OPLS-DA model (M1a) was represented by the size of the circle and the contribution to the pHu– or pHu+ lines were visualized by a gradient going from red (pHu–) to blue (pHu+). The characteristics of this OPLS-DA model (M1a) are 1 predictive and 3 orthogonal components, $R^2Y_{(cum)}$ = 0.74 and $Q^2_{(cum)}$ = 0.56. Position jitter was introduced in the plots to avoid overplotting.

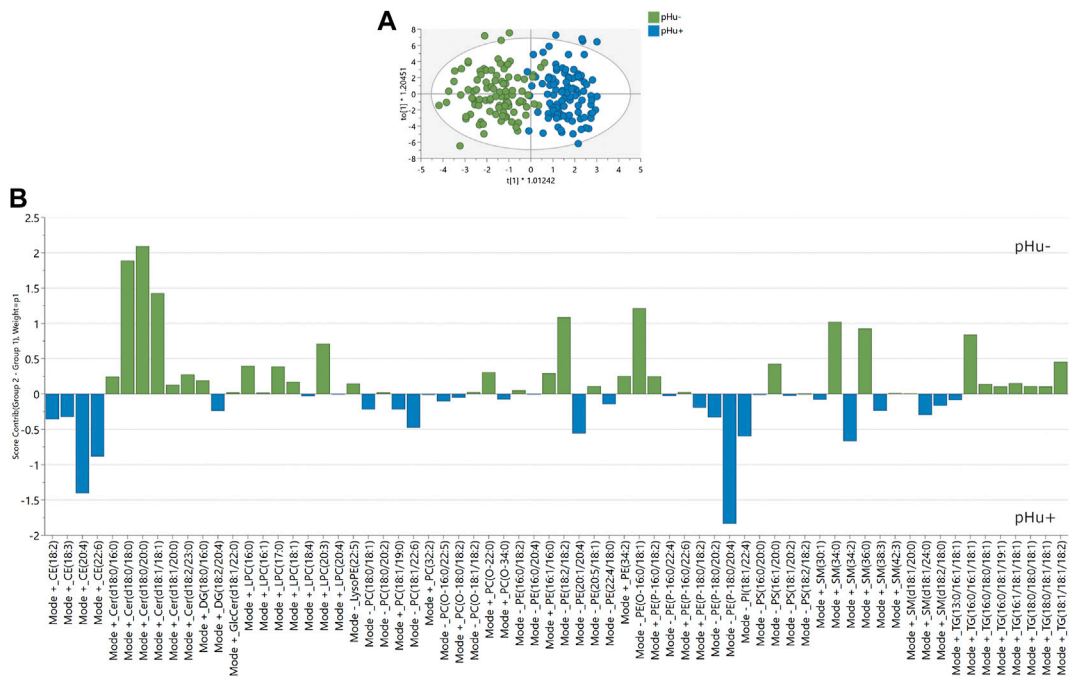

FIGURE 3 | Score and contribution plots following OPLS-DA predictive of the phu line. **(A)** Score plots following OPLS-DA (training dataset) with the chicken lines as categorial factor Y and the lipids as explanatory quantitative variables X. The pHu+ and pHu– individuals were represented by blue and green circles, respectively. The model (M1b) contained 68 lipids, 1 predictive and 3 orthogonal components and its descriptive and predictive performance were $R^2Y_{(cum)}$ = 0.77 and $Q^2_{(cum)}$ = 0.67. **(B)** Contribution plot indicating the contribution of the lipids identified in the OPLS-DA predictive of the pHu lines.

(**Supplementary Figure S2**). GlcCer, PG, and Monoacylglycerols (MG) had low contributions. PS, PE, PC, and SM lipid classes differentially contribute to both lines according to their number of carbon atoms and unsaturation in the acyl chains of the lipids (**Figure 2**). Indeed, the PE with high number of carbons (i.e., ≥ 36; p-value = 0.001) and unsaturation (p-value = 0.009) in their acyl chains and the PC with high unsaturation number in their acyl chains (p-value = 0.005) were more abundant in the serum of the pHu+. Likewise, we observed a tendency (p-value = 0.064) for PC with long acyl chains to be also more abundant in the pHu+.

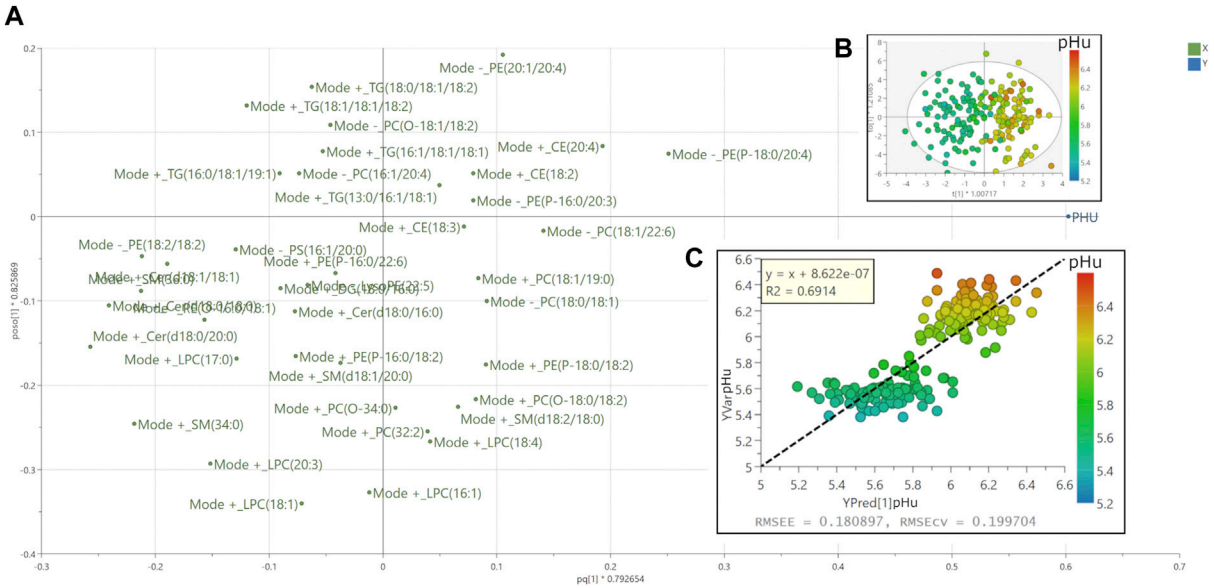

FIGURE 4 | Loadings, scores and observed vs. predicted plots following OPLS model predictive of the pHu value. **(A)** Loadings of the OPLS model (M2; training dataset) with the pHu as quantitative factor Y and the lipids as explanatory quantitative variables X. The model composed of 1 predictive and 2 orthogonal components was fitted to 40 lipids. The cumulative explanatory and predictive performance of this model (M2) were $R^2Y_{(cum)} = 0.69$ and $Q^2_{(cum)} = 0.62$. **(B)** Scores plots following OPLS. Circles correspond to the chicken tags colored according to their measured pHu value in the *Pectoralis major* muscle. **(C)** Observed vs. predicted after 7-fold cross validation plot. The root mean squared error of the estimation (RMSEE) and the root mean squared error after cross validation (RMSECV) were 0.18 and 0.20 pH unit, respectively.

Fitting Predictive Models of pHu Based on Circulating Lipids

Classification Into the Two Genetic Lines

Among the 185 lipids identified in the sera of the pHu+ and pHu− lines fitted to the initial OPLS-DA [M1a; $R^2Y_{(cum)} = 0.74$, $Q^2_{(cum)} = 0.56$], 68 were kept after iteratively excluding the variables with low regression coefficients and wide confidence intervals combined with low VIP until maximum improvement of the quality of the model. Those 68 lipids were included in a new OPLS-DA model (M1b) fitted on 1 predictive and 3 orthogonal components, whose descriptive and predictive performances [$R^2Y_{(cum)} = 0.77$ and $Q^2_{(cum)} = 0.67$, respectively] were improved in comparison to the model M1a without being over-fitted (**Supplementary Figure S3**). The score plot (**Figure 3A**) representing the projection of each chicken tag on the first predictive (x-axis) and first orthogonal (y-axis) components showed that 94% of the pHu− and 97% of the pHu+ were correctly classified by the M1b model. As already observed in the M1a model, the major contributors to the pHu+ belong to the CE and PE classes while the major contributors to the pHu− belong to Cer, LPC, PE, SM, and TG classes (**Figure 3B**). The performance of the M1b model was tested on the 34 birds from each line, selected randomly to constitute the external validation set. It allows the right classification of 88% of the pHu− and 91% of the pHu+ chickens (**Supplementary Figure S4**).

Prediction of the pHu Phenotype

An OPLS model (M2) was trained to predict breast meat pHu values from a set of serum lipids of the broilers from the training dataset composed of 100 pHu+ and 100 pHu−. This model composed of 1 predictive and 2 orthogonal components was fitted to 40 lipids with a descriptive and predictive abilities of $R^2Y_{(cum)} = 0.69$ and $Q^2_{(cum)} = 0.62$, respectively. The similarity of the $R^2Y_{(cum)}$ and $Q^2_{(cum)}$ as well as the permutation plot (**Supplementary Figure S5**) indicated that the model was not over-fitted. The loadings and scores on the first predictive and

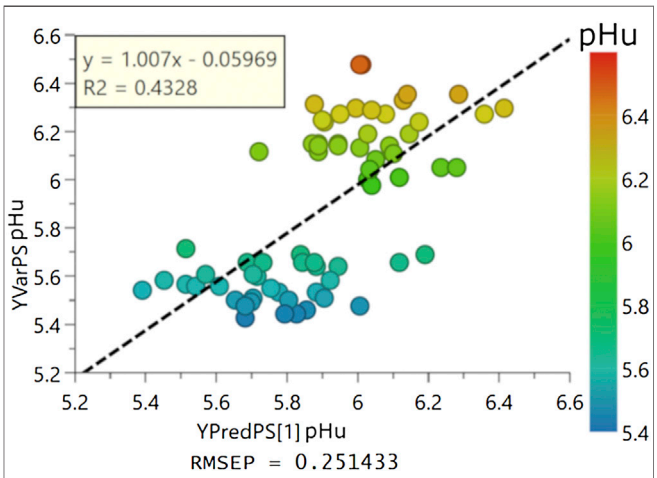

FIGURE 5 | External validation of the OPLS model predictive of the pHu value (M2). Observed vs. predicted plots based on the 34 pHu+ and 34 pHu− broilers selected randomly for external validation. The Root Mean Square Error of Prediction (RMSEP) was 0.25 pH unit.

orthogonal components were presented in **Figures 4A,B**. The predictive performance of the model was further assessed by 1) the plotting of the value of the predicted pHu versus the value to the observed pHu and the fitting of a linear regression model to the data and 2) the computing of the RMSEE and RMSEcv. The equation of the regression was $Y_{obs} = Y_{pred} + 8.622 \times 10^{-7}$ and its coefficient of determination R^2 was 0.69, while the RMSEE and RMSEcv were of 0.18 and 0.20 pH unit, respectively (**Figure 4C**). This model M2 was externally validated on 34 randomly chosen birds from each line. The equation of the linear regression between the pHu observed and predicted in the external validation was Y_{obs} = 1.007 × Ypred - 0.05969 and its R^2 0.43 while the RMSEP was 0.25 pH unit (**Figure 5**).

Thirty-seven of the 40 lipids included in this OPLS model M2 were also included in the OPLS-DA model M1b discriminating the two pHu lines. They were all considered as important in this OPLS (VIP ≥1). Only PC(16:1/20:4), PE (P-16:0/20:3), and TG (18:0/18:1/18:2) were specific to the OPLS model M2 predictive of the pHu value (**Supplementary Table S3**).

DISCUSSION

As extensively illustrated by Brown et al. (2022), metabolomic studies are extremely valuable in understanding the physiology of traits of interest for the poultry industry as metabolism is tightly linked to growth or feed efficiency. Metabolomic analyses also allow detecting sometimes unexpected metabolic evolutions linked to genetic selection. In addition, having access to the metabolic signature of the birds from low-invasive biological samples, such as serum, is of particular interest for identifying biomarkers of phenotypes of interest for poultry production or selection. In this study, we considered lipidomics, a subclass of metabolomics methods that measure lipid-based metabolites. It was applied with success in a recent analysis of serum lipidome of chickens divergently selected for digestive efficiency, a pattern of 10 lipids and lipophile compounds being able to explain 82% of the differences of efficiency between the two lines (Beauclercq et al., 2019). Lipidomics also appeared as a relevant approach for exploring the metabolism of the pHu genetic lines. It helped finding a proxy of muscle carbohydrate reserves and chicken-meat quality, knowing that the pHu+ line exhibited a higher lipid percentage in the egg yolk (Petit et al., 2022) but a lower level of plasma triglycerides at hatch (Métayer-Coustard et al., 2021) and one-week of age after a challenging start (Bergeot et al., 2022). Lipidomic profiles were acquired on 17 days aged birds, at a time when daily feed intake is similar between the two lines but feed efficiency is lower in the pHu+ line compared to the pHu− line (Berger et al., 2022).

Circulating Lipids in Chickens

The circulating lipidome of the broilers analyzed by targeted LC-HRMS lipidomics was composed of 185 lipids belonging to mainly the PC, PE, TG, and SM classes. Those lipid classes were as well the major contributors to the plasma lipidome of mammals, which shows a conserved composition across species (Ishikawa et al., 2015; Kaabia et al., 2018). In birds, most of lipid comparisons were primarily focused on plasma lipoprotein profiles, major lipid components such as total cholesterol, triglycerides and fatty acids, and muscular lipids (Baéza et al., 2015; Mi et al., 2018; Osorio and Flores, 2018). To our knowledge, the only extensive characterization of the circulating lipidome in a bird was done on Quaker parrot (Beaufrère et al., 2020). In this species, the PC and PE were also the major contributors to the serum lipidome with the addition of the fatty acids and conjugates class (FA), PA and PS. By comparison to this untargeted lipidomics study, our lipid database had a similar coverage of most of the lipid classes except the FA, PA, and PI. However, further comparison between the lipidome of those two avian species is limited as their metabolism is most likely very different as it is, for example, the case between mice and rats (Ishikawa et al., 2015). In the same way, a comparison with egg yolk lipid composition, which had been characterized extensively (Meng et al., 2021; Wood et al., 2021), was not relevant.

Impact of the Divergent Selection on Breast Meat pHu on Blood Lipidome

The lipids identified in the blood of the pHu broilers were from 14 classes (PC, PE, TG, SM, LPC, LPE, PS, DG, CE, Cer, PI, GlcCer, PG, MG) belonging to 4 categories: the glycerolipids, the glycerophospholipids, the sterols, and the sphingolipids. Among those 14 classes of lipids only 12 were kept in the OPLS-DA (M1b) model allowing to separate the pHu+ and pHu-lines.

The pHu-line is characterized by higher concentration of glycerolipids (especially TG and DG) that are involved in energy storage. They are provided by diet or are produced from carbohydrates or glycogen during the lipogenesis which involves the synthesis in liver or adipose tissues of FA from acetyl-CoA and an esterification with glycerol 3-phosphate (Everaert et al., 2021). The higher amounts of glycerolipids observed at 4 weeks of age are consistent with the higher plasma triglyceride levels previously observed in the pHu− at hatch and one-week of age (Métayer-Coustard et al., 2021; Bergeot et al., 2022). Metabolomic characterization of the lines early after hatch and at 6 weeks of age had also suggested that TGs and DGs were preferentially used for energy production by β-oxidation in pHu+ animals, whose energy metabolism was found to be more oxidative than that of pHu−, which themselves have higher carbohydrate stores in the muscle. It is also likely that the low availability of carbohydrate in the pHu+ line may limit TG *de novo* synthesis because *de novo* synthesis of FA requires acetyl-CoA and glycerol 3-phosphate themselves produced through glycolysis.

The pHu lines are also discriminated on their content of certain glycerophospholipids (i.e., PC, PE, PS, PI, PG, LPC, LPE). Glycerophospholipids are the major constituents of the membranes and play roles in signaling cascades. Among them, the PC, also known as lecithins, are the most abundant phospholipids found in cell membranes.

Thirty-eight phosphatidylcholines (PC) were identified in the serum of the pHu broilers, which contribute differentially to the two lines. The PC with high number of unsaturations and long

acyl chains were more abundant in the serum of the pHu+, which may suggest in this line a higher activity of the desaturase and elongase during *de novo* synthesis, a greater ability to digest and absorb long PUFA (polyunsaturated fatty acid) or a lower oxidation rate. Indeed, the oxidation rate of medium-chain FA is known to be faster than that of the long-chain fatty acids. In addition, the degree of unsaturation increases the oxidation of FA (Bach et al., 1996; DeLany et al., 2000). The higher concentration of several molecules with antioxidant properties (i.e., betaine, taurine, 1-methylhistidine, and 3-methylhistidine) identified in the pHu+ serum and *Pectoralis major* muscle (Beauclercq et al., 2016) may also exert a protective effect on long-chain PUFA despite a more oxidative energy metabolism in this line (i.e., energy produced from amino acid catabolism and lipid oxidation).

Thirty-four Phosphatidylethanolamine (PE) were identified in the broiler serum, and as for PC, PE with long and polyunsaturated acyl chains were more abundant in pHu+ than in pHu−. Especially, pHu+ were characterized by higher amounts of most of the PE with an (1Z)-alkenyl ether linkage, also referred as neutral plasmalogens. Plasmalogens play a role of antioxidant in addition to their contribution to the decreases in fluidity of the cell membranes and suggested anti-inflammatory properties (Braverman and Moser, 2012; Bozelli et al., 2021). The hydrogen atoms adjacent to the vinyl ether bond have relatively low disassociation energies and are preferentially oxidized when exposed to free radicals. This was proposed to spare the oxidation of polyunsaturated fatty acids and other vulnerable membrane lipids, suggesting a role for plasmalogens as sacrificial oxidants (Braverman and Moser, 2012). The higher serum concentration of plasmogen lipids observed in the pHu+ can reflect a higher adaptive response to oxidative stress due to their propensity for a higher oxidative energy metabolism leading to higher rates of ROS production (Beauclercq et al., 2016).

Lysophosphatidylcholines (LPC) and Lysophosphatidyleth anolamine (LPE) also contribute to the definition of the lines. They are products of the partial hydrolysis (i.e., removes one of the FA chain) of PC and PE in the circulation, respectively. In humans, LPC, *via* G protein-coupled receptor signaling, has harmful effects on various cells that include enhancing inflammatory responses, disrupting mitochondrial integrity, and inducing apoptosis (Law et al., 2019). LPC, and LPE to a lesser extent, are lipids also known to be associated with starch (Gayral et al., 2019). For example, lysophospholids represent 84%–94% of the lipids in starch granules comprised of 70% LPC and 20% LPE in oat or wheat (Autio and Eliasson, 2009; Maningat et al., 2009). The higher quantity of LPC and LPE observed in the serum of the pHu− line is therefore consistent with their better feed efficiency (Berger et al., 2022) and potentially greater ability to absorb LPC and LPE associated with starch, even though carbohydrate digestibility has not yet been specifically evaluated in the two lines.

The sterols represented by the cholesterol esters (CE) are essential structural components of cell membranes and also serve as a precursor for the biosynthesis of steroid hormones, bile acid and vitamin D. They are all over-represented in the pHu+ line, especially those with polyunsaturated and longer acyl chain (i.e., > 20), which could be related to very recent observations (personal communication) that evidenced much lower steroid content in egg yolk of pHu+ compared to the pHu−.

Finally, the serum of pHu− appeared richer in several sphingolipids, including Ceramides (Cer), glucosylceramide (GlcCer), and sphingomyelins. Sphingolipids play important roles in signal transduction and cell recognition. Plasma concentrations of sphingolipids have been associated with increased risk of heart failure in humans (Lemaitre et al., 2019) and used to reveal dietary exposure of chickens to fumonisins (Tardieu et al., 2021). Ceramides (Cer) and glucosylceramides (GlcCer) are sphingolipids with a R group consisting of only a hydrogen atom or a glucose molecule, respectively. Sphingomyelins (SM), one of the few membrane phospholipids not synthesized from glycerol, are the conjugation of a PC and a Cer. High serum level of ceramides and sphingomyelins had been associated with the development of obesity, insulin resistance, and impaired glucose metabolism in several studies in human and rodents (Hanamatsu et al., 2014; Turpin et al., 2014; Kayser et al., 2019). Ceramides antagonize insulin signaling by inhibiting transmission of signals through phosphatidylinositol-3 kinase (PI3K) and blocking activation of the kinase Akt/PKB, inhibiting insulin-stimulated glucose uptake in L6 myotubes, and reducing Glut4 translocation in mammals (Sokolowska and Blachnio-Zabielska, 2019), which results in higher glycemia (Kayser et al., 2019). Therefore, the higher concentration of Cer and GlcCer in the serum of the pHu− line is consistent with the higher glycemia of this line that was observed early post-hatch (Métayer-Coustard et al., 2021) and later during growth (Beauclercq et al., 2016).

In addition to the significant differences in muscle glycogen caused by selection on the ultimate pH of the meat, it was observed a higher occurrence and severity of white striping muscle defects, indicative of more fat deposition along muscle fibers, in the pHu+ line (Alnahhas et al., 2016). Recently, it has been hypothesized that excessive lipid accumulation in muscle (as it is observed in case of white striping and wooden breast defects) can cause lipotoxicity and oxidative stress, which may in turn partly lead to the downregulation of glycolysis and glycogenesis and redirection of glucose to alternative utilization pathways (Lake and Abasht, 2020). Indeed, decreased muscle glucose uptake is unlikely to be involved, as some glucose transporters are overexpressed in birds developing wooden breast syndrome. In addition, susceptibility to the wooden breast defect appears to be associated with an overactivation of lipid metabolism evidenced in muscle as early as 2 weeks of age, as shown by the overexpression of genes coding ankyrin repeat domain 1 but also peroxisome proliferator-activated receptors (gamma and alpha) (Lake et al., 2019). Interestingly, we have previously shown that ANKRD1, a gene involved the regulation of lipid metabolism by the peroxisome proliferator-activated receptor alpha, is overexpressed in 6-week-old pHu+ birds muscles (Beauclercq et al., 2017), and has been identified as a biomarker of interest for ultimate meat pH in pigs (Damon et al., 2013). Regarding genes encoding peroxisome proliferator-activated receptors, they were not differentially expressed in the pHu lines (Beauclercq et al., 2017) but PPARG and PPARD are close to SNPs significantly associated with pHu in these lines (Le Bihan-Duval et al., 2018). Taken together, the transcriptomic and

metabolomic characterizations of the pHu+ and pHu− lines indicate profound changes in carbohydrate and lipid metabolism related to divergent selection. The present study confirms that these changes are expressed at the muscle and blood levels with the expression of metabolic and lipidomic signatures specific to both lines.

Development of Predictive Models of the pHu From Blood Lipidome

One of the challenges for the poultry industry, in particular in the field of selection, is to have access to indicators that are available on live animals. The lipidomic characteristics of each line described here thus open interesting perspectives to search for blood indicators of meat pHu, useful to predict this phenotype on reproducers but also to study the impact of nutritional or farming practices on this trait. The lipidomics data acquired on pHu lines served to adjust a model predictive of the pHu value. The predictive ability of the present model was quite similar to a previous one based on muscle transcriptomic data issued of the two lines (Beauclercq et al., 2017). Indeed, the RMSEE, which reports the differences between the values predicted by a model and the observed values, was 0.16 pH units for the model based on the expression in the *P. major* of 20 genes while it was 0.18 pH units in the present model based on 40 circulating lipids. Concretely, the model based on the lipidome allowed us correctly classifying 76% of the muscles exhibiting a normal value of pHu (between 5.7 and 6.1). The lower performance of the external validation (RMSEP = 0.25 pH unit) may result from the lower representation of birds exhibiting a normal value of pHu in the validation dataset. The main interest of the model developed in the present study comes from the possibility of collecting lipidomic data from blood samples taken from live animals, which is especially crucial for selection, and also to obtain a good quality of prediction quite early during the life of the animal (17 days).

CONCLUSION

This innovative study is the first attempt at the description of the lipidome of modern broilers and its early variation in relation to the pHu. The focus was set on 4 classes of lipids: the glycerolipids, the glycerophospholipids, the sterols, and the sphingolipids. The glycerolipids, which are involved in energy storage, were in higher concentration in the blood of pHu− birds consistently with their higher glycogen storages. The glycerophospholipids, mainly represented by the phosphatidylcholines and the phosphatidylethanolamines, with long and polyunsaturated acyl chains were more abundant in pHu+ than in pHu− while the lysophosphatidylcholines and lysophosphatidylethanolamines, known to be associated with starch, were observed in higher quantity in the serum of the pHu− line. Finally, the concentration of the sterols and the ceramides, belonging to the sphingolipids class, were higher in the pHu+ and pHu−, respectively. The specific lipidomic blood signatures reported here may help to understand what physiological mechanisms are involved in digestion, transport and metabolic utilization of nutrients, but also, after further validation of the models, to predict the propensity of birds to store more or less glycogen in muscles and the associated pHu.

DATA AVAILABILITY STATEMENT

The datasets generated and analyzed during the current study are available in the MetaboLights repository hosted by the EMBL-EBI, https://www.ebi.ac.uk/metabolights/MTBLS2970.

ETHICS STATEMENT

All animal care and experimental procedures needed for this study were conducted in accordance with current European legislation (EU Directive 2010/63/EU) and in agreement with the French National Regulation for human care and use of animals for research purposes and received the authorization number 2019071715406895_V2-21517 from the French Ministry of Higher Education, Research and Innovation, after approval by the animal experimentation ethical committee Pays de Loire CEEA-006.

AUTHOR CONTRIBUTIONS

SB drafted the manuscript, carried out the chemometric, and functional analyses. SM-G and ELB-D designed and supervised the study. CB, SM-G, and ELB-D supervised the preparation of the manuscript. AP prepared the samples and performed the LC-HRMS analyses. QB, SM-G, and ELB-D performed the experiments. AL and PE supervised the lipidomics analyses. SM-C and ST contributed to the biological integration of the lipidomics data. All authors helped to draft the manuscript and approved the final manuscript.

FUNDING

This study was supported by Feed-a-Gene, a project that has received funding from the European Union's Horizon 2020 research and innovation program under grant agreement No. 633531.

ACKNOWLEDGMENTS

We thank the staff of the Poultry Breeding Facilities (INRAE, UE 1295 Pôle d'Expérimentation Avicole de Tours, 37380 Nouzilly, France) for producing the birds, and the Avian Research Unit (INRAE, UMR Biologie des Oiseaux et Aviculture, 37380 Nouzilly, France), and more particularly Séverine Urvoix, Emilie Raynaud, Jérémy Bernard, Patrice Ganier, and Marine Chahnamian.

SUPPLEMENTARY MATERIAL

The Supplementary Material for this article can be found online at: https://www.frontiersin.org/articles/10.3389/fphys.2022.935868/full#supplementary-material

REFERENCES

Alnahhas, N., Berri, C., Boulay, M., Baéza, E., Jégo, Y., Baumard, Y., et al. (2014). Selecting Broiler Chickens for Ultimate pH of Breast Muscle: Analysis of Divergent Selection Experiment and Phenotypic Consequences on Meat Quality, Growth, and Body Composition Traits1. *J. Anim. Sci.* 92, 3816–3824. doi:10.2527/jas.2014-7597

Alnahhas, N., Berri, C., Chabault, M., Chartrin, P., Boulay, M., Bourin, M. C., et al. (2016). Genetic Parameters of White Striping in Relation to Body Weight, Carcass Composition, and Meat Quality Traits in Two Broiler Lines Divergently Selected for the Ultimate pH of the Pectoralis Major Muscle. *BMC Genet.* 17, 61. doi:10.1186/s12863-016-0369-2

Alnahhas, N., le Bihan-Duval, E., Baéza, E., Chabault, M., Chartrin, P., Bordeau, T., et al. (2015). Impact of Divergent Selection for Ultimate pH of Pectoralis Major Muscle on Biochemical, Histological, and Sensorial Attributes of Broiler Meat1. *J. Animal Sci.* 93, 4524–4531. doi:10.2527/jas.2015-9100

Artegoitia, V. M., Foote, A. P., Lewis, R. M., and Freetly, H. C. (2019). Metabolomics Profile and Targeted Lipidomics in Multiple Tissues Associated with Feed Efficiency in Beef Steers. *ACS Omega* 4, 3973–3982. doi:10.1021/ACSOMEGA.8B02494

Autio, K., and Eliasson, A.-C. (2009). "Oat Starch," in *Starch*. Editors J. BeMiller and R. Whistler. Third Edition (San Diego: Academic Press), 589–599. doi:10.1016/B978-0-12-746275-2.00015-X

Bach, A. C., Ingenbleek, Y., and Frey, A. (1996). The Usefulness of Dietary Medium-Chain Triglycerides in Body Weight Control: Fact or Fancy? *J. Lipid Res.* 37, 708–726. doi:10.1016/S0022-2275(20)37570-2

Baéza, E., Guillier, L., and Petracci, M. (2022). Review: Production Factors Affecting Poultry Carcass and Meat Quality Attributes. *Animal* 16, 100331. doi:10.1016/J.ANIMAL.2021.100331

Baéza, E., Jégou, M., Gondret, F., Lalande-Martin, J., Tea, I., le Bihan-Duval, E., et al. (2015). Pertinent Plasma Indicators of the Ability of Chickens to Synthesize and Store Lipids1. *J. Animal Sci.* 93, 107–116. doi:10.2527/JAS.2014-8482

Barbut, S. (1997). Problem of Pale Soft Exudative Meat in Broiler Chickens. *Br. Poult. Sci.* 38, 355–358. doi:10.1080/00071669708418002

Beauclercq, S., Hennequet-Antier, C., Praud, C., Godet, E., Collin, A., Tesseraud, S., et al. (2017). Muscle Transcriptome Analysis Reveals Molecular Pathways and Biomarkers Involved in Extreme Ultimate pH and Meat Defect Occurrence in Chicken. *Sci. Rep.* 7, 1–13. doi:10.1038/s41598-017-06511-6

Beauclercq, S., Nadal-Desbarats, L., Germain, K., Praud, C., Emond, P., Bihan-Duval, E. L., et al. (2019). Does Lipidomic Serum Analysis Support the Assessment of Digestive Efficiency in Chickens? *Poult. Sci.* 98, 1425–1431. doi:10.3382/ps/pey483

Beauclercq, S., Nadal-Desbarats, L., Hennequet-Antier, C., Collin, A., Tesseraud, S., Bourin, M., et al. (2016). Serum and Muscle Metabolomics for the Prediction of Ultimate pH, a Key Factor for Chicken-Meat Quality. *J. Proteome Res.* 15, 1168–1178. doi:10.1021/acs.jproteome.5b01050

Beaufrère, H., Gardhouse, S. M., Wood, R. D., and Stark, K. D. (2020). The Plasma Lipidome of the Quaker Parrot (Myiopsitta Monachus). *PLOS ONE* 15, e0240449. doi:10.1371/JOURNAL.PONE.0240449

Bergeot, M.-A., Collin, A., Travel, A., Pampouille, E., Akakpo, R., Raynaud, E., et al. (2022). *Recherche de nouveaux indicateurs ou biomarqueurs pour l'amélioration génétique de la qualité du poussin*. Tours): Journées de la Recherche Avicole et Palmipèdes à Foie gras, 14.

Berger, Q., Guettier, E., Bernard, J., Ganier, P., Chahnamian, M., le Bihan-Duval, E., et al. (2022). Profiles of Genetic Parameters of Body Weight and Feed Efficiency in Two Divergent Broiler Lines for Meat Ultimate pH. *BMC Genom Data* 23 (1 23), 1–11. doi:10.1186/S12863-022-01035-Z

Berri, C. (2000). Variability of Sensory and Processing Qualities of Poultry Meat. *World's Poult. Sci. J.* 56, 209–224. doi:10.1079/WPS20000016

Bozelli, J. C., Jr., Azher, S., and Epand, R. M. (2021). Plasmalogens and Chronic Inflammatory Diseases. *Front. Physiol.* 12, 730829. doi:10.3389/FPHYS.2021.730829

Braverman, N. E., and Moser, A. B. (2012). Functions of Plasmalogen Lipids in Health and Disease. *Biochimica Biophysica Acta (BBA) - Mol. Basis Dis.* 1822, 1442–1452. doi:10.1016/J.BBADIS.2012.05.008

Brown, L. P., May, A. L., Fisch, A. R., Campagna, S. R., and Voy, B. H. (2022). "Avian Metabolomics," in *Sturkie's Avian Physiology* (Academic Press), 49–63. doi:10.1016/B978-0-12-819770-7.00041-4

Cui, X. Y., Gou, Z. Y., Abouelezz, K. F. M., Li, L., Lin, X. J., Fan, Q. L., et al. (2020). Alterations of the Fatty Acid Composition and Lipid Metabolome of Breast Muscle in Chickens Exposed to Dietary Mixed Edible Oils. *animal* 14, 1322–1332. doi:10.1017/S1751731119003045

Damon, M., Denieul, K., Vincent, A., Bonhomme, N., Wyszynska-Koko, J., and Lebret, B. (2013). Associations between Muscle Gene Expression Pattern and Technological and Sensory Meat Traits Highlight New Biomarkers for Pork Quality Assessment. *Meat Sci.* 95, 744–754. doi:10.1016/j.meatsci.2013.01.016

DeLany, J. P., Windhauser, M. M., Champagne, C. M., and Bray, G. A. (2000). Differential Oxidation of Individual Dietary Fatty Acids in Humans. *Am. J. Clin. Nutr.* 72, 905–911. doi:10.1093/AJCN/72.4.905

Dirong, G., Nematbakhsh, S., Selamat, J., Chong, P. P., Idris, L. H., Nordin, N., et al. (2021). Omics-Based Analytical Approaches for Assessing Chicken Species and Breeds in Food Authentication. *Molecules* 26, 6502. *Page 6502* 26. doi:10.3390/MOLECULES26216502

Everaert, N., Decuypere, E., and Buyse, J. (2021). "Chapter 26: Adipose Tissue and Lipid Metabolism," in *Sturkie's Avian Physiology*. Editors C. G. Scanes and S. Dridi (Academic Press, Elsevier), 627–640.

Fahy, E., Subramaniam, S., Murphy, R. C., Nishijima, M., Raetz, C. R. H., Shimizu, T., et al. (2009). Update of the LIPID MAPS Comprehensive Classification System for Lipids. *J. Lipid Res.* 50 (Suppl. l), S9–S14. doi:10.1194/jlr.R800095-JLR200

Fletcher, D. L., Qiao, M., and Smith, D. P. (2000). The Relationship of Raw Broiler Breast Meat Color and pH to Cooked Meat Color and pH. *Poult. Sci.* 79, 784–788. doi:10.1093/ps/79.5.784

Gayral, M., Fanuel, M., Rogniaux, H. ½. ½., Dalgalarrondo, M. ½., Elmorjani, K., Bakan, B. ½. ½., et al. (2019). The Spatiotemporal Deposition of Lysophosphatidylcholine within Starch Granules of Maize Endosperm and its Relationships to the Expression of Genes Involved in Endoplasmic Reticulum-Amyloplast Lipid Trafficking and Galactolipid Synthesis. *Plant Cell. Physiology* 60, 139–151. doi:10.1093/PCP/PCY198

Gigaud, V., le Bihan-Duval, E., and Berri, C. (2009). *Facteurs de variation de l'aptitude à la transformation de la viande de volaille*, 8. St Malo): Journées de la Recherche Avicole, 124–131.

Guitton, Y., Tremblay-Franco, M., Le Corguillé, G., Martin, J.-F., Pétéra, M., Roger-Mele, P., et al. (2017). Create, Run, Share, Publish, and Reference Your LC-MS, FIA-MS, GC-MS, and NMR Data Analysis Workflows with the Workflow4Metabolomics 3.0 Galaxy Online Infrastructure for Metabolomics. *Int. J. Biochem. Cell. Biol.* 93, 89–101. doi:10.1016/J.BIOCEL.2017.07.002

Guo, Y., Balasubramanian, B., Zhao, Z.-H., and Liu, W.-C. (2021). Heat Stress Alters Serum Lipid Metabolism of Chinese Indigenous Broiler Chickens-A Lipidomics Study. *Environ. Sci. Pollut. Res.* 28, 10707–10717. doi:10.1007/S11356-020-11348-0

Hanamatsu, H., Ohnishi, S., Sakai, S., Yuyama, K., Mitsutake, S., Takeda, H., et al. (2014). Altered Levels of Serum Sphingomyelin and Ceramide Containing Distinct Acyl Chains in Young Obese Adults. *Nutr Diabetes* 4 (10 4), e141. doi:10.1038/nutd.2014.38

Hinterwirth, H., Stegemann, C., and Mayr, M. (2014). Lipidomics. *Circ. Cardiovasc Genet.* 7, 941–954. doi:10.1161/CIRCGENETICS.114.000550

Ishikawa, M., Saito, K., Urata, M., Kumagai, Y., Maekawa, K., and Saito, Y. (2015). Comparison of Circulating Lipid Profiles between Fasting Humans and Three Animal Species Used in Preclinical Studies: Mice, Rats and Rabbits. *Lipids Health Dis.* 14, 1–6. doi:10.1186/S12944-015-0104-4

Jassal, B., Matthews, L., Viteri, G., Gong, C., Lorente, P., Fabregat, A., et al. (2020). The Reactome Pathway Knowledgebase. *Nucleic Acids Res.* 48, D498. doi:10.1093/NAR/GKZ1031

Jlali, M., Gigaud, V., Métayer-Coustard, S., Sellier, N., Tesseraud, S., le Bihan-Duval, E., et al. (2012). Modulation of Glycogen and Breast Meat Processing Ability by Nutrition in Chickens: Effect of Crude Protein Level in 2 Chicken Genotypes1. *J. Anim. Sci.* 90, 447–455. doi:10.2527/jas.2011-4405

Kaabia, Z., Poirier, J., Moughaizel, M., Aguesse, A., Billon-Crossouard, S., Fall, F., et al. (2018). Plasma Lipidomic Analysis Reveals Strong Similarities between Lipid Fingerprints in Human, Hamster and Mouse Compared to Other Animal Species. *Sci. Rep.* 8, 1–9. doi:10.1038/S41598-018-34329-3

Kanehisa, M., and Goto, S. (2000). KEGG: Kyoto Encyclopedia of Genes and Genomes. *Nucleic Acids Res.* 28, 27–30. doi:10.1093/nar/28.1.27

Kayser, B. D., Prifti, E., Lhomme, M., Belda, E., Dao, M.-C., Aron-Wisnewsky, J., et al. (2019). Elevated Serum Ceramides Are Linked with Obesity-Associated Gut Dysbiosis and Impaired Glucose Metabolism. *Metabolomics* 15, 140. doi:10.1007/S11306-019-1596-0

Kehelpannala, C., Rupasinghe, T., Hennessy, T., Bradley, D., Ebert, B., and Roessner, U. (2021). The State of the Art in Plant Lipidomics. *Mol. Omics* 17, 894–910. doi:10.1039/D1MO00196E

Lake, J. A., and Abasht, B. (2020). Glucolipotoxicity: A Proposed Etiology for Wooden Breast and Related Myopathies in Commercial Broiler Chickens. *Front. Physiol.* 11, 169. doi:10.3389/fphys.2020.00169

Lake, J. A., Papah, M. B., and Abasht, B. (2019). Increased Expression of Lipid Metabolism Genes in Early Stages of Wooden Breast Links Myopathy of Broilers to Metabolic Syndrome in Humans. *Genes.* 10, 746. Page 746 10. doi:10.3390/GENES10100746

Law, S.-H., Chan, M.-L., Marathe, G. K., Parveen, F., Chen, C.-H., and Ke, L.-Y. (2019). An Updated Review of Lysophosphatidylcholine Metabolism in Human Diseases. *Ijms* 20, 1149. doi:10.3390/IJMS20051149

le Bihan-Duval, E., Alnahhas, N., Alnahhas, N., Pampouille, E., Berri, C., and Abasht, B. (2020). "Genetics and Genomics of Meat Quality Traits in Poultry Species," in *Advances in Poultry Genetics and Genomics*. Editors S. E. Aggrey, H. Zhou, M. Tixier-Boichard, and D. D. Rhoads (Cambridge, UK: Burleigh Dodds Series in Agricultural Sciences), 127–150. doi:10.19103/as.2020.0065.09

Le Bihan-Duval, E., and Berri, C. (2017). "Genetics and Genomics for Improving Poultry Meat Quality," in *Poultry Quality Evaluation: Quality Attributes and Consumer Values*. Editors M. Petracci and C. Berri (Sawston: Woodhead Publishing), 199–220. doi:10.1016/B978-0-08-100763-1.00008-8

le Bihan-Duval, E., Debut, M., Berri, C. M., Sellier, N., Santé-Lhoutellier, V., Jégo, Y., et al. (2008). Chicken Meat Quality: Genetic Variability and Relationship with Growth and Muscle Characteristics. *BMC Genet.* 9, 53. doi:10.1186/1471-2156-9-53

Lu, J., Lam, S. M., Wan, Q., Shi, L., Huo, Y., Chen, L., et al. (2019). High-coverage Targeted Lipidomics Reveals Novel Serum Lipid Predictors and Lipid Pathway Dysregulation Antecedent to Type 2 Diabetes Onset in Normoglycemic Chinese Adults. *Diabetes Care* 42, 2117–2126. doi:10.2337/DC19-0100/-/DC1

Maningat, C. C., Seib, P. A., Bassi, S. D., Woo, K. S., and Lasater, G. D. (2009). "Wheat Starch," in *Chapter 10 - Wheat Starch: Production, Properties, Modification and UsesStarch*. Editors J. BeMiller and R. Whistler. Third Edition (San Diego: Academic Press), 441–510. doi:10.1016/B978-0-12-746275-2.00010-0

Meng, Y., Qiu, N., Mine, Y., and Keast, R. (2021). Comparative Lipidomics of Chick Yolk Sac during the Embryogenesis Provides Insight into Understanding the Development-Related Lipid Supply. *J. Agric. Food Chem.* 69, 7467–7477. doi:10.1021/acs.jafc.1c01728

Métayer-Coustard, S., Tesseraud, S., Praud, C., Royer, D., Bordeau, T., Coudert, E., et al. (2021). Early Growth and Protein-Energy Metabolism in Chicken Lines Divergently Selected on Ultimate pH. *Front. Physiol.* 12, 144. doi:10.3389/FPHYS.2021.643580

Mi, S., Shang, K., Jia, W., Zhang, C.-H., Li, X., Fan, Y.-Q., et al. (2018). Characterization and Discrimination of Taihe Black-Boned Silky Fowl (Gallus gallus Domesticus Brisson) Muscles Using LC/MS-based Lipidomics. *Food Res. Int.* 109, 187–195. doi:10.1016/J.FOODRES.2018.04.038

Mi, S., Shang, K., Li, X., Zhang, C.-H., Liu, J.-Q., and Huang, D.-Q. (2019). Characterization and Discrimination of Selected China's Domestic Pork Using an LC-MS-based Lipidomics Approach. *Food control.* 100, 305–314. doi:10.1016/J.FOODCONT.2019.02.001

Mir, N. A., Rafiq, A., Kumar, F., Singh, V., and Shukla, V. (2017). Determinants of Broiler Chicken Meat Quality and Factors Affecting Them: a Review. *J. Food Sci. Technol.* 54 (10 54), 2997–3009. doi:10.1007/S13197-017-2789-Z

Osorio, J. H., and Flores, J. D. (2018). Comparación de lípidos sanguíneos entre pollos de engorde y gallinas ponedoras. *Rev. Med. Vet. Zoot.* 65, 27–35. doi:10.15446/rfmvz.v65n1.72021

Pampouille, E., Dusart, L., Bonnouvrier, A., Danel, J., Dauguet, S., Désolé, M., et al. (2021). VOCALIM -Mieux valoriser des matières premières métropolitaines dans l'alimentation des poulets de chair pour améliorer l'autonomie protéique française. *Innov. Agron.* 82, 425–440. doi:10.15454/GYBR-S265

Petit, A., Réhault-Godbert, S., Nadal-Desbarats, L., Cailleau-Audouin, E., Chartrin, P., Raynaud, E., et al. (2022). Nutrient Sources Differ in the Fertilised Eggs of Two Divergent Broiler Lines Selected for Meat Ultimate pH. *Sci. Rep.* 12 (1 12), 1–16. doi:10.1038/s41598-022-09509-x

Qiao, M., Fletcher, D. L., Smith, D. P., and Northcutt, J. K. (2001). The Effect of Broiler Breast Meat Color on pH, Moisture, Water-Holding Capacity, and Emulsification Capacity. *Poult. Sci.* 80, 676–680. doi:10.1093/PS/80.5.676

Smith, C. A., Want, E. J., O'Maille, G., Abagyan, R., and Siuzdak, G. (2006). XCMS: Processing Mass Spectrometry Data for Metabolite Profiling Using Nonlinear Peak Alignment, Matching, and Identification. *Anal. Chem.* 78, 779–787. doi:10.1021/AC051437Y

Sokolowska, E., and Blachnio-Zabielska, A. (2019). The Role of Ceramides in Insulin Resistance. *Front. Endocrinol.* 10, 577. doi:10.3389/FENDO.2019.00577

Sumner, L. W., Amberg, A., Barrett, D., Beale, M. H., Beger, R., Daykin, C. A., et al. (2007). Proposed Minimum Reporting Standards for Chemical Analysis. *Metabolomics* 3, 211–221. doi:10.1007/s11306-007-0082-2

Sun, T., Wang, X., Cong, P., Xu, J., and Xue, C. (2020). Mass Spectrometry-based Lipidomics in Food Science and Nutritional Health: A Comprehensive Review. *Compr. Rev. Food Sci. Food Saf.* 19, 2530–2558. doi:10.1111/1541-4337.12603

Trivedi, D. K., Hollywood, K. A., Rattray, N. J. W., Ward, H., Trivedi, D. K., Greenwood, J., et al. (2016). Meat, the Metabolites: an Integrated Metabolite Profiling and Lipidomics Approach for the Detection of the Adulteration of Beef with Pork. *Analyst* 141, 2155–2164. doi:10.1039/C6AN00108D

Turpin, S. M., Nicholls, H. T., Willmes, D. M., Mourier, A., Brodesser, S., Wunderlich, C. M., et al. (2014). Obesity-induced CerS6-dependent C16:0 Ceramide Production Promotes Weight Gain and Glucose Intolerance. *Cell. Metab.* 20, 678–686. doi:10.1016/J.CMET.2014.08.002

Wang, R., Li, B., Lam, S. M., and Shui, G. (2020). Integration of Lipidomics and Metabolomics for In-Depth Understanding of Cellular Mechanism and Disease Progression. *J. Genet. Genomics* 47, 69–83. doi:10.1016/J.JGG.2019.11.009

Wishart, D. S., Feunang, Y. D., Marcu, A., Guo, A. C., Liang, K., Vázquez-Fresno, R., et al. (2018). HMDB 4.0: the Human Metabolome Database for 2018. *Nucleic Acids Res.* 46, D608–D617. doi:10.1093/nar/gkx1089

Wood, P. L., Muir, W., Christmann, U., Gibbons, P., Hancock, C. L., Poole, C. M., et al. (2021). Lipidomics of the Chicken Egg Yolk: High-Resolution Mass Spectrometric Characterization of Nutritional Lipid Families. *Poult. Sci.* 100, 887–899. doi:10.1016/J.PSJ.2020.11.020

Zhang, Z., Liao, Q., Sun, Y., Pan, T., Liu, S., Miao, W., et al. (2021). Lipidomic and Transcriptomic Analysis of the Longissimus Muscle of Luchuan and Duroc Pigs. *Front. Nutr.* 8, 187. doi:10.3389/FNUT.2021.667622

Conflict of Interest: The authors declare that the research was conducted in the absence of any commercial or financial relationships that could be construed as a potential conflict of interest.

Publisher's Note: All claims expressed in this article are solely those of the authors and do not necessarily represent those of their affiliated organizations, or those of the publisher, the editors and the reviewers. Any product that may be evaluated in this article, or claim that may be made by its manufacturer, is not guaranteed or endorsed by the publisher.

frontiers | Frontiers in Physiology

ORIGINAL RESEARCH
published: 27 June 2022
doi: 10.3389/fphys.2022.935311

The Effect of Commercial Genetic Selection on Somatotropic Gene Expression in Broilers: A Potential Role for Insulin-Like Growth Factor Binding Proteins in Regulating Broiler Growth and Body Composition

Lauren A. Vaccaro[1], *Tom E. Porter*[2] *and Laura E. Ellestad*[1]*

[1]Department of Poultry Science, University of Georgia, Athens, GA, United States, [2]Department of Animal and Avian Sciences, University of Maryland, College Park, MD, United States

OPEN ACCESS

Edited by:
Sandra G. Velleman,
The Ohio State University,
United States

Reviewed by:
Chongxiao Chen,
North Carolina State University,
United States
Paul Siegel,
Virginia Tech, United States

***Correspondence:**
Laura E. Ellestad
lellestad@uga.edu

Specialty section:
This article was submitted to Avian Physiology, a section of the journal Frontiers in Physiology

Received: 03 May 2022
Accepted: 06 June 2022
Published: 27 June 2022

Citation:
Vaccaro LA, Porter TE and Ellestad LE (2022) The Effect of Commercial Genetic Selection on Somatotropic Gene Expression in Broilers: A Potential Role for Insulin-Like Growth Factor Binding Proteins in Regulating Broiler Growth and Body Composition. Front. Physiol. 13:935311. doi: 10.3389/fphys.2022.935311

The somatotropic axis influences growth and metabolism, and many of its effects are a result of insulin-like growth factor (IGF) signaling modulated by IGF-binding proteins (IGFBPs). Modern commercial meat-type (broiler) chickens exhibit rapid and efficient growth and muscle accretion resulting from decades of commercial genetic selection, and it is not known how alterations in the IGF system has contributed to these improvements. To determine the effect of commercial genetic selection on somatotropic axis activity, two experiments were conducted comparing legacy Athens Canadian Random Bred and modern Ross 308 male broiler lines, one between embryonic days 10 and 18 and the second between post-hatch days 10 and 40. Gene expression was evaluated in liver and breast muscle (*pectoralis major*) and circulating hormone concentrations were measured post-hatch. During embryogenesis, no differences in IGF expression were found that corresponded with difference in body weight between the lines beginning on embryonic day 14. While hepatic IGF expression and circulating IGF did not differ between the lines post-hatch, expression of both *IGF1* and *IGF2* mRNA was greater in breast muscle of modern broilers. Differential expression of select IGFBPs suggests their action is dependent on developmental stage and site of production. Hepatic *IGFBP1* appears to promote embryonic growth but inhibit post-hatch growth at select ages. Results suggest that local IGFBP4 may prevent breast muscle growth during embryogenesis but promote it after hatch. Post-hatch, *IGFBP2* produced in liver appears to inhibit body growth, but IGFBP2 produced locally in breast muscle facilitates development of this tissue. The opposite appears true for IGFBP3, which seems to promote overall body growth when produced in liver and restrict breast muscle growth when produced locally. Results presented here suggest that paracrine IGF signaling in breast muscle may contribute to overall growth and muscle accretion in chickens, and that this activity is regulated in developmentally distinct and tissue-specific contexts through combinatorial action of IGFBPs.

Keywords: somatotropic axis, growth, insulin-like growth factor, insulin-like growth factor binding protein, endocrine signaling, paracrine signaling, broiler, Athens-Canadian Random Bred

INTRODUCTION

Growth and body composition in vertebrates are controlled by several highly conserved endocrine axes (Levine, 2012; Vaccaro et al., 2021). In particular, the somatotropic axis is known to regulate growth and development of mammals *via* cellular proliferation and metabolic effects in muscle, bone, and adipose tissue (Clark and Robinson, 1996; Gahete et al., 2016). However, its physiological impact on these processes is not as well understood in birds. Particularly lacking is information regarding how local production of insulin-like growth factor (IGF) 1 and IGF2 in tissues such as muscle impacts growth and body composition and how IGF-binding proteins (IGFBPs) regulate both endocrine and paracrine IGF signaling.

The key effector hormones in the somatotropic axis include IGF1 and IGF2 (Stewart and Rotwein, 1996), which are synthesized in the liver upon growth hormone receptor (GHR) activation (Kajimoto and Rotwein, 1989; Dewil et al., 1999; Herrington and Carter-Su, 2001; Woelfle et al., 2005; Brooks et al., 2008). A dwarf phenotype is observed in chickens deficient in GHR signaling (Hutt, 1959; Burnside et al., 1992; Chen et al., 2009), and this is partially caused by decreased hepatic IGF production (Burnside and Cogburn, 1992). On the cellular level, IGFs downregulate apoptosis while increasing cellular proliferation by binding the type 1 IGF receptor (IGFR1) (Girbau et al., 1989; Duclos and Goddard, 1990; D'Costa et al., 1998). This would imply a direct relationship between IGF signaling and growth in chickens, but studies have been inconclusive. Direct IGF1 administration did not stimulate growth in two to three week-old male chickens (McGuinness and Cogburn, 1991; Czerwinski et al., 1998) or four week-old females (Huybrechts et al., 1992). Increased hepatic *IGF1* mRNA expression has been observed in chickens selected for high body weight (Beccavin et al., 2001), but not consistently (Giachetto et al., 2004). Similarly, fast-growing chickens had greater plasma IGF2 (Scanes et al., 1989), but IGF2 did not induce weight gain when directly administered (Buyse and Decuypere, 1999). Studies investigating levels of growth hormone (GH), which is classically thought to induce IGF secretion from the liver, also yield results inconsistent with the idea that increased somatotropic activity always leads to increased growth. Pituitary GH expression was greater between 3 and 7 weeks of age in male broilers with lower body weight as compared to those with a higher body weight (Ellestad et al., 2019), and the percentage of GH-secreting cells in slow-growing chickens was greater at 5 weeks of age, though fast-growing embryos secreted more GH per hour (Porter, 1998). Circulating GH was also found to be higher in chickens selected for egg production (layers) than those selected for meat production (broilers), despite layers growing slower and having lower body weights (Reiprich et al., 1995).

Cellular effects induced by IGF signaling are regulated by IGFBPs. These proteins are highly conserved across vertebrates (Armstrong et al., 1989; Allander et al., 1995; Schoen et al., 1995; Allander et al., 1997; Kelley et al., 2002), although IGFBP6 has not been retained in birds. Growth modulation occurs when an IGFBP physically binds an IGF to enhance or reduce receptor affinity, extend the hormone's half-life, or alter its tissue specificity (Baxter, 1991; Kim, 2010). For example, *IGFBP1* inhibits protein synthesis in skeletal muscle (Frost and Lang, 1999), while IGFBP2 and IGFBP4 inhibit long bone growth (Mohan et al., 1995; Fisher et al., 2005). In myoblasts, IGFBP5 has a proliferative effect when bound to IGF1 but an inhibitory effect upon binding IGF2 (Ewton et al., 1998). Additionally, some IGFBPs can act independently. For example, IGFBP2 can upregulate apoptosis (Schutt et al., 2004; Klaus et al., 2006), while IGFBP5 can enhance bone cell proliferation (Mohan et al., 1995). As both ligand-dependent and ligand-independent effects of IGFBPs are important in growth regulation, their actions may contribute to the enhanced growth and muscle accretion of commercial modern broiler chickens.

Commercial modern broilers are raised specifically for meat production and have an increased growth rate, greater body weight, reduced feed conversion ratio (FCR; g feed intake/g

TABLE 1 | Primers used for reverse transcription-quantitative PCR.

Gene symbol	Forward primer (5′-3′)	Reverse primer (5′-3′)	Transcript ID[1]	Efficiency
IGFs				
IGF1	TGAGCTGGTTGATGCTCTTC	AGCCTCCTCAGGTCACAACT	20816	0.99
IGF2	AGTCAGAGCGTGACCTCTCC	CTGCGAGCTCTTCTTCTGC	53800	1.05
Hormone receptors				
GHR	TGCTGATTTTTCCTCCTGTG	GGCTGGCTAAGATGGAGTTC	23973	1.08
IGF1R	TGGGGACCTCAAAAGTTACC	ATCCCATCAGCAATCTCTCC	74990	1.04
Hormone binding proteins				
IGFBP1	CAGAGAAGTGGAGGGGACAT	CTTCTGGGGATCCAGGAAT	47713	
IGFBP2	ATCACAACCACGAGGACTCA	GAGGGAGTAGAGGTGCTCCA	18698	0.96
IGFBP3	TTGAGTCCTAGGGGTTTCCA	ATATCCAGGAAGCGGTTGTC	82156	1.02
IGFBP4	AACTTCCACCCCAAGCAG	AATCCAAGTCCCCCTTCAG	68153	0.96
IGFBP5	CTGAAGAGCAGCCAGAGGAT	TTGTCCACACACCAACACAG	38163	0.98
IGFBP7	ATGTGACAGGAGCACAGATCTACCT	TCTGGATACCATACTGTCCTCGAAT	61018	0.95
Reference genes				
GAPDH	AGCCATTCCTCCACCTTTGAT	AGTCCACAACACGGTTGCTGTAT	23323	1.00
18s[2]	AGCCTGCGGCTTAATTTGAC	CAACTAAGAACGGCCATGCA	173612	0.96

[1]*Transcript identification from Ensembl chicken genome assembly GRCg6a (http://www.ensembl.org/Gallus_gallus/Info/Index) preceded by ENSGALT000000.*

[2]*Sequence for 18S rRNA, is not on the assembled chicken genome, and primers were designed based on the sequence in GenBank (Accession Number AF173612).*

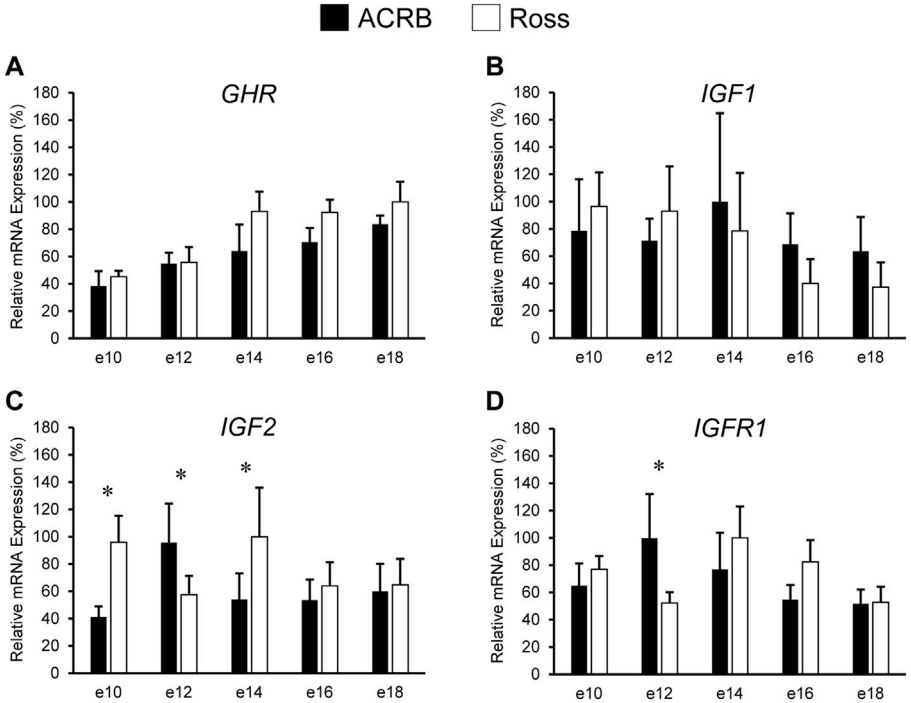

FIGURE 1 | Relative mRNA expression of **(A)** *GHR*, **(B)** *IGF1*, **(C)** *IGF2*, and **(D)** *IGFR1* in liver on embryonic days e 10, 12, 14, 16, and 18 in legacy ACRB and modern Ross 308 male broilers. Relative expression levels were measured using RT-qPCR and normalized to *GAPDH* mRNA ($n = 4$ replicate birds per line at each age). The data (mean + SEM) are expressed relative to the line and age with the highest expression level (equivalent to 100%). No significant line-by-age interactions were detected for **(A)** *GHR* ($p = 0.7777$) or **(B)** *IGF1* ($p = 0.7562$), and main effect means for line and age for these genes are shown in **Tables 2**, **3**, respectively. Significant line-by-age interactions were identified for **(C)** *IGF2* ($p = 0.0003$) and **(D)** *IGFR1* ($p = 0.0235$), and the presence of an asterisk (*) indicates a significant difference in expression between the lines at those ages ($p \leq 0.05$).

TABLE 2 | Means[1] (±SEM) and ANOVA *p*-values of the line main effect for somatotropic gene expression in embryonic male ACRB and Ross 308 broilers.

	ACRB	Ross 308	*p*-value
IGFs and Receptors			
Liver (%)[2]			
GHR	80.6 ± 7.6	100 ± 8.9	0.0640
IGF1	75.2 ± 14.9	100 ± 34.5	0.7004
Muscle (%)[2]			
GHR	100 ± 7.9	90.5 ± 7.4	0.3378
IGF1	93.1 ± 12.1	100 ± 9.9	0.7055
IGF2	100 ± 12.9	88.2 ± 13.5	0.4571
IGF1R	100 ± 10.9	84.5 ± 7.7	0.2150
IGFBPs			
Liver (%)[2]			
IGFBP2	95.5 ± 22.4	100 ± 17.7	0.6238
IGFBP4	87.3 ± 11.4	100 ± 14.7	0.3633
IGFBP5	100 ± 6.1	86.8 ± 5.8	0.0940
IGFBP7	82.1 ± 7.5	100 ± 12.4	0.2619
Muscle (%)[2]			
IGFBP1	99.8 ± 20.1	100 ± 15.8	0.7343
IGFBP2	100 ± 9.4	91.2 ± 5.6	0.6339
IGFBP3	100 ± 7.2	95.9 ± 6.1	0.6978
IGFBP4	100 ± 13.7[a]	69.7 ± 8.0[b]	0.0354
IGFBP5	100 ± 10.5	97.2 ± 8.9	0.8773
IGFBP7	100 ± 13.3	96.3 ± 10.0	0.7269

[1]*Means are only presented for data where a significant line-by-age interaction was not present and were calculated between embryonic day 10 and 18 for each line.*
[2]*Data within each gene are expressed relative to the line with the highest mRNA, level (equal to 100%).*
[a,b]*Values within each gene that do not share a common letter are significantly different ($p \leq 0.05$).*

body weight gain), and higher meat yields (Bartov, 1982; Goddard et al., 1988; Havenstein et al., 1994; Berrong and Washburn, 1998; Havenstein et al., 2003; Collins et al., 2014), all of which are the result of decades of artificial genetic selection by the poultry industry. A useful experimental model to investigate the impact of the somatotropic axis on broiler growth and body composition is the comparison of commercially selected broilers currently used by the poultry industry with non-selected ones. Athens Canadian Random Bred (ACRB) legacy broilers are representative of slower-growing, lower body weight birds prior to the beginning of intensive commercial broiler selection (Hess, 1962; Collins et al., 2014; Marks et al., 2016). Administration of a current commercial-type diet to ACRBs reduced their FCR some but not to the point of a commercial broiler and did not increase growth or body weight (Havenstein et al., 1994), which makes them an ideal genetic control strain. In a recent study where ACRB were compared with Ross 308 commercial broilers to identify effects of commercial genetic selection on the corticotropic and thyrotropic axes, it was reported that Ross 308 body weights were significantly greater than those for ACRB beginning during the last week of embryogenesis, and this difference continued throughout juvenile development (Vaccaro et al., 2021). FCR of ACRB was also significantly higher than of Ross 308, reflecting the improved efficiency of

TABLE 3 | Means[1] (±SEM) and ANOVA *p*-values of the age main effect for somatotropic gene expression in embryonic male ACRB and Ross 308 broilers.

	e10	e12	e14	e16	e18	*p*-value
IGFs and Receptors						
Liver (%)[2]						
GHR	45.5 ± 6.1^{c}	60.0 ± 7.0^{bc}	85.5 ± 13.6^{ab}	88.68 ± 8.3^{ab}	100 ± 8.8^{a}	0.0023
IGF1	51.3 ± 12.4	48.12 ± 10.2	100 ± 50.7	31.84 ± 8.4	29.59 ± 8.9	0.4101
Muscle (%)[2]						
GHR	56.5 ± 8.0^{b}	82.66 ± 8.3^{a}	100 ± 15.3^{a}	92.8 ± 5.8^{a}	81.3 ± 8.9^{a}	0.0243
IGF1	71.8 ± 12.7^{ab}	100 ± 8.9^{a}	85.9 ± 14.6^{ab}	54.1 ± 4.9^{bc}	34.9 ± 2.3^{c}	0.0006
IGF2	96.9 ± 15.9	86.2 ± 24.8	57.2 ± 13.8	96.2 ± 19.8	100 ± 19.3	0.4383
IGF1R	77.9 ± 8.9^{abc}	81.6 ± 6.9^{ab}	100 ± 15.9^{a}	65.6 ± 12.9^{bc}	54.5 ± 10.8^{c}	0.0446
IGFBPs						
Liver (%)[2]						
IGFBP2	15.3 ± 2.1^{c}	24.9 ± 4.7^{c}	67.6 ± 15.5^{b}	100 ± 27.9^{ab}	98.0 ± 15.1^{a}	<0.0001
IGFBP4	69.1 ± 11.0	72.3 ± 14.4	100 ± 26.3	51.9 ± 7.0	69.4 ± 13.8	0.5605
IGFBP5	68.2 ± 8.0^{b}	80.2 ± 9.3^{ab}	100 ± 7.5^{a}	75.8 ± 6.5^{b}	70.3 ± 4.9^{b}	0.0271
IGFBP7	37.5 ± 4.7^{c}	56.3 ± 8.2^{b}	86.5 ± 15.5^{a}	84.5 ± 13.7^{a}	100 ± 7.9^{a}	<0.0001
Muscle (%)[2]						
IGFBP1	100 ± 11.4^{a}	58.9 ± 11.2^{ab}	44.2 ± 26.0^{bc}	36.7 ± 5.4^{bc}	24.2 ± 4.6^{c}	0.0068
IGFBP2	78.8 ± 5.7	64.5 ± 7.4	64.9 ± 7.20	100 ± 11.2	74.3 ± 10.6	0.0808
IGFBP3	90.2 ± 12.0	100 ± 6.7	85.1 ± 10.7	89.2 ± 10.6	81.9 ± 8.5	0.6923
IGFBP4	100 ± 16.9	76.4 ± 16.4	89.4 ± 26.8	75.2 ± 7.8	48.1 ± 8.6	0.0866
IGFBP5	100 ± 12.1	83.8 ± 9.3	82.9 ± 20.4	71.9 ± 6.9	73.6 ± 13.7	0.4908
IGFBP7	40.6 ± 8.8^{c}	46.1 ± 3.3^{c}	60.7 ± 11.2^{bc}	78.8 ± 7.5^{ab}	100 ± 15.1^{a}	0.0009

[1]*Means are only presented for data where a significant line-by-age interaction was not present and were calculated across both lines at each embryonic day (e).*
[2]*Data within each gene are expressed relative to the age with the highest mRNA level (equal to 100%).*
[a,b,c]*Values that do not share a common letter are significantly different (*$p \leq 0.05$*).*

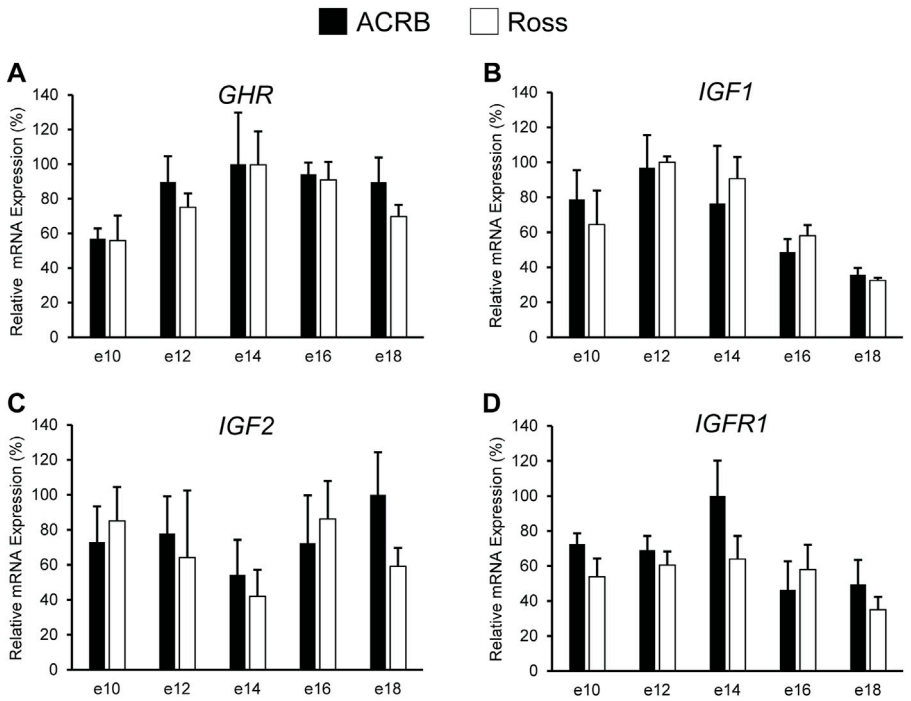

FIGURE 2 | Relative mRNA expression of **(A)** *GHR*, **(B)** *IGF1*, **(C)** *IGF2*, and **(D)** *IGFR1* in breast muscle on embryonic days e 10, 12, 14, 16, and 18 in legacy ACRB and modern Ross 308 male broilers. Relative expression levels were measured using RT-qPCR and normalized to *18S* RNA ($n = 4$ replicate birds per line at each age). The data (mean + SEM) are expressed relative to the line and age with the highest expression level (equivalent to 100%). No significant line-by-age interactions were observed for **(A)** *GHR* ($p = 0.9321$), **(B)** *IGF1* ($p = 0.5901$), **(C)** *IGF2* ($p = 0.6246$), or **(D)** *IGF1R* ($p = 0.4752$), and main effect means of line and age all genes are presented in **Tables 2**, **3**, respectively.

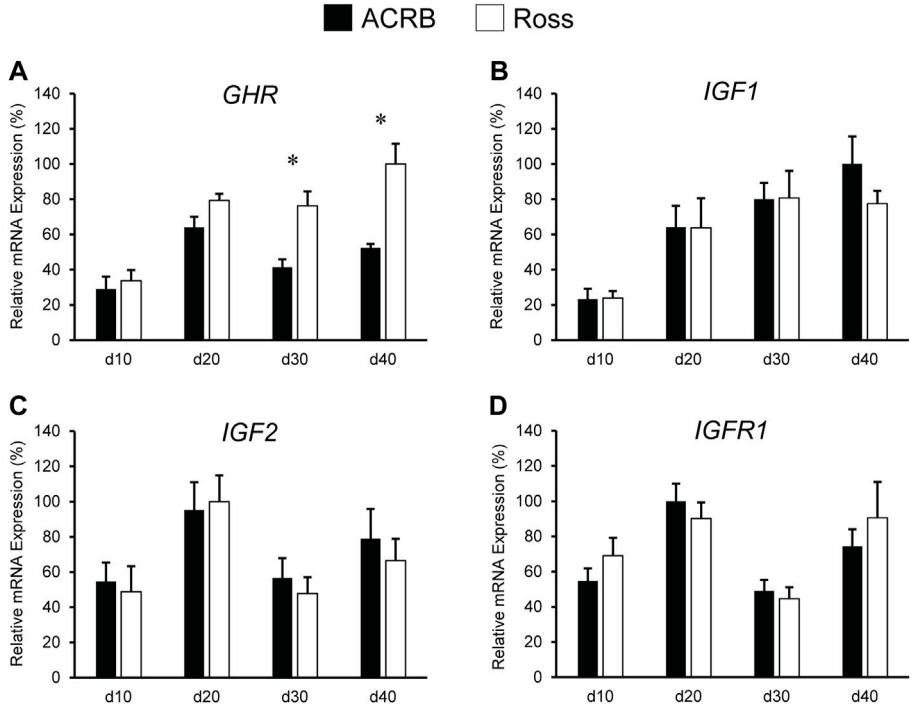

FIGURE 3 | Relative mRNA expression of **(A)** *GHR*, **(B)** *IGF1*, **(C)** *IGF2*, and **(D)** *IGFR1* in liver on post-hatch days d 10, 20, 30, and 40 in legacy ACRB and modern Ross 308 male broilers. Relative expression levels were measured using RT-qPCR and normalized to *GAPDH* mRNA ($n = 8$ replicate birds per line at each age). The data (mean + SEM) are expressed relative to the line and age with the highest expression level (equivalent to 100%). A significant line-by-age interaction was detected for **(A)** *GHR* ($p = 0.0446$), and the presence of an asterisk (*) indicates a significant difference in expression between the lines at the indicated age. No significant line-by-age interactions were detected for **(B)** *IGF1* ($p = 0.6890$), **(C)** *IGF2* ($p = 0.8688$), or **(D)** *IGFR1* ($p = 0.7405$), and main effect means of line and age for these genes are presented in **Tables 4**, **5**, respectively.

feed nutrient use in commercial modern broilers. Together, these results suggest that physiological changes induced by commercial genetic selection begin to appear mid-embryogenesis. Given the conservation of the somatotropic axis across species and its importance in mediating tissue growth and development in mammals, it is likely that IGFs, their receptors, and IGFBPs are linked to improvements in commercial modern broiler growth efficiency. Therefore, the objective of this study was to determine the effect of commercial genetic selection on mRNA expression and circulating hormone concentrations within the somatotropic axis by comparing these parameters between Ross 308 and legacy ACRB broiler lines.

MATERIALS AND METHODS

Animals and Tissue Collection

Samples used for this study were collected from male ACRB and Ross 308 broilers during the same two experiments described in a previously published study (Vaccaro et al., 2021). The first experiment was conducted during embryogenesis, and the second was conducted during post-hatch juvenile development. All experimental procedures using animals were conducted in accordance with University of Georgia and University of Maryland Institutional Animal Care and Use guidelines.

In the first experiment, skin, liver, and breast muscle (*p. major*) were collected from 12 embryos of each line on embryonic days (e) 10, 12, 14, 16, and 18, with e0 being the day eggs were placed in the incubator. Eggs from both lines were co-incubated in the same incubator under identical conditions. The sex of each embryo was determined by PCR analysis of the sexually dimorphic chromo-helicase-DNA binding protein (Fridolfsson and Ellegren, 1999) using genomic DNA extracted from skin tissue, as previously described (Vaccaro et al., 2021). Liver and breast muscle from four male embryos of each line at each age ($n = 4$) were used for gene expression analysis as described below.

In the second experiment, males of each line were raised in separate floor pens ($n = 8$ floor pens per line) within one room, so that environmental conditions were identical. Both lines had free access to water and the same three-phase modern commercial-type diet as previously described (Vaccaro et al., 2021). Liver, breast muscle (*P. major*), and plasma were collected from one bird per pen ($n = 8$ per line) on post-hatch days (d) 10, 20, 30, and 40 as previously described (Vaccaro et al., 2021). Briefly, liver and breast muscle were immediately snap-frozen in liquid nitrogen and stored at −80°C prior to being used for gene expression analysis. Whole blood was collected into syringes coated with lithium heparin and stored on ice for no longer than 60 min prior

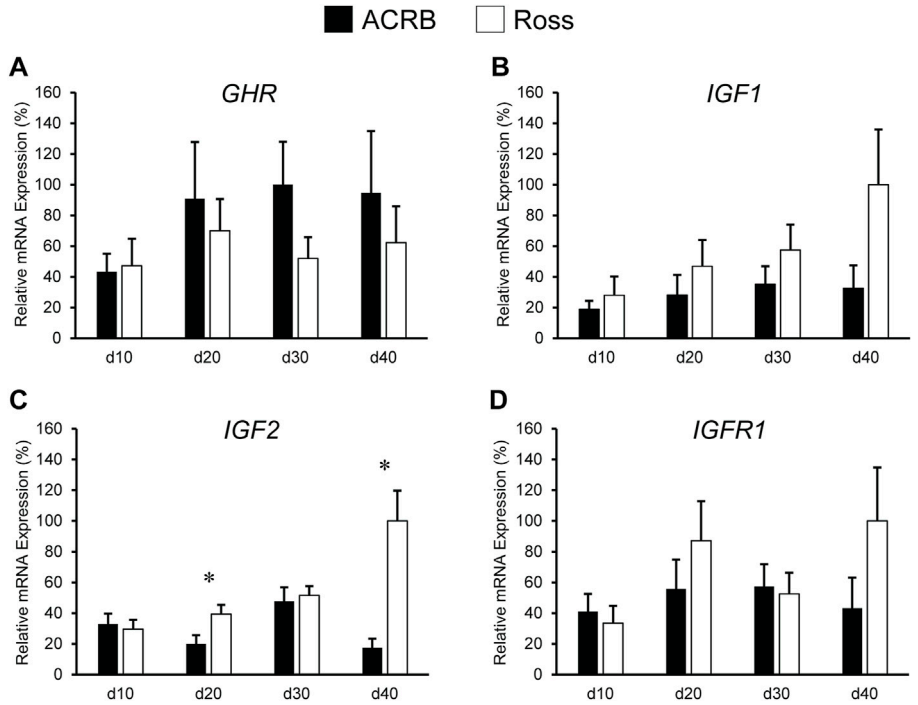

FIGURE 4 | Relative mRNA expression of **(A)** *GHR*, **(B)** *IGF1*, **(C)** *IGF2*, and **(D)** *IGFR1* in breast muscle on post-hatch days d 10, 20, 30, and 40 in legacy ACRB and modern Ross 308 male broilers. Relative expression levels were measured using RT-qPCR and normalized to *18S* RNA (n = 8 replicate birds per line at each age). The data (mean + SEM) are expressed relative to the line and age with the highest expression level (equivalent to 100%). No significant line-by-age interactions were detected for **(A)** *GHR* (p = 0.5112), **(B)** *IGF1* (p = 0.1424), or **(D)** *IGF1R* (p = 0.1258), and main effect means of line and age for these genes are presented in **Tables 4**, **5**, respectively. A significant line-by-age interaction was detected for **(C)** *IGF2* (p = 0.0111), and the presence of an asterisk (*) indicates a significant difference in expression between the lines at the indicated age.

to isolation of plasma by centrifugation at 1,500x g and 4°C for 10 min. Plasma was stored at −20°C prior to use for evaluation of circulating hormone levels, as described below.

Reverse Transcription-Quantitative PCR (RT-qPCR)

Total RNA was isolated from liver and breast muscle using RNeasy Mini kits (Qiagen) with modifications for lipid-rich or fibrous tissues, respectively, and analyzed by RT-qPCR as previously described (Vaccaro et al., 2021). Briefly, total RNA (1 μg) was reverse transcribed with random hexamer primers (ThermoFisher Scientific, Waltham, MA, United States) and M-MuLV reverse transcriptase (New England Biolabs, Ipswich, MA, United States). Resulting cDNA was amplified by qPCR using intron-spanning primers (**Table 1**; Integrated DNA Technologies, Coralville, IA, United States) designed with Primer Express software (Applied Biosystems, Foster City, CA, United States). Serial dilutions of pooled liver and muscle cDNA were analyzed by qPCR to determine amplification efficiency for each primer pair, which was calculated using the following equation: efficiency = $[10^{(-1/\text{slope})}-1]$ (Livak and Schmittgen, 2001; Rutledge and Stewart, 2008).

Transcripts in liver were normalized to glyceraldehyde 3-phosphate dehydrogenase (*GAPDH*), and those in muscle were normalized to 18s ribosomal rRNA (18s rRNA). The equation $(2^{\Delta Ct})_{target}/(2^{\Delta Ct})_{GAPDH\ or\ 18s}$, where $\Delta Ct = Ct_{no\ RT}-CT_{sample}$, was used to transform and normalize data as previously described (Ellestad et al., 2009; Ellestad and Porter, 2013; Ellestad et al., 2015; Payne et al., 2019; Vaccaro et al., 2021). Each transcript's line-by-age interactive data are expressed relative to the line and age with the highest mRNA level, and main effect data are expressed relative to the line or age with the highest mRNA level. As a result, the line-by-age, line, or age value with the highest expression level was 100% in all cases.

Insulin-Like Growth Factor Enzyme-Linked Immunosorbent Assays

Samples were analyzed in duplicate on a VICTOR3 Multilabel Plate Reader (Perkin Elmer, Waltham, MA, United States) using commercially available competitive-binding ELISAs (Cusabio, Houston, TX, United States) for IGF1 and IGF2, which have sensitivity limits of 125 and 62.5 pg/ml, respectively. ELISAs were performed according to manufacturer's instructions with the modification that plates were incubated for 18 h at 4°C instead of 60 min at 37°C after adding the standards or samples and biotinylated IGF. Intra and inter-assay coefficient of variations (CVs) for IGF1 ELISAs were determined to be 4.023 and 6.479, respectively. Intra and inter-assay coefficient of variations (CVs) for IGF2 ELISAs were determined to be 10.0 and 34.6, respectively.

TABLE 4 | Means[1] (±SEM) of the line main effect for gene expression and circulating hormones in post-hatch male broilers.

	ACRB	Ross 308	*p*-value
IGFs and Receptors			
Liver (%)[2]			
IGF1	100 ± 11.1	92.0 ± 10.5	0.6546
IGF2	100 ± 10.2	92.3 ± 10.1	0.4426
IGF1R	94.4 ± 7.3	100 ± 9.4	0.826
Muscle (%)[2]			
GHR	100 ± 18.2[a]	71.4 ± 11.4[b]	0.0447
IGF1	48.4 ± 9.4[b]	100 ± 20.2[a]	0.0009
IGF1R	71.1 ± 11.2	100 ± 17.8	0.242
IGFBPs			
Liver (%)[2]			
IGFBP2	100 ± 32.9[a]	67.9 ± 18.3[b]	0.0073
IGFBP3	83.4 ± 10.8[b]	100 ± 13.3[a]	0.0444
IGFBP4	92.8 ± 11.8	100 ± 15.7	0.9186
IGFBP5	69.0 ± 5.2[b]	100 ± 12.9[a]	0.0234
IGFBP7	66.3 ± 8.5[b]	100 ± 16.5[a]	0.0027
Muscle (%)[2]			
IGFBP1	100 ± 27.5	97.2 ± 38.7	0.3532
IGFBP3	100 ± 10.1[a]	70.08 ± 7.4[b]	0.0041
IGFBP4	54.1 ± 10.19[b]	100 ± 18.05[a]	0.0333
IGFBP5	60.6 ± 5.5[b]	100 ± 14.3[a]	0.0125
IGFBP7	75.2 ± 8.7[b]	100 ± 10.6[a]	0.0308
Hormones			
IGF1 (pg/ml)[3]	776.7 ± 21.5	796.7 ± 24.4	0.5014
IGF2 (pg/ml)[3]	190.9 ± 15.9	167.7 ± 19.8	0.7571

[1]*Means are only presented for data where a significant line-by-age interaction was not present and were calculated between post-hatch day 10 through 40 for each line.*
[2]*Data within each gene are expressed relative to the line with the highest mRNA, level (100%).*
[3]*Circulating hormone data are expressed as absolute concentration.*
[a,b]*Values that do not share a common letter are significantly different (p ≤ 0.05).*

Statistical Analysis

Data were analyzed with a two-way analysis of variance (ANOVA) using the Fit Model Procedure of JMP Pro 14 (SAS Institute, Cary, NC, United States), with relative RT-qPCR data being $\log_2$-transormed prior to analysis. When ANOVA indicated a significant line-by-age effect, line effect, or age effect ($p \leq 0.05$), *post hoc* multiple means comparisons were performed using the test of least significant difference. Main effect means were only calculated and analyzed when there was not a significant interaction ($p > 0.05$).

RESULTS

Insulin-Like Growth Factor and Hormone Receptor Expression During Embryonic Development

Levels of mRNA for IGFs and somatotropic hormone receptors in embryonic ACRB and Ross liver are shown in **Figure 1**. Expression of *GHR* did not exhibit a significant line-by-age effect in embryonic liver (**Figure 1A**; $p > 0.05$), but a near significant main effect of line was observed in which Ross 308 had elevated expression as compared to ACRB (**Table 2**; $p = 0.0640$). A significant main effect of age for *GHR* was also detected in liver, with levels significantly and steadily increasing between e10 and e18 (**Table 3**; $p \leq 0.05$). No significant differences in expression between lines or at different ages were detected for liver *IGF1* during embryogenesis (**Figure 1B**; **Tables 2**, **3**; $p > 0.05$). Significant line-by-age interactive effects were detected for *IGF2* and *IGFR1* in liver, however. *IGF2* was approximately 2-fold greater in Ross on e10 and e14, but a transient decrease in expression in Ross on e12 with a concomitant increase in ACRB expression resulted in reduced levels of Ross *IGF2* at this age (**Figure 1C**; $p \leq 0.05$). A similar though less prominent expression pattern was observed for liver *IGFR1*, with levels in ACRB being approximately two-fold greater than Ross on e12 (**Figure 1D**; $p \leq 0.05$).

As shown in **Figure 2**, no significant line-by-age interactions were detected for any of these genes in embryonic breast muscle (**Figures 2A–D**; $p > 0.05$). However, *GHR*, *IGF1*, and *IGFR1* exhibited age main effects in this tissue (**Table 3**; $p \leq 0.05$). Expression of *GHR* increased in both lines between e10 and e14 and remained elevated thereafter (**Table 3**; $p \leq 0.05$). Expression of *IGF1* began to significantly decrease at e18 (**Table 3**; $p \leq 0.05$). Expression of *IGFR1* dropped between e14 and 16 and remained low on e18 (**Table 3**; $p \leq 0.05$). No main effect of age for *IGF2* was observed in breast muscle (**Table 3**; $p > 0.05$).

Insulin-Like Growth Factor and Hormone Receptor Expression During Post-Hatch Development

Expression levels of somatotropic hormones and receptors in ACRB and Ross post-hatch liver are presented in **Figure 3**. Only *GHR* exhibited a significant line-by-age interaction, in which expression was two-fold greater in Ross liver at both d30 and d40 (**Figure 3A**; $p \leq 0.05$). No line-by-age interactions or main effects of line were observed *IGF1*, *IGF2*, or *IGFR1* (**Figures 3B–D**; $p > 0.05$), but they exhibited main age effects (**Tables 2**, **3**; $p \leq 0.05$). Expression of *IGF1* in both Ross and ACRB liver increased steadily between d10 and d30 and remained elevated through d40 (**Table 3**; $p \leq 0.05$), whereas *IGF2* increased between d10 and d20 before decreasing on d30 and returning to intermediate levels at d40 (**Table 3**; $p \leq 0.05$). Hepatic expression of *IGFR1* exhibited a similar pattern to *IGF2* and went up between d10 and d20, was reduced on d30, and increased again on d40 (**Table 3**; $p \leq 0.05$).

Levels of these genes in post-hatch breast muscle are shown in **Figure 4**. No significant interactive effects were detected for *GHR* and *IGF1* (**Figures 4A,B**; $p > 0.05$), but each exhibited main line effects. Expression was higher overall in ACRB breast muscle for *GHR*, whereas *IGF1* mRNA levels were greater in Ross breast muscle (**Table 4**, $p \leq 0.05$). *GHR* also displayed a main effect of age, increasing from d10 to d20 and remaining stable through d40 in this tissue (**Table 4**; $p \leq 0.05$). Additionally, *IGF1* approached significance for a main effect of age, where breast muscle expression increased between d10 and d40 (**Table 5**; $p = 0.0531$). *IGF2* did demonstrate a significant line-by-age interactive effect, in which expression was two-fold greater in Ross breast muscle on d20 and increased to five-fold greater on d40 (**Figure 4C**; $p \leq 0.05$). A significant interactive effect was not

TABLE 5 | Means[1] (±SEM) of the age main effect for gene expression and circulating hormones in post-hatch male broilers.

	d10	d20	d30	d40	*p*-value
IGFs and Receptors					
Liver (%)[2]					
IGF1	26.6 ± 3.8^{c}	72.0 ± 11.3^{b}	90.6 ± 9.8^{ab}	100 ± 9.9^{a}	<0.0001
IGF2	52.9 ± 9.0^{c}	100 ± 10.7^{a}	53.5 ± 7.3^{bc}	74.5 ± 10.5^{ab}	0.007
IGF1R	65.1 ± 6.6^{bc}	100 ± 6.9^{a}	49.3 ± 4.6^{c}	86.7 ± 11.7^{ab}	0.0002
Muscle (%)[2]					
GHR	56.6 ± 12.4^{b}	100 ± 24.8^{a}	95.2 ± 20.3^{a}	97.1 ± 27.7^{ab}	0.0260
IGF1	33.7 ± 9.3	55.6 ± 15.9	67.6 ± 14.9	100 ± 31.6	0.0531
IGF1R	51.0 ± 10.7	98.6 ± 22.2	74.8 ± 13.1	100 ± 29.2	0.0683
IGFBPs					
Liver (%)[2]					
IGFBP2	3.4 ± 1.2^{c}	100 ± 20.6^{a}	10.4 ± 1.5^{b}	14.1 ± 4.1^{b}	<0.0001
IGFBP3	56.7 ± 11.6^{b}	100 ± 15.6^{a}	57.9 ± 8.5^{b}	84.2 ± 16.6^{a}	<0.0001
IGFBP4	18.1 ± 1.7^{b}	92.1 ± 9.9^{a}	86.9 ± 16.0^{a}	100 ± 17.3^{a}	<0.0001
IGFBP5	45.3 ± 6.6^{c}	100 ± 7.4^{a}	66.2 ± 4.24^{b}	72.6 ± 19.9^{b}	0.0006
IGFBP7	50.3 ± 13.3^{c}	100 ± 20.0^{a}	56.9 ± 6.3^{b}	70.5 ± 18.2^{b}	0.0393
Muscle (%)[2]					
IGFBP1	19.4 ± 6.5^{c}	100 ± 41.9^{a}	49.4 ± 22.3^{ab}	42.4 ± 13.4^{b}	0.0011
IGFBP3	68.4 ± 8.9	71.8 ± 9.3	100 ± 11.6	97.4 ± 18.5	0.1052
IGFBP4	19.4 ± 4.4^{c}	30.4 ± 5.1^{b}	75.7 ± 16.1^{a}	100 ± 21.4^{a}	<0.0001
IGFBP5	36.5 ± 3.6^{b}	48.6 ± 3.4^{b}	79.1 ± 9.5^{a}	100 ± 21.5^{a}	0.0003
IGFBP7	55.2 ± 6.5^{b}	80.5 ± 12.6^{a}	100 ± 13.8^{a}	92.2 ± 15.9^{a}	0.0029
Hormones					
IGF1 (pg/ml)[3]	698.3 ± 26.1^{b}	798.3 ± 42.7^{a}	811.3 ± 18.7^{a}	839.8 ± 26.3^{a}	0.0096
IGF2 (pg/ml)[3]	145.5 ± 13.8^{b}	247.9 ± 27.5^{a}	164.8 ± 21.5^{b}	139.2 ± 23.6^{b}	0.0042

[1]*Means are only presented for data where a significant line-by-age interaction was not present and were calculated across both lines at each post-hatch day (d).*
[2]*Data within each gene are expressed relative to the age with the highest mRNA, level (100%).*
[3]*Circulating hormone data are expressed as absolute concentration.*
[a,b,c]*Values that do not share a common letter are significantly different (p ≤ 0.05).*

observed for *IGFR1* mRNA in breast muscle (**Figure 4D**; $p > 0.05$), but it approached significance for a main effect of age. Expression increased from d10 to d20, decreased at d30, and returned to d20 levels on d40 (**Table 5**; $p = 0.0683$).

Circulating Insulin-Like Growth Factors in Post-Hatch Plasma

Figure 5 shows circulating concentrations of IGF1 and IGF2 in post-hatch broilers, which were determined because of their ability to regulate overall body growth and induce cellular growth and proliferation in breast muscle. There was no significant line-by-age effect for IGF1 (**Figure 5A**; $p > 0.05$), although there was a main effect of age. Levels of IGF1 increased between d10 and d20 and remained elevated through d40 (**Table 5**; $p \leq 0.05$). Circulating IGF2 approached significance for a line-by-age effect, in which IGF2 was greater in Ross at d10 and d20 but higher in ACRB on d40 (**Figure 5B**; $p = 0.0647$). IGF2 also exhibited a main effect of age, with circulating levels peaking on d20 in both lines (**Table 5**; $p \leq 0.05$).

Insulin-Like Growth Factor-Binding Protein Expression During Embryonic Development

The liver is a major producer of IGFBPs (Baxter, 1991), and this protein family is essential for controlling IGF signaling, thus regulates IGF effects on myogenic growth (Ewton et al., 1998; Kamanga-Sollo et al., 2005). Relative IGFBP expression levels measured in embryonic ACRB and Ross liver are presented in **Figure 6**. *IGFBP1* exhibited a significant line-by-age interaction, where ACRB expression at e12 was 4-fold greater than Ross but the opposite was observed at e16 when Ross expression was 2.5-fold greater than ACRB (**Figure 6A**; $p \leq 0.05$). *IGFBP2* did not exhibit an interactive effect (**Figure 6B**; $p > 0.05$), but expression in liver was low from e10 to e12 and increased steadily thereafter through e18, indicating a main age effect (**Table 3**; $p \leq 0.05$). *IGFBP3* exhibited a significant interactive effect and expression was approximately 2-fold greater in Ross liver than in ACRB liver on both e14 and e16 (**Figure 6C**; $p \leq 0.05$). No interactive effects or main effects of line or age were observed for *IGFBP4* in this tissue (**Figure 6D**; **Tables 2**, **3**; $p \leq 0.05$). *IGFBP5* also did not have a significant interactive effect (**Figure 6E**; $p > 0.05$), but it approached significance for a main effect of line where hepatic ACRB expression was greater than that in Ross (**Table 2**; $p = 0.094$). Age was also significant for liver *IGFBP5* expression, increasing between e10 and e14 and decreasing on e16 and e18 (**Table 5**; $p \leq 0.05$). *IGFBP7* displayed a nearly significant line-by-age interaction in embryonic liver (**Figure 6F**; $p = 0.0697$) and was greater in Ross than ACRB on e14. Additionally, its expression increased from e10 to e14, denoting a main effect of age (**Table 3**; $p \leq 0.05$).

The *IGFBPs* did not display any significant interactive effects in embryonic breast muscle (**Figure 7**; $p > 0.05$). *IGFBP1* and *IGFBP7* exhibited a main effect of age, with expression decreasing or increasing between e10 to e18, respectively (**Table 3**; $p \leq 0.05$). No significant main effects of line or age were observed for

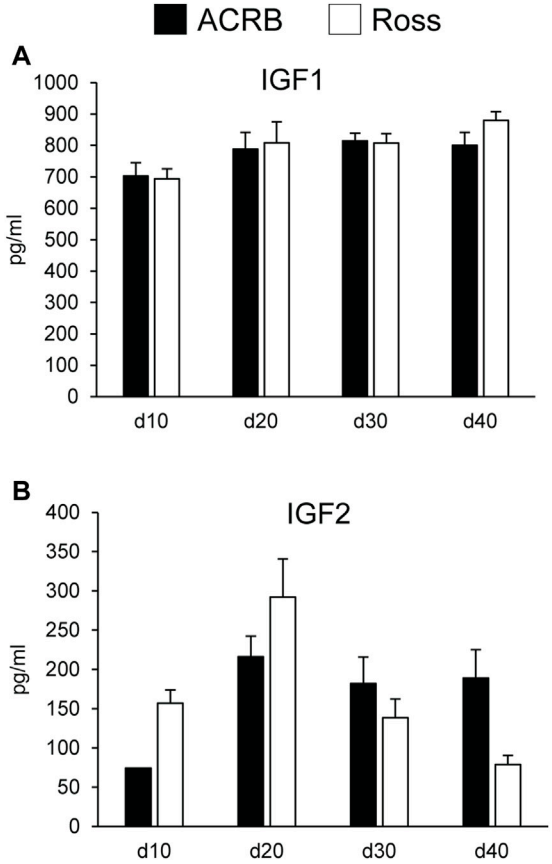

FIGURE 5 | Circulating **(A)** IGF1 and **(B)** IGF2 in legacy ACRB and modern Ross 308 male broilers on post-hatch days d 10, 20, 30, and 40 as determined by ELISA (n = 8 replicate birds per line at each age). No significant line-by-age interactions were observed for **(A)** IGF1 (p = 0.7065) or **(B)** IGF2 (p = 0.0647), and main effect means of line and age are presented in **Tables 4**, **5**, respectively.

IGFBP2, *IGFBP3*, or *IGFBP5* (**Tables 2**, **3**; $p > 0.05$). A line main effect was detected for breast muscle *IGFBP4*, in which levels in Ross were significantly lower (**Table 2**; $p \leq 0.05$).

Insulin-Like Growth Factor-Binding Protein Expression During Post-Hatch Development

IGFBP expression in post-hatch liver is shown in **Figure 8**. Only *IGFBP1* exhibited a significant line-by-age interaction (**Figure 8A**; $p \leq 0.05$), whereas the remaining IGFBPs did not (**Figures 8B–F**; $p > 0.05$). Levels of ACRB *IGFBP1* mRNA were 4-fold higher than Ross at d20 (**Figure 7A**; $p \leq 0.05$) and numerically lower than Ross on d10 and d30. Main effects of line and age were observed for *IGFBP2* and *IGFBP3*, whereas *IGFBP4* only had a main effect of age. Liver expression of *IGFBP2* was greater in ACRB, while expression of *IGFBP3* was greater in Ross (**Table 4**; $p \leq 0.05$). *IGFBP2* was 10- to 30-fold higher on d20 than other age, and *IGFBP3* expression on d20 and d40 was almost twice that of d10 and d30 (**Table 5**; $p \leq 0.05$). After a 5-fold increase in expression between d10 and d20, *IGFBP4* remained high through d40 (**Table 5**; $p \leq 0.05$). *IGFBP5* and *IGFBP7* also exhibited main effects of line and age. Expression of both genes were significantly greater in Ross liver (**Table 4**; $p \leq 0.05$), and their expression increased approximately 2-fold between d10 and d20 and then decreased to intermediate levels of d30 and d40 (**Table 5**; $p \leq 0.05$).

Figure 9 illustrates IGFBP mRNA levels in post-hatch breast muscle. *IGFBP1* did not have a significant interactive effect (**Figure 9A**; $p > 0.05$) or line main effect (**Table 4**; $p > 0.05$) but did exhibit a main effect of age. Expression increased approximately 5-fold between d10 and d20 and was reduced about 2-fold at later ages (**Table 5**; $p \leq 0.05$). *IGFBP2* displayed a significant line-by-age interaction in post-hatch breast muscle and was higher in Ross than ACRB at d40 (**Figure 9B**; $p \leq 0.05$). No significant interactive effects were determined for *IGFBP3*, *IGFBP4*, *IGFBP5*, or *IGFBP7* (**Figures 9C–F**; $p > 0.05$), but each demonstrated a main effect of line (**Table 4**; $p \leq 0.05$). Apart from *IGFBP3*, which was higher in ACRB breast muscle, expression was greater in Ross (**Table 4**; $p \leq 0.05$). Additionally, *IGFBP4*, *IGFBP5*, and *IGFBP7* expression differed significantly across ages. *IGFBP4* expression increased between d10 and d30 and remained high on d40 (**Table 5**; $p \leq 0.05$). Levels of *IGFBP5* mRNA were lower at d10 and d20 than d30 and d40 (**Table 5**; $p \leq 0.05$). Expression of *IGFBP7* increased significantly after d10 and remained high thereafter (**Table 5**; $p \leq 0.05$).

DISCUSSION

The highly conserved nature of the somatotropic axis in vertebrates implies that it plays an important functional role in the growth and development of birds, though how it contributes to the improvements in growth rate and meat production efficiency made through artificial selection of commercial broilers is still not known. Thus, this study examined if components of the somatotropic axis, including hormones, hormone receptors, and hormone binding proteins, differed between a genetic control line (ACRB) and a modern commercial broiler line (Ross 308) during embryonic and post-hatch development. The results suggest that selection has impacted local IGF signaling in breast muscle more than endocrine action of circulating IGFs, and that IGFBPs play an important role in modulating somatotropic axis activity in a tissue-specific manner to affect growth. Multiple lines of evidence from this study suggest that classical somatotopic axis activity might not play a major role in driving chicken embryonic growth, in large part because embryonic IGF levels are likely not influenced by circulating GH. Pituitary GH in chickens increases during the last half of embryonic development (Porter et al., 1995; Ellestad et al., 2006; Lu et al., 2008; Parkinson et al., 2010; Ellestad et al., 2011), around the time that the birds used in this study began diverging in body weight. It was previously shown that Ross embryos were significantly heavier by e14, and body weight differences between the lines continued to increase through d40 (Vaccaro et al., 2021). In liver and breast muscle, neither *GHR* nor *IGF1* expression differed

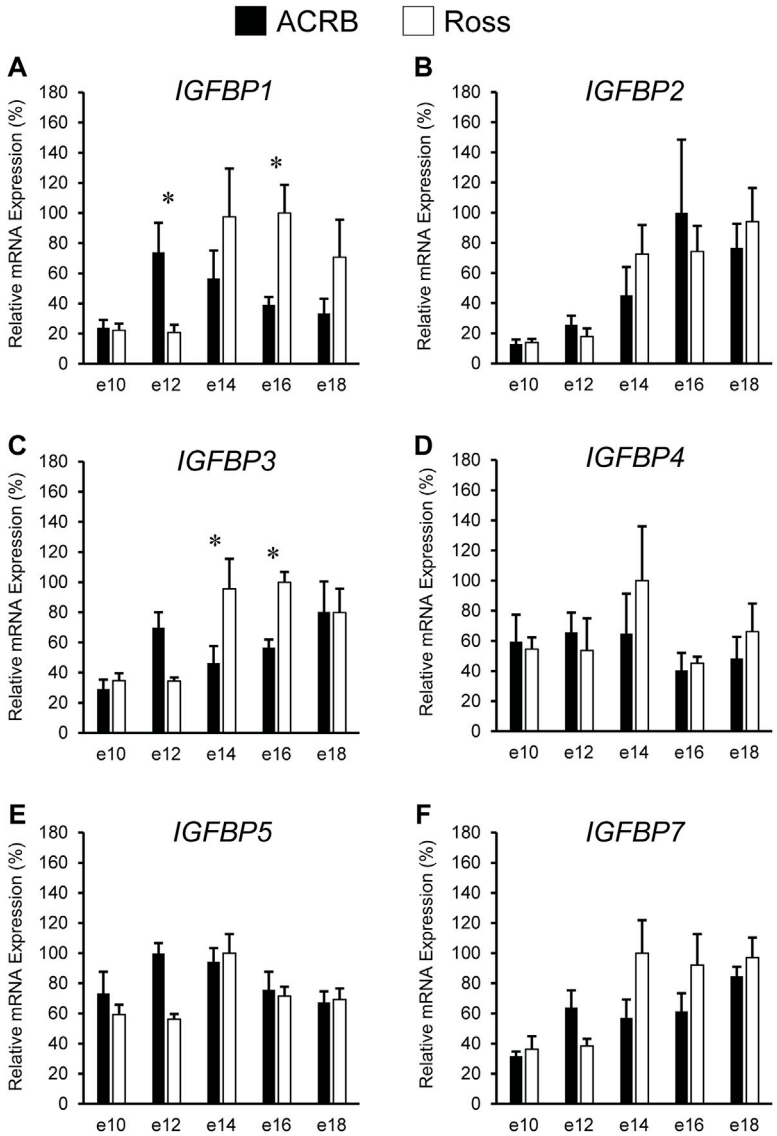

FIGURE 6 | Relative mRNA expression of **(A)** *IGFBP1*, **(B)** *IGFBP2*, **(C)** *IGFBP3*, **(D)** *IGFBP4*, **(E)** *IGFBP5*, and **(F)** *IGFBP7* in liver on embryonic e days 10, 12, 14, 16, and 18 in legacy ACRB and modern Ross 308 male broilers. Relative expression levels were measured using RT-qPCR and normalized to *GAPDH* mRNA (n = 4 replicate birds per line at each age). The data (mean + SEM) are expressed relative to the line and age with the highest expression level (equivalent to 100%). Significant line-by-age interactions were detected for **(A)** *IGFBP1* (p = 0.0038) and **(C)** *IGFBP3* (p = 0.0080), and the presence of an asterisk (*) indicates a significant difference in expression between the lines at the indicated age ($p \leq 0.05$). No significant line-by-age interactions were detected for **(B)** *IGFBP2* (p = 0.3060), **(D)** *IGFBP4* (p = 0.2942), **(E)** *IGFBP5* (p = 0.1055), or **(F)** *IGFBP7* (p = 0.0697), and main effect means of line and age for these genes are presented in **Tables 2**, **3**, respectively.

between the lines during embryonic development, suggesting that GH stimulation of IGF1 is not driving the observed differences in growth. While liver *IGF2* mRNA was higher in Ross 308 on e14, this was not maintained on e16 and 18 despite Ross embryos growing at a faster rate. *GHR* was observed to increase in liver and breast muscle during this period in both lines. However, this increase was accompanied by either no change or inconsistent changes in liver *IGF1*, *IGF2*, and *IGFR1* or a decrease in *IGF1* and *IGFR1* in breast muscle, suggesting that *IGF1*, *IGF2*, and *IGFR1* production are not dependent on GH during late embryonic development. It has been suggested that the somatotropic axis is not fully established until after hatch (Ellestad et al., 2011; Ellestad et al., 2019), and this study provides further evidence that IGF production is likely not GH-dependent in the embryonic somatotropic axis.

Heightened expression of *GHR* mRNA in liver and muscle throughout late embryonic development may be used for GH binding protein (GHBP) synthesis, which is made by cleaving off GHR's extracellular domain (Vleurick et al., 1999; Lau et al., 2007). Human GHBPs form a complex with GH

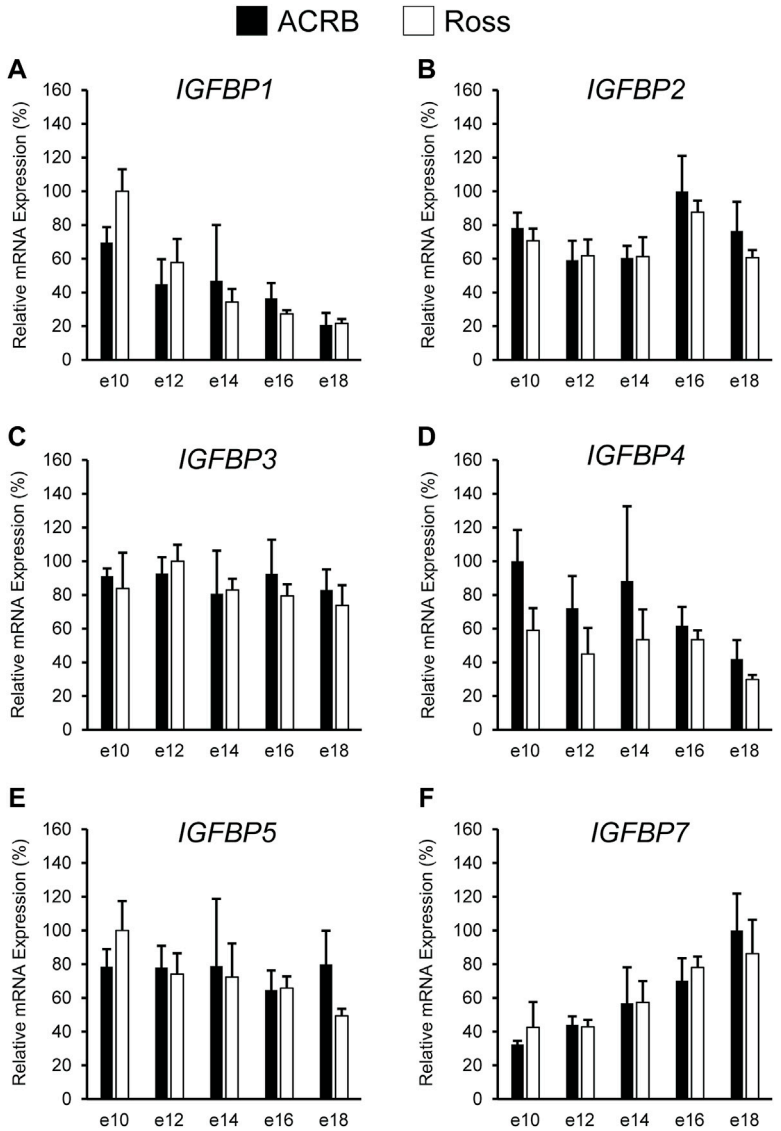

FIGURE 7 | Relative mRNA expression of **(A)** *IGFBP1*, **(B)** *IGFBP2*, **(C)** *IGFBP3*, **(D)** *IGFBP4*, **(E)** *IGFBP5*, and **(F)** *IGFBP7* in breast muscle on embryonic days e 10, 12, 14, 16, and 18 in legacy ACRB and modern Ross 308 male broilers. Relative expression levels were measured using RT-qPCR and normalized to *18S* RNA ($n = 4$ replicate birds per line at each age). The data (mean + SEM) are expressed relative to the line and age with the highest expression level (equivalent to 100%). No significant line-by-age interactions were detected for **(A)** *IGFBP1* ($p = 0.8032$), **(B)** *IGFBP2* ($p = 0.9609$), **(C)** *IGFBP3* ($p = 0.8806$), **(D)** *IGFBP4* ($p = 0.8715$), **(E)** *IGFBP5* ($p = 0.6831$), or **(F)** *IGFBP7* ($p = 0.9480$), and main effect means of line and age for all genes are presented in **Tables 2**, **3**, respectively.

(Baumann et al., 1986), and this may similarly occur in chickens. As pituitary GH production increases late in chicken embryonic development, GHBP might sequester it until target tissues like liver and muscle are responsive to GH after the somatotropic axis is fully established.

It has been reported that pituitary and plasma GH levels are lower in fast-growing birds after hatch (Goddard et al., 1988; Mao et al., 1998; Ellestad et al., 2019). Hepatic *GHR* expression was greater in Ross than ACRB on d30 and d40, and this may reflect a need for increased GH sensitivity to compensate for reduced circulating GH relative to the slower-growing ACRB birds. This could be accomplished by providing additional plasma membrane binding sites for GH and/or by increasing its half-life in plasma *via* GHBP action. Ultimately, however, higher *GHR* in Ross liver does not appear to contribute to increased hepatic *IGF1* or *IGF2* expression or circulating IGF levels in relation to those parameters in to ACRB.

Levels of *IGF1* and *IGF2* mRNA were greater in post-hatch Ross breast muscle as compared to ACRB, suggesting these hormones support the rapid muscle growth observed in commercial modern broilers. Together with the observation

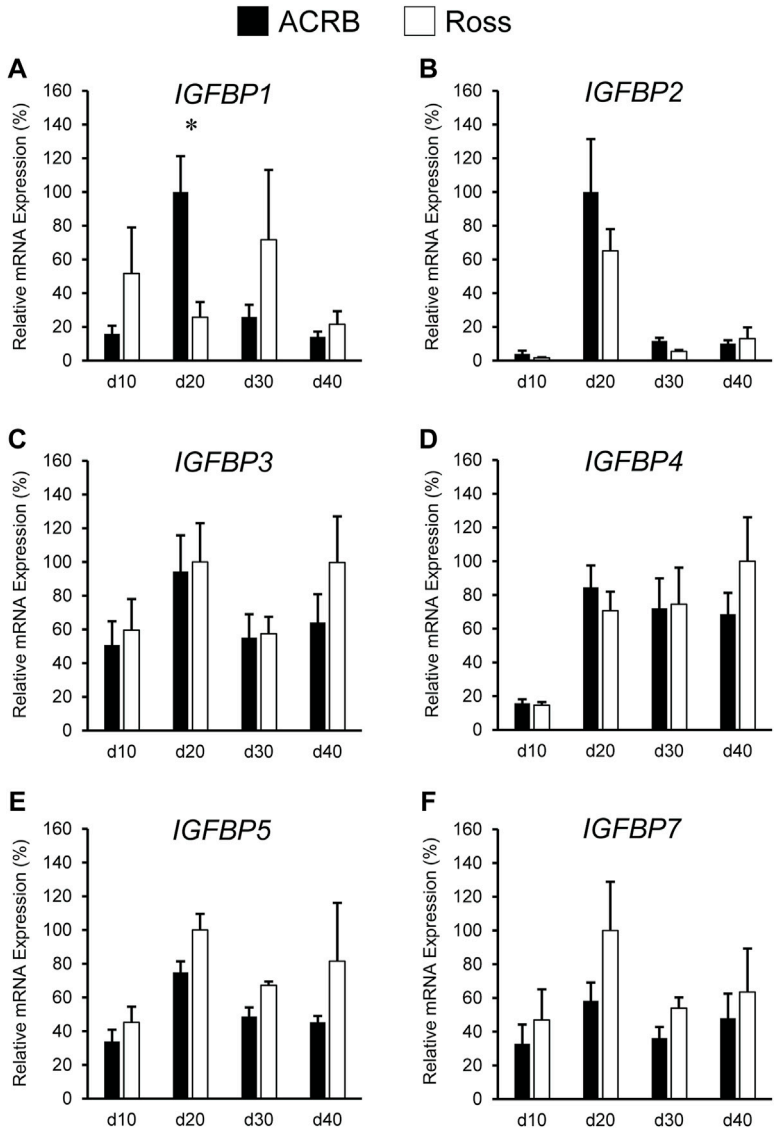

FIGURE 8 | Relative mRNA expression of **(A)** *IGFBP1*, **(B)** *IGFBP2*, **(C)** *IGFBP3*, **(D)** *IGFBP4*, **(E)** *IGFBP5*, and **(F)** *IGFBP7* in liver on post-hatch days d 10, 20, 30, and 40 in legacy ACRB and modern Ross 308 male broilers. Relative expression levels were measured using RT-qPCR and normalized to *GAPDH* mRNA ($n = 8$ replicate birds per line at each age). The data (mean + SEM) are expressed relative to the line and age with the highest expression level (equivalent to 100%). A significant line-by-age interaction was detected for **(A)** *IGFBP1* ($p = 0.0014$), and the presence of an asterisk (*) indicates a significant difference in expression between the lines at the indicated age ($p \leq 0.05$). No significant line-by-age interactions were detected for **(B)** *IGFBP2* ($p = 0.5051$), **(C)** *IGFBP3* ($p = 0.5261$), **(D)** *IGFBP4* ($p = 0.5834$), **(E)** *IGFBP5* ($p = 0.8311$), or **(F)** *IGFBP7* ($p = 0.8716$), and main effect means of line and age for these genes are presented in **Tables 2**, **3**, respectively.

that hepatic and circulating IGFs did not differ between the lines, these results indicate that differential paracrine IGF signaling may impact growth on a tissue-specific basis and contribute to the faster growth and increased muscle accretion in modern birds. Our findings align with the previously proposed theory that IGF signaling in chicken muscle acts in a paracrine fashion, contributing to hypertrophy in a manner similar to mice, rats, and rabbits (Czerwinski et al., 1994; Yang et al., 1997; Duclos et al., 1999).

The IGFBP family mediates IGF effects by enhancing or dampening IGF signaling. This occurs by either increasing IGF-receptor affinity, physically sequestering it to prevent receptor binding, or extending IGF's half-life in circulation. Additionally, many IGFBPs can act independently to induce cellular activity (Kajimoto and Rotwein, 1989; Dewil et al., 1999; Herrington and Carter-Su, 2001; Woelfle et al., 2005; Brooks et al., 2008). Our results suggest that effects of some IGFBPs on broiler growth may differ between embryonic and

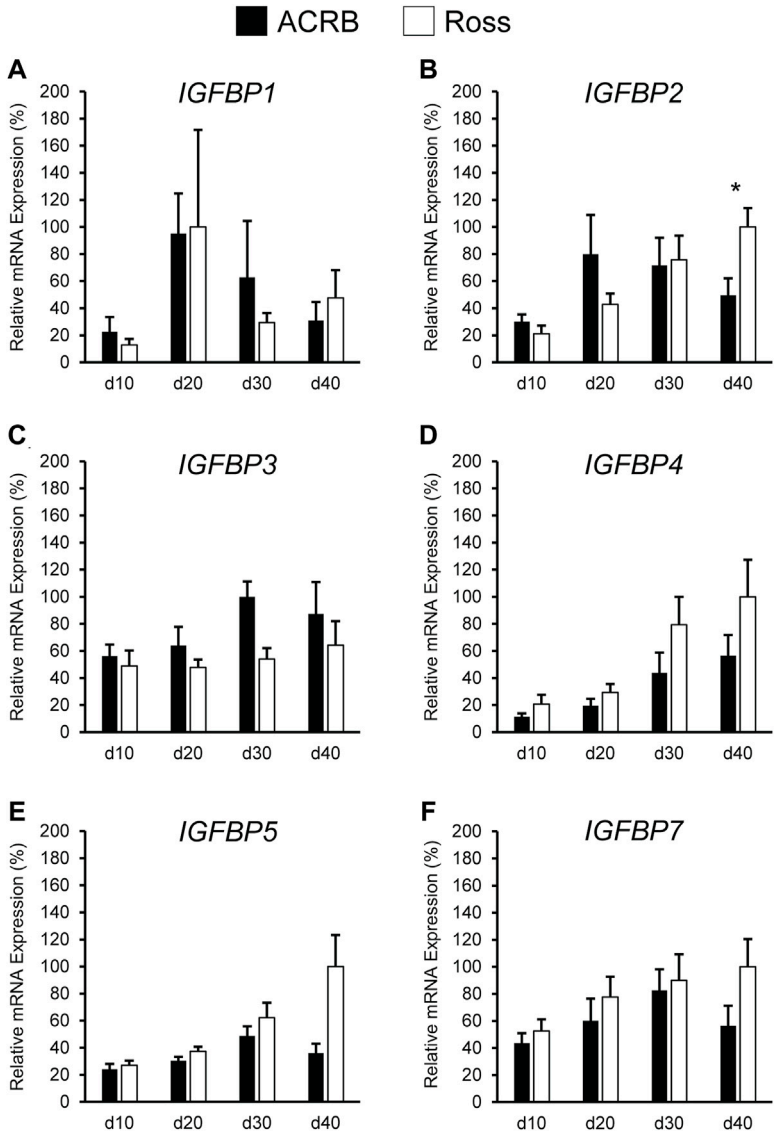

FIGURE 9 | Relative mRNA expression of **(A)** *IGFBP1*, **(B)** *IGFBP2*, **(C)** *IGFBP3*, **(D)** *IGFBP4*, **(E)** *IGFBP5*, and **(F)** *IGFBP7* in breast muscle on post-hatch days d 10, 20, 30, and 40 in legacy ACRB and modern Ross 308 male broilers. Relative expression levels were measured using RT-qPCR and normalized to *18S* RNA ($n = 8$ replicate birds per line at each age). The data (mean + SEM) are expressed relative to the line and age with the highest expression level (equivalent to 100%). A significant line-by-age interaction was identified for **(B)** *IGFBP2* ($p = 0.0022$), and the presence of an asterisk (*) indicates a significant difference in expression between the lines at those ages ($p \leq 0.05$). No significant line-by-age interactions were detected for **(A)** *IGFBP1* ($p = 0.3093$), **(C)** *IGFBP3* ($p = 0.7127$), **(D)** *IGFBP4* ($p = 0.6558$), **(E)** *IGFBP5* ($p = 0.1711$), or **(F)** *IGFBP7* ($p = 0.4647$), and main effect means of line and age for these genes are presented in **Tables 4**, **5**, respectively.

post-hatch development. Expression of *IGFBP1* was greater in ACRB liver at e12 but increased in Ross liver at e16. This correlates with the difference in embryonic body weight between the lines previously observed beginning on e14 (Vaccaro et al., 2021). Here, elevated *IGFBP1* may serve to transport IGF in circulation, as liver *IGF2* in the embryo was greater in Ross at e10 and e14 and could facilitate growth during the last week of embryogenesis. In the liver of post-hatch ACRBs, however, *IGFBP1* was greater at d20, when broilers are growing most rapidly. Work performed in mice indicates *IGFBP1*, when produced in the liver, limits growth (Arany et al., 1994; Gay et al., 1997; Schneider et al., 2000), and it could act similarly in post-hatch chickens. Combined, these results indicate that *IGFBP1* function may change across developmental stages in broilers, in turn altering bird physiology by promoting IGF signaling during embryogenesis and inhibiting it during certain stages of juvenile post-hatch development.

IGFBPs function in an endocrine fashion when secreted into plasma from the liver but a paracrine one when produced locally in peripheral tissues (Allard and Duan, 2018). While levels of *IGFBP4* in liver did not differ between the lines at any stage, differential expression of *IGFBP4* in breast muscle suggests it may

act locally to regulate growth of this tissue and, like *IGFBP1*, may have opposing effects during embryonic and post-hatch developmental stages. In embryonic development, elevated *IGFBP4* mRNA in ACRB breast muscle suggests in acts in an inhibitory manner. This would be consistent with previous reports that *IGFBP4* inhibited growth of mouse skeletal muscle (Jones and Clemmons, 1995; Awede et al., 1999). The effect in breast muscle is likely to be IGF-dependent, because *IGFBP4* inhibits cellular proliferation of myoblasts only in the presence of *IGF1* (Ewton et al., 1998). Since expression of *IGF1* and *IGF2* mRNA in breast muscle did not differ between the lines, it is possible that elevated *IGFBP4* in ACRB reduces IGF signaling in this tissue through its sequestration. On the other hand, during post-hatch development, *IGFBP4* appears to act in a paracrine manner to stimulate breast muscle growth. Levels of *IGFBP4* mRNA in Ross breast muscle post-hatch were almost twice that of ACRB, as were *IGF1* and *IGF2* mRNA. This indicates that, in post-hatch breast muscle, *IGFBP4* could work to perpetuate IGF signaling through increasing the hormones' half-life and/or facilitating their access to *IGFR1*.

IGFBP7 may also regulate skeletal muscle generation in chickens based on results presented here. *IGFBP7* has been shown to limit cell cycle activation in mice, protecting against satellite cell exhaustion to ensure long-term muscle growth (Chen et al., 2020). Increased *IGFBP7* mRNA was observed in Ross broiler breast muscle post-hatch, suggesting it could work in a similar manner to promote muscle growth after hatch by maintaining a healthy satellite cell population. This could contribute to greater breast muscle yield in commercial modern broilers (Schmidt et al., 2009; Collins et al., 2014; Marks et al., 2016) by supporting the satellite cell population and facilitating their differentiation during muscle accretion.

Within the same developmental stage, the effects of a singular IGFBP can also change depending on whether it acts in an endocrine or paracrine manner. Hepatic post-hatch *IGFBP2* was greater in ACRB, aligning with inhibitory *IGFBP2* action observed in zebrafish where it reduced cell proliferation during fasting (Duan et al., 1999). However, *IGFBP2* was greater in post-hatch Ross breast muscle later in development. Since *IGFBP2* has been shown to induce chicken primary myoblast proliferation (Wang et al., 2019), this might mean that endocrine *IGFBP2* released from post-hatch liver inhibits overall body growth but paracrine *IGFBP2* activity in breast muscle facilitates its growth. Data presented here suggest that the inverse may be true for *IGFBP3*, which has a promotive effect on IGF signaling in mammals when acting in an endocrine manner by extending their half-life in the blood (Yamada and Lee, 2009) but may inhibit breast muscle growth by acting in paracrine manner. *IGFBP3* mRNA was greater in Ross embryonic liver at e14 and e16, ages at which they start increasing in size relative to ACRBs. Thus, when synthesized in the liver, *IGFBP3* could extend IGF signaling by maintaining IGFs in the blood of Ross embryos and contribute to their larger size that begins around late embryogenesis. Importantly, elevated hepatic *IGFBP3* in Ross birds continued post-hatch, playing into its established role as a metabolic regulator (Yamada et al., 2010) and suggesting it may also impact body composition and feed efficiency in chickens. Post-hatch *IGFBP3* was reduced in Ross muscle compared to ACRB, suggesting that it may negatively regulate muscle accretion through direct sequestration of IGFs or in another manner. Together, these results are indicative that IGFBPs act in a tissue-specific manner to control IGF signaling through both endocrine and paracrine mechanisms and can have both inhibitory and stimulatory effects depending on their mode of action, as has been observed in mammals.

Like *IGFBP3*, hepatic *IGFBP5* and *IGFBP7* mRNA levels were higher in post-hatch Ross broilers, indicative of an endocrine effect by these proteins that promotes bird growth and muscle accretion. In mice, it was shown that single knockouts for *IGFBP3*, *IGFBP4*, or *IGFBP5* showed little growth impairment, while triple knockout mice were significantly smaller with reduced fat pad accumulation and less skeletal muscle (Ning et al., 2006). This indicates that some IGFBPs exhibit functional redundancy in regulating growth and metabolism in mammals, and a similar phenomenon might exist in birds.

To summarize, we found that expression levels of select somatotropic genes differed between male legacy and commercial modern broilers. Although there were no differences in circulating IGFs, elevated *IGF1* and *IGF2* in post-hatch Ross muscle suggests that paracrine IGF signaling contributes to the increased breast muscle size of commercial modern broilers. Control of IGF signaling by IGFBPs likely also differs between commercial modern and legacy broilers and plays a role in regulating chicken growth. It was observed that select IGFBPs appear to play distinct, and sometimes opposing. growth-promoting or growth-inhibiting roles in a developmental and tissue-specific manner and that functional redundancy among the IGFBPs may exist. In conclusion, these results suggest that rapid growth and increased muscle accretion in commercial modern broilers may be achieved not through increased levels of circulating IGFs but by changing local IGF expression to affect paracrine IGF activity, specifically in muscle. This activity could be further regulated through combinatorial action of IGFBPs, which appear to make up a robust control system acting to support growth within different developmental and physiological contexts.

DATA AVAILABILITY STATEMENT

The raw data supporting the conclusion of this article will be made available by the authors, without undue reservation.

ETHICS STATEMENT

The animal study was reviewed and approved by University of Georgia Institutional Animal Care and Use Committee.

AUTHOR CONTRIBUTIONS

LE and TP conceived the study design, obtained funding, and assisted with sample collection. LV assisted with sample collection, conducted all sample analysis, statistically analyzed the data, and drafted the

manuscript under the guidance of LE. All authors have read and approved the submitted version of the manuscript.

FUNDING

This project was supported by funding from the College of Agricultural and Environmental Sciences, University of Georgia and Agriculture and Food Research Initiative Competitive Grants #2017-67015-26490 (TP and LE) and #2021-67034-35185 (LV and LE) from the USDA National Institute of Food and Agriculture.

ACKNOWLEDGMENTS

Special thanks to Mason Trappio, Monika Proszkowiec-Weglarz, and Jason Payne for their assistance in sample collection, and to Jason Payne and Brett Marshall for constructive feedback during preparation of the manuscript.

REFERENCES

Allander, S. V., Ehrenborg, E., Luthman, H., and Powell, D. R. (1995). Conservation of IGFBP Structure during Evolution: Cloning of Chicken Insulin-like Growth Factor Binding Protein-5. *Prog. Growth Factor Res.* 6 (2), 159–165. doi:10.1016/0955-2235(96)00011-7

Allander, S. V., Coleman, M., Luthman, H., and Powell, D. R. (1997). Chicken Insulin-like Growth Factor Binding Protein (IGFBP)-5: Conservation of IGFBP-5 Structure and Expression during Evolution. *Comp. Biochem. Physiology Part B Biochem. Mol. Biol.* 116 (4), 477–483. doi:10.1016/S0305-0491(96)00289-1

Allard, J. B., and Duan, C. (2018). IGF-binding Proteins: Why Do They Exist and Why Are There So Many? *Front. Endocrinol.* 9, 117. doi:10.3389/fendo.2018.00117

Arany, E., Afford, S., Strain, A. J., Winwood, P. J., Arthur, M. J., and Hill, D. J. (1994). Differential Cellular Synthesis of Insulin-like Growth Factor Binding Protein-1 (IGFBP-1) and IGFBP-3 within Human Liver. *J. Clin. Endocrinol. Metabolism* 79 (6), 1871–1876. doi:10.1210/jcem.79.6.7527416

Armstrong, D. G., McKay, C. O., Morrell, D. J., and Goddard, C. (1989). Insulin-like Growth Factor-I Binding Proteins in Serum from the Domestic Fowl. *J. Endocrinol.* 120 (3), 373–378. doi:10.1677/joe.0.1200373

Awede, B., Thissen, J.-P., Gailly, P., and Lebacq, J. (1999). Regulation of IGF-I, IGFBP-4 and IGFBP-5 Gene Expression by Loading in Mouse Skeletal Muscle. *FEBS Lett.* 461 (3), 263–267. doi:10.1016/S0014-5793(99)01469-6

Bartov, I. (1982). Corticosterone and Fat Deposition in Broiler Chicks: Effect of Injection Time, Breed, Sex and Age. *Br. Poult. Sci.* 23 (2), 161–170. doi:10.1080/00071688208447942

Baumann, G., Stolar, M. W., Amburn, K., Barsano, C. P., and DeVries, B. C. (1986). A Specific Growth Hormone-Binding Protein in Human Plasma: Initial Characterization*. *J. Clin. Endocrinol. Metabolism* 62 (1), 134–141. doi:10.1210/jcem-62-1-134

Baxter, R. C. (1991). Insulin-like Growth Factor (IGF) Binding Proteins: the Role of Serum IGFBPs in Regulating IGF Availability. *Acta Paediatr.* 80 (s372), 107–114. doi:10.1111/j.1651-2227.1991.tb17983.x

Beccavin, C., Chevalier, B., Cogburn, L., Simon, J., and Duclos, M. (2001). Insulin-like Growth Factors and Body Growth in Chickens Divergently Selected for High or Low Growth Rate. *J. Endocrinol.* 168 (2), 297–306. doi:10.1677/joe.0.1680297

Berrong, S. L., and Washburn, K. W. (1998). Effects of Genetic Variation on Total Plasma Protein, Body Weight Gains, and Body Temperature Responses to Heat Stress. *Poult. Sci.* 77 (3), 379–385. doi:10.1093/ps/77.3.379

Brooks, A. J., Wooh, J. W., Tunny, K. A., and Waters, M. J. (2008). Growth Hormone Receptor; Mechanism of Action. *Int. J. Biochem. Cell Biol.* 40 (10), 1984–1989. doi:10.1016/j.biocel.2007.07.008

Burnside, J., and Cogburn, L. A. (1992). Developmental Expression of Hepatic Growth Hormone Receptor and Insulin-like Growth Factor-I mRNA in the Chicken. *Mol. Cell Endocrinol.* 89 (1), 91–96. doi:10.1016/0303-7207(92)90214-Q

Burnside, J., Liou, S. S., Zhong, C., and Cogburn, L. A. (1992). Abnormal Growth Hormone Receptor Gene Expression in the Sex-Linked Dwarf Chicken. *General Comp. Endocrinol.* 88 (1), 20–28. doi:10.1016/0016-6480(92)90190-U

Buyse, J., and Decuypere, E. (1999). The Role of the Somatotrophic axis in the Metabolism of the Chicken. *Domest. Anim. Endocrinol.* 17 (2), 245–255. doi:10.1016/S0739-7240(99)00041-7

Chen, C., Chen, Y. H., Tixier-Boichard, M., Cheng, P. Y., Chang, C. S., Tang, P.-C., et al. (2009). Effects of the Chicken Sex-Linked Dwarf Gene on Growth and Muscle Development. *Asian-australas. J. Anim. Sci.* 22. doi:10.5713/ajas.2009.80689

Chen, Z., Li, L., Wu, W., Liu, Z., Huang, Y., Yang, L., et al. (2020). Exercise Protects Proliferative Muscle Satellite Cells against Exhaustion via the Igfbp7-Akt-mTOR axis. *Theranostics* 10 (14), 6448–6466. doi:10.7150/thno.43577

Clark, R., and Robinson, I. C. (1996). Up and Down the Growth Hormone Cascade. *Cytokine & Growth Factor Rev.* 7 (1), 65–80. doi:10.1016/1359-6101(96)00006-8

Collins, K. E., Kiepper, B. H., Ritz, C. W., McLendon, B. L., and Wilson, J. L. (2014). Growth, Livability, Feed Consumption, and Carcass Composition of the Athens Canadian Random Bred 1955 Meat-type Chicken versus the 2012 High-Yielding Cobb 500 Broiler. *Poult. Sci.* 93 (12), 2953–2962. doi:10.3382/ps.2014-04224

Collins, K. E., Marks, H. L., Aggrey, S. E., Lacy, M. P., and Wilson, J. L. (2016). History of the Athens Canadian Random Bred and the Athens Random Bred Control Populations. *Poult. Sci.* 95 (5), 997–1004. doi:10.3382/ps/pew085

Czerwinski, S. M., Cate, J. M., Francis, G., Tomas, F., Brocht, D. M., and McMurtry, J. P. (1998). The Effect of Insulin-like Growth Factor-I (IGF-I) on Protein Turnover in the Meat-type Chicken (*Gallus domesticus*). *Comp. Biochem. Physiology Part C Pharmacol. Toxicol. Endocrinol.* 119 (1), 75–80. doi:10.1016/s0742-8413(97)00193-x

Czerwinski, S. M., Martin, J. M., and Bechtel, P. J. (1994). Modulation of IGF mRNA Abundance during Stretch-Induced Skeletal Muscle Hypertrophy and Regression. *J. Appl. Physiology* 76 (5), 2026–2030. doi:10.1152/jappl.1994.76.5.2026

D'Costa, A. P., Prevette, D. M., Houenou, L. J., Wang, S., Zackenfels, K., Rohrer, H., et al. (1998). Mechanisms of Insulin-like Growth Factor Regulation of Programmed Cell Death of Developing Avian Motoneurons. *J. Neurobiol.* 36 (3), 379–394. doi:10.1002/(sici)1097-4695(19980905)36:3<379::aid-neu6>3.0.co;2-t

Dewil, E., Darras, V. M., Spencer, G. S. G., Lauterio, T. J., and Decuypere, E. (1999). The Regulation of GH-dependent Hormones and Enzymes after Feed Restriction in Dwarf and Control Chickens. *Life Sci.* 64 (16), 1359–1371. doi:10.1016/S0024-3205(99)00082-X

Duan, C., Ding, J., Li, Q., Tsai, W., and Pozios, K. (1999). Insulin-like Growth Factor Binding Protein 2 Is a Growth Inhibitory Protein Conserved in Zebrafish. *Proc. Natl. Acad. Sci. U.S.A.* 96 (26), 15274–15279. doi:10.1073/pnas.96.26.15274

Duclos, M. J., Beccavin, C., and Simon, J. (1999). Genetic Models for the Study of Insulin-like Growth Factors (IGF) and Muscle Development in Birds Compared to Mammals. *Domest. Anim. Endocrinol.* 17 (2), 231–243. doi:10.1016/S0739-7240(99)00040-5

Duclos, M. J., and Goddard, C. (1990). Insulin-like Growth Factor Receptors in Chicken Liver Membranes: Binding Properties, Specificity, Developmental Pattern and Evidence for a Single Receptor Type. *J. Endocrinol.* 125 (2), 199–206. doi:10.1677/joe.0.1250199

Ellestad, L. E., Carre, W., Muchow, M., Jenkins, S. A., Wang, X., Cogburn, L. A., et al. (2006). Gene Expression Profiling during Cellular Differentiation in the

Embryonic Pituitary Gland Using cDNA Microarrays. *Physiol. Genomics* 25 (3), 414–425. doi:10.1152/physiolgenomics.00248.2005

Ellestad, L. E., Cogburn, L. A., Simon, J., Le Bihan-Duval, E., Aggrey, S. E., Byerly, M. S., et al. (2019). Transcriptional Profiling and Pathway Analysis Reveal Differences in Pituitary Gland Function, Morphology, and Vascularization in Chickens Genetically Selected for High or Low Body Weight. *BMC Genomics* 20 (1), 316. doi:10.1186/s12864-019-5670-9

Ellestad, L. E., Malkiewicz, S. A., Guthrie, H. D., Welch, G. R., and Porter, T. E. (2009). Expression and Regulation of Glucocorticoid-Induced Leucine Zipper in the Developing Anterior Pituitary Gland. *J. Mol. Endocrinol.* 42 (2), 171–183. doi:10.1677/jme-08-0066

Ellestad, L. E., and Porter, T. E. (2013). Ras-dva Is a Novel Pit-1- and Glucocorticoid-Regulated Gene in the Embryonic Anterior Pituitary Gland. *Endocrinology* 154 (1), 308–319. doi:10.1210/en.2012-1566

Ellestad, L. E., Puckett, S. A., and Porter, T. E. (2015). Mechanisms Involved in Glucocorticoid Induction of Pituitary GH Expression during Embryonic Development. *Endocrinology* 156 (3), 1066–1079. doi:10.1210/en.2014-1686

Ellestad, L. E., Saliba, J., and Porter, T. E. (2011). Ontogenic Characterization of Gene Expression in the Developing Neuroendocrine System of the Chick. *General Comp. Endocrinol.* 171 (1), 82–93. doi:10.1016/j.ygcen.2010.12.006

Ewton, D. Z., Coolican, S. A., Mohan, S., Chernausek, S. D., and Florini, J. R. (1998). Modulation of Insulin-like Growth Factor Actions in L6A1 Myoblasts by Insulin-like Growth Factor Binding Protein (IGFBP)-4 and IGFBP-5: a Dual Role for IGFBP-5. *J. Cell. Physiol.* 177 (1), 47–57. doi:10.1002/(sici)1097-4652(199810)177:1<47::aid-jcp5>3.0.co;2-e

Fisher, M. C., Meyer, C., Garber, G., and Dealy, C. N. (2005). Role of IGFBP2, IGF-I and IGF-II in Regulating Long Bone Growth. *Bone* 37 (6), 741–750. doi:10.1016/j.bone.2005.07.024

Fridolfsson, A.-K., and Ellegren, H. (1999). A Simple and Universal Method for Molecular Sexing of Non-ratite Birds. *J. Avian Biol.* 30 (1), 116–121. doi:10.2307/3677252

Frommer, K. W., Reichenmiller, K., Schutt, B. S., Hoeflich, A., Ranke, M. B., Dodt, G., et al. (2006). IGF-independent Effects of IGFBP-2 on the Human Breast Cancer Cell Line Hs578T. *J. Mol. Endocrinol.* 37 (1), 13–23. doi:10.1677/jme.1.01955

Frost, R. A., and Lang, C. H. (1999). Differential Effects of Insulin-like Growth Factor I (IGF-I) and IGF-Binding Protein-1 on Protein Metabolism in Human Skeletal Muscle Cells1. *Endocrinology* 140 (9), 3962–3970. doi:10.1210/endo.140.9.6998

Gahete, M. D., Luque, R. M., and Castaño, J. P. (2016). Models of GH Deficiency in Animal Studies. *Best Pract. Res. Clin. Endocrinol. Metabolism* 30 (6), 693–704. doi:10.1016/j.beem.2016.11.001

Gay, E., Seurin, D., Babajko, S., Doublier, S., Cazillis, M., and Binoux, M. (1997). Liver-Specific Expression of Human Insulin-like Growth Factor Binding Protein-1 in Transgenic Mice: Repercussions on Reproduction, Ante- and Perinatal Mortality and Postnatal Growth1. *Endocrinology* 138 (7), 2937–2947. doi:10.1210/endo.138.7.5282

Giachetto, P. F., Riedel, E. C., Gabriel, J. E., Ferro, M. I. T., Di Mauro, S. M. Z., Macari, M., et al. (2004). Hepatic mRNA Expression and Plasma Levels of Insulin-like Growth Factor-I (IGF-I) in Broiler Chickens Selected for Different Growth Rates. *Genet. Mol. Biol.* 27, 39–44. doi:10.1590/S1415-47572004000100007

Girbau, M., Bassas, L., Alemany, J., and de Pablo, F. (1989). *In Situ* autoradiography and Ligand-dependent Tyrosine Kinase Activity Reveal Insulin Receptors and Insulin-like Growth Factor I Receptors in Prepancreatic Chicken Embryos. *Proc. Natl. Acad. Sci. U.S.A.* 86 (15), 5868–5872. doi:10.1073/pnas.86.15.5868

Goddard, C., Wilkie, R. S., and Dunn, I. C. (1988). The Relationship between Insulin-like Growth Factor-1, Growth Hormone, Thyroid Hormones and Insulin in Chickens Selected for Growth. *Domest. Anim. Endocrinol.* 5 (2), 165–176. doi:10.1016/0739-7240(88)90017-3

Havenstein, G. B., Ferket, P. R., Scheideler, S. E., and Larson, B. T. (1994). Growth, Livability, and Feed Conversion of 1957 vs 1991 Broilers when Fed "Typical" 1957 and 1991 Broiler Diets. *Poult. Sci.* 73 (12), 1785–1794. doi:10.3382/ps.0731785

Havenstein, G., Ferket, P., and Qureshi, M. (2003). Growth, Livability, and Feed Conversion of 1957 versus 2001 Broilers when Fed Representative 1957 and 2001 Broiler Diets. *Poult. Sci.* 82 (10), 1500–1508. doi:10.1093/ps/82.10.1500

Herrington, J., and Carter-Su, C. (2001). Signaling Pathways Activated by the Growth Hormone Receptor. *Trends Endocrinol. Metab.* 12 (6), 252–257. doi:10.1016/S1043-2760(01)00423-4

Hess, C. W. (1962). Randombred Populations of the Southern Regional Poultry Breeding Project. *World's Poult. Sci. J.* 18 (2), 147–152. doi:10.1079/WPS19620019

Hutt, F. B. (1959). Sex-Linked Dwarfism in the Fowl. *J. Hered.* 50 (5), 209–221. doi:10.1093/oxfordjournals.jhered.a106909

Huybrechts, L. M., Decuypere, E., Buyse, J., Kühn, E. R., and Tixier-Boichard, M. (1992). Effect of Recombinant Human Insulin-like Growth Factor-I on Weight Gain, Fat Content, and Hormonal Parameters in Broiler Chickens. *Poult. Sci.* 71 (1), 181–187. doi:10.3382/ps.0710181

Jones, J. I., and Clemmons, D. R. (1995). Insulin-Like Growth Factors and Their Binding Proteins: Biological Actions*. *Endocr. Rev.* 16 (1), 3–34. doi:10.1210/edrv-16-1-3

Kajimoto, Y., and Rotwein, P. (1989). Structure and Expression of a Chicken Insulin-like Growth Factor I Precursor. *Mol. Endocrinol.* 3 (12), 1907–1913. doi:10.1210/mend-3-12-1907

Kamanga-Sollo, E., Pampusch, M. S., White, M. E., Hathaway, M. R., and Dayton, W. R. (2005). Insulin-like Growth Factor Binding Protein (IGFBP)-3 and IGFBP-5 Mediate TGF-β- and Myostatin-Induced Suppression of Proliferation in Porcine Embryonic Myogenic Cell Cultures. *Exp. Cell Res.* 311 (1), 167–176. doi:10.1016/j.yexcr.2005.09.003

Kelley, K., Schmidt, K., Berg, L., Sak, K., Galima, M., Gillespie, C., et al. (2002). Comparative Endocrinology of the Insulin-like Growth Factor-Binding Protein. *J. Endocrinol.* 175 (1), 3–18. doi:10.1677/joe.0.1750003

Kim, J. W. (2010). The Endocrine Regulation of Chicken Growth. *Asian Australas. J. Anim. Sci.* 23 (12), 1668–1676. doi:10.5713/ajas.2010.10329

Lau, J. S., Yip, C. W., Law, K. M., and Leung, F. C. (2007). Cloning and Characterization of Chicken Growth Hormone Binding Protein (cGHBP). *Domest. Anim. Endocrinol.* 33 (1), 107–121. doi:10.1016/j.domaniend.2006.04.012

Levine, J. E. (2012). "An Introduction to Neuroendocrine Systems," in *Handbook of Neuroendocrinology*. Editors G. Fink, D. W. Pfaff, and J. E. Levine (San Diego: Academic Press), 3–19. doi:10.1016/b978-0-12-375097-6.10001-0

Livak, K. J., and Schmittgen, T. D. (2001). Analysis of Relative Gene Expression Data Using Real-Time Quantitative PCR and the 2−ΔΔCT Method. *Methods* 25 (4), 402–408. doi:10.1006/meth.2001.1262

Lu, F. Z., Wang, X. X., Pan, Q. X., Huang, R. H., and Liu, H. L. (2008). Expression of Genes Involved in the Somatotropic, Thyrotropic, and Corticotropic Axes during Development of Langshan and Arbor Acres Chickens. *Poult. Sci.* 87 (10), 2087–2097. doi:10.3382/ps.2007-00493

Mao, J., Burnside, J., Postel-Vinay, M., Pesek, J., Cogburn, L., and Cogburn, L. A. (1998). Ontogeny of Growth Hormone Receptor Gene Expression in Tissue of Growth-Selected Strains of Broiler Chickens. *J. Endocrinol.* 156 (1), 67–75. doi:10.1677/joe.0.1560067

McGuinness, M. C., and Cogburn, L. A. (1991). Response of Young Broiler Chickens to Chronic Injection of Recombinant-Derived Human Insulin-like Growth Factor-I. *Domest. Anim. Endocrinol.* 8 (4), 611–620. doi:10.1016/0739-7240(91)90031-E

Mohan, S., Nakao, Y., Honda, Y., Landale, E., Leser, U., Dony, C., et al. (1995). Studies on the Mechanisms by Which Insulin-like Growth Factor (IGF) Binding Protein-4 (IGFBP-4) and IGFBP-5 Modulate IGF Actions in Bone Cells. *J. Biol. Chem.* 270 (35), 20424–20431. doi:10.1074/jbc.270.35.20424

Ning, Y., Schuller, A. G. P., Bradshaw, S., Rotwein, P., Ludwig, T., Frystyk, J., et al. (2006). Diminished Growth and Enhanced Glucose Metabolism in Triple Knockout Mice Containing Mutations of Insulin-like Growth Factor Binding Protein-3, -4, and -5. *Mol. Endocrinol.* 20 (9), 2173–2186. doi:10.1210/me.2005-0196

Parkinson, N., Collins, M. M., Dufresne, L., and Ryan, A. K. (2010). Expression Patterns of Hormones, Signaling Molecules, and Transcription Factors during Adenohypophysis Development in the Chick Embryo. *Dev. Dyn.* 239 (4), 1197–1210. doi:10.1002/dvdy.22250

Payne, J. A., Proszkowiec-Weglarz, M., and Ellestad, L. E. (2019). Delayed Access to Feed Alters Expression of Genes Associated with Carbohydrate and Amino Acid Utilization in Newly Hatched Broiler Chicks. *Am. J. Physiology-Regulatory, Integr. Comp. Physiology* 317 (6), R864–R878. doi:10.1152/ajpregu.00117.2019

Porter, T. E., Couger, G. S., Dean, C. E., and Hargis, B. M. (1995). Ontogeny of Growth Hormone (GH)-secreting Cells during Chicken Embryonic Development: Initial Somatotrophs Are Responsive to GH-Releasing Hormone. *Endocrinology* 136 (5), 1850–1856. doi:10.1210/endo.136.5.7720629

Porter, T. E. (1998). Differences in Embryonic Growth Hormone Secretion between Slow and Fast Growing Chicken Strains. *Growth Hormone IGF Res.* 8 (2), 133–139. doi:10.1016/S1096-6374(98)80103-2

Reiprich, K., Mühlbauer, E., Decuypere, E., and Grossmann, R. (1995). Characterization of Growth Hormone Gene Expression in the Pituitary and Plasma Growth Hormone Concentrations during Posthatch Development in the Chicken. *J. Endocrinol.* 145 (2), 343–353. doi:10.1677/joe.0.1450343

Rutledge, R. G., and Stewart, D. (2008). Critical Evaluation of Methods Used to Determine Amplification Efficiency Refutes the Exponential Character of Real-Time PCR. *BMC Mol. Biol.* 9 (1), 96. doi:10.1186/1471-2199-9-96

Scanes, C. G., Dunnington, E. A., Buonomo, F. C., Donoghue, D. J., and Siegel, P. B. (1989). Plasma Concentrations of Insulin like Growth Factors (IGF-)I and IGF-II in Dwarf and Normal Chickens of High and Low Weight Selected Lines. *Growth Dev. Aging* 53 (4), 151–157.

Schmidt, C. J., Persia, M. E., Feierstein, E., Kingham, B., and Saylor, W. W. (2009). Comparison of a Modern Broiler Line and a Heritage Line Unselected since the 1950s. *Poult. Sci.* 88 (12), 2610–2619. doi:10.3382/ps.2009-00055

Schneider, M. R., Lahm, H., Wu, M., Hoeflich, A., and Wolf, E. (2000). Transgenic Mouse Models for Studying the Functions of Insulin-like Growth Factor-binding Proteins. *FASEB J.* 14 (5), 629–640. doi:10.1096/fasebj.14.5.629

Schoen, T. J., Bondy, C. A., Zhou, J., Dhawan, R., Mazuruk, K., Arnold, D. R., et al. (1995). Differential Temporal and Spatial Expression of Insulin-like Growth Factor Binding Protein-2 in Developing Chick Ocular Tissues. *Invest. Ophthalmol. Vis. Sci.* 36 (13), 2652–2662.

Schutt, B., Langkamp, M., Rauschnabel, U., Ranke, M., and Elmlinger, M. (2004). Integrin-mediated Action of Insulin-like Growth Factor Binding Protein-2 in Tumor Cells. *J. Mol. Endocrinol.* 32 (3), 859–868. doi:10.1677/jme.0.0320859

Stewart, C. E., and Rotwein, P. (1996). Growth, Differentiation, and Survival: Multiple Physiological Functions for Insulin-like Growth Factors. *Physiol. Rev.* 76 (4), 1005–1026. doi:10.1152/physrev.1996.76.4.1005

Vaccaro, L. A., Porter, T. E., and Ellestad, L. E. (2022). Effects of Genetic Selection on Activity of Corticotropic and Thyrotropic Axes in Modern Broiler Chickens. *Domest. Anim. Endocrinol.* 78, 106649. doi:10.1016/j.domaniend.2021.106649

Vleurick, L., Kühn, E. R., Decuypere, E., Burnside, J., Pezet, A., and Edery, M. (1999). Generation of Chicken Growth Hormone-Binding Proteins by Proteolysis. *General Comp. Endocrinol.* 113 (2), 283–289. doi:10.1006/gcen.1998.7202

Wang, Z., Zhang, X., Li, Z., Abdalla, B. A., Chen, Y., and Nie, Q. (2019). MiR-34b-5p Mediates the Proliferation and Differentiation of Myoblasts by Targeting IGFBP2. *Cells* 8 (4), 360. doi:10.3390/cells8040360

Woelfle, J., Chia, D. J., Massart-Schlesinger, M. B., Moyano, P., and Rotwein, P. (2005). Molecular Physiology, Pathology, and Regulation of the Growth Hormone/insulin-like Growth Factor-I System. *Pediatr. Nephrol.* 20 (3), 295–302. doi:10.1007/s00467-004-1602-1

Yamada, P. M., and Lee, K.-W. (2009). Perspectives in Mammalian IGFBP-3 Biology: Local vs. Systemic Action. *Am. J. Physiology-Cell Physiology* 296 (5), C954–C976. doi:10.1152/ajpcell.00598.2008

Yamada, P. M., Mehta, H. H., Hwang, D., Roos, K. P., Hevener, A. L., and Lee, K. W. (2010). Evidence of a Role for Insulin-like Growth Factor Binding Protein (IGFBP)-3 in Metabolic Regulation. *Endocrinology* 151 (12), 5741–5750. doi:10.1210/en.2010-0672

Yang, S., Alnaqeeb, M., Simpson, H., and Goldspink, G. (1997). Changes in Muscle Fibre Type, Muscle Mass and IGF-I Gene Expression in Rabbit Skeletal Muscle Subjected to Stretch. *J. Anat.* 190 (4), 613–622. doi:10.1046/j.1469-7580.1997.19040613.x

Conflict of Interest: The authors declare that the research was conducted in the absence of any commercial or financial relationships that could be construed as a potential conflict of interest.

Publisher's Note: All claims expressed in this article are solely those of the authors and do not necessarily represent those of their affiliated organizations, or those of the publisher, the editors and the reviewers. Any product that may be evaluated in this article, or claim that may be made by its manufacturer, is not guaranteed or endorsed by the publisher.

frontiers | Frontiers in Physiology

REVIEW
published: 01 July 2022
doi: 10.3389/fphys.2022.942790

The Diverse Roles of 17β-Estradiol in Non-Gonadal Tissues and Its Consequential Impact on Reproduction in Laying and Broiler Breeder Hens

Charlene Hanlon, Clara J. Ziezold and Grégoy Y. Bédécarrats*

Department of Animal Biosciences, University of Guelph, Guelph, ON, Canada

Estradiol-17β (E_2) has long been studied as the primary estrogen involved in sexual maturation of hens. Due to the oviparous nature of avian species, ovarian production of E_2 has been indicated as the key steroid responsible for activating the formation of the eggshell and internal egg components in hens. This involves the integration and coordination between ovarian follicular development, liver metabolism and bone physiology to produce the follicle, yolk and albumen, and shell, respectively. However, the ability of E_2 to be synthesized by non-gonadal tissues such as the skin, heart, muscle, liver, brain, adipose tissue, pancreas, and adrenal glands demonstrates the capability of this hormone to influence a variety of physiological processes. Thus, in this review, we intend to re-establish the role of E_2 within these tissues and identify direct and indirect integration between the control of reproduction, metabolism, and bone physiology. Specifically, the sources of E_2 and its activity in these tissues via the estrogen receptors (ERα, ERβ, GPR30) is described. This is followed by an update on the role of E_2 during sexual differentiation of the embryo and maturation of the hen. We then also consider the implications of the recent discovery of additional E_2 elevations during an extended laying cycle. Next, the specific roles of E_2 in yolk formation and skeletal development are outlined. Finally, the consequences of altered E_2 production in mature hens and the associated disorders are discussed. While these areas of study have been previously independently considered, this comprehensive review intends to highlight the critical roles played by E_2 to alter and coordinate physiological processes in preparation for the laying cycle.

Keywords: estradiol (17ß-estradiol), reproduction, egg formation, sexual maturation, laying persistency, medullary bone, yolk deposition

OPEN ACCESS

Edited by:
Sandra G. Velleman, The Ohio State University, United States

Reviewed by:
Monika Proszkowiec-Weglarz, United States Department of Agriculture, United States
Andrzej Sechman, University of Agriculture in Krakow, Poland

****Correspondence:***
Charlene Hanlon
chanlon@uoguelph.ca

Specialty section:
This article was submitted to Avian Physiology, a section of the journal Frontiers in Physiology

Received: *13 May 2022*
Accepted: *13 June 2022*
Published: *01 July 2022*

Citation:
Hanlon C, Ziezold CJ and Bédécarrats GY (2022) The Diverse Roles of 17β-Estradiol in Non-Gonadal Tissues and Its Consequential Impact on Reproduction in Laying and Broiler Breeder Hens. Front. Physiol. 13:942790. doi: 10.3389/fphys.2022.942790

INTRODUCTION—ESTROGENS AND THEIR RECEPTORS

Estrogens play a fundamental role in controlling female reproduction, with the ovary acting as the primary source. Interestingly, in avian species, estrogen biosynthesis has also been reported in non-gonadal tissues, such as the brain and adrenal glands (Tanabe et al., 1979; Matsunaga et al., 2001). As the synthesis of estrogens in mammals has additionally been observed in the skin, heart, muscle, liver,

adipose tissue, and pancreas (Hemsell et al., 1974; Cui et al., 2013; Barakat et al., 2016), there is a rationale for further investigation in the avian species. Three primary forms of estrogens can be found in circulation: estrone (E_1), estradiol-17β (E_2), and estriol (E_3). In the hen, it has been established that E_1 is a readily reversible estrogen form (MacRae et al., 1959), acting primarily as a precursor and storage form of the most prominent estrogen, E_2 (Raud and Hobkirk, 1968). In avian species, E_2 is primarily produced by small white follicles (SWFs) following their recruitment during sexual maturation of the ovary (Williams and Sharp, 1977; Robinson and Etches, 1986). In fact, E_2 plays an instrumental role in the transition between growth and reproduction in the laying hen. Contrary to mammals, in which E_2 is primarily produced by granulosa cells (Hutz, 1989), E_2 synthesis in birds is localized to the theca externa layer prior to follicular selection into the hierarchy (Porter et al., 1989). In comparison to the influence of E_2, E_3 is a weak, minor form of estrogen (Lague et al., 1975), which is 80-fold less potent than E_2 and acts as a major urinary metabolite rather than playing an active role in controlling reproduction (Mathur et al., 1966).

Three estrogen receptors (ERs) have been characterized, including two intracellular receptors, ER-alpha (ERα, also known as ESR1) and ER-beta (ERβ, also known as ESR2), and one cell surface ER, referred to as GPR30 (also known as GPER-1). E_1 and E_3 have shown a preference for ERα and ERβ, respectively, while E_2 maintains a similar binding capacity for either intracellular receptor (Kuiper et al., 1998). Conversely, much less is known about the activity of GPR30, which was first reported to mediate the response to E_2 in breast cancer cells despite the lack of ERα and ERβ (Filardo et al., 2000; Thomas et al., 2005). Since then, it has been implicated in numerous pathways regulated by E_2, including germ cell proliferation (Olde and Leeb-Lundberg, 2009; Ge et al., 2012). In fact, during embryonic development, GPR30 has been implicated in the renewal of chicken primordial germ cells (PGCs) induced by E_2 (Ge et al., 2012). More recent investigations in mice models have indicated that during follicle-stimulating hormone (FSH)-stimulated aromatase production, E_2 binds to GPR30 to trigger ERK1/2 phosphorylation, resulting in oocyte maturation *in vivo* (Zhao et al., 2020). However, since the discovery of this G-coupled protein ER in chickens is more recent (Acharya and Veney, 2012; Ge et al., 2012), there is little information on its role both in reproduction and metabolic processes. In the case of the intracellular receptors, differences in expression have been identified between the subtypes. Specifically, ERα was identified within the embryonic brain of Japanese quail and chickens (Camacho-Arroyo et al., 2003; Brunström et al., 2009), as well as the hypothalamus of mature laying hens (Hansen et al., 2003), the ovary of mature hens (Hrabia et al., 2004), shell gland (uterus), kidney (Hansen et al., 2003), liver (Li et al., 2014), and bones (Ohashi et al., 1991; Ohashi and Kusuhara, 1993; Turner et al., 1993). In the case of avian ERβ, expression is less widespread, as it was detected in the embryonic brain (Brunström et al., 2009), ovary (Hrabia et al., 2008), and liver (Li et al., 2014).

While both intracellular receptors are expressed in the avian hypothalamus and pituitary, ERα is the predominant subtype (Griffin et al., 1999), and this receptor is primarily implicated in activating the hypothalamic-pituitary-gonadal (HPG) axis. However, expression of ERβ was identified in the embryonic brain region of quail associated with copulatory behaviour in mature males, suggesting a role for the β-subtype in brain differentiation (Brunström et al., 2009). In the ovary, ERα is the predominant ER (Hrabia et al., 2008). While both intracellular ERs are upregulated during follicular development and the ovulatory process (Drummond and Fuller, 2010), the α-subtype in granulosa cells is predominantly involved in triggering follicular recruitment and the maturation of the remainder of the reproductive tract at the time of activation (Kamiyoshi et al., 1986; Hrabia et al., 2004). ERα is also present within the oviduct of hens to trigger the final maturation of the reproductive tract and coordinate the egg formation processes (Hansen et al., 2003; Imamura et al., 2006). In the case of ERβ, this receptor is predominantly involved with the maturation of pre-ovulatory follicles and the ovulatory process (Emmen et al., 2005).

In the bone and liver, ERα once again plays the predominant role (Imamura et al., 2006; Li et al., 2014). While the expression of both ERs in hepatocytes elevates during sexual maturation (Tan et al., 2020), only ERα has been implicated in mediating the upregulation of yolk proteins (Li et al., 2014). GPR30 has also

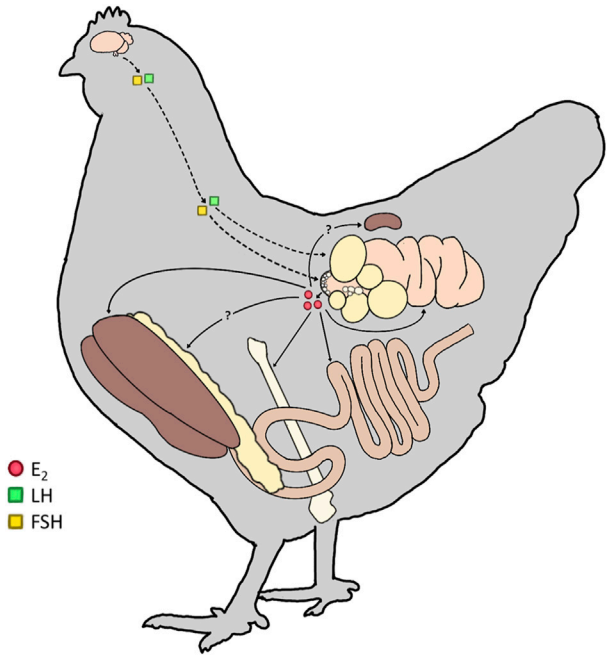

FIGURE 1 | Targets of lowercase (E_2) in mature hens. In the mature laying hen, the upper portion of the hypothalamic-pituitary-gonadal (HPG) axis is activated, resulting in the production of gonadotropins (Luteinizing Hormone; LH and Follicle-Stimulating Hormone; FSH). FSH and LH then act on the ovary (dashed line) to stimulate follicular development and ovulation, respectively. The small white follicle (SWF) pool synthesizes and releases E_2 from the ovary (solid line). E_2 targets estrogen receptors (ERs) in the liver, bone, intestine, and oviduct to participate in all levels of the egg formation process. We hypothesize additional ERs are present in the adipose tissue and kidney of hens to further integrate the physiological processes during sexual maturation and the preparation for lay.

been detected in the liver (Liu et al., 2018), yet little is known regarding its role. Interestingly, in the presence of growth hormone (GH), a significant elevation in ERβ was reported (Hrabia, 2015), suggesting GH may upregulate ERβ in the liver to participate in nutrient partitioning and utilization during lay. ERα is the only receptor subtype reported to support eggshell formation during bone development in the laying hen. Specifically, since ERα is expressed on the surface of osteoblasts (Ohashi et al., 1991; Ohashi and Kusuhara, 1993; Turner et al., 1993), as the hen ages and transitions toward the end of the production cycle, the receptor density declines, reducing the osteogenic effect of E_2 (Hansen et al., 2003). However, the recent determination that modern commercial laying hens can persistently lay up to 100 weeks of age with no detrimental impact on bone or eggshell quality (Hanlon et al., 2022) suggests that genetic selection may have impacted the response to E_2. Thus, further studies are required to determine whether this results from a sustained expression of ERs in these strains.

Furthermore, we hypothesize that ER activity likely extends beyond the investigated tissues, as ERs are expressed in adipose tissue in mammals. In avian species, while the follicle-stimulating hormone receptor (FSH-R) has been identified in adipose tissue (Cui et al., 2012), the presence of ERs has yet to be determined. Therefore, it is possible that E_2, via its receptors, alters adipocyte functions, diverting nutrients and energy toward egg production through the upregulation of ERs by FSH. Thus, for the remainder of this review, the focus is placed on the roles of E_2 as the primary estrogen during sexual differentiation of the embryo, maturation of the hen, and extended laying cycle. Moreover, this review will emphasize the roles of E_2 in yolk formation, skeletal development, and metabolism, which all impact egg production and quality (**Figure 1**). Lastly, the consequences and disorders associated with varying E_2 concentrations are discussed to provide a comprehensive review and demonstrate that beyond the reproductive tract, E_2 is key to altering metabolic processes during the life cycle of a laying hen.

ESTRADIOL AND REPRODUCTION

Embryonic Sexual Differentiation

Aside from the gonadal sources of E_2, studies have reported the presence of maternally derived estrogens in the yolk (Schwabl, 1993; Paitz et al., 2020), potentially implicating estrogen in all stages of embryonic development. A study in quail determined that the E_2 concentration present in yolk is comparable to that of the maternal circulating concentrations (Adkins-Regan et al., 1995). In fact, chicken embryos have concentrations as high as 0.2 ng/g of body weight (Elf and Fivizzani, 2002; Hartmann et al., 2003; Wang et al., 2010), and in other avian species, this concentration is as high as 12 ng/g (Merrill et al., 2019). Since ERα expression has been reported as early as embryonic day 3.5 (E3.5; Andrews et al., 1997; Smith et al., 1997), prior to the production of aromatase (Smith et al., 1997) and E_2 by the gonads (Woods and Erton, 1978), these maternally derived sources of estrogen may be the primary source acting on the ERs during this period. Additional sources of E_2 are produced in the interstitial cells, irrespective of sex, between E3.5–5.5 (Woods and Erton, 1978). However, the role of estrogen in this early developmental period remains to be determined, as it was recently established that E_2 is metabolized to estrone early *in ovo*, then conjugated to sulfates and glucuronides by E5 (Paitz et al., 2020). In female quail treated with estradiol benzoate, female offspring developed right oviducts, resulting in an atypical symmetrical reproductive tract morphology (Adkins-Regan et al., 1995). It has been speculated that the early metabolism of maternally derived E_2 observed by Paitz et al. (2020) suppresses the metabolic capacity for Mullerian duct development on the right side (Zimmerman et al., 2012).

Estrogens have long been implicated in the feminization of the reproductive axis during sexual differentiation, with early exposure to estrogen critical for the normal development of the ovary (Elbrecht and Smith, 1992). Thus, female embryos of turkeys, quail, and chickens have higher circulating E_2 concentrations compared to their male counterparts (Woods and Brazzill, 1981; Schumacher et al., 1988; Abdelnabi et al., 2001; Ottinger et al., 2001; Sechman et al., 2011; Rosati et al., 2021). Recent evidence demonstrates that *JUN* is a critical regulator of sexual differentiation, regulating *DMRT1*, *SOX9*, and *FOXL2*, the genes previously hypothesized to be the determinants of differentiation in avian species. In fact, overexpression of *JUN* results in feminization of ZZ embryos and *JUN* knockout of ZW embryos results in masculinization (Zhang et al., 2021). Upregulation of *JUN* results in the inhibition of Smad2 and the simultaneous production of E_2 within the gonad (Zhang et al., 2021). These gonadal sources of E_2 were detected following the activation of $P450_{17\alpha}$ (CYP17A1) as early as 5–6 days into embryonic development in both the right and left ovaries, with the initiation of cytochrome $P450_{aromatase}$ (CYP19A1) and 3-beta-hydroxysteroid dehydrogenase (3β-HSD) by E6.5 (Yoshida et al., 1996; Andrews et al., 1997; Nakabayashi et al., 1998; Nomura et al., 1999; Nishikimi et al., 2000; **Figure 2**). In fact, the W chromosome has been linked to the early aromatase activation in the female embryo, leading to ovarian development during the first half of the incubation period (Ottinger, 1989; Kagami and Hanada, 1997). It has even been suggested that the presence of CYP19A1 is not only necessary but sufficient to initiate of female sexual differentiation in the embryo (Jin et al., 2020). This elevation in E_2 is key to activating R-spondin-1 (*RSPO1*) expression during early embryonic development, thereby regulating the WNT/β-catenin signalling pathway responsible for controlling cell fate and stem cell pluripotency (Smith et al., 2008).

While the elevated synthesis of E_2 will suppress anti-Mullerian hormone receptor II (AMHRII) to protect the Mullerian duct from apoptosis (Cutting et al., 2014), this protection only occurs in the left ovarian cortex of avian species. This results in an asymmetrical reproductive tract development, as the expression of ERα in the right ovarian cortex is suppressed under the influence of the pituitary homeobox 2 (PITX2) (Nakabayashi et al., 1998). E_2 cannot exert its effects without its receptor present in the cortex, causing the right ovarian cortex to begin regressing as early as E6-6.5 (Ishimaru et al., 2008). Conversely, ERα is expressed in the medulla and germinal epithelium of the left

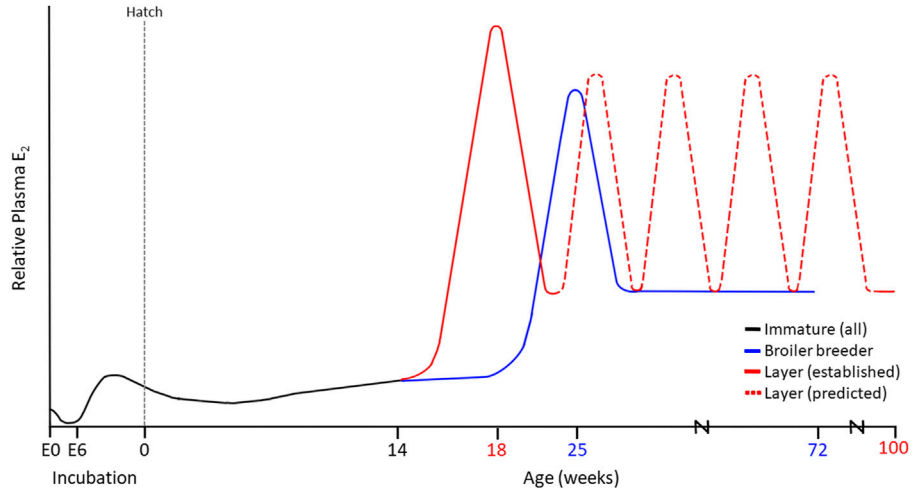

FIGURE 2 | Established and Proposed Estradiol (E_2) Profiles in Modern Commercial Laying Hens (100 weeks) and Broiler Breeder Hens (72 weeks). Maternal sources of E_2 are present in the embryo at day 0 (E0), prior to conjugation during early incubation. At E6.5, the production of aromatase stimulates the ZW left ovarian cortex to produce E_2, driving sexual differentiation. These levels decrease around the time of hatch as the chick ovary remains in a quiescent state. Maturation varies among layers and broiler breeders, yet both demonstrate an initial peak in E_2. In the case of the layer, we propose that up to 5 additional recurrent E_2 elevations occur throughout lay, contributing to the persistency in the cycle that is not observed in broiler breeder hens.

ovary as early as E5.5 (Mizuno et al., 1996; Yoshida et al., 1996; Nakabayashi et al., 1998; Ishimaru et al., 2008). Interestingly, as ERα is temporarily expressed in male embryos between E7-10 (Nakabayashi et al., 1998), embryos can undergo sex reversal following exposure to supraphysiological doses of exogenous E_2. This results in the development of ovotestes at hatch, despite the presence of ZZ chromosomes (Scheib, 1983). However, regardless of E_2 administration, differentiation into testis was shown to eventually occur during sexual maturation (Etches and Kagami, 1997). Interestingly, supraphysiological doses of E_2 are also detrimental to the development of the female reproductive tract, resulting in an intact right ovary and abnormal formation of the left Mullerian duct (Rissman et al., 1984). Therefore, an E_2 threshold likely exists during embryogenesis for normal gonadal development. This may include maternal sources accumulated within the yolk, which may in turn impact hatch rate and future reproductive capacity of offspring.

Estradiol Production and Ovarian Follicular Development

In avian species, the reproductive axis is under the control of a dual stimulatory and inhibitory system, mediated through the hypothalamic neuropeptides, gonadotropin-releasing hormone-I (GnRH-I) and gonadotropin-inhibitory hormone (GnIH) (for review: Bédécarrats, 2015; Bédécarrats et al., 2016; Hanlon et al., 2020). Briefly, long-day breeders, such as the domestic chicken, respond to increasing day lengths, also referred to as photostimulation, by downregulating the expression of GnIH and activating the release of GnRH-I. As GnIH directly suppresses GnRH (Bentley et al., 2003, 2008) and gonadotropins (Tsutsui et al., 2000; Ciccone et al., 2004; Ikemoto and Park, 2005; Ubuka et al., 2006), the downregulation of GnIH allows for the full activation of the reproductive axis (Ikemoto and Park, 2005; Maddineni et al., 2008). In turn, the anterior pituitary gland releases gonadotropins, luteinizing hormone (LH) and FSH, which enter the systemic circulation.

Prior to sexual maturation, LH stimulates a gradual increase in ovarian E_2 production from thousands of SWFs (Williams and Sharp, 1977; Robinson and Etches, 1986; Sechman et al., 2000; **Figure 2**). This E_2 stimulates the final developmental stage of the oviduct by mediating epithelial cell differentiation into tubular gland cells, goblet cells, and ciliated cells (Kohler et al., 1969), thus allowing for albumen synthesis and deposition during egg formation (Palmiter and Wrenn, 1971). Activation of the reproductive axis is concurrent with follicular development via cyclic recruitment, resulting in a mature, functional ovary. Cyclic recruitment in the avian ovary is characterized by a distinct arrangement of prehierarchal and hierarchical (F1-F6) follicles (Johnson, 1993), in which the largest follicle (F1) is ovulated daily (Johnson et al., 1996). FSH supports the maintenance of prehierarchal follicles via proliferative signals (Johnson, 2003) that reduce the susceptibility of developing granulosa cells to apoptosis (Johnson et al., 1996, 1999), thus preventing follicular atresia. Furthermore, LH and FSH are both capable of initiating receptor-mediated cAMP production through their respective receptors, resulting in steroidogenesis (Porter et al., 1989; Kowalski et al., 1991). However, compared to FSH, LH has a more potent effect on steroid hormone secretion (Sharp et al., 1979; Robinson et al., 1988). LH stimulates progesterone (P_4), testosterone (T), and E_2 production from theca cells, with higher steroid concentrations produced by less mature follicles. However, the primary product of the theca interna layer is T, which is subsequently converted to E_2 by the theca externa cells (Porter et al., 1989). In the developing granulosa cells, FSH

induces the necessary steroidogenic competence (Tilly et al., 1991) for P_4 synthesis and LH receptor expression in small yellow follicles and intermediate preovulatory follicles (Calvo and Bahr, 1983; Tilly et al., 1991; Johnson and Bridgham, 2001). As preovulatory follicles mature, granulosa cells lose FSH sensitivity and become exclusively LH-responsive. For instance, in the three largest follicles (F1, F2 and F3), LH increases granulosa cell cAMP production, whereas FSH has no effect (Calvo et al., 1981). In the mature preovulatory follicle (F1), LH stimulates the secretion of high concentrations of P_4 (Yang et al., 1997). This P_4 release exerts positive feedback on GnRH-I, which triggers the preovulatory LH surge (Johnson and van Tienhoven, 1980), inducing ovulation 4–7 h later (Furr et al., 1973). Interestingly, under the influence of the anti-estrogen tamoxifen, egg-laying ceased despite an elevation in E_2 production by SWFs. This occurred concomitantly with declining P_4 concentrations, leading to the inhibition of ovulation (Rzasa et al., 2009).

While E_2 exerts negative and positive feedback on GnRH via kisspeptin neurons in mammals, the absence of kisspeptin in birds may explain the predominantly inhibitory feedback of E_2 on gonadotropins. Removing the primary source of E_2 through ovariectomy induces a substantial rise in circulating LH concentrations in pullets (Knight et al., 1981) and increases pituitary LHβ subunit mRNA levels in mature hens (Terada et al., 1997). Furthermore, E_2 replacement following ovariectomy reduces plasma LH in adult hens (Wilson and Sharp, 1976; Terada et al., 1997) and downregulates pituitary LHβ subunit mRNA levels (Terada et al., 1997). Similarly, E_2 injection suppresses circulating levels of LH and FSH in photostimulated birds; however, this response is age-dependent (Dunn et al., 2003). E_2 may mediate the acquisition of the neuroendocrine response to photostimulation, as E_2 treatment combined with exposure to long daylengths increases plasma gonadotropin concentrations in pullets (Dunn et al., 2003). Likewise, treatment with E_2 or a combination of E_2 and P_4 reduces GnIH-R mRNA abundance in the pituitary of pullets, likely reducing the response to GnIH treatment in adult hens (Maddineni et al., 2008). Interestingly, priming with E_2 is also required to develop the LH positive feedback response to P_4 necessary for ovulation (Wilson and Sharp, 1976), through E_2-induced P_4 receptor (PR) expression in the pituitary gland (Gasc and Baulieu, 1988). At the level of the hypothalamus, continuous E_2 treatment was shown to upregulate PR in immature females, with receptor levels returning to baseline following E_2 withdrawal (Gasc and Baulieu, 1988). This suggests that E_2 plays a stimulatory role in priming the HPG axis for maturation. However, daily tamoxifen injections in mature layers also resulted in elevated ovarian E_2 production (Mao et al., 2018), which indicates that E_2 feedback mechanisms in birds may be more comparable to mammals than hypothesized.

Estradiol and Oviduct Formation

During the development of the chick, implants containing estrogen diethylstilbestrol (DES) triggered cellular proliferation and prevented apoptosis in the developing oviduct (Monroe et al., 2000, 2002). Doses of up 12,000 to 25,000 IU of estradiol benzoate administered to chicks resulted in a 10-fold increase in diameter (Wolff, 1936), and doses of α-estradiol dipropionate at 4 mg per 100-g of body weight led to an 80-fold increase in oviduct weight (Munro and Kosin, 1943). Although the magnum remains an undifferentiated epithelial tube during the immature state, daily injections of estradiol benzoate beginning at 4 days of age can result in an 8-fold increase within 3-days (Palmiter and Wrenn, 1971), indicating that the chick oviduct is already prepared to respond to E_2 stimulation in the days following hatch. This exogenous E_2 during chick growth can also trigger an elevated expression of ovalbumin (Kohler et al., 1969; Palmiter and Wrenn, 1971). These levels will fall quickly in the absence of E_2 stimulation (Schimke et al., 1975). As the hen enters maturity, E_2 mediates the differentiation of tubular gland cells in the magnum, which can be inhibited by the simultaneous administration of P_4 (Oka and Schimke, 1969) through the reduction of cytoplasmic, nuclear, and total ERα (Hsueh et al., 1976; Kraus and Katzenellenbogen, 1993).

The shell gland segment of the oviduct contains a large amount of calbindin 28 K (Corradino et al., 1968) and receptors for cholecalciferol ($1,25(OH)_2D_3$) (Coty, 1980; Haussler, 1986). The binding of cholecalciferol to its receptor triggers an upregulation of the calbindin gene (Theofan et al., 1986; Clemens et al., 1988; Mayel-Afshar et al., 1988). In turn, calbindin protein is responsible for binding calcium and, in the case of the shell gland, depositing this calcium as eggshell in the form of calcium carbonate (Bradfield, 1951; Corradino et al., 1968). Calbindin concentrations are also stimulated by E_2 (Navickis et al., 1979; Nys et al., 1986, 1989), as calbindin is colocalized with ER within the glandular epithelial cells (Jande et al., 1981; Isola, 1990). Thus, levels of this protein increase at the time of sexual maturation (Nys et al., 1989). However, during the formation of the first egg, the expression of calbindin is highly dependent on the transfer of calcium to the shell gland rather than E_2 concentrations (Nys et al., 1989; Striem and Bar, 1991).

Oviductal prolapse is the cause of up to 20% of mortality in laying hens (Shemesh et al., 1984). Evidence has shown increased incidence with declining E_2 levels in the blood (Shemesh et al., 1982). Interestingly, not only has E_2 treatment been shown to support recovery, but spontaneous recovery has also been associated with sudden elevations in E_2 (Shemesh et al., 1984). Recovered birds had higher E_2 in the theca layer of the follicles compared to healthy or prolapsed counterparts (Shemesh et al., 1984). Thus, it has been proposed that prolapse results from systemic E_2 deficiency.

ESTRADIOL AND METABOLISM - YOLK FORMATION

Activation of the Liver

The liver undergoes two metabolic states in hens: pullet growth and active laying (Gruber et al., 1976). Prior to the elevation of E_2 during sexual maturation, the liver primarily contributes to pullet growth. In fact, the liver is responsible for ~90% of fatty acid synthesis (Leveille et al., 1968; O'Hea and Leveille, 1968; Wang et al., 2014), producing a generic VLDL for the transport of

dietary lipids in the blood (Chapman et al., 1977; Walzem, 1996; Walzem et al., 1999). These VLDLs are considerably large (~70 nm diameter) due to their association with 6 identified apolipoproteins, including apoA-1, apoB, and apoC (Walzem, 1996). Thus, these lipids will only be stored in adipose or utilized by peripheral tissues (Walzem, 1996), as they are rapidly processed and energy inefficient, with only ~40% of the substrate used (Griffin et al., 1982). At this time, lipid transport is quite similar to that in mammalian species, with the exception of dietary fat being transported as portomicrons through the portal vein in immature birds (Bensadoun and Rothfeld, 1972) rather than through the lymphatic system in mammals. Upon the initiation of egg-laying, traditional VLDLs are too large to undergo deposition into the growing follicle (Walzem et al., 1999), while intermediate-density lipoproteins (IDLs) and low-density lipoproteins (LDLs) are smaller particles but provide insufficient energy (Griffin et al., 1982). Thus, a modified lipoprotein is required to meet the demands of yolk deposition.

At the time of sexual maturation, ERα present in the liver binds E_2 to elicit the expression of estrogen-dependent genes driving yolk production and enhancing the stability of genes associated with egg white proteins (Bergink and Wallace, 1974; Kirchgessner et al., 1987; Flouriot et al., 1996). Therefore, under the influence of E_2, the liver produces VTG-II (Deeley et al., 1977; Evans et al., 1987), a glycophospholipoprotein that provides the oocyte with glucose, phosphorous, and fat while binding metal ions such as calcium, zinc, and iron (Montorzi et al., 1995). E_2 also stimulates the liver to produce ApoVLDL-II (Chapman et al., 1977; Deeley et al., 1977; Wiskocil et al., 1980; Codina-Salada et al., 1983; Evans et al., 1987; Ratnasabapathy, 1995; Flouriot et al., 1996; Ratnasabapathy et al., 1997; Walzem et al., 1999), an apolipoprotein that inhibits lipoprotein lipase (LPL) to prevent susceptibility to the breakdown of the triglycerides (TAGs) during transport to the oocyte (Griffin et al., 1982; Schneider et al., 1990). Laying hens also have lower LPL activity in the adipose and heart and adipose tissue than their immature counterparts (Husbands, 1972), supporting the redirection of VLDLs to the ovary (Perry and Gilbert, 1979). This Apo-VLDL-II is packaged in a 23:1 ratio with ApoB, combining to form a yolk-targeted TAG-rich VLDL (VLDLy) (Walzem et al., 1999). Due to its association with only two apolipoproteins, the size of VLDLy is reduced by ~50% (30 nm) without sacrificing energy, TAG, or phospholipid content (Griffin et al., 1982; Griffin and Perry, 1985). This allows for easier transport to the ovary, where they can be incorporated into the oocyte via receptor-mediated endocytosis and pass through the granulosa layer (Perry and Gilbert, 1979; Krumins and Roth, 1981; Griffin et al., 1982). Therefore, VLDLy is an ideal candidate for yolk deposition due to the high requirement of energy to be packaged into the follicle for embryo development (Kudzma et al., 1979; Griffin, 1981; Dashti et al., 1983; Lin and McCormick, 1986; Chan et al., 1990; Schneider et al., 1990; Speake et al., 1998; Walzem et al., 1999). These VLDLy particles make up ~30% of the total weight of each yolk, with hens producing up to 5 g of lipids for the daily yolk accumulation (Griffin et al., 1982). Therefore, to keep up with the demand, VLDLy synthesis is significantly upregulated by E_2 compared to the previous production of generic VLDL (Walzem et al., 1999). Furthermore, E_2 has been implicated in the upregulation of lipolytic activities and facilitation of yolk transport during the rapid growth phase of the preovulatory follicles (Brady et al., 1976; Deeley et al., 1977; Wiskocil et al., 1980; Cochrane and Deeley, 1988; Speake et al., 1998; Walzem et al., 1999; Nikolay et al., 2013). Finally, E_2 also stimulates the production of albumen, which is transported to the oviduct during egg formation (Deeley et al., 1975; Cochrane and Deeley, 1988; Evans et al., 1988; Li et al., 2014; Ratna et al., 2016), and is thus critical to the successful formation all internal egg components (**Figure 3**).

Studies have also investigated the impact of exogenous E_2 sources prior to the activation of the HPG axis, and a similar response was observed (Balnave, 1971; Muramatsu et al., 1992; Elnager and Abd-Elhady, 2009), suggesting that ERs are expressed and responsive during pullet growth in preparation for maturation. While it has been established that the populations of both nuclear ER subtypes increase during sexual maturation (Tan et al., 2020), the precise age at which ERs are expressed has not been established. Nonetheless, VLDLy production, along with the associated yolk precursors, apo-VLDL-II and VTG-II, were found to elevate prior to reproductive maturity in response to exogenous E_2 (Muramatsu et al., 1992). This was further associated with increased liver weight and plasma lipid concentrations (Balnave, 1971; Elnager and Abd-Elhady, 2009). In fact, the TAG serum content elevations are associated with a greater number of lipid droplets in the liver of E_2-treated hens than the control (Ren et al., 2021), demonstrating the direct impact of E_2 on liver physiology. Interestingly, while E_2 is required to activate yolk precursors and E_2 concentrations decline in aging hens, a recent study showed that ApoVLDL-II and VTG-II mRNA elevate with age (Cui et al., 2020). A similar result was observed in Li et al. (2020), in which Apo-VLDL-II and ApoB increased over time. This is in line with the hypothesis that the production of yolk precursors may be linked to the recurrent elevations in E_2 observed in commercial strains (Hanlon et al., 2021), suggesting that E_2 may play a larger role in maintaining the egg-laying cycle than previously hypothesized.

Liver Response

More recently, additional estrogen-responsive genes expressed in the liver have been under investigation (Zhang et al., 2020; Ren et al., 2021). Upon exogenous E_2 administration in mature laying hens, a 23-fold elevation in peroxisome-proliferative receptor γ (PPARγ) expression was observed (Lee et al., 2010). This corresponded to increased fatty acids, TAGs, and hepatic lipids (Sato et al., 2009; Lee et al., 2010). Higher hepatic expression of PPARγ has previously been associated with a higher production rate (Chen et al., 2010) and a decline occurs with age (Cui et al., 2020). However, since the expression patterns of ERα increase in aging hens while ERβ does not change (Cui et al., 2020), circulating levels of estrogens are likely the most critical factor.

Apela, which is speculated to be involved in the hepatic lipid metabolism of hens, is activated by E_2 in the liver during

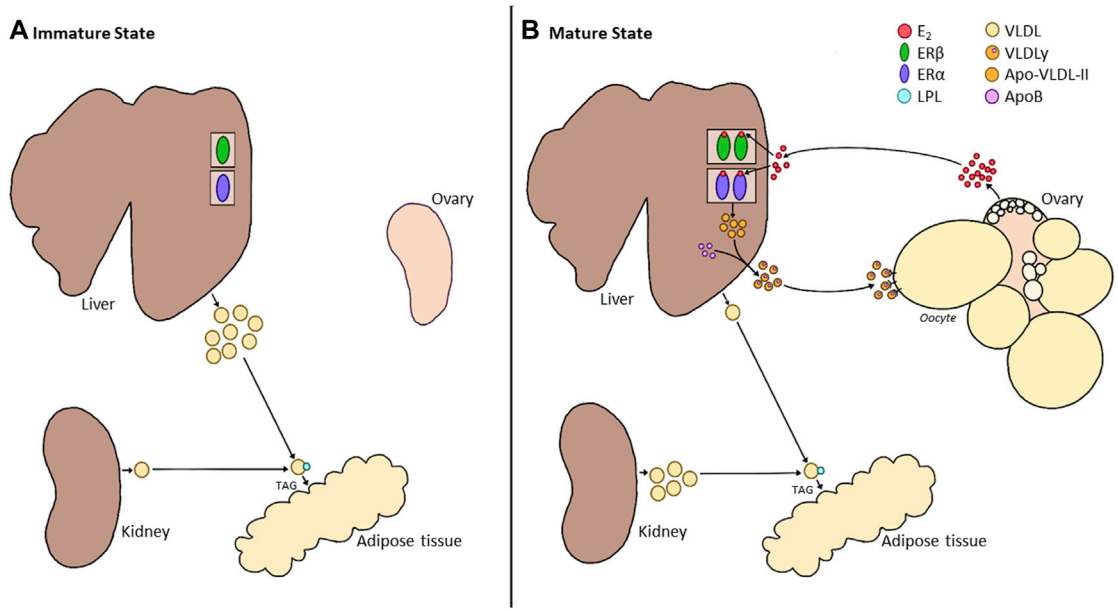

FIGURE 3 | Alterations in Liver Metabolism between the Immature and Mature States of Hens. **(A)**. During the immature state (pullet), the ovary of the bird remains in a quiescent state. While the liver already expresses estrogen receptors (ERα and ERβ), the absence of E_2 results in the production of a generic VLDL. This VLDL is broken down into triglycerides (TAGs) by lipoprotein lipase (LPL) in the circulation and deposited into tissues such as the adipose. During this time, the kidney produces a small amount of generic VLDL and minor production of E_2 by the immature ovary. **(B)**. Once the ovary begins to produce E_2, this hormone binds to its receptors in the liver. While little is known about the role of ERβ in the liver, binding to ERα results in the production of a smaller, more energy-efficient VLDLy, made up of ApoVLDL-II and ApoB in a 23:1 ratio. VLDLy is resistant to LPL, aiding in the deposition of this yolk protein in the rapidly growing follicle. While a small portion of generic VLDL can be produced within the liver, the primary source for peripheral tissues will now be provided by the kidney. However, the role of E_2 in the switch of kidney function is still undetermined.

embryogenesis via ERα. This gene can be induced with exogenous E_2, as demonstrated by the elevated expression at the peak of lay (Tan et al., 2020). Estrogen is also reported to bind to ERα to downregulate *gga-miR-221-5p*, increasing the expression of *ELOVL6* and *SQLE*, responsible for stimulating lipid synthesis, consistent with the role outlined above (Zhang et al., 2020). E_2 binding to ERα also directly targets *miR-144* (Vivacqua et al., 2015), which is known to regulate lipid metabolism through the suppression of *PPARγ-coactivator-1β* (*PGC-1β*; Ren et al., 2021). Furthermore, *PGC-1α* is also influenced by ERα and ERβ (Jiang et al., 2021). However, the action of E_2 on *PGC-1α* remains unclear. Further investigation may reveal a mechanism through which E_2 can directly control lipogenic genes in the liver to influence adipose accumulation and deposition. The involvement of ERα is particularly unique and important to note, as ERβ has been the primary receptor subtype suggested to play a role in the metabolic control of E_2 (Li et al., 2015, 2018). Instead, ERα may be an underappreciated potential target for treating metabolic disorders. However, that does not imply that ERβ is not involved. In fact, *cathepsin E-A like* gene, suggested to play a role in the cleavage and processing of VTGs and ApoB (Wang et al., 2022), acts through the β-receptor (Zhang et al., 2018), demonstrating that both receptors will play a critical role in the yolk formation process.

Activation of the Kidney

Comparable to the liver, the activity of the kidney also depends on the maturity status of the hen. Initially, it was believed that E_2 did not play any role in the synthesis of ApoB in the kidney or intestine (Kirchgessner et al., 1987; Lazier et al., 1994), while it was shown to directly control the production of ApoVLDL-II in the embryonic kidney (Lazier et al., 1994). However, the hen's kidney produces generic VLDL and HDL (Bensadoun and Rothfeld, 1972; Tarugi et al., 1998), with the generic VLDL secreted by cells of the proximal tubules. Thus, generic VLDL from the kidney during the laying cycle was proposed to provide the necessary energy to tissues evaded by VLDLy (Walzem et al., 1999). While a direct or an indirect role for E_2 in the production of generic VLDL is inconclusive, low-density lipoprotein receptor-related protein-2 (LRP2) is primed by E_2 in the kidney during the maturation period (Plieschnig et al., 2012). This endocytic receptor is proposed to be critical in improving the uptake of apolipoproteins to generate and supply generic VLDL to extraoocytic tissues. This is further supported by the elevation of this receptor in the mature hen compared to a mature rooster (Plieschnig et al., 2012). Additionally, ApoB content is higher in the kidney and intestine of laying hens compared to broilers, while no differences are present between breeds in the liver (Zhang et al., 2007). Therefore, it is highly likely that E_2 is involved in the activity of the kidney following the maturation phase.

Fatty Liver Hemorrhagic Syndrome

Fatty liver hemorrhagic syndrome (FLHS) is a metabolic condition typically associated with high-producing laying hens (Trott et al., 2014). This disorder was first described by Couch (1956), with the terminology coined by Wolford and Polin (1972) to distinguish FLHS from non-hemorrhagic fatty liver syndrome (FLS). A high rate of lay has long been attributed to FLS or hepatic steatosis in birds, characterized by the rapid accumulation of lipoproteins in the liver. During this time, the rate of hepatic lipogenesis exceeds that of fat mobilization. FLS is typically observed in modern commercial laying hens since the production cycle requires an exceedingly high rate of lipogenesis, thus overwhelming hepatocytes (Polin and Wolford, 1973; Harms et al., 1982; Hansen and Walzem, 1993; Hermier, 1997; Scheele, 1997). The progression of this disorder eventually leads to a decline in egg production rate (Walzem et al., 1993; Shini and Bryden, 2009; Lee et al., 2010; Jiang et al., 2013; Trott et al., 2014).

While pullets and low-producing hens also have some degree of fat infiltration in the liver (Shini et al., 2020), there are fewer and smaller fenestrae in the sinusoidal endothelium of the liver compared to the mammalian species (Fraser et al., 1986; Braet and Wisse, 2002). It has been hypothesized that the size of fenestrated cells helps avoid dietary fat from overwhelming hepatocytes and prevents atherosclerosis (Fraser et al., 1986). Interestingly, E_2 has also been shown to inhibit coronary atherosclerosis (Hanke et al., 1996; Beaufrère, 2013; Petzinger and Bauer, 2013). Since large particles are blocked from passage, they remain trapped in sinusoids around the central vein, resulting in FLS. This can eventually progress to FLHS with the continued accumulation of fat in the liver, overwhelming the hepatic system (Shini and Bryden, 2009).

Typically, severe cases of FLHS results in the sudden death of older laying hens during their post-peak production (Butler, 1976; Shini et al., 2012), with up to 42% of mortality observed in commercial flocks and up to 74% of caged hen mortality, making this the number one cause of non-infectious laying hen mortality (Shini et al., 2006, 2019; Shini and Bryden, 2009; Mete et al., 2013; Trott et al., 2014). While this metabolic disorder was previously believed to be a result of heat stress (Ringer and Sheppard, 1963; Wolford, 1971; Schexnailder and Griffith, 1973; Pearson and Butler, 1978a; Rozenboim et al., 2016), caged environments (Squires and Leeson, 1988), and high lipid diets (Couch, 1956; Jaussi et al., 1962; Bragg et al., 1973; Haghighi-Rad and Polin, 1982), further evidence has suggested the poorly defined pathogenesis of this disorder is much more complex. Excessive consumption of high energy, low protein (HELP) diets has been clearly established to induce FLHS (Hermier et al., 1994; Lee et al., 2010). While these diets are incredibly effective as a model for this condition, it is well-recognized that the dietary onset of FLHS is also correlated with elevations in E_2 concentrations (Butler, 1976; Polin and Wolford, 1977; Pearson and Butler, 1978b). Even increasing the metabolizable energy in the diet of broiler breeder hens was shown to correspond to higher E_2 concentrations (Hadinia et al., 2020). This resulted in earlier lay, higher GnRH mRNA levels and, as anticipated, higher relative lipid content in the carcass (Hadinia et al., 2020). Therefore, the administration of exogenous E_2 is also highly effective at inducing FLHS independently (Butler, 1976; Polin and Wolford, 1977; Pearson and Butler, 1978b).

Hormonal control of FLHS was first proposed by Butler (1976) since this metabolic disorder was solely accredited to hens presently in lay. Thus, the role of E_2 was investigated, and studies confirmed that exogenous administration stimulates lipogenesis in immature birds, resulting in hepatic steatosis (Lorenz, 1954; Balnave, 1968, 1971; Yu and Marquardt, 1973; Balnave and Pearce, 1974; Harms et al., 1977; Tarlow et al., 1977; Pearson and Butler, 1978b; Kudzma et al., 1979; Dashti et al., 1983; Klimis-Tavantzis et al., 1983). However, this condition was more consistently induced during exogenous E_2 administration in mature layers (Harms et al., 1977; Polin and Wolford, 1977; Pearson and Butler, 1978b; Stake et al., 1981).

Hepatic steatosis has been shown to have detrimental effects on E_2 metabolism in both humans and birds (Adlercreutz, 1970; Haghighi-Rad and Polin, 1981). Despite elevated E_2 levels during sudden FLHS outbreaks, P_4 remains unchanged, and production levels decline as liver fat and FLHS scores increase (Haghighi-Rad and Polin, 1981). This is followed by the rapid regression of the ovary and oviduct (Stake et al., 1981). Reduced LPL activity associated with sexual maturation and the switch in liver metabolism at this time results in reduced clearance of fat in the adipose tissue and increased deposition in the liver (Hasegawa et al., 1980). Thus, the liver fat content of laying hens, typically ~40% of dry weight, can reach up to 70% (Squires and Leeson, 1988). Additionally, E_2 will trigger hypercholesterolemia and hypertriglyceridemia (Shini et al., 2020) as the clearance rate of E_2 falls short of its production by the ovary (Hawkins et al., 1969; Johnson and van Tienhoven, 1981; Tsang and Grunder, 1984), resulting in further impaired liver function (Shini et al., 2020). This suggests E_2 concentrations may become detrimental above a threshold level. Interestingly, white strains are more tolerant to higher and persistent E_2 concentrations (Stake et al., 1981).

While it has been proposed that a combination of E_2 and a positive energy balance via high-energy diets is required to induce FLHS (Harms et al., 1977; Polin and Wolford, 1977; Pearson and Butler, 1978b; Stake et al., 1981; Haghighi-Rad and Polin, 1982), Walzem et al. (1994) hypothesized that providing excessive energy to these hens results in decreased E_2. This reduction would effectively shut down ApoVLDL-II synthesis and secretion, returning the VLDL particles to their larger, generic size (Walzem et al., 1994). However, further investigation demonstrated that E_2-treated hens with low feed intake have the greatest incidence of FLHS (Stake et al., 1981), concluding that this disorder is primarily under the control of E_2, and the remainder of the associated factors may be co-morbidities. Additionally, the administration of tamoxifen, an E_2 inhibitor, reduced the severity of hepatic hemorrhages (Stake et al., 1981). With the updated E_2 profiles of recurrent elevations linked to persistency, we hypothesize this will impact liver lipogenesis, and

it is critical to determine if these elevated concentrations result in the induction of FLHS.

ESTROGENS AND BONE FORMATION

Hormonal Regulation of Calcium Homeostasis

There are two phases of calcium homeostasis regulation in avian species. The first corresponds to structural bone growth occurring throughout the development of the skeletal frame. The second corresponds to the accumulation of medullary bone, which serves as an available pool of calcium for successful egg production. Thus, at the time of sexual maturation, calcium homeostasis shifts from bone growth to calcium storage (Dacke et al., 1993). Regardless of the phase, plasma calcium levels are controlled by the release of parathyroid hormone (PTH), calcitonin (CT), and 1,25-dihydroxycholicaciferol ($1,25(OH)_2D_3$), acting similarly to most mammalian species. However, in the case of chickens, once the hen enters sexual maturity, E_2 has a major impact on calcium metabolism (Etches, 1987; Newman and Leeson, 1997; Deluca, 2004; Bar, 2008, 2009).

In growing pullets, the majority of calcium is stored as hydroxyapatite ($Ca_{10}(PO_4)_6(OH)_2$), requiring a tight regulation between calcium and phosphorus and adequate dietary inclusion of both minerals for successful bone development (Hurwitz and Bar, 1965; Whitehead and Fleming, 2000). While phosphorus is required to form several egg components, including yolk and albumen (Keshavarz, 1998), requirements remain constant during the laying cycle. Since calcium destined for the eggshell is deposited as calcium carbonate ($CaCO_3$), phosphorous is not necessary during this process. Thus, the breakdown of medullary bone results in phosphorous being primarily excreted (Kebreab et al., 2009).

Under natural light, 7-dehydrocholesterol is a precursor synthesized in the liver and transported to the skin to interact with UV light and synthesize cholecalciferol, also known as Vitamin D_3 (Klassing, 1998b). This form of Vitamin D is the most efficiently metabolized in chickens (Valinietse and Bauman, 1981), thus meeting the demands of the birds without requiring supplementation. However, artificial lighting programs in commercial settings lack UV light, resulting in the inability of birds to synthesize adequate Vitamin D levels (Sharp, 1996). Thus, dietary supplementation with exogenous sources is required, forming $25(OH)D_3$ in the liver (Lund and Deluca, 1966). This form undergoes further hydroxylation in the kidney by the rate-limiting enzyme, 1α-hydroxylase, to produce $1,25(OH)_2D_3$ (Lund and Deluca, 1966; Gray et al., 1972; DeLuca, 1974, 1976; Haussler, 1974; Knutson and DeLuca, 1974; Rosol et al., 2000). Therefore, 1α-hydroxylase is upregulated during periods of hypocalcemia (Deluca, 1980).

Hypocalcemia also triggers the synthesis and release of PTH, a hormone produced by the chief cells of the parathyroid glands in response to signals by calcium-sensing receptors (Brown, 1991; Yarden et al., 2000) to regulate calcium within the bone, kidney, and small intestine (Laverty and Clark, 1989; Nys, 1993; Dacke et al., 2015). Specifically, PTH binds to its receptor on the cell surface of osteoblasts to alter their morphology and inactivate osteogenesis (Hurwitz, 1989). Additionally, PTH stimulation promotes calcium reabsorption in the kidney (Laverty and Clark, 1989). Simultaneously, PTH promotes the resorption of bone by stimulating osteoclasts to develop a ruffled border secreting enzymes and acid (Miller et al., 1984; Sugiyama and Kusuhara, 1994). If the hen is instead in a period of hypercalcemia, calcitonin is produced and secreted by the ultimobranchial glands (reviewed by: Dacke, 1979), acting in opposition of PTH. Calcitonin supports the development of bone by promoting osteoblasts to return to their original state, while inhibiting osteoclastic activity (Sugiyama and Kusuhara, 1993, 1996). As hens are under intensive calcium demands during a laying cycle, this hormone will primarily be responsible for downregulating the activity of PTH to support normokalemia. Calcium homeostasis is maintained throughout the life of the bird, from early embryogenesis to the end of a laying cycle. However, the production of E_2 during sexual maturation promotes adaptive changes to calcium homeostasis to further support skeletal maintenance while stimulating eggshell formation.

Development of the Skeletal Frame

Since the development of the skeletal frame begins during embryogenesis, the fully formed yolk also contains all the required Vitamin D_3 and phosphorous *in ovo*, along with 1% of the total calcium required (Klassing, 1998a; 1998b). This is sufficient for the initial formation of hyaline cartilage, which occurs during the first 7–10 days of incubation (Richards and Packard, 1996). Once this source of calcium has been depleted, the chorioallantoic membrane (CAM) will mobilize calcium carbonate from the shell membrane. Meanwhile, carbonic anhydrase dissolves calcium from the shell, which diffuses through the shell membrane, binding to calcium-binding proteins on the surface of the ectoderm by E13 (Tuan and Scott, 1977). Thus, the role of E_2 in breeder hens during eggshell formation directly impacts the success of skeletal development during embryogenesis, preventing metabolic disorders that occur later in the laying cycle of the offspring.

Once hatched, bones continue to grow in width and length via intermembranous and endochondral ossification, respectively (Pechak et al., 1986a, 1986b; Whitehead, 2004). During this period of growth, the structural bone develops as two types of lamellar bone: cortical and trabecular (Whitehead and Fleming, 2000). Intramembranous ossification contributes to bone thickness, with mesenchymal stem cells differentiating into bone until the period of sexual maturation (Pechak et al., 1986a, 1986b; Whitehead, 2004). Longitudinal growth occurs at the epiphyseal growth plates, with bone formation initiated in the lower hypertrophic zone. Chondroclasts reabsorb the cartilage matrix in this region to create space and support mineralization via the formation of hydroxyapatite crystals and infiltration of bone-building cells, referred to as osteoblasts (Whitehead, 2004). Bone development and remodelling progresses through the coordination of calcium deposition by osteoblasts and calcium breakdown triggered by

osteoclasts (Roodman, 1999; Suda et al., 2001; Dacke et al., 2015). Prior to sexual maturation, the skeletal frame should have reached its maximum length and optimal thickness. This emphasizes the importance of managing the pullet prior to the increase in sex steroids to prevent the development of metabolic disorders later in the cycle, such as osteoporosis and cage layer fatigue, resulting in fragile skeletal structures (Whitehead and Fleming, 2000).

Medullary Bone and the Laying Cycle

As mentioned above, the increase in circulating E_2 associated with maturation leads to alterations in the control of calcium, Vitamin D, and PTH levels. The direct impact of E_2 extends to the upregulation of $1,25(OH)_2D_3$ receptors within the gut mucosa to improve the absorption of dietary sources of calcium. E_2 has also been reported to increase the responsiveness of the kidney to PTH and promote the production of medullary bone (Pfeiffer and Gardner, 1938).

Particularly, upon activation of the reproductive axis, the hen terminates all further calcium deposition for the sole purpose of structural development. At this time, hens entering lay transition to the formation of the medullary bone (Bloom et al., 1941; Miller, 1992; Turner et al., 1994). This is a readily mobilizable source of calcium stored on the inner endosteal surface of the marrow cavities of long bones to provide calcium for future eggshell formation (Bloom et al., 1958; Mccoy and Reilly, 1996). This occurs primarily in the long bones, such as the femur and tibia but is also present in the pubic bone, ribs, ulna, toes, and scapula (Jacob and Pescatore, 2013). Studies have suggested medullary bone forms at the expense of structural bone since it has not been linked to direct improvements in strength (Whitehead and Wilson, 1992). However, additional findings have indicated a decline in fracture rate related to increased total content in the cavity (Fleming et al., 1998; Whitehead and Fleming, 2000), implying that medullary bone may play a beneficial role in the bone health of hens.

Medullary bone has been established to develop as early as 12–14 days preceding the first egg (Bloom et al., 1941; Miller, 1992; Turner et al., 1994), which is concomitant with the rise in E_2 produced by the ovary during early follicular development (Benoit and Clavert, 1945; Common et al., 1948; Simkiss, 1961; Senior, 1974; Tanabe et al., 1981; Johnson et al., 1986; Miller, 1992). However, a recent study has demonstrated that the rise in E_2 occurs at the time of age of first egg (AFE) in current commercial laying hens (Hanlon et al., 2021). Interestingly, this is further altered in broiler breeder hens, with the E_2 peak occurring 2 weeks after the AFE (Takeshima, 2018; Takeshima et al., 2019). Thus, rather than require the peak concentration of E_2, we hypothesize that there may be a threshold E_2 concentration that must be achieved to trigger the initiation of medullary bone formation.

As ERα mRNA is expressed in osteoblasts, binding to E_2 alters the morphology of these spindle-shaped cells and terminates the formation of structural bone while stimulating the initiation of medullary bone (Dacke et al., 1993, 2015). Simultaneously, osteoclasts are deactivated as they take on a cuboidal shape (Dacke et al., 2015). While PTH and $1,25(OH)_2D_3$ levels typically regulate osteoclasts, E_2 has been shown to indirectly influence the formation of this cell type (Oursler et al., 1991; Dacke et al., 1993). In mice models, E_2 regulates the formation of osteoclasts by inhibiting a protein kinase pathway, resulting in indirect inhibition of the PTH-stimulated formation (Kanatani et al., 1998). However, as E_2 also prevents apoptosis of osteocytes, this hormone supports the balance between the formation and resorption of bone during maturation (Tomkinson et al., 1998). Male quail treated with anti-estrogen displayed an elevation in the osteoclast population (Ohashi et al., 1987), suggesting that an inverse relationship between E_2 and osteoclast activity is conserved in poultry. Unlike osteoblasts, early studies determining the presence of ERs on the surface of osteoclasts led to conflicting reports in the literature (Ohashi et al., 1991; Oursler et al., 1991). However, it is now largely accepted that osteoclasts will not express either ER subtype (Ohashi et al., 1991). Presently, most evidence suggests that E_2 will play an indirect inhibitory role in bone resorption and a direct stimulatory role in bone formation (Oursler et al., 1991, 1993; Ali, 1992; Price and Russell, 1992; **Figure 4**).

In commercial laying hens, 2.2-g of calcium, or 10% of total calcium stores, is required for each eggshell (Nys et al., 1999; Bouvarel et al., 2011; Bain et al., 2016). While approximately 50% of this requirement can be covered by dietary calcium absorbed within the intestine daily (Kerschnitzki et al., 2014), about 33% is directly provided by the medullary bone (Bouvarel et al., 2011). Interestingly, this bone source stores ~12% of the total bone calcium content within the hen's body (Nys and le Roy, 2018). Since laying consists of active and inactive eggshell formation periods (Miller, 1977), medullary bone provides a source of calcium for the active shell formation, which primarily occurs during the scotophase (Clunies and Leeson, 1995). Specifically, the ovum reaches the shell gland ~5 h post-ovulation, with eggshell formation occurring between 7 and 20 h post-ovulation (van de Velde et al., 1984).

Osteocalcin (OC) is a major non-collagenous protein produced by osteoblasts (Ugar and Karaca, 1999) and used to evaluate bone remodelling (Christenson, 1997; Ugar and Karaca, 1999; Seibel, 2005). Studies have suggested that calcium in the bone matrix is bound by OC (Christenson, 1997). However, comparisons of brown and white laying strains unexpectedly showed that brown strains have higher OC levels while white strains have higher E_2 levels (Habig et al., 2021). This suggests that brown strains would have improved bone quality, despite the E_2 differences observed. This hypothesis was confirmed by several studies (Eusemann et al., 2018a; Jansen et al., 2020; Habig et al., 2021). Thus, elevated OC in brown strains (Habig et al., 2021) may explain the lower prevalence of keel bone deformities (Eusemann et al., 2018a). This has led to speculated strain differences regarding the proportion of calcium mobilized from each source to form the eggshell. Habig et al. (2021) suggested that brown laying strains mobilize a more significant proportion of calcium from the bone compared to white layers. In contrast, white strains were hypothesized to meet calcium requirements via intestinal absorption. This may partially explain the improved feed conversion rate in white versus brown strains (Jansen et al., 2020). In addition, while the

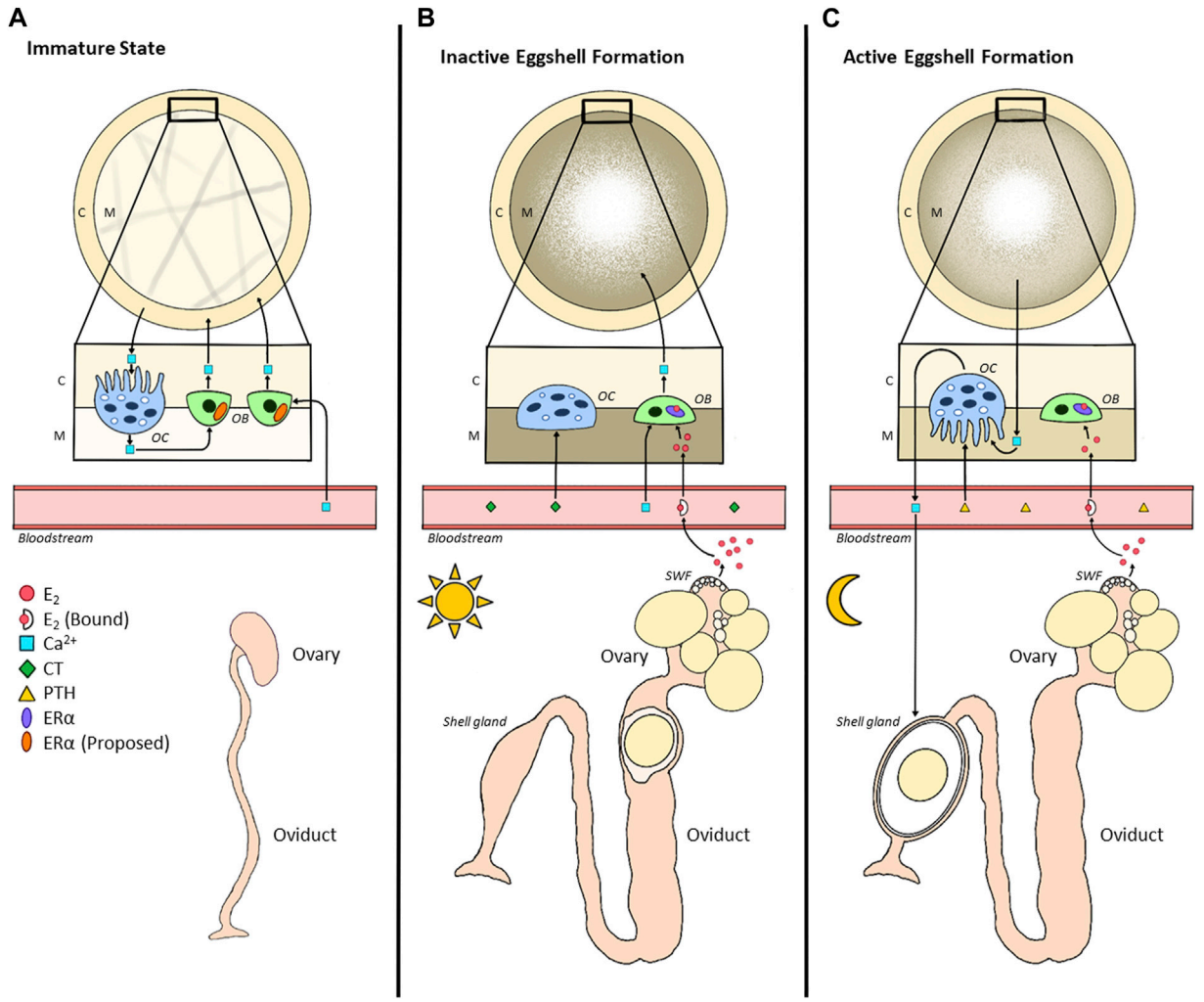

FIGURE 4 | Alterations in Bone Metabolism between Immature and Mature States of Hens. **(A)**. During the immature state (pullet), calcium (Ca^{2+}) is deposited by osteoblasts as cortical bone (C), serving as a structural source. Continuous bone remodelling occurs due to the resorptive capacity of osteoclasts. While the immature ovary produces very little E_2 during this time, we propose that osteoblasts already express ERα in the immature state. Once the hen reaches maturation **(B,C)**, in each 24-h egg formation cycle, there will be inactive and active eggshell formation. **(B)**. Inactive eggshell formation occurs when the egg is present in the early portion of the oviduct (infundibulum, magnum, isthmus), usually during photophase. During this time, E_2 enters the circulation where it binds to its carrier protein; a portion of free E_2 then enters the cavity of the bone to bind to ERα expressed in osteoblasts. This triggers a morphological alteration in the shape of the osteoblast, interrupting the formation of cortical bone, instead opting for the formation of medullary bone (M), a readily mobilizable storage site of calcium for eggshell development. Calcium homeostasis is regulated by calcitonin (CT) at this time, downregulating the activity of osteoblasts via morphological alterations. **(C)**. Active eggshell formation begins once the egg enters the shell gland (uterus), typically during scotophase. Therefore, due to the unavailability of dietary calcium, medullary bone undergoes resorption to provide the shell gland with calcium. The morphological alterations in osteoclasts are triggered by the upregulation of parathyroid hormone (PTH). Simultaneously, although E_2 binds to its receptor, the absence of additional calcium prevents the active formation of medullary bone at this time.

cumulative production was not found to differ between strains, the total proportion of eggshell was higher in white strains (Jansen et al., 2020), indicating that these hens may require more calcium for eggshell formation. Interestingly, while E_2 did not differ between strains during lay, prior to maturation at 17 weeks of age (woa), white strains were found to have significantly higher E_2 concentrations than the brown (Habig et al., 2021), possibly triggering a larger recruitment of calcium. This suggests that further studies are required to identify if there are differences in E_2 involvement during maturation and active lay between white and brown strains.

Calcium Homeostasis in the Aging Hen

Throughout the laying cycle, hens have been reported to undergo a progressive loss of mineralized structural bone (Webster, 2004). Previously, this was associated with declining E_2 as the hen ages, causing medullary bone accumulation to cease and a breakdown of the cortical bone to supply calcium for the eggshell (Yamada et al., 2021). In fact, this decrease in E_2 production coincides with the depletion of SWFs from the follicular pool, the associated decline in calcium availability for the shell formation, and slower follicular development, ultimately leading to the termination of lay. The depletion of medullary and cortical bone during the end

of lay led to concerns regarding hen health and welfare, along with diminishing egg quality for the breeder and table egg industries. However, intensive genetic selection for extended laying periods resulted in commercial layer breeds adapted to meet these demands without impacting bone or eggshell quality (Hanlon et al., 2021, 2022). In fact, our latest studies suggest that modern strains of layers display recurrent elevations in E_2 throughout a laying cycle. We hypothesize that this results in continuous stimulation of medullary bone formation, providing the hen with sufficient calcium storage to keep up with the demands of producing over 500 eggs in 100 weeks of life (Hanlon et al., 2021, 2022). Furthermore, these recurrent elevations in E_2 were positively correlated with medullary bone mineral density (BMD) and negatively correlated with cortical BMD, yet cortical bone thickness did not change between 12 and 100 woa. Meanwhile, eggshell thickness and breaking strength did decline over time but never below an acceptable grade A quality (Hanlon et al., 2022). This is partially attributed to the selection for maintained egg size during extended lay (Bouvarel et al., 2011), since it has been determined that a constant quantity of calcium will be supplied to the shell regardless of the weight of the egg (Roland, 1979; Buss, 1988). Thus, understanding the impact of these additional E_2 elevations will help understand the physiological needs associated with extended production cycles and adjust dietary calcium and Vitamin D accordingly to promote calcium uptake as the hen ages. As a matter of fact, current knowledge and guidelines, including NRC recommendations (NRC, 1994), may be outdated as it is based on reports that 1α-hydroxylase and intestinal calbindin production will decline with age contributing to the decline in Vitamin D metabolism (Abe et al., 1982; Joyner et al., 1987). However, as E_2 promotes the uptake of $1,25(OH)_2D_3$ within the digestive tract (Pfeiffer and Gardner, 1938), we propose that the unintended selection for recurrent E_2 peaks has likely resulted in better Vitamin D absorption and synthesis.

Calcium Tetany and Estradiol

Calcium tetany is a condition during which muscle weakness or even paralysis results from hypocalcemia (Turner and Debeer, 2009). While this is a common issue in commercial broiler breeder production systems, this disorder has been poorly characterized within the literature. It has been established that calcium tetany has similar outcomes to the well-described cage layer fatigue in layers, yet the timing of these conditions is vastly different. In the case of laying hens, this is an osteoporotic onset occurring at the end of the reproductive cycle and is typically associated with aging (Whitehead and Fleming, 2000). However, in broiler breeders, hens have been reported to exhibit these symptoms during sexual maturation up until the peak of lay, with a consequential spike in mortality observed (Turner and Debeer, 2009). Numerous management strategies have been recommended ranging from maximizing pullet uniformity to avoiding high calcium diets during the maturation period of breeders. This opposes the dietary recommendation in the laying hen industry, as a pre-lay diet is typically provided to these hens to slowly elevate calcium for the initial formation of the medullary bone ~10 days prior to the onset of lay. This pre-lay diet includes ~2% calcium, increasing to ~4% once hens reach 5% production and remaining constant through the active laying phase (Lohmann-Tierzucht, 2015). Interestingly, breeding companies like Aviagen have suggested that broiler breeder hens should not be provided with elevated dietary calcium until they reach ~5% production (Turner and Debeer, 2009).

The current literature has alluded that calcium regulation mechanisms initiated during sexual maturation are not responsive to higher calcium inclusion until the onset of lay has commenced (Turner and Debeer, 2009). In support of this hypothesis, studies in our laboratory identified that the initial E_2 peak in the laying hen occurs at the time of AFE (Hanlon et al., 2021). In contrast, this elevation in E_2 typically associated with sexual maturation occurred 2 weeks after the AFE in the broiler breeder hen (Takeshima, 2018; Takeshima et al., 2019). This could potentially explain the differing responsiveness to dietary calcium between laying hens and broiler breeders. As eggshell formation is initiated, calcium levels are depleted, resulting in a decline in PTH levels. This significantly reduces calcium excretion and increases $1,25(OH)_2D_3$ levels to stimulate calcium absorption (Pfeiffer and Gardner, 1938; Laverty and Clark, 1989). However, without an early elevation in E_2 to enhance $1,25(OH)_2D_3$ and calbindin receptors in the intestine, along with the morphological alterations to osteoblast and osteoclast activity, providing dietary calcium too early in broiler breeder hens will result in extreme calcium imbalances. Without the influences of E_2, calcium retention will not be able to compensate for the excretion rate. However, further studies are required to validate this hypothesis and understand the integration between E_2, AFE, and calcium supplementation to provide better management recommendations in broiler breeder hens.

Osteoporosis and Estradiol

Bone fractures and keel bone deviations have long been attributed to high rates of lay (Gregory and Wilkins, 1989; Rufener and Makagon, 2020), although the etiology of bone disorders has recently been an area of discussion (Jansen et al., 2020; Dunn et al., 2021). However, it is undisputed that keel bone fractures can occur in up to 97% of commercial laying flocks (Wilkins et al., 2011; Richards et al., 2012; Petrik et al., 2014; Heerkens et al., 2016). In laying hens, osteoporosis was previously associated with caged housing systems, hence its designation as cage layer fatigue (Grumbles, 1959). However, the onset of osteoporosis and declining bone quality is much more complex than simply being under the control of the environment. E_2 has been negatively associated with cortical BMD while positively correlated with medullary BMD (Hanlon et al., 2022), indicating that the onset of lay predisposes hens to the onset of osteoporosis. This is supported by evidence suggesting that medullary bone adds no structural integrity (Wilson and Thorp, 1998). Regardless, declining E_2 in the aging hen results in decreased calcium absorptive capacity, which leads to an overall negative association between E_2 and osteoporosis (Abe et al., 1982; Joyner et al., 1987). Altogether, these reports suggest the relationship between this hormone and metabolic condition may be much more complex. The sustained release of the GnRH

agonist, deslorelin acetate, diminishes the prevalence of keel bone damage at the expense of the laying cycle (Eusemann et al., 2018b). This supports the hypothesis that lower E_2 levels are critical for maintaining skeletal structure integrity (Beck and Hansen, 2004). However, this comes at the expense of egg production and is thus impractical for commercial production. Although research from the early 1960s suggested that bone fragility was induced by E_2-treatment, resulting in a thinner cortex (Urist and Deutsch, 1960), recent studies indicate that this may no longer be a primary concern (Hanlon et al., 2022).

Interestingly, osteoporosis has also been associated with obesity (Rosen and Bouxsein, 2006; Zhao et al., 2007). Specifically, visceral fat has been shown to play a detrimental role in the structural integrity of bone (Janicka et al., 2007; Gilsanz et al., 2009). This is consistent with the increased risk of developing osteoporosis under FLHS (Pardee et al., 2012; Yilmaz, 2012). Inducing FLHS via HELP diets results in upregulated bone turnover and detectable damage to skeletal integrity (Jiang et al., 2013). This suggests an additional link between the roles of E_2 on fat metabolism and bone development. As a matter of fact, the inclusion of long-term dietary lipids has been detrimental to bone remodelling (Liu et al., 2003, 2004), bone formation rate (Watkins et al., 1997), and bone mineral content (Liu et al., 2004). Specifically, OC alleviated liver damage caused by this high-lipid diet (Wu et al., 2021). OC levels are highest in the pullet phase, slowly declining to reach the lowest levels at the end of a laying cycle (Jiang et al., 2013; Nys and le Roy, 2018), thus displaying an inverse relationship with E_2 during maturation. Wu et al. (2021) proposed that OC can counteract the onset of FLHS in older laying hens. Taking that one step further, we hypothesize that the recurrent elevations in E_2 we reported (Hanlon et al., 2021) are key to sustaining extended reproduction and balancing the activation of bone and liver metabolism to support egg formation.

CONCLUSION

In conclusion, the involvement of E_2 in activating the reproductive axis, liver metabolism, and medullary bone formation demonstrates that this hormone contributes to and may coordinate all aspects of egg formation. However, while the success of the breeder and table egg industries is highly dependent on E_2, little research has considered the underlying endocrinological alterations responsible for improvements in laying rate. These effects are primarily mediated through ERα, resulting in the production of yolk proteins in the liver and the storage of calcium in the medullary bone while also coordinating their transport to the reproductive tract. However, by diverting nutrients and energy towards egg formation, E_2 can also contribute to the onset of metabolic disorders, such as FLHS and calcium tetany. Nonetheless, decades of genetic selection for egg production have impacted the patterns of E_2 production, which may have helped accommodate the further demands in modern strains of commercial laying hens. Interestingly, this may not be the case in broiler breeder hens undergoing selection for rapid growth, as a delay in the initial rise in E_2 is associated with calcium tetany during sexual maturation. Thus, it is apparent that rather than absolute concentrations, the timing of E_2 production is key to successful reproduction, which requires tight coordination with metabolic processes to prevent liver and skeletal damage. As ERs are present in several additional metabolic organs, including adipose and kidney in mammals, future investigations should consider the impact this hormone may have on the control of energy partitioning between growth and reproductive process, particularly during the preparation for lay.

AUTHOR CONTRIBUTIONS

CH was the primary author and performed most of the literature search. CZ contributed to the estradiol and reproduction section, created the figures, and participated in the redaction of all sections. GB participated in the redaction of all sections and supported CH throughout the project as the supervisor. All authors contributed to the article and approved the submitted version.

FUNDING

This review was in partly supported by funding from the Canada First Research Excellence Fund (Food from Thought - Agricultural Systems for a Healthy Planet), Egg Farmers of Canada, the Ontario Ministry of Agriculture and Rural Affairs (OMAFRA) Ontario Agri-Food Innovation Alliance Program (#UofG2018-3148) and the Natural Sciences and Engineering Research Council of Canada (NSERC CRDPJ program #CRDPJ543662-19).

REFERENCES

Abdelnabi, M. A., Richards, M. P., and Ottinger, M. A. (2001). Comparison of Gonadal Hormone Levels in Turkey Embryos Incubated in Long-Term Shell-Less Culture and in Ovo. *Poult. Sci.* 80, 666–669. doi:10.1093/ps/80.5.666

Abe, E., Horikawa, H., Masumura, T., Sugahara, M., Kubota, M., and Suda, T. (1982). Disorders of Cholecaiciferol Metabolism in Old Egg-Laying Hens. *J. Nutr.* 112, 436–446. doi:10.1093/jn/112.3.436

Acharya, K. D., and Veney, S. L. (2012). Characterization of the G-Protein-Coupled Membrane-Bound Estrogen Receptor GPR30 in the Zebra Finch Brain Reveals a Sex Difference in Gene and Protein Expression. *Devel Neurobio* 72, 1433–1446. doi:10.1002/dneu.22004

Adkins-Regan, E., Ottinger, M. A., and Park, J. (1995). Maternal Transfer of Estradiol to Egg Yolks Alters Sexual Differentiation of Avian Offspring. *J. Exp. Zool.* 271, 466–470. doi:10.1002/jez.1402710608

Adlercreutz, H. (1970). Oestrogen Metabolism in Liver Disease. *J. Endorcr.* 46, 129–163. doi:10.1677/joe.0.0460129

Ali, S. Y. (1992). "Matrix Formation and Mineralisation in Bone," in *Bone Biology and Skeletal Disorders in Poultry*. Editor C. C. Whitehead (Oxfordshire, UK: Carfax Publishing Co), 19–38.

Andrews, J. E., Smith, C. A., and Sinclair, A. H. (1997). Sites ofEstrogen ReceptorandAromataseExpression in the Chicken Embryo. *General Comp. Endocrinol.* 108, 182–190. doi:10.1006/gcen.1997.6978

Bain, M. M., Nys, Y., and Dunn, I. C. (2016). Increasing Persistency in Lay and Stabilising Egg Quality in Longer Laying Cycles. What Are the Challenges? *Br. Poult. Sci.* 57, 330–338. doi:10.1080/00071668.2016.1161727

Balnave, D. (1968). Influence of Dietary Linoleic Acid on Egg Fatty Acid Composition in Hens Deficient in Essential Fatty Acids. *J. Sci. Food Agric.* 19, 266–269. doi:10.1002/jsfa.2740190507

Balnave, D., and Pearce, J. (1974). Induction by Gonadal Hormones of Hepatic Lipogenic Enzyme Activity in Immature Pullets. *J. Endocrinol.* 61, 29–43. doi:10.1677/joe.0.0610029

Balnave, D. (1971). The Influence of Exogenous Oestrogens and the Attainment of Sexual Maturity on Fatty Acid Metabolism in the Immature Pullet. *Comp. Biochem. Physiology Part B Comp. Biochem.* 40, 189–197. doi:10.1016/0305-0491(71)90075-7

Bar, A. (2008). Calcium Homeostasis and Vitamin D Metabolism and Expression in Strongly Calcifying Laying Birds. *Comp. Biochem. Physiology Part A Mol. Integr. Physiology* 151, 477–490. doi:10.1016/j.cbpa.2008.07.006

Bar, A. (2009). Differential Regulation of Calbindin in the Calcium-Transporting Organs of Birds with High Calcium Requirements. *J. Poult. Sci.* 46, 267–285. doi:10.2141/jpsa.46.267

Barakat, R., Oakley, O., Kim, H., Jin, J., and Ko, C. J. (2016). Extra-gonadal Sites of Estrogen Biosynthesis and Function. *BMB Rep.* 49, 488–496. doi:10.5483/BMBRep.2016.49.9.141

Beaufrère, H. (2013). Atherosclerosis: Comparative Pathogenesis, Lipoprotein Metabolism, and Avian and Exotic Companion Mammal Models. *J. Exot. Pet Med.* 22, 320–335. doi:10.1053/j.jepm.2013.10.016

Beck, M. M., and Hansen, K. K. (2004). Role of Estrogen in Avian Osteoporosis. *Poult. Sci.* 83, 200–206. doi:10.1093/ps/83.2.200

Bédécarrats, G. Y., Baxter, M., and Sparling, B. (2016). An Updated Model to Describe the Neuroendocrine Control of Reproduction in Chickens. *General Comp. Endocrinol.* 227, 58–63. doi:10.1016/j.ygcen.2015.09.023

Bédécarrats, G. Y. (2015). Control of the Reproductive axis: Balancing Act between Stimulatory and Inhibitory Inputs. *Poult. Sci.* 94, 810–815. doi:10.3382/ps/peu042

Benoit, J., and Clavert, J. (1945). Role indispensable des parathyroids dans la calcification de l'osfolliculinque chez le canard domestique. *Cr. Seanc. Soc. Biol.* 139, 743.

Bensadoun, A., and Rothfeld, A. (1972). The Form of Absorption of Lipids in the Chicken, *Gallus domesticus*. *Exp. Biol. Med.* 141, 814–817. doi:10.3181/00379727-141-36878

Bentley, G. E., Perfito, N., Ukena, K., Tsutsui, K., and Wingfield, J. C. (2003). Gonadotropin-inhibitory Peptide in Song Sparrows (Melospiza Melodia) in Different Reproductive Conditions, and in House Sparrows (*Passer domesticus*) Relative to Chicken-Gonadotropin-Releasing Hormone. *J. Neuroendocrinol.* 15, 794–802. doi:10.1046/j.1365-2826.2003.01062.x

Bentley, G. E., Ubuka, T., McGuire, N. L., Chowdhury, V. S., Morita, Y., Yano, T., et al. (2008). Gonadotropin-inhibitory Hormone and its Receptor in the Avian Reproductive System. *General Comp. Endocrinol.* 156, 34–43. doi:10.1016/j.ygcen.2007.10.003

Bergink, E. W., and Wallace, R. A. (1974). Precursor-Product Relationship between Amphibian Vitellogenin and the Yolk Proteins, Lipovitellin and Phosvitin. *J. Biol. Chem.* 249, 2897–2903. doi:10.1016/s0021-9258(19)42715-4

Bloom, M. A., Domm, L. V., Nalbandov, A. V., and Bloom, W. (1958). Medullary Bone of Laying Chickens. *Am. J. Anat.* 102, 411–453. doi:10.1002/aja.1001020304

Bloom, W., Bloom, M. A., and McLean, F. C. (1941). Calcification and Ossification. Medullary Bone Changes in the Reproductive Cycle of Female Pigeons. *Anat. Rec.* 81, 443–475. doi:10.1002/ar.1090810404

Bouvarel, I., Nys, Y., and Lescoat, P. (2011). "Hen Nutrition for Sustained Egg Quality," in *Improving the Safety and Quality of Eggs and Egg Products, Vol 1: Egg Chemistry, Production and Consumption*. Editors Y. Nys, M. Bain, and F. van Immerseel (Cambridge, UK: Woodhead Publishing Ltd), 261–299. doi:10.1533/9780857093912.3.261

Bradfield, J. R. G. (1951). Radiographic Studies on the Formation of the Hen'S Egg Shell. *J. Exp. Biol.* 28, 125–140. doi:10.1242/jeb.28.2.125

Brady, L., Romsos, D. R., and Leveille, G. A. (1976). *In Vivo* Estimation of Fatty Acid Synthesis in the Chicken (Gallus Domesticus) Utilizing 3H2O. *Comp. Biochem. Physiology Part B Comp. Biochem.* 54, 403–407. doi:10.1016/0305-0491(76)90265-0

Braet, F., and Wisse, E. (2002). Structural and Functional Aspects of Liver Sinusoidal Endothelial Cell Fenestrae: A Review. *Comp. Hepatol.* 1, 1–17. doi:10.1186/1476-5926-1-1

Bragg, D. B., Sim, J. S., and Hodgson, G. C. (1973). Influence of Dietary Energy Source on Performance and Fatty Liver Syndrome in White Leghorn Laying Hens. *Poult. Sci.* 52, 736–740. doi:10.3382/ps.0520736

Brown, E. M. (1991). Extracellular Ca2+ Sensing, Regulation of Parathyroid Cell Function, and Role of Ca2+ and Other Ions as Extracellular (First) Messengers. *Physiol. Rev.* 71, 371–411. doi:10.1152/physrev.1991.71.2.371

Brunström, B., Axelsson, J., Mattsson, A., and Halldin, K. (2009). Effects of Estrogens on Sex Differentiation in Japanese Quail and Chicken. *General Comp. Endocrinol.* 163, 97–103. doi:10.1016/j.ygcen.2009.01.006

Buss, E. G. (1988). "Correlation of Egg Shell Weight with Egg Weight, Body Weight, and Percent Shell," in *Proceedings of the XVIII World's Poultry Congress*, 348–349. Available at: https://naldc.nal.usda.gov/download/CAT10414984/PDF (Accessed June 7, 2022).

Butler, E. J. (1976). Fatty Liver Diseases in the Domestic Fowl - A Review. *Avian Pathol.* 5, 1–14. doi:10.1080/03079457608418164

Calvo, F. O., and Bahr, J. M. (1983). Adenylyl Cyclase System of the Small Preovulatory Follicles of the Domestic Hen: Responsiveness to Follicle-Stimulating Hormone and Luteinizing Hormone 1. *Biol. Reproduction* 29, 542–547. doi:10.1095/biolreprod29.3.542

Calvo, F. O., Wang, S.-C., and Bahr, J. M. (1981). LH-stimulable Adenylyl Cyclase Activity during the Ovulatory Cycle in Granulosa Cells of the Three Largest Follicles and the Postovulatory Follicle of the Domestic Hen (*Gallus domesticus*). *Biol. Reproduction* 25, 805–812. doi:10.1095/biolreprod25.4.805

Camacho-Arroyo, I., González-Arenas, A., González-Agüero, G., Guerra-Araiza, C., and González-Morán, G. (2003). "Changes in the Content of Progesterone Receptor Isoforms and Estrogen Receptor Alpha in the Chick Brain during Embryonic Development," in *Comparative Biochemistry and Physiology - A Molecular and Integrative Physiology* (Elsevier), 136, 447–452. doi:10.1016/S1095-6433(03)00204-6*Comp. Biochem. Physiology Part A Mol. Integr. Physiology*

Chan, C. Z., Sato, K., and Shimada, Y. (1990). Three-dimensional Electron Microscopy of the Sarcoplasmic Reticulum and T-System in Embryonic Chick Skeletal Muscle Cells *In Vitro*. *Protoplasma* 154, 112–121. doi:10.1007/bf01539838

Chapman, M. J., Goldstein, S., and Laudat, M.-H. (1977). Characterization and Comparative Aspects of the Serum Very Low and Low Density Lipoproteins and Their Apoproteins in the Chicken (*Gallus domesticus*). *Biochemistry* 16, 3006–3015. doi:10.1021/bi00632a031

Chen, L.-R., Lee, S.-C., Lin, Y.-P., Hsieh, Y.-L., Chen, Y.-L., Yang, J.-R., et al. (2010). Prostaglandin-D Synthetase Induces Transcription of the LH Beta Subunit in the Primary Culture of Chicken Anterior Pituitary Cells via the PPAR Signaling Pathway. *Theriogenology* 73, 367–382. doi:10.1016/j.theriogenology.2009.09.020

Christenson, R. H. (1997). Biochemical Markers of Bone Metabolism: An Overview. *Clin. Biochem.* 30, 573–593. doi:10.1016/s0009-9120(97)00113-6

Ciccone, N. A., Dunn, I. C., Boswell, T., Tsutsui, K., Ubuka, T., Ukena, K., et al. (2004). Gonadotrophin Inhibitory Hormone Depresses Gonadotrophin Alpha and Follicle-Stimulating Hormone Beta Subunit Expression in the Pituitary of the Domestic Chicken. *J. Neuroendocrinol.* 16, 999–1006. doi:10.1111/j.1365-2826.2005.01260.x

Clemens, T. L., Garrett, K. P., Zhou, X.-Y., Pike, J. W., Haussler, M. R., and Dempster, D. W. (1988). Immunocytochemical Localization of the 1,25-Dihydroxyvitamin D3Receptor in Target Cells*. *Endocrinology* 122, 1224–1230. doi:10.1210/endo-122-4-1224

Clunies, M., and Leeson, S. (1995). Effect of Dietary Calcium Level on Plasma Proteins and Calcium Flux Occurring during a 24 H Ovulatory Cycle. *Can. J. Anim. Sci.* 75, 439–444. doi:10.4141/cjas95-064

Cochrane, A. W., and Deeley, R. G. (1988). Estrogen-dependent Activation of the Avian Very Low Density Apolipoprotein II and Vitellogenin Genes. *J. Mol. Biol.* 203, 555–567. doi:10.1016/0022-2836(88)90192-1

Codina-Salada, J., Moore, J. P., and Chan, L. (1983). Kinetics of Primary and Secondary Stimulation of the mRNA for Apovldl-II, a Major Yolk Protein, in the Cockerel Liver by Estrogen. *Endocrinology* 113, 1158–1160. doi:10.1210/endo-113-3-1158

Common, R. H., Rutledge, W. A., and Hale, R. W. (1948). Observations on the Mineral Metabolism of Pullets: VIII. The Influence of Gonadal Hormones on Retention of Calcium and Phosphorus. *J. Agric. Sci.* 38, 64–80. doi:10.1017/s0021859600005153

Corradino, R. A., Wasserman, R. H., Pubols, M. H., and Chang, S. I. (1968). Vitamin D3 Induction of a Calcium-Binding Protein in the Uterus of the Laying Hen. *Archives Biochem. Biophysics* 125, 378–380. doi:10.1016/0003-9861(68)90674-7

Coty, W. A. (1980). A Specific, High Affinity Binding Protein for 1α,25-Dihydroxy Vitamin D in the Chick Oviduct Shell Gland. *Biochem. Biophysical Res. Commun.* 93, 285–292. doi:10.1016/s0006-291x(80)80278-6

Couch, J. R. (1956). Fatty Livers in Laying Hens - a Condition Which May Occur as a Result of Increased Strain. *Feedstuffs* 28, 46–53.

Cui, H., Zhao, G., Liu, R., Zheng, M., Chen, J., and Wen, J. (2012). FSH Stimulates Lipid Biosynthesis in Chicken Adipose Tissue by Upregulating the Expression of its Receptor FSHR. *J. Lipid Res.* 53, 909–917. doi:10.1194/jlr.M025403

Cui, J., Shen, Y., and Li, R. (2013). Estrogen Synthesis and Signaling Pathways during Aging: From Periphery to Brain. *Trends Mol. Med.* 19, 197–209. doi:10.1016/j.molmed.2012.12.007

Cui, Z., Amevor, F. K., Feng, Q., Kang, X., Song, W., Zhu, Q., et al. (2020). Sexual Maturity Promotes Yolk Precursor Synthesis and Follicle Development in Hens via Liver-Blood-Ovary Signal axis. *Animals* 10, 1–14. doi:10.3390/ani10122348

Cutting, A. D., Ayers, K., Davidson, N., Oshlack, A., Doran, T., Sinclair, A. H., et al. (2014). Identification, Expression, and Regulation of Anti-müllerian Hormone Type-II Receptor in the Embryonic Chicken Gonad. *Biol. Reprod.* 90, 106–112. doi:10.1095/biolreprod.113.116491

Dacke, C. G., Arkle, S., Cook, D. J., Wormstone, I. M., Jones, S., Zaidi, M., et al. (1993). Medullary Bone and Avian Calcium Regulation. *J. Exp. Biol.* 184, 63–88. doi:10.1242/jeb.184.1.63

Dacke, C. G. (1979). *Calcium Regulation in Sub-mammalian Vertebrates*. London, UK: Academic Press.

Dacke, C. G., Sugiyama, T., and Gay, C. V. (2015). "The Role of Hormones in the Regulation of Bone Turnover and Eggshell Calcification," in *Sturkie's Avian Physiology* (London, UK: Academic Press), 549–575. doi:10.1016/b978-0-12-407160-5.00025-7

Dashti, N., Kelley, J. L., Thayer, R. H., and Ontko, J. A. (1983). Concurrent Inductions of Avian Hepatic Lipogenesis, Plasma Lipids, and Plasma Apolipoprotein B by Estrogen. *J. Lipid Res.* 24, 368–380. doi:10.1016/s0022-2275(20)37977-3

Deeley, R. G., Gordon, J. I., Burns, A. T., Mullinix, K. P., Binastein, M., and Goldberg, R. F. (1977). Primary Activation of the Vitellogenin Gene in the Rooster. *J. Biol. Chem.* 252, 8310–8319. doi:10.1016/s0021-9258(17)40972-0

Deeley, R., Mullinix, D., Wetekam, W., Kronenberg, H., Meyers, M., Eldridge, J., et al. (1975). Vitellogenin Synthesis in the Avian Liver. Vitellogenin Is the Precursor of the Egg Yolk Phosphoproteins. *J. Biol. Chem.* 250, 9060–9066. doi:10.1016/s0021-9258(19)40693-5

Deluca, H. F. (2004). Overview of General Physiologic Features and Functions of Vitamin D. *Am. J. Clin. Nutr.* 80, 1689S–96S. doi:10.1093/ajcn/80.6.1689S

Deluca, H. F. (1980). William C. Rose Lectureship in Biochemistry and Nutrition. Some New Concepts Emanating from a Study of the Metabolism and Function of Vitamin D. *Nutr. Rev.* 38, 169–182. doi:10.1111/j.1753-4887.1980.tb05887.x

DeLuca, H. F. (1976). Metabolism of Vitamin D: Current Status. *Am. J. Clin. Nutr.* 29, 1258–1270. doi:10.1093/ajcn/29.11.1258

DeLuca, H. F. (1974). Vitamin D: The Vitamin and the Hormone. *Ref. Proc.* 33, 2211–2219.

Drummond, A. E., and Fuller, P. J. (2010). The Importance of ERβ Signalling in the Ovary. *J. Endocrinol.* 205, 15–23. doi:10.1677/JOE-09-0379

Dunn, I. C., de Koning, D.-J., McCormack, H. A., Fleming, R. H., Wilson, P. W., Andersson, B., et al. (2021). No Evidence that Selection for Egg Production Persistency Causes Loss of Bone Quality in Laying Hens. *Genet. Sel. Evol.* 53, 1–13. doi:10.1186/s12711-021-00603-8

Dunn, I., Lewis, P., Wilson, P., and Sharp, P. (2003). Acceleration of Maturation of FSH and LH Responses to Photostimulation in Prepubertal Domestic Hens by Oestrogen. *Reproduction* 126, 217–225. doi:10.1530/rep.0.1260217

Elbrecht, A., and Smith, R. G. (1992). Aromatase Enzyme Activity and Sex Determination in Chickens. *Science* 255, 467–470. doi:10.1126/science.1734525

Elf, P. K., and Fivizzani, A. J. (2002). Changes in Sex Steroid Levels in Yolks of the Leghorn chicken,*Gallus domesticus*, during Embryonic Development. *J. Exp. Zool.* 293, 594–600. doi:10.1002/jez.10169

Elnager, S., and Abd-Elhady, A. (2009). Exogenous Estradiol: Productive and Reproductive Performance and Physiological Profile of Japanese Quail Hens. *Int. J. Poult. Sci.* 8, 634–641. doi:10.3923/ijps.2009.634.641

Emmen, J. M. A., Couse, J. F., Elmore, S. A., Yates, M. M., Kissling, G. E., and Korach, K. S. (2005). *In Vitro* Growth and Ovulation of Follicles from Ovaries of Estrogen Receptor (ER)α and ERβ Null Mice Indicate a Role for ERβ in Follicular Maturation. *Endocrinology* 146, 2817–2826. doi:10.1210/en.2004-1108

Etches, R. J. (1987). Calcium Logistics in the Laying Hen. *J. Nutr.* 117, 619–628. doi:10.1093/jn/117.3.619

Etches, R., and Kagami, H. (1997). "Genotypic and Phenotypic Sex Reversal," in *Perspectives in Avian Endocrinology*. Editors S. Harvey and R. Etches (Bristol: Journal of Endocrinology Ltd), 57–67.

Eusemann, B. K., Baulain, U., Schrader, L., Thöne-Reineke, C., Patt, A., and Petow, S. (2018a). Radiographic Examination of Keel Bone Damage in Living Laying Hens of Different Strains Kept in Two Housing Systems. *PLoS ONE* 13, e0194974–17. doi:10.1371/journal.pone.0194974

Eusemann, B. K., Sharifi, A. R., Patt, A., Reinhard, A.-K., Schrader, L., Thöne-Reineke, C., et al. (2018b). Influence of a Sustained Release Deslorelin Acetate Implant on Reproductive Physiology and Associated Traits in Laying Hens. *Front. Physiol.* 9, 1–11. doi:10.3389/fphys.2018.01846

Evans, M. I., O'Malley, P. J., Krust, A., and Burch, J. B. (1987). Developmental Regulation of the Estrogen Receptor and the Estrogen Responsiveness of Five Yolk Protein Genes in the Avian Liver. *Proc. Natl. Acad. Sci. U.S.A.* 84, 8493–8497. doi:10.1073/pnas.84.23.8493

Evans, M. I., Silva, R., and Burch, J. B. (1988). Isolation of Chicken Vitellogenin I and III cDNAs and the Developmental Regulation of Five Estrogen-Responsive Genes in the Embryonic Liver. *Genes Dev.* 2, 116–124. doi:10.1101/gad.2.1.116

Filardo, E. J., Quinn, J. A., Bland, K. I., Frackelton, A. R., and Williams, R. (2000). Estrogen-Induced Activation of Erk-1 and Erk-2 Requires the G Protein-Coupled Receptor Homolog, GPR30, and Occurs via Trans-activation of the Epidermal Growth Factor Receptor through Release of HB-EGF. *Mol. Endocrinol.* 14, 1649–1660. doi:10.1210/mend.14.10.0532

Fleming, R. H., McCormack, H. A., Mcteir, L., and Whitehead, C. C. (1998). Medullary Bone and Humeral Breaking Strength in Laying Hens. *Res. Veterinary Sci.* 64, 63–67. doi:10.1016/s0034-5288(98)90117-5

Flouriot, G., Pakdel, F., and Valotaire, Y. (1996). Transcriptional and Post-transcriptional Regulation of Rainbow Trout Estrogen Receptor and Vitellogenin Gene Expression. *Mol. Cell. Endocrinol.* 124, 173–183. doi:10.1016/s0303-7207(96)03960-3

Fraser, R., Day, W. A., and Fernando, N. S. (1986). Review: the Liver Sinusoidal Cells. Their Role in Disorders of the Liver, Lipoprotein Metabolism and Atherogenesis. *Pathology* 18, 5–11. doi:10.3109/00313028609090821

Furr, B. J. A., Bonney, R. C., England, R. J., and Cunningham, F. J. (1973). Luteinizing Hormone and Progesterone in Peripheral Blood during the Ovulatory Cycle of the Hen Gallus Domesticus. *J. Endocrinol.* 57, 159–169. doi:10.1677/joe.0.0570159

Gasc, J.-M., and Baulieu, E.-E. (1988). Regulation by Estradiol of the Progesterone Receptor in the Hypothalamus and Pituitary: An Immunohistochemical Study in the Chicken. *Endocrinology* 122, 1357–1365. doi:10.1210/endo-122-4-1357

Ge, C., Yu, M., and Zhang, C. (2012). G Protein-Coupled Receptor 30 Mediates Estrogen-Induced Proliferation of Primordial Germ Cells via EGFR/Akt/β-Catenin Signaling Pathway. *Endocrinology* 153, 3504–3516. doi:10.1210/en.2012-1200

Gilsanz, V., Chalfant, J., Mo, A. O., Lee, D. C., Dorey, F. J., and Mittelman, S. D. (2009). Reciprocal Relations of Subcutaneous and Visceral Fat to Bone

Structure and Strength. *J. Clin. Endocrinol. Metabolism* 94, 3387–3393. doi:10.1210/jc.2008-2422

Gray, R. W., Omdahl, J. L., Ghazarian, J. G., and DeLuca, H. F. (1972). 25-Hydroxycholecalciferol-1-hydroxylase. *J. Biol. Chem.* 247, 7528–7532. doi:10.1016/s0021-9258(19)44557-2

Gregory, N. G., and Wilkins, L. J. (1989). Broken Bones in Domestic Fowl: Handling and Processing Damage in End-of-lay Battery Hens. *Br. Poult. Sci.* 30, 555–562. doi:10.1080/00071668908417179

Griffin, C., Flouriot, G., Sonntag-buck, V., and Gannon, F. (1999). Two Functionally Different Protein Isoforms Are Produced from the Chicken Estrogen Receptor-α Gene. *Mol. Endocrinol.* 13, 1571–1587. doi:10.1210/mend.13.9.0336

Griffin, H. D., and Perry, M. M. (1985). Exclusion of Plasma Lipoproteins of Intestinal Origin from Avian Egg Yolk Because of Their Size. *Comp. Biochem. Physiology Part B Comp. Biochem.* 82, 321–325. doi:10.1016/0305-0491(85)90248-2

Griffin, H., Grant, G., and Perry, M. (1982). Hydrolysis of Plasma Triacylglycerol-Rich Lipoproteins from Immature and Laying Hens (*Gallus domesticus*) by Lipoprotein Lipase *In Vitro*. *Biochem. J.* 206, 647–654. doi:10.1042/bj2060647

Griffin, H. P. (1981). Plasma Very Low Density Lipoproteins (VLDL) in Immature and Laying Hens (*Gallus domesticus*). *Biochem. Soc. Trans.* 155, 1. doi:10.1042/bst009155p

Gruber, M., Bos, E. S., and Ab, G. (1976). Hormonal Control of Vitellogenin Synthesis in Avian Liver. *Mol. Cell. Endocrinol.* 5, 41–50. doi:10.1016/0303-7207(76)90069-1

Grumbles, L. C. (1959). Cage Layer Fatigue (Cage Paralysis). *Avian Dis.* 3, 122–125. doi:10.2307/1587714

Habig, C., Weigend, A., Baulain, U., Petow, S., and Weigend, S. (2021). Influence of Age and Phylogenetic Background on Blood Parameters Associated with Bone Metabolism in Laying Hens. *Front. Physiol.* 12, 1–9. doi:10.3389/fphys.2021.678054

Hadinia, S. H., Carneiro, P. R. O., Fitzsimmons, C. J., Bédécarrats, G. Y., and Zuidhof, M. J. (2020). Post-photostimulation Energy Intake Accelerated Pubertal Development in Broiler Breeder Pullets. *Poult. Sci.* 99, 2215–2229. doi:10.1016/j.psj.2019.11.065

Haghighi-Rad, F., and Polin, D. (1982). Lipid Alleviates Fatty Liver Hemorrhagic Syndrome. *Poult. Sci.* 61, 2465–2472. doi:10.3382/ps.0612465

Haghighi-Rad, F., and Polin, D. (1981). The Relationship of Plasma Estradiol and Progesterone Levels to the Fatty Liver Hemorrhagic Syndrome in Laying Hens ,. *Poult. Sci.* 60, 2278–2283. doi:10.3382/ps.0602278

Hanke, H., Hanke, S., Bruck, B., Brehme, U., Gugel, N., Finking, G., et al. (1996). Inhibition of the Protective Effect of Estrogen by Progesterone in Experimental Atherosclerosis. *Atherosclerosis* 121, 129–138. doi:10.1016/0021-9150(95)05710-2

Hanlon, C., Ramachandran, R., Zuidhof, M. J., and Bédécarrats, G. Y. (2020). Should I Lay or Should I Grow: Photoperiodic versus Metabolic Cues in Chickens. *Front. Physiol.* 11, 707–724. doi:10.3389/fphys.2020.00707

Hanlon, C., Takeshima, K., and Bédécarrats, G. Y. (2021). Changes in the Control of the Hypothalamic-Pituitary Gonadal Axis across Three Differentially Selected Strains of Laying Hens (Gallus gallus Domesticus). *Front. Physiol.* 12, 1–20. doi:10.3389/fphys.2021.651491

Hanlon, C., Takeshima, K., Kiarie, E. G., and Bédécarrats, G. Y. (2022). Bone and Eggshell Quality throughout an Extended Laying Cycle in Three Strains of Layers Spanning 50 Years of Selection. *Poult. Sci.* 101, 101672. doi:10.1016/j.psj.2021.101672

Hansen, K., Kittok, R., Sarath, G., Toombs, C., Caceres, N., and Beck, M. (2003). Estrogen Receptor-Alpha Populations Change with Age in Commercial Laying Hens. *Poult. Sci.* 82, 1624–1629. doi:10.1093/ps/82.10.1624

Hansen, R. J., and Walzem, R. L. (1993). Avian Fatty Liver Hemorrhagic Syndrome: a Comparative Review. *Adv. Vet. Sci. Comp. Med.* 37, 451–468.

Harms, R. H., Costa, P. T., and Miles, R. D. (1982). Daily Feed Intake and Performance of Laying Hens Grouped According to Their Body Weight. *Poult. Sci.* 61, 1021–1024. doi:10.3382/ps.0611021

Harms, R. H., Roland, D. A., and Simpson, C. F. (1977). Experimentally Induced "Fatty Liver Syndrome" Condition in Laying Hens. *Poult. Sci.* 56, 517–520. doi:10.3382/ps.0560517

Hartmann, C., Johansson, K., Strandberg, E., and Rydhmer, L. (2003). Genetic Correlations between the Maternal Genetic Effect on Chick Weight and the Direct Genetic Effects on Egg Composition Traits in a White Leghorn Line. *Poult. Sci.* 82, 1–8. doi:10.1093/ps/82.1.1

Hasegawa, S., Sato, K., Hikami, Y., and Mizuno, T. (1980). Effect of Estrogen on Adipose Tissue Accumulation in Chicks, with Reference to Changes in its Chemical Composition and Lipase Activity. *Nihon Chikusan Gakkaiho* 51, 360–367. doi:10.2508/chikusan.51.360

Haussler, M. R. (1974). Vitamin D: Mode of Action and Biomedical Applications. *Nutr. Rev.* 32, 257–266. doi:10.1111/j.1753-4887.1974.tb00970.x

Haussler, M. R. (1986). Vitamin D Receptors: Nature and Function. *Annu. Rev. Nutr.* 6, 527–562. doi:10.1146/annurev.nu.06.070186.002523

Hawkins, R. A., Heald, P. J., and Taylor, P. (1969). The Uptake of (6,7-3H) 17β-Oestradiol by Tissues of the Domestic Fowl during an Ovulation Cycle. *Acta Endocrinol.* 60, 210–215. doi:10.1530/acta.0.0600210

Heerkens, J. L. T., Delezie, E., Rodenburg, T. B., Kempen, I., Zoons, J., Ampe, B., et al. (2016). Risk Factors Associated with Keel Bone and Foot Pad Disorders in Laying Hens Housed in Aviary Systems. *Poult. Sci.* 95, 482–488. doi:10.3382/ps/pev339

Hemsell, D. L., Grodin, J. M., Brenner, P. F., Siiteri, P. K., and Macdonald, P. C. (1974). Plasma Precursors of Estrogen. II. Correlation of the Extent of Conversion of Plasma Androstenedione to Estrone with Age1. *J. Clin. Endocrinol. Metabolism* 38, 476–479. doi:10.1210/jcem-38-3-476

Hermier, D. (1997). Lipoprotein Metabolism and Fattening in Poultry. *J. Nutr.* 127, 805–808. doi:10.1093/jn/127.5.805s

Hermier, D., Rousselot-Pailley, D., Peresson, R., and Sellier, N. (1994). Influence of Orotic Acid and Estrogen on Hepatic Lipid Storage and Secretion in the Goose Susceptible to Liver Steatosis. *Biochimica Biophysica Acta (BBA) - Lipids Lipid Metabolism* 1211, 97–106. doi:10.1016/0005-2760(94)90143-0

Hrabia, A. (2015). Growth Hormone Production and Role in the Reproductive System of Female Chicken. *General Comp. Endocrinol.* 220, 112–118. doi:10.1016/j.ygcen.2014.12.022

Hrabia, A., Paczoska-Eliasiewicz, H., and Rząsa, J. (2004). Effect of Prolactin on Estradiol and Progesterone Secretion by Isolated Chicken Ovarian Follicles. *folia Biol. (krakow)* 52, 197–203. doi:10.3409/1734916044527494

Hrabia, A., Wilk, M., and Rząsa, J. (2008). Expression of α and β Estrogen Receptors in the Chicken Ovary. *folia Biol. (krakow)* 56, 187–191. doi:10.3409/fb.56_3-4.187-191

Hsueh, A. J. W., Peck, E. J., and Clark, J. H. (1976). Control of Uterine Estrogen Receptor Levels by Progesterone. *Endocrinology* 98, 438–444. doi:10.1210/endo-98-2-438

Hurwitz, S., and Bar, A. (1965). Absorption of Calcium and Phosphorus along the Gastrointestinal Tract of the Laying Fowl as Influenced by Dietary Calcium and Egg Shell Formation. *J. Nutr.* 86, 433–438. doi:10.1093/jn/86.4.433

Hurwitz, S. (1989). "Parathyroid Hormone," in *Vertebrate Endocrinology: Fundamentals and Biomedical Implications*. Editors P. K. T. Pang and M. P. Schreibman (New York, USA: Academic Press), 45–77.

Husbands, D. R. (1972). The Distribution of Lipoprotein Lipase in Tissues of the Domestic Fowl and the Effects of Feeding and Starving. *Br. Poult. Sci.* 13, 85–90. doi:10.1080/00071667208415919

Hutz, R. J. (1989). Disparate Effects of Estrogens on *In Vitro* Steroidogenesis by Mammalian and Avian Granulosa Cells1. *Biol. Reproduction* 40, 709–713. doi:10.1095/biolreprod40.4.709

Ikemoto, T., and Park, M. K. (2005). Chicken RFamide-Related Peptide (GnIH) and Two Distinct Receptor Subtypes: Identification, Molecular Characterization, and Evolutionary Considerations. *J. Reproduction Dev.* 51, 359–377. doi:10.1262/jrd.16087

Imamura, T., Sugiyama, T., and Kusuhara, S. (2006). Expression and Localization of Estrogen Receptors Alpha and Beta mRNA in Medullary Bone of Laying Hens. *Anim. Sci. J.* 77, 223–229. doi:10.1111/j.1740-0929.2006.00341.x

Ishimaru, Y., Komatsu, T., Kasahara, M., Katoh-Fukui, Y., Ogawa, H., Toyama, Y., et al. (2008). Mechanism of Asymmetric Ovarian Development in Chick Embryos. *Development* 135, 677–685. doi:10.1242/dev.012856

Isola, J. J. (1990). Distribution of Estrogen and Progesterone Receptors and Steroid-Regulated Gene Products in the Chick Oviduct. *Mol. Cell. Endocrinol.* 69, 235–243. doi:10.1016/0303-7207(90)90017-3

Jacob, J., and Pescatore, T. (2013). *Avian Skeletal System*. Lexington, KY: Cooperative Extension Service University of Kentucky College of Agriculture, Food and Environment, 1–2. Available at: www.ca.uky.edu.

Jande, S. S., Tolnai, S., and Lawson, D. E. M. (1981). Immunohistochemical Localization of Vitamin D-dependent Calcium-Binding Protein in

Duodenum, Kidney, Uterus and Cerebellum of Chickens. *Histochemistry* 71, 99–116. doi:10.1007/bf00592574

Janicka, A., Wren, T. A. L., Sanchez, M. M., Dorey, F., Kim, P. S., Mittelman, S. D., et al. (2007). Fat Mass Is Not Beneficial to Bone in Adolescents and Young Adults. *J. Clin. Endocrinol. Metabolism* 92, 143–147. doi:10.1210/jc.2006-0794

Jansen, S., Baulain, U., Habig, C., Weigend, A., Halle, I., Scholz, A. M., et al. (2020). Correction: Jansen, S., et al. Relationship between Bone Stability and Egg Production in Genetically Divergent Chicken Layer Lines. Animals 2020, 10, 850. *Animals* 10, 2355–5. doi:10.3390/ani10122355

Jaussi, A. W., Newcomer, W. S., and Thayer, R. H. (1962). Hyperlipemic Effect of ACTH Injections in the Chicken. *Poult. Sci.* 41, 528–532. doi:10.3382/ps.0410528

Jiang, S., Cheng, H. W., Cui, L. Y., Zhou, Z. L., and Hou, J. F. (2013). Changes of Blood Parameters Associated with Bone Remodeling Following Experimentally Induced Fatty Liver Disorder in Laying Hens. *Poult. Sci.* 92, 1443–1453. doi:10.3382/ps.2012-02800

Jiang, Z., Yang, Z., Zhang, H., Yao, Y., and Ma, H. (2021). Genistein Activated Adenosine 5′-Monophosphate-Activated Protein Kinase-Sirtuin1/peroxisome Proliferator-Activated Receptor γ Coactivator-1α Pathway Potentially through Adiponectin and Estrogen Receptor β Signaling to Suppress Fat Deposition in Broiler Chickens. *Poult. Sci.* 100, 246–255. doi:10.1016/j.psj.2020.10.013

Jin, K., Zuo, Q., Song, J., Zhang, Y., Chen, G., and Li, B. (2020). CYP19A1 (Aromatase) Dominates Female Gonadal Differentiation in Chicken (Gallus gallus) Embryos Sexual Differentiation. *Biosci. Rep.* 40, 1–10. doi:10.1042/BSR20201576

Johnson, A. L., Bridgham, J. T., and Jensen, T. (1999). Bcl-Xlong Protein Expression and Phosphorylation in Granulosa Cells1. *Endocrinology* 140, 4521–4529. doi:10.1210/endo.140.10.7022

Johnson, A. L., and Bridgham, J. T. (2001). Regulation of Steroidogenic Acute Regulatory Protein and Luteinizing Hormone Receptor Messenger Ribonucleic Acid in Hen Granulosa Cells*. *Endocrinology* 142, 3116–3124. doi:10.1210/endo.142.7.8240

Johnson, A. L., Bridgham, J. T., Witty, J. P., and Tilly, J. L. (1996). Susceptibility of Avian Ovarian Granulosa Cells to Apoptosis Is Dependent upon Stage of Follicle Development and Is Related to Endogenous Levels of Bcl-Xlong Gene Expression. *Endocrinology* 137, 2059–2066. doi:10.1210/endo.137.5.8612548

Johnson, A. L. (2003). Intracellular Mechanisms Regulating Cell Survival in Ovarian Follicles. *Animal Reproduction Sci.* 78, 185–201. doi:10.1016/S0378-4320(03)00090-3

Johnson, A. L. (1993). Regulation of Follicle Differentiation by Gonadotropins and Growth Factors. *Poult. Sci.* 72, 867–873. doi:10.3382/ps.0720867

Johnson, A. L., and van Tienhoven, A. (1981). Hypothalamo-Hypophyseal Sensitivity to Hormones in the Hen. II. Plasma Concentrations of LH, Progesterone, and Testosterone in Response to Peripheral and Central Injections of LHRH or Testosterone. *Biol. Reproduction* 25, 153–161. doi:10.1095/biolreprod25.1.153

Johnson, A. L., and van Tienhoven, A. (1980). Plasma Concentrations of Six Steroids and LH during the Ovulatory Cycle of the Hen, *Gallus domesticus*1. *Biol. Reproduction* 23, 386–393. doi:10.1095/biolreprod23.2.386

Johnson, P. A., Dickerman, R. W., and Bahr, J. M. (1986). Decreased Granulosa Cell Luteinizing Hormone Sensitivity and Altered Thecal Estradiol Concentration in the Aged Hen, Gallus Domesticus1. *Biol. Reproduction* 35, 641–646. doi:10.1095/biolreprod35.3.641

Joyner, C. J., Peddie, M. J., and Taylor, T. G. (1987). The Effect of Age on Egg Production in the Domestic Hen. *General Comp. Endocrinol.* 65, 331–336. doi:10.1016/0016-6480(87)90117-1

Kagami, H., and Hanada, H. (1997). Current Knowledge of Sexual Differentiation in Domestic Fowl. *World's Poult. Sci. J.* 53, 111–123. doi:10.1079/wps19970012

Kamiyoshi, M., Niwa, T., and Tanaka, K. (1986). Nuclear Estrogen Receptor Bindings in Granulosa Cells and Estradiol-17β Contents in Follicular Membranes of the Ovary of the Hen during the Ovulatory Cycle. *General Comp. Endocrinol.* 61, 428–435. doi:10.1016/0016-6480(86)90229-7

Kanatani, M., Sugimoto, T., Takahashi, Y., Kaji, H., Kitazawa, R., and Chihara, K. (1998). Estrogen via the Estrogen Receptor Blocks cAMP-Mediated Parathyroid Hormone (PTH)-stimulated Osteoclast Formation. *J. Bone Min. Res.* 13, 854–862. doi:10.1359/jbmr.1998.13.5.854

Kebreab, E., France, J., Kwakkel, R. P., Leeson, S., Kuhi, H. D., and Dijkstra, J. (2009). Development and Evaluation of a Dynamic Model of Calcium and Phosphorus Flows in Layers. *Poult. Sci.* 88, 680–689. doi:10.3382/ps.2008-00157

Kerschnitzki, M., Zander, T., Zaslansky, P., Fratzl, P., Shahar, R., and Wagermaier, W. (2014). Rapid Alterations of Avian Medullary Bone Material during the Daily Egg-Laying Cycle. *Bone* 69, 109–117. doi:10.1016/j.bone.2014.08.019

Keshavarz, K. (1998). Investigation on the Possibility of Reducing Protein, Phosphorus, and Calcium Requirements of Laying Hens by Manipulation of Time of Access to These Nutrients. *Poult. Sci.* 77, 1320–1332. doi:10.1093/ps/77.9.1320

Kirchgessner, T. G., Heinzmann, C., Svenson, K. L., Gordon, D. A., Nicosia, M., Lebherz, H. G., et al. (1987). Regulation of Chicken Apolipoprotein B: Cloning, Tissue Distribution, and Estrogen Induction of mRNA. *Gene* 59, 241–251. doi:10.1016/0378-1119(87)90332-5

Klassing, K. C. (1998a). "Minerals," in *Comparative Avian Nutrition*. Editor K. C. Klassing (Oxford and New York: Oxford University Press), 234–276.

Klassing, K. C. (1998b). "Vitamins," in *Comparative Avian Nutrition*. Editor K. Klassing (Oxford and New York: Oxford University Press), 277–329.

Klimis-Tavantzis, D. J., Kris-Etherton, P. M., and Leach, R. M. (1983). The Effect of Dietary Manganese Deficiency on Cholesterol and Lipid Metabolism in the Estrogen-Treated Chicken and the Laying Hen. *J. Nutr.* 113, 320–327. doi:10.1093/jn/113.2.320

Knight, P. G., Gladwell, R. T., and Cunningham, F. J. (1981). Effect of Gonadectomy on the Concentrations of Catecholamines in Discrete Areas of the Diencephalon of the Domestic Fowl. *J. Endocrinol.* 89, 389–397. doi:10.1677/joe.0.0890389

Knutson, J. C., and DeLuca, H. F. (1974). 25-Hydroxyvitamin D3-24-Hydroxylase. Subcellular Location and Properties. *Biochemistry* 13, 1543–1548. doi:10.1021/bi00704a034

Kohler, P. O., Grimley, P. M., and O'malley, B. W. (1969). Estrogen-Induced Cytodifferentiation of the Ovalbumin-Secreting Glands of the Chick Oviduct. *J. Cell Biol.* 40, 8–27. doi:10.1083/jcb.40.1.8

Kowalski, K. I., Tilly, J. L., and Johnson, A. L. (1991). Cytochrome P450 Side-Chain Cleavage (P450scc) in the Hen Ovary. I. Regulation of P450scc Messenger RNA Levels and Steroidogenesis in Theca Cells of Developing Follicles1. *Biol. Reproduction* 45, 955–966. doi:10.1095/biolreprod45.6.955

Kraus, W. L., and Katzenellenbogen, B. S. (1993). Regulation of Progesterone Receptor Gene Expression and Growth in the Rat Uterus: Modulation of Estrogen Actions by Progesterone and Sex Steroid Hormone Antagonists. *Endocrinology* 132, 2371–2379. doi:10.1210/endo.132.6.8504742

Krumins, S. A., and Roth, T. F. (1981). High-affinity Binding of Lower-Density Lipoproteins to Chicken Oocyte Membranes. *Biochem. J.* 196, 481–488. doi:10.1042/bj1960481

Kudzma, D. J., Swaney, J. B., and Ellis, E. N. (1979). Effects of Estrogen Administration on the Lipoproteins and Apoproteins of the Chicken. *Biochim. Biophys. Acta* 572, 257–268. doi:10.1016/0005-2760(79)90041-9

Kuiper, G. G. J. M., Lemmen, J. G., Carlsson, B., Corton, J. C., Safe, S. H., van der Saag, P. T., et al. (1998). Interaction of Estrogenic Chemicals and Phytoestrogens with Estrogen Receptor β. *Endocrinology* 139, 4252–4263. doi:10.1210/endo.139.10.6216

Lague, P. C., van Tienhoven, A., and Cunningham, F. J. (1975). Concentrations of Estrogens, Progesterone and LH during the Ovulatory Cycle of the Laying Chicken [*Gallus domesticus*]. *Biol. Reproduction* 12, 590–598. doi:10.1095/biolreprod12.5.590

Laverty, G., and Clark, N. B. (1989). "The Kidney," in *Vertebrate Endocrinology: Fundamentals and Biomedical Implications*. Editors P. K. T. Pang and M. P. Schreibman (New York, USA: Academic Press), 277–317.

Laziera, C. B., Wiktorowicza, M., DiMattiaa, G. E., Gordonb, D. A., Binderb, R., and Williamsb, D. L. (1994). Apolipoprotein (Apo) B and apoII Gene Expression Are Both Estrogen-Responsive in Chick Embryo Liver but Only apoII Is Estrogen-Responsive in Kidney. *Mol. Cell. Endocrinol.* 106, 187–194. doi:10.1016/0303-7207(94)90202-x

Lee, B. K., Kim, J. S., Ahn, H. J., Hwang, J. H., Kim, J. M., Lee, H. T., et al. (2010). Changes in Hepatic Lipid Parameters and Hepatic Messenger Ribonucleic Acid Expression Following Estradiol Administration in Laying Hens (*Gallus domesticus*). *Poult. Sci.* 89, 2660–2667. doi:10.3382/ps.2010-00686

Leveille, G. A., O'Hea, E. K., and Chakrabarty, K. (1968). *In Vivo* lipogenesis in the Domestic Chicken. *Exp. Biol. Med.* 128, 398–401. doi:10.3181/00379727-128-33022

Li, H., Li, Y., Yang, L., Zhang, D., Liu, Z., Wang, Y., et al. (2020). Identification of a Novel Lipid Metabolism-Associated Hepatic Gene Family Induced by Estrogen via ERα in Chicken (Gallus gallus). *Front. Genet.* 11, 1–16. doi:10.3389/fgene.2020.00271

Li, H., Wang, T., Xu, C., Wang, D., Ren, J., Li, Y., et al. (2015). Transcriptome Profile of Liver at Different Physiological Stages Reveals Potential Mode for Lipid Metabolism in Laying Hens. *BMC Genomics* 16, 1–13. doi:10.1186/s12864-015-1943-0

Li, J., Leghari, I. H., He, B., Zeng, W., Mi, Y., and Zhang, C. (2014). Estrogen Stimulates Expression of Chicken Hepatic Vitellogenin II and Very Low-Density Apolipoprotein II through ER-α. *Theriogenology* 82, 517–524. doi:10.1016/j.theriogenology.2014.05.003

Li, Q., Zhao, X., Wang, S., and Zhou, Z. (2018). Letrozole Induced Low Estrogen Levels Affected the Expressions of Duodenal and Renal Calcium-Processing Gene in Laying Hens. *General Comp. Endocrinol.* 255, 49–55. doi:10.1016/j.ygcen.2017.10.005

Lin, L.-Y., and McCormick, C. C. (1986). Quantitation of Chick Tissue Zinc-Metallothionein by Gel Electrophoresis and Silver Stain Enhancement. *Comp. Biochem. Physiology Part C Comp. Pharmacol.* 85, 75–84. doi:10.1016/0742-8413(86)90054-x

Liu, D., Veit, H. P., and Denbow, D. M. (2004). Effects of Long-Term Dietary Lipids on Mature Bone Mineral Content, Collagen, Crosslinks, and Prostaglandin E2 Production in Japanese Quail. *Poult. Sci.* 83, 1876–1883. doi:10.1093/ps/83.11.1876

Liu, D., Veit, H., Wilson, J., and Denbow, D. (2003). Long-Term Supplementation of Various Dietary Lipids Alters Bone Mineral Content, Mechanical Properties and Histological Characteristics of Japanese Quail. *Poult. Sci.* 82, 831–839. doi:10.1093/ps/82.5.831

Liu, X.-t., Lin, X., Mi, Y.-l., Zeng, W.-d., and Zhang, C.-q. (2018). Age-related Changes of Yolk Precursor Formation in the Liver of Laying Hens. *J. Zhejiang Univ. Sci. B* 19, 390–399. doi:10.1631/jzus.B1700054

Lohmann-Tierzucht (2015). *Lohmann Management Guide*. Germany: Cuxhaven.

Lorenz, F. W. (1954). Effects of Estrogens on Domestic Fowl and Applications in the Poultry Industry. *Vitamins Hormones* 12, 235–275. doi:10.1016/s0083-6729(08)61014-6

Lund, J., and Deluca, H. F. (1966). Biologically Active Metabolite of Vitamin D3 from Bone, Liver, and Blood Serum. *J. Lipid Res.* 7, 739–744. doi:10.1016/s0022-2275(20)38950-1

MacRae, H. F., Layne, D. S., and Common, R. H. (1959). Formation of Estrone, Estriol and an Unidentified Steroid from Estradiol in the Laying Hen. *Poult. Sci.* 38, 684–687. doi:10.3382/ps.0380684

Maddineni, S. R., Ocón-Grove, O. M., Krzysik-Walker, S. M., Hendricks, G. L., and Ramachandran, R. (2008). Gonadotropin-inhibitory Hormone (GnIH) Receptor Gene Is Expressed in the Chicken Ovary: Potential Role of GnIH in Follicular Maturation. *Reproduction* 135, 267–274. doi:10.1530/rep-07-0369

Mao, Y., Wu, X., An, L., Li, X., Li, Z., and Zhu, G. (2018). Tamoxifen Activates Hypothalamic L-Dopa Synthesis to Stimulate Ovarian Estrogen Production in Chicken. *Biochem. Biophysical Res. Commun.* 496, 1257–1262. doi:10.1016/j.bbrc.2018.01.182

Mathur, R. S., Anastassiadis, P. A., and Common, R. H. (1966). Urinary Excretion of Estrone and of 16-Epi-Estriol Plus 17-Epi-Estriol by the Hen „. *Poult. Sci.* 45, 946–952. doi:10.3382/ps.0450946

Matsunaga, M., Ukena, K., and Tsutsui, K. (2001). Expression and Localization of Cytochrome P450 17α-Hydroxylase/c17,20-Lyase in the Avian Brain. *Brain Res.* 899, 112–122. doi:10.1016/s0006-8993(01)02217-x

Mayel-Afshar, S., Lane, S. M., and Lawson, D. E. (1988). Relationship between the Levels of Calbindin Synthesis and Calbindin mRNA in Chick Intestine. Quantitation of Calbindin mRNA. *J. Biol. Chem.* 263, 4355–4361. doi:10.1016/s0021-9258(18)68933-1

Mccoy, M. A., Reilly, G. A. C., and Kilpatrick, D. J. (1996). Density and Breaking Strength of Bones of Mortalities Among Caged Layers. *Res. Veterinary Sci.* 60, 185–186. doi:10.1016/s0034-5288(96)90017-x

Merrill, L., Chiavacci, S. J., Paitz, R. T., and Benson, T. J. (2019). Quantification of 27 Yolk Steroid Hormones in Seven Shrubland Bird Species: Interspecific Patterns of Hormone Deposition and Links to Life History, Development, and Predation Risk. *Can. J. Zool.* 97, 1–12. doi:10.1139/cjz-2017-0351

Mete, A., Giannitti, F., Barr, B., Woods, L., and Anderson, M. (2013). Causes of Mortality in Backyard Chickens in Northern California: 2007-2011. *Avian Dis.* 57, 311–315. doi:10.1637/10382-092312-Case.1

Miller, S. C., Bowman, B. M., and Myers, R. L. (1984). Morphological and Ultrastructural Aspects of the Activation of Avian Medullary Bone Osteoclasts by Parathyroid Hormone. *Anat. Rec.* 208, 223–231. doi:10.1002/ar.1092080209

Miller, S. C. (1992). "Calcium Homeostasis and Mineral Turnover in the Laying Hen," in *Bone Biology and Skeletal Disorders in Poultry*. Editor C. C. Whitehead (Oxfordshire: Carfax Publishing Co.), 103–116.

Miller, S. (1977). Osteoclast Cell-Surface Changes during the Egg-Laying Cycle in Japanese Quail. *J. Cell Biol.* 75, 104–118. doi:10.1083/jcb.75.1.104

Monroe, D. G., Berger, R. R., and Sanders, M. M. (2002). Tissue-Protective Effects of Estrogen Involve Regulation of Caspase Gene Expression. *Mol. Endocrinol.* 16, 1322–1331. doi:10.1210/mend.16.6.0855

Monroe, D. G., Jin, D. F., and Sanders, M. M. (2000). Estrogen Opposes the Apoptotic Effects of Bone Morphogenetic Protein 7 on Tissue Remodeling. *Mol. Cell Biol.* 20, 4626–4634. doi:10.1128/mcb.20.13.4626-4634.2000

Montorzi, M., Falchuk, K. H., and Vallee, B. L. (1995). Vitellogenin and Lipovitellin: Zinc Proteins of *Xenopus laevis* Oocytes. *Biochemistry* 34, 10851–10858. doi:10.1021/bi00034a018

Munro, S. S., and Kosin, I. L. (1943). Dramatic Response of the Chick Oviduct to Estrogen. *Poult. Sci.* 22, 330–331. doi:10.3382/ps.0220330

Muramatsu, T., Tsuchiya, S., Okumura, J.-i., and Miyoshi, S. (1992). Genetic Differences in Steroid-Induced Protein Synthesis *In Vivo* of the Liver and Magnum in Immature Chicks (Gallus Domesticus). *Comp. Biochem. Physiology Part B Comp. Biochem.* 102, 905–909. doi:10.1016/0305-0491(92)90100-6

Mizuno, S., Nakabayashi, O., Kikuchi, H., and Kikuchi, T. (1996). "Expression of Genes Involved in Estrogen Synthesis and Expression of the Estrogen Receptor Gene During Early Gonadal Development of Chickens. *Poultry Avian Biol. Rev.*," in Abstracts of the 6th International Symposium on Avian Endocrinology, 306.

Nakabayashi, O., Kikuchi, H., Kikuchi, T., and Mizuno, S. (1998). Differential Expression of Genes for Aromatase and Estrogen Receptor during the Gonadal Development in Chicken Embryos. *J. Endocrinol.* 20, 193–202. doi:10.1677/jme.0.0200193

Navickis, R. J., Katzenellenbogen, B. S., and Nalbandov, A. V. (1979). Effects of the Sex Steroid Hormones and Vitamin D3 on Calcium-Binding Proteins in the Chick Shell Gland1. *Biol. Reproduction* 21, 1153–1162. doi:10.1095/biolreprod21.5.1153

Newman, S., and Leeson, S. (1997). Skeletal Integrity in Layers at the Completion of Egg Production. *World's Poult. Sci. J.* 53, 265–277. doi:10.1079/wps19970021

Nikolay, B., Plieschnig, J. A., Šubik, D., Schneider, J. D., Schneider, W. J., and Hermann, M. (2013). A Novel Estrogen-Regulated Avian Apolipoprotein. *Biochimie* 95, 2445–2453. doi:10.1016/j.biochi.2013.09.005

Nishikimi, H., Kansaku, N., Saito, N., Usami, M., Ohno, Y., and Shimada, K. (2000). Sex Differentiation and mRNA Expression of P450c17, P450arom and AMH in Gonads of the Chicken. *Mol. Reprod. Dev.* 55, 20–30. doi:10.1002/(sici)1098-2795(200001)55:1<20::aid-mrd4>3.0.co;2-e

Nomura, O., Nakabayashi, O., Nishimori, K., Yasue, H., and Mizuno, S. (1999). Expression of Five Steroidogenic Genes Including Aromatase Gene at Early Developmental Stages of Chicken Male and Female Embryos. *J. Steroid Biochem. Mol. Biol.* 71, 103–109. doi:10.1016/s0960-0760(99)00127-2

NRC (1994). *National Research Council. Nutrient Requirements of Poultry*. Washington, DC: National Academy Press. 9th rev. e.

Nys, Y., Hincke, M. T., Garcia-ruiz, J. M., and Solomon, S. (1999). Avian Eggshell Mineralization. *Poult. Avian Biol. Rev.* 10, 143–166.

Nys, Y., and le Roy, N. (2018). "Calcium Homeostasis and Eggshell Biomineralization in Female Chicken," in *Vitamin D*. Fourth Edition(Elsevier), 361–382. doi:10.1016/B978-0-12-809965-0.00022-7

Nys, Y., Mayel-Afshar, S., Bouillon, R., Van Baelen, H., and Lawson, D. E. M. (1989). Increases in Calbindin D 28K mRNA in the Uterus of the Domestic Fowl Induced by Sexual Maturity and Shell Formation. *General Comp. Endocrinol.* 76, 322–329. doi:10.1016/0016-6480(89)90164-0

Nys, Y., N'Guyen, T. M., Williams, J., and Etches, R. J. (1986). Blood Levels of Ionized Calcium, Inorganic Phosphorus, 1,25-dihydroxycholecalciferol and

Gonadal Hormones in Hens Laying Hard-Shelled or Shell-Less Eggs. *J. Endocrinol.* 111, 151–157. doi:10.1677/joe.0.1110151

Nys, Y. (1993). "Regulation of Plasma 1,25-(OH)2D3, of Osteocalcin and of Intestinal and Uterine Calbindin in Hens," in *Avian Endocrinology*. Editor P. J. Sharp (Bristol, UK: Journal of Endocrinology Ltd.), 345–357.

Ohashi, T., and Kusuhara, S. (1993). Immunoelectron Microscopic Detection of Estrogen Target Cells in the Bone Marrow of Estrogen-Treated Male Japanese Quail. *Bone Mineral* 20, 31–39. doi:10.1016/s0169-6009(08)80035-9

Ohashi, T., Kusuhara, S., and Ishida, K. (1987). Effects of Oestrogen and Anti-oestrogen on the Cells of the Endosteal Surface of Male Japanese Quail. *Br. Poult. Sci.* 28, 727–732. doi:10.1080/00071668708417008

Ohashi, T., Kusuhara, S., and Ishida, K. (1991). Estrogen Target Cells during the Early Stage of Medullary Bone Osteogenesis: Immunohistochemical Detection of Estrogen Receptors in Osteogenic Cells of Estrogen-Treated Male Japanese Quail. *Calcif. Tissue Int.* 49, 124–127. doi:10.1007/bf02565134

O'Hea, E. K., and Leveille, G. A. (1968). Lipogenesis in Isolated Adipose Tissue of the Domestic Chick (Gallus Domesticus). *Comp. Biochem. Physiology* 26, 111–120.

Oka, T., and Schimke, R. T. (1969). Interaction of Estrogen and Progesterone in Chick Oviduct Development. *J. Cell Biol.* 43, 123–137. doi:10.1083/jcb.43.1.123

Olde, B., and Leeb-Lundberg, L. M. F. (2009). GPR30/GPER1: Searching for a Role in Estrogen Physiology. *Trends Endocrinol. Metabolism* 20, 409–416. doi:10.1016/j.tem.2009.04.006

Ottinger, M. A., Pitts, S., and Abdelnabi, M. A. (2001). Steroid Hormones during Embryonic Development in Japanese Quail: Plasma, Gonadal, and Adrenal Levels. *Poult. Sci.* 80, 795–799. doi:10.1093/ps/80.6.795

Ottinger, M. A. (1989). Sexual Differentiation of Neuroendocrine Systems and Behavior ,. *Poult. Sci.* 68, 979–989. doi:10.3382/ps.0680979

Oursler, M. J., Landers, J. P., Riggs, B. L., and Spelsberg, T. C. (1993). Oestrogen Effects on Osteoblasts and Osteoclasts. *Ann. Med.* 25, 361–371. doi:10.3109/07853899309147298

Oursler, M. J., Osdoby, P., Pyfferoen, J., Riggs, B. L., and Spelsberg, T. C. (1991). Avian Osteoclasts as Estrogen Target Cells. *Proc. Natl. Acad. Sci. U.S.A.* 88, 6613–6617. doi:10.1073/pnas.88.15.6613

Paitz, R. T., Angles, R., and Cagney, E. (2020). In Ovo Metabolism of Estradiol to Estrone Sulfate in Chicken Eggs: Implications for How Yolk Estradiol Influences Embryonic Development. *General Comp. Endocrinol.* 287, 113320–113326. doi:10.1016/j.ygcen.2019.113320

Palmiter, R. D., and Wrenn, J. T. (1971). Interaction of Estrogen and Progesterone in Chick Oviduct Development. *J. Cell Biol.* 50, 598–615. doi:10.1083/jcb.50.3.598

Pardee, P. E., Dunn, W., and Schwimmer, J. B. (2012). Non-alcoholic Fatty Liver Disease Is Associated with Low Bone Mineral Density in Obese Children. *Alimentary Pharmacol. Ther.* 35, 248–254. doi:10.1111/j.1365-2036.2011.04924.x

Pearson, A. W., and Butler, E. J. (1978a). Environmental Temperature as a Factor in the Aetiology of Fatty Liver-Haemorrhagic Syndrome in the Fowl. *Res. Veterinary Sci.* 25, 133–138. doi:10.1016/s0034-5288(18)32967-9

Pearson, A. W., and Butler, E. J. (1978b). The Oestrogenised Chick as an Experimental Model for Fatty Liver-Haemorrhagic Syndrome in the Fowl. *Res. Veterinary Sci.* 24, 82–86. doi:10.1016/s0034-5288(18)33103-5

Pechak, D. G., Kujawa, M. J., and Caplan, A. I. (1986a). Morphological and Histochemical Events during First Bone Formation in Embryonic Chick Limbs. *Bone* 7, 441–458. doi:10.1016/8756-3282(86)90004-9

Pechak, D. G., Kujawa, M. J., and Caplan, A. I. (1986b). Morphology of Bone Development and Bone Remodeling in Embryonic Chick Limbs. *Bone* 7, 459–472. doi:10.1016/8756-3282(86)90005-0

Perry, M. M., and Gilbert, A. B. (1979). Yolk Transport in the Ovarian Follicle of the Hen (Gallus Domesticus): Lipoprotein-like Particles at the Periphery of the Oocyte in the Rapid Growth Phase. *J. Cell Sci.* 39, 257–272. doi:10.1242/jcs.39.1.257

Petrik, M. T., Guerin, M. T., and Widowski, T. M. (2015). On-farm Comparison of Keel Fracture Prevalence and Other Welfare Indicators in Conventional Cage and Floor-Housed Laying Hens in Ontario, Canada. *Poult. Sci.* 94, 579–585. doi:10.3382/ps/pev039

Petzinger, C., and Bauer, J. E. (2013). Dietary Considerations for Atherosclerosis in Common Companion Avian Species. *J. Exot. Pet Med.* 22, 358–365. doi:10.1053/j.jepm.2013.10.013

Pfeiffer, C. A., and Gardner, W. U. (1938). Skeletal Changes and Blood Serum Calcium Level in Pigeons Receiving Estrogens. *Endocrinology* 23, 485–491. doi:10.1210/endo-23-4-485

Plieschnig, J. A., Gensberger, E. T., Bajari, T. M., Schneider, W. J., and Hermann, M. (2012). Renal LRP2 Expression in Man and Chicken Is Estrogen-Responsive. *Gene* 508, 49–59. doi:10.1016/j.gene.2012.07.041

Polin, D., and Wolford, J. H. (1973). Factors Influencing Food Intake and Caloric Balance in Chickens. *Fed. Proc.* 32, 1720–1726.

Polin, D., and Wolford, J. H. (1977). Role of Estrogen as a Cause of Fatty Liver Hemorrhagic Syndrome. *J. Nutr.* 107, 873–886. doi:10.1093/jn/107.5.873

Porter, T. E., Hargis, B. M., Silsby, J. L., and Halawani, M. E. E. (1989). Differential Steroid Production between Theca Interna and Theca Externa Cells: A Three-Cell Model for Follicular Steroidogenesis in Avian Species*. *Endocrinology* 125, 109–116. doi:10.1210/endo-125-1-109

Price, J. S., and Russell, R. G. G. (1992). "Bone Remodeling: Regulation by Systemic and Local Factors," in *Bone Biology and Skeletal Disorders in Poultry*. Editor C. C. Whitehead (Oxfordshire, UK: Carfax Publishing Co.), 39–60.

Ratna, W. N., Bhatt, V. D., Chaudhary, K., Ariff, A. B., Bavadekar, S. A., and Ratna, H. N. (2016). Estrogen-responsive Genes Encoding Egg Yolk Proteins Vitellogenin and Apolipoprotein II in Chicken Are Differentially Regulated by Selective Estrogen Receptor Modulators. *Theriogenology* 85, 376–383. doi:10.1016/j.theriogenology.2015.08.015

Ratnasabapathy, R. (1995). *In Vitro* characterization of an Estrogen-Regulated mRNA Stabilizing Activity in the Avian Liver. *Cell Mol. Biol. Res.* 41, 583–594.

Ratnasabapathy, R., Tom, M., and Post, C. (1997). Modulation of the Hepatic Expression of the Estrogen-Regulated mRNA Stabilizing Factor by Estrogenic and Antiestrogenic Nonsteroidal Xenobiotics. *Biochem. Pharmacol.* 53, 1425–1434. doi:10.1016/s0006-2952(97)00084-1

Raud, H. R., and Hobkirk, R. (1968). *In Vitro* metabolism of estrone-4-14C and Estrone-6,7-3h-3-Sulfate by Laying Hen Liver Homogenates. *Can. J. Biochem.* 46, 759–764. doi:10.1139/o68-116

Ren, J., Tian, W., Jiang, K., Wang, Z., Wang, D., Li, Z., et al. (2021). Global Investigation of Estrogen-Responsive Genes Regulating Lipid Metabolism in the Liver of Laying Hens. *BMC Genomics* 22, 1–14. doi:10.1186/s12864-021-07679-y

Richards, G. J., Wilkins, L. J., Knowles, T. G., Booth, F., Toscano, M. J., Nicol, C. J., et al. (2012). Pop Hole Use by Hens with Different Keel Fracture Status Monitored throughout the Laying Period. *Veterinary Rec.* 170, 494. doi:10.1136/vr.100489

Richards, M., and Packard, M. (1996). Mineral Metabolism in Avian Embryos. *Avian Poult. Biol. Rev.* 7, 143–161.

Ringer, R., and Sheppard, C. (1963). Report of Fatty-Liver Syndrome in a Michigan Caged Layer Operation. *Q. Bull. Mich. State Univ. Agric. Exp. Stn.* 45, 426–427.

Rissman, E. F., Ascenzi, M., Johnson, P., and Adkins-Regan, E. (1984). Effect of Embryonic Treatment with Oestradiol Benzoate on Reproductive Morphology, Ovulation and Oviposition and Plasma LH Concentrations in Female Quail (*Coturnix coturnix* Japonica). *Reproduction* 71, 411–417. doi:10.1530/jrf.0.0710411

Robinson, F. E., Etches, R. J., Anderson-Langmuir, C. E., Burke, W. H., Cheng, K.-W., Cunningham, F. J., et al. (1988). Steroidogenic Relationships of Gonadotrophin Hormones in the Ovary of the Hen (*Gallus domesticus*). *General Comp. Endocrinol.* 69, 455–466. doi:10.1016/0016-6480(88)90038-x

Robinson, F. E., and Etches, R. J. (1986). Ovarian Steroidogenesis during Foillicular Maturation in the Domestic Fowl (Gallus Domesticus)1. *Biol. Reprod.* 35, 1096–1105. doi:10.1095/biolreprod35.5.1096

Roland, D. A. (1979). Factors Influencing Shell Quality of Aging Hens. *Poult. Sci.* 58, 774–777. doi:10.3382/ps.0580774

Roodman, G. D. (1999). Cell Biology of the Osteoclast. *Exp. Hematol.* 27, 1229–1241. doi:10.1016/s0301-472x(99)00061-2

Rosati, L., Falvo, S., Chieffi Baccari, G., Santillo, A., and di Fiore, M. M. (2021). The Aromatase-Estrogen System in the Testes of Non-mammalian Vertebrates. *Animals* 11, 1–12. doi:10.3390/ani11061763

Rosen, C. J., and Bouxsein, M. L. (2006). Mechanisms of Disease: Is Osteoporosis the Obesity of Bone? *Nat. Rev. Rheumatol.* 2, 35–43. doi:10.1038/ncprheum0070

Rosol, T. J., Chew, D. J., and Nagode, L. A. (2000). "Disorders of Calcium: Hypercalcemia and Hypocalcaemia," in *Fluid Therapy in Small Animal*

Clinical Practice. Editor S. P. DiBartola (Philadelphia, USA: WB Saunders), 108–161.

Rozenboim, I., Mahato, J., Cohen, N. A., and Tirosh, O. (2016). Low Protein and High-Energy Diet: A Possible Natural Cause of Fatty Liver Hemorrhagic Syndrome in Caged White Leghorn Laying Hens. *Poult. Sci.* 95, 612–621. doi:10.3382/ps/pev367

Rufener, C., and Makagon, M. M. (2020). Keel Bone Fractures in Laying Hens: A Systematic Review of Prevalence across Age, Housing Systems, and Strains. *J. Animal Sci.* 98, S36–S51. doi:10.1093/JAS/SKAA145

Rząsa, J., Sechman, A., Paczoska-Eliasiewicz, H., and Hrabia, A. (2009). Effect of Tamoxifen on Sex Steroid Concentrations in Chicken Ovarian Follicles. *Acta Veterinaria Hung.* 57, 85–97. doi:10.1556/AVet.57.2009.1.9

Sato, K., Abe, H., Kono, T., Yamazaki, M., Nakashima, K., Kamada, T., et al. (2009). Changes in Peroxisome Proliferator-Activated Receptor Gamma Gene Expression of Chicken Abdominal Adipose Tissue with Different Age, Sex and Genotype. *Animal Sci. J.* 80, 322–327. doi:10.1111/j.1740-0929.2009.00639.x

Scheele, C. W. (1997). Pathological Changes in Metabolism of Poultry Related to Increasing Production Levels. *Veterinary Q.* 19, 127–130. doi:10.1080/01652176.1997.9694756

Scheib, D. (1983). Effects and Role of Estrogens in Avian Gonadal Differentiation. *Differentiation* 1, 87–92. doi:10.1007/978-3-642-69150-8_15

Schexnailder, R., and Griffith, M. (1973). Liver Fat and Egg Production of Laying Hens as Influenced by Choline and Other Nutrients. *Poult. Sci.* 52, 1188–1194. doi:10.3382/ps.0521188

Schimke, R. T., McKnight, G. S., Shapiro, D. J., Sullivan, D., and Palacios, R. (1975). Hormonal Regulation of Ovalbumin Synthesis in the Chick Oviduct. *Proc. 1974 Laurent. Hormone Conf.* 1, 175–211. doi:10.1016/b978-0-12-571131-9.50009-8

Schneider, W., Carroll, R., Severson, D., and Nimpf, J. (1990). Apolipoprotein VLDL-II Inhibits Lipolysis of Triglyceride-Rich Lipoproteins in the Laying Hen. *J. Lipid Res.* 31, 507–513. doi:10.1016/s0022-2275(20)43172-4

Schumacher, M., Sulon, J., and Balthazart, J. (1988). Changes in Serum Concentrations of Steroids during Embryonic and Post-hatching Development of Male and Female Japanese Quail (*Coturnix coturnix* Japonica). *J. Endocr.* 118, 127–134. doi:10.1677/joe.0.1180127

Schwabl, H. (1993). Yolk Is a Source of Maternal Testosterone for Developing Birds. *Proc. Natl. Acad. Sci. U.S.A.* 90, 11446–11450. doi:10.1073/pnas.90.24.11446

Sechman, A., Paczoska-Eliasiewicz, H., Rzasa, J., and Hrabia, A. (2000). Simultaneous Determination of Plasma Ovarian and Thyroid Hormones during Sexual Maturation of the Hen (*Gallus domesticus*). *Folia Biol. (Krakow)* 48, 7–12.

Sechman, A., Hrabia, A., Lis, M. W., and Niedziółka, J. (2011). Effect of 2,3,7,8-Tetrachlorodibenzo-P-Dioxin (TCDD) on Steroid Concentrations in Blood and Gonads of Chicken Embryo. *Toxicol. Lett.* 205, 190–195. doi:10.1016/j.toxlet.2011.06.004

Seibel, M. J. (2005). Biochemical Markers of Bone Turnover: Part I: Biochemistry and Variability. *Clin. Biochem. Rev.* 26, 97–122.

Senior, B. E. (1974). Oestradiol Concentration in the Peripheral Plasma of the Domestic Hen from 7 Weeks of Age until the Time of Sexual Maturity. *Reproduction* 41, 107–112. doi:10.1530/jrf.0.0410107

Sharp, P. J., Scanes, C. G., Williams, J. B., Harvey, S., and Chadwick, A. (1979). Variations in Concentrations of Prolactin, Luteinizing Hormone, Growth Hormone and Progesterone in the Plasma of Broody Bantams (*Gallus domesticus*). *J. Endocrinol.* 80, 51–57. doi:10.1677/joe.0.0800051

Sharp, P. J. (1996). Strategies in Avian Breeding Cycles. *Animal Reproduction Sci.* 42, 505–513. doi:10.1016/0378-4320(96)01556-4

Shemesh, M., Shore, L., Bendheim, U., Lavi, S., and Weisman, Y. (1982). Correlation between Serum Estrogen Concentrations, Light and Prolapsed Uterus in Laying Hens. *Adv. Pathology* 1, 273–276.

Shemesh, M., Shore, L., Lavi, S., Ailenberg, M., Bendheim, U., Totach, A., et al. (1984). The Role of 17β-Estradiol in the Recovery from Oviductal Prolapse in Layers. *Poult. Sci.* 63, 1638–1643. doi:10.3382/ps.0631638

Shini, A., Shini, S., and Bryden, W. L. (2019). Fatty Liver Haemorrhagic Syndrome Occurrence in Laying Hens: Impact of Production System. *Avian Pathol.* 48, 25–34. doi:10.1080/03079457.2018.1538550

Shini, A., Shini, S., Filippich, L., Anderson, S., and Bryden, W. (2012). *Role of Inflammation in the Pathogenesis of Fatty Liver Haemorrhagic Syndrome in Laying Hens*. University of Sydney Poultry Foundation: Australian Poultry Science Symposium. 193.

Shini, S., and Bryden, W. (2009). *Occurrence and Control of Fatty Liver Haemorrhagic Syndrome (FLHS) in Caged Hens*. Sydney: Austrian Egg Corporation, 44–48.

Shini, S., Shini, A., and Bryden, W. L. (2020). Unravelling Fatty Liver Haemorrhagic Syndrome: 1. Oestrogen and Inflammation. *Avian Pathol.* 49, 87–98. doi:10.1080/03079457.2019.1674444

Shini, S., Stewart, G., Shini, A., and Bryden, W. (2006). "Mortality Rates and Causes of Death in Laying Hens Kept in Cage and Alternative Housing Systems," in *12th European Poultry Conference*. Editor D. Martin (Verona: World Poultry Science Association), 601.

Simkiss, K. (1961). Calcium Metabolism and Avian Reproduction. *Biol. Rev.* 36, 321–359. doi:10.1111/j.1469-185x.1961.tb01292.x

Smith, C. A., Andrews, J. E., and Sinclair, A. H. (1997). Gonadal Sex Differentiation in Chicken Embryos: Expression of Estrogen Receptor and Aromatase Genes. *J. Steroid Biochem. Mol. Biol.* 60, 295–302. doi:10.1016/s0960-0760(96)00196-3

Smith, C. A., Roeszler, K. N., Bowles, J., Koopman, P., and Sinclair, A. H. (2008). Onset of Meiosis in the Chicken Embryo; Evidence of a Role for Retinoic Acid. *BMC Dev. Biol.* 8, 85–19. doi:10.1186/1471-213X-8-85

Speake, B. K., Murray, A. M. B., and C. Noble, R. (1998). Transport and Transformations of Yolk Lipids during Development of the Avian Embryo. *Prog. Lipid Res.* 37, 1–32. doi:10.1016/s0163-7827(97)00012-x

Squires, E. J., and Leeson, S. (1988). Aetiology of Fatty Liver Syndrome in Laying Hens. *Br. Veterinary J.* 144, 602–609. doi:10.1016/0007-1935(88)90031-0

Stake, P. E., Fredrickson, T. N., and Bourdeau, C. A. (1981). Induction of Fatty Liver-Hemorrhagic Syndrome in Laying Hens by Exogenous B-Estradiol. *Avian Dis.* 25, 410–422. doi:10.2307/1589933

Striem, S., and Bar, A. (1991). Modulation of Quail Intestinal and Egg Shell Gland Calbindin (Mr 28,000) Gene Expression by Vitamin D3, 1,25-dihydroxyvitamin D3 and Egg Laying. *Mol. Cell. Endocrinol.* 75, 169–177. doi:10.1016/0303-7207(91)90232-H

Suda, T., Kobayashi, K., Jimi, E., Udagawa, N., and Takahashi, N. (2001). The Molecular Basis of Osteoclast Differentiation and Activation. *Novartis Found. Symp.* 232, 235–250. doi:10.1002/0470846658.ch16

Sugiyama, T., and Kusuhara, S. (1994). Efect of Parathyroid Hormone on Osteoclasts in Organ-Cultured Medullary Bone. *Jpn. Poult. Sci.* 31, 392–399. doi:10.2141/jpsa.31.392

Sugiyama, T., and Kusuhara, S. (1996). "Morphological Changes of Osteoclasts on Hen Medullary Bone during the Egg-Laying Cycle and Their Regulation," in *Comparative Endocrinology of Calcium Regulating Hormones*. Editors C. G. Dacke, J. Danks, G. Flik, and I. Caple (Bristol, UK: Journal of Endocrinology Ltd), 149–160.

Sugiyama, T., and Kusuhara, S. (1993). Ultrastructural Changes of Osteoclasts on Hen Medullary Bone during the Egg-laying Cycle. *Br. Poult. Sci.* 34, 471–477. doi:10.1080/00071669308417602

Takeshima, K. (2018). Optimizing Lighting for Precision Broiler Breeder Feeding. [Master's Thesis].

Takeshima, K., Zuidhof, M., Hanlon, C., and Bédécarrats, G. (2019). "Differential Effects of Constant Supplemental Light Wavelength on Plasma Estradiol and Melatonin Levels, Body Weight, and Egg Production in Female Broiler Breeders," in *Poult. Sci.* (Montreal, Canada, 261. 98.E-suppl. 1

Tan, W., Zheng, H., Wang, D., Tian, F., Li, H., and Liu, X. (2020). Expression Characteristics and Regulatory Mechanism of Apela Gene in Liver of Chicken (Gallus gallus). *PLoS ONE* 15, e0238784–16. doi:10.1371/journal.pone.0238784

Tanabe, Y., Nakamura, T., Fujioka, K., and Doi, O. (1979). Production and Secretion of Sex Steroid Hormones by the Testes, the Ovary, and the Adrenal Glands of Embryonic and Young Chickens (*Gallus domesticus*). *General Comp. Endocrinol.* 39, 26–33. doi:10.1016/0016-6480(79)90189-8

Tanabe, Y., Nakamura, T., Tanase, H., and Doi, O. (1981). Comparisons of Plasma LH, Progesterone, Testosterone and Estradiol Concentrations in Male and Female Chickens (*Gallus domesticus*) from 28 to 1141 Days of Age. *Endocrinol. Jpn.* 28, 605–613. doi:10.1507/endocrj1954.28.605

Tarlow, D. M., Watkins, P. A., Reed, R. E., Miller, R. S., Zwergel, E. E., and Lane, M. D. (1977). Lipogenesis and the Synthesis and Secretion of Very Low Density Lipoprotein by Avian Liver Cells in Nonproliferating Monolayer Culture. Hormonal Effects. *J. Cell Biol.* 73, 332–353. doi:10.1083/jcb.73.2.332

Tarugi, P., Ballarini, G., Pinotti, B., Franchini, A., Ottaviani, E., and Calandra, S. (1998). Secretion of apoB- and apoA-I-Containing Lipoproteins by Chick Kidney. *J. Lipid Res.* 39, 731–743. doi:10.1016/s0022-2275(20)32562-1

Terada, O., Shimada, K., and Saito, N. (1997). Effect of Oestradiol Replacement in Ovariectomized Chickens on Pituitary LH Concentrations and Concentrations of mRNAs Encoding LH and Subunits. *Reproduction* 111, 59–64. doi:10.1530/jrf.0.1110059

Theofan, G., Nguyen, A. P., and Norman, A. W. (1986). Regulation of Calbindin-D28k Gene Expression by 1,25-dihydroxyvitamin D3 Is Correlated to Receptor Occupancy. *J. Biol. Chem.* 261, 16943–16947. doi:10.1016/s0021-9258(19)75981-x

Thomas, P., Pang, Y., Filardo, E. J., and Dong, J. (2005). Identity of an Estrogen Membrane Receptor Coupled to a G Protein in Human Breast Cancer Cells. *Endocrinology* 146, 624–632. doi:10.1210/en.2004-1064

Tilly, J. L., Kowalski, K. I., and Johnson, A. L. (1991). Cytochrome P450 Side-Chain Cleavage (P450scc) in the Hen Ovary. II. P450scc Messenger RNA, Immunoreactive Protein, and Enzyme Activity in Developing Granulosa Cells1. *Biol. Reprod.* 45, 967–974. doi:10.1095/biolreprod45.6.967

Tomkinson, A., Gevers, E. F., Wit, J. M., Reeve, J., and Noble, B. S. (1998). The Role of Estrogen in the Control of Rat Osteocyte Apoptosis. *J. Bone Min. Res.* 13, 1243–1250. doi:10.1359/jbmr.1998.13.8.1243

Trott, K. A., Giannitti, F., Rimoldi, G., Hill, A., Woods, L., Barr, B., et al. (2014). Fatty Liver Hemorrhagic Syndrome in the Backyard Chicken. *Vet. Pathol.* 51, 787–795. doi:10.1177/0300985813503569

Tsang, C. P. W., and Grunder, A. A. (1984). Production, Clearance Rates and Metabolic Fate of Estradiol-17β in the Plasma of the Laying Hen. *Steroids* 43, 71–84. doi:10.1016/0039-128X(84)90059-X

Tsutsui, K., Saigoh, E., Ukena, K., Teranishi, H., Fujisawa, Y., Kikuchi, M., et al. (2000). A Novel Avian Hypothalamic Peptide Inhibiting Gonadotropin Release. *Biochem. Biophysical Res. Commun.* 275, 661–667. doi:10.1006/bbrc.2000.3350

Tuan, R. S., and Scott, W. A. (1977). Calcium-binding Protein of Chorioallantoic Membrane: Identification and Development Expression. *Proc. Natl. Acad. Sci. U.S.A.* 74, 1946–1949. doi:10.1073/pnas.74.5.1946

Turner, B. J., and Debeer, M. (2009). Calcium Tetany in Broiler Breeder Hens: Update. *Aviagen Brief.* 1, 1–5.

Turner, R. T., Riggs, B. L., and Spelsberg, T. C. (1994). Skeletal Effects of Estrogen. *Endocr. Rev.* 15, 275–300. doi:10.1210/edrv-15-3-275

Turner, R. T., Bell, N. H., and Gay, C. V. (1993). Evidence that Estrogen Binding Sites Are Present in Bone Cells and Mediate Medullary Bone Formation in Japanese Quail. *Poult. Sci.* 72, 728–740. doi:10.3382/ps.0720728

Ubuka, T., Ukena, K., Sharp, P. J., Bentley, G. E., and Tsutsui, K. (2006). Gonadotropin-Inhibitory Hormone Inhibits Gonadal Development and Maintenance by Decreasing Gonadotropin Synthesis and Release in Male Quail. *Endocrinology* 147, 1187–1194. doi:10.1210/en.2005-1178

Ugar, D., and Karaca, I. (1999). Serum Osteocalcin as a Biochemical Bone Formation Marker. *Biochem. Arch.* 15, 379–382.

Urist, M. R., and Deutsch, N. M. (1960). Osteoporosis in the Laying Hen1. *Endocrinology* 66, 377–391. doi:10.1210/endo-66-3-377

Valinietse, M. I. U., and Bauman, V. K. (1981). Comparative Antirachitic Activity of Vitamins D2 and D3 in the Body of Chicks. *Prikl. Biokhim Mikrobiol.* 17, 712–719.

van de Velde, J. P., Vermeiden, J. P. W., Touw, J. J. A., and Veldhuijzen, J. P. (1984). Changes in Activity of Chicken Medullary Bone Cell Populations in Relation to the Egg-Laying Cycle. *Metabolic Bone Dis. Relat. Res.* 5, 191–193. doi:10.1016/0221-8747(84)90029-8

Vivacqua, A., de Marco, P., Santolla, M. F., Cirillo, F., Pellegrino, M., and Panno, M. L. (2015). Estrogenic Gper Signaling Regulates Mir144 Expression in Cancer Cells and Cancer-Associated Fibroblasts (Cafs). *Oncotarget* 6, 16573–16587. doi:10.18632/oncotarget.4117

Walzem, R. L. (1996). Lipoproteins and the Laying Hen: Form Follows Function. *Poultry Avian Biol. Rev.* 7, 31–64.

Walzem, R. L., Hansen, R. J., Williams, D. L., and Hamilton, R. L. (1999). Estrogen Induction of VLDLy Assembly in Egg-Laying Hens. *J. Nutr.* 129, 467S–472S. doi:10.1093/jn/129.2.467S

Walzem, R. L., Davis, P. A., and Hansen, R. J. (1994). Overfeeding Increases Very Low Density Lipoprotein Diameter and Causes the Appearance of a Unique Lipoprotein Particle in Association with Failed Yolk Deposition. *J. Lipid Res.* 35, 1354–1366. doi:10.1016/s0022-2275(20)40077-x

Walzem, R. L., Simon, C., Morishita, T., Lowenstine, L., and Hansen, R. J. (1993). Fatty Liver Hemorrhagic Syndrome in Hens Overfed a Purified Diet. Selected Enzyme Activities and Liver Histology in Relation to Liver Hemorrhage and Reproductive Performance ,. *Poult. Sci.* 72, 1479–1491. doi:10.3382/ps.0721479

Wang, Q.-l., Zhang, A.-z., Pan, X., and Chen, L.-r. (2010). Simultaneous Determination of Sex Hormones in Egg Products by ZnCl2 Depositing Lipid, Solid-phase Extraction and Ultra Performance Liquid Chromatography/electrospray Ionization Tandem Mass Spectrometry. *Anal. Chim. Acta* 678, 108–116. doi:10.1016/j.aca.2010.08.014

Wang, X., Yang, L., Wang, H., Shao, F., Yu, J., Jiang, H., et al. (2014). Growth Hormone-Regulated mRNAs and miRNAs in Chicken Hepatocytes. *PLoS ONE* 9, e112896–15. doi:10.1371/journal.pone.0112896

Wang, Y., Wang, J., Shi, Y., Ye, H., Luo, W., and Geng, F. (2022). Quantitative Proteomic Analyses during Formation of Chicken Egg Yolk. *Food Chem.* 374, 1–11. doi:10.1016/j.foodchem.2021.131828

Watkins, B. A., Shen, C.-L., Mcmurtry, J. P., Xu, H., Bain, S. D., Allen, K. G. D., et al. (1997). Dietary Lipids Modulate Bone Prostaglandin E2 Production, Insulin-like Growth Factor-I Concentration and Formation Rate in Chicks. *Biochem. Mol. Roles Nutrients Diet. Lipids Modul. Bone Prostaglandin E 2 Prod. Nutr* 127, 1084–1091. doi:10.1093/jn/127.6.1084

Webster, A. B. (2004). Welfare Implications of Avian Osteoporosis. *Poult. Sci.* 83, 184–192. doi:10.1093/ps/83.2.184

Whitehead, C. C., and Fleming, R. H. (2000). Osteoporosis in Cage Layers. *Poult. Sci.* 79, 1033–1041. doi:10.1093/ps/79.7.1033

Whitehead, C. C. (2004). Overview of Bone Biology in the Egg-Laying Hen. *Poult. Sci.* 83, 193–199. doi:10.1093/ps/83.2.193

Whitehead, C. C., and Wilson, S. (1992). "Characteristics of Osteopenia in Hens," in *Bone Biology and Skeletal Disorders in Poultry*. Editor C. C. Whitehead (Oxfordshire, UK: Carfax Publishing Co.), 265–280.

Wilkins, L. J., McKinstry, J. L., Avery, N. C., Knowles, T. G., Brown, S. N., Tarlton, J., et al. (2011). Influence of Housing System and Design on Bone Strength and Keel Bone Fractures in Laying Hens. *Veterinary Rec.* 169, 414. doi:10.1136/vr.d4831

Williams, J. B., and Sharp, P. J. (1977). A Comparison of Plasma Progesterone and Luteinizing Hormone in Growing Hens from Eight Weeks of Age to Sexual Maturity. *J. Endocrinol.* 75, 447–448. doi:10.1677/joe.0.0750447

Wilson, S. C., and Sharp, P. J. (1976). Induction of Luteinizing Hormone Release by Gonadal Steroids in the Ovariectomized Domestic Hen. *J. Endocrinol.* 71, 87–98. doi:10.1677/joe.0.0710087

Wilson, S., and Thorp, B. H. (1998). Estrogen and Cancellous Bone Loss in the Fowl. *Calcif. Tissue Int.* 62, 506–511. doi:10.1007/s002239900470

Wiskocil, R., Bensky, P., Dower, W., Goldberger, R. F., Gordon, J. I., and Deeley, R. G. (1980). Coordinate Regulation of Two Estrogen-dependent Genes in Avian Liver. *Proc. Natl. Acad. Sci. U.S.A.* 77, 4474–4478. doi:10.1073/pnas.77.8.4474

Wolff, E. (1936). L'action de l'oestrone sur 1'oviducte et la cloaque des poussins femelles, intersexues et males. *Compt. Rend. Soc. De. Biol.* 123, 235–236.

Wolford, J. H., and Polin, D. (1972). Lipid Accumulation and Hemorrhage in Livers of Laying Chickens. *Poult. Sci.* 51, 1707–1713. doi:10.3382/ps.0511707

Wolford, J. H. (1971). The Effect of Temperature and Iodinated Casein on Liver Lipids of Laying Chickens. *Poult. Sci.* 50, 1331–1335. doi:10.3382/ps.0501331

Woods, J. E., and Brazzill, D. M. (1981). Plasma 17β-Estradiol Levels in the Chick Embryo. *General Comp. Endocrinol.* 44, 37–43. doi:10.1016/0016-6480(81)90353-1

Woods, J. E., and Erton, L. H. (1978). The Synthesis of Estrogens in the Gonads of the Chick Embryo. *General Comp. Endocrinol.* 36, 360–370. doi:10.1016/0016-6480(78)90117-x

Wu, X. L., Zou, X. Y., Zhang, M., Hu, H. Q., Wei, X. L., Jin, M. L., et al. (2021). Osteocalcin Prevents Insulin Resistance, Hepatic Inflammation, and Activates Autophagy Associated with High-Fat Diet-Induced Fatty Liver Hemorrhagic Syndrome in Aged Laying Hens. *Poult. Sci.* 100, 73–83. doi:10.1016/j.psj.2020.10.022

Yamada, M., Chen, C., Sugiyama, T., and Kim, W. K. (2021). Effect of Age on Bone Structure Parameters in Laying Hens. *Animals* 11, 570–578. doi:10.3390/ani11020570

Yang, J., Long, D. W., and Bacon, W. L. (1997). Changes in Plasma Concentrations of Luteinizing Hormone, Progesterone, and Testosterone in turkey Hens during

the Ovulatory Cycle. *General Comp. Endocrinol.* 106, 281–292. doi:10.1006/gcen.1997.6884

Yarden, N., Lavelin, I., Genina, O., Hurwitz, S., Diaz, R., Brown, E. M., et al. (2000). Expression of Calcium-Sensing Receptor Gene by Avian Parathyroid Gland *In Vivo*: Relationship to Plasma Calcium. *General Comp. Endocrinol.* 117, 173–181. doi:10.1006/gcen.1999.7405

Yilmaz, Y. (2012). Review Article: Non-alcoholic Fatty Liver Disease and Osteoporosis - Clinical and Molecular Crosstalk. *Aliment. Pharmacol. Ther.* 36, 345–352. doi:10.1111/j.1365-2036.2012.05196.x

Yoshida, K., Shimada, K., and Saito, N. (1996). Expression of P45017αHydroxylase and P450 Aromatase Genes in the Chicken Gonad before and after Sexual Differentiation. *General Comp. Endocrinol.* 102, 233–240. doi:10.1006/gcen.1996.0064

Yu, J. Y.-L., and Marquardt, R. R. (1973). Effects of Estradiol and Testosterone on the Immature Female Chicken (*Gallus domesticus*)-II. Immunodiffusional Patterns of Yolk Lipoproteins in the Liver and Plasma. *Comp. Biochem. Physiology Part B Comp. Biochem.* 46, 759–767. doi:10.1016/0305-0491(73)90120-x

Zhang, D.-D., Wang, D.-D., Wang, Z., Wang, Y.-B., Li, G.-X., Sun, G.-R., et al. (2020). Estrogen Abolishes the Repression Role of Gga-miR-221-5p Targeting ELOVL6 and SQLE to Promote Lipid Synthesis in Chicken Liver. *Ijms* 21, 1–18. doi:10.3390/ijms21051624

Zhang, M., Xu, P., Sun, X., Zhang, C., Shi, X., Li, J., et al. (2021). JUN Promotes Chicken Female Differentiation by Inhibiting Smad2. *Cytotechnology* 73, 101–113. doi:10.1007/s10616-020-00447-y

Zhang, S., Shi, H., and Li, H. (2007). Cloning and Tissue Expression Characterization of the ChickenAPOBGene. *Anim. Biotechnol.* 18, 243–250. doi:10.1080/10495390701574887

Zhang, X. Y., Wu, M. Q., Wang, S. Z., Zhang, H., Du, Z. Q., Li, Y. M., et al. (2018). Genetic Selection on Abdominal Fat Content Alters the Reproductive Performance of Broilers. *Animal* 12, 1232–1241. doi:10.1017/s1751731117002658

Zhao, H., Ge, J., Wei, J., Liu, J., Liu, C., Ma, C., et al. (2020). Effect of FSH on E2/GPR30-Mediated Mouse Oocyte Maturation *In Vitro*. *Cell. Signal.* 66, 1–13. doi:10.1016/j.cellsig.2019.109464

Zhao, L.-J., Liu, Y.-J., Liu, P.-Y., Hamilton, J., Recker, R. R., and Deng, H.-W. (2007). Relationship of Obesity with Osteoporosis. *J. Clin. Endocrinol. Metabolism* 92, 1640–1646. doi:10.1210/jc.2006-0572

Zimmerman, L. M., Paitz, R. T., Clairardin, S. G., Vogel, L. A., and Bowden, R. M. (2012). No Evidence that Estrogens Affect the Development of the Immune System in the Red-Eared Slider Turtle, *Trachemys scripta*. *Hormones Behav.* 62, 331–336. doi:10.1016/j.yhbeh.2012.04.009

Conflict of Interest: The authors declare that the research was conducted in the absence of any commercial or financial relationships that could be construed as a potential conflict of interest.

Publisher's Note: All claims expressed in this article are solely those of the authors and do not necessarily represent those of their affiliated organizations, or those of the publisher, the editors and the reviewers. Any product that may be evaluated in this article, or claim that may be made by its manufacturer, is not guaranteed or endorsed by the publisher.

frontiers | Frontiers in Physiology

ORIGINAL RESEARCH
published: 08 July 2022
doi: 10.3389/fphys.2022.936768

Molecular Pathways and Key Genes Associated With Breast Width and Protein Content in White Striping and Wooden Breast Chicken Pectoral Muscle

Martina Bordini[1†], *Francesca Soglia*[2†], *Roberta Davoli*[1], *Martina Zappaterra*[1*], *Massimiliano Petracci*[2] *and Adele Meluzzi*[1]

[1]Department of Agricultural and Food Sciences (DISTAL), Alma Mater Studiorum—University of Bologna, Bologna, Italy, [2]Department of Agricultural and Food Sciences (DISTAL), Alma Mater Studiorum—University of Bologna, Cesena, Italy

OPEN ACCESS

Edited by:
Kent M. Reed,
University of Minnesota Twin Cities,
United States

Reviewed by:
Giri Athrey,
Texas A&M University, United States
Erin Brannick,
University of Delaware, United States

***Correspondence:**
Martina Zappaterra
martina.zappaterra2@unibo.it

[†]These authors have contributed equally to this work

Specialty section:
This article was submitted to Avian Physiology, a section of the journal Frontiers in Physiology

Received: 05 May 2022
Accepted: 17 June 2022
Published: 08 July 2022

Citation:
Bordini M, Soglia F, Davoli R, Zappaterra M, Petracci M and Meluzzi A (2022) Molecular Pathways and Key Genes Associated With Breast Width and Protein Content in White Striping and Wooden Breast Chicken Pectoral Muscle. Front. Physiol. 13:936768. doi: 10.3389/fphys.2022.936768

Growth-related abnormalities affecting modern chickens, known as White Striping (WS) and Wooden Breast (WB), have been deeply investigated in the last decade. Nevertheless, their precise etiology remains unclear. The present study aimed at providing new insights into the molecular mechanisms involved in their onset by identifying clusters of co-expressed genes (i.e., modules) and key loci associated with phenotypes highly related to the occurrence of these muscular disorders. The data obtained by a Weighted Gene Co-expression Network Analysis (WGCNA) were investigated to identify hub genes associated with the parameters breast width (W) and total crude protein content (PC) of *Pectoralis major* muscles (PM) previously harvested from 12 fast-growing broilers (6 normal vs. 6 affected by WS/WB). W and PC can be considered markers of the high breast yield of modern broilers and the impaired composition of abnormal fillets, respectively. Among the identified modules, the turquoise (r = -0.90, $p < 0.0001$) and yellow2 (r = 0.91, $p < 0.0001$) were those most significantly related to PC and W, and therefore respectively named "protein content" and "width" modules. Functional analysis of the width module evidenced genes involved in the ubiquitin-mediated proteolysis and inflammatory response. GTPase activator activity, PI3K-Akt signaling pathway, collagen catabolic process, and blood vessel development have been detected among the most significant functional categories of the protein content module. The most interconnected hub genes detected for the width module encode for proteins implicated in the adaptive responses to oxidative stress (i.e., *THRAP3* and *PRPF40A*), and a member of the inhibitor of apoptosis family (i.e., *BIRC2*) involved in contrasting apoptotic events related to the endoplasmic reticulum (ER)-stress. The protein content module showed hub genes coding for different types of collagens (such as *COL6A3* and *COL5A2*), along with *MMP2* and *SPARC*, which are implicated in Collagen type IV catabolism and biosynthesis. Taken together, the present findings suggested that an ER stress condition may underly the inflammatory responses and apoptotic events taking place within affected PM muscles. Moreover, these results support the hypothesis of a role of the Collagen type IV in the cascade of events leading to the occurrence of WS/WB and identify novel actors probably involved in their onset.

Keywords: white striping, wooden breast, WGCNA, functional analysis, gene network

INTRODUCTION

The intensive breeding programs implemented in the last half-century to improve broilers' production traits have been accompanied by the appearance of severe conditions mainly affecting the *Pectoralis major* muscle (PM) of fast-growing and high breast-yield hybrids (Lake and Abasht, 2020). These conditions include the White Striping (WS) and Wooden Breast (WB) defects (Petracci et al., 2019) which are known as "growth-related abnormalities," as their occurrence is strongly connected to the high breast yield reached thanks to the selection programs carried out to develop the modern chicken hybrids (Kuttappan et al., 2013; Clark and Velleman, 2016). These conditions are responsible for detrimental alterations at the microscopic level. Indeed, the affected pectoral muscles exhibit extensive muscle degeneration which results in lower crude protein contents in the forthcoming meat (Wold et al., 2017; Dalle Zotte et al., 2020; Xing et al., 2020; Oliveira et al., 2021). Due to their adverse impact on meat quality and consumer acceptability (Kuttappan et al., 2012; Oliveira et al., 2021), these defects are responsible for significant economic losses for the poultry meat industry (Baldi et al., 2018; Zanetti et al., 2018). Indeed, severe degrees of these myopathies determine negative effects on the technological and nutritional properties of chicken meat, as suggested by the occurrence of lipid infiltration, collagen deposition, and protein degradation characterizing abnormal fillets (Tasoniero et al., 2016; Baldi et al., 2018; Huang and Ahn, 2018). Although characterized by distinctive phenotypes (Kuttappan et al., 2016), these muscular abnormalities share similar microscopic features (Petracci et al., 2013; Sihvo et al., 2014), thus suggesting the existence of potentially common causative mechanisms (Soglia et al., 2021). Briefly, fillets affected by WS are characterized by the appearance of white striations parallel to the fiber direction, while the WB-affected ones show the presence of hard, pale, and out-bulging areas mainly in the cranial and/or caudal area of breast muscle (Baldi et al., 2018; Huang and Ahn, 2018).

In this context, notable efforts have been made to discover the causal factors of these growth-related abnormalities. Several years of studies led to an extensive description of phenotypic and molecular perturbations that characterize these abnormalities and that may underly their occurrence. Some speculations have been made to try elucidating the mechanisms underlying these defects (Boerboom et al., 2018; Lake et al., 2020; Velleman, 2020; Ayansola et al., 2021). Among them, recent studies have highlighted a possible role of the development of oxidative stress (Hubert and Athrey, 2022), mitochondrial dysfunction (Papah et al., 2017), and energy metabolism dysregulations (Papah and Abasht, 2019) in the cascade of events triggering the occurrence of WS and WB. Several studies focused also on the decreased vascularization of modern broilers' PM (Kuttappan et al., 2013; Lake and Abasht, 2020), which may result in hypoxic conditions due to the impaired oxygen supply at the muscular level, possibly triggering or exacerbating the WS and WB myopathic conditions (Soglia et al., 2019). More recently, it has been suggested that the endoplasmic reticulum stress caused by an accumulation of misfolded proteins may be one of the first phenomena leading to the development of these myopathic conditions (Bordini et al., 2021; Soglia et al., 2021). However, despite the considerable increase in the knowledge regarding the complex etiology associated with the development of these defects, the precise factors triggering the cascade of events leading to their occurrence remain to be elucidated. In this regard, there is still a need to further explore the pathophysiological mechanisms underlying the progression of these myopathic conditions.

Over the past decades, great strides in new high-throughput technologies have provided the scientific community with a remarkable opportunity to investigate the genetic architecture and the regulatory mechanisms of complex traits and diseases (Rotival and Petretto, 2014). In particular, co-expression network analysis has rapidly become a prevalent and powerful approach to elucidate the specific molecular processes underlying physiological mechanisms and pathological pathways (Hocquette et al., 2009; van Dam et al., 2018). Currently, Weighted Gene Co-expression Network Analyses (WGCNA) have been successfully employed in the study of various human diseases, most notably in different cancer research (Bai et al., 2020; Jia et al., 2020; Chen et al., 2021), to identify patterns of co-expressed genes (i.e., modules) associated with specific disease features. Combining the identification of key gene modules with hub gene analyses has proved to be useful in detecting molecular mechanisms and candidate genes that may be at the base of the physiological changes characterizing different human and animal disorders (van Dam et al., 2018). In our previous work performed on 52-day-old broilers (Bordini et al., 2021), WGCNA analysis evidenced pathways involved in the extracellular matrix organization, collagen metabolism, and unfolded protein response as some of the most significant functional categories probably involved in the cascade of biological reactions that result in onset of the growth-related myopathies. Moreover, the Collagen type IV (COL4) coding genes were found as the most significant hubs. Considering the strong similarities between the histological and molecular features that characterize COL4-related disorders in humans (Guerci et al., 2012) and the growth-related myopathies in broilers, COL4 genes may be interesting candidates possibly involved in the onset and/or progression of events leading to WS and WB abnormal conditions. However, the approach used in our previous work did not allow us to explore gene networks and hub genes possibly associated with phenotypes not yet investigated and significantly related to the broiler breast abnormalities occurrence. Therefore, for the present study, we decided to consider and investigate two traits that strongly characterize the WS/WB emergency in fast-growing chickens: the first one directly related to the breast dimensions of modern hybrids, the breast width, and the second one related to one of the major meat quality traits of affected breasts, the crude protein content.

Within this context, this study aimed at providing new insights into the molecular basis underlying the onset of WS/WB through the analysis of key modules and hub genes associated with breast width and total crude protein content of broiler PM: two traits chosen as indicative markers of the broiler breast yield and the impaired composition of the affected breasts, respectively. In

particular, our study aims to further investigate the gene expression networks involved in the biochemical and physiological changes characterizing broiler breast muscles affected by WS and WB. As far as we know, this is the first study trying to investigate co-expression patterns and hub genes associated to the protein content and breast width of fast-growing chickens' pectoral muscles.

MATERIALS AND METHODS

Data Collection and Co-Expression Network Analysis

The present study was carried out by using the set of samples collected in our previous research (Zambonelli et al., 2016). This set of samples consisted of 12 *Pectoralis major* muscles (6 macroscopically normal vs. 6 severe WS/WB) belonging to 52-day-old fast-growing broilers selected from the same flock of Ross 708 (males, weighing around 3.7 kg), and slaughtered in a commercial abattoir. A detailed description of samples' selection and preparation is reported in Zambonelli et al. (2016). Briefly, 49 meat quality parameters (including technological and morphological traits as well as those related to the proximate composition of samples) were analyzed together with the microarray profiles (18,308 probes) of the 12 broiler breast fillets. The same phenotypic and gene expression data have been used in the present research to perform the Weighted Gene Co-expression Network Analysis, using the "WGCNA" package (Langfelder and Horvath, 2008) in R environment (R Core Team., 2020).

The gene expression profile of each sample was used to construct the co-expression network by creating an adjacency matrix in which the nodes correspond to the gene expression level and the edges between genes are represented by their pairwise correlation (calculated using the Pearson's correlation coefficient), as previously described by Zappaterra et al. (2021). In particular, to establish the adjacency matrix, an appropriate soft threshold power (β value) of 10 was chosen applying the approximate scale-free topology criterion (Zhang and Horvath 2005; Langfelder and Horvath 2008). The topological overlap matrix (TOM) and the corresponding dissimilarity (dissTOM = 1-TOM) were used to construct the adjacency matrix (Langfelder and Horvath, 2008). Finally, the blockwiseModules R function was used to build the network of gene co-expression patterns with the dissTOM values used as the distance measure for the gene hierarchical clustering. In particular, the latter allowed us to identify groups of co-expressed genes (i.e., modules) by employing the Dynamic Tree Cut algorithm (Langfelder and Horvath, 2008).

Module-Trait Association Study

Once the list of gene modules (i.e., groups of highly interconnected genes) had been identified and named using different color labels, the module eigengene (ME) of each module was calculated using the principal component analysis criterion to assess the relationship between modules and traits (Langfelder and Horvath, 2008). In fact, the ME represented a weighted average expression level of the considered module, and it was used to identify the "module-trait association" by calculating the Pearson's correlation between every ME and trait.

Identification of the Most Significant Traits and Modules

In the current research, two traits measured in Zambonelli et al. (2016) and not yet considered in our previous study (Bordini et al., 2021), were investigated to deepen the knowledge on the molecular mechanisms underlying WS/WB abnormalities in broiler breast meat. For this purpose, in the present study, width (expressed in mm; W) and protein content (expressed in %; PC) of PM were considered in light of their highly significant association with the onset of WS and WB myopathies ($p < 0.0001$) (Zambonelli et al., 2016) and their relevance as phenotypic markers of the high breast yield and impaired muscle composition, respectively.

For the next steps of our analysis, we focused on those modules identified by WGCNA that showed the highest absolute value of module-trait correlation with the considered traits (i.e., W and PC). For each selected module, the software calculated the gene significance (GS; i.e., the gene-trait correlation value) and module membership (MM; i.e., the intramodular connectivity) of genes belonging to the selected modules (Langfelder and Horvath, 2008).

Functional Enrichment Analyses of Selected Modules

Functional enrichment analysis was performed using the Database for Annotation, Visualization and Integrated Discovery (DAVID) version 6.8 (Huang et al., 2008) to understand the biological meaning and functional grouping of the proteins coded by the genes entering the modules most significantly related to W and PC. Moreover, this analysis may be relevant to identify potential pathways involved in molecular processes associated with the WS/WB occurrence. More in detail, each gene list belonging to the modules selected for functional analyses has been individually analyzed using the Functional Annotation Clustering tool by considering the Biological processes (BP), Molecular function (MF), and Cellular components (CC) GO categories included in the DAVID Knowledgebase for the gene functional characterization. Besides, KEGG pathways (Kanehisa and Goto, 2000) and UP_KEYWORDS categories have been considered for the enrichment analysis. For the present analysis, a Benjamini-adjusted *p*-value of 0.05 was chosen as the significance threshold to identify the most significant functional categories.

The functional characterization of the gene modules most strongly associated with the traits of interest was also performed using "ClueGo" (Bindea et al., 2009), a Cytoscape software 3.8.2 plugin (Shannon et al., 2003). First of all, we individually exported the selected module gene lists to the Cytoscape software by using the export Network To Cytoscape function ("WGCNA" package). Secondly, we used the "GeneMANIA" plugin (Montojo et al., 2010) to create the gene networks in Cytoscape, and then "ClueGo" plugin to obtain a functional

characterization of the corresponding modules. Besides, the plugin displayed an "annotation network" by clustering functional terms in different groups based on their similarities. To do this, the plugin calculates the term-term similarity using the corrected kappa statistic, which determines the association strength between the terms (Bindea et al., 2009). Also, this plugin provided an insightful view of functional interrelations by grouping similar terms by the same color (Bindea et al., 2009). In the ClueGO analysis, the p-value was adjusted using the Benjamini–Hochberg method, and a threshold for significance of $p < 0.05$ was chosen.

Homo sapiens was used as the reference organism for both DAVID and Cytoscape enrichment analyses.

Hub Gene Analysis

The hub genes analysis was performed using "cytoHubba" (Chin et al., 2014), a Cytoscape plug-in that allowed us to identify the most interconnected genes (i.e., the hub genes) belonging to each gene network considered in the present study (i.e., the turquoise and yellow2 modules). In particular, cytoHubba enabled us to explore important nodes in the considered biological networks using the Maximal Clique Centrality (MCC) algorithm, developed by Chin et al. (2014), as a topological analysis method. In detail, the MCC algorithm identifies hub nodes by calculating the number of "maximal cliques," which represents how many connections the node displays. Then, the software created the hub gene network, in which nodes are colored from red to yellow depending on their importance (the most important in dark red vs. less important in light-yellow).

RESULTS

Co-expression Network Construction and Modules Detection

In the current research, two new traits not yet investigated in our previous work (i.e., the breast width and the total crude protein content of PM muscles) were selected and analyzed using the same methodological approach already reported in Bordini et al. (2021). In particular, we decided to focus our investigation on two traits that can be considered phenotypical markers of high breast yield (i.e., the breast width; W) and muscle degeneration (i.e., the total crude reduced protein content of breast muscle; PC) which usually characterize the WS/WB affected fillets. Then, we analyzed the modules that were characterized by the highest absolute value of correlation with the considered traits of W and PC, namely the yellow2 and turquoise modules. In particular, the yellow2 (named as "width module" hereafter) was found positively associated with W ($r = +0.92$; $p < 0.001$), while the turquoise module (named as "protein content module" hereafter) was negatively related to PC ($r = -0.90$; $p < 0.001$). Thus, due to their highest absolute value of correlation with the considered traits, the width and protein content modules have been selected for the following analysis. The correlation values between each module and the two considered traits (W and PC) are reported in **Supplementary Table S1**.

Figure 1 reports the WGCNA outputs representing the absolute Gene Significance (GS) of genes belonging respectively to the width (**Figure 1A**) and protein (**Figure 1B**) modules, plotted against the corresponding gene module membership (MM). The graphs show that genes characterized by a high absolute value of GS also displayed a high gene MM value. The lists of GS values and the relative p-value between all genes and the considered traits (W and PC) are reported in **Supplementary Table S2**. Also, the complete lists of gene MM values and the relative p-values of all genes considered for the present analysis are reported in **Supplementary Table S3**.

DAVID Functional Annotation

The lists of genes entering in the width and protein content modules were individually submitted to DAVID online tool to perform functional enrichment analysis. Functional categories of both modules identified as significant analysis are reported in **Table 1**. With reference to the width module, the "hsa04120: Ubiquitin mediated proteolysis" KEGG pathway was found as unique significant functional term ($p < 0.01$). Considering the protein content module, instead, several significant function terms have been identified, as reported in **Table 1**. Some of the GO terms correlated with the WS/WB defects were enriched with the "positive regulation of GTPase activity" and "collagen catabolic process," along with the "ECM-receptor interaction" and "PI3K-Akt signaling pathway" as KEGG pathways. Both for the width and protein content modules, the detailed results obtained by the DAVID Annotation Tool are reported in **Supplementary Table S4**.

ClueGO Enrichment Analysis

The same modules were subsequently submitted to Cytoscape with the aim of deepening the enrichment analysis of the width and protein content modules and showing the functional categories interconnections. **Figure 2** reports the ClueGO enrichment analysis for the width module. This analysis has shown several genes enriched in categories linked to the interleukin-4 receptor activity, negative regulation of electron transfer activity, and regulation of Ripoptosome assembly involved in the necroptotic process. **Figure 3** shows the results obtained by analyzing genes belonging to the protein content module. Among the functional categories identified by ClueGO for this module, several terms were the same found as significant by DAVID tools, such as the GTPase activator activity, focal adhesion assembly, phosphatidylinositol 3-kinase signaling. In addition, the present analysis showed different GO terms related to the regulation of actin cytoskeleton organization, blood vessel development, regulation of fibroblast migration, and regulation of apoptotic signaling pathway.

All the data obtained by the ClueGO analysis for both considered modules are reported in **Supplementary Table S5**.

Detection of Hub Genes

Using the Cytoscape plugin "cytoHubba" we performed a hub gene analysis of selected modules that allowed us to identify genes that may play a pivotal role in the biological networks significantly related to the W and PC traits: the width and protein content modules, respectively. Indeed, this analysis allowed us to identify genes characterized by a high degree of

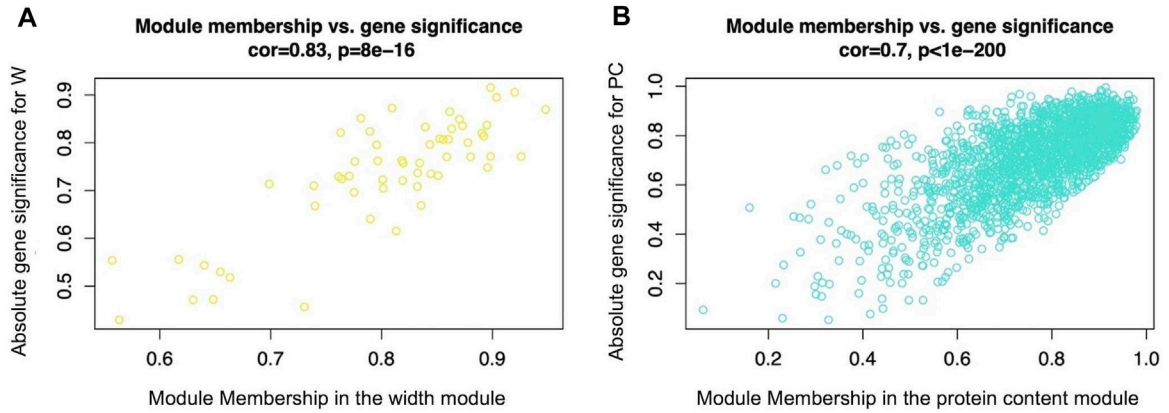

FIGURE 1 | Scatterplot of absolute gene significance (GS, *y*-axis) plotted against the gene module membership (MM, *x*-axis) of the modules selected for further analysis: the width module Figure 1**(A)**, which was the module most significantly related to breast muscle width (W trait) (evaluated in 52-day-old broilers' *Pectoralis major* muscles), and the protein content module **(B)**, which was the most significant module related to breasts protein contents (PC trait) (evaluated in 52-day-old broilers' *Pectoralis major* muscles).

TABLE 1 | The significantly enriched GO terms, KEGG pathways and UP_KEYWORDS identified by DAVID tools considering the genes comprised in the width (yellow2) and protein content (turquoise) modules and whose mRNA level covaried with the crude protein content and breast width in normal and White Striping/Wooden Breast affected *Pectoralis major* muscles in 52-day-old broilers. Benjamini-adjusted *p* value < 0.05 was chosen as the significance threshold.

Width module (yellow2)			
Category	**Term**	**Gene count**	***p* value**
KEGG	hsa04120: Ubiquitin mediated proteolysis	10	0.006
Protein content module (turquoise)			
Category	**Term**	**Gene count**	***p* value**
KEGG	hsa04510: Focal adhesion	54	5.55E-10
	hsa04512: ECM-receptor interaction	29	2.33E-07
	hsa04151: PI3K-Akt signaling pathway	64	6.37E-0.6
GOTERM_BP	GO:0043547~positive regulation of GTPase activity	82	3.42E-0.4
	GO:0051056~regulation of small GTPase mediated signal transduction	30	6.41E-04
	GO:0030574~collagen catabolic process	17	0.01
GOTERM_MF	GO:0005096~GTPase activator activity	51	2.73E-05
	GO:0098641~cadherin binding involved in cell-cell adhesion	44	0.01
GOTERM_CC	GO:0005913~cell-cell adherens junction	49	5.89E-04
	GO:0005581~collagen trimer	20	0.002
UP_KEYWORDS	Glycoprotein	427	1.29E-08
	GTPase activation	34	1.16E-04
	Hydroxylation	20	8.39E-04
	Collagen	20	0.001

interconnection with other genes belonging to the network (i.e., "hub genes").

Considering the width module, cytoHubba detected 10 genes (**Figure 4**) that can be considered hub nodes: *Pre-mRNA processing factor 40 homolog A* (*PRPF40A*), *Formin like 2* (*FMNL2*), *Thyroid hormone receptor associated protein 3* (*THRAP3*), *Zinc finger CCHC-type containing 8* (*ZCCHC8*), *ASXL transcriptional regulator 2* (*ASXL2*), *UTP20 small subunit processome component* (*UTP20*), *Baculoviral IAP repeat containing 2* (*BIRC2*), *Zinc finger protein 451* (*ZNF451*), *interleukin 1 receptor accessory protein* (*IL1RAP*), and *Programmed cell death 7* (*PDCD7*).

Regarding the protein content module, the output of the hub gene analysis is reported in **Figure 5**. Intriguingly, most of the genes identified as hub nodes by cytoHubba encode for proteins related to the connective tissue and extracellular matrix (ECM) composition and organization, which are: *Collagen type V alpha 2 chain* (*COL5A2*), *Collagen type VI alpha 3 chain* (*COL6A3*), *Collagen type XV alpha 1 chain* (*COL15A1*), *Collagen type I alpha 2 chain* (*COL1A2*), *Matrix metallopeptidase 2* (*MMP*), *Fibroblast activation protein alpha* (*FAP*), *Fibrillin 1* (*FBN1*), *Collagen type III alpha 1 chain* (*COL3A1*), *Secreted protein acidic and cysteine rich* (*SPARC*), and *Platelet derived growth factor receptor beta* (*PDGFRB*).

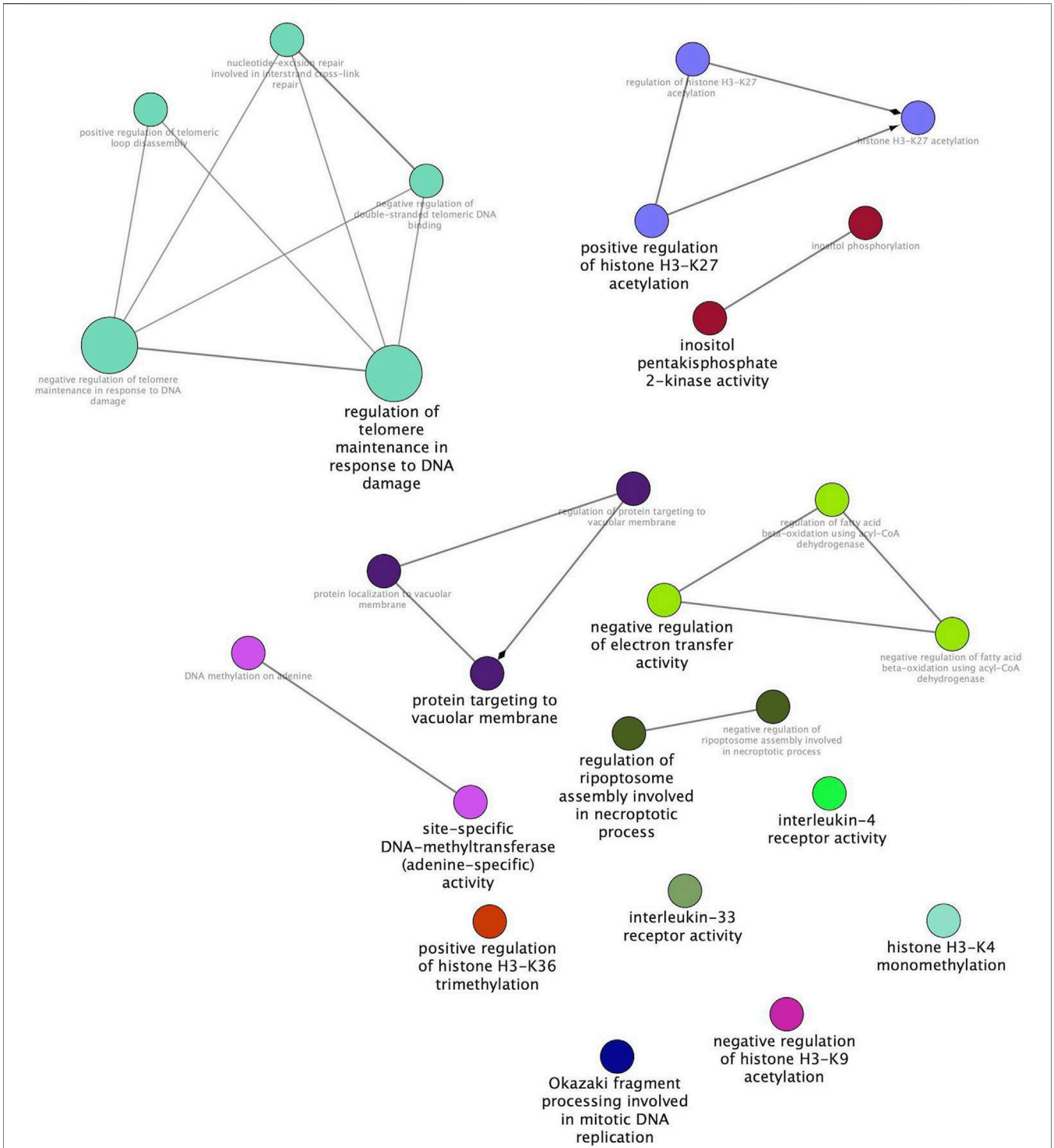

FIGURE 2 | Width module functional network. This image shows functional terms identified by ClueGO, considering genes belonging to the width module and whose mRNA level covaried with the breast width in normal and White Striping/Wooden Breast affected *Pectoralis major* muscles in 52-day-old broilers. Connections show how functional categories interact with each other. Terms belonging to the same functional group are colored with the same color. Black bold terms indicate the leading group term identified by the highest level of significance, using the Benjamini–Hochberg *p*-value and setting $p < 0.05$ as the significant threshold.

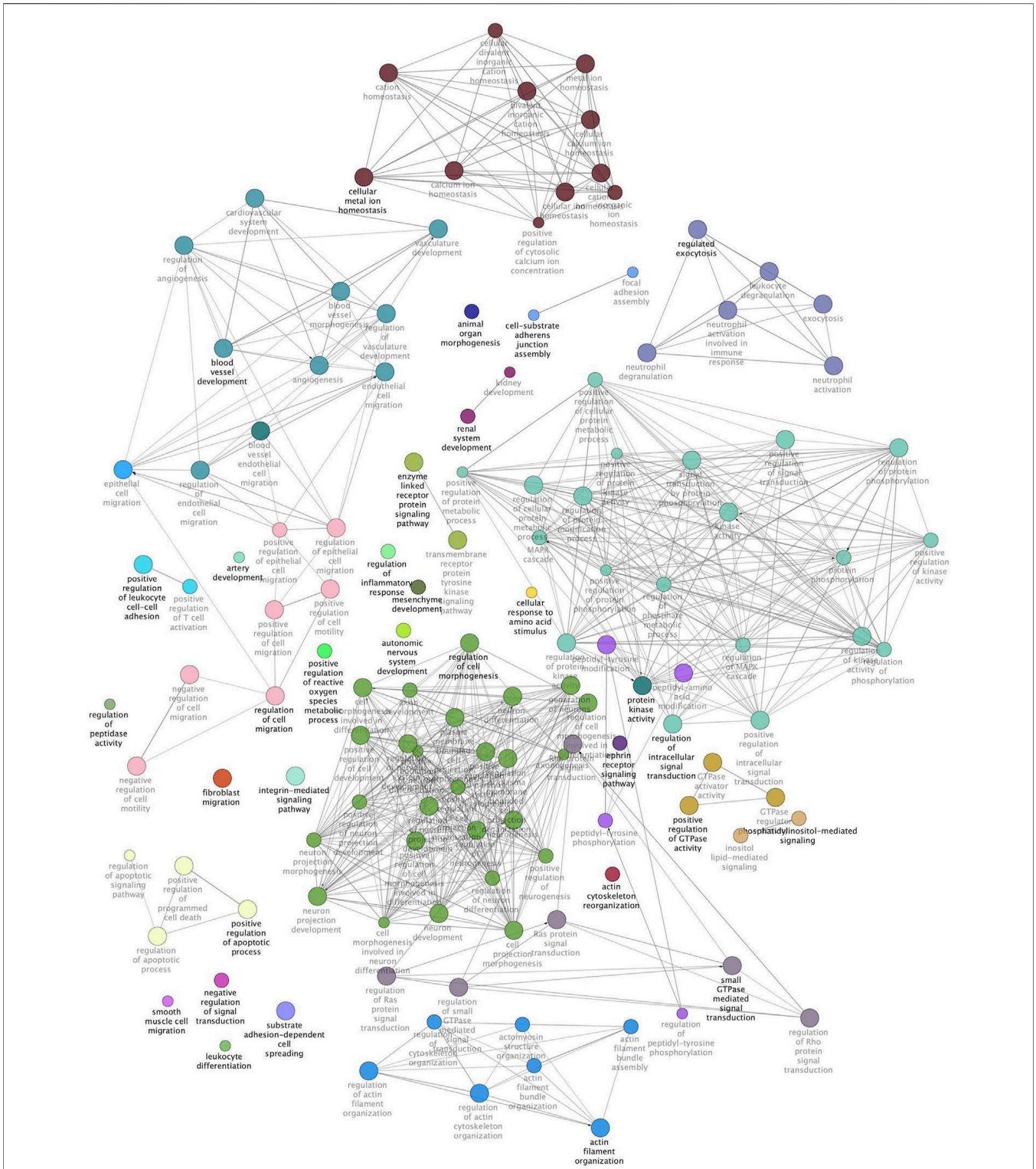

FIGURE 3 | Protein content module functional network. This image shows functional terms identified by ClueGO considering genes belonging to the protein content module and whose mRNA level covaried with the crude protein content in normal and White Striping/Wooden Breast affected *Pectoralis major* muscles in 52-day-old broilers. Connections show how functional categories interact with each other. Terms belonging to the same functional group are colored with the same color, while terms belonging to two different functional groups have both colors of groups they belong to. Black bold terms indicate the leading group term identified by the highest level of significance, using the Benjamini–Hochberg *p*-value and setting $p < 0.05$ as significant threshold.

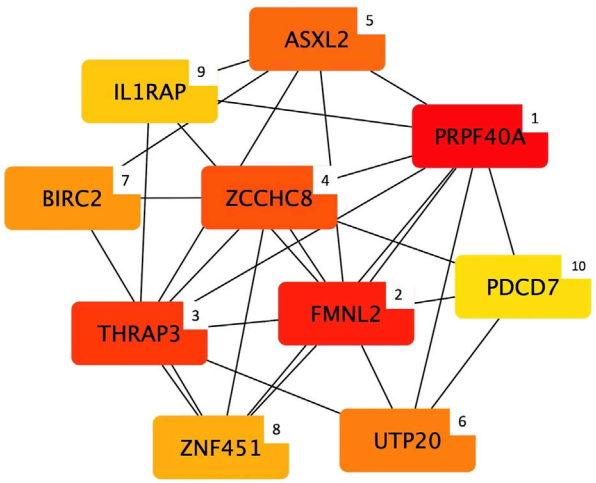

FIGURE 4 | Top 10 hub genes entering the width module (i.e., group of co-expressed genes and whose mRNA level covaried with the breast width in normal and White Striping/Wooden Breast affected *Pectoralis major* muscles in 52-day-old broilers. Connections show how functional categories interact with each other). The cytoHubba output shows hub nodes with the most significant MCC values (i.e., genes characterized by the highest number of connections in the considered network). Besides, the plugin classifies the 10 hub genes by ranking them considering their MCC value and using a color-ranging scale: from the dark red (most important hub gene) to the light-yellow (less important hub gene), also indicated by a numerical scale from 1 (most important) to 10 (less important).

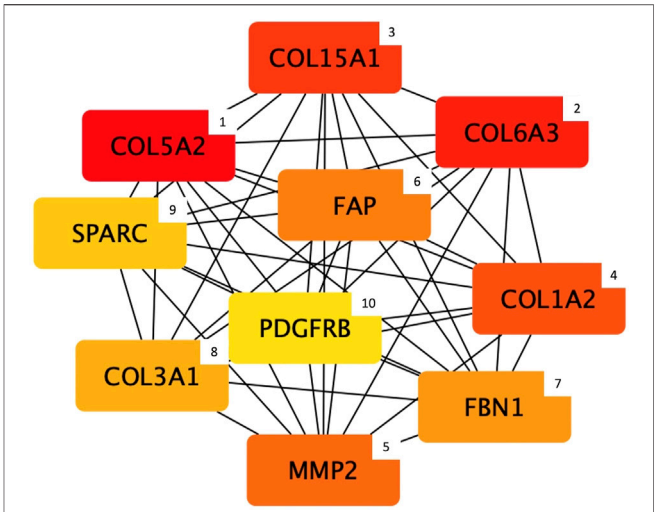

FIGURE 5 | Top 10 hub genes entering the protein content module (i.e., group of co-expressed genes and whose mRNA level covaried with the crude protein content in normal and White Striping/Wooden Breast affected *Pectoralis major* muscles in 52-day-old broilers. Connections show how functional categories interact with each other). The cytoHubba output shows hub nodes with the most significant MCC values (i.e., genes characterized by the highest number of connections in the considered network). Besides, the plugin classifies the 10 hub genes by ranking them considering their MCC value and using a color-ranging scale: from the dark red (most important hub gene) to the light-yellow (less important hub gene), also indicated by a numerical scale from 1 (most important) to 10 (less important).

DISCUSSION

The present research explored new patterns of co-expressed genes not yet considered in our previous study (Bordini et al., 2021) by investigating two PM muscles traits (i.e., breast width- W, and protein content- PC) that were found in Zambonelli et al. (2016) to be significantly associated with the WS/WB onset, and that have not yet been analyzed in depth. The traits examined in this study can be considered markers of the modern broiler growth rate and of the meat quality impairment characterizing the affected fillets. Indeed, the breast width (W) is indicative of the high breast yield of the fast-growing broilers, and the reduced total crude protein content (PC) depicts the impaired composition (as a result of the extensive necrosis of the fibers) characterizing abnormal fillets. Hence, we decided to investigate these traits to better clarify and bring new knowledge on key pathways and molecular players (i.e., hub genes) potentially associated to the complexity of mechanisms underlying these abnormalities. For this purpose, the WGCNA approach allowed us to identify molecular patterns and their most interconnected genes that may have a role in the pathophysiological processes underlying the phenotypic characteristics of PM muscle affected by WS and WB. In fact, the enrichment analysis carried out considering the lists of genes belonging to the width and protein content modules (i.e., the two modules most significantly correlated to the W and PC traits respectively) has provided biological insights for each module examined.

Considering the width module, the "ubiquitin-mediated proteolysis" was the unique functional category identified as significant by DAVID tools. In accordance with this outcome, genes involved in ubiquitin-specific proteases have been found differentially expressed in myopathic affected broilers, thus suggesting their involvement in the higher level of degradation of muscular proteins featuring the PM of affected chickens when compared to the normal counterpart (Kuttappan et al., 2017; Malila et al., 2020; Ayansola et al., 2021; Maharjan et al., 2021). The ubiquitin proteolytic system consists of a cascade of molecular events involved in a broad variety of cellular processes, with particular reference to the degradation of aberrant proteins (Glickman & Ciechanover, 2002; Wertz & Dixit, 2008; Berner et al., 2018). Interestingly, the ubiquitination of aberrant proteins is in line with the hypothesis suggested in our previous paper where it was hypothesized that the endoplasmic reticulum (ER) stress induced by the accumulation of misfolded/unfolded proteins may lead to the cascade of cellular events underlying the onset of these (Bordini et al., 2021). However, it could not be excluded that the activation of this process may result from the myofiber's alterations characterizing the WS/WB progression. Thus, further studies will be necessary to assess if these conditions could be considered the cause or the effect of these breast abnormalities complex picture.

Moreover, the protein ubiquitination mechanism has recently been reported as a key regulatory process influencing numerous aspects of pathways involved in the repair of damaged DNA

(Ghosh and Saha, 2012). Thus, ubiquitination mechanisms could be linked to the functional category "regulation of telomere maintenance in response to DNA damage" identified by ClueGO. Oxidative stress has been demonstrated to accelerate telomere shortening in humans and mice (Barnes et al., 2019). More in detail, oxidative stress in cultured human fibroblasts resulted in increased shortening of telomeres, as well as mitochondrial oxidative stress was shown to induce telomere erosion in human cardiovascular disease (Gordona et al., 2022). Similarly, a recent study by Hubert and Athrey (2022) pointed out the potential relationship between mitochondrial dysfunction, oxidative stress, and the longevity-assurance processes (a complex network of processes linked to the cell maintenance and repair mechanisms including telomere length) (Rattan, 1998) in fast-growing broilers. In light of the above, it could be hypothesized that, similarly to what was evidenced in human and animal models, the accumulation of oxidative damage (for instance due to mitochondrial dysfunction) may determine telomere shortening rates, thus leading to faster cellular senescence. In this scenario, this outcome seems to evidence that telomeres maintenance, as well as the response to DNA damage, could be potentially involved in the complexity of WS/WB underlying mechanisms. As far as we know, this is the first research evidencing a potential association between the telomere maintenance in response to DNA damage with the mechanisms probably involved in the WS/WB occurrence.

With regard to the mitochondrial dysfunction, Papah et al. (2017) evidenced mitochondrial architecture alteration (i.e., disintegration of mitochondrial cristae) in degenerating myofibrils of six-weeks-old wooden breast chickens. The same Authors suggested that alterations of mitochondrial morphology and cristae disruption may lead to an impaired bioenergetics balance of breast muscle fibers, resulting in increased susceptibility to muscle damage. In agreement with this hypothesis, since the mitochondrial electron transport chain is localized in the mitochondrial cristae (Cogliati et al., 2021), our results evidencing the "negative regulation of electron transfer activity" as a significant functional category seem to agree with the findings obtained by Papah et al. (2017). Thus, this result supports the hypothesis of a potential implication of mitochondrial dysfunction in the cascade of events involved in the WS/WB occurrence and/or progression. However, additional studies would be necessary to verify if the alterations in mitochondrial electron transfer activity may be one of the primary causes of abnormal modern broilers' PM.

Moreover, the ClueGO enrichment analysis of the genes comprised in the width module confirmed the relevance of the muscular inflammation status as one of the main phenomena taking place in WS/WB fillets (Zambonelli et al., 2016; Papah et al., 2017; Xing et al., 2021), and supposedly involved in the activation of signaling pathways leading also to the induction of regenerative processes that characterize myopathic breasts. In fact, ClueGO also identified the "interleukin-4 receptor activity" as a significant functional category. In particular, the muscle-secreted interleukin 4 (IL4) is a cytokine involved not only in the inflammatory response as an anti-inflammatory agent (Gadani et al., 2012) but also in the muscle regeneration process (Guerci et al., 2012; Yang & Hu, 2018; Costa et al., 2021): injured muscles release IL4 and other cytokines (e.g., interleukin 6, IL6; tumor necrosis factor, TNF) as signals in response to muscular damage in hypertrophic muscles with the aim of facilitating the myoblasts migration and their fusion into myotubes (Nierobisz et al., 2008; Świerczek-Lasek et al., 2019). In agreement with these statements, Pampouille et al. (2019) reported that cytokines released during inflammatory response could play a relevant role in muscle regeneration of myopathic chickens by promoting satellite cells (i.e., muscle stem cells; SC) proliferation and differentiation.

Referring to the multiple aspects of the inflammatory condition of the affected PM muscles, ClueGO has also evidenced the "regulation of Ripoptosome assembly involved in the necroptotic process" functional category, which is related to a particular type of necrosis, the necroptotic process. Interestingly, this process is an inflammation-induced form of necrosis initiated by the TNF cytokine secretion (Feoktistova and Leverkus, 2015; Liu et al., 2016) well-described in muscular dystrophies affecting humans, such as the Duchenne Muscular Dystrophy (Morgan et al., 2018; Sreenivasan et al., 2020). Accordingly, the involvement of the TNF-induced necroptosis in the muscle-wasting condition characterizing abnormal chickens' breasts can be supported also by our results.

Concerning PC trait, the results obtained from the functional enrichment analysis of the protein content module evidenced that genes of this module are functionally related to the reorganization of the actin cytoskeleton. This process is well represented by two of the significant functional categories identified in this study: the "positive regulation of GTPase" and the "actin cytoskeleton organization". In this regard, several studies highlighted the relevant role of the GTPase superfamily in the actin organization (Matsumoto et al., 1997; Gu et al., 2014) and Mutryn et al. (2015) found several proteins belonging to the GTPase family as up-regulated in woody breasts when compared with fillets exhibiting normal appearance. The same Authors hypothesized that the altered expression of GTPase genes may be linked to the phenomena of disruption and subsequent repair of the actin cytoskeleton manifested in abnormal breasts (Mutryn et al., 2015). Besides having a role in the re-organization of the altered sarcomere architecture characterizing muscles affected by the growth-related myopathies (Velleman et al., 2018), the rearrangement of the actin cytoskeleton has an important role in modulating angiogenesis (Bayless et al., 2011). In this regard, the "blood vessel development" was found among the functional terms identified by ClueGO. Noteworthy, compromised angiogenesis is widely considered as one of the potential causative/major predisposing factors at the basis of the occurrence of growth-related myopathies, as an inadequate development of blood vessels in PM could lead to impaired oxygen and nutrient supply at the muscular level and impaired waste removal (Sihvo et al., 2018; Brothers et al., 2019; Petracci et al., 2019). A large body of literature detected in WS/WB affected muscles consistent changes in the expression level of genes related to the regulation of angiogenesis (Mutryn et al., 2015; Abasht et al., 2016; Zambonelli et al., 2016; Sihvo et al., 2018; Marchesi et al., 2019; Ayansola et al., 2021), suggesting that impaired angiogenesis is a common feature in WS/WB affected PM.

In terms of regulation of the angiogenetic process, genes belonging to the protein content module were also functionally annotated with the "PI3K-Akt signaling pathway." This pathway plays a critical role in many cellular functions and biological processes including not only angiogenesis but also a wider domain of biological actions concerning proliferation, metabolisms and apoptosis (Bader et al., 2005). In particular, the PI3K pathway influences the endothelial cells' growth by mediating the vascular endothelial growth factor (VEGF) (Karar and Maity, 2011). These results, considered with the above-mentioned blood vessel development category, strengthen the hypothesis of potential involvement of pathways regulating the angiogenesis process in relation to the reduced vascularization characterizing modern broilers' PM. Moreover, it is worth mentioning that the PI3K/Akt can also inhibit the expression of genes encoding for the E3 ubiquitin ligases that, as previously stated, regulate the ubiquitin-mediated protein degradation (Yoshida and Delafontaine, 2020). Thus, the functional analysis of the investigated modules allowed us to assume that the traits considered as markers of the WS and WB disorders (i.e., breast width and breast protein content) are associated with groups of co-expressed genes interconnected between each other (for example considering the PI3K/Akt and the ubiquitin-mediated proteolysis). Hence, it could be hypothesized that these groups of genes may contribute together to build the complex pathological framework characterizing WS/WB defects.

Most importantly, the weighted gene network analysis allowed us not only to detect gene expression patterns (i.e., modules) significantly related to the phenotypic variability of the considered traits in normal and WS/WB affected PM muscles, but also to identify central players within the considered modules: the hub genes. Indeed, these genes are characterized by a high number of interactions with other genes belonging to the same network, and generally have crucial roles in regulating biological processes (Yu et al., 2017). Therefore, since hub genes can be considered key regulators in their biological networks (Langfelder et al., 2013), which in turn are significantly related to phenotypic traits considered as indicative markers of WS/WB occurrence, their involvement in the phenotypic variability that characterizes breast muscles affected by WS and WB defects might be hypothesized.

In this context, *BIRC2* is one of the top 10 hub genes identified by CytoHubba for the width module. This gene, also known as *cIAP1* (Cellular Inhibitor of Apoptosis Protein 1), encodes for the homonymous protein that belongs to a group of anti-apoptosis proteins: the IAPs (i.e., inhibitors of apoptotic proteins) (Li et al., 2011). In general, this group of proteins exerts an anti-apoptotic role by inhibiting the caspases signaling system during the apoptosis process (Budihardjo et al., 1999; Fan et al., 2005; Li et al., 2011) and, particularly, it has been demonstrated that Birc2 protein has a relevant role in maintaining endothelial cell survival and vascular homeostasis during vascular tissue development of zebrafish embryos (Santoro et al., 2007). The *BIRC2* gene expression is regulated by the activation of the nuclear factor kappa B (NF-κB) pathway, which is involved in the immune and inflammatory responses by regulating pro-inflammatory cytokine production (Lawrence, 2009). However, it has also been demonstrated an anti-apoptotic function of NF-κB through the regulation of the expression level of genes involved in the anti-apoptosis process, such as the IAPs protein family (Dolcet et al., 2005; Lawrence, 2009). As regards NF-κB activation, different mechanisms have been reported in the literature. Among them, the so-called "canonical NF-κB activation" is directly linked to the ubiquitination of the NF-κB inhibitors (IkBs) via the E3 ubiquitin-protein ligases activity (Santoro et al., 2007; Li et al., 2011; Saleem et al., 2013), which could be probably associated with the "ubiquitin-mediated proteolysis" functional category discussed above in this paper.

Based on these considerations, it is important to note that the ER stress in WB/WS muscle may induce the NF-κB activation in the early phase of the unfolded protein response (UPR) (Kitamura, 2011), thus inducing the expression of several anti-apoptotic genes, including *BIRC2* (Brown et al., 2016). These statements support that ER stress occurring at the endothelial level could be one of the factors potentially involved in the cascade of events that result in the onset and/or progression of the growth-related abnormalities. In these conditions of muscular and/or endothelial dysfunctions likely triggering apoptotic events, it could be hypothesized the role of the hub gene *BIRC2* in contrasting the ER-stress apoptosis by acting against the altered cellular functionality induced by the ER stress.

Moreover, the *BIRC2* gene could be in turn regulated by *IL1RAP,* another hub gene belonging to the width module. *IL1RAP* encodes for the interleukin 1 receptor accessory protein: a coreceptor essential for the transmission of interleukin-1 (IL1) signaling (Ågerstam et al., 2015). IL1 is a pro-inflammatory cytokine implicated in several types of cellular stress responses (Goshen and Yirmiya, 2009; Chen et al., 2012) that can also activate the transcription factor NF-κB. As previously discussed, NF-κB regulates in its turn the expression of several genes involved both in the inflammatory and apoptosis processes (Wang et al., 2002). Therefore, *IL1RAP* may be one of the regulators of the NF-κB, ultimately triggering the expression of *BIRC2*, which contrasts the ER stress-induced apoptosis. Thus, these results confirm the impressive inflammatory status and cellular stress response observed in WS/WB affected muscles by previous studies (Kuttappan et al., 2013; Zambonelli et al., 2016; Papah et al., 2018).

In terms of cellular stress responses, the Cytohubba analysis also detected hub genes involved in the molecular response to hypoxia and oxidative stress conditions: the *PRPF40A* and *THRAP3* genes. In fact, in the literature, it is reported that an over-expression of the *PRPF40A* gene is associated with an upregulation of biochemical pathways linked to hypoxia and oxidative stress conditions (Oleksiewicz et al., 2017), and it is reported that *PRPF40A* expression level could be considered a reliable marker of hypoxia-induced stress in human lung cancer (Huo et al., 2019; Ancel et al., 2021). Similarly, the protein encoded by *THRAP3* has a role in the DNA repair process during oxidative stress events (Jungmichel et al., 2013; Vohhodina et al., 2017). Indeed, Jungmichel et al. (2013) demonstrated that the human *THRAP3* gene exerts a critical role in maintaining DNA genomic stability under oxidative stress

conditions by regulating alternative splicing events of genes coding for key proteins of the DNA damage response. Therefore, the present results suggest that this gene could participate in the oxidative stress responses characterizing WS/WB breasts (Abasht et al., 2016; Brothers et al., 2019) and, overall, these findings are in line with the hypothesis that hypoxic conditions could be one of the possible causative processes underlying the occurrence of growth-related muscular disorders affecting modern chickens.

Considering the protein content module, most of the genes identified as "hubs" encode for proteins constituting different types of collagens (i.e., collagen type I, III, V, VI, and XV), and that are involved in their assembly (i.e., secreted protein acidic and cysteine-rich; SPARC) and catabolism (i.e., matrix metallopeptidase 2; MMP2). Collagens are the most abundant proteins belonging to the ECM of connective tissues, and they contribute to the proper development and maintenance of musculoskeletal tissues (Bailey, 1985; Velleman, 2015; Gatseva et al., 2019; Mienaltowski et al., 2021). Because of its importance in the ECM structure, alteration in the deposition and assembly of different types of collagens determine numerous congenital myopathies widely described in humans and other species (Ahmad et al., 2020). For instance, mutations in *COL1A2*, *COL3A1*, and *COL5A2* human genes (identified as hub genes in the present research) are at least in part the genetic basis of the Ehlers-Danlos syndrome: a systemic connective tissue disorder caused by defects in fibrillar collagen deposition (Nuytinck et al., 2000; Mao & Bristow, 2001; Malfait et al., 2005). Besides, of particular interest is *COL6A3* gene, encoding for one of the three alpha chains composing type VI collagen, that in turn is associated with Bethlem and Ullrich congenital human myopathies (Bertini and Pepe, 2002). Recent studies hypothesized that this gene could be considered one of the candidate genes potentially involved in the onset of the WS and WB defects (Pampouille et al., 2018). Accordingly, Papah et al. (2018) and Praud et al. (2020) showed an upregulation of *COL6A3* expression in muscles severely affected by both WS and WB, in agreement with the great amount of fibrosis characterizing myopathic muscles. In this respect, numerous Authors identified genes directly involved in fibrosis development as overexpressed in abnormal breasts (Papah et al., 2018; Brothers et al., 2019; Pampouille et al., 2019; Praud et al., 2020).

With regards to the fibrotic conditions of abnormal breasts, *PDGFRB* was found as a further key node in the protein content module gene network. In general, several Authors suggested that the activation of this pathway may participate in the aberrant deposition of ECM components, which in its turn may lead to the impressive fibrosis which is commonly observed in WB (Papah et al., 2018; Pampouille et al., 2019; Malila et al., 2021). Intriguingly, PDGFR-receptors are implicated in the proliferation, differentiation and migration of myogenic cells (Contreras et al., 2021), and a higher expression level of *PDGFRB* was found in developing and regenerative mice' skeletal muscles (Jin et al., 1991), as well as in WB fillets (Pampouille et al., 2019; Praud et al., 2020).

In accordance with this statement, recent studies suggested that increasing PDGF-receptors expression supports the activation of fibro-adipogenic progenitors (FAPs) that are involved in the ECM remodeling and, more specifically, in the regulation of regeneration and repair processes of the injured muscles (Contreras et al., 2019, 2021). Interestingly, the *FAP* gene, which encodes for a fibroblast activation protein, was found to be one of the hub nodes belonging to the gene expression network negatively related to the PC trait. Intriguingly, several studies identified genes involved in fibroblasts proliferation and function (e.g., FAPs) as differentially expressed in PM exhibiting myopathic conditions, suggesting their involvement in the abnormal collagen deposition (Mutryn et al., 2015; Papah et al., 2018; Praud et al., 2020). In terms of ECM remodeling, the Matrix Metalloproteinases (MMPs) represent a group of endopeptidases primarily involved in the degradation of almost all ECM components, such as the cross-linked collagen and elastin fibers (Gomes et al., 2012) and therefore involved in the ECM remodeling process. In the present study, the *MMP2* gene was detected as another important hub node belonging to the protein content module gene network. This result can be considered particularly interesting in consideration of the findings obtained in our previous study (Bordini et al., 2021) in which Collagen type IV alpha 1 chain (COL4A1) was identified as the most significant hub gene in the considered gene network. In fact, MMP2 is typically associated with the cleavage of the collagen type IV (COL4) (Zeng et al., 1999), the most abundant component of the basement membranes (BMs) of many tissues (e.g., endothelial cells and muscle fibers). Furthermore, the MMP2 activity is indirectly associated with blood vessel development, thus perfectly overlapping with the results obtained by the functional analysis. Indeed, the degradation of COL4 determines the production of bioactive collagen fragments that can inhibit the angiogenesis process, such as the so-called "Arresten" fragment resulting from the degradation of the COL4 non-collagenous domain (Monaco et al., 2006; Aikio et al., 2012). Therefore, it can be hypothesized that alterations in COL4 degradation that leads to the production of anti-angiogenic fragments could be considered likely involved in the compromised vascularization that characterizes breast muscles of modern chickens (Hoving-Bolink et al., 2000; Sihvo et al., 2017).

Within this framework, the Cytohubba Cytoscape plugin identified *SPARC* as another interesting hub gene that might play a role in the cascade of molecular and physiological events characterizing these myopathic conditions. This gene encodes for the homonymous protein that has a critical role in ensuring the proper secretion and assembly of COL4-networks at the BM level in both vertebrates and invertebrate organisms (Chioran et al., 2017). This COL4-network consists of interactions between COL4 heterotrimers (i.e., protomers) forming a polygonal structure that interacts with integrins and serves as a scaffold for the deposition of other ECM components (e.g., laminins and perlecans) (Chioran et al., 2017; Gatseva et al., 2019). Interestingly, SPARC is a transient component of ECM that works as an extracellular chaperone-like protein necessary for the correct integration of COL4 at the BM level (Martinek et al.,

2008; Morrissey et al., 2016). Hence, it is important to note that this result could be considered in line with the hypothesis that alteration in the COL4 network assembly and/or in its intracellular accumulation may results in the occurrence of ER stress condition in muscular cells, thus leading to an alteration of the ECM structure and apoptosis process in abnormal breast muscles. Therefore, these results may suggest that this alteration in the protein assembly and/or secretion may be at least partially due to errors in the SPARC chaperone-like activities. Taken together, these results support the hypothesis that alteration in COL4 secretion and/or assembly of the COL4 network resulting from either an abnormal synthesis of the protein (Bordini et al., 2021) or linked to disorders in collagen-associated chaperone activities (e.g., SPARC), could represent a potential pathological mechanism underlying the onset of growth-related abnormalities.

Overall, the present research has allowed us to obtain a more complete understanding of the complex framework of biological and physiological events at the basis of the growth-related myopathies affecting modern chicken hybrids, along with new insights on genes that may have a role in regulating molecular pathways underlying WS/WB occurrence. In fact, through the functional analysis and hub gene identification, the current research allowed us to identify new candidate genes characterized by a high degree of interconnections with other genes belonging to the same expression pattern. Thus, it could be assumed that these candidate genes could play key roles in the pathogenesis of these abnormalities, such as the genes involved in contrasting apoptotic events (e.g., *BIRC2*) and that may be implicated in collagen degradation and assembly (e.g., *MMP2* and *SPARC*). Furthermore, the consistency between the present results and what we have found in our previous study (Bordini et al., 2021) highlights that the traits most significantly associated with the manifestation of WS and WB defects are related in particular to changes in the expression level of genes linked to ER stress condition and ECM remodeling.

In conclusion, the present findings supported the relevance of ER stress condition in association with inflammatory responses, apoptotic events and degenerative processes taking place within the affected PM, as depicted by both the functional and hub gene analyses. These results are also in line with the hypothesis formulated by Lake et al. (2020) suggesting that abnormal lipid accumulation at the perivascular level may lead to ER and mitochondrial stress, thus resulting in the cascade of events involved in the WS/WB occurrence and development. Moreover, these findings may also support our previous hypothesis that an altered architecture and/or degradation of the type IV collagen may be at least in part involved in the WS/WB onset. Indeed, alteration in the assembly of the COL4 network at the BM level could be the cause of ER stress both at the endothelial and muscular levels, thus leading to apoptosis promoted by the UPR activation and that in turn may be responsible for the activation of pro-inflammatory and anti-apoptotic events (e.g., NF-κB pathway). In this process, the involvement of the *SPARC* gene could be hypothesized as a key player in COL4-network stability. Furthermore, it might be speculated that an abnormal degradation of COL4 protein carried out by MMP2, which can determine the production of fragments having anti-angiogenetic activities, might be involved in the vascular damage of PM muscles exhibiting these myopathic conditions. Although the present study seems to corroborate the hypothesis that COL4 may be one of the players involved in the onset of these myopathies, it could not be excluded that its alterations may be the result of the aberrant conditions characterizing abnormal PM muscles at the collagen level. To summarize, the main findings obtained in the present study, and that could be considered remarkable points for a more complete picture of the WS/WB complexity, highlighted molecular pathways directly related to the blood vessel development and cellular responses to several types of stress conditions: oxidative, mitochondrial, and ER stress. Besides, our results identified hub players potentially involved in the occurrence and/or progression of WS/WB, due to their important role in counteracting ER stress-induced apoptosis (*BIRC2* and *ILRAP1*) and ECM composition (*SPARC* and *MMP2*).

DATA AVAILABILITY STATEMENT

The datasets presented in this study can be found in online repositories. The names of the repository/repositories and accession number(s) can be found below: https://www.ncbi.nlm.nih.gov/geo/, GSE79276.

AUTHOR CONTRIBUTIONS

All the Authors have made a substantial contribution to the work and approved it for the publication. MZ, MB, RD, and FS have conceptualized the study. MB performed the analysis. All the Authors have made the interpretation of data. MB, RD, MZ, and FS drafted the manuscript, and AM and MP supervised it. All the Authors have substantively revised the work.

SUPPLEMENTARY MATERIAL

The Supplementary Material for this article can be found online at: https://www.frontiersin.org/articles/10.3389/fphys.2022.936768/full#supplementary-material

REFERENCES

Abasht, B., Mutryn, M. F., Michalek, R. D., and Lee, W. R. (2016). Oxidative Stress and Metabolic Perturbations in Wooden Breast Disorder in Chickens. *PLoS One* 11, e0153750. doi:10.1371/JOURNAL.PONE.0153750

Ågerstam, H., Karlsson, C., Hansen, N., Sandén, C., Askmyr, M., Von Palffy, S., et al. (2015). Antibodies Targeting Human IL1RAP (IL1R3) Show Therapeutic Effects in Xenograft Models of Acute Myeloid Leukemia.

Proc. Natl. Acad. Sci. U.S.A. 112, 10786–10791. doi:10.1073/PNAS.1422749112

Ahmad, K., Shaikh, S., Ahmad, S. S., Lee, E. J., and Choi, I. (2020). Cross-Talk Between Extracellular Matrix and Skeletal Muscle: Implications for Myopathies. *Front. Pharmacol.* 11, 1–8. doi:10.3389/fphar.2020.00142

Aikio, M., Alahuhta, I., Nurmenniemi, S., Suojanen, J., Palovuori, R., Teppo, S., et al. (2012). Arresten, a Collagen-Derived Angiogenesis Inhibitor, Suppresses Invasion of Squamous Cell Carcinoma. *PLoS One* 7, e51044. doi:10.1371/JOURNAL.PONE.0051044

Ancel, J., Perotin, J.-M., Dewolf, M., Launois, C., Mulette, P., Nawrocki-Raby, B., et al. (2021). Hypoxia in Lung Cancer Management: A Translational Approach. *Cancers* 13, 3421. doi:10.3390/CANCERS13143421

Ayansola, H., Liao, C., Dong, Y., Yu, X., Zhang, B., and Wang, B. (2021). Prospect of Early Vascular Tone and Satellite Cell Modulations on White Striping Muscle Myopathy. *Poult. Sci.* 100, 100945. doi:10.1016/J.PSJ.2020.12.042

Bader, A. G., Kang, S., Zhao, L., and Vogt, P. K. (20052005). Oncogenic PI3K Deregulates Transcription and Translation. *Nat. Rev. Cancer* 5 (5), 921–929. doi:10.1038/nrc1753

Bai, K. H., He, S. Y., Shu, L. L., Wang, W. D., Lin, S. Y., Zhang, Q. Y., et al. (2020). Identification of Cancer Stem Cell Characteristics in Liver Hepatocellular Carcinoma by WGCNA Analysis of Transcriptome Stemness Index. *Cancer Med.* 9, 4290–4298. doi:10.1002/cam4.3047

Bailey, A. J. (1985). The Role of Collagen in the Development of Muscle and its Relationship to Eating Quality. *J. Anim. Sci.* 60, 1580–1587. doi:10.2527/JAS1985.6061580X

Baldi, G., Soglia, F., Mazzoni, M., Sirri, F., Canonico, L., Babini, E., et al. (2018). Implications of White Striping and Spaghetti Meat Abnormalities on Meat Quality and Histological Features in Broilers. *Animal* 12, 164–173. doi:10.1017/S1751731117001069

Barnes, R. P., Fouquerel, E., and Opresko, P. L. (2019). The Impact of Oxidative DNA Damage and Stress on Telomere Homeostasis. *Mech. Ageing Dev.* 177, 37–45. doi:10.1016/j.mad.2018.03.013

Bayless, K. J., and Johnson, G. A. (2011). Role of the Cytoskeleton in Formation and Maintenance of Angiogenic Sprouts. *J. Vasc. Res.* 48 (5), 369–385. doi:10.1159/000324751

Berner, N., Reutter, K.-R., and Wolf, D. H. (2018). Protein Quality Control of the Endoplasmic Reticulum and Ubiquitin-Proteasome-Triggered Degradation of Aberrant Proteins: Yeast Pioneers the Path. *Annu. Rev. Biochem.* 87, 751–782. doi:10.1146/annurev-biochem-062917-012749

Bertini, E., and Pepe, G. (2002). Collagen Type VI and Related Disorders: Bethlem Myopathy and Ullrich Scleroatonic Muscular Dystrophy. *Eur. J. Paediatr. Neurology* 6, 193–198. doi:10.1053/EJPN.2002.0593

Bindea, G., Mlecnik, B., Hackl, H., Charoentong, P., Tosolini, M., Kirilovsky, A., et al. (2009). ClueGO: A Cytoscape Plug-In to Decipher Functionally Grouped Gene Ontology and Pathway Annotation Networks. *Bioinformatics* 25, 1091–1093. doi:10.1093/bioinformatics/btp101

Boerboom, G., van Kempen, T., Navarro-Villa, A., and Pérez-Bonilla, A. (2018). Unraveling the Cause of White Striping in Broilers Using Metabolomics. *Poult. Sci.* 97 (11), 3977–3986. doi:10.3382/ps/pey266

Bordini, M., Zappaterra, M., Soglia, F., Petracci, M., and Davoli, R. (2021). Weighted Gene Co-expression Network Analysis Identifies Molecular Pathways and Hub Genes Involved in Broiler White Striping and Wooden Breast Myopathies. *Sci. Rep.* 11, 1776. doi:10.1038/s41598-021-81303-7

Brothers, B., Zhuo, Z., Papah, M. B., and Abasht, B. (2019). RNA-Seq Analysis Reveals Spatial and Sex Differences in Pectoralis Major Muscle of Broiler Chickens Contributing to Difference in Susceptibility to Wooden Breast Disease. *Front. Physiol.* 10, 764. doi:10.3389/FPHYS.2019.00764/BIBTEX

Brown, M., Strudwick, N., Suwara, M., Sutcliffe, L. K., Mihai, A. D., Ali, A. A., et al. (2016). An Initial Phase of JNK Activation Inhibits Cell Death Early in the Endoplasmic Reticulum Stress Response. *J. Cell Sci.* 129 (12), 2317–2328. doi:10.1242/jcs.179127

Budihardjo, I., Oliver, H., Lutter, M., Luo, X., and Wang, X. (1999). Biochemical Pathways of Caspase Activation during Apoptosis. *Annu. Rev. Cell Dev. Biol.* 15, 269–290. doi:10.1146/annurev.cellbio.15.1.269

Chen, Q., Tan, Y., Zhang, C., Zhang, Z., Pan, S., An, W., et al. (2021). A Weighted Gene Co-Expression Network Analysis–Derived Prognostic Model for Predicting Prognosis and Immune Infiltration in Gastric Cancer. *Front. Oncol.* 11, 221. doi:10.3389/FONC.2021.554779/BIBTEX

Chen, R., Li, M., Zhang, Y., Zhou, Q., and Shu, H.-B. (2012). The E3 Ubiquitin Ligase MARCH8 Negatively Regulates IL-1β-induced NF-κB Activation by Targeting the IL1RAP Coreceptor for Ubiquitination and Degradation. *Proc. Natl. Acad. Sci. U.S.A.* 109, 14128–14133. doi:10.1073/PNAS.1205246109

Chin, C.-H., Chen, S.-H., Wu, H.-H., Ho, C.-W., Ko, M.-T., and Lin, C.-Y. (2014). cytoHubba: Identifying Hub Objects and Sub-networks from Complex Interactome. *BMC Syst. Biol.* 8, S11. doi:10.1186/1752-0509-8-S4-S11

Chioran, A., Duncan, S., Catalano, A., Brown, T. J., and Ringuette, M. J. (2017). Collagen IV Trafficking: The Inside-Out and beyond Story. *Dev. Biol.* 431, 124–133. doi:10.1016/j.ydbio.2017.09.037

Clark, D. L., and Velleman, S. G. (2016). Spatial Influence on Breast Muscle Morphological Structure, Myofiber Size, and Gene Expression Associated with the Wooden Breast Myopathy in Broilers. *Poult. Sci.* 95 (12), 2930–2945. doi:10.3382/ps/pew243

Cogliati, S., Cabrera-Alarcón, J. L., and Enriquez, J. A. (2021). Regulation and Functional Role of the Electron Transport Chain Supercomplexes. *Biochem. Soc. Trans.* 49 (6), 2655–2668. doi:10.1042/BST20210460

Contreras, O., Córdova-Casanova, A., and Brandan, E. (2021). PDGF-PDGFR Network Differentially Regulates the Fate, Migration, Proliferation, and Cell Cycle Progression of Myogenic Cells. *Cell. Signal.* 84, 110036. doi:10.1016/J.CELLSIG.2021.110036

Contreras, O., Cruz-Soca, M., Theret, M., Soliman, H., Tung, L. W., Groppa, E., et al. (2019). The Cross-Talk between TGF-β and PDGFRα Signaling Pathways Regulates Stromal Fibro/adipogenic Progenitors' Fate. *J. Cell Sci.* 132, jcs232157. doi:10.1242/JCS.232157

Core Team (2020). R: A Language and Environment for Statistical Computing R Foundation. Available at: https://www.r-project.org/.

Costa, M. L., Jurberg, A. D., and Mermelstein, C. (2021). The Role of Embryonic Chick Muscle Cell Culture in the Study of Skeletal Myogenesis. *Front. Physiol.* 12, 686. doi:10.3389/FPHYS.2021.668600/BIBTEX

Dalle Zotte, A., Ricci, R., Cullere, M., Serva, L., Tenti, S., and Marchesini, G. (2020). Research Note: Effect of Chicken Genotype and White Striping-Wooden Breast Condition on Breast Meat Proximate Composition and Amino Acid Profile. *Poult. Sci.* 99 (3), 1797–1803. doi:10.1016/j.psj.2019.10.066

Dolcet, X., Llobet, D., Pallares, J., and Matias-Guiu, X. (2005). NF-kB in Development and Progression of Human Cancer. *Virchows Arch.* 446, 475–482. doi:10.1007/S00428-005-1264-9/FIGURES/5

Fan, T.-J., Han, L.-H., Cong, R.-S., and Liang, J. (2005). Caspase Family Proteases and Apoptosis. *Acta. Biochim. Biophys. Sin.* 37 (11), 719–727. doi:10.1111/j.1745-7270.2005.00108.x

Feoktistova, M., and Leverkus, M. (2015). Programmed Necrosis and Necroptosis Signalling. *FEBS J.* 282, 19–31. doi:10.1111/febs.13120

Gadani, S. P., Cronk, J. C., Norris, G. T., and Kipnis, J. (2012). IL-4 in the Brain: A Cytokine to Remember. *J. I.* 189, 4213–4219. doi:10.4049/JIMMUNOL.1202246

Gatseva, A., Sin, Y. Y., Brezzo, G., and Van Agtmael, T. (2019). Basement Membrane Collagens and Disease Mechanisms. *Essays Biochem.* 63, 297–312. doi:10.1042/EBC20180071

Ghosh, S., and Saha, T. (2012). Central Role of Ubiquitination in Genome Maintenance: DNA Replication and Damage Repair. *ISRN Mol. Biol.* 2012, 1–9. doi:10.5402/2012/146748

Glickman, M. H., and Ciechanover, A. (2002). The Ubiquitin-Proteasome Proteolytic Pathway: Destruction for the Sake of Construction. *Physiol. Rev.* 82, 373–428. doi:10.1152/physrev.00027.2001

Gomes, L. R., Terra, L. F., Wailemann, R. A., Labriola, L., and Sogayar, M. C. (2012). TGF-β1 Modulates the Homeostasis between MMPs and MMP Inhibitors through P38 MAPK and ERK1/2 in Highly Invasive Breast Cancer Cells. *BMC Cancer* 12, 26. doi:10.1186/1471-2407-12-26/FIGURES/10

Gordon, C.-A., Madamanchi, N. R., Runge, M. S., and Jarstfer, M. B. (2022). Effect of Oxidative Stress on Telomere Maintenance in Aortic Smooth Muscle Cells. *Biochimica Biophysica Acta (BBA) - Mol. Basis Dis.* 1868, 166397. doi:10.1016/j.bbadis.2022.166397

Goshen, I., and Yirmiya, R. (2009). Interleukin-1 (IL-1): a Central Regulator of Stress Responses. *Front. Neuroendocrinol.* 30, 30–45. doi:10.1016/J.YFRNE.2008.10.001

Gu, C., Chang, J., Shchedrina, V. A., Pham, V. A., Hartwig, J. H., Suphamungmee, W., et al. (2014). Regulation of Dynamin Oligomerization in Cells: The Role of Dynamin-Actin Interactions and its GTPase Activity. *Traffic* 15, 819–838. doi:10.1111/TRA.12178

Guerci, A., Lahoute, C., Hébrard, S., Collard, L., Graindorge, D., Favier, M., et al. (2012). Srf-Dependent Paracrine Signals Produced by Myofibers Control Satellite Cell-Mediated Skeletal Muscle Hypertrophy. *Cell Metab.* 15, 25–37. doi:10.1016/J.CMET.2011.12.001

Hocquette, J. F., Cassar-Malek, I., Scalbert, A., and Guillou, F. (2009). Contribution of Genomics to the Understanding of Physiological Functions. *J. Physiol. Pharmacol.* 60 Suppl 3, 5–16.

Hoving-Bolink, A. H., Kranen, R. W., Klont, R. E., Gerritsen, C. L. M., and De Greef, K. H. (2000). Fibre Area and Capillary Supply in Broiler Breast Muscle in Relation to Productivity and Ascites. *Meat Sci.* 56, 397–402. doi:10.1016/S0309-1740(00)00071-1

Huang, D. W., Sherman, B. T., and Lempicki, R. A. (2008). Systematic and Integrative Analysis of Large Gene Lists Using DAVID Bioinformatics Resources. *Nat. Protoc.* 4, 44–57. doi:10.1038/nprot.2008.211

Huang, X., and Ahn, D. U. (2018). The Incidence of Muscle Abnormalities in Broiler Breast Meat - A Review. *Korean J. Food Sci. Anim. Resour.* 38, 835–850. doi:10.5851/kosfa.2018.e2

Hubert, S., and Athrey, G. (2022). Transcriptomic Signals of Mitochondrial Dysfunction and OXPHOS Dynamics in Fast-Growth Chicken. *PeerJ* 10, e13364. doi:10.7717/peerj.13364

Huo, Z., Zhai, S., Weng, Y., Qian, H., Tang, X., Shi, Y., et al. (2019). PRPF40A as a Potential Diagnostic and Prognostic Marker Is Upregulated in Pancreatic Cancer Tissues and Cell Lines: an Integrated Bioinformatics Data Analysis. *OncoTargets Ther.* 12, 5037–5051. doi:10.2147/OTT.S206039

Jia, R., Zhao, H., and Jia, M. (2020). Identification of Co-expression Modules and Potential Biomarkers of Breast Cancer by WGCNA. *Gene* 750, 144757. doi:10.1016/J.GENE.2020.144757

Jin, P., Sejersen, T., and Ringertz, N. R. (1991). Recombinant Platelet-Derived Growth Factor-BB Stimulates Growth and Inhibits Differentiation of Rat L6 Myoblasts. *J. Biol. Chem.* 266, 1245–1249. doi:10.1016/S0021-9258(17)35307-3

Jungmichel, S., Rosenthal, F., Altmeyer, M., Lukas, J., Hottiger, M. O., and Nielsen, M. L. (2013). Proteome-wide Identification of poly(ADP-Ribosyl)ation Targets in Different Genotoxic Stress Responses. *Mol. Cell* 52, 272–285. doi:10.1016/J.MOLCEL.2013.08.026

Kanehisa, M., and Goto, S. (2000). KEGG: Kyoto Encyclopedia of Genes and Genomes. *Nucleic Acids Res.* 28, 27–30. doi:10.1093/NAR/28.1.27

Karar, J., and Maity, A. (2011). PI3K/AKT/mTOR Pathway in Angiogenesis. *Front. Mol. Neurosci.* 4, 51. doi:10.3389/FNMOL.2011.00051

Kitamura, M. (2011). Control of NF-κB and Inflammation by the Unfolded Protein Response. *Int. Rev.Immunol.* 30 (1), 4–15. doi:10.3109/08830185.2010.522281

Kuttappan, V. A., Bottje, W., Ramnathan, R., Hartson, S. D., Coon, C. N., Kong, B.-W., et al. (2017). Proteomic Analysis Reveals Changes in Carbohydrate and Protein Metabolism Associated with Broiler Breast Myopathy. *Poult. Sci.* 96, 2992–2999. doi:10.3382/ps/pex069

Kuttappan, V. A., Hargis, B. M., and Owens, C. M. (2016). White Striping and Woody Breast Myopathies in the Modern Poultry Industry: A Review. *Poult. Sci.* 95, 2724–2733. doi:10.3382/ps/pew216

Kuttappan, V. A., Lee, Y. S., Erf, G. F., Meullenet, J.-F. C., Mckee, S. R., and Owens, C. M. (2012). Consumer Acceptance of Visual Appearance of Broiler Breast Meat with Varying Degrees of White Striping. *Poult. Sci.* 91, 1240–1247. doi:10.3382/ps.2011-01947

Kuttappan, V. A., Shivaprasad, H. l., Shaw, D. P., Valentine, B. A., Hargis, B. M., Clark, F. D., et al. (2013). Pathological Changes Associated with White Striping in Broiler Breast Muscles. *Poult. Sci.* 92, 331–338. doi:10.3382/ps.2012-02646

Lake, J. A., and Abasht, B. (2020). Glucolipotoxicity: A Proposed Etiology for Wooden Breast and Related Myopathies in Commercial Broiler Chickens. *Front. Physiol.* 11, 169. doi:10.3389/fphys.2020.00169

Lake, J. A., Brannick, E. M., Papah, M. B., Lousenberg, C., Velleman, S. G., and Abasht, B. (2020). Blood Gas Disturbances and Disproportionate Body Weight Distribution in Broilers with Wooden Breast. *Front. Physiol.* 11, 304. doi:10.3389/fphys.2020.00304

Langfelder, P., and Horvath, S. (2008). WGCNA: An R Package for Weighted Correlation Network Analysis. *BMC Bioinforma.* 9. doi:10.1186/1471-2105-9-559

Langfelder, P., Mischel, P. S., and Horvath, S. (2013). When Is Hub Gene Selection Better Than Standard Meta-Analysis? *PLoS One* 8, e61505. doi:10.1371/JOURNAL.PONE.0061505

Lawrence, T. (2009). The Nuclear Factor NF- B Pathway in Inflammation. *Cold Spring Harb. Perspect. Biol.* 1, a001651. doi:10.1101/CSHPERSPECT.A001651

Li, W., Li, B., Giacalone, N. J., Torossian, A., Sun, Y., Niu, K., et al. (2011). BV6, an IAP Antagonist, Activates Apoptosis and Enhances Radiosensitization of Non-small Cell Lung Carcinoma *In Vitro*. *J. Thorac. Oncol.* 6, 1801–1809. doi:10.1097/JTO.0B013E318226B4A6

Liu, X., Shi, F., Li, Y., Yu, X., Peng, S., Li, W., et al. (2016). Post-Translational Modifications as Key Regulators of TNF-Induced Necroptosis. *Cell Death Dis.* 7, e2293. doi:10.1038/cddis.2016.197

Maharjan, P., Beitia, A., Weil, J., Suesuttajit, N., Hilton, K., Caldas, J., et al. (2021). Woody Breast Myopathy Broiler Show Age-dependent Adaptive Differential Gene Expression in Pectoralis Major and Altered *In-Vivo* Triglyceride Kinetics in Adipogenic Tissues. *Poult. Sci.* 100, 101092. doi:10.1016/J.PSJ.2021.101092

Malfait, F., Coucke, P., Symoens, S., Loeys, B., Nuytinck, L., and De Paepe, A. (2005). The Molecular Basis of Classic Ehlers-Danlos Syndrome: a Comprehensive Study of Biochemical and Molecular Findings in 48 Unrelated Patients. *Hum. Mutat.* 25, 28–37. doi:10.1002/HUMU.20107

Malila, Y., Uengwetwanit, T., Thanatsang, K. V., Arayamethakorn, S., Srimarut, Y., Petracci, M., et al. (2021). Insights into Transcriptome Profiles Associated With Wooden Breast Myopathy in Broilers Slaughtered at the Age of 6 or 7 Weeks. *Front. Physiol.* 12, 691194. doi:10.3389/FPHYS.2021.691194/FULL

Malila, Y., Uengwetwanit, T., Arayamethakorn, S., Srimarut, Y., Thanatsang, K. V., Soglia, F., et al. (2020). Transcriptional Profiles of Skeletal Muscle Associated With Increasing Severity of White Striping in Commercial Broilers. *Front. Physiol.* 11, 580. doi:10.3389/FPHYS.2020.00580/BIBTEX

Mao, J.-R., and Bristow, J. (2001). The Ehlers-Danlos Syndrome: On beyond Collagens. *J. Clin. Invest.* 107, 1063–1069. doi:10.1172/JCI12881

Marchesi, J. A. P., Ibelli, A. M. G., Peixoto, J. O., Cantão, M. E., Pandolfi, J. R. C., Marciano, C. M. M., et al. (2019). Whole Transcriptome Analysis of the Pectoralis Major Muscle Reveals Molecular Mechanisms Involved with White Striping in Broiler Chickens. *Poult. Sci.* 98, 590–601. doi:10.3382/ps/pey429

Martinek, N., Shahab, J., Saathoff, M., and Ringuette, M. (2008). Haemocyte-derived SPARC Is Required for Collagen-IV-dependent Stability of Basal Laminae in Drosophila Embryos. *J. Cell Sci.* 121, 1671–1680. doi:10.1242/JCS.021931

Matsumoto, K., Asano, T., and Endo, T. (1997). Novel Small GTPase M-Ras Participates in Reorganization of Actin Cytoskeleton. *Oncogene* 15, 2409–2417. doi:10.1038/sj.onc.1201416

Mienaltowski, M. J., Gonzales, N. L., Beall, J. M., and Pechanec, M. Y. (2021). Basic Structure, Physiology, and Biochemistry of Connective Tissues and Extracellular Matrix Collagens. *Adv. Exp. Med. Biol.* 1348, 5–43. doi:10.1007/978-3-030-80614-9_2/FIGURES/8

Monaco, S., Sparano, V., Gioia, M., Sbardella, D., Di PierroDiMarini, D. S., Marini, S., et al. (2006). Enzymatic Processing of Collagen IV by MMP-2 (Gelatinase A) Affects Neutrophil Migration and it Is Modulated by Extracatalytic Domains. *Protein Sci.* 15, 2805–2815. doi:10.1110/PS.062430706

Montojo, J., Zuberi, K., Rodriguez, H., Kazi, F., Wright, G., Donaldson, S. L., et al. (2010). GeneMANIA Cytoscape Plugin: Fast Gene Function Predictions on the Desktop. *Bioinformatics* 26, 2927–2928. doi:10.1093/BIOINFORMATICS/BTQ562

Morgan, J. E., Prola, A., Mariot, V., Pini, V., Meng, J., Hourde, C., et al. (2018). Necroptosis Mediates Myofibre Death in Dystrophin-Deficient Mice. *Nat. Commun.* 9, 3655. doi:10.1038/s41467-018-06057-9

Morrissey, M. A., Jayadev, R., Miley, G. R., Blebea, C. A., Chi, Q., Ihara, S., et al. (2016). SPARC Promotes Cell Invasion *In Vivo* by Decreasing Type IV Collagen Levels in the Basement Membrane. *PLoS Genet.* 12 (2), e1005905. doi:10.1371/journal.pgen.1005905

Mutryn, M. F., Brannick, E. M., Fu, W., Lee, W. R., and Abasht, B. (2015). Characterization of a Novel Chicken Muscle Disorder through Differential Gene Expression and Pathway Analysis Using RNA-Sequencing. *BMC Genomics* 16, 1–19. doi:10.1186/s12864-015-1623-0

Nierobisz, L. S., Mozdziak, P. E., Author, C., and Mozdziak, P. (2008). Factors Influencing Satellite Cell Activity during Skeletal Muscle Development in Avian and Mammalian Species. *Asian Australas. J. Anim. Sci.* 21 (3), 456–464. doi:10.5713/ajas.2008.r.02

Nuytinck, L., Freund, M., Lagae, L., Pierard, G. E., Hermanns-Le, T., and De Paepe, A. (2000). Classical Ehlers-Danlos Syndrome Caused by a Mutation in Type I Collagen. *Am. J. Hum. Genet.* 66, 1398–1402. doi:10.1086/302859

Oleksiewicz, U., Liloglou, T., Tasopoulou, K.-M., Daskoulidou, N., Gosney, J. R., Field, J. K., et al. (2017). COL1A1, PRPF40A, and UCP2 Correlate with Hypoxia Markers in Non-small Cell Lung Cancer. *J. Cancer Res. Clin. Oncol.* 143, 1133–1141. doi:10.1007/S00432-017-2381-Y/FIGURES/3

Oliveira, R. F. d., Mello, J. L. M. d., Ferrari, F. B., Cavalcanti, E. N. F., Souza, R. A. d., Pereira, M. R., et al. (2021). Physical, Chemical and Histological Characterization of Pectoralis Major Muscle of Broilers Affected by Wooden Breast Myopathy. *Animals* 11, 596. doi:10.3390/ANI11030596

Pampouille, E., Berri, C., Boitard, S., Hennequet-Antier, C., Beauclercq, S. A., Godet, E., et al. (2018). Mapping QTL for White Striping in Relation to Breast Muscle Yield and Meat Quality Traits in Broiler Chickens. *BMC Genomics* 19, 1–14. doi:10.1186/s12864-018-4598-9

Pampouille, E., Hennequet-Antier, C., Praud, C., Juanchich, A., Brionne, A., Godet, E., et al. (2019). Differential Expression and Co-expression Gene Network Analyses Reveal Molecular Mechanisms and Candidate Biomarkers Involved in Breast Muscle Myopathies in Chicken. *Sci. Rep.* 9, 1–17. doi:10.1038/s41598-019-51521-1

Papah, M. B., and Abasht, B. (2019). Dysregulation of Lipid Metabolism and Appearance of Slow Myofiber-specific Isoforms Accompany the Development of Wooden Breast Myopathy in Modern Broiler Chickens. *Sci. Rep.* 9 (1), 17170. doi:10.1038/s41598-019-53728-8

Papah, M. B., Brannick, E. M., Schmidt, C. J., and Abasht, B. (2017). Evidence and Role of Phlebitis and Lipid Infiltration in the Onset and Pathogenesis of Wooden Breast Disease in Modern Broiler Chickens. *Avian Pathol.* 46, 623–643. doi:10.1080/03079457.2017.1339346

Papah, M. B., Brannick, E. M., Schmidt, C. J., and Abasht, B. (2018). Gene Expression Profiling of the Early Pathogenesis of Wooden Breast Disease in Commercial Broiler Chickens Using RNA-Sequencing. *PLoS One* 13, e0207346–25. doi:10.1371/journal.pone.0207346

Petracci, M., Sirri, F., Mazzoni, M., and Meluzzi, A. (2013). Comparison of Breast Muscle Traits and Meat Quality Characteristics in 2 Commercial Chicken Hybrids. *Poult. Sci.* 92, 2438–2447. doi:10.3382/ps.2013-03087

Petracci, M., Soglia, F., Madruga, M., Carvalho, L., Ida, E., and Estévez, M. (2019). Wooden-Breast, White Striping, and Spaghetti Meat: Causes, Consequences and Consumer Perception of Emerging Broiler Meat Abnormalities. *Compr. Rev. Food Sci. Food Saf.* 18, 565–583. doi:10.1111/1541-4337.12431

Praud, C., Jimenez, J., Pampouille, E., Couroussé, N., Godet, E., Le Bihan-Duval, E., et al. (2020). Molecular Phenotyping of White Striping and Wooden Breast Myopathies in Chicken. *Front. Physiol.* 11, 633. doi:10.3389/FPHYS.2020.00633/BIBTEX

Rattan, S. I. S. (1998). The Nature of Gerontogenes and Vitagenes: Antiaging Effects of Repeated Heat Shock on Human Fibroblasts. *Ann. N. Y. Acad. Sci.* 854, 54–60. doi:10.1111/j.1749-6632.1998.tb09891.x

Rotival, M., and Petretto, E. (2014). Leveraging Gene Co-expression Networks to Pinpoint the Regulation of Complex Traits and Disease, with a Focus on Cardiovascular Traits. *Briefings Funct. Genomics* 13, 66–78. doi:10.1093/bfgp/elt030

Saleem, M., Qadir, M. I., Perveen, N., Ahmad, B., Saleem, U., Irshad, T., et al. (2013). Inhibitors of Apoptotic Proteins: New Targets for Anticancer Therapy. *Chem. Biol. Drug Des.* 82, 243–251. doi:10.1111/CBDD.12176

Santoro, M. M., Samuel, T., Mitchell, T., Reed, J. C., and Stainier, D. Y. R. (2007). Birc2 (cIap1) Regulates Endothelial Cell Integrity and Blood Vessel Homeostasis. *Nat. Genet.* 39, 1397–1402. doi:10.1038/ng.2007.8

Shannon, P., Markiel, A., Ozier, O., Baliga, N. S., Wang, J. T., Ramage, D., et al. (2003). Cytoscape: A Software Environment for Integrated Models of Biomolecular Interaction Networks. *Genome Res.* 13, 2498–2504. doi:10.1101/gr.1239303

Sihvo, H.-K., Airas, N., Lindén, J., and Puolanne, E. (2018). Pectoral Vessel Density and Early Ultrastructural Changes in Broiler Chicken Wooden Breast Myopathy. *J. Comp. Pathology* 161, 1–10. doi:10.1016/J.JCPA.2018.04.002

Sihvo, H.-K., Immonen, K., and Puolanne, E. (2014). Myodegeneration With Fibrosis and Regeneration in the Pectoralis Major Muscle of Broilers. *Vet. Pathol.* 51, 619–623. doi:10.1177/0300985813497488

Sihvo, H.-K., Lindén, J., Airas, N., Immonen, K., Valaja, J., and Puolanne, E. (2017). Wooden Breast Myodegeneration of Pectoralis Major Muscle Over the Growth Period in Broilers. *Vet. Pathol.* 54, 119–128. doi:10.1177/0300985816658099

Soglia, F., Mazzoni, M., and Petracci, M. (2019). Spotlight on Avian Pathology: Current Growth-Related Breast Meat Abnormalities in Broilers. *Avian Pathol.* 48, 1–3. doi:10.1080/03079457.2018.1508821

Soglia, F., Petracci, M., Davoli, R., and Zappaterra, M. (2021). A Critical Review of the Mechanisms Involved in the Occurrence of Growth-Related Abnormalities Affecting Broiler Chicken Breast Muscles. *Poult. Sci.* 100, 101180. doi:10.1016/J.PSJ.2021.101180

Sreenivasan, K., Ianni, A., Künne, C., Strilic, B., Günther, S., Perdiguero, E., et al. (2020). Attenuated Epigenetic Suppression of Muscle Stem Cell Necroptosis Is Required for Efficient Regeneration of Dystrophic Muscles. *Cell Rep.* 31, 107652. doi:10.1016/J.CELREP.2020.107652

Świerczek-Lasek, B., Neska, J., Kominek, A., Tolak, Ł., Czajkowski, T., Jańczyk-Ilach, K., et al. (2019). Interleukin 4 Moderately Affects Competence of Pluripotent Stem Cells for Myogenic Conversion. *Ijms* 20, 3932. doi:10.3390/IJMS20163932

Tasoniero, G., Cullere, M., Cecchinato, M., Puolanne, E., and Dalle Zotte, A. (2016). Technological Quality, Mineral Profile, and Sensory Attributes of Broiler Chicken Breasts Affected by White Striping and Wooden Breast Myopathies. *Poult. Sci.* 95, 2707–2714. doi:10.3382/PS/PEW215

van Dam, S., Võsa, U., van der Graaf, A., Franke, L., and de Magalhães, J. P. (2018). Gene Co-expression Analysis for Functional Classification and Gene-Disease Predictions. *Brief. Bioinform.* 19, 575–592. doi:10.1093/bib/bbw139

Velleman, S. G., Clark, D. L., and Tonniges, J. R. (2018). The Effect of the Wooden Breast Myopathy on Sarcomere Structure and Organization. *Avian Dis.* 62, 28–35. doi:10.1637/11766-110217-reg.1

Velleman, S. G. (2020). Pectoralis Major (Breast) Muscle Extracellular Matrix Fibrillar Collagen Modifications Associated With the Wooden Breast Fibrotic Myopathy in Broilers. *Front. Physiol.* 11, 1–7. doi:10.3389/fphys.2020.00461

Velleman, S. G. (2015). Relationship of Skeletal Muscle Development and Growth to Breast Muscle Myopathies: A Review. *Avian Dis.* 59, 525–531. doi:10.1637/11223-063015-review.1

Vohhodina, J., Barros, E. M., Savage, A. L., Liberante, F. G., Manti, L., Bankhead, P., et al. (2017). The RNA Processing Factors THRAP3 and BCLAF1 Promote the DNA Damage Response through Selective mRNA Splicing and Nuclear Export. *Nucleic Acids Res.* 45, 12816–12833. doi:10.1093/NAR/GKX1046

Wang, T., Zhang, X., and Li, J. J. (2002). The Role of NF-κB in the Regulation of Cell Stress Responses. *Int. Immunopharmacol.* 2, 1509–1520. doi:10.1016/S1567-5769(02)00058-9

Wertz, I. E., and Dixit, V. M. (2008). Ubiquitin-mediated Regulation of TNFR1 Signaling. *Cytokine & Growth Factor Rev.* 19, 313–324. doi:10.1016/J.CYTOGFR.2008.04.014

Wold, J. P., Veiseth-Kent, E., Høst, V., and Løvland, A. (2017). Rapid On-Line Detection and Grading of Wooden Breast Myopathy in Chicken Fillets by Near-Infrared Spectroscopy. *PLoS One* 12 (3), e0173384. doi:10.1371/journal.pone.0173384

Xing, T., Pan, X., Zhang, L., and Gao, F. (2021). Hepatic Oxidative Stress, Apoptosis, and Inflammation in Broiler Chickens with Wooden Breast Myopathy. *Front. Physiol.* 12, 659777. doi:10.3389/FPHYS.2021.659777/FULL

Xing, T., Zhao, X., Xu, X., Li, J., Zhang, L., and Gao, F. (2020). Physiochemical Properties, Protein and Metabolite Profiles of Muscle Exudate of Chicken Meat Affected by Wooden Breast Myopathy. *Food Chem.* 316, 126271. doi:10.1016/j.foodchem.2020.126271

Yang, W., and Hu, P. (2018). Skeletal Muscle Regeneration Is Modulated by Inflammation. *J. Orthop. Transl.* 13, 25–32. doi:10.1016/J.JOT.2018.01.002

Yoshida, T., and Delafontaine, P. (2020). Mechanisms of IGF-1-Mediated Regulation of Skeletal Muscle Hypertrophy and Atrophy. *Cells* 9, 1970. doi:10.3390/CELLS9091970

Yu, D., Lim, J., Wang, X., Liang, F., and Xiao, G. (2017). Enhanced Construction of Gene Regulatory Networks Using Hub Gene Information. *BMC Bioinforma.* 18 (1), 186. doi:10.1186/s12859-017-1576-1

Zambonelli, P., Zappaterra, M., Soglia, F., Petracci, M., Sirri, F., Cavani, C., et al. (2016). Detection of Differentially Expressed Genes in Broiler Pectoralis Major Muscle Affected by White Striping - Wooden Breast Myopathies. *Poult. Sci.* 95, 2771–2785. (accession number GSE79276). doi:10.3382/ps/pew268

Zanetti, M. A., Tedesco, D. C., Schneider, T., Teixeira, S. T. F., Daroit, L., Pilotto, F., et al. (2018). Economic Losses Associated with Wooden Breast and White Striping in Broilers. *Sca* 39, 887–892. doi:10.5433/1679-0359.2018v39n2p887

Zappaterra, M., Gioiosa, S., Chillemi, G., Zambonelli, P., and Davoli, R. (2021). Dissecting the Gene Expression Networks Associated with Variations in the Major Components of the Fatty Acid Semimembranosus Muscle Profile in Large White Heavy Pigs. *Animals* 11, 628. doi:10.3390/ANI11030628

Zeng, Z.-S., Cohen, A. M., Guillem, J. G., and Guillem, G. (1999). Loss of Basement Membrane Type IV Collagen Is Associated with Increased Expression of Metalloproteinases 2 and 9 (MMP-2 and MMP-9) during Human Colorectal Tumorigenesis. *Carcinogenesis* 20 (5), 749–755. doi:10.1093/carcin/20.5.749

Zhang, B., and Horvath, S. (2005). A General Framework for Weighted Gene Co-expression Network Analysis. *Stat. Appl. Genet. Mol. Biol.* 4, 17. doi:10.2202/1544-6115.1128

Conflict of Interest: The authors declare that the research was conducted in the absence of any commercial or financial relationships that could be construed as a potential conflict of interest.

Publisher's Note: All claims expressed in this article are solely those of the authors and do not necessarily represent those of their affiliated organizations, or those of the publisher, the editors and the reviewers. Any product that may be evaluated in this article, or claim that may be made by its manufacturer, is not guaranteed or endorsed by the publisher.

frontiers | Frontiers in Physiology

ORIGINAL RESEARCH
published: 18 July 2022
doi: 10.3389/fphys.2022.920777

Immunization of Broiler Chickens With a Killed Chitosan Nanoparticle *Salmonella* Vaccine Decreases *Salmonella* Enterica Serovar Enteritidis Load

Keila Acevedo-Villanueva[1], *Gabriel Akerele*[1], *Walid Al-Hakeem*[1], *Daniel Adams*[1], *Renukaradhy Gourapura*[2] *and Ramesh Selvaraj*[1]*

[1]Department of Poultry Science, College of Agricultural and Environmental Sciences, University of Georgia, Athens, GA, United States, [2]Ohio Agricultural Research and Development Center, College of Food, Agricultural, and Environmental Sciences, The Ohio State University, Columbus, OH, United States

There is a critical need for an oral-killed *Salmonella* vaccine for broilers. Chitosan nanoparticle (CNP) vaccines can be used to deliver *Salmonella* antigens orally. We investigated the efficacy of a killed *Salmonella* CNP vaccine on broilers. CNP vaccine was synthesized using *Salmonella* enterica serovar Enteritidis (*S*. Enteritidis) outer membrane and flagella proteins. CNP was stable at acidic conditions by releasing 14% of proteins at pH 5.5. At 17 h post-incubation, the cumulative protein release for CNP was 75% at pH 7.4. Two hundred microliters of PBS with chicken red blood cells incubated with 20 µg/ml CNP released 0% hemoglobin. Three hundred chicks were allocated into 1) Control, 2) Challenge, 3) Vaccine + Challenge. At d1 of age, chicks were spray-vaccinated with PBS or 40 mg CNP. At d7 of age, chicks were orally-vaccinated with PBS or 20 µg CNP/bird. At d14 of age, birds were orally-challenged with PBS or 1×10^7 CFU/bird of *S*. Enteritidis. The CNP-vaccinated birds had higher antigen-specific IgY/IgA and lymphocyte-proliferation against flagellin ($p < 0.05$). At 14 days post-infection, CNP-vaccinated birds reversed the loss in gut permeability by 13% ($p < 0.05$). At 21 days post-infection, the CNP-vaccinated birds decreased *S*. Enteritidis in the ceca and spleen by 2 Log_{10} CFU/g, and in the small intestine by 0.6 Log_{10} CFU/g ($p < 0.05$). We conclude that the CNP vaccine is a viable alternative to conventional *Salmonella* poultry vaccines.

Keywords: Salmonella, Enteritidis, vaccines, broilers, nanoparticles

OPEN ACCESS

Edited by:
Sandra G. Velleman, The Ohio State University, United States

Reviewed by:
Kazi Mirajul Hoque, University of Maryland, United States
Francesca Soglia, University of Bologna, Italy

***Correspondence:**
Ramesh Selvaraj
selvaraj@uga.edu

Specialty section:
This article was submitted to Avian Physiology, a section of the journal Frontiers in Physiology

Received: *15 April 2022*
Accepted: *18 May 2022*
Published: *18 July 2022*

Citation:
Acevedo-Villanueva K, Akerele G, Al-Hakeem W, Adams D, Gourapura R and Selvaraj R (2022) Immunization of Broiler Chickens With a Killed Chitosan Nanoparticle Salmonella Vaccine Decreases Salmonella Enterica Serovar Enteritidis Load. Front. Physiol. 13:920777. doi: 10.3389/fphys.2022.920777

1 INTRODUCTION

Salmonella is a zoonotic pathogen that is currently responsible for approximately four billion dollars in total costs of foodborne illness in the United States of America (United States) (Economic Research Service United States Department of Agriculture, 2021). Poultry is a core reservoir of *Salmonella* and it is linked to approximately seventy percent of salmonellosis foodborne cases (Andino and Hanning, 2015). *Salmonella* control strategies in the poultry industry consist of combined pre-harvest and post-harvest preventative strategies that aim to decrease *Salmonella* "on-farm" and also minimize the introduction of *Salmonella* at poultry processing plants when broilers

reach market age. Broilers are considered to be at market age when they reach slaughter weight typically between 28 and 49 days of age (Setyohadi, Octavia and Puspitasari, 2018; Lakhmir; Singh & Manjit Kaur, 2021). One of the successful preventative strategies against *Salmonella* includes vaccinating at an early age. This strategy is facilitated by high throughput methods, like gel-spray vaccination, on the day of hatch.

For chickens, spray vaccination is a standard method for delivering respiratory vaccines, such as Newcastle Disease or Infectious Bronchitis (Tizard, 2021). Spray vaccination is especially convenient when vaccinating birds for the first time as it can be done in high throughput and an automated manner in the hatchery while the chicks are still grouped in chicken crates. Spray vaccination is one of the delivery methods that can induce mucosal immunity. For example, one way the respiratory vaccines for broilers induce mucosal immunity upon being delivered by spray is by entering the chicks' mucosal cells in the eyes and upper respiratory tract (Nochi et al., 2018). For this study, the gel-spray method was used to deliver the CNP vaccine to newly hatched chicks. When the vaccine was sprayed on the chicks, the colored gel droplets attached to the chicks' feathers were ingested as a form of oral vaccination when hungry newly-hatched chicks preened each other or themselves in chicken crates.

Selecting the most efficient delivery route for vaccines is vital because pathogens have different natures that allow them to thrive against the host immune defenses. For example, the oral vaccination route is key to developing mucosal immune responses against enteric pathogens, such as *Salmonella*. The oral route provides a more tailored and effective defense against *Salmonella* because systemic and mucosal immune responses are highly segregated (Li et al., 2020). However, the delivery route for conventional *Salmonella* killed vaccines for broilers are subcutaneous or intramuscular injections. The challenge is that injected vaccines induce poor mucosal immunity because they elicit specific T-cell responses in the bloodstream, resulting in predominantly IgY responses. Mucosal vaccines, however, stimulate the production of secretory immunoglobulin A (sIgA) along the gastrointestinal tract (GIT) (Lamm, 1997; Levine, 2000; Neutra and Kozlowski, 2006). The sIgA maintains homeostasis between the commensal microorganisms in the GIT and contributes to the late clearance of *Salmonella* enterica serovars from the GIT (Berthelot-Hérault et al., 2003; Forbes, Eschmann and Mantis, 2008). In addition, currently available *Salmonella* vaccines for oral delivery in broilers are live-attenuated vaccines. Live attenuated vaccines have the probability of the vaccine strain regaining its virulence (Tak W. Mak, 2006) and compromising the flock. Thus, killed *Salmonella* vaccines are preferred. Unfortunately, there are currently no commercially available oral-killed *Salmonella* vaccines for broilers. For this reason, chitosan nanoparticle (CNP) vaccines against *Salmonella* are studied as alternative vaccine candidates.

Chitosan is a natural polymer that is known for being mucoadhesive, biodegradable, non-toxic, and biologically compatible. Further, chitosan-based nanoparticles have been proved to be one of the most effective nanocarriers for the oral delivery of antigens (Imam et al., 2021). The CNP vaccine is synthesized with outer membrane proteins (OMPs) and flagella proteins extracted from *Salmonella* enterica serovar Enteritidis (Sankar Renu, Ashley D. Markazi, Santosh Dhakal, Yashavanth Shaan Lakshmanappa, Revathi Shanmugasundaram, 2018a). The synthesized CNP has (1) high cationic charge, (2) average particle size distribution of approximately 500 nm, (3) 70% encapsulation efficacy for entrapped antigens, and (4) 40% encapsulation efficacy for surface-conjugated antigens (Renu Sankar et al., 2018). In different studies, the CNP vaccine has shown to be biocompatible with broilers and layers, have no adverse effects on the production performance of broilers or layers, to successfully deliver the antigens to the Peyer's Patches *via* oral delivery, to significantly increase the antigen-specific mucosal immune response against *Salmonella*, and to decrease *Salmonella* enterica serovar Enteritidis (*S.* Enteritidis) in the ceca (Renu, D. Markazi, et al., 2018; Acevedo-Villanueva et al., 2020; Renu, Markazi, et al., 2020a; Y. Han et al., 2020a).

Previous studies have explored the potential for mass vaccination delivery of the CNP vaccine through oral gavage, water, feed, *in-ovo*, and in a combined live followed by killed vaccination scheme (Acevedo-Villanueva et al., 2020; Renu, Han, et al., 2020; Renu, Markazi, et al., 2020; Y.; Han et al., 2020a; Yi; Han et al., 2020b; Acevedo-Villanueva et al., 2021; Acevedo-Villanueva, Renu and Gourapura, Renukaradhya, Selvaraj, 2021). Therefore, the objective of this study was to examine the efficacy of a killed *Salmonella* CNP vaccine delivered through gel-spray vaccination on broilers at d35 of age. We hypothesize that the CNP vaccine can elicit significant amounts of antigen-specific IgA and can significantly decrease the cecal and intestinal load of *S.* Enteritidis in broilers. We tested our hypothesis by (1) quantifying serum, cloacal, and bile anti-*Salmonella* OMPs IgY and IgA antibodies, (2) quantifying *S.* Enteritidis loads in the gizzard, pancreas, small intestine, spleen, liver, ceca, heart, and blood, (3) quantifying the antigen-recall response, (4) quantifying key cytokines and Toll-like receptors (TLRs) mRNA amounts, (5) quantifying fluorescein isothiocyanate dextran (FITC-d) levels in the serum, and (6) monitoring the body-weight-gain (BWG) and feed-conversion-ratio (FCR) of immunized and challenged broilers.

2 MATERIALS AND METHODS

2.1 Ethical Considerations

All animal protocols were approved by the Institutional Animal Care and Use Committee (IACUC) at the University of Georgia (IACUC # A2021 04-014-Y1-A1). Experimental procedures were performed following the pertinent guidelines concerning animal handling, care, and welfare.

2.2 Synthesis of Chitosan Nanoparticle Vaccine

2.2.1 Isolation of *S.* Enteritidis Outer Membrane Proteins

A crude protein extract of *S.* Enteritidis OMPs was used for the preparation of the CNP vaccine. The isolation of *S.* Enteritidis OMPs was done as described previously (Renu, Markazi, et al., 2020; Acevedo-Villanueva et al., 2021). In brief, a pure culture of wild-type *S.* Enteritidis was grown in Tryptic Soy Broth for 48 h at 37°C, with shaking. The grown culture was resuspended with 1 × Phosphate-Buffered Saline (PBS; pH 7.4) and centrifuged three times at 4,800 ×g for 40 min. The cell pellet was collected, washed three times using 10 mM TRIS Base buffer (pH 7.5), and heat-killed at 75 C for 20 min. The cell pellet was subsequently treated with 2% Triton X-100 in 10 mM Tris HCl buffer (pH 7.5) and disrupted using a homogenizer (OMNI Inc., GA, United States) for two rounds of 3 min each, with a cooling period on ice of 1 min in between each round. Afterward, the cell suspension was centrifuged at 4,800 ×g for 30 min and the supernatant was collected and centrifuged at 100,000 ×g for 3 h. The protein concentration was estimated using a Pierce™ BCA Protein Assay Kit (Thermo Fisher Scientific, United States), as per the manufacturer's instructions. The final product was freeze-dried with 5% sucrose and stored until further use.

2.2.2 Isolation of *S.* Enteritidis Flagellar Proteins

A crude protein extract of *S.* Enteritidis flagellin was used for the preparation of the CNP vaccine. The flagellin proteins were isolated from *S.* Enteritidis, as described previously (Renu, Markazi, et al., 2020; Acevedo-Villanueva et al., 2021). A pure culture of wild-type *S.* Enteritidis was grown in Brain Heart Infusion Broth (Sigma-Aldrich, MO, United States) for 48 h at 37°C, without shaking. The grown culture was resuspended with 1 × PBS (pH 7.4) and centrifuged three times at 4,000 ×g for 40 min. The suspension was subsequently treated with 3M Potassium Thiocyanate in 1 × PBS (pH 7.4) for 2 h at 25°C, with magnetic stirring. The treated cell suspension was centrifuged at 35,000 ×g for 30 min. The supernatant was dialyzed against 1 × PBS (pH 7.4), followed by overnight dialysis in Milli-Q water. The protein concentration was estimated using a Pierce™ BCA Protein Assay Kit, as per the manufacturer's instructions. The end product was freeze-dried using 5% sucrose and stored until further use.

2.2.3 Preparation of the Loaded Chitosan Nanoparticle Vaccine

The loaded CNP was synthesized using the ionic gelation method, as described previously (Renu, Markazi, et al., 2020; Acevedo-Villanueva et al., 2021). First, a solution of 1.0% (w/v) low molecular weight chitosan (Sigma-Aldrich, MO, United States) was made by slowly dissolving the chitosan in an aqueous solution of 4.0% acetic acid. The chitosan solution was magnetically stirred overnight, the pH was adjusted to 4.3, and the overnight stirring was repeated once more. The dissolved chitosan solution was collected and filtered using a 0.44 µm syringe filter. Afterward, 5 mL of the 1.0% chitosan solution were added to 5 ml of deionized water and magnetically stirred for 15 min. Then, the solution was incubated with 2.5 mg OMPs and flagella proteins for 15 min, with magnetic stirring. To form the nanoparticles, 2.5 ml of 1% (w/v) Sodium Tripolyphosphate (TPP) was dissolved in 2.5 ml deionized water and was subsequently added to the solution that contained the OMPs and flagella proteins, under magnetic stirring at 25°C. Finally, 2.5 mg of flagellin protein in 1 × PBS (pH 7.4) were added to the nanoparticles and the suspension was incubated for 3 h at 25 C, with magnetic stirring. The CNP vaccines were collected by centrifuging the above suspension at 10,500 ×g for 10 min. The end-product was freeze-dried using 5% sucrose and stored until further use.

2.2.4 Preparation of the Loaded Chitosan Nanoparticle Vaccine in Gel-Pac Solution

The Gel-pac solution used for this study was kindly provided by Animal Science Products, Inc. and was prepared as per the manufacturer's instructions (ASP, Inc., LOT 200507). In brief, one hundred grams of Gel-pac were dissolved into 4 L of cold water. The solution was thoroughly homogenized using a high-speed handheld emulsifier until a uniform distribution of the green coloring in the gel spray solution was obtained. For the vaccination, a total of 40 mg of loaded CNP vaccine diluted in PBS (pH 7.4) were added to the Gel-pac solution for a total volume of 500 ml stock solution. The vaccine solution was delivered in a concentration/volume of 2 mg CNP/25 ml Gel-Pac solution per box of 100 hatched chicks, to account for the delivery of 20 µg/bird. For the mock Gel-pac vaccine solution PBS (pH 7.4) was added to the Gel-pac stock solution.

2.2.5 The Entrapment Efficiency of Total Proteins for Synthesized CNP Vaccine

After centrifuging the loaded CNP, the entrapment efficiency for the synthesized CNP was estimated by quantifying the amount of proteins that were left in the supernatant, as described previously (Akerele et al., 2020). In brief, the protein content in 200 µL of the supernatant was determined by using a Pierce™ BCA Protein Assay Kit, as per the manufacturer's instructions. Afterward, the entrapment efficiency was determined as Entrapment efficiency (%) = (Total protein for the nanoparticle synthesis–Total protein left in the supernatant)/Total protein for the nanoparticle synthesis × 100.

2.2.6 Cumulative Protein Release Assay and pH Stability Assay of Synthesized CNP Vaccine

The cumulative protein release of the CNP was measured by using a cumulative protein release assay, as described previously (Dhakal et al., 2018). In brief, suspensions of 0.2 mg/ml of CNP in 3 ml of 1× PBS (7.4 pH) were incubated at 37 C for 2, 3, 10, and 17 h. For each time point, a total of 350 µL of the supernatant was collected and subsequently centrifuged at 10,000 ×g at 4 C in triplicates. Two hundred microliters of the supernatant were collected, and the protein content was determined using a Pierce™ BCA Protein Assay Kit, as per the manufacturer's instructions. The cumulative protein released for each time

point was determined as Cumulative protein release (%) = (cumulative protein released in the supernatant/0.2) × 100.

A pH stability assay was used to measure the stability of the CNP at different acidic and alkaline pH, as described previously (Akerele et al., 2020). In brief, the stability of the CNP was measured by reconstituting 0.5 mg/ml of CNP in 1 × PBS at 3.5, 4.0, 4.5, 5.5, 6.5, and 7.5 pH. All the CNP suspensions were incubated at 37 °C for 6 h and subsequently centrifuged at 10,000 ×g for 5 min at 4 C. Two hundred microliters of the supernatant were collected, and the protein content was determined using a Pierce™ BCA Protein Assay Kit, as per the manufacturer's instructions. The cumulative protein release at each pH was determined as Protein release (%) = (protein released in the supernatant/0.5) × 100.

2.2.7 Hemolysis Assay- Effect of CNP Vaccine on Chicken Red Blood Cells

A hemolysis assay was done to study the biocompatibility of the CNP with chicken red blood cells (cRBCs) (Pan et al., 2016). In brief, 1 ml of blood from 4-week-old broilers was collected and centrifuged at 750 ×g to obtain the cRBCs. The cRBCs were washed four times with 1 × PBS (7.4 pH) and reconstituted in 3 ml of 1 × PBS (7.4 pH). Afterward, a total of 10 µL of cRBC suspension were incubated with 0.5 ml of 1 × PBS at 7.4 pH (negative control), pure deionized water (positive control), or 20 µg/ml, 50 µg/ml, or 100 µg/ml of CNP. All the suspensions were incubated for 3 h at 37 °C with agitation at 100 rpm. Subsequently, the suspensions were centrifuged at 750 ×g for 6 min. Two hundred microliters of the supernatant were collected, and their absorbance values were determined at 570 nm. The cRBCs hemolysis was determined as: Hemolysis (%) = (OD 595 nm Absorbance (treatment—negative control))/(OD 595 nm Absorbance (positive control–negative control)) × 100.

2.3 Experimental Animals

Broiler birds (Cobb-Vantress hatchery, Inc.) had access to *ad libitum* feed and water during the experimental period. Broiler birds were monitored twice a day for (1) dehydration, (2) refusal to eat food, (3) loss of body weight, (4) diarrhea, (5) bloody feces, and (6) lethargy during the experimental period. Broiler birds were euthanized with CO_2, as per the IACUC standards.

2.3.1 Treatment Groups

At d1 of age, three hundred chicks were randomly allocated into three treatment groups: 1) Control, 2) Challenge, and 3) Vaccine + Challenge. At d1 of age, all treatments were delivered using a spray cabinet (Spraycox® II, K Supply Co. Inc.). Non-vaccine groups were given PBS as a mock vaccination. The vaccine group was given the CNP vaccine. At d7 of age, birds in the control and the challenge groups were given a mock booster vaccination of 0.5 ml 1 × PBS/bird, by oral gavage; while birds in the vaccine + challenge group were given a booster vaccination of 20 µg CNP/bird, by oral gavage. After vaccination, each pen was assigned 16 replicates as birds per pen. At d14 of age, birds in the control group were given a mock challenge of 0.5 ml 1 × PBS/bird by oral gavage, and birds in the challenge and the vaccine + challenge groups were orally challenged with 1×10^7 CFU/bird of nalidixic acid-resistant *S.* Enteritidis. For this study, the experimental unit was the pen (n = 6 pen/treatment). A summary of the experimental treatment groups is provided in **Table 1**.

2.3.2 Sample Collection and Preparation

In this study, the experimental unit was the pen. Treatments consisted of n = 6 pens per treatment, with 16 birds per pen as replicates. On the day of hatch, all chicks were screened for *Salmonella* prevalence. In brief, cloacal swab samples were enriched in Tetrathionate Broth (Neogen, MI) for 6 h. Subsequently, 10 µL of the enriched supernatant were inoculated to Modified Semi-Solid Rappaport-Vassiliadis (MSRV) Agar (Neogen, MI). Samples were subsequently incubated at 41°C for 24 h. Detection of *Salmonella* was negative on the day of hatch.

For the experimental challenge, a pure culture of wild-type *S.* Enteritidis was selected for nalidixic acid resistance on Xylose Lactose Tergitol™ 4 (XLT4) (Neogen, MI) agar at 500 mg/L. The nalidixic acid-resistant colonies were grown at 37°C for 24 h on Tryptic Soy Broth (G-Biosciences, MO, United States) containing 500 mg/L nalidixic acid and further used for the experimental challenge.

At d1 of age, one hundred birds per group were gel-spray vaccinated with either mock PBS or CNP vaccine. At 12 h post-vaccination, cecal tonsils were collected to analyze IL-1β, TNF-α, IFN-γ, IL-6, and TLR 5 mRNA expression by RT-PCR. At d7 of age, birds were treated as follows: (1) the control group and the challenge group were boosted with 1 × PBS (7.4 pH), and (2) the vaccine + challenge group was boosted with CNP vaccine. At d14 of age, birds were treated as follows: (1) the control group was given a mock challenge of 0.5 ml 1 × PBS/bird by oral gavage, and (2) the challenge group and the vaccine + challenge group were orally challenged with 1×10^7 CFU/bird of nalidixic acid-resistant *S.* Enteritidis. At 12 h post-challenge, cecal tonsils were collected to analyze induced nitric oxide synthase (iNOS), IFN-γ, TNF-α, IL-10, IL-6, IL-17, TGF-β, K 60, and TLR 4 mRNA levels by RT-PCR. Bodyweight and feed consumption were recorded weekly. The BWG and FCR were calculated. Blood, bile, and cloacal swabs were collected before the experimental challenge at d14 and d35 of age. The serum, bile, and cloacal swab samples were analyzed by enzyme-linked immunosorbent assay (ELISA) for anti-OMPs IgY and IgA antibodies, respectively. At d12 of age, primary splenocytes were isolated and stimulated with either *S.* Enteritidis OMPs, *S.* Enteritidis flagellin, *S.* Enteritidis heat-killed antigen (HKA), *S.* Typhimurium HKA, *S.* Kentucky HKA, *S.* Infantis HKS, *S.* Heidelberg HKA, *S.* Hadar HKA, *S.* Litchfield HKA, or *S.* Newport HKA, to determine the recall response. At 14 days post-infection (dpi), one bird per pen was given an oral gavage of 2.2 mg FITC-d/bird, and serum was collected after 2 h for a gut permeability assay. At 21 dpi, the birds' gizzard, pancreas, small intestine, spleen, liver, ceca, heart, and blood were collected for *S.* Enteritidis quantification by plating. At 21 dpi, cecal tonsils were collected to analyze IL-1β, TNF-α, IL-6, TGF-β, and IL-10 mRNA levels by RT-PCR, and jejunum samples were collected to analyze Claudin-1 and Zona Occludens-1 mRNA levels by RT-PCR. Spleen samples for the

TABLE 1 | Summary of experimental treatment groups. For all experimental groups, the experimental unit was the pen, $n = 6$ pen/treatment, with 16 technical replicates as birds/pen. For the gel-spray vaccination, 2 mg of CNP vaccine was reconstituted in 25 ml of Gel-Pac solution and sprayed on 100 chicks. For the mock gel-spray vaccination, PBS (pH 7.4) was added to the Gel-pac stock solution. For the oral gavage booster vaccination, birds in the experimental group were given 20 μg CNP/bird, and birds in the control groups were given 0.5 ml PBS/bird. At d14 of age birds in the negative control group were given a mock challenge of 0.5 ml PBS/bird and birds in the positive control and the treatment group were orally challenged with 1×10^7 CFU/bird of S. Enteritidis (nalidixic acid-resistant).

Group	1st Gel-spray vaccination	Oral gavage booster vaccination	Experimental challenge
Control	PBS	PBS	PBS
Challenge	PBS	PBS	1×10^7 CFU/bird *S.* Enteritidis
Vaccine + Challenge	CNP	CNP	1×10^7 CFU/bird *S.* Enteritidis

ex-vivo splenocyte recall assay were collected from two birds per pen, otherwise, samples were collected from one bird per pen ($n = 6$) at each time point.

2.3.3 Antigen-Specific IgY and IgA Antibodies in Serum, Cloacal Swabs, and Bile of Vaccinated Birds

Antigen-specific IgY and IgA antibodies in serum, cloacal swab, and bile samples were assessed by ELISA, as described earlier (Renu, Markazi, et al., 2020). In brief, OMPs were diluted in 0.05 M sodium-bicarbonate coating buffer (9.6 pH) and used to coat high-binding 96-well plates (ThermoFisher Scientific, MA) with either 2 μg/ml of OMP for IgG or 7.5 μg/ml of OMP for IgA (Renu, Markazi, et al., 2020). The OMP-coated plates were incubated overnight at 4°C, with no shaking. The incubated plates were washed three times with 0.05% PBS-Tween 20 (PBS-T; pH 7.4) and were subsequently blocked with 5% non-fat dry milk powder in PBS-T for 1 h at 37°C. The unbound antigens were removed by washing the plates three times with PBS-T. A two-fold serial dilution for a total of 100 μL per well was carried out for each sample. Serum and bile samples were diluted with 2.5% non-fat dry milk and cloacal swabs samples were diluted in 1 × PBS (pH 7.4). Negative serum was used as a control for serum samples, negative bile was used as a control for bile samples, and sterile 1 × PBS (pH 7.4) was used as a control for cloacal swabs samples. The samples were incubated for 2 h at 37°C and subsequently washed three times with PBS-T. Fifty microliters of the HRP-conjugated goat anti-chicken IgG (Southern Biotech, AL) were added at 1: 10,000 in 2.5% non-fat dry milk powder in PBS-T or 50 μL of the HRP-conjugated goat anti-chicken IgA (Bethyl Laboratories, TX) were added at 1: 3,000 in 2.5% skim milk powder in PBS-T. The secondary antibodies were incubated for 2 h at 37°C. Plates were subsequently washed three times with PBS-T, and 50 μL per well of TMB peroxidase substrate (KPL, MD) were added. After 5 min, the reaction was stopped by adding 50 μL per well of 2M Sulfuric Acid (J.T. Baker Inc., NJ, United States). The Optical Density (OD) was measured at 450 nm using a spectrophotometer and the corrected OD was calculated by subtracting the treatment OD from the blank OD. Results were reported as geometric mean titers (GMT). The cut-off values were determined by the mean (x) and standard deviation (SD) of the negative sera for serum samples, negative bile for bile samples, and PBS controls for cloacal swabs samples. The cut-off value was taken as x + 3SD, as described previously (Lunn et al., 2012). The GMT was calculated with the use of the log-transformed values and taken as the antilog of the mean of the transformed values, as described previously (Perkins, 1958; Belshe et al., 2004). The percent increase was determined as [(GMT of Vaccine + Challenge)—(GMT of Control)] ÷ (GMT of Control) × 100.

2.3.4 Recall-Response of Spleenocytes of Vaccinated Birds

For this study, the spleen samples were collected from two birds per pen ($n = 6$) at d12 of age. The recall-response was determined using an *ex-vivo* recall assay, as previously described (Acevedo-Villanueva et al., 2021). Briefly, the whole spleen was passed through a cell strainer with 3 ml of sterile 1 × PBS (7.4 pH) to obtain a single-cell suspension of PBMCs. The single-cell suspension was slowly added onto 3 ml of Ficoll-paque plus solution (Fisher Scientific, MA, United States). To remove the red blood cells the suspension was centrifuged at 450 × g for 30 min at 4°C. Subsequently, the splenocytes in the interface were slowly harvested. The cells were reconstituted using 100 μL of RPMI-1640 (Sigma Aldrich, MO, United States) supplemented with 10% fetal bovine serum and 1% Penicillin and Streptomycin. The cell suspension was plated at 5×10^6 cells per well in duplicates. For the first recall response assay, the cells were stimulated with 20 μg/ml of OMPs crude protein extract or 20 μg/ml of flagellin crude protein extract and incubated for 3 days at 37°C in the presence of 5% CO_2. For the second recall response assay, cells were stimulated with 20 μg/ml of either *S.* Enteritidis HKA, *S.* Typhimurium HKA, *S.* Kentucky HKA, *S.* Infantis HKS, *S.* Heidelberg HKA, *S.* Hadar HKA, *S.* Litchfield HKA, or *S.* Newport HKA. The HKA was prepared by boiling the bacterial stock for 15 min, sonicating to make soluble antigen, and centrifuging at 1,000 ×g for 15 min to obtain the bacterial suspension. The protein concentration was assessed using the Pierce™ BCA Protein Assay Kit, as per the manufacturer's instructions. Further, a Sodium Dodecyl Sulphate–Polyacrylamide Gel Electrophoresis (SDS-PAGE) analysis was done to visualize the *S.* Enterica serovars heat-killed whole-antigenic crude extract (**Supplementary Figure S1**). Before stimulation, the bacterial suspension was re-suspended in the enriched RPMI-1640. As a negative control for both recall response assays, splenocytes were stimulated with 0.0 μg/ml proteins. As a positive control for both recall response assays, splenocytes were stimulated with 20 μg/ml of Concanavalin A (Con A). The proliferation of spleenocytes was measured using an MTT assay, as described previously

(Zhao et al., 2012). The optical density was measured at 570 nm using a spectrophotometer.

2.3.5 *Salmonella* Loads in the Gizzard, Pancreas, Small Intestine, Spleen, Liver, Ceca, Heart, and Blood of Vaccinated Birds

Gizzard, pancreas, small intestine, spleen, liver, ceca, heart, and blood samples were analyzed for *S.* Enteritidis loads by plating. All feed was removed from organs by washing with approximately 3 ml of 1 × PBS (pH 7.4). All samples were stored in stomacher bags and placed on ice. At the laboratory, samples were diluted with 1× (wt/vol) 1 × PBS (pH 7.4), mashed with a rubber mallet, and then stomached for 2 min. A volume of 100 µL of ceca was serially diluted into 900 µL of 1 × PBS (pH 7.4) and from every dilution, a volume of 10 µL was plated in duplicates on XLT4 agar plates. Plates were then incubated for 24 h at 41°C for the confirmation of black colonies. When no growth was observed, to corroborate true negative samples, the samples were further enriched in Tetrathionate Broth for 6 h followed by the inoculation of 10 µL of the enriched solution to XLT4 agar or MSRV Agar. The inoculated media were then incubated for 24 h at 41°C for the confirmation or the absence of black colonies on XLT-4 agar plates or the confirmation of positive or negative samples on MSRV selective motility-enrichment media. Upon double confirmation of the absence of growth, the samples were considered to be negative for *Salmonella* colonization. Data were recorded as CFU/g of organ and then transformed to Log 10 CFU/g of organ for statistical analysis. Further, the prevalence of *S.* Enteritidis in colonized organs was also calculated. In addition, the organ weight was further used to observe the CNP vaccine effect on the relative weight of different organs by calculating the organ index as Weight Index (%) = (organ weight (g))/(live weight (g)) × (100).

2.3.6 FITC-d Concentration in the Serum of Vaccinated Birds

To determine the serum FITC-d levels at 14 dpi, one bird per pen was given FITC-d (MW 3–5 kDa; Sigma-Aldrich Co., St. Louis, MO, United States) by oral gavage at a dose of 2.2 mg FITC-d per bird (Liu et al., 2021). After 2 h the chicks were euthanized by CO_2 inhalation and blood samples were collected. As a control, serum was taken from one broiler chicken of each treatment group that was not given FITC-d. The blood samples were collected and centrifuged at 3,000 rpm for 12 min at 4°C. The serum was then collected and diluted at 1:5. The OD was measured at 485 nm using a spectrophotometer.

2.3.7 Gene Expression in the Cecal Tonsils or Jejunum of Vaccinated Birds

Cecal tonsils were collected to monitor the mRNA expression of key cytokines of the gut-associated lymphoid tissue. Jejunum samples were also collected to monitor the expression of key cytokines of tight-junction proteins in the gut. For this study, cecal tonsil and jejunum samples were collected from one bird per pen ($n = 6$) at 21 dpi. For gene expression analysis samples were analyzed in duplicates. The TRIzol reagent (Invitrogen, CA, United States) was used for the total RNA extraction, as per the manufacturer's instructions. The extracted RNA was dissolved in Tris-EDTA buffer (pH 7.5) and the cDNA synthesis was executed using 2 µg of total RNA template in a 20 µL reaction volume, as described previously (Acevedo-Villanueva et al., 2021). The cecal tonsils mRNA transcripts were analyzed for IL-1β, TNF-α, IFN-γ, IL-6, and TLR 5 mRNA levels at 12 h post-vaccination, or analyzed for iNOS, IFN-γ, TNF-α, IL-10, IL-6, IL-17, TGF-β, K 60, and TLR 4 mRNA levels at 12 h post-challenge, or analyzed for IL-1β, TNF-α, IL-6, TGF-β, and IL-10 mRNA levels at 21 dpi by RT-PCR (CFX96 Touch Real-Time System, BioRad). The jejunum mRNA transcripts were analyzed for Claudin-1 and Zona Occludens-1 mRNA levels at 21 dpi by RT-PCR. All reactions were carried out using iQ™ SYBR® Green Supermix (ThermoFisher Scientific, MA), as described previously (Acevedo-Villanueva et al., 2021). The housekeeping gene Ribosomal Protein S13 (RPS13) was used as a reference gene to normalize the Ct values (de Jonge et al., 2007). The fold change from the reference was determined using the delta-delta Ct method, as explained previously (Schmittgen and Livak, 2008). Results were reported as the fold-change ($2^{-\Delta\Delta Ct}$ method). The primers sequences used for RT-PCR analysis are described in **Table 2**.

2.4 Statistical Analysis

The experimental unit was the pen, where $n = 6$ pens per treatment, with 16 replicates as birds per pen. At each time point, samples were taken from one bird per pen, except for the spleen samples, which were taken from two birds per pen. For this study, all the samples were analyzed in duplicates. Data for the antigen-specific recall response of immunized birds against different *Salmonella* enterica serovars HKA was analyzed by parametric Student t-test. For the multiple comparisons of other data, if data were normally distributed the analysis was done using a one-way analysis of variance (ANOVA), followed by a Tukey's post-hoc test. Otherwise, the statistical differences were determined using a Kruskal-Wallis test and followed by Dunn's post-hoc test. Statistical analysis was performed using JMP Pro 14 (SAS Institute Inc., United States) and results were statistically significant at $p < 0.05$.

3 RESULTS

3.1 *In-vitro* Analysis of Synthesized CNP Vaccine

3.1.1 The Entrapment Efficiency of Total Proteins for Synthesized CNP Vaccine

The entrapment efficiency for the total protein content of the CNP vaccine was 87% (data not shown).

3.1.2 The pH Stability Assay and Cumulative Protein Release Assay of Synthesized CNP Vaccine

At 6 h post-incubation the CNP released 3, 9, 10, 14, 31 and 26% of proteins from 3.5 to 7.5 pH, respectively (**Table 3**).

At 2 h post-incubation the CNP had released 11% of its protein cargo, at 3 h post-incubation the CNP had released

TABLE 2 | Primers and PCR conditions for RT-PCR.

Target Gene	Sequence (5′—3′)	T_a (°C)	Reference
IL-1β (F)	TCCTCCAGCCAGAAAGTGA	57.0	Morris et al. (2014)
IL-1β (R)	CAGGCGGTAGAAGATGAAGC		
IFN-γ (F)	GTGAAGAAGGTGAAAGTATCATGGA	57.0	Kaiser, Underwood and Davison, (2003)
IFN-γ (R)	GCTTTGCGCTGGATTCTCA		
IL-10 (F)	CATGCTGCTGGGCCTGAA	57.5	Rothwell et al. (2004)
IL-10 (R)	CGTCTCCTTGATCTGCTTGATG		
iNOS (F)	AGTGGTATGCTCTGCCTGCT	60.0	Selvaraj and Klasing, (2006)
iNOS (R)	CCAGTCCCATTCTTCTTCC		
TGF-β (F)	AGGATCTGCAGTGGAGTGGAT	54.0	Han et al. (2020b)
TGF-β (R)	CCCCGGGTTGTGTTGGT		
IL-6 (F)	CAAGGTGACGGAGGAGGAC	57.5	Hong et al. (2012)
IL-6 (R)	TGGCGAGGAGGGATTTCT		
TNF-α (F)	ATCCTCACCCCTACCCTGTC	56.0	Han et al. (2020b)
TNF-α (R)	GGCGGTCATAGAACAGCACT		
IL-17 (F)	GCAGATGCTGGATGCCTAAC	55.5	Markazi et al. (2018)
IL-17 (R)	ATGGAGCCAGTGAGCGTTT		
TLR 4 (F)	ACCTACCCATCGGACACTTG	60.0	Markazi, et al. (2018)
TLR 4 (R)	TGCCTGAGAGAGGTCAGGTT		
TLR 5 (F)	CCTTGTGCTTTGAGGAACGAGA	52.3	Xu et al. (2015)
TLR 5 (R)	CACCCATCTTTGAGAAACTGCC		
K60 (F)	ATTTCCTCCTGCCTCCTACA	55.0	Hong et al. (2006)
K60 (R)	GTGACTGGCAAAAATGACTCC		
Claudin-1 (F)	TGTAGCCACAGCAAGAGGTG	55.0	Chen et al. (2017)
Claudin-1 (R)	GACAGCCATCCGCATCTTCT		
Zona Occludens-1 (F)	TGTAGCCACAGCAAGAGGTG	55.0	Oxford and Selvaraj, (2019)
Zona Occludens-1 (R)	CTGGAATGGCTCCTTGTGGT		
RPS13 (F)	CAAGAAGGCTGTTGCTGTTCG	55.5	Hutsko. (2017)
RPS13 (R)	GGCAGAAGCTGTCGATGATT		

TABLE 3 | The pH stability assay and cumulative protein release assay of the synthesized CNP vaccine. The CNP was incubated in 1 × PBS at multiple pH's for 6 h.

pH stability of the CNP vaccine	
pH	**Protein release (%)**
3.5	3
4.0	9
4.5	10
5.5	14
6.5	31
7.5	26

TABLE 4 | The pH stability assay and cumulative protein release assay of the synthesized CNP vaccine. The CNP were incubated in 1 × PBS at 7.4 pH and the cumulative antigen release was assessed at different time points. Means +SD. $n = 2$.

Cumulative protein release of the CNP vaccine	
Hours	**CPR (%)**
2	11
3	14
10	21
17	75

TABLE 5 | Effect of CNP on chicken red blood cells. The CNP was synthesized by entrapping a crude-enriched extract of OMP and Flagellin proteins from *Salmonella* enterica serovar Enteritidis. Mean ± SD. $n = 2$.

cRBCs hemolysis (%)		
20 μg/ml	**50 μg/ml**	**100 μg/ml**
0.07 ± 0.030	0.09 ± 0.007	0.94 ± 0.021

14% of its protein cargo, at 10 h post-incubation the CNP had released 21% of its protein cargo, and at 17 h post-incubation the CNP had released 75% of its protein cargo (**Table 4**).

3.1.3 Hemolysis Assay- Effect of CNP Vaccine on Chicken Red Blood Cells

The cRBC incubated with 20 μg/ml, 50 μg/ml, and 100 μg/ml of CNP had 0.07, 0.09 and 0.9% hemolysis respectively (**Table 5**).

3.2 The Effects of *Salmonella* CNP Vaccine on the Production Performance of Vaccinated Birds

The CNP vaccine had no adverse effect on the production performance of the vaccinated birds. There were no significant differences ($p > 0.05$) between treatments in the BWG or FCR of birds at all the time points, compared to control; hence, results

TABLE 6 | The GMT of anti-*S.* Enteritidis OMP IgY and IgA antibodies. Blood, bile, and cloacal swabs samples were collected at d14 of age (pre-challenge) and d35 of age (post-challenge). Samples were analyzed for anti-*Salmonella* OMP IgY and OMP IgA levels by ELISA ($n = 6$). Results were reported as geometric mean titers (GMT). Values with no common superscript differ ($p < 0.05$). The percent increase was determined as [(GMT of Vaccine + Challenge)–(GMT of Control)] ÷ (GMT of Control) × 100.

OMP					
Sample	**Day of age**	**Treatment group**	**GMT**	**% CV**	***p*-value**
Serum	d14	Control	228[b]	69	$p < 0.05$
		Challenge	128[ab]	79	
		Vaccine + Challenge	724[a]	49	
	d35	Control	144	20	$p = 0.05$
		Challenge	1448	42	
		Vaccine + Challenge	1290	47	
Bile	d14	Control	645[c]	82	$p < 0.05$
		Challenge	724[b]	63	
		Vaccine + Challenge	4096[a]	0	
	d35	Control	512[b]	59	$p < 0.05$
		Challenge	4096[a]	0	
		Vaccine + Challenge	3250[a]	31	
Cloacal swabs	d14	Control	23	67	$p = 0.05$
		Challenge	51	20	
		Vaccine + Challenge	2298	52	
	d35	Control	161[b]	89	$p < 0.05$
		Challenge	2580[a]	49	
		Vaccine + Challenge	1824[a]	68	

The meaning of the symbol for (a, b) in Table is in indicated in the figure legend as "Values with no common superscript differ (p < 0.05)." It indicates the significance of the data.

were reported as cumulative BWG (**Supplementary Figure S2A**) and FCR from d0 to d35 of age (**Supplementary Figure S2B**).

3.3 The Effects of *Salmonella* CNP Vaccine on Antigen-Specific IgY and IgA Antibodies of Vaccinated Birds

At d14 of age, the birds that were vaccinated with CNP had significantly increased anti-*S.* Enteritidis OMP IgY serum titers by 218%, when compared to the control group ($p < 0.05$) (**Table 6**). At d35 of age, there were no significant differences in anti-*S.* Enteritidis OMP IgY titers from serum samples between any of the treatment groups when compared to the control group ($p = 0.05$) (**Table 6**). At d14 of age, the birds that were vaccinated with CNP had significantly increased anti-*S.* Enteritidis OMP IgA bile titers by 535%, when compared to the control group ($p < 0.05$) (**Table 6**). At d35 of age, the birds that were vaccinated with CNP had significantly increased anti-*S.* Enteritidis OMP IgA bile

TABLE 7 | The GMT of anti-*S.* Enteritidis Flagellin IgY and IgA antibodies. Blood, bile, and cloacal swabs samples were collected at d14 of age (pre-challenge) and d35 of age (post-challenge). Samples were analyzed for anti-*Salmonella* Flagellin IgY and Flagellin IgA levels by ELISA ($n = 6$). Results were reported as geometric mean titers (GMT). Values with no common superscript differ ($p < 0.05$). The percent increase was determined as [(GMT of Vaccine + Challenge)–(GMT of Control)] ÷ (GMT of Control) × 100.

Flagellin					
Sample	**Day of age**	**Treatment group**	**GMT**	**% CV**	***p*-value**
Serum	d14	Control	512	0	$p > 0.05$
		Challenge	181	70	
		Vaccine + Challenge	1024	56	
	d35	Control	574	35	$p > 0.05$
		Challenge	1024	59	
		Vaccine + Challenge	812	75	
Bile	d14	Control	456[b]	68	$p < 0.05$
		Challenge	813 [ab]	72	
		Vaccine + Challenge	1448[a]	37	
	d35	Control	512[b]	0	$p < 0.05$
		Challenge	2047[a]	0	
		Vaccine + Challenge	1824[a]	22	
Cloacal swabs	d14	Control	57	34	$p > 0.05$
		Challenge	18	32	
		Vaccine + Challenge	91	30	
	d35	Control	80[b]	82	$p < 0.05$
		Challenge	813[a]	70	
		Vaccine + Challenge	1448[ab]	85	

The meaning of the symbol for (a, b) in Table is in indicated in the figure legend as "Values with no common superscript differ (p < 0.05)." It indicates the significance of the data.

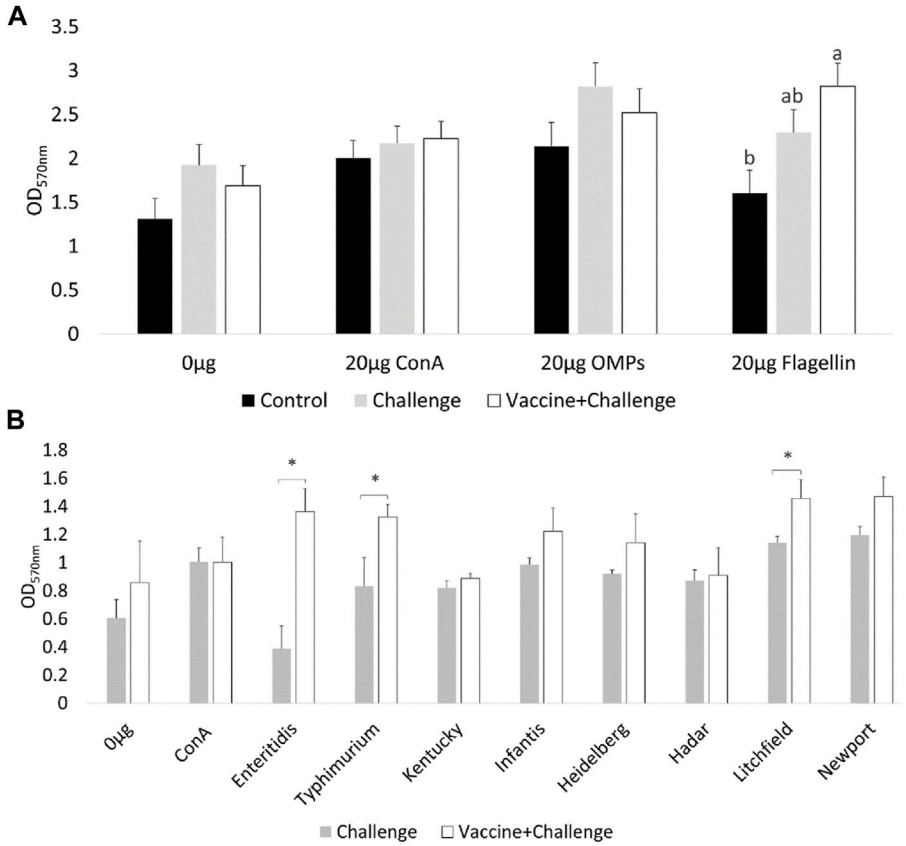

FIGURE 1 | *Ex-vivo* recall-response of spleenocytes of vaccinated birds. At d12 of age, splenocytes PBMCs were stimulated with either 20 µg/ml OMP, 20 µg/ml Flagellin or 20 µg/ml proteins of different *S*. Enterica serovars HKA for 3 days. As a negative control splenocytes were stimulated with 0.0 µg/ml of antigen. As a positive control splenocytes were stimulated with 20 µg/ml Con A. **(A)** OMP and Flagellin. Bars (+SE) with no common superscript differ ($p < 0.05$); **(B)** HKA from *S*. Enterica serovars. Means + SE Bars. $n = 6$. "*" signifies $p < 0.05$.

titers by 535%, when compared to the control group ($p < 0.05$) (**Table 6**). At d14 of age, there were no significant differences in anti-*S*. Enteritidis OMP IgA titers from cloacal swab samples between any of the treatment groups when compared to the control group ($p = 0.05$) (**Table 6**). At d35 of age, the birds that were vaccinated with CNP had significantly increased anti-*S*. Enteritidis OMP IgA cloacal titers by 1033%, when compared to the control group ($p < 0.05$) (**Table 6**).

At d14 of age and d35 of age, there were no significant differences in anti-*S*. Enteritidis Flagellin IgY titers from serum samples between any of the treatment groups when compared to control ($p > 0.05$) (**Table 7**). At d14 of age, the birds that were vaccinated with CNP had significantly increased anti-*S*. Enteritidis Flagellin IgA bile titers by 218%, when compared to the control group ($p < 0.05$) (**Table 7**). At d35 of age, the birds that were vaccinated with CNP had significantly increased anti-*S*. Enteritidis Flagellin IgA bile titers by 256%, when compared to the control group ($p < 0.05$) (**Table** 7). At d14 of age, there were no significant differences in anti-*S*. Enteritidis Flagellin IgA titers from cloacal swabs samples between any of the treatment groups when compared to control ($p > 0.05$) (**Table 7**). At d35 of age, the birds that were vaccinated with CNP had significantly increased anti-*S*. Enteritidis Flagellin IgA cloacal titers by 1710%, when compared to the control group ($p < 0.05$) (**Table 7**).

3.4 The Effects of *Salmonella* CNP Vaccine on the Antigen Recall Response of Vaccinated Birds

At d12 of age, the spleenocytes from birds that were immunized with the CNP vaccine had significant ($p < 0.05$) T-lymphocyte proliferation when they were stimulated with 20 µg/ml Flagellin, compared to control (**Figure 1A**). There were no significant differences in T-lymphocyte proliferation when the spleenocytes were stimulated with 20 µg/ml OMP, compared to control (**Figure 1A**).

At d12 of age, the spleenocytes from birds that were immunized with the CNP vaccine had significant ($p < 0.05$) T-lymphocyte proliferation when they were stimulated with 20 µg/mL *S*. Enteritidis HKA, 20 µg/mL *S*. Typhimurium HKA, and 20 µg/mL *S*. Litchfield HKA, compared to control (**Figure 1B**).

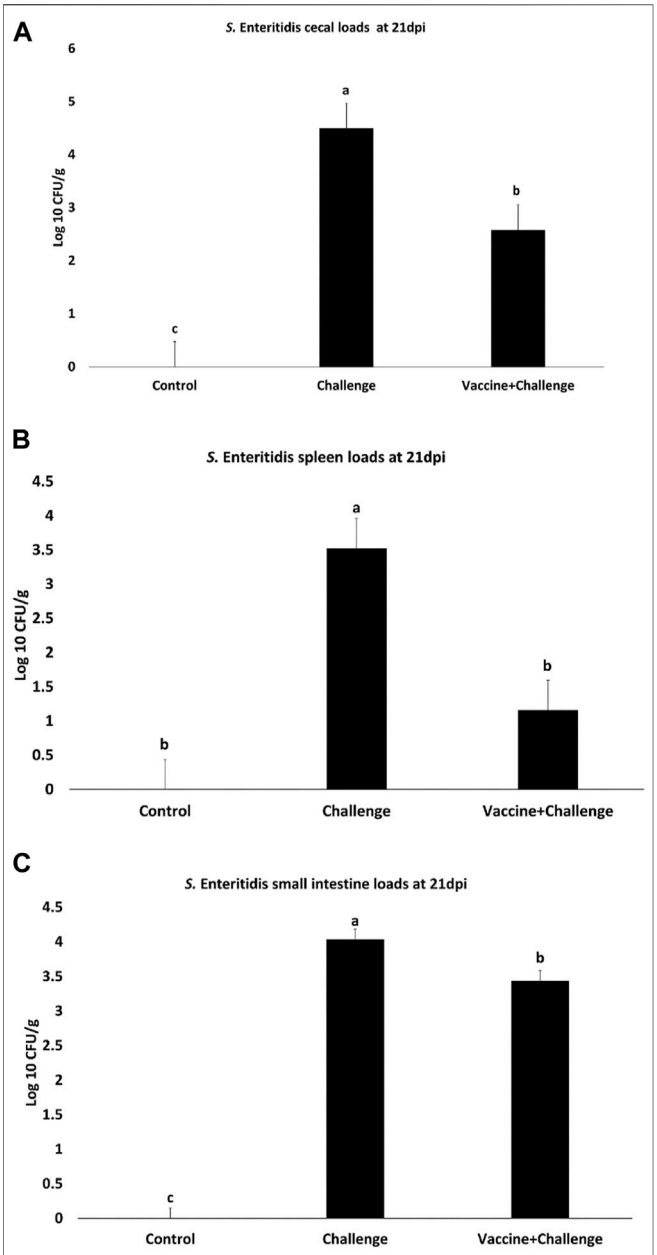

FIGURE 2 | *Salmonella* loads in the ceca, spleen, and small intestines of vaccinated birds. Organ samples were collected from 1 bird per pen ($n = 6$) at 21 dpi. Samples were analyzed for *S*. Enteritidis loads by plating. Samples that were double negative for *S*. Enteritidis presence after selective enrichment were considered negative for *Salmonella* colonization. Data were recorded as CFU/g of organ and transformed to Log 10 CFU/g of organ for statistical analysis. **(A)** Ceca; **(B)** Spleen; **(C)** Small intestine. Bars (+SE) with no common superscript differ ($p < 0.05$).

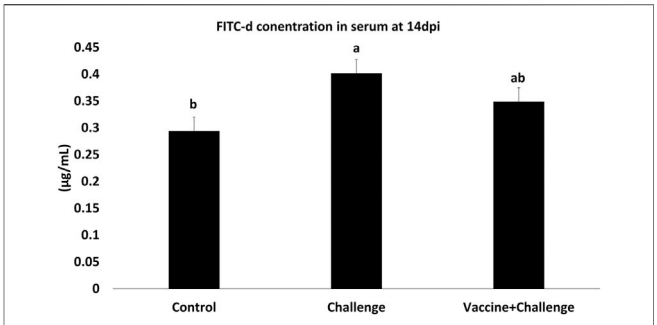

FIGURE 3 | FITC-d concentration in the serum of vaccinated birds. At d1 of age birds were allocated into treatment groups: 1) Control; 2) Challenge; or 3) Vaccine + Challenge. At d1 and d7 of age birds in the negative and positive control groups were mock vaccinated with PBS and birds in the treatment group were vaccinated with CNP. At d14 of age birds in the negative control group were given a mock challenge of 0.5 ml PBS/bird and birds in the positive control and the treatment group were orally challenged with 1×10^7 CFU/bird of *S*. Enteritidis. At 14 dpi, one bird per pen was given 2.2 mg FITC-d by oral gavage. After 2 h blood samples were collected. The Optical Density (OD) was measured at 485 nm. Bars (+SE) with no common superscript differ ($p < 0.05$).

3.5 The Effects of *Salmonella* CNP Vaccine on *Salmonella* Loads in Gizzard, Pancreas, Small Intestine, Spleen, Liver, Ceca, Heart, and Blood of Vaccinated Birds

At 21 dpi the CNP-vaccinated birds had a 2 Log_{10} CFU/g, 2 Log_{10} CFU/g, 0.6 Log_{10} CFU/g decrease in *S*. Enteritidis loads in the ceca (**Figure 2A**), spleen (**Figure 2B**), and small intestine (**Figure 2C**), respectively, compared to that in the control ($p < 0.05$). There was no *S*. Enteritidis detection in gizzard, pancreas, liver, heart, and blood when compared to control ($p > 0.05$).

The prevalence of *S*. Enteritidis in the ceca of the immunized birds was 33% for *Salmonella* negative birds and 67% for *Salmonella* positive birds (**Supplementary Figure S3A**). The prevalence of *S*. Enteritidis in the spleen of the immunized birds was 67% for *Salmonella* negative birds and 33% for *Salmonella* positive birds (**Supplementary Figure S3B**). The prevalence of *S*. Enteritidis in the small intestine of the immunized birds was 17% for *Salmonella* negative birds and 83% for *Salmonella* positive birds (**Supplementary Figure S3C**).

Further, there were no significant differences between any treatment groups for the organ index when compared to control ($p > 0.05$) (**Supplementary Figure S4**).

3.6 The Effects of *Salmonella* CNP Vaccine on FITC-d Concentration in the Serum of Vaccinated Birds

The gut permeability was assessed by measuring the amounts of FITC-d in the serum of immunized birds. At 14 dpi the challenge group had a 27% increase in gut permeability, whereas the vaccine + challenge group reversed the increase in gut permeability by 13% ($p < 0.05$) (**Figure 3**).

3.7 The Effects of *Salmonella* CNP Vaccine on Gene Expression in the Cecal Tonsils or Jejunum of Vaccinated Birds

At 12 h post-vaccination, the TNF-α mRNA amounts were 2-fold higher in the cecal tonsils of immunized birds when compared to control ($p < 0.05$) (**Figure 4A**). At 12 h post-vaccination, the TLR

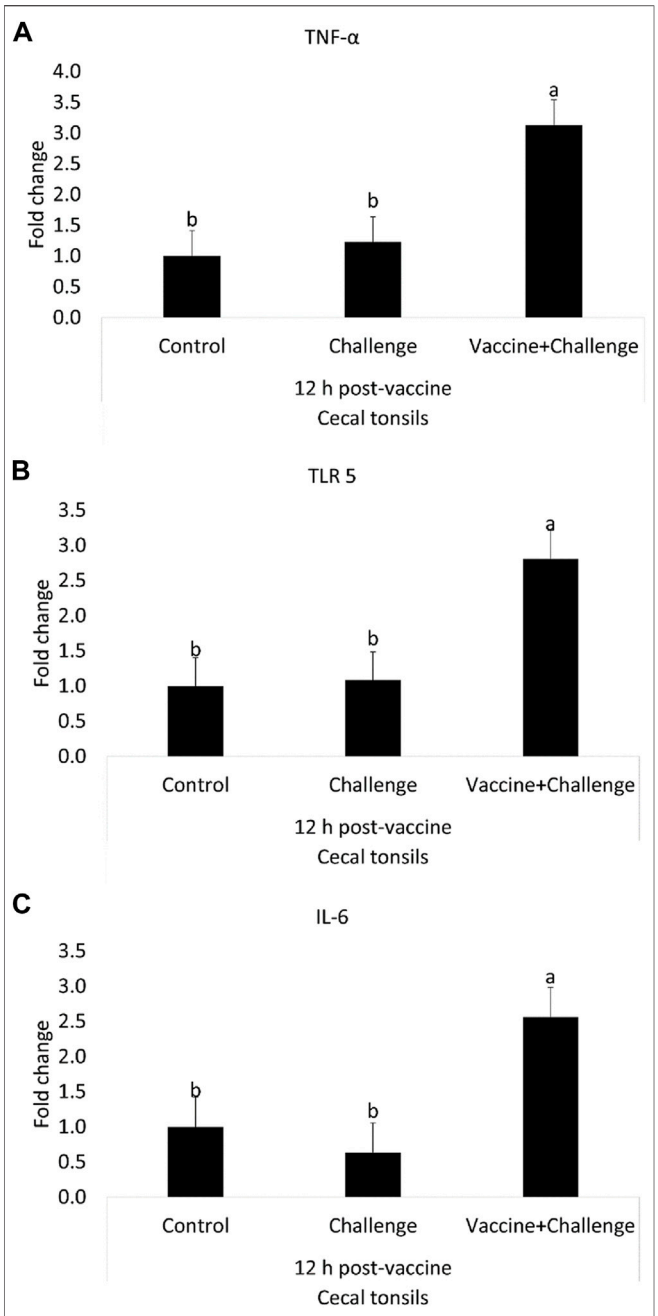

FIGURE 4 | The Effects of *Salmonella* CNP Vaccine on Gene Expression in the Cecal Tonsils of Vaccinated Birds at 12 h post-vaccination. At d1 of age birds were allocated into treatment groups: 1) Control; 2) Challenge; or 3) Vaccine + Challenge. At d1 and d7 of age birds in the negative and positive control groups were mock vaccinated with PBS and birds in the treatment group were vaccinated with CNP. At d14 of age birds in the negative control group were given a mock challenge of 0.5 ml PBS/bird and birds in the positive control and the treatment group were orally challenged with 1×10^7 CFU/bird of *S*. Enteritidis. Cecal tonsils were collected from one bird/pen ($n = 6$) at 12 h post-vaccination. Data represented as fold change compared to control. **(A)** TNF-α mRNA; **(B)** TLR 5 mRNA; **(C)** IL-6 mRNA. Bars (+SE) with no common superscript differ ($p < 0.05$).

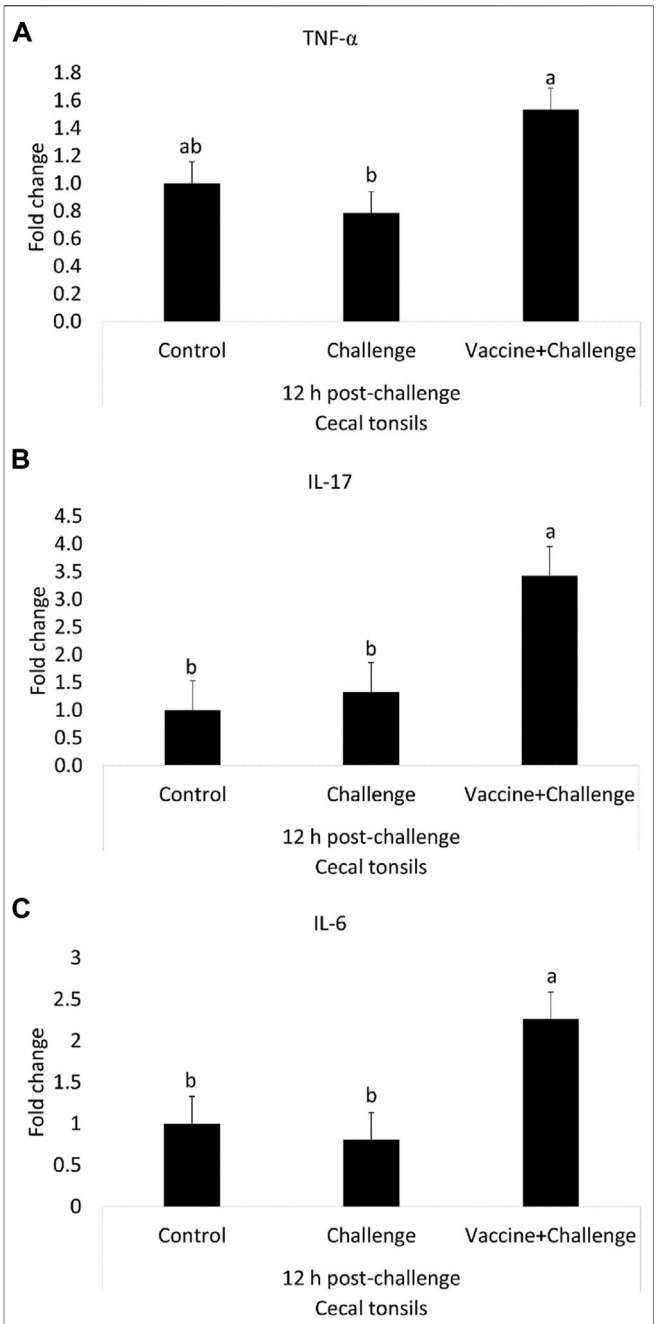

FIGURE 5 | The Effects of *Salmonella* CNP Vaccine on Gene Expression in the Cecal Tonsils of Vaccinated Birds at 12 h post-challenge. At d1 of age birds were allocated into treatment groups: 1) Control; 2) Challenge; or 3) Vaccine + Challenge. At d1 and d7 of age birds in the negative and positive control groups were mock vaccinated with PBS and birds in the treatment group were vaccinated with CNP. At d14 of age birds in the negative control group were given a mock challenge of 0.5 ml PBS/bird and birds in the positive control and the treatment group were orally challenged with 1×10^7 CFU/bird of *S*. Enteritidis. Cecal tonsils were collected from one bird/pen ($n = 6$) at 12 h post-challenge. Data represented as fold change compared to control. **(A)** TNF-α mRNA; **(B)** IL-17 mRNA; **(C)** IL-6 mRNA. Bars (+SE) with no common superscript differ ($p < 0.05$).

5 mRNA amounts were 2-fold higher in the cecal tonsils of immunized birds when compared to control ($p < 0.05$) (**Figure 4B**). At 12 h post-vaccination, the IL-6 mRNA amounts were 2-fold higher in the cecal tonsils of immunized birds when compared to control ($p < 0.05$) (**Figure 4C**). At 12 h post-vaccination, there were no significant differences between any of the treatment groups for IFN-γ and IL-1β mRNA amounts in the cecal tonsils, compared to control ($p > 0.05$) (**Supplementary Figure S5**).

At 12 h post-challenge, the TNF-α mRNA amounts were 0.5-fold higher in the cecal tonsils of immunized birds when compared to control ($p < 0.05$) (**Figure 5A**). At 12 h post-challenge, the IL-17 mRNA amounts were 2-fold higher in the cecal tonsils of immunized birds when compared to control ($p < 0.05$) (**Figure 5B**). At 12 h post-challenge, the IL-6 mRNA amounts were 1.3-fold higher in the cecal tonsils of immunized birds when compared to control ($p < 0.05$) (**Figure 5C**). At 12 h post-challenge, there were no significant differences between any of the treatment groups for IFN-γ, TLR 4, IL-10, iNOS, K60, and TGF-β mRNA amounts in the cecal tonsils when compared to control ($p > 0.05$) (**Supplementary Figure S6**).

At 12 h post-challenge, there were no significant differences for Claudin-1 and Zona Occludens-1 mRNA amounts in jejunum samples, compared to control ($p > 0.05$) (**Supplementary Figure S6**).

At d 35 of age, there were no significant differences between any of the treatment groups for TGF-β, IL-10, IL-6, TNF-α, and IL-1β mRNA amounts in the cecal tonsils, compared to control ($p > 0.05$) (**Supplementary Figure S7**).

4 DISCUSSION

Currently, polymeric chitosan nanoparticles are studied as antigen-delivery tools for killed *Salmonella* vaccine antigens. Previous studies with broiler and layer birds have investigated the efficacy of the oral *Salmonella* CNP vaccine when delivered by oral gavage, water, feed, *in-ovo*, and in a combined live followed by killed vaccination scheme (Acevedo-Villanueva et al., 2020; Renu, Han, et al., 2020; Renu, Markazi, et al., 2020; Y.; Han et al., 2020a; Yi; Han et al., 2020b; Acevedo-Villanueva et al., 2021; Acevedo-Villanueva, Renu and Gourapura, Renukaradhya, Selvaraj, 2021). Findings have demonstrated that the oral *Salmonella* CNP vaccine is a potential alternative to existing *Salmonella* vaccines for broilers and layers. When compared to uncoated CNPs and soluble OMP and flagellin antigens, previous studies demonstrated that flagellin-coated CNPs are readily uptaken by ileal Peyer Patch's M cells by passing through mucus layer, elicited *Salmonella*-specific mucosal IgA and T cell responses and induced the expression of Th1 and Th2 cytokines mRNA expression (Renu, Han, et al., 2020). In this study, we assessed the efficacy of the *Salmonella* CNP vaccine delivered through gel-spray on broilers. All birds were vaccinated with PBS or CNP vaccine by gel-spray delivery at d1 of age and were given a booster vaccination of PBS or CNP vaccine at d7 of age by oral gavage. A shorter prime-boost interval was carried out because (1) unlike commercial breeders, broilers have a shorter life span, (2) *Salmonella* vaccines require two doses that are three to 4 weeks apart, and (3) *Salmonella* vaccines have a withdrawal period of 21 days before processing (Acevedo-villanueva et al., 2021). Thus, a shorter prime-boost approach takes into account the broiler's short life span while complying with the 21-days withdrawal restriction. Previous research also explored the shorter prime-boost interval approach and found that the CNP can significantly reduce *S.* Enteritidis when it is orally delivered as a one-dose vaccination or as a booster vaccination (Acevedo-Villanueva et al., 2021).

In this study, we found that 87% of the antigens were successfully entrapped into the nanoparticle. To ensure the safe delivery of the antigens to the gut, we assessed the stability of the CNP vaccine at biological pH levels that range from the crop to the small intestine of broilers (Ravindran, 2013). According to literature, the vaccine must resist the pH from the crop to the gizzard at pH 3.5–5.5 to reach the small intestine intact at pH 6–7.5 (Gauthier, 2002). The delivery of the CNP vaccine antigens at the pH of the small intestine is essential to provide a stimulus to the immune system (Fredriksen and Grip, 2012). Results show that at pH 6.5 the CNP releases 31% of the antigen load, and at pH 7.5 the CNP releases 26% of the antigen load. The *in-vitro* results indicate that when the CNP vaccine is at the pH range of the small intestine, it would be releasing approximately 57% of its antigen load.

The average transit time of feed particles from the crop to the small intestine is approximately 70 min (Ravindran, 2013); hence, we assessed the cumulative protein release of antigens for the CNP at the initial stages after delivery for up to 17 h. The cumulative protein release of antigens for the CNP was determined to be 75% of its total protein after 17 h of incubation at a pH of 7.4. Previous research has reported that CNP loaded with Newcastle disease virus F-protein employed a slow release of 28% of their protein load at 18 h of incubation (Zhao et al., 2012). Another study reported that CNP loaded with native or toxoids of extracellular proteins of *Clostridium perfringens* and surface-tagged with *Salmonella* flagellin proteins had a cumulative release of approximately 10 and 16%, respectively, after 17 h of incubation (Akerele et al., 2020). Compared to other studies, our results show an increased cumulative protein release at 17 h of incubation. This difference could be due to the different TPP ratios among nanoparticle formulations, as it has been shown that as the TPP ratio increases in the vaccine formulation the protein loading efficiency decreases, and protein release from the nanoparticle increases (Hou et al., 2012).

When incubating the cRBCs with 20 μg/ml CNP and with 100 μg/ml CNP, the cRBCs released less than 1% and approximately 1% of hemoglobin, respectively, indicating no adverse effect of CNP on cRBCs. In previous research where CNP was loaded with native extracellular proteins of *Clostridium perfringens* and surface-tagged with *Salmonella* flagellin proteins, the CNP released less than 3% from cRBC (Akerele et al., 2020), further substantiating our results. The CNP loaded with Newcastle disease virus F-protein has also

been demonstrated to be safe in chicken embryo kidney cells (Zhao et al., 2012).

Salmonella enterica serovars infections are not a problem to poultry health as they are asymptomatic carriers and look healthy during infection. The main concern with *Salmonella* and poultry infections arises when humans interact with infected live poultry or consume infected poultry meat or poultry-derived products and develop *Salmonellosis* (Centers for Disease Control and Prevention, 2021). However, in this study, all birds were monitored twice a day for dehydration, refusal to eat food, diarrhea, bloody feces, and lethargy during the experimental period. Further, production performance parameters were also monitored during the experimental period. As expected, the birds in the challenge and the vaccine + challenge groups showed no *Salmonella* symptoms during the experimental period. Moreover, the *S.* Enteritidis challenge had no significant effects on the BWG or FCR of the challenged birds during the experimental period. Our *in-vivo* study also found that CNP vaccination did not significantly affect BWG or FCR, as seen by the BWG and FCR of the birds that were vaccinated with the CNP vaccine and challenged with *S.* Enteritidis. Results are in accord with existing research where the CNP vaccine had no adverse effects on the production performance parameters of broilers or layers (Zhao et al., 2012; Acevedo-Villanueva et al., 2020; Akerele et al., 2020; Renu, Markazi, et al., 2020; Y.; Han et al., 2020a; Yi; Han et al., 2020b; Acevedo-Villanueva et al., 2021; Acevedo-Villanueva, Renu and Gourapura, Renukaradhya, Selvaraj, 2021).

Oral vaccination elicits a greater mucosal response through the production of substantial amounts of IgA against the pathogen of interest (Neutra and Kozlowski, 2006). In this study, the OMP IgY antibody titers in the serum of vaccinated birds significantly increased after the booster vaccination, when compared to the unvaccinated control birds. A significant antigen-specific IgY antibody increase can be seen as an immunological advantage, as indicated by various studies showing that IgG can also partake in the host defense against enteric pathogens (Holmgren and Czerkinsky, 2005; Brandtzaeg, 2009). Previous findings are in agreement with our results showing that the *Salmonella* CNP vaccine can elicit significant IgY antibody levels (Acevedo-Villanueva et al., 2020; Acevedo-Villanueva et al., 2021; Renu, Markazi, et al., 2020; Acevedo-Villanueva, Renu and Gourapura, Renukaradhya, Selvaraj, 2021).

IgA in the serum is actively and selectively transported from the blood to the bile by the liver (Davis and Sell, 1989). Further, mucosal IgA functions as the primary defense mechanism against enteric pathogens, like *Salmonella*. For this study, the OMP IgA and Flagellin IgA antibody titers in the bile of vaccinated birds significantly increased after the booster vaccination, when compared to the unvaccinated control birds. The CNP vaccine was able to induce significantly greater levels of antigen-specific antibodies against *S.* Enteritidis before the experimental challenge. Further, the OMP and Flagellin IgA antibody titers in the bile of vaccinated birds also had a significant increase in response to the *S.* Enteritidis challenge, when compared to the unvaccinated control birds. The significant increase in OMP IgA and Flagellin IgA antibody titers in the bile of vaccinated birds at d35 of age were from birds that had already significantly decreased the *S.* Enteritidis colonization. Their antigen-specific antibody titers were similar to that of the antibody titers observed in the unvaccinated-challenge birds. However, the unvaccinated-challenged birds were still struggling to clear the *S.* Enteritidis infection, as indicated by the significant increase of *S.* Enteritidis colonization. These findings indicate that the CNP vaccine can produce significant antigen-specific IgA titers, similar to that of infection, and can also aid in the clearance of *S.* Enteritidis in the gut. However, the primary mechanism of *Salmonella* clearance in the gut of the vaccinated birds seems to be directed towards the cell-mediated component of the immune response. This is relevant because killed vaccines elicit weak cell-mediated responses when compared to live vaccines (Wodi AP and Morelli V, 2021). However, our findings demonstrate that the CNP vaccine can elicit a significant cellular immune response, as seen by its capability to elicit a significant antigen-specific lymphocyte proliferation against *S.* Enteritidis flagellin antigens. For this reason, future research should further explore the cellular immune mechanisms behind the vaccine. Further, results are in agreement with previous research demonstrating that in chickens an infection with *Salmonella* enterica serovar Typhimurium induces high levels of antigen-specific antibodies, but B-cells do not play an essential role in the clearance of the primary infection (Beal et al., 2006). Currently, it is not clear what non-B cell mechanism mediates *Salmonella* clearance; which could be beneficial to developing a successful *Salmonella* vaccine for broilers. For this study, results demonstrated that the CNP vaccine can induce protective OMP and Flagellin IgA antibody titers in bile. Also, further research is needed to better understand the cellular and humoral advantages that the CNP can convey.

In chickens, cloacal swabs are an easy and reliable way to evaluate mucosal IgA concentration (Merino-Guzmán et al., 2017). For this study, the OMP and Flagellin IgA antibody titers in the cloacal swabs of vaccinated birds also had a significant increase in response to the *S.* Enteritidis challenge, when compared to the unvaccinated control birds. Results are in agreement with previous studies that have reported that the CNP vaccine can elicit significant antigen-specific IgA antibody titers against *S.* Enteritidis (Acevedo-Villanueva et al., 2020; Renu, Han, et al., 2020; Renu, Markazi, et al., 2020; Y.; Han et al., 2020a; Yi; Han et al., 2020b; Acevedo-Villanueva et al., 2021; Acevedo-Villanueva, Renu and Gourapura, Renukaradhya, Selvaraj, 2021).

An antigen-specific lymphocyte proliferation assay was carried out to evaluate the cell-mediated response of birds that are vaccinated with CNP against *S.* Enteritidis antigens. The CNP vaccine was surface-coated with a flagellin crude protein extract as an adjuvant that is capable of being recognized by the host TLR 5 and triggering the immune system. Our results indicate that 20 μg/ml of flagellin crude protein extract can induce a substantial antigen-specific proliferation response against *Salmonella*, making it is a suitable choice as an adjuvant for the CNP vaccine. This study also found that the TLR 5 mRNA expression was significantly upregulated at 12 h post-vaccination in birds that were immunized with the CNP vaccine. The observed results are in agreement with previous studies regarding the PBMCs recall response against loaded CNP

antigen stimulation (Renu, Markazi, et al., 2020; Y.; Han et al., 2020b; Yi; Han et al., 2020c; Acevedo-Villanueva et al., 2021) and a previous study that assessed the upregulation of TLR 5 by the CNP vaccine (Renu, Han, et al., 2020). Further, the numerical differences ($p > 0.05$) in cell proliferation of birds in the control and the challenge groups at d12 of age can be due to individual variations. Variations among individuals of the same species can result in differences in the immune responses (Nature Education, 2014; Urban, 2020).

For this study, we also investigated if spleenocytes from birds that were vaccinated with the CNP, loaded with the *S.* Enteritidis antigens, can also recognize antigens from other prominent *Salmonella* enterica serovars. The *ex-vivo* assessment was done to study the CNP vaccine's potential to provide cross-protection against heterologous *Salmonella* serovars. Cross-protection against heterologous *Salmonella* serovars requires vaccine antigens that share conserved sequences (Vojtek et al., 2019). Conserved sequences allow the immune system of the vaccinated birds to recognize multiple *Salmonella* serovars, which benefits the poultry industry. The *ex-vivo* results indicate that the T-lymphocytes from immunized birds responded in an antigen-specific manner when stimulated with 20 μg/ml of either *S.* Enteritidis, *S.* Typhimurium, or *S.* Litchfield HK. Results indicate that the CNP vaccine could significantly provide cross-protection against other *Salmonella* enterica serovars. The CNP vaccine was loaded with a crude-enriched extract of OMP and flagellin proteins from *S.* Enteritidis. It is expected that vaccines that are synthesized with either the Enteritidis or Typhimurium serovar can provide cross-protection against both because *S.* Enteritidis and *S.* Typhimurium porin OMP C contains several amino acid sequences that are highly conserved (Valero-Pacheco et al., 2020), making them suitable vaccine candidates. Further, *S.* Enteritidis and *S.* Litchfield have been linked to a massive multi-state outbreak in 2018 that was traced to live poultry (Robertson et al., 2019). Further research found that *S.* Enteritidis and *S.* Litchfield contain significant homology in their genetic sequence, making cross-protection possible during an *S.* Enteritidis vaccination (Robertson et al., 2019). Future research should consider the *in-vivo* study of the *Salmonella* CNP vaccine against experimental challenges of *S.* Typhimurium or *S.* Litchfield to fully explore the vaccine's potential for cross-protection.

Salmonella control and prevention requires a coordinated and multifaceted approach with several intervention strategies of which vaccination is only one. Currently, *Salmonella* vaccines alone cannot fully eradicate *Salmonella* in poultry, but they are strongly recommended to significantly help reduce the *Salmonella* loads in poultry production. Early interventions at the live stage of the birds can significantly contribute to decreasing the *Salmonella* load at the market age of 35–49 days of age. A previous study identified that *S.* Enteritidis can colonize the spleen, liver, small intestine, cecum contents, stomach, heart, pancreas, and the blood of broilers during 21 days, from highest to lowest distribution (Zeng et al., 2018). For this reason, the current study aimed to explore the efficacy of the CNP vaccine in decreasing the colonization of *S.* Enteritidis in the internal organs of broilers at d35 of age. Broilers are asymptomatic carriers of non-typhoidal *Salmonella* (Shanmugasundaram et al., 2015), while healthy individuals require the presence of 1×10^6 bacterial cells to cause infection (Alena Klochko, 2019). Thus, all birds in the challenge and the vaccine + challenge groups were given an oral challenge of 1×10^7 CFU/bird of *S.* Enteritidis. Our findings demonstrate that the CNP vaccine can aid in significantly reducing the *S.* Enteritidis colonization by 2 Log in the ceca and spleen, and by 0.6 Log in the small intestine of immunized and experimentally challenged birds at d35 of age. A 2 Log reduction in two of the organs that have been reported to have the highest *S.* Enteritidis loads places the CNP as a viable vaccine candidate for *Salmonella* in poultry. Further, a significant 2 Log reduction of *Salmonella* at market age is of biological importance because combining the CNP vaccine with active "on-farm" and processing interventions can significantly reduce the number of contaminated carcasses. Future research should explore the vaccine's potential to reduce the *Salmonella* load in ready-to-eat carcasses of broilers.

Gut integrity is a crucial indicator of both health and critical illness, as damage to the intestinal epithelia induces "hyper-permeability" that can lead to bacterial translocation and subsequent systemic infection (Otani and Coopersmith, 2019). In this study, results indicate that the CNP vaccine treatment significantly reduced the loss in gut permeability, as seen by decreased levels of FITC-d in the serum of birds that were vaccinated with CNP. Results were further confirmed by the significant increase in FITC-d levels in the serum of birds in the challenge group when compared to control. Additionally, the mRNA expression levels of both Claudin-1 and Zona Occludens-1 at 12 h post-challenge were decreased ($p > 0.05$) in the jejunum samples of the challenge group. Previous findings demonstrate that *S.* Typhimurium is known to increase intestinal permeability of the chicken gut due to its ability to induce tight junction protein damage, as seen by the decreased expression of a few key markers, such as Claudin-1 and Zona Occludens-1 (Tafazoli, Magnusson and Zheng, 2003; Wang et al., 2018; Leyva-Diaz et al., 2021). Further, a study with rats found that *S.* Enteritidis can increase gut permeability as the result of environmental stress which can increase the *Salmonella* virulence factors (Ten Bruggencate et al., 2005). Future research should further explore the impact of CNP in the gut permeability of chickens that are challenged with *S.* Enteritidis.

For this study, we explored the CNP vaccine effect on key immune-related gene expressions of biological relevance to *Salmonella* infections in broilers. The induction of immune relevant cytokines and proteins, such as IL-1β, TNF-α, IFN-γ, IL-6, IL-10, IL-17, TLR 4, TLR 5, iNOS, TGF-β, K 60, Claudin-1, and Zona Occludens-1, following *Salmonella* infection of chickens have been studied previously (Van Immerseel et al., 2002; Withanage et al., 2004; Berndt et al., 2007; Ivanov et al., 2008; Crhanova et al., 2011; He, Genovese and Kogut, 2011; Matulova et al., 2012; Renu, Markazi, et al., 2020; Shanmugasundaram et al., 2021). The ability of a vaccine to induce significant levels of pro-inflammatory cytokines upon vaccination mimics the natural inflammatory response seen in the initial stages of infection, which is key to successfully triggering an immune response against the desired antigen. In mammals, the synthesis and release of pro-inflammatory cytokines, such as TNF-α and IL-6, are increased especially during the early stages of inflammation (Abbas Abul, 2014). Further, TNF-α and IL-6 are pleiotropic cytokines, so they can act as both pro-inflammatory and anti-inflammatory. In this study, birds that were immunized with the CNP vaccine had significantly higher mRNA expression of TNF-

α and IL-6 at 12 h post-vaccination and 12 h post-challenge. These results highlight the ability of the CNP vaccine to induce a significant pro-inflammatory response against the loaded antigens, similar to that which is observed in a *Salmonella* infection. Results are in agreement with *in-vitro* findings that report that CNP vaccines can elicit increased secretion of TNF-α and IL-6 in immunized pig cells (Dhakal et al., 2018). Future studies will also explore the mRNA levels of key cytokines in serum samples of immunized birds.

IL-17 is predominantly produced by T helper 17 (Th17) cells (Xu and Cao, 2010). There is a significant gap in research regarding Th17 cells and *Salmonella* in chickens, and the research to date is contradicting. Further, there is no research regarding CNP effects in IL-17 cells or Th17 cytokines in chickens challenged with *Salmonella*. According to literature, Th17 cells and Th17 cytokines play an important role in the resistance to mucosal *Salmonella* infections across different species (Raffatellu M, George MD, Akiyama Y, 2009; Griffin and McSorley, 2011), including chickens (Crhanova et al., 2011). It has also been reported that chicken IL-17RA expression remains unchanged in *Salmonella* infection (Kim et al., 2014). However, in this study, our findings show that the birds that were immunized with the CNP vaccine had significantly higher IL-17 mRNA expression in response to the *S*. Enteritidis challenge when compared to the control groups. At 12 h post-challenge, both the control and the challenge groups had similar and significantly lower levels of IL-17. Thus, we hypothesize that the increased levels of Th17 mRNA can be due to a synergistic effect of the vaccine-loaded antigens and the increased IL-6 mRNA amounts induced by the CNP vaccine. Our hypothesis is based on previous research in mice that indicates that *Salmonella*-specific Th17 cells can recognize *Salmonella* flagellin (Lee et al., 2012) and that *Salmonella* Flagellin antigen has also shown an intrinsic ability to elicit IL-1 and IL-6 production (Salazar-Gonzalez and McSorley, 2005; Mizel and Bates, 2010). Moreover, it has been reported that IL-6 is a non-redundant differentiation factor for Th17 cells (Korn and Hiltensperger, 2021) in which significantly increased levels of IL-6 can promote the generation of Th17 cells (Hou et al., 2014) and result in IL-6 and IL-17 cytokines. So, the recognition of the vaccine's flagellin by TLR 5 and its ability to induce significant IL-6 mRNA may be the force driving the Th17 response against *Salmonella* in the cecal tonsils during *S*. Enteritidis infection in chickens. These results also support the hypothesis that the primary mechanism of *Salmonella* clearance in the gut is due to the cellular component of the immune response (Beal et al., 2006). Future research regarding the effect of the CNP vaccine on *Salmonella* Th17 cells and IL-17 cytokines is needed to explore the IL-17 and *Salmonella* research gap in chickens.

5 CONCLUSION

This study analyzed the efficacy of a CNP vaccine against *Salmonella* delivered by gel-spray to broilers. The CNP vaccine (1) can overcome the hurdles of conventional vaccines; (2) had no negative effects on production performance of broilers; (3) elicited antigen-specific systemic and mucosal immune responses; (4) elicited antigen-specific recall response against *S*. Enteritidis Flagellin, *S*. Enteritidis HKA, *S*. Typhimurium HKA, and S. Litchfield HKA; (5) reduced the *Salmonella* load in the ceca, spleen and small intestine of broilers at d35 of age; (6) decreased the loss in gut permeability caused by *S*. Enteritidis; and (7) increased IL-6, IL- 17, and TNF-α mRNA in cecal tonsils. Future studies will examine the CNP vaccine potential to convey cross-protection against heterologous *Salmonella* serovars, the efficacy of the CNP vaccine in reducing *S*. Enteritidis loads in ready-to-eat carcasses, and the relationship between the CNP vaccine and the Th17/IL-17 immune response to explore the role of Th17 cells and IL-17 cytokines on *Salmonella* infections in broilers. We conclude that the CNP vaccine is a viable alternative to conventional *Salmonella* vaccines for poultry.

DATA AVAILABILITY STATEMENT

The original contributions presented in the study are included in the article/**Supplementary Material**, further inquiries can be directed to the corresponding author.

ETHICS STATEMENT

The animal study was reviewed and approved by IACUC # A2021 04-014-Y1-A1.

AUTHOR CONTRIBUTIONS

KA-V roles: formal analysis, investigation, methodology, writing–original draft, writing–review and editing; GA roles: investigation, writing–review and editing; WA-H roles: investigation, writing–review and editing; DA roles: writing–review and editing; RG roles: resources, writing–review and editing; RS roles: funding acquisition, project administration, resources, supervision, validation, visualization; writing–review and editing.

FUNDING

This research was partially supported by the Hatch grant, USDA-NIFA grant 2017-05035, and 58-6040-8-034 USDA-ARS awarded to RS.

ACKNOWLEDGMENTS

We acknowledge Dr. Brian Jordan from the University of Georgia as well as the Poultry Research Complex staff and the Complex Carbohydrate Research Center staff at the University of Georgia.

SUPPLEMENTARY MATERIAL

The Supplementary Material for this article can be found online at: https://www.frontiersin.org/articles/10.3389/fphys.2022.920777/full#supplementary-material

REFERENCES

Abbas Abul, K., Lichtman, A. H., and Pillai, S. (2014). *Cellular and Molecular Immunology*. Amsterdam: Elsevier.

Acevedo-Villanueva, K., Renu, S., Gourapura, R., and Selvaraj, R. (2021a). Efficacy of a Nanoparticle Vaccine Administered In-Ovo against Salmonella in Broilers. *PLoS ONE.* 16, e0247938–16. doi:10.1371/journal.pone.0247938

Acevedo-villanueva, K. Y., Akerele, G. O., Al Hakeem, W. G., Renu, S., Shanmugasundaram, R., and Selvaraj, R. K. (2021b). A Novel Approach against Salmonella: A Review of Polymeric Nanoparticle Vaccines for Broilers and Layers. *Vaccines(Basel).* 9, 1041.doi:10.3390/vaccines9091041

Acevedo-Villanueva, K. Y., Lester, B., Renu, S., Han, Y., Shanmugasundaram, R., Gourapura, R., et al. (2020). Efficacy of Chitosan-Based Nanoparticle Vaccine Administered to Broiler Birds Challenged with Salmonella. *PLoS ONE* 15, e0231998. doi:10.1371/journal.pone.0231998

Acevedo-Villanueva, K. Y., Renu, S., Shanmugasundaram, R., Akerele, G. O., Gourapura, R. J., and Selvaraj, R. K. (2021c). Salmonella Chitosan Nanoparticle Vaccine Administration Is Protective against Salmonella Enteritidis in Broiler Birds. *Plos One* 16 (11), e0259334. doi:10.1371/journal.pone.0259334

Akerele, G., Ramadan, N., Renu, S., Renukaradhya, G. J., Shanmugasundaram, R., and Selvaraj, R. K. (2020), *In Vitro* characterization and Immunogenicity of Chitosan Nanoparticles Loaded with Native and Inactivated Extracellular Proteins from a Field Strain of Clostridium perfringens Associated with Necrotic Enteritis. *Veterinary Immunol. Immunopathol.*224, 110059. Elsevier. doi:10.1016/j.vetimm.2020.110059

Andino, A., and Hanning, I. (2015). Salmonella enterica: Survival, Colonization, and Virulence Differences Among Serovars. *Sci. World J.* 2015, 1–16. doi:10.1155/2015/520179

Beal, R. K., Powers, C., Davison, T. F., Barrow, P. A., and Smith, A. L. (2006). Clearance of Enteric Salmonella enterica Serovar Typhimurium in Chickens Is Independent of B-Cell Function. *Infect. Immun.* 74 (2), 1442–1444. doi:10.1128/IAI.74.2.1442-1444.2006

Belshe, R. B., Newman, F. K., Cannon, J., Duane, C., Treanor, J., Van Hoecke, C., et al. (2004). Serum Antibody Responses after Intradermal Vaccination against Influenza. *N. Engl. J. Med.* 351 (22), 2286–2294. doi:10.1056/nejmoa043555

Berndt, A., Wilhelm, A., Jugert, C., Pieper, J., Sachse, K., and Methner, U. (2007). Chicken Cecum Immune Response to Salmonella enterica Serovars of Different Levels of Invasiveness. *Infect. Immun.* 75 (12), 5993–6007. doi:10.1128/IAI.00695-07

Berthelot-Hérault, F., Mompart, F., Zygmunt, M. S., Dubray, G., and Dushet-Suchaux, M. (2003). Antibody Responses in the Serum and Gut of Chicken Lines Differing in Cecal Carriage of Salmonella Enteritidis. *Veterinary Immunol. Immunopathol.* 96 (1–2), 43–52. doi:10.1016/S0165-2427(03)00155-7

Brandtzaeg, P. (2009). Mucosal Immunity: Induction, Dissemination, and Effector Functions. *Scand. J. Immunol.* 70, 505–515. doi:10.1111/j.1365-3083.2009.02319.x

Centers for Disease Control and Prevention (2021). Salmonella Outbreaks Linked to Backyard Poultry. *Investig. Not.*, 1. Available at: https://www.cdc.gov/salmonella/backyardpoultry-05-21/index.html.

Chen, Y. P., Cheng, Y. F., Li, X. H., Yang, W. L., Wen, C., Zhuang, S., et al. (2017). Effects of Threonine Supplementation on the Growth Performance, Immunity, Oxidative Status, Intestinal Integrity, and Barrier Function of Broilers at the Early Age. *Poult. Sci.* 96 (2), 405–413. doi:10.3382/ps/pew240

Crhanova, M., Hradecka, H., Faldynova, M., Matulova, M., Havlickova, H., Sisak, F., et al. (2011). Immune Response of Chicken Gut to Natural Colonization by Gut Microflora and to Salmonella enterica Serovar Enteritidis Infection. *Infect. Immun.* 79 (7), 2755–2763. doi:10.1128/IAI.01375-10

Davis, C. Y., and Sell, J. L. (1989). Immunoglobulin Concentrations in Serum and Tissues of Vitamin A-Deficient Broiler Chicks after Newcastle Disease Virus Vaccination. *Poult. Sci.* 68 (1), 136–144. doi:10.3382/ps.0680136

de Jonge, H. J. M., Fehrmann, R. S. N., de Bont, E. S. J. M., Hofstra, R. M. W., Gerbens, F., Kamps, W. A., et al. (2007). Evidence Based Selection of Housekeeping Genes. *PLoS ONE* 2 (9), e898–5. doi:10.1371/journal.pone.0000898

Dhakal, S., Renu, S., Ghimire, S., Shaan Lakshmanappa, Y., Hogshead, B. T., Feliciano-Ruiz, N., et al. (2018). Mucosal Immunity and Protective Efficacy of Intranasal Inactivated Influenza Vaccine Is Improved by Chitosan Nanoparticle Delivery in Pigs. *Front. Immunol.* 9, 934. doi:10.3389/fimmu.2018.00934

Economic Research Service United States Department of Agriculture (2021). Cost Estimates of Foodborne Illnesses- Total Cost of Foodborne Illness Estimates for 15 Leading Foodborne Pathogens, 1. Available at: https://www.ers.usda.gov/data-products/cost-estimates-of-foodborne-illnesses/.

Forbes, S. J., Eschmann, M., and Mantis, N. J. (2008). Inhibition of Salmonella enterica Serovar Typhimurium Motility and Entry into Epithelial Cells by a Protective Antilipopolysaccharide Monoclonal Immunoglobulin a Antibody. *Infect. Immun.* 76 (9), 4137–4144. doi:10.1128/IAI.00416-08

Fredriksen, B. N., and Grip, J. (2012). PLGA/PLA Micro- and Nanoparticle Formulations Serve as Antigen Depots and Induce Elevated Humoral Responses after Immunization of Atlantic Salmon (Salmo salar L.). *Vaccine* 30 (3), 656–667. doi:10.1016/j.vaccine.2011.10.105

Gauthier, R. (2002). "Intestinal Health, The Key to Productivity: The Case of Organic Acids," in Proceedings of the XXVII Convencion American Association of Avian Pathologists-Western Poultry Diseases Conference, 8–10.

Griffin, A. J., and McSorley, S. J. (2011). Development of Protective Immunity to Salmonella, a Mucosal Pathogen with a Systemic Agenda. *Mucosal Immunol.* 4, 371–382. doi:10.1038/mi.2011.2

Han, Y., Renu, S., Patil, V., Schrock, J., Feliciano-Ruiz, N., Selvaraj, R., et al. (2020a). Immune Response to Salmonella Enteritidis Infection in Broilers Immunized Orally With Chitosan-Based Salmonella Subunit Nanoparticle Vaccine. *Front. Immunol.* 11, 935. doi:10.3389/fimmu.2020.00935

Han, Y., Renu, S., Patil, V., Schrock, J., Feliciano-Ruiz, N., Selvaraj, R., et al. (2020b). Mannose-modified Chitosan-Nanoparticle-Based salmonella Subunit Oralvaccine-Induced Immune Response and Efficacy in a Challenge Trial in Broilers. *Vaccines* 8 (2), 299–316. doi:10.3390/vaccines8020299

Han, Y., Renu, S., Schrock, J., Acevedo-Villanuev, K. Y., Lester, B., Selvaraj, R. K., et al. (2020c). Temporal Dynamics of Innate and Adaptive Immune Responses in Broiler Birds to Oral Delivered Chitosan Nanoparticle-Based Salmonella Subunit Antigens. *Veterinary Immunol. Immunopathol.* 228, 110111. doi:10.1016/j.vetimm.2020.110111

He, H., Genovese, K. J., and Kogut, M. H. (2011). Modulation of Chicken Macrophage Effector Function by TH1/TH2 Cytokines. *Cytokine* 53 (3), 363–369. doi:10.1016/j.cyto.2010.12.009

Holmgren, J., and Czerkinsky, C. (2005). Mucosal Immunity and Vaccines. *Nat. Med.* 11, S45–S53. doi:10.1038/nm1213

Hong, Y. H., Lillehoj, H. S., Lee, S. H., Dalloul, R. A., and Lillehoj, E. P. (2006). Analysis of Chicken Cytokine and Chemokine Gene Expression Following Eimeria Acervulina and Eimeria Tenella Infections. *Veterinary Immunol. Immunopathol.* 114 (3–4), 209–223. doi:10.1016/j.vetimm.2006.07.007

Hong, Y. H., Song, W., Lee, S. H., and Lillehoj, H. S. (2012). Differential Gene Expression Profiles of β-defensins in the Crop, Intestine, and Spleen Using a Necrotic Enteritis Model in 2 Commercial Broiler Chicken Lines. *Poult. Sci.* 91 (5), 1081–1088. Poultry Science Association Inc. doi:10.3382/ps.2011-01948

Hou, W., Jin, Y.-H., Kang, H. S., and Kim, B. S. (2014). Interleukin-6 (IL-6) and IL-17 Synergistically Promote Viral Persistence by Inhibiting Cellular Apoptosis and Cytotoxic T Cell Function. *J. Virol.* 88 (15), 8479–8489. doi:10.1128/jvi.00724-14

Hou, Y., Hu, J., Park, H., and Lee, M. (2012). Chitosan-based Nanoparticles as a Sustained Protein Release Carrier for Tissue Engineering Applications. *J. Biomed. Mat. Res.* 100, 939–947. doi:10.1002/jbm.a.34031

Hutsko, S. (2017). The Effects of an Anti-Coccidial Vaccination in Conjunction with Supplemental Protease Vitamin C and Differing Levels of Dietary Protein on the Production and Gut Barrier Function in Young Broiler Chickens. Doctoral dissertation. Columbus (US): The Ohio State University. Available at: https://etd.ohiolink.edu/apexprod/rws_etd/send_file/send?accession=osu1511167090610371&disposition=inline.

Imam, S. S., Alshehri, S., Ghoneim, M. M., Zafar, A., Alsaidan, O. A., Alruwaili, N. K., et al. (2021). Recent Advancement in Chitosan-Based Nanoparticles for Improved Oral Bioavailability and Bioactivity of Phytochemicals: Challenges and Perspectives. *Polymers* 13 (22), 4036. doi:10.3390/polym13224036

Ivanov, I. I., Frutos, R. d. L., Manel, N., Yoshinaga, K., Rifkin, D. B., Sartor, R. B., et al. (2008). Specific Microbiota Direct the Differentiation of IL-17-

Producing T-Helper Cells in the Mucosa of the Small Intestine. *Cell Host Microbe* 4, 337–349. doi:10.1016/j.chom.2008.09.009

Kaiser, P., Underwood, G., and Davison, F. (2003). Differential Cytokine Responses Following Marek's Disease Virus Infection of Chickens Differing in Resistance to Marek's Disease. *J. Virol.* 77, 762–768. doi:10.1128/jvi.77.1.762-768.2003

Kim, W. H., Jeong, J., Park, A. R., Yim, D., Kim, S., Chang, H. H., et al. (2014). Downregulation of Chicken Interleukin-17 Receptor A during Eimeria Infection. *Infect. Immun.* 82 (9), 3845–3854. doi:10.1128/IAI.02141-14

Klochko, A. (2019). Salmonella Infection (Salmonellosis). *Medscape*, 1. Available at: https://emedicine.medscape.com/article/228174-overview#a5.

Korn, T., and Hiltensperger, M. (2021). Role of IL-6 in the Commitment of T Cell Subsets. *Cytokine* 146, 155654. Elsevier Ltd. doi:10.1016/j.cyto.2021.155654

Lamm, M. E. (1997). Interaction of Antigens and Antibodies at Mucosal Surfaces. *Annu. Rev. Microbiol.* 51, 311–340. PMID: 9343353. doi:10.1146/annurev.micro.51.1.311

Lee, S.-J., McLachlan, J. B., Kurtz, J. R., Fan, D., Winter, S. E., Baumler, A. J., et al. (2012). Temporal Expression of Bacterial Proteins Instructs Host CD4 T Cell Expansion and Th17 Development. *PLoS Pathog.* 8 (1), e1002499. doi:10.1371/journal.ppat.1002499

Levine, M. M. (2000). Immunization against Bacterial Diseases of the Intestine. *J. Pediatr. Gastroenterology Nutr.* 31, 336–355. PMID: 11045827. doi:10.1097/00005176-200010000-00003

Leyva-Diaz, A. A., Hernandez-Patlan, D., Solis-Cruz, B., Adhikari, B., Kwon, Y. M., Latorre, J. D., et al. (2021). Evaluation of Curcumin and Copper Acetate against Salmonella Typhimurium Infection, Intestinal Permeability, and Cecal Microbiota Composition in Broiler Chickens. *J. Anim. Sci. Biotechnol.* 12 (1), 1–12. doi:10.1186/s40104-021-00545-7

Li, Y., Jin, L., and Chen, T. (2020). The Effects of Secretory IgA in the Mucosal Immune System. *BioMed Res. Int.* 2020, 1–6. doi:10.1155/2020/2032057

Liu, J., Teng, P.-Y., Kim, W. K., and Applegate, T. J. (2021). Assay Considerations for Fluorescein Isothiocyanate-Dextran (FITC-D): an Indicator of Intestinal Permeability in Broiler Chickens. *Poult. Sci.* 100 (7), 101202 Elsevier Inc. doi:10.1016/j.psj.2021.101202

Lunn, J. A., Lee, R., Smaller, J., MacKay, B. M., King, T., Hunt, G. B., et al. (2012). Twenty Two Cases of Canine Neural Angiostrongylosis in Eastern Australia (2002-2005) and a Review of the Literature. *Parasites Vectors* 5 (1), 70. doi:10.1186/1756-3305-5-70

Mak, T. W., and Saunders, M. E. (2006). "Vaccines and Clinical Immunization," in *The Immune Response* (Cambridge: Academic Press), 695–749. doi:10.1016/B978-012088451-3.50025-9

Markazi, A., Luoma, A., Shanmugasundaram, R., Mohnl, M., Raj Murugesan, G., and Selvaraj, R. (2018). Effects of Drinking Water Synbiotic Supplementation in Laying Hens Challenged with Salmonella. *Poult. Sci.* 97, 3510–3518. doi:10.3382/ps/pey234

Matulova, M., Stepanova, H., Sisak, F., Havlickova, H., Faldynova, M., Kyrova, K., et al. (2012). Cytokine Signaling in Splenic Leukocytes from Vaccinated and Non-vaccinated Chickens after Intravenous Infection with salmonella Enteritidis. *PLoS ONE* 7 (2), e32346. doi:10.1371/journal.pone.0032346

Merino-Guzmán, R., Latorre, J. D., Delgado, R., Hernandez-Velasco, X., Wolfenden, A. D., Teague, K. D., et al. (2017). Comparison of Total Immunoglobulin A Levels in Different Samples in Leghorn and Broiler Chickens. *Asian Pac. J. Trop. Biomed.* 7 (2), 116–120. doi:10.1016/j.apjtb.2016.11.021

Mizel, S. B., and Bates, J. T. (2010). Flagellin as an Adjuvant: Cellular Mechanisms and Potential. *J. I.* 185, 5677–5682. doi:10.4049/jimmunol.1002156

Morris, A., Shanmugasundaram, R., Lilburn, M. S., and Selvaraj, R. K. (2014). 25-Hydroxycholecalciferol Supplementation Improves Growth Performance and Decreases Inflammation during an Experimental Lipopolysaccharide Injection. *Poult. Sci.* 93, 1951–1956. doi:10.3382/ps.2014-03939

Nature Education (2014). The Genetic Variation in a Population Is Caused by Multiple Factors. *Scitable*, 10. Available at: https://www.nature.com/scitable/topicpage/the-genetic-variation-in-a-population-is-6526354/#:~:text=Genetic variation describes naturally occurring,face of changing environmental circumstances.

Neutra, M. R., and Kozlowski, P. A. (2006). Mucosal Vaccines: The Promise and the Challenge. *Nat. Rev. Immunol.* 6, 148–158. doi:10.1038/nri1777

Nochi, T., Jansen, C. A., Toyomizu, M., and Eden, W. v. (2018). The Well-Developed Mucosal Immune Systems of Birds and Mammals Allow for Similar Approaches of Mucosal Vaccination in Both Types of Animals. *Front. Nutr.* 5, 60. doi:10.3389/fnut.2018.00060

Otani, S., and Coopersmith, C. M. (2019). Gut Integrity in Critical Illness. *J. intensive care* 7 (1), 1–7. doi:10.1186/s40560-019-0372-6

Oxford, J. H., and Selvaraj, R. K. (2019). Effects of Glutamine Supplementation on Broiler Performance and Intestinal Immune Parameters During an Experimental Coccidiosis Infection. *J. Appl. Poult. Res.* 28 (4), 1279–1287. Poultry Science Association Inc. doi:10.3382/japr/pfz095

Pan, D., Vargas-Morales, O., Zern, B., Anselmo, A. C., Gupta, V., Zakrewsky, M., et al. (2016). The Effect of Polymeric Nanoparticles on Biocompatibility of Carrier Red Blood Cells. *PLoS ONE* 11 (3), e0152074–17. doi:10.1371/journal.pone.0152074

Perkins, F. T. (1958). A Ready Reckoner for the Calculation of Geometric Mean Antibody Titres. *J. general Microbiol.* 19 (3), 540–541. doi:10.1099/00221287-19-3-540

Raffatellu, M., George, M. D., Akiyama, Y., Hornsby, M. J., Nuccio, S.-P., Paixao, T. A., et al. (2009). Lipocalin-2 Resistance Confers an Advantage to Salmonella enterica Serotype Typhimurium for Growth and Survival in the Inflamed Intestine. *Cell Host Microbe* 5, 476–486. doi:10.1016/j.chom.2009.03.011

Ravindran, V. (2013). Feed Enzymes: The Science, Practice, and Metabolic Realities. *J. Appl. Poult. Res.* 22 (3), 628–636. doi:10.3382/japr.2013-00739

Renu, S., Markazi, A. D., Dhakal, S., Lakshmanappa, Y. S., and Shanmugasundaram, R., Ramesh, K. S., et al. (2018b). Engineering of Targeted Mucoadhesive Chitosan Based Salmonella Nanovaccine for Oral Delivery in Poultry. *J. Immunol.* 200 (1), 118–215.

Renu, S., Han, Y., Dhakal, S., Lakshmanappa, Y. S., Ghimire, S., Feliciano-Ruiz, N., et al. (2020a). Chitosan-adjuvanted Salmonella Subunit Nanoparticle Vaccine for Poultry Delivered through Drinking Water and Feed. *Carbohydr. Polym.* 243, 116434. doi:10.1016/j.carbpol.2020.116434

Renu, S., Markazi, A. D., Dhakal, S., Lakshmanappa, Y. S., Gourapura, S. R., Shanmugasundaram, R., et al. (2018a). Surface Engineered Polyanhydride-Based Oral Salmonella Subunit Nanovaccine for Poultry. *Ijn* 13, 8195–8215. doi:10.2147/ijn.s185588

Renu, S., Markazi, A. D., Dhakal, S., Shaan Lakshmanappa, Y., Shanmugasundaram, R., Selvaraj, R. K., et al. (2020b). Oral Deliverable Mucoadhesive Chitosan-Salmonella Subunit Nanovaccine for Layer Chickens. *Ijn* 15, 761–777. doi:10.2147/IJN.S238445

Robertson, S. A., Sidge, J. L., Koski, L., Hardy, M. C., Stevenson, L., Signs, K., et al. (2019). Onsite Investigation at a Mail-Order Hatchery Following a Multistate Salmonella Illness Outbreak Linked to Live poultry-United States, 2018. *Poult. Sci. Univ. Press behalf Poult. Sci. Assoc.* 98 (12), 6964–6972. The Author(s) 2019Published by. doi:10.3382/ps/pez529

Rothwell, L., Young, J. R., Zoorob, R., Whittaker, C. A., Hesketh, P., Archer, A., et al. (2004). Cloning and Characterization of Chicken IL-10 and Its Role in the Immune Response toEimeria Maxima. *J. Immunol.* 173, 2675–2682. doi:10.4049/jimmunol.173.4.2675

Salazar-Gonzalez, R. M., and McSorley, S. J. (2005). Salmonella Flagellin, a Microbial Target of the Innate and Adaptive Immune System. *Immunol. Lett.* 101 (2), 117–122. doi:10.1016/j.imlet.2005.05.004

Schmittgen, T. D., and Livak, K. J. (2008). Analyzing Real-Time PCR Data by the Comparative CT Method. *Nat. Protoc.* 3 (6), 1101–1108. doi:10.1038/nprot.2008.73

Selvaraj, R. K., and Klasing, K. C. (2006). Lutein and Eicosapentaenoic Acid Interact to Modify iNOS mRNA Levels through the PPARγ/RXR Pathway in Chickens and HD11 Cell Lines. *J. Nutr.* 136, 1610–1616. doi:10.1093/jn/136.6.1610

Setyohadi, D. P. S., Octavia, R. A., and Puspitasari, T. D. (2018). An Expert System for Diagnosis of Broiler Diseases Using Certainty Factor. *J. Phys. Conf. Ser.* 953 (1), 012118. doi:10.1088/1742-6596/953/1/012118

Shanmugasundaram, R., Acevedo, K., Mortada, M., Akerele, G., Applegate, T. J., Kogut, M. H., et al. (2021). Effects of Salmonella enterica Ser. Enteritidis and Heidelberg on Host CD4+CD25+ Regulatory T Cell Suppressive Immune Responses in Chickens. *PLoS ONE* 16 (11), e0260280–16. doi:10.1371/journal.pone.0260280

Shanmugasundaram, R., Kogut, M. H., Arsenault, R. J., Swaggerty, C. L., Cole, K., Reddish, J. M., et al. (2015). Effect of Salmonella Infection on Cecal Tonsil Regulatory T Cell Properties in Chickens. *Poult. Sci.* 94 (8), 1828–1835. doi:10.3382/ps/pev161

Singh, L., and Kaur, M. (2021). *Foundation Course for NEET (Part 3): Biology Class 9*. 1st Edn. New Delhi, India: S. Chand Publishing.

Tafazoli, F., Magnusson, K.-E., and Zheng, L. (2003). Disruption of Epithelial Barrier Integrity by Salmonella enterica Serovar Typhimurium Requires Geranylgeranylated Proteins. *Infect. Immun.* 71 (2), 872–881. doi:10.1128/IAI.71.2.872-881.2003

Ten Bruggencate, S. J. M., Bovee-Oudenhoven, I. M. J., Lettink-Wissink, M. L. G., and Van der Meer, R. (2005). Dietary Fructooligosaccharides Increase Intestinal Permeability in Rats. *J. Nutr.* 135 (4), 837–842. doi:10.1093/jn/135.4.837

Tizard, I. R. (2021). "Chapter 19 - Poultry Vaccines," in *Vaccines for Veterinarians* (Amsterdam: Elsevier), 243–266. doi:10.1016/B978-0-323-68299-2.00028-9

Urban, J. (2020). *Individual Genetic Variation in Immune System May Affect Severity of COVID-19*. Washington, D.C: American Society for Microbiology. Available at: https://asm.org/Press-Releases/2020/Individual-Genetic-Variation-in-Immune-System-May#:~:text=Genetic variation explains some of,pathogen%2C or other foreign entity (Accessed: August 3, 2022).

Valero-Pacheco, N., Blight, J., Aldapa-Vega, G., Kemlo, P., Pérez-Toledo, M., Wong-Baeza, I., et al. (2020). Conservation of the OmpC Porin Among Typhoidal and Non-Typhoidal Salmonella Serovars. *Front. Immunol.* 10, 1–11. doi:10.3389/fimmu.2019.02966

Van Immerseel, F., De Buck, J., De Smet, I., Mast, J., Haesebrouck, F., and Ducatelle, R. (2002). Dynamics of Immune Cell Infiltration in the Caecal Lamina Propria of Chickens after Neonatal Infection with a Salmonella Enteritidis Strain. *Dev. Comp. Immunol.* 26 (4), 355–364. doi:10.1016/S0145-305X(01)00084-2

Vojtek, I., Buchy, P., Doherty, T. M., and Hoet, B. (2019). Would Immunization Be the Same without Cross-Reactivity? *Vaccine* 37 (4), 539–549. doi:10.1016/j.vaccine.2018.12.005

Wang, L., Li, L., Lv, Y., Chen, Q., Feng, J., and Zhao, X. (2018). Lactobacillus Plantarum Restores Intestinal Permeability Disrupted by Salmonella Infection in Newly-Hatched Chicks. *Sci. Rep.* 8 (1), 1–10. doi:10.1038/s41598-018-20752-z

Withanage, G. S. K., Kaiser, P., Wigley, P., Powers, C., Mastroeni, P., Brooks, H., et al. (2004). Rapid Expression of Chemokines and Proinflammatory Cytokines in Newly Hatched Chickens Infected with Salmonella enterica Serovar Typhimurium. *Infect. Immun.* 72 (4), 2152–2159. doi:10.1128/iai.72.4.2152-2159.2004

Wodi, A. P., and Morelli, V. (2021) 'Chapter 1: Principles of Vaccination', in *Epidemiology and Prevention of Vaccine-Preventable Diseases*. Editor E. Hall, A. Kroger, G. Redmon, J. Hamborsky, and S. Wolfe. 14th edn. Washinghton, D.C: Public Health Foundation, Centers for Disease Control and Prevention.

Xu, S., and Cao, X. (2010). Interleukin-17 and its Expanding Biological Functions. *Cell Mol. Immunol.* 7 (3), 164–174. doi:10.1038/cmi.2010.21

Xu, Y., Zhang, T., Xu, Q., Han, Z., Liang, S., Shao, Y., et al. (2015). Differential Modulation of Avian β-defensin and Toll-like Receptor Expression in Chickens Infected with Infectious Bronchitis Virus. *Appl. Microbiol. Biotechnol.* 99 (21), 9011–9024. doi:10.1007/s00253-015-6786-8

Zeng, J., Lei, C., Wang, Y., Chen, Y., Zhang, X., Kang, Z., et al. (2018). Distribution of Salmonella Enteritidis in Internal Organs and Variation of Cecum Microbiota in Chicken after Oral Challenge. *Microb. Pathog.* 122 (29), 174–179. Elsevier Ltd. doi:10.1016/j.micpath.2018.06.022

Zhao, K., Chen, G., Shi, X.-m., Gao, T.-t., Li, W., Zhao, Y., et al. (2012). Preparation and Efficacy of a Live Newcastle Disease Virus Vaccine Encapsulated in Chitosan Nanoparticles. *PLoS ONE* 7, e53314. doi:10.1371/journal.pone.0053314

Conflict of Interest: The authors declare that the research was conducted in the absence of any commercial or financial relationships that could be construed as a potential conflict of interest.

The handling editor SV declared a shared parent affiliation with the author RG at the time of review.

Publisher's Note: All claims expressed in this article are solely those of the authors and do not necessarily represent those of their affiliated organizations, or those of the publisher, the editors and the reviewers. Any product that may be evaluated in this article, or claim that may be made by its manufacturer, is not guaranteed or endorsed by the publisher.

frontiers | Frontiers in Physiology

TYPE Review
PUBLISHED 22 July 2022
DOI 10.3389/fphys.2022.961392

OPEN ACCESS

EDITED BY
Sandra G. Velleman,
The Ohio State University, United States

REVIEWED BY
Francesca Soglia,
University of Bologna, Italy
Orna Halevy,
Hebrew University of Jerusalem, Israel

*CORRESPONDENCE
Ana Gabriela Jimenez,
ajimenez@colgate.edu

SPECIALTY SECTION
This article was submitted to Avian Physiology,
a section of the journal
Frontiers in Physiology

RECEIVED 04 June 2022
ACCEPTED 29 June 2022
PUBLISHED 22 July 2022

CITATION
Swanson DL, Zhang Y and Jimenez AG (2022), Skeletal muscle and metabolic flexibility in response to changing energy demands in wild birds.
Front. Physiol. 13:961392.
doi: 10.3389/fphys.2022.961392

Skeletal muscle and metabolic flexibility in response to changing energy demands in wild birds

David L. Swanson[1], Yufeng Zhang[2] and Ana Gabriela Jimenez[3]*

[1]Department of Biology, University of South Dakota, Vermillion, SD, United States, [2]College of Health Science, University of Memphis, Memphis, TN, United States, [3]Department of Biology, Colgate University, Hamilton, NY, United States

Phenotypically plastic responses of animals to adjust to environmental variation are pervasive. Reversible plasticity (i.e., phenotypic flexibility), where adult phenotypes can be reversibly altered according to prevailing environmental conditions, allow for better matching of phenotypes to the environment and can generate fitness benefits but may also be associated with costs that trade-off with capacity for flexibility. Here, we review the literature on avian metabolic and muscle plasticity in response to season, temperature, migration and experimental manipulation of flight costs, and employ an integrative approach to explore the phenotypic flexibility of metabolic rates and skeletal muscle in wild birds. Basal (minimum maintenance metabolic rate) and summit (maximum cold-induced metabolic rate) metabolic rates are flexible traits in birds, typically increasing with increasing energy demands. Because skeletal muscles are important for energy use at the organismal level, especially to maximum rates of energy use during exercise or shivering thermogenesis, we consider flexibility of skeletal muscle at the tissue and ultrastructural levels in response to variations in the thermal environment and in workloads due to flight exercise. We also examine two major muscle remodeling regulatory pathways: myostatin and insulin-like growth factor -1 (IGF-1). Changes in myostatin and IGF-1 pathways are sometimes, but not always, regulated in a manner consistent with metabolic rate and muscle mass flexibility in response to changing energy demands in wild birds, but few studies have examined such variation so additional study is needed to fully understand roles for these pathways in regulating metabolic flexibility in birds. Muscle ultrastrutural variation in terms of muscle fiber diameter and associated myonuclear domain (MND) in birds is plastic and highly responsive to thermal variation and increases in workload, however, only a few studies have examined ultrastructural flexibility in avian muscle. Additionally, the relationship between myostatin, IGF-1, and satellite cell (SC) proliferation as it relates to avian muscle flexibility has not been addressed in birds and represents a promising avenue for future study.

KEYWORDS

muscle, hypertrophy, myostatin, IGF-1, myonuclear domain

Introduction

Phenotypically plastic responses of morphology, behavior and physiology to environmental variation are ubiquitous among living organisms (Pigliucci 2005; Morel-Journel et al., 2020; Sommer 2020). Genetic variation for plastic responses to environmental variation occurs among organisms (Pigliucci 2005), such that individual organisms differ predictably in plastic responses, including plasticity of metabolic rates (Norin and Metcalfe 2019). Phenotypic plasticity includes developmental plasticity, where environmental conditions experienced during development impact adult phenotypes, and reversible plasticity (i.e., phenotypic flexibility, Piersma and Drent 2003), where adult phenotypes can be reversibly altered according to prevailing environmental conditions. Such flexible responses allow better matching of adult phenotypes to the environment and can generate positive fitness benefits (Piersma and Van Gils 2011; Petit et al., 2017; Latimer et al., 2018).

The primary functions of skeletal muscle in birds are locomotion and thermogenesis. Powered flight is supported by large flight muscles, which comprise 10%–25% of total body mass in volant birds (Hartman 1961; DuBay et al., 2020). For more terrestrial species, leg muscles comprise larger fractions of total musculature (Hartman 1961; Bennett 1996). Thermogenesis in birds may be accomplished by both shivering and non-shivering mechanisms, and, although evidence continues to accumulate for muscular non-shivering thermogenesis in chicks or growing birds (for reviews see Rowland et al., 2015), thermogenesis in adult birds appears to occur primarily through shivering (Hohtola 1982; Cheviron and Swanson 2017; Stager and Cheviron 2020). Changing energetic demands for locomotion or thermoregulation throughout the annual cycle of birds, such as migration or cold winters, may result in flexible changes to the volume, ultrastructure, or aerobic capacity of skeletal muscles (Dawson et al., 1983; Marsh and Dawson 1989; Swanson 2010; Jimenez 2020).

Organismal metabolic and flight muscle flexibility in response to temperature

Birds resident in highly seasonal climates typically upregulate their maximum capacity for thermogenesis, known as summit metabolic rate (M_{sum}), in winter (Swanson 2010; Swanson and Vézina 2015). This elevation in M_{sum} is associated with improved capacities for cold tolerance and endurance under submaximal levels of cold exposure (Marsh and Dawson 1989; Swanson 2001; Swanson and Liknes 2006). In addition, M_{sum} is positively related to overwinter survival for small birds in cold climates (Petit et al., 2017; Latimer et al., 2018). Basal metabolic rate (BMR, miniumum maintenance metabolic rate) also often increases in winter in birds from cold climates or with cold acclimation in birds, although this trend is far from universal (Marsh and Dawson 1989; Swanson 2010, Table 1). As a recent example, Li et al. (2020) documented a 102% increase in BMR in winter relative to late spring in Eurasian tree sparrows (*Passer montanus*) from the relatively mild winter climate of southeastern China. BMR may also be associated with overwinter survival in birds, but on a fluctuating basis, with high BMR favored in cold winters and low BMR favored in warm winters (Nilsson and Nilsson 2016).

For birds wintering in warmer subtropical or tropical climates, seasonal patterns of variation in M_{sum} are much more variable (McKechnie et al., 2015), with winter increases, winter decreases or no seasonal change evident for various bird species (Smit and McKechnie 2010; Wells and Schaeffer 2012; Van de Ven et al., 2013; Thompson et al., 2015; Noakes et al., 2017; Pollock et al., 2019; Noakes and McKechnie, 2020). This suggests that thermoregulatory demand is an important determinant of M_{sum} in birds (Swanson and Garland 2009; Stager et al., 2016; Stager et al., 2020; Stager et al., 2021). The migratory condition (especially the more rapid spring migration; Nilsson et al., 2013; Horton et al., 2016; Schmaljohann et al., 2017) in birds also appears to generally result in an upregulation of M_{sum}, perhaps as a by-product of enhancement of flight capacities (Swanson 1995; Swanson and Dean 1999; Vézina et al., 2007; Petit and Vézina 2014a; Corder and Schaeffer 2015).

Because M_{sum} is primarily a function of skeletal muscle metabolism, increases in M_{sum} are likely mediated by changes in skeletal muscle. Increases in M_{sum} at the organismal level can be accomplished by changes in either the size of the skeletal muscles involved in thermogenesis or in the cellular metabolic intensity of individual muscle fibers (Swanson 2010). For birds, the prevailing dogma is that changes in muscle mass (especially the pectoralis, which is the largest muscle in the body of volant birds and, therefore, the principal thermogenic organ, Marsh and Dawson 1989) are regular contributors to changes in M_{sum}, but that variation in cellular metabolic intensity is a less consistent mediator of flexibility of M_{sum} in response to changing energy demands associated with seasonal thermogenesis or migration (Swanson and Vézina 2015).

Recent evidence, however, suggests that, although muscle hypertrophy is still a common correlate of increases in BMR and M_{sum} at the organismal level, that tight coupling between muscle hypertrophy and increases in M_{sum} is not as consistent as previously believed (Figure 1; Table 1). BMR is positively correlated with pectoralis mass or flight muscle mass for many bird species, including house sparrows (Chappell et al., 1999) and non-breeding European starlings (Vézina and Williams 2003). Several recent studies also document the expected positive relationships between pectoralis muscle mass and BMR or M_{sum}. For example, pectoralis muscle mass was positively correlated with M_{sum} in summer-acclimatized captive American goldfinches (*Spinus tristis,* Swanson et al., 2013). In addition, even when acclimation- or acclimatization-induced

TABLE 1 Results of recent studies (since 2010) of natural seasonal or migratory acclimatization, temperature acclimation, or experimental flight training effects on pectoralis/flight muscle mass or size and metabolic rates (BMR or M_{sum}) in birds.

Species	Acclimatization or acclimation condition	Trend in pectoralis muscle mass or size	Trend in metabolic Rates	Reference
Black-capped chickadee *Poecile atricapillus*	Seasonal acclimatization to cold winter	Dry mass increase by 10%	M_{sum} increase by 22%	Petit et al. (2014)
Snow bunting *Plectrophenax nivalis*	Outdoor captive all year in winter range	Ultrasound thickness increase by 8%	M_{sum} increase by 23%	Le Pogam et al. (2020)
Chinese bulbul *Pycnonotus sinensis*	Seasonal acclimatization to cool winter	Dry mass increase by 12%	BMR increase by 21%	Zheng et al. (2014)
Chinese hwamei *Garrulax canorus*	Acclimated to 15 and 35°C	Dry mass increase by 20%	BMR increase by 40%	Zhou et al. (2016)
Eurasian tree sparrow *Passer montanus*	Acclimated to 10 and 30°C; varying photoperiod	No sig. change in dry mass of skeletal muscle	BMR increase by 45%	Li et al. (2020)
Chinese bulbul *Pycnonotus sinensis*	Seasonal acclimatization to cool winter	No sig. change in dry mass	BMR increase by 42%	Wang et al. (2019)
Chinese hwamei *Garrulax canorus*	Acclimated to 10 and 30°C; varying photoperiod	No sig. change in dry mass	BMR increase by 18%	Hu et al. (2017)
Dark-eyed junco *Junco hyemalis*	Acclimated to 3 and 24°C; varying photoperiod	No significant change in wet mass	M_{sum} increase by 18%	Swanson et al. (2014a)
White-throated sparrow *Zonotrichia albicollis*	Acclimated to -8 and 28°C	No sig. change in dry mass	M_{sum} increase by 19% BMR increase by 15%	Barcelo et al. (2017)
Black-capped chickadee *Poecile atricapillus*	Acclimated to -10 and 27°C	No sig. change in dry mass	M_{sum} increase by 20% BMR increase by 5%	Milbergue et al. (2018)
Snow bunting *Plectrophenax nivalis*	Seasonal acclimatization cold winter, Arctic summer	Winter ultrasound thickness increase by 3.1%	No significant change in M_{sum}	Le Pogam et al. (2021)
White-browed sparrow-weaver *Plocepasser mahali*	Seasonal acclimatization to mild winter	Dry mass increase by 5%	M_{sum} decrease by 26%	Noakes et al. (2020)
House sparrow *Passer domesticus*	Acute, repeated exposure to severe cold	Wet mass increase by 5%	M_{sum} increase by 14.6% BMR increase by 10.3%	Zhang et al. (2015)
Gray catbird *Dumetella carolinensis*	Natural migratory acclimatization	Wet mass increase by 8.7% in migrants	M_{sum} increase by 19-29%	DeMoranville et al. (2019)
Warbling vireo *Vireo gilvus*	Natural migratory acclimatization	Wet mass increase by 10.3% in spring	M_{sum} increase by 18.3%	King et al. (2015) Swanson (1995)
Yellow warbler *Setophaga petechia*	Natural migratory acclimatization	Wet mass increase by 14.7% in spring	M_{sum} increase by 23.3%	King et al. (2015) Swanson and Dean (1999)
Yellow-rumped warbler *Setophaga coronata*	Natural migratory acclimatization	No significant seasonal change in wet mass	M_{sum} increase by 19.8% in spring vs. fall	King et al. (2015) Swanson and Dean (1999)
Black-capped chickadee *Poecile atricapillus*	Feather clipping to increase flight costs	Muscle score increase	M_{sum} increase by 17%	Petit and Vézina (2014a)
House sparrow *Passer domesticus*	Experimental flight training	Wet mass increase by 7%	M_{sum} increase by 15.5% BMR decrease by 37.9%	Zhang et al. (2015)

changes in pectoralis or skeletal muscle masses are not concordant with similar changes in M_{sum} or BMR (Table 1), muscle masses and metabolic rates may still show positive correlations (Barcelo et al., 2017; Milbergue et al., 2018; Li et al., 2020). These data suggest that muscle masses, especially mass of the flight muscles, are important determinants of organismal metabolic rates. In addition to changes in muscle masses, changes in muscle ultrastructure in response to winter or cold may also be evident. For example, black-capped chickadees acclimated to −5°C had 23% larger pectoralis fiber diameter than

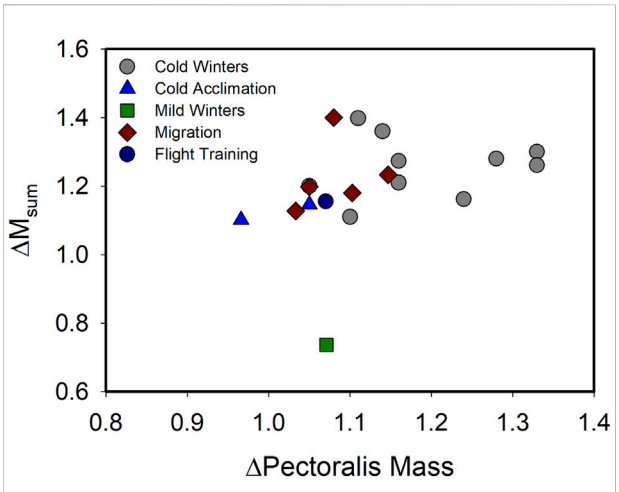

FIGURE 1
Relationship of variation in pectoralis muscle mass (ΔPectoralis Mass) with variation in summit metabolic rate (ΔM_{sum}) across a range of natural acclimatization (winter *vs.* summer in climate with cold or mild winters, migratory *vs.* non-migratory conditions) and experimental acclimation (cold *vs.* warm, flight training *vs.* control) for birds. A linear regression on these data indicated no significant relationship ($F_{1,17}$ = 1.918, p = 0.184), including after removal of the "Mild Winters" data point ($F_{1,16}$ = 2.775, p = 0.115), suggesting that despite increases in both M_{sum} and pectoralis muscle mass often occurring under conditions of increasing energy demand in birds, the two traits are not tightly coupled. Data from Swanson (1990), Swanson (1991), Swanson (1995), O'Connor (1995a), O'Connor (1995b), Cooper (2002), Cooper and Swanson (1994), Petit et al. (2014), Liknes and Swanson (2011), Sgueo et al. (2012), Swanson et al. (2014a,b), Milbergue et al. (2018), Noakes et al. (2020), DeMoranville et al. (2019), King et al. (2015), Zhang et al. (2015), Vézina et al. (2006).

birds acclimated to 20°C (Vézina et al., 2020). When birds in these temperature treatments were exposed to a 3 h temperature drop of 15°C, cold-acclimated birds increased the number of capillaries per muscle fiber and the number of nuclei per fiber by 22%, whereas no changes occurred in warm-acclimated birds, suggesting that cold-acclimated birds had an increased capacity for response to an acute temperature decrease (Vézina et al., 2020), but how these changes relate to acute changes in M_{sum} is not known.

In contrast to these studies, a number of other recent studies suggest that seasonal or cold-induced changes in muscle size do not necessarily accompany changes in metabolic capacities in birds (Table 1). In addition to study results summarized in Table 1 showing a lack of congruence in seasonal or cold-induced variation in muscle masses and organismal metabolic rates, Bai et al. (2016) found no significant correlations between pectoralis mass residuals and BMR residuals in brambling (*Fringilla montifringilla*), little bunting (*Emberiza pusilla*), and Eurasian tree sparrow (*P. montanus*). The overall generalization from recent work on flexibility in pectoralis mass and metabolic capacities in birds in response to winter or cold exposure is well-stated by Milbergue et al. (2018), who noted in the title of their paper that "large muscles are beneficial but not required for improving thermogenic capacity in small birds." Such a result indicates that cellular and biochemical adjustments, such as alterations of the number of mitochondria, aerobic enzyme activities, substrate transport pathways, and, potentially, mechanisms promoting muscular non-shivering thermogenesis, can also contribute to changes in organismal thermogenic capacity in response to temperature (Swanson 2010; Milbergue et al., 2018).

Organismal metabolic and flight muscle flexibility in response to migration or flight training

In addition to winter acclimatization or cold acclimation influences on muscle masses and metabolic rates in birds, development of migratory disposition is also typically associated with increases in flight muscle mass of up to 35% (Swanson 2010; Piersma and Van Gils 2011). Such increases in flight muscle mass can occur over periods as short as a few days and apparently do not require exercise as a cue for hypertrophy (Dietz et al., 1999; Piersma and Van Gils 2011). Examples of such rapid hypertrophy associated with migration include an approximately 19% increase in lean dry pectoralis muscle mass over the last few days of a 24-days stopover in red knots (*Calidris canutus*, Piersma et al., 1999). Similarly, Bar-tailed godwits (*Limosa lapponica*) showed increases in lean dry pectoralis mass of 21 and 27% in males and females, respectively, between early and late stopover phases (Landys-Ciannelli et al., 2003). More recent studies also generally support the trend of muscle hypertrophy during the migratory period for birds. For example, pectoralis muscle mass and fiber diameter both increased (by approximately 17 and 35%, respectively) with development of migratory condition in outdoor captive Snow buntings (Vézina et al., 2021). Concurrently with this change, myonuclear domain (MND) also increased during migration (Vézina et al., 2021; more on this below). Velten et al. (2016) compared winter flocks of white-crowned sparrows (*Zonotrichia leucophrys*) in central California with birds just arriving from migration in May in Alaska and found that flight muscle mass was greater upon arrival in Alaska than during winter or just prior to departure in April in California. Flight training also typically results in increases in pectoralis muscle mass in birds. Fight-trained European starlings (*Sturnus vulgaris*) increased pectoralis mass by 8% compared to untrained birds (DeMoranville et al., 2020). Zhang et al. (2018a) forced Zebra finches (*Taeniopygia guttata*) to hover while feeding, thus increasing flight costs, which resulted in a 9% increase in pectoralis mass for females, but not for males.

Oftentimes, these increases in pectoralis mass with migration or flight training are correlated with increases in metabolic capacities in birds (Table 1). For example, M_{sum} was positively

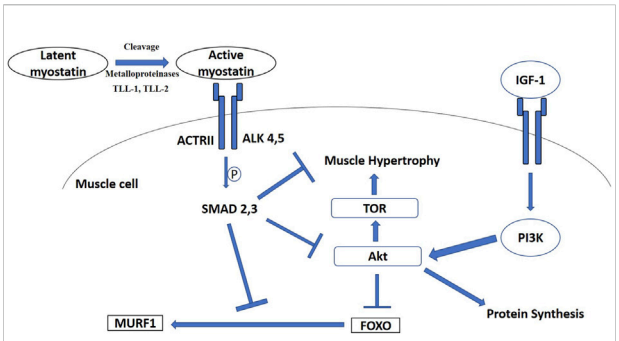

FIGURE 2
Signaling diagram illustrating myostatin and insulin-like growth factor−1 (IGF-1) pathways. ActRII, activin receptor II; ALK, type I activin receptors; Akt, protein kinase B; PI3K, phosphatidylinositol 3-kinase; TOR, target of rapamycin; TLL, Tolloid-like protein; FOXO, Forkhead Box-O; MURF1, muscle-specific E3 ubiquitin ligase muscle RING-finger 1.

correlated with breast muscle size measured by ultrasonography in migratory and cold acclimated red knots (Vézina et al., 2006; Vézina et al., 2007). In addition, male Ruby-crowned kinglets (*Regulus calendula*) elevated M_{sum} by 10.9% between spring and fall migration, although female kinglets showed statistically stable M_{sum} between spring and fall, consistent with a more rapid pace of migration in spring (Swanson and Dean 1999). Results from recent studies are also generally consistent with elevated pectoralis mass being positively associated with elevations in M_{sum}, although this does not occur for all birds studied (Table 1).

The signaling pathways regulating muscle mass

As noted above, one major factor often supporting increases in thermogenic and exercise capacity in small birds is pectoralis muscle hypertrophy (O'Connor 1995a; Swanson, 2010; Swanson and Merkord, 2013; Swanson et al., 2013). However, the signaling pathways and cellular and molecular mechanisms regulating muscle and organ mass changes underlying phenotypic flexibility in wild, free-living, birds have received relatively little research attention to date (Swanson, 2010). Two major candidates for signaling pathways regulating flexibility in muscle mass are myostatin and insulin-like growth factor -1 (IGF-1) pathways (Favier et al., 2008; Hennebry et al., 2017). While myostatin acts by inhibiting muscle growth, IGF-1 signals an increase in protein synthesis and, therefore, an increase muscle mass (Figure 2; Hennebry et al., 2017). The interaction of these signaling pathways with cellular and molecular mechanisms influencing muscle growth and function are important determinants of muscle mass and should be tightly regulated in birds (Lozier et al., 2018; Sartori et al., 2021).

Myostatin signaling pathway

Of these two major pathways, the myostatin signaling pathway is better studied in avian phenotypic flexibility. Myostatin (MSTN), also known as growth differentiation factor 8 (GDF-8), is a TGF-β superfamily growth factor (McPherron et al., 1997; Lee, 2004; Sharma et al., 2015). Myostatin is a potent autocrine/paracrine inhibitor of muscle growth in mammals and birds, and is a highly conserved protein, with the active peptide being identical in birds and mammals, such as mice, rats, humans, pigs, dogs, chickens and turkeys (Lee, 2004; McFarland et al., 2006; McFarland et al., 2007). Similar to other TGF-β superfamily members, myostatin is synthesized in skeletal muscle in an inactive form (52 kDa) that requires two proteolytic cleavages for activation (McPherron et al., 1997; Lee and McPherron, 2001). An initial cleavage of the propeptide from mature myostatin by furin or other propeptide convertases produces a latent form with the propeptide non-covalently bound to the mature myostatin (Lee, 2008; Pirruccello-Straub et al., 2018). Cleavage of the NH_2-terminal propeptide domain from mature myostatin results in formation of the active COOH-terminal dimer, which binds to myostatin receptors and is required for myostatin activity (Thomas et al., 2000; Lee, 2008). Metalloproteinases, including BMP-1/tolloid family members TLL-1 and TLL-2, can perform this second cleavage to activate myostatin (Wolfman et al., 2003). Because of these enzymatic cleavages, a 36/40 kDa Latency Associated Peptide and a 12.5/26 kDa mature peptide, corresponding to a C-terminal monomer or dimer respectively, have been observed (Thomas et al., 2000; Lee and McPherron, 2001; McFarlane et al., 2005). Both mature and LAP forms of myostatin are secreted into the circulation (Lee and McPherron, 2001; Hill et al., 2002), allowing myostatin to function in an autocrine, paracrine, or endocrine manner.

Active mature myostatin binds to the type II activin receptors A and B (ActRIIA and ActRIIB) (Lee et al., 2005), which recruit and activate type I activin receptors four and five (Alk4 and Alk5) (Rebbapragada et al., 2003). These events stimulate phosphorylation and activation of the transcriptional factors Smad2 and Smad3, which join with Smad4 into a Smad2/3/4 complex that triggers gene transcription (Figure 2; Zhu et al., 2004). Additionally, myostatin decreases Akt (protein kinase B) phosphorylation (Trendelenburg et al., 2009), which is accompanied by the accumulation of dephosphorylated active Forkhead Box-O1 (FOXO1) and FOXO3 (Allen and Unterman, 2007), followed by upregulation of components of the ubiquitin-proteasome pathway, such as atrogin-1 and the muscle-specific E3 ubiquitin ligase muscle RING-finger1 (MURF1) (McFarlane et al., 2006) (Figure 2). As one of the master regulators of muscle mass and protein synthesis, regulation of myostatin could also occur at the post-transcriptional (regulating microRNAs) (Clop et al., 2006) and post-translational (regulating protein-protein interaction) levels (Sharma et al., 2015). Moreover, myostatin

could also promote quiescence of satellite cells in skeletal muscle so that they fail to become incorporated into the muscle fiber and inhibit self-renewal of satellite cells (McCroskery et al., 2003; McFarland et al., 2007).

Mutations in the myostatin gene and blockage of myostatin action result in dramatic increases in muscle growth (McPherron and Lee, 1997; Lee, 2004; Chen and Lee, 2016). In mammals, treatment of adult mice with an inhibitory antibody to myostatin resulted in muscle hypertrophy, suggesting that myostatin is an important mechanism for muscle remodeling in adult animals (Whittemore et al., 2003). In poultry, myostatin tightly regulates pectoralis muscle mass and inhibition of myostatin dramatically increased pectoralis mass in chicken, turkey, domestic pigeon, duck, and Japanese quail (McFarland et al., 2006; Xu et al., 2013; Shin et al., 2015; Liu et al., 2019; Zhao et al., 2019; Kim et al., 2020). Phenotypic flexibility in wild, free-living, birds could be more complicated since birds can modify flight muscle independent of workload (Swaddle and Biewener, 2000) and changes in flight muscle mass can occur without training (Dietz et al., 1999). Because of the prominent role of myostatin in muscle remodeling, it is reasonable to hypothesize that myostatin is involved in phenotypic flexibility of muscle mass in birds generally, potentially playing roles in muscle size changes associated with different periods of the annual cycle (e.g., winter acclimation, migration, molt) where phenotypic flexibility of muscle mass occurs.

Myostatin in avian phenotypic flexibility

Investigation of a role for myostatin in avian metabolic flexibility was first examined in house sparrows during winter acclimatization where increases in pectoralis muscle mass occurred in response to winter cold (Swanson et al., 2009). In this study, myostatin and TLL-1 gene expression were both lower in pectoralis muscle of house sparrows during winter than during summer, suggesting reductions in myostatin levels and myostatin processing capacity in winter consistent with winter increases in muscle mass and metabolic capacities. However, in a follow-up study (Swanson et al., 2014b), results for both American goldfinches (*S. tristis*) or black-capped chickadees (*Poecile atricapillus*) between summer and winter were not consistent with house sparrows. Swanson et al. (2014b) found that pectoralis muscle mass increased in winter for naturally acclimatized American goldfinches (by 15%) but not for black-capped chickadees, despite chickadees typically showing winter increases in pectoralis mass and M_{sum} (Cooper and Swanson, 1994; Liknes and Swanson, 2011; Petit and Vézina, 2014b; Petit et al., 2014). Myostatin gene or protein expression did not vary significantly between summer and winter for goldfinches, although there was a tendency toward lower levels in winter, but both TLL-1 and TLL-2 were reduced in winter goldfinches, suggesting a lower capacity for processing and activation of myostatin in winter consistent with a winter increase in pectoralis muscle mass (Swanson et al., 2014b). For chickadees, myostatin gene and protein expression showed only non-siginificant decreases and TLL-1 also showed no significant seasonal variation, but TLL-2 exhibited a significant winter decrease (Swanson et al., 2014b). Thus, although changes in muscle mass and expression of the myostatin system were generally consistent with a role for the myostatin pathway in regulating seasonal changes in muscle mass and thermogenic capacity in chickadees and goldfinches, these changes were not uniform for both species.

Swanson et al. (2017) examined within-winter variation in pectoralis muscle mass and expression of the myostatin system in dark-eyed juncos and house sparrows and found that pectoral muscle mass residuals were positively correlated with Short-term (ST; 0–7 days prior to measurement) temperature variables for both species, which was opposite of predictions and suggests that cold temperatures resulted in catabolism of skeletal muscles over the short term. Pectoralis gene or protein expression of myostatin and the TLL proteases were only weakly correlated with ST and medium-term (MT; 14–30 days prior to measurement) temperature variables, and myostatin expression was negatively related with ST and MT temperatures for juncos but positively related with long-term (30-years average temperatures) and MT temperatures for house sparrows (Swanson et al., 2017), so no consistent regulation of the myostatin system in response to acute temperature variation within winters was evident, despite within-winter variation in basal and summit metabolic rates in response to ST and MT temperature variables in small birds (Swanson and Olmstead, 1999).

For migration-induced muscle mass changes, myostatin gene expression did not vary significantly during the migratory season (spring and fall) compared to the non-migratory season (winter) in white-throated sparrows (*Zonotrichia albicollis*) (Price et al., 2011). Moreover, pectoralis and heart mRNA expression of myostatin, TLL-1 and TLL-2 also did not differ significantly among seasons for yellow warblers (*Setophaga petechia*), warbling vireos (*Vireo gilvus*), and yellow-rumped warblers (*Setophaga coronata*), either between migratory seasons (spring of fall) or compared to summer (King et al., 2015). In contrast, myostatin protein levels in pectoralis muscle were lowest during the spring migratory season, concomitant with the greatest pectoralis muscle mass for all three species (King et al., 2015). Similar to winter acclimatization, these data offered mixed support for a regulatory role for myostatin in supporting increases in muscle masses during migration and suggest that patterns of gene and protein expression of the myostatin system do not vary in lockstep. These results further suggest a potentially important role for post-transcriptional regulation of the myostatin pathway in bird responses to seasonally changing energy demands.

Other than natural winter and migratory adjustments, experimental photoperiod, temperature and flight training treatments have been employed to examine a potential role for myostatin in avian metabolic flexibility. Photoperiod (short- *vs.* long-day) and temperature (3°C or 24°C) treatments did not significantly alter gene expression of myostatin or the TLLs nor myostatin protein levels in dark-eyed juncos (*Junco hyemalis*) (Zhang et al., 2018a). Photoperiod-stimulated white-throated sparrows showed higher myostatin mRNA expression for long-day (migratory) compared to short-day (winter) treatments, despite long-day sparrows having greater flight muscle dry mass (Price et al., 2011). In addition to regulating muscle mass, myostatin is also known to increase fat accumulation in adipose tissue in mammals (Lin et al., 2002; McPherron and Lee, 2002; Rebbapragada et al., 2003) by either directly acting on receptors on adipocytes or indirectly saving energy from decreased musculature (Guo et al., 2009). Consequently, elevated myostatin levels might function in adipogenesis in photo-stimulated birds in migratory disposition, which must gain fat mass in preparation for migration.

Compared with seasonal changes, myostatin's role in muscle remodeling in birds during experimental manipulation was more consistent. Experimental increases in foraging costs of zebra finches (*T. guttata*), accomplished by forcing birds to forage while hovering, resulted in female, but not male, finches showing lower myostatin protein levels than controls (Zhang et al., 2018b). It is important to note here that female zebra finches average shorter wings and higher wing loading than males, so increased flight costs might be expected to disproportionately affect females. Indeed, only female zebra finches in the high foraging group in this study showed reduced total fat masses and increased pectoralis muscle masses, whereas male finches had similar fat and pectoralis mass between groups (Zhang et al., 2018b). Gene expression of myostatin and the TLLs, however, did not vary significantly after high foraging cost treatments for either sex. Other than experimentally increasing foraging costs, flight exercise training has been employed to study the role of myostatin in avian muscle remodeling. Two-week incremental wind tunnel flight training did not significantly modify myostatin or TLL-1 gene expression in European starlings (*S. vulgaris*) (Price et al., 2011). However, this training protocol also did not significantly affect flight muscle mass after controlling for body mass. In another study, Zhang et al. (2015) used experimental cold exposure and exercise training protocols in house sparrows and both training protocols increased pectoralis muscle mass and reduced pectoralis myostatin protein levels. However, gene expression of pectoralis myostatin did not change significantly and gene expression of the TLLs increased for both training protocols. Again, these studies offer partial support for the hypothesis that the myostatin system plays a regulatory role in muscle mass changes in response to changing energy demands in birds and suggest that gene and protein expression of the myostatin system do not necessarily vary in tandem, highlighting again the potential importance of post-transcriptional regulation of this system.

IGF-1 signaling pathway

In addition to myostatin, the growth hormone/Insulin-like growth factor 1 (IGF-1) axis stimulates growth and accounts for up to 83% of postnatal growth and skeletal muscle hypertrophy in young mammals (Hennebry et al., 2017). Locally produced IGF-1 is now considered to have the predominant influence on tissue growth and local delivery of IGF-1 to skeletal muscle is essential for muscle hypertrophy (Shavlakadze et al., 2010). IGF-1 activates the IGF-1 receptor and phosphorylates PI3 kinase (PI3K) and Akt (Figure 2; Rommel et al., 2001). This process stimulates protein synthesis in myocytes and also satellite cell proliferation, leading to hypertrophy (Snijders et al., 2015). As mentioned above, the PI3K/Akt pathway is also common to the myostatin system, so there appears to be cross-regulation between myostatin and IGF-1 (Figure 2; Morissette et al., 2009; Yoshida and Delafontaine, 2020). However, the myostatin knockout mouse model also suggested that IGF-1 could stimulate muscle hypertrophy in the absence of myostatin, indicating distinct mechanisms for myostatin and IGF-1 regulation of skeletal muscle mass (Hennebry et al., 2017). IGF-1 also promotes skeletal muscle growth through the PI3K/Akt pathway in chickens (Deng et al., 2014; Yu et al., 2015; Nakashima and Ishida, 2018; Nakashima and Ishida, 2019). Even though the IGF-1 axis is a prime target for muscle remodeling in poultry (e.g., Tomas et al., 1998; Saneyasu et al., 2016; Saneyasu et al., 2017; Chen et al., 2018), the IGF-1 axis has received much less research attention in wild birds, with reference to muscle remodeling for phenotypic flexibility, compared with the myostatin signaling pathway. Adélie penguins chicks (*Pygoscelis adeliae*) expressed high IGF-1 mRNA in pectoralis muscle during a rapid growth period, indicating that it plays an important role in the development of an enhanced muscle phenotype (Dégletagne et al., 2013). Gene expression of IGF-1 increased in the pectoralis muscle of migratory Gambel's white-crowned sparrows (*Zonotrichia leucophrys gambelii*), but decreased in the gastrocnemius muscle at pre-departure stage (Pradhan et al., 2019). On the other hand, IGF-1 mRNA expression in pectoralis of white-throated sparrows was stable during migratory seasons (spring and fall) compared to winter (Price et al., 2011). Flight-trained European starlings showed higher IGF-1 mRNA expression than untrained controls, even though flight muscle mass did not vary significantly between these two groups (Price et al., 2011). Taken together, these data suggest that the IGF-1 signaling pathway might play an important role, independent of myostatin, in modulating avian phenotypic flexibility, but the results to date remain tentative and inconclusive due to limited data.

In addition, transcriptomic analyses on dark-eyed juncos under different temperature and photoperiod treatments indicated that very few genes associated with the mammalian target of rapamycin (mTOR) signaling pathway that governs protein synthesis, and with which myostatin and IGF-1 interact (Amirouche et al., 2009; Ma et al., 2018), were changed, and those genes were counterintuitively upregulated in warm-acclimated birds (Stager et al., 2015). Cheviron and Swanson (2017), however, examined seasonal transcriptomic variation in naturally seasonally acclimatized black-capped chickadees and American goldfinches and found winter upregulation in *mTOR* and genes in the BMP-signaling cascade (*TOB1* and *BMPR2*) in pectoralis muscle, suggesting possible involvement of these pathways in seasonal phenotypic flexibility.

Ultrastructural changes associated with flexibility in muscle mass

Myonuclear domain and its significance to muscle function

Skeletal muscle is a multinucleated syncitium. As such, nuclei are each supported by linker of nucleoskeleton and cytoskeleton (LINC) complexes that preserve nuclear positioning (Azevedo and Baylies 2020), so as to minimize transport distances (Snijders et al., 2020). This multinucleation develops through a well-coordinated and seemingly conserved process in vertebrates (Azevedo and Baylies 2020). Progenitor myoblasts are first specified in the embryonic mesoderm to undergo cell-cell fusion events that increase nuclear and cytoplasmic mass to form syncytial myotubes (Azevedo and Baylies 2020). Through myogenesis, these nascent myotubes undergo changes and movements to develop into mature myofibers with specifically determined nuclear positioning and internuclear distances (Azevedo and Baylies 2020). However, not all myoblasts participate in embryonic myogenesis. Such "unfused" myoblasts are termed satellite cells (SCs) and constitute a multipotential mesenchymal stem cell population with the ability to undergo myogenesis or alternative trans-differentiation programs (Velleman 2015). Though undifferentiated, SCs are heterogenous in that distinct sub-populations express a particular set of cell surface markers, differ in activation kinetics, and exhibit unique self-renewal timeframes that make them fiber-type specific and dictate their ability to proliferate and differentiate during post-embryonic muscle growth and regeneration (Velleman 2015; Forcina et al., 2019; Jankowski et al., 2020). In birds, as well as other vertebrates, a SC population surrounds mature myofibers and is key to enabling the post-hatch growth and regeneration of terminally differentiated myofibers in response to mechanical stimuli, injury, and homeostatic factors, including environmental changes (Mauro 1961; Kuang et al., 2007; Forcina et al., 2019). Protected between the basal lamina and sarcolemma of each muscle fiber that preserves their survival and niche behavior, SCs remain in a non-growing, quiescent state with low transcriptional activity until they receive the appropriate signals that restore their proliferative activity by stimulating their re-entrance into the cell cycle (Mauro 1961; Forcina et al., 2019). Then, they can undergo symmetric and asymmetric divisions that maintain the stem cell pool while simultaneously producing cells with reactivated transcriptional expression that allow for differentiation and contribution to muscle plasticity (Kuang et al., 2007; Forcina et al., 2019). Afterwards, they can fuse with existing myofibers to add nuclei, enhance diameter and length, and augment protein synthesis potential through hypertrophic accretion (Forcina et al., 2019; Jankowski et al., 2020; Murach et al., 2021), otherwise DNA may become limiting in larger cells (Cramer et al., 2020). Most muscle growth in adult organisms happens via hypertrophy, that is, an increase in muscle fiber diameter (Kinsey et al., 2007). Because muscle is a post-mitotic, multinucleated tissue, new adult muscle growth via hypertrophy may necessitate either an upregulation of the protein synthesis machinery by existing myonuclei or new nuclei to be drawn into the muscle fiber from a population of SCs. Each myonucleus in a muscle fiber is responsible for servicing a certain volume of cytoplasm known as a myonuclear domain (MND) (Rosser et al., 2003; Qaisar and Larsson, 2014). The cytoplasm of a muscle fiber must be highly organized to compartmentalize the necessary metabolic and contractile machinery. One could, therefore, think of the regulation of muscle fiber diameter and/or cross-sectional area in terms of the balance between production and degradation of cytoplasmic components (Hughes and Schiaffino, 1999; Van der Meer et al., 2011).

Other circulating factors that may activate proliferation of SC in non-injury states into myofibers include growth hormone, follistatin (a myostatin antagonist), and IGF-1, among others (Forcina et al., 2019; Murach et al., 2021). Additionally, increases in lactate concentrations may act as a signaling molecule for increased proliferation of SCs (Nalbandian et al., 2020), and others have suggested that glycolytic enzymes are necessary for optimal muscle growth, at least in *Drosophila* models (Graca et al., 2021). However, it is unclear how regulation to either add new nuclei or upregulate existing myonuclear activity is accomplished within muscle fibers (Cramer et al., 2020).

Myonuclear domain and muscle remodeling in mammals with respect to energy demand

MND regulation is much more extensively studied in mammals than in birds, so an exploration of mammalian regulation of MND can provide the necessary background to examine similar MND regulation in birds. In mammals, hypertrophy can be initiated and sustained for a time in the

absence of SCs in adult mice, but hypertrophy maintained for 8 weeks or more is dampened without additional SCs (Murach et al., 2021), and large changes to MND during muscle hypertrophy do not persist (Snijders et al., 2020). In mammals, myonuclear number is positively correlated with muscle protein synthesis, and the number of nuclei is also positively correlated with myofiber size (Snijders et al., 2020; Ato and Ogasawara 2021), but muscle protein synthesis was negatively correlated with myofiber size (Ato and Ogasawara 2021). Scaling properties of adult human and mice muscle fibers are the same for myonuclei number and cell volume (Hansson et al., 2020). MND may differ between fiber types in mammals, where slow-oxidative fibers have a smaller MND compared with glycolytic fibers (Tseng et al., 1994; Liu et al., 2009; Van der Meer et al., 2011; Omairi et al., 2016). This difference originates from fewer myogenic nuclei in glycolytic fibers rather than a smaller fiber volume in slow-oxidative fibers (Van der Meer et al., 2011). Thus, MND is inversely related to oxidative capacity of the muscle fiber itself, because slow-oxidative fibers should need faster protein turnover rates than fast-glycolytic fibers (Tseng et al., 1994; Liu et al., 2009; Van der Meer et al., 2011; Omairi et al., 2016). Fast-glycolytic fibers demonstrate high flexibility in MND (Murach et al., 2018). Furthermore, manipulating Myostatin or Akt pathways that are associated with hypertrophy also increases fiber diameter without myonuclear accretion in fast-glycolytic fibers (Murach et al., 2018). SCs also respond to increases in IGF-1 by stimulating proliferation (Scicchitano et al., 2016; Forcina et al., 2019). Exercise in mammals typically promotes SC activation. In mice, after 4 weeks of training, SC activation can happen within 24 h of acute exercise (Wen et al., 2021).

Myonuclear domain and muscle remodeling in birds with respect to temperature changes

Post-natal development of muscle fibers involves an increase in fiber size and a concomitant increase in the number of nuclei (derived from SCs) (Hughes and Schiaffino, 1999; Brack et al., 2005). In adult birds, SCs may proliferate following stretching (Winchester and Gonyea, 1992). In black-capped chickadees, when fiber diameter increases in colder seasons via hypertrophy, MND also increases (Jimenez et al., 2019). This indicates that each myonucleus must regulate synthesis and degradation for a greater area of the muscle fiber (Van der Meer et al., 2011). Additionally, this implies that increases in thermogenic capacity are coupled with remodeling of muscle tissue protein processing such that each myonucleus may need to respond to an increased demand for protein turnover. It is, however, possible that MND increases prior to SCs being incorporated into the myofiber. Cold-acclimated chickadees exposed to a sudden 15°C drop in temperature are able to modify their pectoralis ultrastructure within 3 h of the temperature decrease (Vézina et al., 2020). Within 3 h, these birds were able to increase the number of nuclei per millimeter of fiber by 15%, and decrease MND by the same amount. This may suggest that the addition of SCs into existing myofibers can be rapid (Vézina et al., 2020). Others have also demonstrated that cultured muscle SCs have rapid proliferation rates (Young et al., 2021a). After muscle injury, 73% of the myonuclei found at the periphery of the fiber migrated to the site of injury within 5 h in adult mice, thus, movement of nuclei within a myofiber seems to be rapid and dynamic (Roman et al., 2021). These additional nuclei may originate from either symmetrical or asymmetrical divisions of SCs (Kuang et al., 2007), as DNA content per myonucleus (or genome size) of avian muscle does not increase during muscle remodeling (Jimenez and Lencyk 2021). Thus, winter-phenotype chickadees facing a sudden cold drop may have activated SCs.

A further implication of these data is that, whereas avian muscle seems more phenotypically flexible than mammalian muscle, the biological processes surrounding myonuclear function may be more closely related to those of mammals (Jimenez 2020; Jimenez and Lencyk 2021). SCs have capacity for self-renewal and their ability to retain stem cell properties in mammals is well documented (Sobolewska et al., 2011; Shimizu-Motohashi and Asakura, 2014; Forcina et al., 2019; Abreu and Kowaltowski, 2020). Because ploidy number does not change in bird muscle tissue, phenotypic flexibility of avian muscle may be limited by self-renewal capacities of SCs (Jimenez and Lencyk 2021). If avian SCs are capable of self-renewal and act as stem cells, as they apparently do in mammals (Forcina et al., 2019), especially during exercise or exercise-induced injury, then activating new satellite cells into the muscle fiber under conditions promoting hypertrophy might not be a limiting factor for birds. Additionally, Pax7 (a marker for adult SCs) expression in aging chickens was not different from that in young chickens, highlighting that Pax7 protein expression does not decrease with age in birds as it does in mammals (Jankowski et al., 2020). This is consistent with proliferative capacities of SCs being maintained across the lifespan of birds (Brown et al., 2019).

Jimenez and De Jesus (2021a) found that fast-growing quail subjected to an acute temperature increase had lower numbers of nuclei per mm of fiber than control quail. In opposition, in house sparrow pectoralis muscle, higher numbers of nuclei per mm of fiber occurred in the control (winter phenotype) group compared with the heat-shocked and recovery group (De Jesus and Jimenez 2021). Both fast-growing quail and winter phenotype sparrows likely grow adult muscle fibers via hypertrophy. Thus, the control group of sparrows should have higher numbers of nuclei, compared with the heat-shocked and recovery group, as their winter phenotype pectoralis muscle should have undergone hypertrophic accretion, similar to fast-growing quail, suggesting a similar physiological mechanism of control. Additionally, tropical bird species (exposed to a thermally stable warm climate) had more nuclei per mm of muscle fiber compared with their temperate counterparts, but no differences in MND (Jimenez and De Jesus 2021b).

Changing environmental temperatures can affect chick muscle development (Modrey and Nichelmann, 1992), which is mediated by SCs. The neonatal period in chick muscle growth is when SCs are most active (Halevy et al., 2000). SC proliferation increases with temperature during late embryogenesis or early life in chicks (Halevy et al., 2000; Loyau et al., 2013; Piestun et al., 2017), yielding increases in muscle mass. SCs isolated from turkeys and exposed to differing environmental temperatures also demonstrated increased proliferation rates with increased temperatures, but decreased proliferation and differentiation rates at ambient temperatures lower than control values of 38°C (Clark et al., 2016). Furthermore, just 24 h of transitory heat stress in a chick's first week of life promoted increased SC proliferation and differentiation (Halevy et al., 2000). Mild heat stress, even at 3 weeks of age, may also increase SC proliferation into existing myotubes, at least in birds with slower growth rates (Jimenez and De Jesus 2021a). The reason SC profiferation may not be the same in faster-growing birds could result from either the availability of SCs, the environment in which SCs occur (Murach et al., 2018; Forcina et al., 2019), or dramatic increases in muscle fiber size without proportional addition of myonuclei (Velleman et al., 2003).

SC activities including proliferation and differentiation are highly responsive to environmental temperatures, especially early in life (Halevy et al., 2006; Xu et al., 2022), suggesting that muscle fiber diameter and temperature are related (Clark et al., 2016; Xu et al., 2021). Cultured adult turkey pectoralis major muscle SCs demonstrated heightened proliferation and differentiation when temperature was increased from 33 to 43°C. Thus, temperature increases seem to be a signal for avian SCs to increase activity, proliferation and *MyoD* expression (Clark et al., 2016; Xu et al., 2021). However, this may happen over a series of days and it is most pronounced within the first week of life. In contrast, 24 h of heat shock in adult house sparrows reduced the number of nuclei per millimeter of fiber and increased MND, both of which were not corrected by 24 h of recovery (De Jesus and Jimenez 2021). This implies that the timing of thermal challenges may be important with respect to the response of SCs within the avian pectoralis muscle. Secondly, the SCs could have been partially activated by the heat, but instead lacked the proper environment and vasculature needed for full activation, termed the muscle stem cell niche (Velleman, 2015). Additionally, thermal stress can change SC proliferation and differentiation through the mTOR/S6K pathway with faster-growing birds showing greater SC activity compared to those with slower growth rates (Xu et al., 2022).

Myonuclear domain and muscle remodeling in birds with respect to flight exercise

Besides thermally induced remodeling in avian muscle, the number of nuclei per fiber is positively associated with flight velocity in black-legged kittiwakes, likely because higher power output needed by faster-flying birds required plasticity for muscle fiber recruitment (Lalla et al., 2020). The number of nuclei per muscle fiber increases with muscle training, even preceding hypertrophic muscle growth (Bruusgaard et al., 2010), supporting our hypothesis that a higher number of nuclei per fiber is associated with faster flight speeds. It should be noted, however, that the hypothesis that muscle has "memory" after training such that nuclei are maintained after detraining has been challenged (Dungan et al., 2019; Murach et al., 2020). Research in this area of study is severely lacking and would be extremely informative.

Potential mechanisms driving MND flexibility in birds

Flexibility around MND, including hypertrophic growth (Murach et al., 2018), appears to be the mechanism employed by avian muscle in response to decreases in temperature and to migration (Jimenez 2020). Such hypertrophic and MND responses appear to be dominated by the number of nuclei within a fiber. Acquiring new nuclei may benefit muscle function more than upregulating the output of existing nuclei when MND is increased (Cramer et al., 2020). Thus, mechanisms of avian muscle flexibility, including increases in muscle mass and muscle fiber diameter, may involve mammalian-like processes (Jimenez 2020). For example, it is generally assumed that SC-dependent myonuclear accretion, which is required for adult skeletal muscle hypertrophy, is the first step for increasing muscle fiber diameter, though hypertrophy may occur without SC addition (Murach et al., 2018). SC fusion within a myotube increases DNA content, but how this relates to muscle fiber protein output is unclear (Kirby et al., 2016). When DNA content is held constant, however, myonuclei upregulate transcriptional activity (Kirby et al., 2016). It is generally assumed that fiber diameter regulation is related to protein turnover potential in muscle fibers, such that fiber diameter is positively correlated with protein turnover rates (Kirby et al., 2016; Figueiredo 2019). Muscle hypertrophy in response to exercise results from repeated short-term increases in protein synthesis (likely of myofibril proteins) following each bout of exercise (Figueiredo 2019). These increases in RNA content during hypertrophy are likely due to increases in transcriptional activity (Kirby et al., 2016). That birds increase muscle fiber diameter not only for migratory flights or in response to decreases in temperature, but prior to winter or migration may suggest that muscle growth may be dictated by differing mechanisms in birds than in mammals (Driedzic et al., 1993). Hypertrophic adaptation by mechanical stimuli (exercise) may fundamentally differ from non-mechanically mediated hypertrophy (growth) (Murach et al., 2018). It would be of great interest to develop a framework to tease apart

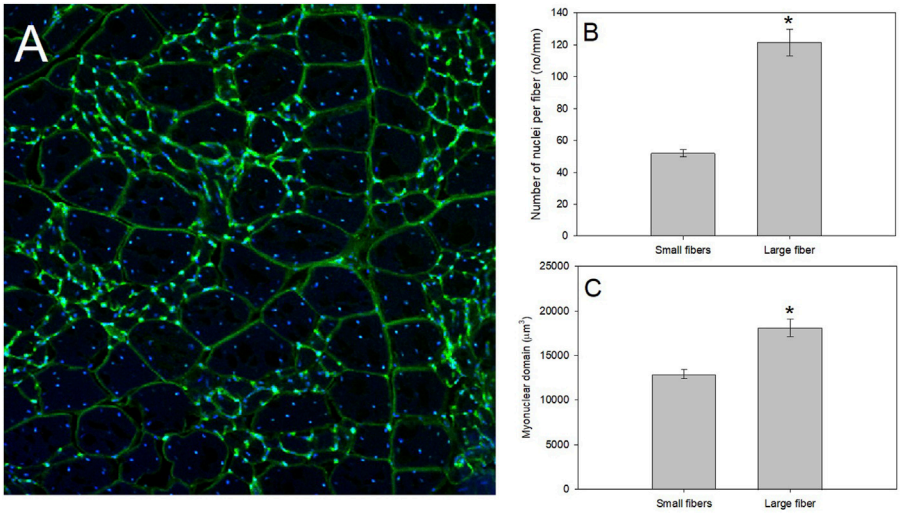

FIGURE 3
A productive model system to study regulation of muscle fiber size as whole-animal energetics change for birds is that of the pectoralis of mourning doves. **(A)** After fixing the pectoralis muscle in 4% paraformaldehyde, we placed fixed muscle tissue in 25% sucrose for 24 h to cryo-protect the samples. Tissues were then flash frozen in isopentane cooled in liquid nitrogen, mounted at resting length in Optimal Cutting Temperature (O.C.T.) compound and allowed to equilibrate to −19°C in a Leica 1800 cryocut microtome before sectioning. Sections were cut at 30 μm, picked up on slides, air-dried at room temperature, stained with a 250 μg/ml solution of wheat germ agglutinin (WGA) labeled with Alexa Fluor 488 (in green), and 4′,6-diamidino-2-phenylindole (DAPI; in blue), for 30 min, and rinsed in avian ringer's for 60 min. WGA is a lectin that binds to glycoproteins on the basement membrane of the fiber sarcolemma, and effectively outlines the fiber periphery to allow measurements of fiber size, whereas DAPI irreversibly binds to nuclei. Stained slides were examined with an Olympus Fluoview 1000 laser filter confocal microscope, and pictures were taken at a magnification of ×20. Mourning dove pectoralis muscle contain a population of small muscle fibers with a myonuclear domain (MND) surrounded by a population of large muscle fibers. **(B,C)** Using data from Jimenez and De Jesus (2021b), we isolated the number of nuclei per fiber and MND of $N = 4$ mourning doves ($N = 135$ small fibers and $N = 63$ large fibers). Using a one-way ANOVA, the small fibers demonstrated a significantly fewer nuclei per mm of fiber ($F = 108.83$, $p < 0.0001$; Panel **(B)**, and a significantly smaller MND ($F = 27.48$, $p < 0.001$; Panel **(C)**.

mechanistic differences between these two modes of hypertrophic muscle growth in birds.

Regarding the relationship between SCs and muscle remodeling pathways, studies addressing the relationship between myostatin and SCs proliferation in mammals provide mixed results. For example, some studies suggest that muscle hypertrophy driven by decreases in myostatin does not result in more nuclei per fiber and SC proliferation rates do not change in the absence of myostatin (Amthor et al., 2009). Others have found that myostatin inhibits SC proliferation and self-renewal (McCroskery et al., 2003). In contrast, increases in IGF-1 seem to increase the activation of SCs (Machida and Booth, 2004). How these two pathways affect SC activation and proliferation in adult wild birds warrants future study (Duclos et al., 1999; Halevy et al., 2001).

Conclusion and future directions

In summary, avian muscle remodeling is a common component of flexible responses to changes in energy demand, such as cold temperatures or migratory flights. Studies focusing on the signaling pathways regulating avian muscle remodeling, however, are still limited, inconclusive and biased towards myostatin. Strategies and the underlying signaling pathways employed by birds might be species- or context-specific (Zhang et al., 2018a). In order to cope with such complexity, we first encourage researchers to employ an integrative approach to study these signaling pathways and phenotypes they produce at a variety of biological levels (Zhang and Wong, 2021). Moreover, using genetic manipulation of primary avian muscle cells (Young et al., 2021a; Young et al., 2021b), or pharmaceutical activators/inhibitors (such as follistatin for myostatin) might provide alternative and/or more comprehensive answers. Secondly, intracellular signaling pathways controlling muscle mass, such as the Akt/TSC2/mTOR pathway (Saxton and Sabatini, 2017), have also received limited research attention relating to phenotypic flexibility in wild birds. Further study targeting genes in these pathways under conditions of increased energy demand in wild birds seems warranted. Moreover, studies to date on myostatin or IGF-1 and phenotypic flexibility in wild birds are correlative in nature, so functional roles for myostatin and IGF-1 in flexible responses of muscle to changes in energy demand have yet to be demonstrated. Future studies experimentally manipulating myostatin or IGF-1 levels in wild birds followed by

examination of changes in SCs, MND, mitochondria, muscle fiber diameter, muscle mass and organismal metabolic capacities would be useful in validating roles for myostatin and IGF-1 pathways in regulating muscular and metabolic flexibility in wild birds. Thirdly, besides regulating protein synthesis, skeletal muscle mass can also be regulated through transduction pathways that control protein degradation. Situations altering the synthesis/degradation balance of myofibrillar proteins may thus contribute to muscle hypertrophy or atrophy. Unfortunately, pathways associated with protein degradation in muscles, such as ubiquitin proteasome system and FOXO-mediated signals have not been investigated in the context of avian phenotypic flexibility.

MND-related questions in the avian study model are still in a primitive state, with only a few studies addressing this concept. Regulation of MND in birds appears to be dominated by some of the same mechanisms as mammals, however, its ability to adjust to thermal or workload changes may be faster, potentially due to avian SCs ability to proliferate quickly (Young et al., 2021a). Future studies in this field would benefit from addressing communication of these exogenous cues across the myotube. Myonuclei in the syncytium may organize by dividing transcriptional labor to achieve specific functions (Wen et al., 2021), but how these functions are shared across the myotube is unclear. Thus, experiments surrounding the activation of myonuclei with differing stressors (cell-wide vs. sarcolemmal, for example), would be valuable in deciphering protein expression patterns within the myotube. An interesting avian study model to address this question is mourning dove (*Zenaida macroura*), which demonstrated a pectoralis muscle fiber population including very small and very large muscle fibers (Figure 3). These size differences within one muscle tissue should allow studies of the functionality of a syncytium and how MND labor is dictated. Additionally, determining how regulation to either add nuclei or upregulate existing nuclear activity and under what ecological or environmental conditions such changes occur in birds would be another fruitful topic for study (Machida and Booth, 2004; Noakes and McKechnie, 2020; Attwaters and Hughes, 2021; Snijders et al., 2021).

Author contributions

DS developed the idea and wrote the first part of the manuscript. YZ wrote the molecular pathway part of the manuscript. AJ wrote the myonuclear domain part of the manuscript. All authors edited the manuscript together.

Funding

Much of the recent work of the laboratory of DS related to this topic was funded by National Science Foundation (NSF) IOS-1021218. All of the MND work in the laboratory of AJ was funded by NSF IBN 0212587 and Colgate University.

Conflict of interest

The authors declare that the research was conducted in the absence of any commercial or financial relationships that could be construed as a potential conflict of interest.

Publisher's note

References

Abreu, P., and Kowaltowski, A. J. (2020). Satellite cell self-renewal in endurance exercise is mediated by inhibition of mitochondrial oxygen consumption. *J. Cachexia, Sarcopenia Muscle* 11 (6), 1661–1676. doi:10.1002/jcsm.12601

Allen, D. L., and Unterman, T. G. (2007). Regulation of myostatin expression and myoblast differentiation by FoxO and SMAD transcription factors. *Am. J. Physiology-Cell Physiology* 292 (1), C188–C199. doi:10.1152/ajpcell.00542.2005

Amirouche, A., Durieux, A.-C., Banzet, S., Koulmann, N., Bonnefoy, R., Mouret, C., et al. (2009). Down-regulation of Akt/mammalian target of rapamycin signaling pathway in response to myostatin overexpression in skeletal muscle. *Endocrinology* 150, 286–294. doi:10.1210/en.2008-0959

Amthor, H., Otto, A., Vulin, A., Rochat, A., Dumonceaux, J., Garcia, L., et al. (2009). Muscle hypertrophy driven by myostatin blockade does not require stem/precursor-cell activity. *Proc. Natl. Acad. Sci. U.S.A.* 106 (18), 7479–7484. doi:10.1073/pnas.0811129106

Ato, S., and Ogasawara, R. (2021). The relationship between myonuclear number and protein synthesis in individual rat skeletal muscle fibres. *J. Exp. Biol.* 224 (10), jeb242496. doi:10.1242/jeb.242496

Attwaters, M., and Hughes, S. M. (2021). Cellular and molecular pathways controlling muscle size in response to exercise. *FEBS J.* 289, 1428–1456. doi:10.1111/febs.15820

Azevedo, M., and Baylies, M. K. (2020). Getting into position: Nuclear movement in muscle cells. *Trends Cell Biol.* 30 (4), 303–316. doi:10.1016/j.tcb.2020.01.002

Bai, M., Wu, X., Cai, K., Zheng, W., and Liu, J. (2016). Relationships between interspecific differences in the mass of internal organs, biochemical markers of metabolic activity, and the thermogenic properties of three small passerines. *Avian Res.* 7 (1), 11. doi:10.1186/s40657-016-0046-1

Barceló, G., Love, O. P., and Vézina, F. (2017). Uncoupling basal and summit metabolic rates in white-throated sparrows: Digestive demand drives maintenance costs, but changes in muscle mass are not needed to improve thermogenic capacity. *Physiological Biochem. Zoology* 90 (2), 153–165. doi:10.1086/689290

Bennett, M. B. (1996). Allometry of the leg muscles of birds. *J. Zoology* 238, 435–443. doi:10.1111/j.1469-7998.1996.tb05404.x

Brack, A. S., Bildsoe, H., and Hughes, S. M. (2005). Evidence that satellite cell decrement contributes to preferential decline in nuclear number from large fibres

during murine age-related muscle atrophy. *J. Cell Sci.* 118 (20), 4813–4821. doi:10.1242/jcs.02602

Brown, K., Jimenez, A. G., Whelan, S., Lalla, K., Hatch, S. A., Elliott, K. H., et al. (2019). Muscle fiber structure in an aging long-lived seabird, the black-legged kittiwake (Rissa tridactyla). *J. Morphol.* 280 (7), 1061–1070. doi:10.1002/jmor.21001

Bruusgaard, J. C., Johansen, I. B., Egner, I. M., Rana, Z. A., and Gundersen, K. (2010). Myonuclei acquired by overload exercise precede hypertrophy and are not lost on detraining. *Proc. Natl. Acad. Sci. U.S.A.* 107 (34), 15111–15116. doi:10.1073/pnas.0913935107

Chappell, M. A., Bech, C., and Buttemer, W. A. (1999). The relationship of central and peripheral organ masses to aerobic performance variation in house sparrows. *J. Exp. Biol.* 202 (17), 2269–2279. doi:10.1242/jeb.202.17.2269

Chen, P. R., and Lee, K. (2016). Invited review: Inhibitors of myostatin as methods of enhancing muscle growth and development1. *J. Anim. Sci.* 94 (8), 3125–3134. doi:10.2527/jas.2016-0532

Chen, R., Zhuang, S., Chen, Y. P., Cheng, Y. F., Wen, C., Zhou, Y. M., et al. (2018). Betaine improves the growth performance and muscle growth of partridge shank broiler chickens via altering myogenic gene expression and insulin-like growth factor-1 signaling pathway. *Poult. Sci.* 97 (12), 4297–4305. doi:10.3382/ps/pey303

Cheviron, Z. A., and Swanson, D. L. (2017). Comparative transcriptomics of seasonal phenotypic flexibility in two North American songbirds. *Integr. Comp. Biol.* 57 (5), 1040–1054. doi:10.1093/icb/icx118

Clark, D. L., Coy, C. S., Strasburg, G. M., Reed, K. M., and Velleman, S. G. (2016). Temperature effect on proliferation and differentiation of satellite cells from turkeys with different growth rates. *Poult. Sci.* 95 (4), 934–947. doi:10.3382/ps/pev437

Clop, A., Marcq, F., Takeda, H., Pirottin, D., Tordoir, X., Bibé, B., et al. (2006). A mutation creating a potential illegitimate microRNA target site in the myostatin gene affects muscularity in sheep. *Nat. Genet.* 38 (7), 813–818. doi:10.1038/ng1810

Cooper, S. J. (2002). Seasonal metabolic acclimatization in mountain chickadees and juniper titmice. *Physiol. Biochem. Zool.* 75 (4), 386–395. doi:10.1086/342256

Cooper, S. J., and Swanson, D. L. (1994). Seasonal acclimatization of thermoregulation in the black-capped chickadee. *Condor* 96 (3), 638–646. doi:10.2307/1369467

Corder, K. R., and Schaeffer, P. J. (2015). Summit metabolic rate exhibits phenotypic flexibility with migration, but not latitude in a neotropical migrant, Parkesia noveboracensis. *J. Ornithol.* 156 (2), 547–550. doi:10.1007/s10336-015-1157-x

Cramer, A. A., Prasad, V., Eftestøl, E., Song, T., Hansson, K. A., Dugdale, H. F., et al. (2020). Nuclear numbers in syncytial muscle fibers promote size but limit the development of larger myonuclear domains. *Nat. Commun.* 11 (1), 6287. doi:10.1038/s41467-020-20058-7

Dawson, W. R., Marsh, R. L., and Yacoe, M. E. (1983). Metabolic adjustments of small passerine birds for migration and cold. *Am. J. Physiology-Regulatory, Integr. Comp. Physiology* 245 (6), R755–R767. doi:10.1152/ajpregu.1983.245.6.R755

De Jesus, A. D., and Jimenez, A. G. (2021). Effects of acute temperature increases on House sparrow (*Passer domesticus*) pectoralis muscle myonuclear domain. *J. Exp. Zool. Pt A* 337, 150–158. doi:10.1002/jez.2544

Dégletagne, C., Roussel, D., Rouanet, J. L., Baudimont, F., Moureaux, E. M., Harvey, S., et al. (2013). Growth prior to thermogenesis for a quick fledging of adélie penguin chicks (pygoscelis adeliae). *PLoS One* 8 (9), e74154. doi:10.1371/journal.pone.0074154

DeMoranville, K. J., Carter, W. A., Pierce, B. J., and McWilliams, S. R. (2020). Flight training in a migratory bird drives metabolic gene expression in the flight muscle but not liver, and dietary fat quality influences select genes. *Am. J. Physiology-Regulatory, Integr. Comp. Physiology* 319 (6), R637–R652. doi:10.1152/ajpregu.00163.2020

DeMoranville, K. J., Corder, K. R., Hamilton, A., Russell, D. E., Huss, J. M., Schaeffer, P. J., et al. (2019). PPAR expression, muscle size, and metabolic rates across the Gray catbird's annual cycle are greatest in preparation for fall migration. *J. Exp. Biol.* 222 (14), jeb198028. doi:10.1242/jeb.198028

Deng, H., Zheng, A., Liu, G., Chang, W., Zhang, S., Cai, H., et al. (2014). Activation of mammalian target of rapamycin signaling in skeletal muscle of neonatal chicks: Effects of dietary leucine and age. *Poult. Sci.* 93 (1), 114–121. doi:10.3382/ps.2013-03287

Dietz, M. W., Piersma, T., and Dekinga, A. (1999). Body-building without power training: Endogenously regulated pectoral muscle hypertrophy in confined shorebirds. *J. Exp. Biol.* 202 (20), 2831–2837. doi:10.1242/jeb.202.20.2831

Driedzic, W. R., Crowe, H. L., Hicklin, P. W., and Sephton, D. H. (1993). Adaptations in pectoralis muscle, heart mass, and energy metabolism during premigratory fattening in semipalmated sandpipers (Calidris pusilla). *Can. J. Zool.* 71 (8), 1602–1608. doi:10.1139/z93-226

DuBay, S. G., Wu, Y., Scott, G. R., Qu, Y., Liu, Q., Smith, J. H., et al. (2020). Life history predicts flight muscle phenotype and function in birds. *J. Anim. Ecol.* 89 (5), 1262–1276. doi:10.1111/1365-2656.13190

Duclos, M. J., Beccavin, C., and Simon, J. (1999). Genetic models for the study of insulin-like growth factors (IGF) and muscle development in birds compared to mammals. *Domest. Anim. Endocrinol.* 17 (2-3), 231–243. doi:10.1016/s0739-7240(99)00040-5

Dungan, C. M., Murach, K. A., Frick, K. K., Jones, S. R., Crow, S. E., Englund, D. A., et al. (2019). Elevated myonuclear density during skeletal muscle hypertrophy in response to training is reversed during detraining. *Am. J. Physiology-Cell Physiology* 316 (5), C649–C654. doi:10.1152/ajpcell.00050.2019

Favier, F. B., Benoit, H., and Freyssenet, D. (2008). Cellular and molecular events controlling skeletal muscle mass in response to altered use. *Pflugers Arch. - Eur. J. Physiol.* 456 (3), 587–600. doi:10.1007/s00424-007-0423-z

Figueiredo, V. C. (2019). Revisiting the roles of protein synthesis during skeletal muscle hypertrophy induced by exercise. *Am. J. Physiology-Regulatory, Integr. Comp. Physiology* 317 (5), R709–R718. doi:10.1152/ajpregu.00162.2019

Forcina, L., Miano, C., Pelosi, L., and Musarò, A. (2019). An overview about the biology of skeletal muscle satellite cells. *Curr. Genomics* 20 (1), 24–37. doi:10.2174/1389202920666190116094736

Graca, F. A., Sheffield, N., Puppa, M., Finkelstein, D., Hunt, L. C., Demontis, F., et al. (2021). A large-scale transgenic RNAi screen identifies transcription factors that modulate myofiber size in Drosophila. *PLoS Genet.* 17 (11), e1009926. doi:10.1371/journal.pgen.1009926

Guo, T., Jou, W., Chanturiya, T., Portas, J., Gavrilova, O., McPherron, A. C., et al. (2009). Myostatin inhibition in muscle, but not adipose tissue, decreases fat mass and improves insulin sensitivity. *PloS one* 4 (3), e4937. doi:10.1371/journal.pone.0004937

Halevy, O., Geyra, A., Barak, M., Uni, Z., and Sklan, D. (2000). Early posthatch starvation decreases satellite cell proliferation and skeletal muscle growth in chicks. *J. Nutr.* 130 (4), 858–864. doi:10.1093/jn/130.4.858

Halevy, O., Krispin, A., Leshem, Y., McMurtry, J. P., and Yahav, S. (2001). Early-age heat exposure affects skeletal muscle satellite cell proliferation and differentiation in chicks. *Am. J. Physiology-Regulatory, Integr. Comp. Physiology* 281 (1), R302–R309. doi:10.1152/ajpregu.2001.281.1.R302

Halevy, O., Yahav, S., and Rozenboim, I. (2006). Enhancement of meat production by environmental manipulations in embryo and young broilers. *World's. Poult. Sci. J.* 62 (3), 485–497. doi:10.1017/s0043933906001103

Hansson, K. A., Eftestøl, E., Bruusgaard, J. C., Juvkam, I., Cramer, A. W., Malthe-Sørenssen, A., et al. (2020). Myonuclear content regulates cell size with similar scaling properties in mice and humans. *Nat. Commun.* 11 (1), 6288. doi:10.1038/s41467-020-20057-8

Hartman, F. A. (1961). Maurice blanchot: Philosopher-novelist. *Smithson. Misc. Coll.* 15, 1–91. doi:10.2307/25293657

Hennebry, A., Oldham, J., Shavlakadze, T., Grounds, M. D., Sheard, P., Fiorotto, M. L., et al. (2017). IGF1 stimulates greater muscle hypertrophy in the absence of myostatin in male mice. *J. Endocrinol.* 234 (2), 187–200. doi:10.1530/JOE-17-0032

Hill, J. J., Davies, M. V., Pearson, A. A., Wang, J. H., Hewick, R. M., Wolfman, N. M., et al. (2002). The myostatin propeptide and the follistatin-related gene are inhibitory binding proteins of myostatin in normal serum. *J. Biol. Chem.* 277 (43), 40735–40741. doi:10.1074/jbc.M206379200

Hohtola, E. S. A. (1982). Thermal and electromyographic correlates of shivering thermogenesis in the pigeon. *Comp. Biochem. Physiology Part A Physiology* 73 (2), 159–166. doi:10.1016/0300-9629(82)90049-4

Horton, K. G., Van Doren, B. M., Stepanian, P. M., Farnsworth, A., and Kelly, J. F. (2016). Seasonal differences in landbird migration strategies. *Auk* 133 (4), 761–769. doi:10.1642/auk-16-105.1

Hu, S. N., Zhu, Y. Y., Lin, L., Zheng, W. H., and Liu, J. S. (2017). Temperature and photoperiod as environmental cues affect body mass and thermoregulation in Chinese bulbuls Pycnonotus sinensis. *J. Exp. Biol.* 220 (5), 844–855. doi:10.1242/jeb.143842

Hughes, S. M., and Schiaffino, S. (1999). Control of muscle fibre size: A crucial factor in ageing. *Acta Physiol. Scand.* 167 (4), 307–312. doi:10.1046/j.1365-201x.1999.00622.x

Jankowski, M., Mozdziak, P., Petitte, J., Kulus, M., and Kempisty, B. (2020). Avian satellite cell plasticity. *Animals.* 10 (8), 1322. doi:10.3390/ani10081322

Jimenez, A. G., and De Jesus, A. D. (2021b). Comparison of myonuclear domain in phylogenetically paired tropical and temperate bird species. *J. Avian Biol.* 52 (11), 2880. doi:10.1111/jav.02880

Jimenez, A. G., and De Jesus, A. D. (2021a). Do thermal acclimation and an acute heat challenge alter myonuclear domain of control- and fast-growing quail? *J. Therm. Biol.* 100, 103050. doi:10.1016/j.jtherbio.2021.103050

Jimenez, A. G., and Lencyk, E. G. (2022). Lack of variation in nuclear DNA content in avian muscle. *Genome* 65 (999), 219–227. doi:10.1139/gen-2021-0052

Jimenez, A. G., O'Connor, E. S., Brown, K. J., and Briggs, C. W. (2019). Seasonal muscle ultrastructure plasticity and resistance of muscle structural changes during temperature increases in resident black-capped chickadees (Poecile atricapillus) and rock pigeons (*Columba livia*). *J. Exp. Biol.* 222 (12), jeb201855. doi:10.1242/jeb.201855

Jimenez, A. G. (2020). Structural plasticity of the avian pectoralis: A case for geometry and the forgotten organelle. *J. Exp. Biol.* 223 (23), jeb234120. doi:10.1242/jeb.234120

Kim, D. H., Choi, Y. M., Suh, Y., Shin, S., Lee, J., Hwang, S., et al. (2020). Research Note: Association of temporal expression of myostatin with hypertrophic muscle growth in different Japanese quail lines. *Poult. Sci.* 99 (6), 2926–2930. doi:10.1016/j.psj.2019.12.069

King, M. O., Zhang, Y., Carter, T., Johnson, J., Harmon, E., Swanson, D. L., et al. (2015). Phenotypic flexibility of skeletal muscle and heart masses and expression of myostatin and tolloid-like proteinases in migrating passerine birds. *J. Comp. Physiol. B* 185 (3), 333–342. doi:10.1007/s00360-015-0887-7

Kinsey, S. T., Hardy, K. M., and Locke, B. R. (2007). The long and winding road: Influences of intracellular metabolite diffusion on cellular organization and metabolism in skeletal muscle. *J. Exp. Biol.* 210 (20), 3505–3512. doi:10.1242/jeb.000331

Kirby, T. J., Patel, R. M., McClintock, T. S., Dupont-Versteegden, E. E., Peterson, C. A., McCarthy, J. J., et al. (2016). Myonuclear transcription is responsive to mechanical load and DNA content but uncoupled from cell size during hypertrophy. *Mol. Biol. Cell* 27 (5), 788–798. doi:10.1091/mbc.E15-08-0585

Kuang, S., Kuroda, K., Le Grand, F., and Rudnicki, M. A. (2007). Asymmetric self-renewal and commitment of satellite stem cells in muscle. *Cell* 129 (5), 999–1010. doi:10.1016/j.cell.2007.03.044

Lalla, K. M., Whelan, S., Brown, K., Patterson, A., Jimenez, A. G., Hatch, S. A., et al. (2020). Accelerometry predicts muscle ultrastructure and flight capabilities in a wild bird. *J. Exp. Biol.* 223 (22), jeb234104. doi:10.1242/jeb.234104

Landys-Ciannelli, M. M., Piersma, T., and Jukema, P. (2003). Strategic size changes of internal organs and muscle tissue in the bar-tailed godwit during fat storage on a spring stopover site. *Funct. Ecol.* 17, 151–159. doi:10.1046/j.1365-2435.2003.00715.x

Latimer, C. E., Cooper, S. J., Karasov, W. H., and Zuckerberg, B. (2018). Does habitat fragmentation promote climate-resilient phenotypes? *Oikos* 127 (8), 1069–1080. doi:10.1111/oik.05111

Le Pogam, A., Love, O. P., Régimbald, L., Dubois, K., Hallot, F., Milbergue, M., et al. (2020). Wintering snow buntings elevate cold hardiness to extreme levels but show no changes in maintenance costs. *Physiological Biochem. Zoology* 93 (6), 417–433. doi:10.1086/711370

Le Pogam, A., O'Connor, R. S., Love, O. P., Drolet, J., Régimbald, L., Roy, G., et al. (2021). Snow buntings maintain winter-level cold endurance while migrating to the high arctic. *Front. Ecol. Evol.* 9, 642. doi:10.3389/fevo.2021.724876

Lee, S. J. (2008). Genetic analysis of the role of proteolysis in the activation of latent myostatin. *PloS one* 3 (2), e1628. doi:10.1371/journal.pone.0001628

Lee, S. J., and McPherron, A. C. (2001). Regulation of myostatin activity and muscle growth. *Proc. Natl. Acad. Sci. U.S.A.* 98 (16), 9306–9311. doi:10.1073/pnas.151270098

Lee, S. J., Reed, L. A., Davies, M. V., Girgenrath, S., Goad, M. E., Tomkinson, K. N., et al. (2005). Regulation of muscle growth by multiple ligands signaling through activin type II receptors. *Proc. Natl. Acad. Sci. U.S.A.* 102 (50), 18117–18122. doi:10.1073/pnas.0505996102

Lee, S. J. (2004). Regulation of muscle mass by myostatin. *Annu. Rev. Cell Dev. Biol.* 20, 61–86. doi:10.1146/annurev.cellbio.20.012103.135836

Li, L., Ge, J., Zheng, S., Hong, L., Zhang, X., Li, M., et al. (2020). Thermogenic responses in Eurasian Tree Sparrow (*Passer montanus*) to seasonal acclimatization and temperature-photoperiod acclimation. *Avian Res.* 11 (1), 35. doi:10.1186/s40657-020-00222-9

Liknes, E. T., and Swanson, D. L. (2011). Phenotypic flexibility of body composition associated with seasonal acclimatization in passerine birds. *J. Therm. Biol.* 36 (6), 363–370. doi:10.1016/j.jtherbio.2011.06.010

Lin, J., Arnold, H. B., Della-Fera, M. A., Azain, M. J., Hartzell, D. L., Baile, C. A., et al. (2002). Myostatin knockout in mice increases myogenesis and decreases adipogenesis. *Biochem. Biophysical Res. Commun.* 291 (3), 701–706. doi:10.1006/bbrc.2002.6500

Liu, J. X., Höglund, A. S., Karlsson, P., Lindblad, J., Qaisar, R., Aare, S., et al. (2009). Myonuclear domain size and myosin isoform expression in muscle fibres from mammals representing a 100 000-fold difference in body size. *Exp. Physiol.* 94 (1), 117–129. doi:10.1113/expphysiol.2008.043877

Liu, H. H., Mao, H. G., Dong, X. Y., Cao, H. Y., Liu, K., Yin, Z. Z., et al. (2019). Expression of MSTN gene and its correlation with pectoralis muscle fiber traits in the domestic pigeons (*Columba livia*). *Poult. Sci.* 98 (11), 5265–5271. doi:10.3382/ps/pez399

Loyau, T., Berri, C., Bedrani, L., Métayer-Coustard, S., Praud, C., Duclos, M. J., et al. (2013). Thermal manipulation of the embryo modifies the physiology and body composition of broiler chickens reared in floor pens without affecting breast meat processing quality1. *J. Anim. Sci.* 91 (8), 3674–3685. doi:10.2527/jas.2013-6445

Lozier, N. R., Kopchick, J. J., and de Lacalle, S. (2018). Relative contributions of myostatin and the GH/IGF-1 Axis in body composition and muscle strength. *Front. Physiol.* 9, 1418. doi:10.3389/fphys.2018.01418

Ma, B., He, X., Lu, Z., Zhang, L., Li, J., Jiang, Y., et al. (2018). Chronic heat stress affects muscle hypertrophy, muscle protein synthesis and uptake of amino acid in broilers via insulin like growth factor-mammalian target of rapamycin signal pathway. *Poult. Sci.* 97, 4150–4158. doi:10.3382/ps/pey291

Machida, S., and Booth, F. W. (2004). Insulin-like growth factor 1 and muscle growth: Implication for satellite cell proliferation. *Proc. Nutr. Soc.* 63 (2), 337–340. doi:10.1079/PNS2004354

Marsh, R. L., and Dawson, W. R. (1989). "Avian adjustments to cold," in *Animal adaptation to cold* (Berlin, Heidelberg: Springer), 205–253. doi:10.1007/978-3-642-74078-7_6

Mauro, A. (1961). Satellite cell of skeletal muscle fibers. *J. Biophys. Biochem. Cytol.* 9 (2), 493–495. doi:10.1083/jcb.9.2.493

McCroskery, S., Thomas, M., Maxwell, L., Sharma, M., and Kambadur, R. (2003). Myostatin negatively regulates satellite cell activation and self-renewal. *J. Cell Biol.* 162 (6), 1135–1147. doi:10.1083/jcb.200207056

McFarland, D. C., Velleman, S. G., Pesall, J. E., and Liu, C. (2006). Effect of myostatin on Turkey myogenic satellite cells and embryonic myoblasts. *Comp. Biochem. Physiology Part A Mol. Integr. Physiology* 144 (4), 501–508. doi:10.1016/j.cbpa.2006.04.020

McFarland, D. C., Velleman, S. G., Pesall, J. E., and Liu, C. (2007). The role of myostatin in chicken (*Gallus domesticus*) myogenic satellite cell proliferation and differentiation. *General Comp. Endocrinol.* 151 (3), 351–357. doi:10.1016/j.ygcen.2007.02.006

McFarlane, C., Langley, B., Thomas, M., Hennebry, A., Plummer, E., Nicholas, G., et al. (2005). Proteolytic processing of myostatin is auto-regulated during myogenesis. *Dev. Biol.* 283 (1), 58–69. doi:10.1016/j.ydbio.2005.03.039

McFarlane, C., Plummer, E., Thomas, M., Hennebry, A., Ashby, M., Ling, N., et al. (2006). Myostatin induces cachexia by activating the ubiquitin proteolytic system through an NF-κB-independent, FoxO1-dependent mechanism. *J. Cell. Physiol.* 209 (2), 501–514. doi:10.1002/jcp.20757

McKechnie, A. E., Noakes, M. J., and Smit, B. (2015). Global patterns of seasonal acclimatization in avian resting metabolic rates. *J. Ornithol.* 156 (1), 367–376. doi:10.1007/s10336-015-1186-5

McPherron, A. C., Lawler, A. M., and Lee, S. J. (1997). Regulation of skeletal muscle mass in mice by a new TGF-p superfamily member. *Nature* 387 (6628), 83–90. doi:10.1038/387083a0

McPherron, A. C., and Lee, S. J. (1997). Double muscling in cattle due to mutations in the myostatin gene. *Proc. Natl. Acad. Sci. U.S.A.* 94 (23), 12457–12461. doi:10.1073/pnas.94.23.12457

McPherron, A. C., and Lee, S. J. (2002). Suppression of body fat accumulation in myostatin-deficient mice. *J. Clin. Invest.* 109 (5), 595–601. doi:10.1172/JCI1356210.1172/jci0213562

Milbergue, M. S., Blier, P. U., and Vézina, F. (2018). Large muscles are beneficial but not required for improving thermogenic capacity in small birds. *Sci. Rep.* 8 (1), 14009. doi:10.1038/s41598-018-32041-w

Modrey, P., and Nichelmann, M. (1992). Development of autonomic and behavioural thermoregulation in turkeys (*Meleagris gallopavo*). *J. Therm. Biol.* 17 (6), 287–292. doi:10.1016/0306-4565(92)90035-e

Morel-Journel, T., Thuillier, V., Pennekamp, F., Laurent, E., Legrand, D., Chaine, A. S., et al. (2020). A multidimensional approach to the expression of phenotypic plasticity. *Funct. Ecol.* 34 (11), 2338–2349. doi:10.1111/1365-2435.13667

Morissette, M. R., Cook, S. A., Buranasombati, C., Rosenberg, M. A., and Rosenzweig, A. (2009). Myostatin inhibits IGF-I-induced myotube hypertrophy through Akt. *Am. J. Physiology-Cell Physiology* 297 (5), 1124–1132. doi:10.1152/ajpcell.00043.2009

Murach, K. A., Englund, D. A., Dupont-Versteegden, E. E., McCarthy, J. J., and Peterson, C. A. (2018). Myonuclear domain flexibility challenges rigid assumptions on satellite cell contribution to skeletal muscle fiber hypertrophy. *Front. Physiol.* 9, 635. doi:10.3389/fphys.2018.00635

Murach, K. A., Mobley, C. B., Zdunek, C. J., Frick, K. K., Jones, S. R., McCarthy, J. J., et al. (2020). Muscle memory: Myonuclear accretion, maintenance, morphology, and miRNA levels with training and detraining in adult mice. *J. Cachexia, Sarcopenia Muscle* 11 (6), 1705–1722. doi:10.1002/jcsm.12617

Murach, K. A., Fry, C. S., Dupont-Versteegden, E. E., McCarthy, J. J., and Peterson, C. A. (2021). Fusion and beyond: Satellite cell contributions to loading-induced skeletal muscle adaptation. *FASEB J.* 35 (10), e21893. doi:10.1096/fj.202101096R

Nakashima, K., and Ishida, A. (2018). Regulation of autophagy in chick myotubes: Effects of insulin, insulin-like growth factor-I, and amino acids. *J. Poult. Sci.* 55, 257–262. doi:10.2141/jpsa.0170196

Nakashima, K., and Ishida, A. (2020). Regulation of autophagy in chick skeletal muscle: Effect of mTOR inhibition. *J. Poult. Sci.* 57, 77–83. doi:10.2141/jpsa.0190008

Nalbandian, M., Radak, Z., and Takeda, M. (2020). Lactate metabolism and satellite cell fate. *Front. Physiol.* 11, 610983. doi:10.3389/fphys.2020.610983

Nilsson, C., Klaassen, R. H., and Alerstam, T. (2013). Differences in speed and duration of bird migration between spring and autumn. *Am. Nat.* 181 (6), 837–845. doi:10.1086/670335

Nilsson, J. F., and Nilsson, J.-Å. (2016). Fluctuating selection on basal metabolic rate. *Ecol. Evol.* 6 (4), 1197–1202. doi:10.1002/ece3.1954

Noakes, M. J., and McKechnie, A. E. (2020). Phenotypic flexibility of metabolic rate and evaporative water loss does not vary across a climatic gradient in an Afrotropical passerine bird. *J. Exp. Biol.* 223 (7), jeb220137. doi:10.1242/jeb.220137

Noakes, M. J., Wolf, B. O., and McKechnie, A. E. (2017). Seasonal metabolic acclimatization varies in direction and magnitude among populations of an Afrotropical passerine bird. *Physiological Biochem. Zoology* 90 (2), 178–189. doi:10.1086/689030

Noakes, M. J., Karasov, W. H., and McKechnie, A. E. (2020). Seasonal variation in body composition in an afrotropical passerine bird: Increases in pectoral muscle mass are, unexpectedly, associated with lower thermogenic capacity. *J. Comp. Physiol. B* 190 (3), 371–380. doi:10.1007/s00360-020-01273-6

Norin, T., and Metcalfe, N. B. (2019). Ecological and evolutionary consequences of metabolic rate plasticity in response to environmental change. *Phil. Trans. R. Soc. B* 374 (1768), 20180180. doi:10.1098/rstb.2018.0180

O'Connor, T. P. (1995a). Metabolic characteristics and body composition in house finches: Effects of seasonal acclimatization. *J. Comp. Physiol. B* 165 (4), 298–305. doi:10.1007/bf00367313

O'Connor, T. P. (1995b). Seasonal acclimatization of lipid mobilization and catabolism in house finches (*Carpodacus mexicanus*). *Physiol. Zool.* 68 (6), 985–1005. doi:10.1086/physzool.68.6.30163790

Omairi, S., Matsakas, A., Degens, H., Kretz, O., Hansson, K. A., Solbrå, A. V., et al. (2016). Enhanced exercise and regenerative capacity in a mouse model that violates size constraints of oxidative muscle fibres. *Elife* 5, e16940. doi:10.7554/eLife.16940

Petit, M., Lewden, A., and Vézina, F. (2014). How does flexibility in body composition relate to seasonal changes in metabolic performance in a small passerine wintering at northern latitude? *Physiological Biochem. Zoology* 87 (4), 539–549. doi:10.1086/676669

Petit, M., Clavijo-Baquet, S., and Vézina, F. (2017). Increasing winter maximal metabolic rate improves intrawinter survival in small birds. *Physiological Biochem. Zoology* 90 (2), 166–177. doi:10.1086/689274

Petit, M., and Vézina, F. (2014a). Phenotype manipulations confirm the role of pectoral muscles and haematocrit in avian maximal thermogenic capacity. *J. Exp. Biol.* 217 (6), 824–830. doi:10.1242/jeb.095703

Petit, M., and Vézina, F. (2014b). Reaction norms in natural conditions: How does metabolic performance respond to weather variations in a small endotherm facing cold environments? *PLoS One* 9 (11), e113617. doi:10.1371/journal.pone.0113617

Piersma, T., and Drent, J. (2003). Phenotypic flexibility and the evolution of organismal design. *Trends Ecol. Evol.* 18 (5), 228–233. doi:10.1016/s0169-5347(03)00036-3

Piersma, T., Gudmundsson, G. A., and Lilliendahl, K. (1999). Rapid changes in the size of different functional organ and muscle groups during refueling in a long-distance migrating shorebird. *Physiological Biochem. Zoology* 72 (4), 405–415. doi:10.1086/316680

Piersma, T., and Van Gils, J. A. (2011). *The flexible phenotype: A body-centred integration of ecology, physiology, and behaviour*. Oxford University Press.

Piestun, Y., Patael, T., Yahav, S., Velleman, S. G., and Halevy, O. (2017). Early posthatch thermal stress affects breast muscle development and satellite cell growth and characteristics in broilers. *Poult. Sci.* 96 (8), 2877–2888. doi:10.3382/ps/pex065

Pigliucci, M. (2005). Evolution of phenotypic plasticity: Where are we going now? *Trends Ecol. Evol.* 20 (9), 481–486. doi:10.1016/j.tree.2005.06.001

Pirruccello-Straub, M., Jackson, J., Wawersik, S., Webster, M. T., Salta, L., Long, K., et al. (2018). Blocking extracellular activation of myostatin as a strategy for treating muscle wasting. *Sci. Rep.* 8 (1), 2292. doi:10.1038/s41598-018-20524-9

Pollock, H. S., Brawn, J. D., Agin, T. J., and Cheviron, Z. A. (2019). Differences between temperate and tropical birds in seasonal acclimatization of thermoregulatory traits. *J. Avian Biol.* 50 (4), jav.02067. doi:10.1111/jav.02067

Pradhan, D. S., Ma, C., Schlinger, B. A., Soma, K. K., and Ramenofsky, M. (2019). Preparing to migrate: Expression of androgen signaling molecules and insulin-like growth factor-1 in skeletal muscles of Gambel's white-crowned sparrows. *J. Comp. Physiol. A* 205 (1), 113–123. doi:10.1007/s00359-018-1308-7

Price, E. R., Bauchinger, U., Zajac, D. M., Cerasale, D. J., McFarlan, J. T., Gerson, A. R., et al. (2011). Migration- and exercise-induced changes to flight muscle size in migratory birds and association with IGF1 and myostatin mRNA expression. *J. Exp. Biol.* 214 (17), 2823–2831. doi:10.1242/jeb.057620

Qaisar, R., and Larsson, L. (2014). What determines myonuclear domain size? *Indian J. Physiol. Pharmacol.* 58 (1), 1–12.

Rebbapragada, A., Benchabane, H., Wrana, J. L., Celeste, A. J., and Attisano, L. (2003). Myostatin signals through a transforming growth factor β-like signaling pathway to block Adipogenesis. *Mol. Cell. Biol.* 23 (20), 7230–7242. doi:10.1128/mcb.23.20.7230-7242.2003

Roman, W., Pinheiro, H., Pimentel, M. R., Segalés, J., Oliveira, L. M., García-Domínguez, E., et al. (2021). Muscle repair after physiological damage relies on nuclear migration for cellular reconstruction. *Science* 374 (6565), 355–359. doi:10.1126/science.abe5620

Rommel, C., Bodine, S. C., Clarke, B. A., Rossman, R., Nunez, L., Stitt, T. N., et al. (2001). Mediation of IGF-1-induced skeletal myotube hypertrophy by PI(3)K/Akt/mTOR and PI(3)K/Akt/GSK3 pathways. *Nat. Cell Biol.* 3 (11), 1009–1013. doi:10.1038/ncb1101-1009

Rosser, B. W., Dean, M. S., and Bandman, E. (2003). Myonuclear domain size varies along the lengths of maturing skeletal muscle fibers. *Int. J. Dev. Biol.* 46 (5), 747–754.

Rowland, L. A., Bal, N. C., and Periasamy, M. (2015). The role of skeletal-muscle-based thermogenic mechanisms in vertebrate endothermy. *Biol. Rev.* 90 (4), 1279–1297. doi:10.1111/brv.12157

Saneyasu, T., Inui, M., Kimura, S., Yoshimoto, Y., Tsuchii, N., Shindo, H., et al. (2016). The IGF-1/Akt/S6 signaling pathway is age-dependently downregulated in the chicken breast muscle. *J. Poult. Sci.* 53, 213–219. doi:10.2141/jpsa.0150171

Saneyasu, T., Tsuchihashi, T., Kitashiro, A., Tsuchii, N., Kimura, S., Honda, K., et al. (2017). The IGF-1/Akt/S6 pathway and expressions of glycolytic myosin heavy chain isoforms are upregulated in chicken skeletal muscle during the first week after hatching. *Anim. Sci. J.* 88 (11), 1779–1787. doi:10.1111/asj.12847

Sartori, R., Romanello, V., and Sandri, M. (2021). Mechanisms of muscle atrophy and hypertrophy: Implications in health and disease. *Nat. Commun.* 12 (1), 330. doi:10.1038/s41467-020-20123-1

Saxton, R. A., and Sabatini, D. M. (2017). mTOR signaling in growth, metabolism, and disease. *Cell* 169 (6), 361–371. doi:10.1016/j.cell.2017.03.035

Schmaljohann, H., Lisovski, S., and Bairlein, F. (2017). Flexible reaction norms to environmental variables along the migration route and the significance of stopover duration for total speed of migration in a songbird migrant. *Front. Zool.* 14 (1), 17. doi:10.1186/s12983-017-0203-3

Scicchitano, B. M., Sica, G., and Musarò, A. (2016). Stem cells and tissue niche: Two faces of the same coin of muscle regeneration. *Eur. J. Transl. Myol.* 26 (4), 6125. doi:10.4081/ejtm.2016.6125

Sgueo, C., Wells, M. E., Russell, D. E., and Schaeffer, P. J. (2012). Acclimatization of seasonal energetics in northern cardinals (*Cardinalis cardinalis*) through plasticity of metabolic rates and ceilings. *J. Exp. Biol.* 215 (14), 2418–2424. doi:10.1242/jeb.061168

Sharma, M., McFarlane, C., Kambadur, R., Kukreti, H., Bonala, S., Srinivasan, S., et al. (2015). Myostatin: Expanding horizons. *IUBMB life* 67 (8), 589–600. doi:10.1002/iub.1392

Shavlakadze, T., Chai, J., Maley, K., Cozens, G., Grounds, G., Winn, N., et al. (2010). A growth stimulus is needed for IGF-1 to induce skeletal muscle hypertrophy *in vivo*. *J. Cell Sci.* 123 (6), 960–971. doi:10.1242/jcs.061119

Shimizu-Motohashi, Y., and Asakura, A. (2014). Angiogenesis as a novel therapeutic strategy for Duchenne muscular dystrophy through decreased ischemia and increased satellite cells. *Front. Physiol.* 5, 50. doi:10.3389/fphys.2014.00050

Shin, S., Song, Y., Ahn, J., Kim, E., Chen, P., Yang, S., et al. (2015). A novel mechanism of myostatin regulation by its alternative splicing variant during

myogenesis in avian species. *Am. J. Physiology-Cell Physiology* 309 (10), C650–C659. doi:10.1152/ajpcell.00187.2015

Smit, B., and McKechnie, A. E. (2010). Avian seasonal metabolic variation in a subtropical desert: Basal metabolic rates are lower in winter than in summer. *Funct. Ecol.* 24 (2), 330–339. doi:10.1111/j.1365-2435.2009.01646.x

Snijders, T., Holwerda, A. M., Loon, L. J., and Verdijk, L. B. (2021). Myonuclear content and domain size in small versus larger muscle fibres in response to 12 weeks of resistance exercise training in older adults. *Acta Physiol.* 231 (4), e13599. doi:10.1111/apha.13599

Snijders, T., Nederveen, J. P., McKay, B. R., Joanisse, S., Verdijk, L. B., and Van Loon, L. J. (2015). Satellite cells in human skeletal muscle plasticity. *Front. Physiol.* 6 (4), 283.

Sobolewska, A., Elminowska-Wenda, G., Bogucka, J., Szpinda, M., Walasik, K., Bednarczyk, M., et al. (2011). Myogenesis - possibilities of its stimulation in chickens. *folia Biol. (krakow)* 59 (3-4), 85–90. doi:10.3409/fb59_3-4.85-90

Sommer, R. J. (2020). Phenotypic plasticity: From theory and genetics to current and future challenges. *Genetics* 215 (1), 1–13. doi:10.1534/genetics.120.303163

Stager, M., and Cheviron, Z. A. (2020). Is there a role for sarcolipin in avian facultative thermogenesis in extreme cold? *Biol. Lett.* 16 (6), 20200078. doi:10.1098/rsbl.2020.0078

Stager, M., Swanson, D. L., and Cheviron, Z. A. (2015). Regulatory mechanisms of metabolic flexibility in the dark-eyed junco (Junco hyemalis). *J. Exp. Biol.* 218 (5), 767–777. doi:10.1242/jeb.113472

Stager, M., Pollock, H. S., Benham, P. M., Sly, N. D., Brawn, J. D., Cheviron, Z. A., et al. (2016). Disentangling environmental drivers of metabolic flexibility in birds: The importance of temperature extremes versus temperature variability. *Ecography* 39 (8), 787–795. doi:10.1111/ecog.01465

Stager, M., Senner, N. R., Tobalske, B. W., and Cheviron, Z. A. (2020). Body temperature maintenance acclimates in a winter-tenacious songbird. *J. Exp. Biol.* 223 (12), jeb221853. doi:10.1242/jeb.221853

Stager, M., Senner, N. R., Swanson, D. L., Carling, M. D., Eddy, D. K., Greives, T. J., et al. (2021). Temperature heterogeneity correlates with intraspecific variation in physiological flexibility in a small endotherm. *Nat. Commun.* 12 (1), 4401. doi:10.1038/s41467-021-24588-6

Swaddle, J. P., and Biewener, A. A. (2000). Exercise and reduced muscle mass in starlings. *Nature* 406 (6796), 585–586. doi:10.1038/35020695

Swanson, D. L. (1990). Seasonal variation in cold hardiness and peak rates of cold-induced thermogenesis in the dark-eyed junco (*Junco hyemalis*). *Auk* 107 (3), 561–566. doi:10.1093/auk/107.3.561

Swanson, D. L. (1991). Seasonal adjustments in metabolism and insulation in the dark-eyed junco. *Condor* 93 (3), 538–545. doi:10.2307/1368185

Swanson, D. L. (1995). Seasonal variation in thermogenic capacity of migratory warbling vireos. *Auk* 112 (4), 870–877. doi:10.2307/4089019

Swanson, D. L. (2001). Are summit metabolism and thermogenic endurance correlated in winter-acclimatized passerine birds? *J. Comp. Physiology B Biochem. Syst. Environ. Physiology* 171 (6), 475–481. doi:10.1007/s003600100197

Swanson, D. L. (2010). "Seasonal metabolic variation in birds: Functional and mechanistic correlates," in *Current ornithology volume 17* (New York, NY: Springer), 75–129. doi:10.1007/978-1-4419-6421-2_3

Swanson, D. L., and Dean, K. L. (1999). Migration-induced variation in thermogenic capacity in migratory passerines. *J. avian Biol.* 30, 245. doi:10.2307/3677350

Swanson, D. L., and Garland, Jr., T., Jr (2009). The evolution of high summit metabolism and cold tolerance in birds and its impact on present-day distributions. *Evolution* 63 (1), 184–194. doi:10.1111/j.1558-5646.2008.00522.x

Swanson, D. L., and Liknes, E. T. (2006). A comparative analysis of thermogenic capacity and cold tolerance in small birds. *J. Exp. Biol.* 209 (3), 466–474. doi:10.1242/jeb.02024

Swanson, D. L., and Merkord, C. (2013). Seasonal phenotypic flexibility of flight muscle size in small birds: A comparison of ultrasonography and tissue mass measurements. *J. Ornithol.* 154 (1), 119–127. doi:10.1007/s10336-012-0877-4

Swanson, D. L., and Olmstead, K. L. (1999). Evidence for a proximate influence of winter temperature on metabolism in passerine birds. *Physiol. Biochem. Zool.* 72 (5), 566–575. doi:10.1086/316696

Swanson, D. L., and Vézina, F. (2015). Environmental, ecological and mechanistic drivers of avian seasonal metabolic flexibility in response to cold winters. *J. Ornithol.* 156 (1), 377–388. doi:10.1007/s10336-015-1192-7

Swanson, D. L., Sabirzhanov, B., VandeZande, A., and Clark, T. G. (2009). Seasonal variation of myostatin gene expression in pectoralis muscle of house sparrows (*Passer domesticus*) is consistent with a role in regulating thermogenic capacity and cold tolerance. *Physiological Biochem. Zoology* 82 (2), 121–128. doi:10.1086/591099

Swanson, D. L., Zhang, Y., and King, M. O. (2013). Individual variation in thermogenic capacity is correlated with flight muscle size but not cellular metabolic capacity in American goldfinches (Spinus tristis). *Physiological Biochem. Zoology* 86 (4), 421–431. doi:10.1086/671447

Swanson, D., Zhang, Y., Liu, J. S., Merkord, C. L., and King, M. O. (2014a). Relative roles of temperature and photoperiod as drivers of metabolic flexibility in dark-eyed juncos. *J. Exp. Biol.* 217 (6), 866–875. doi:10.1242/jeb.096677

Swanson, D. L., King, M. O., and Harmon, E. (2014b). Seasonal variation in pectoralis muscle and heart myostatin and tolloid-like proteinases in small birds: A regulatory role for seasonal phenotypic flexibility? *J. Comp. Physiol. B* 184 (2), 249–258. doi:10.1007/s00360-013-0798-4

Swanson, D. L., King, M. O., Culver, W., III, and Zhang, Y. (2017). Within-winter flexibility in muscle masses, myostatin, and cellular aerobic metabolic intensity in passerine birds. *Physiological Biochem. Zoology* 90 (2), 210–222. doi:10.1086/688956

Thomas, M., Langley, B., Berry, C., Sharma, M., Kirk, S., Bass, J., et al. (2000). Myostatin, a negative regulator of muscle growth, functions by inhibiting myoblast proliferation. *J. Biol. Chem.* 275 (51), 40235–40243. doi:10.1074/jbc.M004356200

Thompson, L. J., Brown, M., and Downs, C. T. (2015). Circannual rhythm of resting metabolic rate of a small Afrotropical bird. *J. Therm. Biol.* 51, 119–125. doi:10.1016/j.jtherbio.2015.04.003

Tomas, F. M., Pym, R. A., McMurtry, J. P., and Francis, G. L. (1998). Insulin-like growth factor (IGF)-I but not IGF-II promotes lean growth and feed efficiency in broiler chickens. *General Comp. Endocrinol.* 110 (3), 262–275. doi:10.1006/gcen.1998.7072

Trendelenburg, A. U., Meyer, A., Rohner, D., Boyle, J., Hatakeyama, S., Glass, D. J., et al. (2009). Myostatin reduces Akt/TORC1/p70S6K signaling, inhibiting myoblast differentiation and myotube size. *Am. J. Physiology-Cell Physiology* 296 (6), C1258–C1270. doi:10.1152/ajpcell.00105.2009

Tseng, B. S., Kasper, C. E., and Edgerton, V. R. (1994). Cytoplasm-to-myonucleus ratios and succinate dehydrogenase activities in adult rat slow and fast muscle fibers. *Cell Tissue Res.* 275 (1), 39–49. doi:10.1007/BF00305374

van de Ven, T. M., Mzilikazi, N., and McKechnie, A. E. (2013). Seasonal metabolic variation in two populations of an Afrotropical euplectid bird. *Physiological Biochem. Zoology* 86 (1), 19–26. doi:10.1086/667989

Van der Meer, S. F. T., Jaspers, R. T., and Degens, H. (2011). Is the myonuclear domain size fixed? *J. Musculoskelet. Neuronal Interact.* 11, 286–297.

Velleman, S. G., Anderson, J. W., Coy, C. S., and Nestor, K. E. (2003). Effect of selection for growth rate on muscle damage during Turkey breast muscle development. *Poult. Sci.* 82 (7), 1069–1074. doi:10.1093/ps/82.7.1069

Velleman, S. G. (2015). Relationship of skeletal muscle development and growth to breast muscle myopathies: A review. *Avian Dis.* 59 (4), 525–531. doi:10.1637/11223-063015-Review.1

Velten, B. P., Welch, K. C., Jr, and Ramenofsky, M. (2016). Altered expression of pectoral myosin heavy chain isoforms corresponds to migration status in the white-crowned sparrow (Zonotrichia leucophrys gambelii). *R. Soc. Open Sci.* 3 (11), 160775. doi:10.1098/rsos.160775

Ve´zina, F., Jalvingh, K. M., Dekinga, A., and Piersma, T. (2006). Acclimation to different thermal conditions in a northerly wintering shorebird is driven by body mass-related changes in organ size. *J. Exp. Biol.* 209 (16), 3141–3154. doi:10.1242/jeb.02338

Vézina, F., Jalvingh, K. M., Dekinga, A., and Piersma, T. (2007). Thermogenic side effects to migratory predisposition in shorebirds. *Am. J. Physiology-Regulatory, Integr. Comp. Physiology* 292 (3), R1287–R1297. doi:10.1152/ajpregu.00683.2006

Vézina, F., Cornelius Ruhs, E., O'Connor, E. S., Le Pogam, A., Régimbald, L., Love, O. P., et al. (2020). Consequences of being phenotypically mismatched with the environment: Rapid muscle ultrastructural changes in cold-shocked black-capped chickadees (poecile atricapillus). *Am. J. Physiology-Regulatory, Integr. Comp. Physiology* 318 (2), R274–R283. doi:10.1152/ajpregu.00203.2019

Vézina, F., O'Connor, R. S., Le Pogam, A., De Jesus, A. D., Love, O. P., Jimenez, A. G., et al. (2021). Snow buntings preparing for migration increase muscle fiber size and myonuclear domain in parallel with a major gain in fat mass. *J. Avian Biol.* 52 (5), jav.02668. doi:10.1111/jav.02668

Vézina, F., and Williams, T. D. (2003). Plasticity in body composition in breeding birds: What drives the metabolic costs of egg production? *Physiological Biochem. Zoology* 76 (5), 716–730. doi:10.1086/376425

Wang, Y., Shan, S., Zhang, H., Dong, B., Zheng, W., Liu, J., et al. (2019). Physiological and biochemical thermoregulatory responses in male Chinese hwameis to seasonal acclimatization: Phenotypic flexibility in a small passerine. *Zool. Stud.* 58, e6. doi:10.6620/ZS.2019.58-06

Wells, M. E., and Schaeffer, P. J. (2012). Seasonality of peak metabolic rate in non-migrant tropical birds. *J. avian Biol.* 43 (6), 481–485. doi:10.1111/j.1600-048x.2012.05709.x

Wen, Y., Englund, D. A., Peck, B. D., Murach, K. A., McCarthy, J. J., Peterson, C. A., et al. (2021). Myonuclear transcriptional dynamics in response to exercise following satellite cell depletion. *Iscience* 24 (8), 102838. doi:10.1016/j.isci.2021.102838

Whittemore, L. A., Song, K., Li, X., Aghajanian, J., Davies, M., Girgenrath, S., et al. (2003). Inhibition of myostatin in adult mice increases skeletal muscle mass and strength. *Biochem. Biophysical Res. Commun.* 300 (4), 965–971. doi:10.1016/s0006-291x(02)02953-4

Winchester, P. K., and Gonyea, W. J. (1992). Regional injury and the terminal differentiation of satellite cells in stretched avian slow tonic muscle. *Dev. Biol.* 151 (2), 459–472. doi:10.1016/0012-1606(92)90185-j

Wolfman, N. M., McPherron, A. C., Pappano, W. N., Davies, M. V., Song, K., Tomkinson, K. N., et al. (2003). Activation of latent myostatin by the BMP-1/tolloid family of metalloproteinases. *Proc. Natl. Acad. Sci. U.S.A.* 100 (26), 15842–15846. doi:10.1073/pnas.2534946100

Xu, T. S., Gu, L. H., Zhang, X. H., Ye, B. G., Liu, X. L., Hou, S. S., et al. (2013). Characterization of myostatin gene (MSTN) of Pekin duck and the association of its polymorphism with breast muscle traits. *Genet. Mol. Res.* 12 (3), 3166–3177. doi:10.4238/2013.February.28.18

Xu, J., Strasburg, G. M., Reed, K. M., and Velleman, S. G. (2021). Response of Turkey pectoralis major muscle satellite cells to hot and cold thermal stress: Effect of growth selection on satellite cell proliferation and differentiation. *Comp. Biochem. Physiology Part A Mol. Integr. Physiology* 252, 110823. doi:10.1016/j.cbpa.2020.110823

Xu, J., Strasburg, G. M., Reed, K. M., and Velleman, S. G. (2022). Thermal stress affects proliferation and differentiation of Turkey satellite cells through the mTOR/S6K pathway in a growth-dependent manner. *Plos one* 17 (1), e0262576. doi:10.1371/journal.pone.0262576

Yoshida, T., and Delafontaine, P. (2020). Mechanisms of IGF-1-mediated regulation of skeletal muscle hypertrophy and atrophy. *Cells* 9 (9), 1970. doi:10.3390/cells9091970

Young, K. G., Regnault, T. R., and Guglielmo, C. G. (2021a). Extraordinarily rapid proliferation of cultured muscle satellite cells from migratory birds. *Biol. Lett.* 17 (8), 20210200. doi:10.1098/rsbl.2021.0200

Young, K. G., Vanderboor, C. M., Regnault, T. R., and Guglielmo, C. G. (2021b). Species-specific metabolic responses of songbird, shorebird, and murine cultured myotubes to n-3 polyunsaturated fatty acids. *Am. J. Physiology-Regulatory, Integr. Comp. Physiology* 320 (3), R362–R376. doi:10.1152/ajpregu.00249.2020

Yu, M., Wang, H., Xu, Y., Yu, D., Li, D., Liu, X., et al. (2015). Insulin-like growth factor-1 (IGF-1) promotes myoblast proliferation and skeletal muscle growth of embryonic chickens via the PI3K/Akt signalling pathway. *Cell Biol. Int.* 39 (8), 910–922. doi:10.1002/cbin.10466

Zhang, Y., Eyster, K., Liu, J. S., and Swanson, D. L. (2015). Cross-training in birds: Cold and exercise training produce similar changes in maximal metabolic output, muscle masses and myostatin expression in house sparrows,*Passer domesticus*. *J. Exp. Biol.* 218 (14), 2190–2200. doi:10.1242/jeb.121822

Zhang, Y., Eyster, K., and Swanson, D. L. (2018a). Context-dependent regulation of pectoralis myostatin and lipid transporters by temperature and photoperiod in dark-eyed juncos. *Curr. Zool.* 64 (1), 23–31. doi:10.1093/cz/zox020

Zhang, Y., Yap, K. N., Williams, T. D., and Swanson, D. L. (2018b). Experimental increases in foraging costs affect pectoralis muscle mass and myostatin expression in female, but not male, zebra finches (*Taeniopygia guttata*). *Physiological Biochem. Zoology* 91 (3), 849–858. doi:10.1086/697153

Zhang, Y., and Wong, H. S. (2021). Are mitochondria the main contributor of reactive oxygen species in cells? *J. Exp. Biol.* 224 (5), jeb221606. doi:10.1242/jeb.221606

Zhao, X. H., Li, M. Y., Xu, S. S., Sun, J. Y., and Liu, G. J. (2019). Expression of myostatin (Mstn) and myogenin (Myog) genes in Zi and Rhine goose and their correlation with carcass traits. *Rev. Bras. Cienc. Avic.* 21 (1), 1–6. doi:10.1590/1806-9061-2017-0710

Zheng, W. H., Liu, J. S., and Swanson, D. L. (2014). Seasonal phenotypic flexibility of body mass, organ masses, and tissue oxidative capacity and their relationship to resting metabolic rate in Chinese bulbuls. *Physiological Biochem. Zoology* 87 (3), 432–444. doi:10.1086/675439

Zhou, L. M., Xia, S. S., Chen, Q., Wang, R. M., Zheng, W. H., Liu, J. S., et al. (2016). Phenotypic flexibility of thermogenesis in the hwamei (garrulax canorus): Responses to cold acclimation. *Am. J. Physiology-Regulatory, Integr. Comp. Physiology* 310 (4), R330–R336. doi:10.1152/ajpregu.00259.2015

Zhu, X., Topouzis, S., Liang, L. F., and Stotish, R. L. (2004). Myostatin signaling through Smad2, Smad3 and Smad4 is regulated by the inhibitory Smad7 by a negative feedback mechanism. *Cytokine* 26 (6), 262–272. doi:10.1016/j.cyto.2004.03.007

frontiers | Frontiers in Physiology

ORIGINAL RESEARCH
published: 22 July 2022
doi: 10.3389/fphys.2022.954399

Estradiol-17ß Is Influenced by Age, Housing System, and Laying Performance in Genetically Divergent Laying Hens (*Gallus gallus* f.d.)

Julia Mehlhorn[1]*, *Anja Höhne*[2], *Ulrich Baulain*[3], *Lars Schrader*[2], *Steffen Weigend*[3] and *Stefanie Petow*[2]*

[1]Institute for Anatomy I, Medical Faculty and University Hospital, Heinrich-Heine-University Düsseldorf, Düsseldorf, Germany, [2]Friedrich-Loeffler-Institut, Institute of Animal Welfare and Animal Husbandry, Celle, Germany, [3]Friedrich-Loeffler-Institut, Institute of Farm Animal Genetics, Mariensee, Germany

The estrogen estradiol-17ß is known as one of the major gonadal steroid hormones with different functions in reproduction. In this study we analyzed estradiol-17ß concentration in laying hens of four pure bred chicken laying lines at four different time intervals of the laying period (17th–19th week of age, 33rd–35th week of age, 49th–51st week of age, and 72nd week of age). The high performing white egg (WLA) and brown egg (BLA) layer lines as well as the low performing white (R11) and brown (L68) layer lines were kept in both single cages and a floor housing system. We investigated whether there were differences in estradiol -17ß concentrations between lines at different ages that could be related to selection for high egg production or phylogenetic origin of the animals, and whether there was an influence of housing conditions on estradiol-17ß. Estradiol-17ß concentrations differed between high and low performing layer lines at all time intervals studied. High performing hens showed higher estradiol-17ß concentrations compared to low performing hens. In all lines, highest estradiol-17ß concentration was measured at their 49th to their 51st week of age, whereas the peak of laying intensity was observed at their 33rd to their 35th week of age. Additionally, hens with fewer opportunities for activity housed in cages showed higher estradiol-17ß concentrations than hens kept in a floor housing system with more movement possibilities. We could show that laying performance is strongly linked with estradiol -17ß concentration. This concentration changes during laying period and is also influenced by the housing system.

Keywords: estradiol, laying hen, egg laying performance, laying intensity, housing condition, floor housing, cage housing, keel bone damage

OPEN ACCESS

Edited by:
Sandra G. Velleman, The Ohio State University, United States

Reviewed by:
Gregoy Y. Bedecarrats, University of Guelph, Canada
Paul Siegel, Virginia Tech, United States

***Correspondence:**
Julia Mehlhorn
julia.mehlhorn@hhu.de
Stefanie Petow
Stefanie.Petow@fli.de

Specialty section:
This article was submitted to Avian Physiology, a section of the journal Frontiers in Physiology

Received: *27 May 2022*
Accepted: *24 June 2022*
Published: *22 July 2022*

Citation:
Mehlhorn J, Höhne A, Baulain U, Schrader L, Weigend S and Petow S (2022) Estradiol-17ß Is Influenced by Age, Housing System, and Laying Performance in Genetically Divergent Laying Hens (Gallus gallus f.d.). Front. Physiol. 13:954399. doi: 10.3389/fphys.2022.954399

INTRODUCTION

Commercial laying hens are continuously bred for high laying performance and have an average laying performance of more than 320 eggs in 13 laying months per hen housed (Preisinger, 2018). At the same time husbandry systems and nutritional requirements of the animal have changed drastically due to high laying performance. Modern laying hens have been bred to have no brood drive, and progressive sexual maturity and shortening of the clutch length interval have

been critical factors in significantly improving egg production (Hanlon et al., 2021). To date, little attention has been paid to the underlying physiological changes that made this possible.

The hypothalamic-pituitary-gonadal (HPG) axis plays a central role in controlling reproduction and sexual maturation of animals (Dunn and Sharp, 1990; Bédécarrats et al., 2009). In the HPG axis, Gonadotrophin-releasing hormone (GnRH), a hypothalamic decapeptide, stimulates the secretion of luteinizing hormone (LH) and follicle-stimulating hormone (FSH) in the adenohypophysis. Subsequently, LH regulates the estradiol-17ß synthesis in the ovaries (Clarke and Pompolo, 2005). Through a feedback mechanism, LH and estradiol-17ß inhibit increased GnRH secretion in the brain (Kawashima et al., 1993; Ottinger et al., 2002). As a result, less estradiol-17ß is released. However, modern laying hens have consistently high plasma estradiol-17ß levels (Eusemann et al., 2018a) and it is suggested that this feedback mechanism is disrupted in high performing laying hens or at least changes have occurred in the control of the HPG axis (Hanlon et al., 2021). But the detailed endocrine control mechanism of the laying cycle of the modern laying hen is still little understood, and the feedback between the ovarian follicles and the hypothalamo-hypophysial system which controls follicular development is particularly nebulous.

Estradiol-17ß is the most abundant estrogen and one of the most important gonadal steroids with various functions in the regulation of the female reproduction, e.g., yolk precursor production, oviduct development and reproductive behavior (Yu et al., 1971; Gahr, 2001; Williams et al., 2004). In addition, estradiol-17ß is known to be a triggering factor in calcium and bone metabolism and has a positive effect on bone turnover and regeneration in adults (Bar et al., 1996; Väänänen and Härkötnen, 1996; Johnson, 2000; Beck and Hansen, 2004). Estradiol-17ß is synthesized and permanently produced mainly in granulosa- and theca cells in growing follicles (Marrone and Hertelendy, 1983) with the highest concentrations in small, early-stage follicles and 6–4 h prior the ovulation in laying hens (Johnson and van Tienhoven, 1980; Bahr et al., 1983). During the lifetime of a laying hen, estradiol-17ß concentrations gradually increases until week 20 (onset of laying) and then remain high for the next several weeks (Whitehead and Fleming, 2000; Beck and Hansen, 2004). The exact time course of estradiol-17ß secretion patterns after the peak of production is not clear; only few studies have systematically monitored plasma estradiol over the entire production period. Previous studies have shown that estradiol levels are closely related to the laying performance with estradiol concentrations being highest during the peak of egg production, decreasing during the production year and low during molting (Senior, 1974; Hoshino et al., 1988; Hansen et al., 2003; Ebeid et al., 2008; Habig et al., 2021a). Habig et al. (2021b) also showed differences between different high performing lines during their reproduction cycle. In the pre-laying period (17th week), the estradiol-17ß level of high performing white-egg layers (WLA) was more than twice as high as the level for phylogenetically divergent high performing brown-egg layers (BLA), but much lower than after the onset of laying. In the laying period (25–69 weeks) no significant differences could be observed between the lines, while the estradiol-17ß level continuously increased with age (Habig et al., 2021a; Hanlon et al., 2021).

The influence of estradiol-17ß on egg production was also demonstrated in studies in which egg production was selectively suppressed by the synthetic GnRH agonist deslorelin acetate (Eusemann et al., 2018a). Here, treated hens showed not only lower egg laying performance, but also significantly lower estradiol-17ß levels compared to untreated hens. In addition, there is a correlation between laying performance and estradiol-17ß concentration. Hens of high performing lines achieved higher estradiol-17ß plasma concentrations than hens of low performing lines (Eusemann et al., 2020; Eusemann et al., 2022).

One possible consequence of high laying performance could be the occurrence of keel bone alterations, which are often manifested in reduced bone stability, deviations and fractures. In commercial systems, keel bone damage often affects over 90% of the hens in a flock (Wilkins et al., 2004; Rodenburg et al., 2008; Wilkins et al., 2011; Heerkens et al., 2016). At the onset of sexual maturity, osteoblasts start producing so-called medullary bone. This type of bone is unique to birds (and crocodilians) and serves as a source of calcium for shell formation. At the onset of sexual maturity, osteoblasts begin to form the medullary bone (Whitehead, 2004). Thus, in laying hens, keel bone damage is thought to be related to high laying performance and substantial calcium requirements during eggshell formation (Kerschnitzki et al., 2014). High performing layer lines not only had higher estradiol-17ß concentrations than low performing layer lines, but could also have a significantly higher risk of fracture, a lower degree of mineralization of the cortical bone, and a lower relative amount of medullary bone (Eusemann et al., 2020; Eusemann et al., 2022). The formation of the medullary bone is estrogen and androgen dependent and starts with the onset of ovarian follicle maturation which is part of the hypothalamic-pituitary-gonadal axis (Beck and Hansen, 2004). Therefore, it is likely, that there is a close relationship between laying performance, keel bone damage, and estradiol-17ß concentration.

The influence of different housing conditions of laying hens on the behavior and performance of laying hens in different housing systems has been the subject of numerous studies. Conventional cage systems restrict behavioral expression and increase the risk of skeletal degradation, but floor- or free-range systems evoke difficulties in terms of disease and pest control or higher incidences of skeletal injuries (Whitehead, 2004; Lay et al., 2011; Weeks et al., 2016; Eusemann et al., 2018b). It is obvious that the housing condition have an influence on keel bone damage. The proportion of deviated keel bones was significantly higher in laying hens kept in cages than in floor-housed laying hens whereas fractures occur more often in floor-housed hens (Eusemann et al., 2018b). Additionally, there is a presumption that housing conditions have an influence on laying performance, but the data are inconsistent. At least in enriched and barren cages, egg production seems to be similar (Ylmaz Dikmen et al., 2016; Onbasilar et al., 2020; Philippe et al., 2020) and it is assumed that the differences between the studies are due to the investigated lines and characteristics of the enrichment materials. For free-range hens, Ylmaz Dikmen et al. (2016) described a higher egg production compared to cage housed

hens, whereas Philippe et al. (2020) and Shimmura et al. (2010) found lower egg laying rates in hens housed in aviaries or free-range systems compared to cage housed hens. Lower egg laying rates were also found in floor-housed hens compared to cage-housed hens (Voslarova et al., 2006; Ketta et al., 2020). The authors assumed that this could be related to higher animal activity and competition for facilities/resources. Wan et al. (2021) compared two different non-caged systems, namely a plastic-net housing system and a floor-littered housing system and revealed that the plastic-net housing system enhanced the production performance, antioxidant capacity and intestinal health of hens. It should be kept in mind that different findings in different studies could be due to differences in chicken breeds and environmental conditions. Whether the estradiol-17ß concentration is also influenced by the housing system has not yet been investigated.

We hypothesize that activation and function of the HPG axis changed in high performing laying hens to support the significant increase in egg production. Therefore, the aim of the current study was to characterize and compare the estradiol-17ß concentration in pure bred genetically divergent lines with a particular attention to the production cycle and the housing system. We hypothesized that lines with a high ovulation rate would have higher estradiol concentrations compared to low performing lines and that the highest estradiol concentration will be measured at the laying peak. Additionally, we expect that housing condition influences estradiol-17ß concentration, which could explain the lower laying performance in floor-kept hens compared to cage-housed hens as described in previous studies (e.g., Voslarova et al., 2006; Ketta et al., 2020).

MATERIALS AND METHODS

Animals and Housing Conditions

All experiments were performed in accordance with the German Animal Protection Law and were approved by the Lower Saxony State Office for Consumer Protection and Food Safety (No. 33.9-42502-05-10A079).

In this study, we compared phylogenetically divergent high performing white (WLA, $n = 20$) and brown egg laying (BLA, $n = 20$) purebred chicken lines with low performing white (R11, $n = 20$) and brown laying lines (L68, $n = 20$). WLA and BLA originated as purebred lines from the breeding program of Lohmann Breeders and have been kept at the Institute of Farm Animal Genetics of the Friedrich-Loeffler-Institute since 2012. L68, and R11 are very old laying lines that have been maintained as conservation lines at the institute for decades. This four-line animal model was developed as part of a multidisciplinary collaboration at the Friedrich-Loeffler-Institute and first presented by Lieboldt et al. (2015), who described the growth and performance of the four chicken lines. Since then, a number of studies have been conducted, including bone traits (Habig et al., 2017; Dudde et al., 2020) and keel bone damage (Eusemann et al., 2018a; Eusemann et al., 2020; Habig et al., 2021a).

All animals hatched at the same day and were raised separately in a floor housing system until 16 weeks of age. Rearing compartments (6 m × 4 m) were littered with wood-shavings and straw and were equipped with perches. Food (week 1–7: 12.97 MJ AMEN/kg DM, 189.61 g/kg crude protein, 31.38 g/kg crude fat, 9.14 g/kg Ca, 6.94 g/kg P; week 8–16: 12.82 MJ AMEN/kg DM, 151.67 g/kg crude protein, 30.21 g/kg crude fat, 15.83 g/kg Ca, 8.11 g/kg P) and water was provided *ad libitum*. A standard light-programme was applied during rearing period. At 16 weeks of age 10 hens of each line were moved to a single cage housing system equipped with a food trough, two drinking nipples and a perch. Other 10 hens of each line were kept in floor pens (each 2.0 m × 4.0 m) separated by line. The animals were distributed between two pens per line. Both housing conditions were in the same room. Floor pens were littered with wood-shavings and equipped with perches and nests mounted on a slatted floor 0.5 m above the litter area. In both housing systems animals had *ad libitum* access to food (11.68 MJ AMEN/kg DM, 168.11 g/kg crude protein, 29.43 g/kg crude fat, 50.05 g/kg Ca, 5.06 g/kg P) and water. The light period increased from 9 to 14 h from 16th until 20th week of age and was maintained at 14 h for the remainder of the laying cycle (to 72 weeks of age).

Laying performance was recorded individually of all hens in the single cages and summarized for every week. However, recording laying performance in the floor-housed hens at individual level was not possible, therefore, we determined the total number of eggs per week and chicken line. For analyses, we calculated the laying intensity (in %) based on the number of eggs laid during the experimental weeks of age and the number of hen days (number of hens x number of days).

We investigated four time periods, the first period from the 17th, 18th, and 19th week of age (before start of laying), the second period from the 33rd, 34th, and 35th week of age (maximum of egg production), the third period from the 49th, 50th, and 51st week of age (decrease in egg production in low producing lines) and the last period in the 72nd week of age (end of experiment).

Blood Sampling

In each of the four experimental periods blood was collected once a week between 2.00 and 5.00 p.m. For this, ten hens of each line and housing condition were selected (resulting in a total of 80 hens). Blood was collected from the wing vein (*V. ulnaris*) using needles with a gauge of 21 and 2 ml syringes (both Henry Schein, Hamburg, Germany). After collection, blood samples were immediately transferred to K_3-EDTA covered tubes (Greiner, Solingen, Germany) to avoid coagulation, and centrifuged at 4°C for 10 min at 2750 rcf. Tubes were placed on ice, and plasma phase was pipetted into 1.5 ml Eppendorf® cups (Fisher Scientific, Schwerte, Germany) and frozen at −20°C until analysis.

Hormone Assays

For estradiol-17ß analysis a commercial estradiol-17ß ELISA Kit (IBL International, Hamburg, Germany) was used. Assays were conducted following the manufacturer's instructions and samples were analyzed in duplicates. The kit used detects the entire E2. The absorption of the plate was detected with an ELISA

microplate reader (Tecan, Crailsheim, Germany) at 450 nm with a reference wavelength at 620 nm.

The concentrations and coefficients of variation of the assays were calculated using the microplate reader software (Magellan® Version 7.1, Tecan Austria, Salzburg, Austria). For estradiol the intraassay coefficient of variation was 6% and the interassay coefficient of variation was 9%.

Statistical Analysis

Data were statistically analyzed using JMP, version 15.0 (Statistical Analysis System Institute, Cary, NC, United States). Estradiol-17ß content was examined using a linear mixed model. Individual hen was included as random factor in order to account for repeated measurements within animal. Layer line, housing condition, age and the three two-way interactions were considered as fixed effects. The 3-fold interaction between housing condition, line and age did not show a significant effect on the Estradiol concentration, therefore it was removed from the model (model 1).

Laying performance of single caged hens was analyzed using a linear mixed model, too, including individual hen as random effect. Layer line, age and the interaction of layer line x age were considered as fixed effects (model 2). The influence of layer line and age on group laying performance of floor housed hens (two pens per line) was analyzed using a two-way ANOVA including layer line and age with interaction (model 3).

Differences between Least Squares means (LSM) were tested by means of the Tukey-Kramer Test, adjusting for multiple comparisons. Differences were regarded as statistically significant at $p < 0.05$.

RESULTS

From **Table 1** it is evident that estradiol-17ß plasma concentration was significantly affected by housing condition, layer line, age and by the interaction of line*age ($p < 0.05$). The laying performance, analyzed separately by housing condition, was significantly influenced by layer line, age and also by the line*age interaction ($p < 0.001$).

Estradiol-17ß Concentration in Different Layer Lines

High performing laying hens (BLA, WLA) started in week 17 with estradiol-17ß plasma concentrations almost twice as high as low performing laying hens (L68, R11) and showed a higher increase from week 18 to week 19 compared to the low performance lines (**Figure 1A**; Supplementary Table S1). In the period of maximum laying performance (weeks 33–35) the high performing lines showed a tendency towards higher estradiol-17ß concentrations than those of low performing lines.

In all lines, estradiol-17ß concentration increased until week 50 or 51 (3rd period), reaching more than 500 pg/ml in high performing hens (WLA: 527.03 ± 22.04 pg/ml, BLA: 550.42 ± 22.01 pg/ml) and about 400 pg/ml in low performing hens (L68: 429.58 ± 22.54 pg/ml, R11: 415.21 ± 22.04 pg/ml). After week 51, estradiol-17ß concentration decreased to 248.58 ± 23.59 pg/ml in WLA, 255.00 ± 22.64 pg/ml in BLA, 199.50 ± 22.54 pg/ml in R11 and 182.00 ± 23.14 pg/ml in L68 in week 72.

Estradiol-17ß Concentration in Different Housing Systems

There is a significant main effect of the housing system on estradiol-17ß concentration in laying hens (**Figure 1B**, Supplementary Table S1). In all study periods, caged hens tended to have higher estradiol-17ß concentrations than floor-housed hens, with the difference being statistically significant only at 51 weeks of life. (**Figure 1B**; Supplementary Table S2). Within both housing systems, estradiol-17ß concentrations differed significantly between all the 4 periods. In both, floor pens and cages, estradiol-17ß concentrations increased until the 3rd period and were highest between week 49 and 51 (floor: 445.16 ± 15.76 ng/ml, cage: 523.81 ± 15.57 ng/ml). In week 72, estradiol-17ß concentration decreased to 206.24 ± 16.89 ng/ml in floor-housed hens and 236.29 ± 15.58 ng/ml in cage-housed hens, respectively.

Laying Intensity

Laying intensity of cage housed hens was significantly affected by the interaction between week of age and breeding line ($p <$

TABLE 1 | Significance of fixed effects (*p*-values).

Source	Estradiol-17ß [a]	Laying intensity [b]	Laying intensity [c]
		Cage housing	Floor housing
Housing condition (HC)	**0.0019**	–	–
Layer line (LL)	**<0.0001**	**<0.0001**	**<0.0001**
Week of age	**<0.0001**	**<0.0001**	**<0.0001**
HC * LL	0.8415	–	–
HC * week of age	0.1113	–	–
LL * week of age	**<0.0001**	**0.0001**	**<0.0001**
HC * LL * week of age	0.2422	–	–

[a]*Model (1).*
[b]*Model (2).*
[c]*Model (3).*

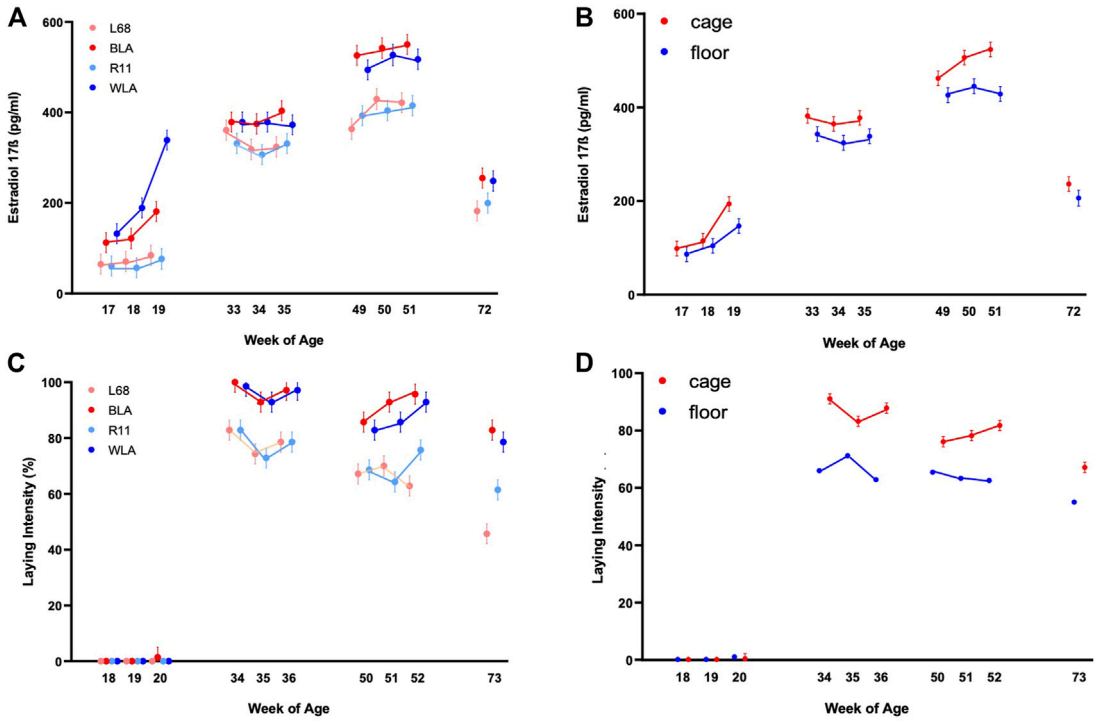

FIGURE 1 | Estradiol-17ß blood plasma concentration (pg/ml) and laying intensity (%) of four different layer lines kept in different housing systems and investigated at four time periods (17th, 18th, and 19th week of age (before start of laying); 33rd, 34th, and 35th week of age (maximum of egg production); 49th, 50th, and 51st week of age (decrease in egg production in low producing lines) and 72nd week of age (end of experiment). The laying intensity is shown after each week of blood sampling **(A)** Estradiol-17ß concentration of the two high performing layer lines (WLA, BLA) and the two low performing layer lines (L68, R11) respectively cage-housed and floor-housed laying hens **(B)**, consisting of WLA, BLA, L68, and R11 hens) during their laying period **(C)** Laying intensity of all four-layer lines and of cage-housed and floor-housed laying hens **(D)** during their laying period.

0.0001); Supplementary Table S3 and **Figure 1C** show that within the first period hens had not yet started laying. In the second period all lines reached the maximum egg laying rate in the 34th week of life (BLA: 100.00% ± 3.60, WLA: 98.57% ± 3.60, L68, and R11: 82.86 ± 3.60). In all periods high performing layers showed a higher laying intensity compared to low performing layers, with statistically significances in the 2nd, 3rd, and 4th period. Since the laying performance of hens kept in floors was not recorded individually, we only note descriptively that hens kept in cages had a higher laying intensity than hens kept in floor systems in time periods 2, 3, and 4 (**Figure 1D**; Supplementary Table S3), without this being statistically verifiable.

DISCUSSION

Genetic selection for earlier sexual maturation and extended production cycles in laying hens has significantly improved reproductive efficiency (Hanlon et al., 2021). and allowed modern layers to double their reproductive capacity compared to their 1960s counterparts. Breeding improvement in egg production has led to a continuous improvement in laying performance, with a trend of an increase of about 2–3 eggs per hen per year in a 13-months production cycle (Preisinger, 2018) However, the underlying physiological changes throughout the laying period and the correlation between these changes and laying performance have received limited attention. Hence, the effect of housing conditions, genotype, and laying performance and their interactions on estradiol concentration is not fully understood.

In this study, we investigated the relationship between blood estradiol-17ß levels and egg production at four different time points during the laying period in two high performing laying lines (WLA and BLA) and two low performing laying lines (L68 and R11). All lines showed low estradiol-17ß concentrations in the beginning of the 1st investigated time period (17th week of age), followed by a strong increase in the 2nd period (33rd–35th week of age) and an even higher estradiol-17ß concentration in the 3rd period (49th–51st week of age). In the 4th period (72nd week of age) estradiol-17ß concentration decreased to a level between the first and 2nd period. Low estradiol-17ß concentrations at the beginning of the first period are not unexpected because at this time, hens are just starting to lay and are not yet sexually matured. WLA and BLA not only showed higher estradiol-17ß concentrations but also a higher increase from week 18 to week 19 compared to the low performance lines.

Our finding that there are differences in estradiol-17ß concentrations between WLA and BLA in the pre-laying

period is in line with Habig et al. (2021b). Probably, these differences are due to the different phylogenetic background of these lines.

Interestingly, estradiol-17ß concentration in the second period is high, but it is still exceeded by the concentration of the third period. Due to its involvement in the regulation of egg production (Yu et al., 1971; Williams et al., 2004) we expected highest estradiol concentrations at the maximum of egg laying rather than in the following period. Next to its function in the female reproduction cycle, estradiol-17ß is also involved in calcium and bone metabolism and has an impact on bone stability (Bar et al., 1996; Väänänen and Härkötnen, 1996; Johnson, 2000; Beck and Hansen, 2004). Previous studies have shown that most keel bone fractures occur or were already present at this week of age, when we measured the highest estradiol-17ß concentrations (Petrik et al., 2015; Stratmann et al., 2015; Eusemann et al., 2018b). Estradiol-17ß can also counteract the reduction of bone strength and loss of structural bone as a consequence of increased egg production (Whitehead and Fleming, 2000). The medullary bone, which presents a calcium reservoir for egg shell building, is formed at the onset of egg laying (Senior, 1974; Johnson, 2000; Whitehead and Fleming, 2000; Dojana et al., 2015). The key role of Estradiol-17ß in the modelling of the medullary bone is well described (e.g., Hiyama et al., 2012; Squire et al., 2017; Eusemann et al., 2022) Thus, our results may support the relationship between estradiol-17ß and bone health. In the investigation of Eusemann et al. (2020) the authors could show, that hormonally castrated hens have significantly less fractures than the non-castrated control group. The increase of estradiol-17ß after the peak of egg production in our study might be related with its function in regeneration in adult bone turnover particularly in the high performing selected lines. Interestingly, this is different to non-poultry birds like starlings. Here, estradiol-17ß concentrations decrease after onset of laying well before the final yolky follicle was ovulated (Williams et al., 2004). Apparently, ovary and oviduct size and their function are maintained despite lower estradiol-17ß concentration. The authors suggest that one reason for this might be that there are negative, non-reproductive effects of high estradiol-17ß levels which would foster rapid down-regulation, e.g., suppression of hematopoiesis or immunosuppression, or decreased embryo viability. Alternatively, the observed decrease in estradiol-17ß concentration in starlings could be a pre-requisite for rapid oviduct regression at the end of laying, because estrogens also oppose the induction of apoptosis that is involved in oviduct regression (Williams and Ames, 2004). It is not surprising, that such a decrease would be not observed in laying hens, or at least only at a much later point of reproduction cycle, because of their extended laying period and extended end of reproduction period.

Estradiol-17ß concentration in cage-housed hens was higher compared to floor-housed hens where birds had more opportunities for activity. Aguado et al. (2015) described a reduced bone mass and bone quality in hypoactive chickens. There are two possible explanations for this: either, the stimulating effect of activity/exercises on bone strength is related to the degree of biomechanical load experienced by the bone [following the concept of causal histogenesis (Pauwels, 1960)] or it is caused by a lower estradiol-17ß concentration. Although we cannot state whether the higher estradiol-17ß concentration in cage-housed hens is the consequence or the cause of less activity, it seems likely that there is a correlation between these two parameters. Besides, the estradiol-17ß concentration depends on the number of maturing follicles. Thus, the lower laying intensity may also be an explanation for the lower estradiol-17ß concentration in floor-housed hens compared to cage-housed hens. Recent studies showed that, at least in premenopausal women, high physical activity was associated with lower levels of estrone and estradiol (Matthews et al., 2012; Dallal et al., 2016). These findings suggest that physical activity may induce changes in estrogen metabolism possibly through more extensive hydroxylation of parent estrogens, leading to increased excretion. Given the exploratory nature of these studies, findings should be interpreted cautiously, but in our opinion, there could be a negative relationship between activity and estradiol-17ß level in the blood as floor-housed laying hens are more active/more mobile than cage housed hens.

The laying performance of the lines used in our study was significantly affected by the genotype which agrees with previous studies (e.g., Lieboldt et al., 2015). WLA and BLA were classified as high performing lines with a laying intensity of more than 93%–95% at the maximum of egg production and when housed in cages, whereas cage-housed low performing L68 and R11 showed a lower egg production of 67%–74%. Besides, laying maturity, defined as age at the first egg laid, was reached by the hens of the high performing genotypes four to 5 weeks earlier than in hens of the low performing genotypes, namely in the 20th week of age (Lieboldt et al., 2015). In our study we did not investigate the exact age of reaching laying maturity but observed that laying intensity in week 20 was still 0% in WLA, L68, and R11 and just 1.4% in BLA. Thus, reaching laying maturity must be a little bit later in our study. However, laying intensity of all four lines was even a little bit higher as shown in Lieboldt et al. (2015) and all four lines reached their maximum egg production in the 34th week of age.

Determining laying performance in floor-housed hens is always a challenge. Some eggs might be laid in the litter and were not easily counted, an assignment to the individual hen is difficult and it is possible that eggs were completely destroyed and the remains buried in the litter. Another problem could be that there might be hens among the floor housed hens, that have not laid and therefore have low estradiol-17ß levels. In order to exclude the possibility that these animals decrease the estradiol-17ß level of the whole group, we checked it and would have excluded all hens with values with the level of the 1st period. But this was not the case, apparently all floor-housed hens always have laid regularly.

The observation that high performing lines showed higher concentrations of estradiol-17ß compared to both low performing layer lines, independent of the phylogenetic origin,

supports our hypothesis that selection for egg production resulted in higher concentrations of estradiol-17ß. It seems that high estradiol-17ß concentrations are related to production level and might be a result of human directed selection. Hanlon et al. (2021) hypothesized that modifications in the control of the hypothalamic-pituitary gonadal axis have occurred in modern laying hens. They compared estradiol-17ß concentration and mRNA levels of key genes involved in the HPG axis of current commercial hens (Lohmann LSL-lite) with Shaver White leghorns as 2000s commercial equivalents and Smoky Joe hens as 1960s commercial equivalents. Their results showed that the extended laying persistency in Lohmann LSL lite hens was supported by sustained pituitary sensitivity to GnRH and recurrent increases in follicle-stimulating hormone (FSH) and estradiol-17ß. This is in line with our finding about higher estradiol concentration in high performing layers compared to low performing layers. In Hanlon et al. (2021) the highest estradiol-17ß concentrations were found (in all strains) at the beginning of laying at week 19–21. Up to 100th week of age, there are recurrent elevations of estradiol concentration, but they do not reach the level of the first peak. This does not agree with our results where there was just one peak of estradiol-17ß concentration and much later at week 50–51. However, these differences could be caused by the different genotypes of the used lines or differences in e.g. feeding, light regime or rearing. Besides, blood sampling in Hanlon et al. (2021) was taken in the morning and not in the afternoon as in our study what makes a direct comparison difficult. It is known, that there are circadian fluctuations in estradiol-17ß concentrations since the highest concentrations of estradiol-17ß was observed 6–4 h prior the ovulation in laying hens (Johnson and van Tienhoven, 1980; Bahr et al., 1983). In the course of the daily egg laying cycle blood concentrations clearly reflected the stage of egg formation (Habig et al., 2021a). The egg-laying cycle of modern laying hens lasts about 24 h and oviposition followed 24 h after ovulation (Bain et al., 2016). As modern layer lines lay their eggs all about the same time (more likely in the morning), ovulation and peak of estradiol-17ß concentration should be as well at the same time. Thus, it cannot be excluded that estradiol-17ß concentrations measured in the afternoon differ from estradiol-17ß concentrations measured in the morning. However, Habig et al. (2021b) also showed that the daily variations of the estradiol-17ß concentrations were rather small compared to differences between different ages or the phylogenetic origin of chicken lines.

Habig et al. (2021b) showed differences between the estradiol-17ß level of WLA compared to BLA in the pre-laying period (17th week) and assumed that this might be indication that brown-egg layers were further from sexual maturity than white-egg layers (although start of egg laying was similar). In our study we found the same results but shifted to the 19th week of age. Here, the WLA hens were as twice as high as the BLA hens in their estradiol-17ß concentrations.

As modern laying hens further selected for improved laying performance, the physiological implications of this intensive selection must be considered. Here, many factors play a role but are not fully described for the laying hen. There are particularly open questions regarding the physiological and neuronally controlled mechanisms for a high laying performance and there are still ambiguities about the influence of the housing system. In addition to pituitary-derived gonadotropins, which are essential for steroid production, chicken ovarian steroidogenesis is under regulatory influence of several endocrine, paracrine and autocrine factors (Sechman, 2013), thus, further investigations are necessary to investigate all parameters which are involved in reproductivity over the whole laying period.

DATA AVAILABILITY STATEMENT

The original contributions presented in the study are included in the article/**Supplementary Material**, further inquiries can be directed to the corresponding authors.

ETHICS STATEMENT

All experiments were reviewed and approved by the Lower Saxony State Office for Consumer Protection and Food Safety (No. 33.9-42502-05-10A079).

AUTHOR CONTRIBUTIONS

JM, AH, UB, SP, and LS: study concept, design, data acquisition, analysis and interpretation of data; JM, AH, and SP: drafting of the manuscript and preparing the figures; SW and LS: initiated the multidisciplinary research using the four-line-chicken model and have participated in the writing of the manuscript.

ACKNOWLEDGMENTS

We would like to thank Silke Werner, Maik Przyklenk, Silvia Wittig, Elke Albrecht †, and Daniel Piotrowski for technical assistance.

SUPPLEMENTARY MATERIAL

The Supplementary Material for this article can be found online at: https://www.frontiersin.org/articles/10.3389/fphys.2022.954399/full#supplementary-material

REFERENCES

Aguado, E., Pascaretti-Grizon, F., Goyenvalle, E., Audran, M., and Chappard, D. (2015). Bone Mass and Bone Quality Altered by Hypoactivity in Chicken. *PLoS One* 10, e0116763. doi:10.1371/journal.pone.0116763

Bahr, J. M., Wang, S.-C., Huang, M. Y., and Calvo, F. O. (1983). Steroid Concentrations in Isolated Theca and Granulosa Layers of Preovulatory Follicles during the Ovulatory Cycle of the Domestic Hen. *Biol. Reprod.* 29, 326–334.

Bain, M. M., Nys, Y., and Dunn, I. C. (2016). Increasing Persistency in Lay and Stabilising Egg Quality in Longer Laying Cycles. What Are the Challenges? *Brit. Poult. Sci.* 57, 330–338. doi:10.1080/00071668.2016.1161727

Bar, A., Vax, E., Hunziker, W., Halevy, O., and Striem, S. (1996). The Role of Gonadal Hormones in Gene Expression of Calbindin (Mr 28,000) in the Laying Hen. *Gen. Comp. Endocrinol.* 103, 115–122.

Beck, M. M., and Hansen, K. K. (2004). Role of Estrogen in Avian Osteoporosis. *Poult. Sci.* 83, 200–206. doi:10.1093/ps/83.2.200

Bédécarrats, G. Y., McFarlane, H., Maddineni, S. R., and Ramachandran, R. (2009). Gonadotropin- Inhibitory Hormone Receptor Signaling and its Impact on Reproduction in Chickens. *Gen. Comp. Endocrinol.* 163, 7–11. doi:10.1016/j.ygcen.2009.03.010

Clarke, I. J., and Pompolo, S. (2005). Synthesis and Secretion of GnRH. *Animal Reproduction Sci.* 88, 29–55. doi:10.1016/j.anireprosci.2005.05.003

Dallal, C. M., Brinton, L. A., Matthews, C. E., Pfeiffer, R. M., Hartman, T. J., Lissowska, J., et al. (2016). Association of Active and Sedentary Behaviors with Postmenopausal Estrogen Metabolism. *Med. Sci. Sports Exerc* 48, 439–448. doi:10.1249/mss.0000000000000790

Dojana, N., Cotor, G., Codreanu, I., and Balaceanu, R. (2015). The Effect of Experimental 17-beta Estradiol Administering on Calcium Metabolism Regulation in Young Laying Hens. *Vet. Med.* 72 (1), 90–92. doi:10.15835/buasvmcn-vm:10854

Dudde, A., Weigend, S., Krause, E. T., Jansen, S., Habig, C., and Schrader, L. (2020). Chickens in Motion: Effects of Egg Production Level and Pen Size on the Motor Abilities and Bone Stability of Laying Hens (Gallus gallus Forma Domestica). *Appl. Anim. Behav. Sci.* 227. 104998. doi:10.1016/j.applanim.2020.104998

Dunn, I. C., and Sharp, P. J. (1990). Photoperiodic Requirements for LH Release in Juvenile Broiler and Egg-Laying Strains of Domestic Chickens Fed Ad Libitum or Restricted Diets. *J. Reprod. Fertil.* 90, 329–335. doi:10.1530/jrf.0.0900329

Ebeid, T. A., Eid, Y. Z., El-Abd, E. A., and EL-Habbak, M. M. (2008). Effects of Catecholamines on Ovary Morphology, Blood Concentrations of Estradiol-17ß, Progesterone, Zinc, Triglycerides and Rate of Ovulation in Domestic Hens. *Theriogenology* 69, 870–876. doi:10.1016/j.theriogenology.2008.01.002

Eusemann, B. K., Baulain, U., Schrader, L., Thöne-Reineke, C., Patt, A., and Petow, S. (2018a). Radiographic Examination of Keel Bone Damage in Living Laying Hens of Different Strains Keptin Two Housing Systems. *PloS ONE* 13 (5), e0194974. doi:10.1371/journal.pone.0194974

Eusemann, B. K., Patt, A., Schrader, L., Weigend, S., Thöne-Reineke, C., and Petow, S. (2020). The Role of Egg Production in the Etiology of Keel Bone Damage in Laying Hens. *Front. Vet. Sci.* 7, 81. doi:10.3389/fvets.2020.00081

Eusemann, B. K., Sharifi, A. R., Patt, A., Reinhard, A. K., Schrader, L., and Petow, S. (2018b). Influence of a Sustained Release Deslorelin Acetate Implant on Reproductive Physiology and Associated Traits in Laying Hens. *Front. Physiol.* 9, 1846. doi:10.3389/fphys.2018.01846

Eusemann, B. K., Ulrich, K., Sanchez-Rodriguez, E., Benavides-Reyes, C., Dominguez-Gasca, N., Rodriguez-Navarro, A. B., et al. (2022). Bone Quality and Composition Are Influenced by Egg Production, Layer Line, and Estradiol-17ß in Laying Hens. *Avian Pathol.* 51:267. doi:10.1080/03079457.2022.2050671

Gahr, M. (2001). Distribution of Sex Steroid Hormone Receptors in the Avian Brain: Functional Implications for Neural Sex Differences and Sexual Behaviors. *Microsc. Res. Tech.* 55, 1–11. doi:10.1002/jemt.1151

Habig, C., Baulain, U., Henning, M., Scholz, A. M., Sharifi, A. R., Janisch, S., et al. (2017). How Bone Stability in Laying Hens Is Affected by Phylogenetic Background and Performance Level. *Eur. Poult. Sci.* 81. doi:10.1399/eps.2017.200

Habig, C., Henning, M., Baulain, U., Jansen, S., Scholz, A. M., and Weigend, S. (2021a). Keel Bone Damage in Laying Hens—Its Relation to Bone Mineral Density, Body Growth Rate and Laying Performance. *Animals* 11, 1546. doi:10.3390/ani11061546

Habig, C., Weigend, A., Baulain, U., Petow, S., and Weigend, S. (2021b). Influence of Age and Phylogenetic Background on Blood Parameters Associated with Bone Metabolism in Laying Hens. *Front. Physiol.* 12, 678054. doi:10.3389/fphys.2021.678054

Hanlon, C., Takeshima, K., and Bédécarrats, G. Y. (2021). Changes in the Control of the Hypothalamic-Pituitary Gonadal Axis Across Three Differentially Selected Strains of Laying Hens (*Gallus gallus Domesticus*). *Front. Physiol.* 12, 651491. doi:10.3389/fphys.2021.651491

Hansen, K. K., Kittok, R. J., Sarath, G., Toombs, C. F., Caceres, N., and Beck, M. M. (2003). Estrogen Receptor-Alpha Populations Change with Age in Commercial Laying Hens. *Poult. Sci.* 82, 1624–1629. doi:10.1093/ps/82.10.1624

Heerkens, J. L., Delezie, E., Ampe, B., Rodenburg, T. B., and Tuyttens, F. A. (2016). Ramps and Hybrid Effects on Keel Bone and Foot Pad Disorders in Modified Aviaries for Laying Hens. *Poult. Sci.* 95 (11), 2479–2488. doi:10.3382/ps/pew157.PMID.27143777

Hiyama, S., Sugiyama, T., Kusuhara, S., and Uchida, T. (2012). Sequential Expression of Osteoblast Phenotypic Genes during Medullary Bone Formation and Resorption in Estrogen-Treated Male Japanese Quails. *J. Exp. Zool. B Mol. Dev. Evol.* 318 (5), 344–352. doi:10.1002/jez.b.22451

Hoshino, S., Suziki, M., Kakegawa, T., Imai, K., Wakita, M., Kobayashi, Y., et al. (1988). Changes in Plasma Thyroid Hormones, Luteinizing Hormone (LH), Estradiol, Progesteron and Corticosterone of Laying Hens during a Forced Molt. *Comp. Biochem. Physiol.* 90A, 355–359.

Johnson, A. L. (2000). "Reproduction in the Female". In: *Sturkie's Avian Physiol.*, Editor G. Causey Whittow (Amsterdam: Academic Press, Elsevier), 569–596. doi:10.1016/b978-012747605-6/50023-7

Johnson, A. L., and van Tienhoven, A. (1980). Plasma Concentrations of Six Steroids and LH during the Ovulatory Cycle of the Hen, *Gallus domesticus*. *Biol. Reprod.* 23, 386–393.

Kawashima, M., Kamiyoshi, M., and Tanaka, K. (1993). Estrogen Receptor Binding in the Hen Hypothalamus and Pituitary during the Ovulatory Cycle. *Poult. Sci.* 72, 839–847.

Kerschnitzki, M., Zander, T., Zaslansky, P., Fratzl, P., Shahar, R., and Wagermaier, W. (2014). Rapid Alterations of Avian Medullary Bone Material during the Daily Egg-Laying Cycle. *Bone* 69, 109–117. doi:10.1016/j.bone.2014.08.019

Ketta, M., Tůmová, E., Englmaierová, M., and Chodová, D. (2020). Combined Effect of Genotype, Housing System, and Calcium on Performance and Eggshell Quality of Laying Hens. *Anim. (Basel)* 10, 2120. doi:10.3390/ani10112120

Lay, D. C., Fulton, R. M., Hester, P. Y., Karcher, D. M., Kjaer, J. B., Mench, J. A., et al. (2011). Hen Welfare in Different Housing Systems. *Poult. Sci.* 90, 278–294. doi:10.3382/ps.2010-00962

M.-A. Lieboldt, M. A., Ingrid Halle, I., Jana Frahm, J., L. Schrader, L., U. Baulain, U., Martina Henning, M., et al. (2015). Phylogenic versus Selection Effects on Growth Development, Egg Laying and Egg Quality in Purebred Laying Hens. *Eur. Poult. Sci.* 79, 1612–9199. doi:10.1399/eps.2015.89

Marrone, B. L., and Hertelendy, F. (1983). Steroidogenesis by Avian Ovarian Cells: Effects of Luteinizing Hormone and Substrate Availability. *Am. J. Physio.* 244 (5), E487–E493.

Matthews, C. E., Fortner, R. T., Xu, X., Hankinson, S. E., Eliassen, A. H., and Ziegler, R. G. (2012). Association between Physical Activity and Urinary Estrogens and Estrogen Metabolites in Premenopausal Women. *J. Clin. Endocrinol. Metab.* 97, 3724–3733. doi:10.1210/jc.2012-1732

Onbaşılar, E. E., Kahraman, M., Güngör, Ö. F., Kocakaya, A., Karakan, T., Pirpanahi, M., et al. (2020). Effects of Cage Type on Performance, Welfare, and Microbiological Properties of Laying Hens during the Molting Period and the Second Production Cycle. *Trop. Anim. Health Prod.* 52, 3713–3724. doi:10.1007/s11250-020-02409-0

Ottinger, M. A., Wu, J., and Pelican, K. (2002). Neuroendocrine Regulation of Reproduction in Birds and Clinical Applications of GnRH Analogues in Birds and Mammals. *Semin. Avian Exot. Pet. Med.* 11, 71–79. doi:10.1053/saep.2002.122896

Pauwels, F. (1960). A New Theory on the Influence of Mechanical Stimuli on the Differentiation of, Supporting Tissue. The Tenth Contribution to the Functional Anatomy and Causal Morphology of the Supporting Structure. *Z. Anat. Entwicklungsgesch.* 121, 478–515.

Petrik, M. T., Guerin, M. T., and Widowski, T. M. (2015). On-farm Comparison of Keel Fracture Prevalence and Other Welfare Indicators in Conventional Cage and Floor-Housed Laying Hens in Ontario, Canada. *Poult. Sci.* 94, 579–585. doi:10.3382/ps/pev039

Philippe, F. X., Mahmoudi, Y., Cinq-Mars, D., Lefrancois, M., Moula, N., Palacios, J., et al. (2020). Comparison of Egg Production, Quality and Composition in Three Production Systems for Laying Hens. *Livest. Sci.* 232, 103917. doi:10.1016/j.livsci.2020.103917

Preisinger, R. (2018). Innovative Layer Genetics to Improve Egg Production. *LOHMANN Inf.* 52 (1), 4–11. doi:10.1080/00071668.2018.1401828

Rodenburg, T. B., Tuyttens, F. A., De Reu, K., Herman, L., Zoons, J., and Sonck, B. (2008). Welfare Assessment of Laying Hens in Furnished Cages and Non-cage Systems: an On-Farm Comparison. *Anim. Welf.* 17 (4), 363–373.

Sechman, A. (2013). The Role of Thyroid Hormones in Regulation of Chicken Ovarian Steroidogenesis. *Gen. Comp. Endocrinol.* 190, 68–75. doi:10.1016/j.ygcen.2013.04.012

Senior, B. E. (1974). Oestradiol Concentration in the Peripheral Plasma of the Domestic Hen from 7weeks of Age until the Time of Sexual Maturity. *J. Reprod. Fert.* 41, 107–112.

Shimmura, T., Hirahara, S., Azuma, T., Suzuki, T., Eguchi, Y., Uetake, K., et al. (2010). Multi-factorial Investigation of Various Housing Systems for Laying Hens. *Brit.Poult. Sci.* 51, 31–42. doi:10.1080/00071660903421167

Squire, M. E., Veglia, M. K., Drucker, K. A., Brzeal, K. R., Hahn, T. P., and Watts, H. E. (2017). Estrogen Levels Influence Medullary Bone Quantity and Density in Female House Finches and Pine Siskins. *Gen. Comp. Endocrinol.* 246 (15), 249–257. doi:10.1016/j.ygcen.2016.12.015

Stratmann, A., Fröhlich, E. K. F., Harlander-Matauschek, A., Schrader, L., Toscano, M. J., Würbel, H., et al. (2015). Soft Perches in an Aviary System Reduce Incidence of Keel Bone Damage in Laying Hens. *Plos One* 10 (3), e0122568. doi:10.1371/journal.pone.0122568

Väänänen, H. K., and Härkötnen, P. L. (1996). Estrogen Anti Bone Metabolism. *Maturitas* 23, 65–69.

Voslarova, E., Hanzalek, Z., Vecerek, V., Strakova, E., and Suchy, P. (2006). Comparison between Laying Hen Performance in the Cage System and the Deep Litter System on a Diet Free Fromanimal Protein. *Acta Veterinaria Brno* 75, 219–225. doi:10.2754/avb200675020219

Wan, Y., Yang, H., Zhang, H., Ma, R., Qi, R., Li, J., et al. (2021). Effects ofDifferent Non-Cage Housing Systems on the Production Performance, Serum Parameters and Intestinal Morphology of Laying Hens. *Animals* 11, 1673. doi:10.3390/ani11061673

Weeks, C. A., Lambton, S. L., and Williams, A. G. (2016). Implications for Welfare, Productivity Andsustainability of the Variation in Reported Levels of Mortality for Laying Hen Flocks Kept Indifferent Housing Systems: a Meta-Analysis of Ten Studies. *PLoS One* 11, e0146394.

Whitehead, C. C., and Fleming, R. H. (2000). Osteoporosis in Cage Layers. *Poult. Sci.* 79, 1033–1041. doi:10.1093/ps/79.7.1033

Whitehead, C. C. (2004). Overview of Bone Biology in the Egg-Laying Hen. *Poult. Sci.* 83, 193–199. doi:10.1093/ps/83.2.193

Wilkins, L., Brown, S. N., Zimmerman, P. H., Leeb, C., and Nicol, C. J. (2004). Investigation of Palpation as a Method for Determining the Prevalence of Keel and Furculum Damage in Laying Hens. *Vet. Rec.* 155 (18), 547–549. doi:10.1136/vr.155.18.547

Wilkins, L. J., McKinstry, J. L., Avery, N. C., Knowles, T. G., Brown, S. N., Tarlton, J., et al. (2011). Influence of Housing System and Design on Bone Strength and Keel Bone Fractures in Laying Hens. *Veterinary Rec.* 169, 414. doi:10.1136/vr.d4831

Williams, T. D., and Ames, C. A. (2004). Top-down Regression of the Avian Oviduct during Lateoviposition in a Small Passerine Bird. *J. Exp. Biol.* 207, 263–268. doi:10.1242/jeb.00740

Williams, T. D., Kitaysky, A. S., and Vezina, F. (2004). Individual Variation in Plasma Estradiol-17β and Androgen Levels during Egg Formation in the European Starling *Sturnus vulgaris*: Implications for Regulation of Yolk Steroids. *Gen. Comp. Endocrinol.* 136, 346–352. doi:10.1016/j.ygcen.2004.01.010

Yilmaz Dikmen, B., İpek, A., Şahan, Ü., Petek, M., and Sözcü, A. (2016). Egg Production Andwelfare of Laying Hens Kept in Different Housing Systems (Conventional, Enriched Cage, and Free Range). *Poult. Sci.* 95, 1564–1572. doi:10.3382/ps/pew082

Yu, J. Y.-L., Campbell, L. D., and Marquardt, R. R. (1971). Sex Hormone Control Mechanisms. I. Effect of Estrogen and Progesterone on Major Cellular Components in Chicken (*Gallus domesticus*) Oviducts. *Can. J. Biochem.* 49 (3), 348–356.

Conflict of Interest: The authors declare that the research was conducted in the absence of any commercial or financial relationships that could be construed as a potential conflict of interest.

Publisher's Note: All claims expressed in this article are solely those of the authors and do not necessarily represent those of their affiliated organizations, or those of the publisher, the editors and the reviewers. Any product that may be evaluated in this article, or claim that may be made by its manufacturer, is not guaranteed or endorsed by the publisher.

frontiers | Frontiers in Physiology

ORIGINAL RESEARCH
published: 22 July 2022
doi: 10.3389/fphys.2022.934660

Subclinical Doses of Combined Fumonisins and Deoxynivalenol Predispose *Clostridium perfringens*–Inoculated Broilers to Necrotic Enteritis

R. Shanmugasundaram[1], D. Adams[2], S. Ramirez[3], G. R. Murugesan[3], T. J. Applegate[2], S. Cunningham[1], A. Pokoo-Aikins[1] and A. E. Glenn[1]*

[1]Toxicology and Mycotoxin Research Unit, U.S. National Poultry Research Center, Agricultural Research Service, U.S. Department of Agriculture, Athens, GA, United States, [2]Department of Poultry Science, University of Georgia, Athens, GA, United States, [3]DSM Animal Nutrition and Health, Kaiseraugst, Switzerland

OPEN ACCESS

Edited by:
Francesca Soglia, University of Bologna, Italy

Reviewed by:
Marco Zampiga, University of Bologna, Italy
Ahmed Ragab Elbestawy, Damanhour University, Egypt

***Correspondence:**
R. Shanmugasundaram
revathi.shan@usda.gov

Specialty section:
This article was submitted to Avian Physiology, a section of the journal Frontiers in Physiology

Received: *02 May 2022*
Accepted: *13 June 2022*
Published: *22 July 2022*

Citation:
Shanmugasundaram R, Adams D, Ramirez S, Murugesan GR, Applegate TJ, Cunningham S, Pokoo-Aikins A and Glenn AE (2022) Subclinical Doses of Combined Fumonisins and Deoxynivalenol Predispose Clostridium perfringens–Inoculated Broilers to Necrotic Enteritis. Front. Physiol. 13:934660. doi: 10.3389/fphys.2022.934660

Fumonisins (FB) and deoxynivalenol (DON) are mycotoxins which may predispose broiler chickens to necrotic enteritis (NE). The objective of this study was to identify the effects of subclinical doses of combined FB and DON on NE. A total of 480 day-old male broiler chicks were divided into four treatment groups; 1) control group (basal diet + *Clostridium perfringens*); 2) necrotic enteritis group (basal diet + *Eimeria maxima* + *C. perfringens*); 3) FB + DON group (basal diet + 3 mg/kg FB + 4 mg/kg DON + *C. perfringens*); and 4) FB + DON + NE group (basal diet + 3 mg/kg FB + 4 mg/kg DON + *E. maxima* + *C. perfringens*). Birds in NE and FB + DON + NE groups received 2.5×10^3 *E. maxima* on day 14. All birds were inoculated with *C. perfringens* on days 19, 20, and 21. On day 35, birds in the NE, FB + DON, and FB + DON + NE groups had 242, 84, and 339 g lower BWG and a 19-, 2-, and 22-point increase in FCR respectively, than in the control group. Subclinical doses of FB + DON increased ($p < 0.05$) the NE lesion scores compared to the control group on day 21. On day 21, birds in the NE, FB + DON, and FB + DON + NE groups had increased ($p < 0.05$) serum FITC-D, lower ($p < 0.05$) jejunal tight junction protein mRNA, and increased ($p < 0.05$) cecal tonsil IL-1 mRNA compared to control group. On day 21, birds in the NE group had decreased ($p < 0.05$) villi height to crypt depth ratio compared to the control group and the presence of FB + DON in NE-induced birds further decreased the villi height to crypt depth ratio. Birds in the NE, FB + DON, and FB + DON + NE groups had increased ($p < 0.05$) *C. perfringens*, lower ($p < 0.05$) *Lactobacillus* loads in the cecal content, and a lower ($p < 0.05$) $CD8^+$: $CD4^+$ cell ratio in the cecal tonsils compared to the control group. It can be concluded that subclinical doses of combined FB and DON predispose *C. perfringens*-inoculated birds to NE, and the presence of FB + DON in NE-induced birds exacerbated the severity of NE.

Keywords: fumonisins, deoxynivalenol, necrotic enteritis, tight junction proteins, immune response, broiler chicken

INTRODUCTION

Corn is one of the major components of poultry feed, and up to 65% of finished poultry feed can be comprised of corn and corn byproducts (Alqaisi et al., 2017). Poultry diets are often contaminated with more than one mycotoxin. Fumonisins (FB) and deoxynivalenol (DON) are secondary mycotoxin metabolites produced by *Fusarium verticillioides* and *Fusarium graminearum*, respectively (Glenn, 2007). According to the 2021 survey by Biomin, FB and DON are the most prevalent mycotoxins in poultry feed samples in North America and were detected in 64% and 47% of poultry diets, respectively (Biomin, 2021). Recent surveys have identified that, on average, the amount of DON in corn and cereal grain was 808 μg/kg and 1,721 μg/kg, respectively; the amount of FB in corn was 2,405 μg/kg. Furthermore, DON and FB can co-occur in poultry feed ingredients, and 92% of feed samples analyzed in 2021 had more than one mycotoxin (Biomin, 2021). Though negative effects of FB have been reported when FB are present at 100 mg/kg in chicken feed, FB has been suggested to cause negative effects even at a lower dose when co-occurring with other mycotoxins such as aflatoxins, DON, and zearalenone in poultry (Ogbuewu, 2011). Co-occurrence of mycotoxins decreases the tolerance to individual mycotoxins and, therefore, the existence of multiple mycotoxins in poultry feed even at subclinical levels can be expected to exacerbate the pathology of individual mycotoxins in poultry.

European Food Safety Authority (EFSA) and Food and Drug Administration (FDA) have set guidelines for maximal permissible levels of major mycotoxins in poultry feed. However, subclinical doses of FB (20 mg/kg diet) and DON (5 mg/kg diet), alone (Antonissen et al., 2014; Antonissen et al., 2015) or in combination (Grenier et al., 2016), cause metabolic and immunological disturbances that amplify the severity of necrotic enteritis (NE), coccidiosis, and increase the susceptibility to bacterial diseases in chickens. Mycotoxin interactions within the animal system are mainly additive, but depending on the endpoint assessment these interactions can also be synergistic or antagonistic (Grenier and Oswald, 2011).

Currently, NE is an economically important disease affecting the modern broiler industry. Subclinical NE affects broilers between 2–5-weeks of age and is characterized by intestinal mucosal damage, with no apparent clinical signs or mortality (Hofacre et al., 2018). Subclinical NE leads to decreased digestion and absorption of nutrients, reduced weight gain, and impaired feed conversion rate in poultry (Immerseel et al., 2004). Coccidiosis and feed contaminated with mycotoxins, particularly FB and DON (Antonissen et al., 2015), are considered to be the predisposing factors for NE. In addition, mycotoxins reduce the efficacy of coccidiosis vaccines and, therefore, contribute to NE incidence in chickens (Broom, 2017). Recent restrictions on the use of antibiotics and ionophores in broiler production led to an increase in the occurrence of NE by altering the composition and microbial balance in the gut microbiome (Smith, 2019). The causative organism for NE is *Clostridium perfringens,* a commensal bacterium in the gastrointestinal tract of healthy broilers. *C. perfringens* loads range up to 1×10^5 CFU/g of digesta in healthy chickens, while in chickens with clinical NE symptoms, *C. perfringens* loads increase to 1×10^6 to 1×10^8 CFU/g of digesta, along with associated toxins that include necrotic toxin enteritis B-like (NetB) (Timbermont et al., 2011; Mora et al., 2020).

In the past, FB below 50 mg/kg feed and DON at 5 mg/kg feed were considered not to cause negative effects in poultry (Dänicke et al., 2001; Filazi et al., 2017). However, recent studies have identified that a combined dose of 20 mg/kg FB and 1.5 mg/kg DON decreases the production performances, causes gut damage, and increases coccidiosis severity (Antonissen et al., 2014; Antonissen et al., 2015; Grenier et al., 2016), which can be expected to predispose the broilers to NE. Information regarding the role of chronic exposure of subclinical doses, even at doses much lower than previous studies, of mycotoxins is lacking. Continuous exposure to mycotoxins is expected to damage the gut wall and increase gut permeability to negatively affect the FDA recommendation on NE, gut health, and immune response in chickens. Therefore, the objective of this study was to evaluate the combined effects of FB (3 mg/kg diet) and DON (4 mg/kg diet) on gut health and immune parameters and evaluate the role of mycotoxins as a predisposing factor in inducing and increasing the severity of a NE in poultry.

TABLE 1 | Ingredient and nutrient composition of basal diets (as-fed basis).

Ingredients (%)	Starter	Finisher
Corn	56.29	64.86
Soybean meal, 48% CP	37.87	28.44
Soybean oil	2.18	3.80
Dicalcium phosphate	1.48	0.84
Calcium carbonate	0.91	0.78
Sodium chloride	0.40	0.40
MHA	0.37	0.32
L-lysine	0.21	0.22
Trace mineral premix	0.10	0.10
Choline chloride (60%)	0.07	0.08
L-threonine	0.06	0.07
Vitamin premix	0.05	0.05
Phytase (500 ftu)	0.01	0.01

Nutrients, vitamins, and minerals were provided in the form and amount described in the NRC, standard reference diet for chickens (Council, 1994).

MATERIALS AND METHODS

Diet Formulation

A non-medicated corn–soybean meal-based mash diet was applied as a basal diet (**Table 1**). The feeding study was divided into two experimental phases: 1) d0–18, starter feed, and 2) d19–35, finisher feed. Two strains of *Fusarium*, *F. graminearum* strain PH-1 and *F. verticillioides* strain M3125 were cultured for DON and FB production, respectively (Altpeter and Posselt, 1994). In brief, *Fusarium* strains were cultured separately in carboxymethyl cellulose liquid media and shaken for 5 days (*F. verticillioides*) or 7 days

TABLE 2 | Analyzed mycotoxin content of experimental diets.

	Aflatoxin (ppm)	Fumonisin (ppm)	Deoxynivalenol (ppm)	Zearalenone (ppm)	Nivalenol (ppm)
Starter diet					
Control	0.04[a]	0.4[b]	0.1	<0.05	<0.1
Treatment	0.03[a]	2.8[b]	4.3	0.3	<0.1
Finisher diet					
Control	0.003[a]	1.5[b]	0.2	0.07	<0.1
Treatment	0.002[a]	2.9[b]	4.0	0.4	0.2

[a]*Total aflatoxins (B1 + B2).*
[b]*Total fumonisins (B1 + B2 + B3).*
The final diets were analyzed by LC-MS/MS, at Romer Labs, Union, MO, United States.

TABLE 3 | Primers and PCR conditions for PCR.

Gene	Primer sequence1 (5′- 3′)	Annealing temperature (°C)	Reference
IL1-β	F: TCCTCCAGCCAGAAAGTGA R: CAGGCGGTAGAAGATGAAGC	57.5	Shanmugasundaram and Selvaraj. (2012)
IL10	F: CATGCTGCTGGGCCTGAA R: CGTCTCCTTGATCTGCTTGATG	57.5	Shanmugasundaram and Selvaraj. (2012)
LITAF	F: ATCCTCACCCCTACCCTGTC R: GGCGGTCATAGAACAGCACT	55	Markazi et al. (2019)
IFN-γ	F: GGCGTGAAGAAGGTGAAAGA R: CCTCTGAGACTGGCTCCTTTT	57.4	Shanmugasundaram et al. (2021)
RPS-13	F: CAAGAAGGCTGTTGCTGTTCG R: GGCAGAAGCTGTCGATGATT	55	Shanmugasundaram et al. (2019c)
Claudin-1	F: CATACTCCTGGGTCTGGTTGGT R: GACAGCCATCCGCATCTTCT	55	Chen et al. (2017)
Claudin-2	F: CCTGCTCACCCTCATTGGAG R: GCTGAACTCACTCTTGGGCT	55	Li et al. (2015)
Zona occluden-1	F: TGTAGCCACAGCAAGAGGTG R: CTGGAATGGCTCCTTGTGGT	56	Zhang et al. (2017)
C. perfringens	F: AAAGGAAGATTAATACCGCATAA R: ATCTTGCGACCGTACTCCCC	55	Shanmugasundaram et al. (2020)
Lactobacillus	F: CATCCAGTGCAAACCTAAGAG R: CCACCGTTACACCGGGAA	55	Wang et al. (1996)
Bifidobacterium	F: GGGTGGTAATGCCGGATG R: CCACCGTTACACCGGGAA	57	Langendijk et al. (1995)

(*F. graminearum*), and spores were collected. Fungal spores were added separately to rice media and incubated until mycotoxin content was analyzed. The homogenized rice cultures with FB and DON were mixed with a small portion of the basal diet and re-mixed with the appropriate amount of basal feed to create the experimental diets. The starter diet (d0–18) and the finisher diet were formulated to contain 3 mg/kg FB and 4 mg/kg DON, respectively. The final diets were analyzed by LC-MS-MS to determine the actual content of FB and DON and the content of other major mycotoxins (Romer Labs, Union, MO, United States). The mycotoxin content of the formulated experimental diet is provided in **Table 2**.

Birds and Housing

This 35-day feeding trial was conducted with 480 day-old male Ross × Ross 708 strain broiler chicks (Aviagen, Blairsville, GA, United States). The animal care practices and use procedures were followed under the Guide for the Care and Use of Agricultural Animals in Research and Teaching (McGlone, 2010). All animal protocols were approved by the Institutional Animal Care and Use Committee at the Southern Poultry Research Group, Athens, GA. The birds were raised under the supervision of a licensed poultry veterinarian. All birds were euthanized by methods approved by the American Veterinary Medical Association (AVMA). Day-old broiler chicks were raised in 1.5 m × 1.5 m floor pens (stocking density of 15 birds/m^2) on new shavings/litter following standard industry practice in North America and raised under ambient humidity. Chickens were weighed individually and randomly distributed into either one of the four treatment groups. The experimental treatment groups were 1) control group (basal diet + *C. perfringens* challenge), 2) NE group (basal diet + *E. maxima* + *C. perfringens*), 3) FB + DON group (basal diet + 3 mg/kg FB +4 mg/kg DON + *C. perfringens*), and 4) FB + DON + NE group (basal diet + 3 mg/kg FB + 4 mg/kg DON + *E. maxima* + *C. perfringens*). Each treatment was replicated in 8 pens with 15 birds/pen in a completely randomized design. Chicks had *ad libitum* access to the feed and water throughout the experimental period. The mortality of the birds was recorded daily. The birds were

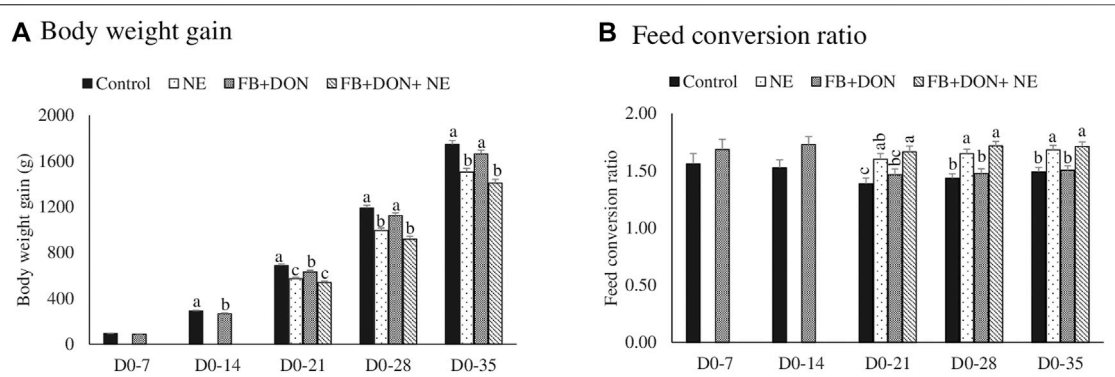

FIGURE 1 | Effect of subclinical dose of FB + DON and *E. maxima/C. perfringens* challenge on production performances. Day-old chicks were distributed into four treatment groups: control, necrotic enteritis (NE), fumonisin + deoxynivalenol (FB + DON), and FB + DON + NE groups. Birds in the NE and FB + DON + NE groups received 2.5×10^3 *Eimeria maxima* oocyst per bird on day 14. All birds received 1×10^8 CFU/bird of *Clostridium perfringens* on days 19, 20, and 21. Body weight and feed consumption was measured on days 0, 7, 14, 21, 28, and 35 of age to calculate body weight gain (Panel 1A) and feed consumption ratio (Panel 1B). Mortality-corrected body weight gain and feed conversion ratio are presented. Bars (+SEM) without a common superscript differ significantly ($p < 0.05$). $n = 8$ pens of 15 birds/pen.

TABLE 4 | Effect of subclinical dose of FB + DON and *E. maxima/C. perfringens* challenge on necrotic enteritis lesion score at 21 days of age.

Treatment	Score 0	Score 1	Score 2	Score 3	Rank scores mean	Chi sq. *p*-value
Control	21	3	0	0	22.4	0.01
NE	1	14	9	0	60.5	
FB + DON	18	6	0	0	37.3	
FB + DON + NE	0	9	15	0	73.8	

Day-old chicks were distributed into four treatment groups: control, necrotic enteritis (NE), fumonisin + deoxynivalenol (FB + DON), and FB + DON + NE groups. Birds in the NE and FB + DON + NE groups received 2.5 × 10³ Eimeria maxima *oocyst per bird on day 14. All birds received 1 × 10⁸ CFU/bird of* Clostridium perfringens *on days 19, 20, and 21. On day 21, three birds were scored for NE lesion scores on a 0 to 3 scale wherein 0 is normal, 1 shows slight mucus covering the small intestine, 2 has a necrotic small intestinal mucosa, and 3 shows sloughed cells and blood in the small intestinal mucosa and contents. Lesion scores were analyzed by a non-parametric test, and Wilcoxon/Kruskal–Wallis rank-sum test was used to separate the means.*

housed in floor pens equipped with nipple-type waterers and thermostatically controlled heaters.

Production Performances and NE Lesion Score

On day 14, 2.5×10^3 *Eimeria maxima* sporulated oocysts/bird were mixed in the feed of NE and FB + DON + NE groups. On days 19, 20, and 21, birds in all treatment groups were challenged with 1×10^8 CFU/bird *C. perfringens* (strain #6) through the feed to target 3%–5% NE mortality as described earlier (Hofacre et al., 1998). Before the *C. perfringens* challenge, feed and water were withdrawn for 4 h and 2 h, respectively. Three birds from each pen were randomly sacrificed and examined for the NE lesion score on day 21. Lesion scoring was based on a 0 to 3 scale as described earlier (Hofacre et al., 1998), wherein 0 is normal, 1 is a slight mucus covering the small intestine, 2 is a necrotic small intestinal mucosa, and 3 is a sloughed cells and blood in the small intestinal mucosa and contents. Bodyweight and feed intake were measured at 0, 7, 14, 21, 27, and 35 days of age. Average feed intake and body weight gain (BWG) were corrected for mortality for calculating the feed conversion ratio (FCR) for each pen.

Gut Permeability to FITC-Dextran

Gut permeability was measured using the FITC-D assay as described earlier (Kuttappan et al., 2015). On days 21, 28, and 35, one bird/pen ($n = 8$) was orally gavaged with 1 ml of fluorescein isothiocyanate dextran (FITC-D, MW 4000; Sigma-Aldrich, United States) 2.2 mg/bird. 2 h later, the birds were euthanized, and blood was collected by cardiac puncture. Blood samples were centrifuged at 450 × g for 10 min to separate the serum from red blood cells. The serum was diluted in PBS with pH 7.4 at a 1:1 ratio. The serum FITC-D concentration was determined based on a standard curve. A standard curve with 0, 0.2, 0.4, 0.6, 0.8, 1.0, and 2 μg/ml FITC-D was drawn using Gen5 software on the same plate as the samples. The samples and standards were measured at an excitation wavelength of 485 nm and emission wavelength of 528 nm (Synergy HT, multi-mode microplate reader, BioTek Instruments, Inc., VT).

Spleen and Cecal Tonsil $CD8^+$: $CD4^+$ Ratio

On days 21, 28, and 35, post-challenge, the effect of FB and DON on the spleen and cecal tonsil $CD4^+$ and $CD8^+$ cell percentages were determined by flow cytometry as described previously (Shanmugasundaram et al., 2015). In brief, single-cell

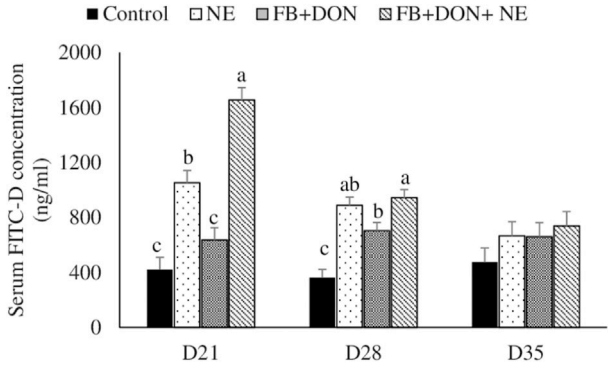

FIGURE 2 | Effect of subclinical dose of FB + DON and *E. maxima/C. perfringens* challenge on gut permeability to FITC-dextran. Day-old chicks were distributed into four treatment groups: control, necrotic enteritis (NE), fumonisin + deoxynivalenol (FB + DON), and FB + DON + NE groups. Birds in the NE and FB + DON + NE groups received 2.5×10^3 *Eimeria maxima* oocyst per bird on day 14. All birds received 1×10^8 CFU/bird of *Clostridium perfringens* on days 19, 20, and 21. One bird/pen was orally gavaged with 2.2 mg/bird of 4,000 MW fluorescein isothiocyanate dextran (FITC-D), and blood was collected 2 h later. Serum FITC-D concentration was determined in a microplate reader. Bars (+SEM) without a common superscript differ significantly ($p < 0.05$). $n = 8$ (8 pens of 15 birds/pen).

suspensions from the spleen and cecal tonsils were enriched for mononuclear cells by density centrifugation over Histopaque (1.077 g/ml, Sigma-Aldrich, St. Louis, MO) for 15 min at 400 g. The cells were incubated with a 1:250 dilution of fluorescent-isothiocyanate conjugated mouse anti-chicken $CD4^+$ (Southern Biotech, Birmingham, AL), 1:450 dilution of phycoerythrin-conjugated mouse anti-chicken $CD8^+$ (Southern Biotech, Birmingham, AL), and 1:200 dilution of unlabeled mouse IgG for 15 min. The unbound antibodies were removed by centrifugation, the percentages of $CD4^+$ and $CD8^+$ cells were analyzed using a flow cytometer (Guava EasyCyte, Millipore, MA), and $CD8^+$: $CD4^+$ ratio was calculated.

Jejunal Tight Junction Protein and Cecal Tonsil Cytokine mRNA Expression

On days 21, 28, and 35, 1 bird per pen ($n = 8$) was euthanized by cervical dislocation. A portion of distal-jejunum and proximal ileum (1 cm proximal and 1 cm distal to the Meckel's diverticulum) and cecal tonsils were collected in cryovials containing RNAlater® (Ambion Inc., Austin, TX, United States) and stored at −70°C until further analysis. The jejunum was analyzed for claudin-1, claudin-2, and zona-occluden-1 tight junction protein mRNAs, and cecal tonsils were analyzed for pro-and anti-inflammatory cytokines IL-1β, IL-10, LITAF, and IFN-γ mRNA expression, as described previously (Shanmugasundaram and Selvaraj, 2012).

Total RNA was extracted from all experimental groups using the TRI reagent (Molecular Research Center, Cincinnati, OH) following the manufacturer's instructions. RNA concentration and purity were determined using an Epoch spectrophotometer (BioTek, Winooski, VT, United States), using the 260/280 and 260/230 ratios. 2 mg RNA was reverse transcribed into cDNA and analyzed for IL-1β, IL-10, LITAF, IFN-γ, claudin-1, claudin-2, and zona-occluden-1 by real-time PCR (CFX96 Touch Real-Time System, BioRad, Hercules, CA) using SYBR Green. Primer sequences and annealing temperature are provided in **Table 3**. Each well contained 10 µl SYBR Green PCR master mix, 7 µl RNAse-free water using C1000 TouchTM Thermal cycler (BioRad, Hercules, CA), 2 µl (~600 ng/µl) cDNA, 0.5 µl forward primer (5 µM), and 0.5 µl reverse primer (5 µM). To perform real-time PCR, the following settings were used for all genes: an initial denaturation of 95°C for 10 min (1 cycle); followed by 95°C for 15 s; and 60°C for 45 s (40 cycles). The melting profile was determined by heating samples at 65°C for 30 s and then increasing the temperature at a linear rate of 10°C/s to 95°C while continuously monitoring fluorescence. Housekeeping genes of β-actin, glyceraldehyde-3-phosphate dehydrogenase (GAPDH), and ribosomal protein S13 (RPS13) were selected, and the stability was analyzed using Normfinder software (Department of Molecular Medicine, Aarhus University Hospital, Denmark) as described previously (Shanmugasundaram et al., 2018). The RPS13 gene was selected for data normalization because it was the most stable expression among the set of housekeeping genes analyzed for normalization. The cecal tonsil IL-1β, IL-10, LITAF, and IFN-γ, the jejunal claudin-1, claudin-4, and zona-occluden-1 mRNAs were normalized with RPS13. The $2^{-\Delta\Delta Ct}$ method, as previously described (Livak and Schmittgen, 2001), where Ct is the threshold cycle, was used to calculate the mRNA fold change. The fold change was calculated as $2^{(Ct\ Sample\ -\ housekeeping)}/2^{\ (Ct\ Reference\ -\ housekeeping)}$. The reference group was the control group.

C. perfringens, Total *Lactobacillus,* and Total *Bifidobacteria* Loads in the Cecal Content

On days 21, 28, and 35, cecal content from one bird/pen ($n = 8$) was collected and stored at −20°C until further use. The DNA from the cecal microflora DNA was extracted as described earlier (Amit-Romach et al., 2004; Shanmugasundaram et al., 2019a). The DNA pellet was resuspended in TE buffer (10 mM Tris-HCl, 1 mM EDTA, pH 8.0) and stored at −20°C until further use. The final concentration of the isolated DNA was determined using an Epoch spectrophotometer (BioTek, Winooski, VT, United States). The DNA samples were diluted to a final concentration of 100 ng/µl. The primers for *Lactobacillus*, *Bifidobacterium*, and *C. Perfringens* were adapted from an earlier publication (Amit-Romach et al., 2004). The Ct values were converted into CFU/g using a standard curve as described previously (Shanmugasundaram et al., 2019b). The PCR efficiency and the slope and intercept of the standard curve were determined by the CFX software (Bio-Rad, Hercules, CA). The PCR efficiency of the *C. perfringens*, *Lactobacillus*, and *Bifidobacteria* standard curve analysis was 98%, 99%, and 99%, respectively.

Jejunal and Ileal Histomorphology

On 21, 28, and 35 days, jejunal and ileal samples were collected from one bird/pen ($n = 8$) from each replication post-challenge. Approximately 4 cm of jejunal and ileal samples were cut proximal

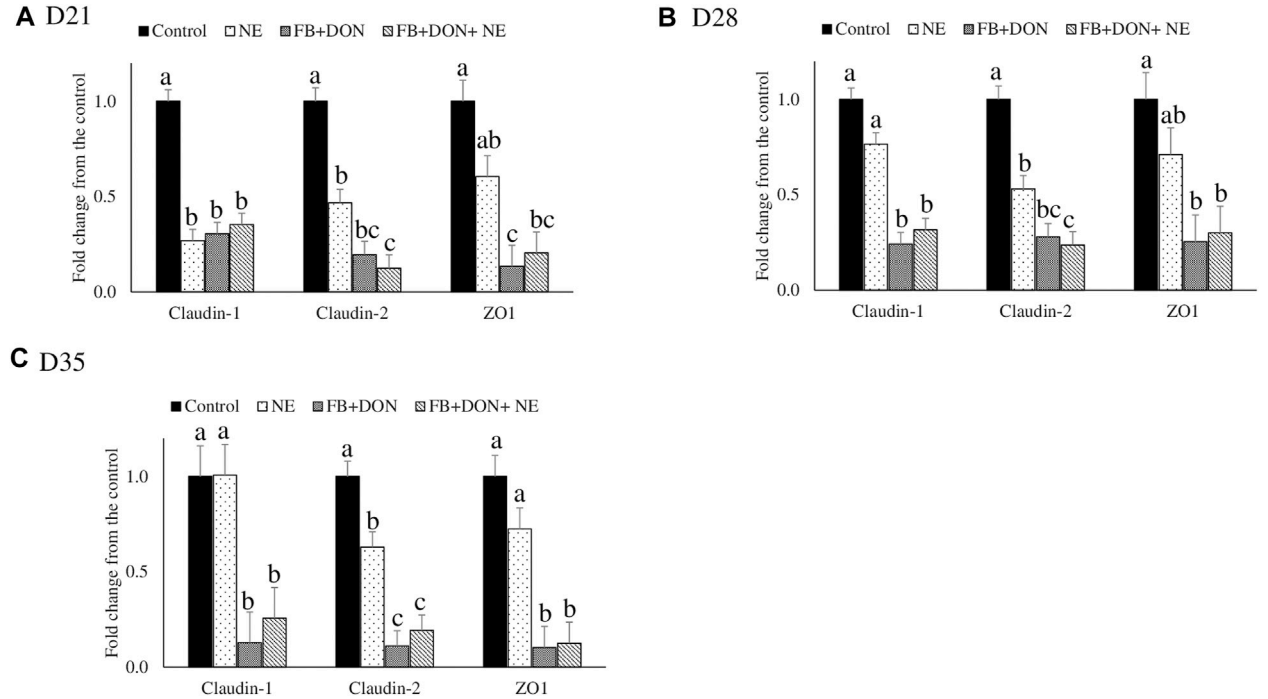

FIGURE 3 | Effect of subclinical dose of FB + DON and *E. maxima/C. perfringens* challenge on jejunal tight junction protein mRNA expression. Day-old chicks were distributed into four treatment groups: control, necrotic enteritis (NE), fumonisin + deoxynivalenol (FB + DON), and FB + DON + NE groups. Birds in the NE and FB + DON + NE groups received 2.5×10^3 *Eimeria maxima* oocyst per bird on day 14. All birds received 1×10^8 CFU/bird of *Clostridium perfringens* on days 19, 20, and 21. Tight junction protein mRNA content was analyzed after correcting for the housekeeping gene RPS13 mRNA content and normalizing to the mRNA content of the control group at D21 **(A)**, D28 **(B)** and D35 **(C)**, so all bars represent fold change compared to the control group. Bars (+SEM) without a common superscript differ significantly ($p < 0.05$). $n = 8$ (8 pens of 15 birds/pen).

and distal to the Meckel's diverticulum and stored in buffered formalin. The jejunal and ileal samples were processed at room temperature in a graded series of alcohols (15 min in 50% ethanol, 15 min in 70% ethanol, 15 min in 96% ethanol, and 30 min in 100% ethanol with one change at 15 min), cleared in Pro-par (Anatech, Battle Creek, MI) for 45 min with 2 changes at 15 and 30 min, and infiltrated with paraffin at 60°C overnight with one change at 15 min using a tissue processor (Sakura Finetek USA, Inc., Torrance, CA, United States). Paraffin blocks were cut into 5-µm cross-sections and mounted on super frost slides (Thermo Fisher Scientific, Waltham, MA, United States). Slides were then stained with hematoxylin and eosin. Cross-sections were viewed using the cellSens Imaging software (Olympus America, Central Valley, PA) to measure villi length and crypt depth. Ten intact lamina propria villi and crypts per section and 5 sections per sample were analyzed as described earlier (Shanmugasundaram et al., 2020). The tip of the villus to the villus–crypt junction was measured as villus height. The crypt depth was defined by the depth of the invagination between adjacent villi. All the samples in a time point were collected from the same bird, except for the gut permeability analysis for which a second bird was used.

Statistical Analysis

A one-way ANOVA (JMP Pro 15 software, Cary, NC) was used to examine the effects of the subclinical dose of FB + DON on dependent variables, with the pen being considered as the experimental unit. When the main effects were significant ($p < 0.05$), differences between means were analyzed by Tukey's least-square means comparison. Values reported are least-squares means ± SEM. The lesion scores were analyzed by a non-parametric test, and a Wilcoxon/Kruskal–Wallis rank-sum test was used to separate the means. The heatmap was rendered with JMP's plotting library (Šefcová et al., 2020).

RESULTS

Effect of Subclinical Dose of FB + DON and *E. maxima/C. perfringens* Challenge on Production Performances

There were significant ($p < 0.05$) treatment effects on body weight gain on days 14, 21, 28, and 35 (**Figure 1A**). On day 14, birds in the FB + DON had lower BWG compared to the birds in the control group. On day 35, birds in the NE and FB + DON + NE groups had 242 g ($p < 0.05$) and 339 g ($p < 0.05$) lower BWG than the birds in the control group, respectively.

There were significant ($p < 0.05$) treatment effects on the FCR on days 21, 28, and 35 (**Figure 1B**). On day 14, birds in the FB + DON group had 21 points ($p = 0.05$) increase in FCR compared to the birds in the control group. On day 35, birds in the NE and FB

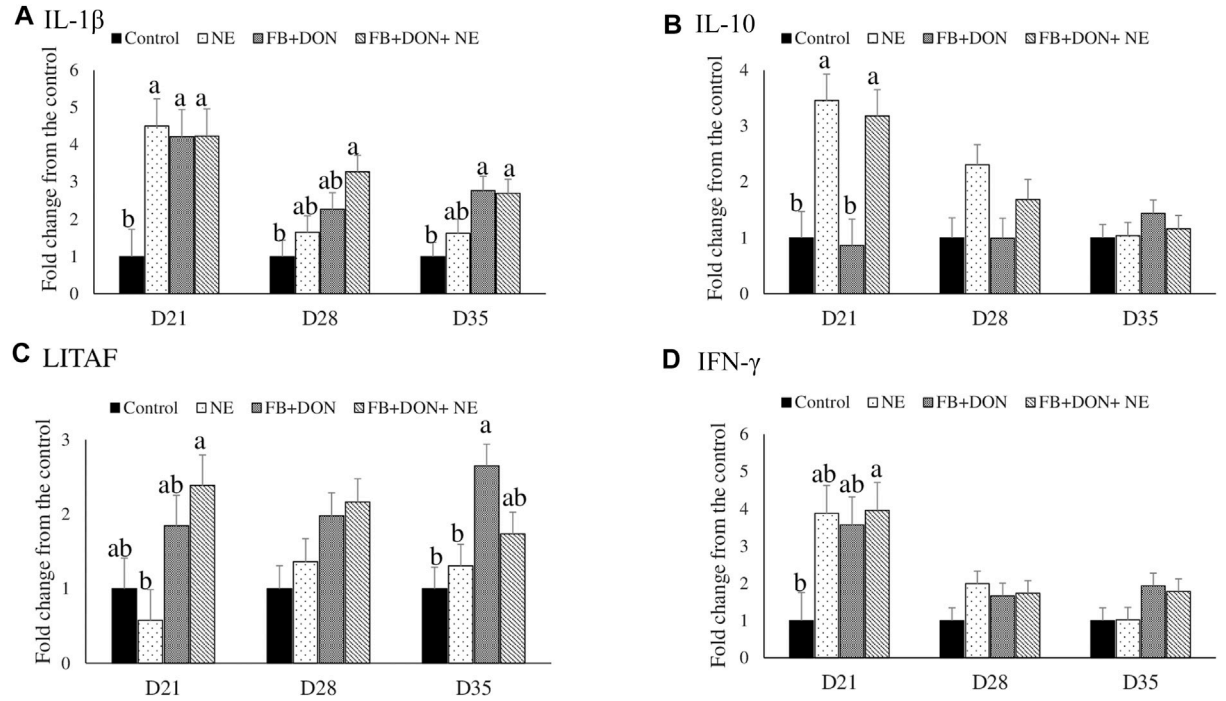

FIGURE 4 | Effect of subclinical dose of FB + DON and *E. maxima/C. perfringens* challenge on cecal tonsil cytokine mRNA expression. Day-old chicks were distributed into four treatment groups: control, necrotic enteritis (NE), fumonisin + deoxynivalenol (FB + DON), and FB + DON + NE groups. Birds in the NE and FB + DON + NE groups received 2.5×10^3 *Eimeria maxima* oocyst per bird on day 14. All birds received 1×10^8 CFU/bird of *Clostridium perfringens* on days 19, 20, and 21. IL-1β, IL-10, LITAF, and IFN-γ mRNA content was analyzed after correcting for the housekeeping gene RPS13 mRNA content and normalizing to the mRNA content of the control group, so all bars represent fold change compared to the control group. Bars (+SEM) without a common superscript differ significantly ($p < 0.05$). $n = 8$ (8 pens of 15 birds/pen).

+ DON + NE groups had 19 points and 22 points significant increase in FCR than those in the control group.

Effect of Subclinical Dose of FB + DON and *E. maxima/C. perfringens* Challenge on NE Lesion Score

There were significant ($p < 0.05$) treatment effects on the NE lesion score on day 21 (**Table 4**). Birds in the control group had the lowest Wilcoxon/Kruskal–Wallis score means for lesion scores. In birds with induced NE, 4.2% (1 out of 24) had a NE lesion score of 0, 58.3% (14 out of 24) had a NE lesion score of 1, 37.5% (9 out of 24) had a NE lesion score of 2, and 0% had a NE lesion score of 3. In birds exposed to FB + DON and induced with NE, 0% had a NE lesion score of 0 , 37.5% (9 out of 24) had a NE lesion score of 1, 62.5% (15 out of 24) had a NE lesion score of 2, and 0% had a NE lesion score of 3. Birds in the NE group had higher ($p < 0.05$) Wilcoxon/Kruskal–Wallis Score Means for lesion scores than scores observed in the control group. Subclinical dose of FB + DON increased ($p < 0.05$) the Wilcoxon/Kruskal–Wallis Score Means for lesion scores compared with the control group on day 21. The presence of FB + DON in NE-challenged birds increased ($p < 0.05$) the Wilcoxon/Kruskal–Wallis Score Means for lesion scores compared to the NE group.

Effect of Subclinical Dose of FB + DON and *E. maxima/C. perfringens* Challenge on Gut Permeability to FITC-Dextran

There were significant ($p < 0.05$) treatment effects on the serum FITC-D concentration on days 21 and 28 (**Figure 2**). On day 21, birds in the NE, FB + DON, and FB + DON + NE groups had a 150% ($p < 0.05$), 51% ($p > 0.05$), and 293% ($p < 0.05$) increase in serum FITC-D compared to the birds in the control group. Similar trends were observed on day 28. The presence of FB + DON in NE-challenged birds increased ($p < 0.05$) the serum FITC-D concentration further by 57%, compared with NE group on day 21.

Effect of Subclinical Dose of FB + DON and *E. maxima/C. perfringens* Challenge on Jejunal Tight Junction Protein mRNA Expression

There were significant ($p < 0.05$) treatment effects on the jejunal mRNA expression on days 21, 28, and 35 (**Figure 3**). On day 21, birds in the NE, FB + DON, and FB + DON + NE groups had lower claudin-1, claudin-2, and zona occludens-1 mRNA expression compared to the birds in the control group. On days 28 and 35, birds in the NE group had similar claudin-1 and zona occludens-1 mRNA expression when compared with the control group, but birds in the FB + DON and FB + DON + NE groups still had

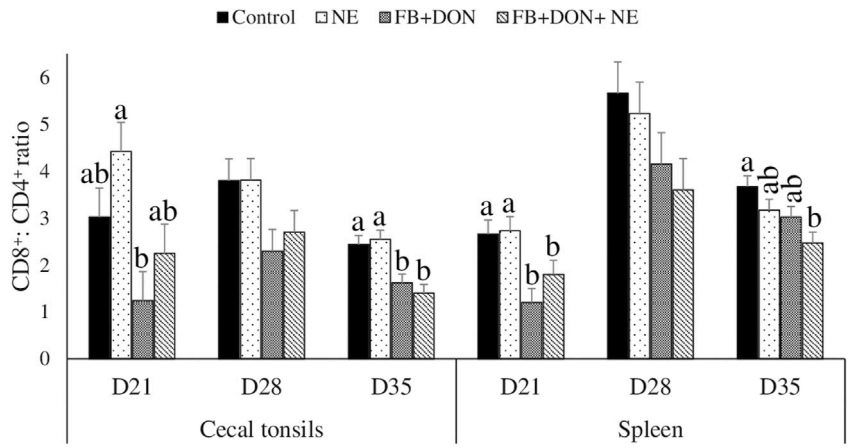

FIGURE 5 | Effect of subclinical dose of FB + DON and *E. maxima/C. perfringens* challenge on the spleen and cecal tonsil $CD8^+$: $CD4^+$ ratio. Day-old chicks were distributed into four treatment groups: control, necrotic enteritis (NE), fumonisin + deoxynivalenol (FB + DON), and FB + DON + NE groups. Birds in the NE and FB + DON + NE groups received 2.5×10^3 *Eimeria maxima* oocyst per bird on day 14. All birds received 1×10^8 CFU/bird of *Clostridium perfringens* on days 19, 20, and 21. $CD4^+$ and $CD8^+$ cells were identified using fluorescent-linked anti-chicken CD4 and CD8 in a flow cytometer. Bars (+SEM) without a common superscript differ significantly ($p < 0.05$). $n = 8$ (8 pens of 15 birds/pen).

downregulated claudin-1 and zona occludens-1 mRNA compared to the control group. Similar trends were observed on days 28 and 35.

Effect of Subclinical Dose of FB + DON and *E. maxima/C. perfringens* Challenge on Cytokine mRNA Expression

There were significant ($p < 0.05$) treatment effects on the cecal tonsil IL-1β, IL-10, LITAF, and IFN-γ jejunal mRNA expression on day 21 (**Figure 4**). On day 21, birds in the NE, FB + DON, and FB + DON + NE groups had an approximately 4-fold increase in IL-1β mRNA compared to the birds in the control group. Similar trends were observed on days 28 and 35.

On day 21, birds in the NE and FB + DON + NE groups had an approximately 3-fold increase in IL-10 mRNA compared to the birds in the control group.

On day 21, birds in the FB + DON + NE group had higher LITAF mRNA compared to the birds in the NE group. On day 35, birds in the FB + DON group had higher LITAF mRNA compared to the birds in the control group.

On day 21, birds in the FB + DON + NE group had an approximately 4-fold increase in IFN-γ mRNA compared to the birds in the control group.

Effect of Subclinical Dose of FB + DON and *E. maxima/C. perfringens* Challenge on the Spleen and Cecal Tonsil $CD8^+$: $CD4^+$ Ratio

On day 21, birds in the FB + DON group had a lower $CD8^+$: $CD4^+$ ratio in the cecal tonsils compared to the birds in the control group (**Figure 5**). On day 35, birds in the FB + DON and FB + DON + NE groups had a lower $CD8^+$: $CD4^+$ ratio in the cecal tonsils compared to the birds in the control group

On day 21, birds in the FB + DON and FB + DON + NE groups had a lower $CD8^+$:$CD4^+$ ratio in the spleen compared to that in the birds in the control group. On day 35, birds in the FB + DON + NE group had a lower $CD8^+$:$CD4^+$ ratio in the spleen compared to the birds in the control group.

Effect of Subclinical Dose of FB + DON and *E. maxima/C. perfringens* Challenge on Jejunal and Ileal Histomorphology

On day 21, birds in the NE group had a 24% decrease ($p > 0.05$) in villi height to crypt depth ratio compared to the birds in the control group and the presence of FB + DON in NE-induced birds further decreased the villi height to crypt depth ratio by 8.4% when compared with NE group (**Figure 6**). Similar results were observed in the ileum on day 21.

Effect of Subclinical Dose of FB + DON and *E. maxima/C. perfringens* Challenge on *C. perfringens*, *Lactobacillus* spp., and *Bifidobacterium* spp. Loads in the Cecal Content

On days 21, 28, and 35, birds in the NE, FB + DON, and FB + DON + NE groups had an approximately 1.3 Log increase in *C. perfringens* loads in the cecal tonsils compared to the birds in the control group (**Figure 7**).

On day 21, birds in the FB + DON group had lower ($p < 0.05$) *Lactobacillus* spp. compared to the birds in the control group.

Heat Map Representing Pearson's Correlation Coefficient Matrix Between Cytokine Amounts and Body Weight Gain

The negative value of Pearson's coefficient indicated that IL-1β and IL10- mRNA expression on days 21 and 28 were inversely related to body weight (**Figure 8**).

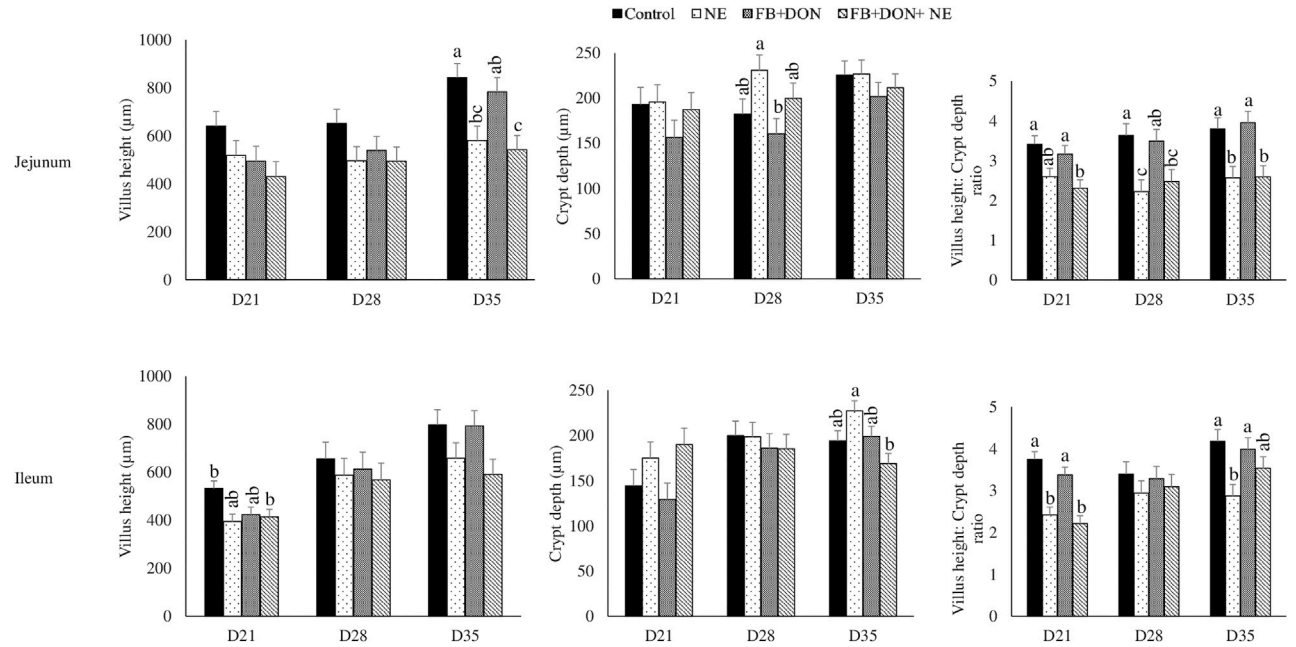

FIGURE 6 | Effect of subclinical dose of FB + DON and *E. maxima/C. perfringens* challenge on jejunal and ileal histomorphology. Day-old chicks were distributed into four treatment groups: control, necrotic enteritis (NE), fumonisin + deoxynivalenol (FB + DON), and FB + DON + NE groups. Birds in the NE and FB + DON + NE groups received 2.5×10^3 *Eimeria maxima* oocyst per bird on day 14. All birds received 1×10^8 CFU/bird of *Clostridium perfringens* on days 19, 20, and 21. Jejunal and ileal sections were stained with hematoxylin and eosin. Villi height and crypt depth were measured using cellSens Imaging software, and villi height:crypt depth ratio was calculated. Bars (+SEM) without a common superscript differ significantly ($p < 0.05$). $n = 8$ (8 pens of 15 birds/pen).

DISCUSSION

Corn is the major energy source in poultry feed and constitutes 50%–80% of the finished poultry feeds in the United States and Europe (Guerre, 2016). Mycotoxins are ubiquitous in nature (Shimshoni et al., 2013), and under practical conditions, it is difficult to produce clean corn without mycotoxin contamination. In this study, the starter basal diets in the control group were naturally contaminated with 40 µg/kg aflatoxin, 400 µg/kg FB, and 100 µg/kg DON, and the finisher basal diets in the control group were contaminated with 3 µg/kg aflatoxin, 1,500 µg/kg FB, and 200 µg/kg DON. Because there is an increase in the occurrence of mycotoxins contamination of poultry feed under field conditions, there is a growing concern regarding the negative effects of combined mycotoxins, even when present at subclinical doses, on gut health. Hence, this study aimed to identify whether the combined presence of FB and DON at subclinical concentration predisposed broiler chickens to NE and acerbated the severity of NE lesions.

In the current study, a combined dose of 3 mg/kg FB and 4 mg/kg DON decreased the chickens' body weight on day 14 even before the birds were inoculated with *E. maxima*. In birds that were induced with NE, FB and DON further decreased the body weight gain. Our data suggest that a combined dose of 3 mg/kg FB and 4 mg/kg DON in the poultry diet increased gut permeability and decreased villi height to crypt depth ratio, which can be expected to decrease body weight and increase the FCR. An earlier study identified that combination of FB and DON either at 20 and 1.5 mg/kg or 20 and 5.0 mg/kg feed, respectively, increases the feed conversion ratio. A similar result was observed in piglets when feeding 6 mg/kg FB and 3 mg/kg DON in combination, which decreased the production performance (Grenier and Oswald, 2011). Broilers exposed to multiple mycotoxins at subclinical doses in the starter to finisher diets exhibit decreased production broiler performance and impaired health (Wang et al., 2005). Earlier reports have identified that poultry feed contaminated with 5 mg/kg DON alone did not alter the chicken production performance (Awad et al., 2011). Similarly, FB alone at 300 mg (Brown et al., 1992) or 50 mg (Yu et al., 2022) did not cause a decrease in production performance in broiler birds. Considering that when FB or DON was individually fed, they did not decrease the production performance even when present at 300 mg/kg and 5 mg/kg. It should be noted that subclinical doses of FB + DON had numerical changes, rather than statistical significance, on production performances. It has been suggested that the interpretation of *p* values should not be a dichotomous conclusion as either significant or nonsignificant, but it should be interpreted based on the real-world implication of the observed change in the data points (Andrade, 2019). FB + DON decreased the body weight gain by 87 g, further decreased the body weight by 97 g, and worsened the FCR by 3 points in birds induced with NE on day 35. FB + DON at subclinical dose can thus lead to a loss of up to 184 g per bird, which accounts for approximately 10.5% of live body weight. Thus, it can be concluded that in this present study, the combined

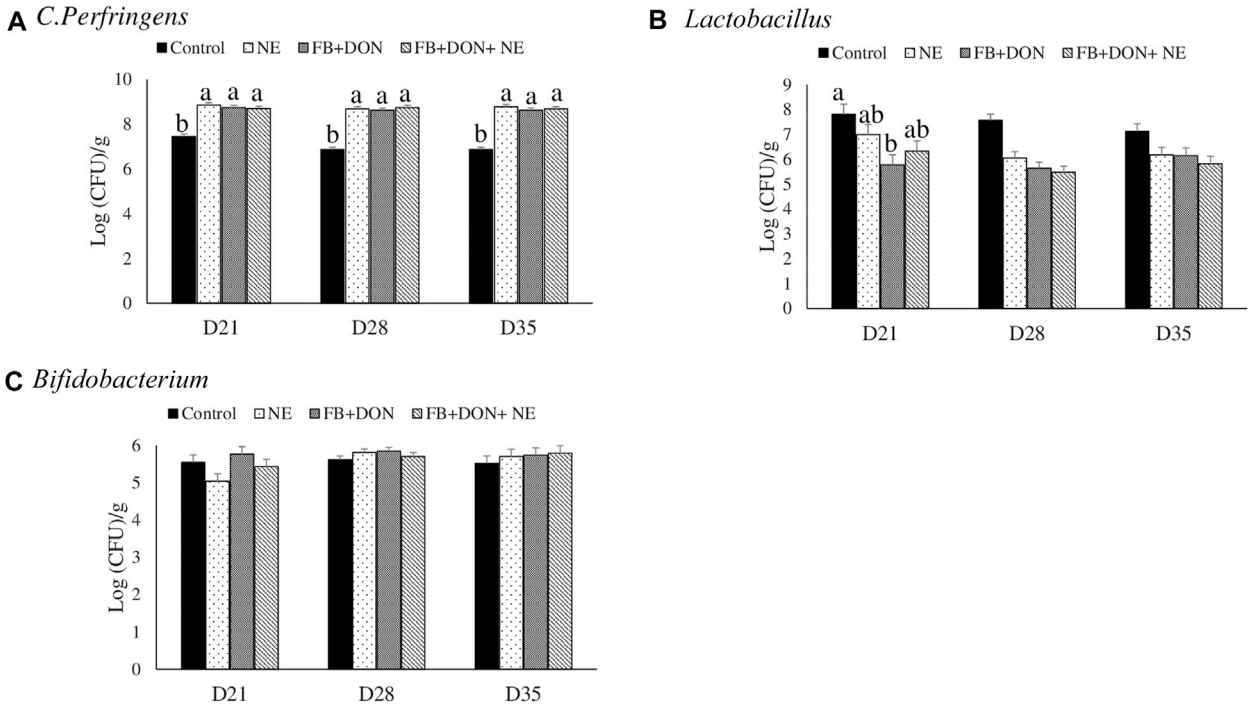

FIGURE 7 | Effect of subclinical dose of FB + DON and *E. maxima/C. perfringens* challenge on *C. perfringens*, total *Lactobacillus,* and total *Bifidobacteria* loads in the cecal content. Day-old chicks were distributed into four treatment groups: control, necrotic enteritis (NE), fumonisin + deoxynivalenol (FB + DON), and FB + DON + NE groups. Birds in the NE and FB + DON + NE groups received 2.5×10^3 *Eimeria maxima* oocyst per bird on day 14. All birds received 1×10^8 CFU/bird of *Clostridium perfringens* on days 19, 20, and 21. Cecal content was analyzed for *C. perfringens*, **(A)** total *Lactobacillus,* **(B)** and total *Bifidobacteria* **(C)** through PCR. Bars (+SEM) without a common superscript differ significantly ($p < 0.05$). $n = 8$ (8 pens of 15 birds/pen).

dose of DON and FB had a synergistic negative effect on body weight gain and feed conversion ratio.

The presence of both FB and DON increased the severity of the NE lesions in birds induced with NE. However, FB and DON did not increase NE mortality (23.3% and 21.2% mortality in FB + DON and FB + DON + NE group). In the NE model studied, the control group was inoculated with *C. perfringens* and, hence, the *C. perfringens* loads were approximately 7 logs/g of cecal content. In the absence of accompanying intestinal wall damage because of *E. maxima* or mycotoxins, the control group had no NE lesions. These findings suggest that combined subclinical doses of FB and DON increase the severity of the NE lesion without increasing the associated mortality. NE lesion scores, but not the associated mortality, should be used to assess the cost of subclinical doses of FB and DON under field conditions.

Previous studies have identified that chronic exposure to FB1 at 100 mg/kg concentration for 28 days or 300 mg/kg for 14 days decreases the jejunum villus height and villus: crypt depth ratio and causes mild villus atrophy and goblet cell hyperplasia in broiler chicks (Rauber et al., 2013). This study identified that the presence of FB and DON combination decreased villi height to crypt depth ratio similar to that in the NE group. The villi length to crypt depth ratio is an indicator of the intestinal renovation rate and a higher villi to crypt ratio indicates a lower intestinal turnover (Brown et al., 1992; Van Nevel et al., 2005). Thus, subclinical doses of FB and DON combination increased the intestinal turnover and contributed to the observed decrease in FCR and loss in body weight gain during NE.

FB and DON acerbated the loss in the tight junction protein and increase in gut permeability associated with NE. FB and DON combination decreased the jejunal claudin-1, claudin-2, and zona-occluden-1 in the intestine. The decrease in the jejunal tight junction protein owing to subclinical mycotoxin was comparable to the loss in the tight junction in the birds induced with NE. Earlier studies have identified that chronic exposure to FB decreases the proliferation of intestinal epithelial cells and breaks down the gut barrier in pigs (Bouhet et al., 2004). Tight junction proteins are comprised of transmembrane proteins such as claudins and occludens, and cytoplasmic proteins, such as zona occludens (Findley and Koval, 2009). Tight junction proteins act as a barrier to pathogens and harmful toxins while permitting the entry of nutrients, ions, and water (Tomaszewska et al., 2021). Caco-2 cells exposed to a combination of aflatoxin and ochratoxin had significantly decreased tight junction proteins (Gao et al., 2018). FB inhibits ceramide synthase, which results in the accumulation of sphingoid bases and their metabolites, leading to the depletion of complex sphingolipids (Wang et al., 1991). In addition, FB leads to the accumulation of sphinganine (Riley et al., 1999) and increases calmodulin, an apoptotic protein. Alteration in the sphingolipid metabolic products, sphingosine content, and calmodulin can be expected to decrease intestinal cell viability and loss in tight junction proteins (Bouhet et al., 2004). Furthermore, chronic exposure to FB

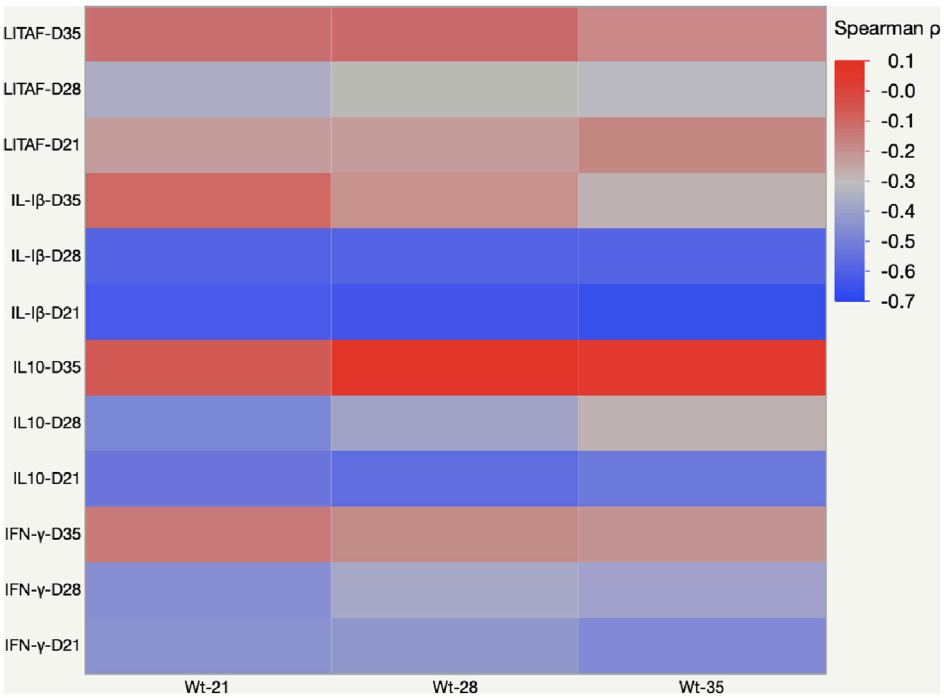

FIGURE 8 | Heat map representing Pearson's r correlation coefficient matrix between cytokine amounts and body weight gain. Heat map showing the transcriptional fold change of LITAF, IL-1β, IL-10, and IFN-γ in the cecal tonsils of birds fed mycotoxin contaminated diet and induced with necrotic enteritis. The color scale, −1 (blue) to +1 (red), and the negative value of the coefficient indicate that increased IL-1β and IL-10 mRNA expression levels are inversely affected the body weight.

+ DON enhances the claudin-1, claudin-2, and zona-occluden internalization by endocytosis (Fujita et al., 2000). This results in the reduction of claudins at a cellular level and a lack of new molecules to replace the damaged tight junction proteins (Hopkins et al., 2003).

During NE infection, the integrity of intestinal epithelial cells is compromised due to either inflammation or toxins or the associated gut dysbiosis. Quantification of serum FITC-d is commonly used as an indicator for assessing intestinal paracellular permeability and magnitude of severity (Kuttappan et al., 2015). The oral administration of FITC-D passes through the disrupted intestinal epithelium and enters systemic circulation, which can be quantified in the blood (Liu et al., 2021). In this current study, the presence of FB and DON caused a loss in gut integrity, and this loss in gut integrity was acerbated in birds challenged with NE. The observed increase in serum FITC-D level correlated with decreased tight junction proteins in the ileum. A decrease in the tight junction proteins of the intestine leads to a loss in gut integrity and an increase in gut permeability, and it can explain the observed increase in serum FITC-D concentration. This current study suggests that chronic exposure to even subclinical doses of mycotoxins could adversely damage the intestinal gut epithelium.

FB and DON increased the cecal tonsil IL-1β, an inflammatory cytokine. Upregulation of interleukins is observed normally during various bacterial and parasitic infections (Mensikova et al., 2013). Immune system activation includes changes in cytokines such as tumor necrosis factor (TNF-α, IL-1β, IFN-γ, and IL-10 (Wallach et al., 2014). Activated macrophages secrete IL-1β to induce inflammation (Bhat and Fitzgerald, 2014). In mice, a single dose of *in vivo* DON exposure increases TNF-α, IL-1β, IFN-γ, and IL-10 in $CD4^+$ cells isolated from spleen and Peyer's patches (Zhou et al., 1997). *In vitro* treatment of chicken splenocytes with DON increases the concentrations of IL-1β, IL-10, and IFN-γ (Azcona-Olivera et al., 1995; Ren et al., 2015). In this present study, birds exposed to FB and DON had increased cecal tonsil IFN-γ mRNA transcription at levels similar to that in the birds undergoing a NE challenge. IFN-γ plays an important role in the host's defense against intracellular pathogens such as coccidiosis. This increased IFN-γ mRNA transcription at D21 in the combined toxin group suggests that FB and DON could have had a synergistic effect on IFN-γ mRNA transcription. Cecal tonsils of *Eimeria*-challenged birds had an increase in IFN-γ mRNA transcription when chickens were fed *Fusarium* mycotoxins contaminated diet (Girgis et al., 2010). Chronic exposure to combined FB + DON activates the NF-kB pathway to upregulate pro-inflammatory cytokines (Pinton and Oswald, 2014; Taranu et al., 2015). Several studies have identified that the dietary mycotoxins, at doses even below EU guidance, could upregulate both pro and anti-inflammatory cytokines in the duodenum and jejunum (Bracarense et al., 2012; Lucke et al., 2018; Guo et al., 2021). Similarly, in this present study, 4 mg/kg DON and 3 mg/kg FB increased the pro- and anti-inflammatory cytokines, suggesting that combined

toxins could have adverse effects on intestinal epithelial cells to modify the cecal tonsils cytokines expression in broilers. Furthermore, Pearson's correlation analysis identified significant negative correlations ($p < 0.05$) between IL-1β, IL-10, and body weight. The negative coefficient indicated that the chronic exposure to mycotoxins increased the IL-1β and IL-10 mRNA transcripts, coinciding with an ultimate decrease in body weight gain. Activation of the immune system and cytokines production requires energy resources and affects the production performance, resulting in a trade-off between immune function and growth (van der Most et al., 2011). NE infection by itself increased proinflammatory cytokines, and further synergism between FB, DON, and NE acerbated the loss in body weight gain in the FB + DON + NE group.

T cell proliferation involves the activation and differentiation of T cells into effector and memory subsets which is critical for the adaptive immune system. $CD8^+$: $CD4^+$ ratio is a marker of immune dysfunction (Roitt, 1992; Martin et al., 2016). The impairment in $CD4^+$ T cell regeneration and persistent elevation of $CD8^+$ T cells are indicators of inflammation that involves gut microbial translocation (Hirakawa et al., 2020; Ruhnau et al., 2020). In this present study, the presence of FB + DON decreased the $CD8^+$: $CD4^+$ cell ratio in the cecal tonsils, and this effect was acerbated in the FB + DON + NE group compared to the control group. Similar results were observed in chickens' peripheral mononuclear cells (PBMCs) when they were fed contaminated diets containing up to 3.8 μg/g deoxynivalenol (DON), 0.3 μg/g 15-acetyl DON, and 0.2 μg/g zearalenone (Girgis et al., 2008). Furthermore, broilers fed 20 mg/kg FB and 1.5 mg/kg of DON had an increased percentage of T lymphocytes, and $CD4^+CD25^+$ in the cecal tonsils (Grenier et al., 2016). In bovine and porcine PBMCs, a similar kind of trend was observed when they were fed DON contaminated diet. In porcine PBMCs, *in vitro* studies with DON at 0.4 mM or higher concentration have decreased the proliferation of $CD8^+$ and $CD4^+$ cells (Novak et al., 2018). Similarly, beef cattle exposed to 1.7 mg DON and 3.5 mg FB for 21 days has significantly decreased the $CD8^+$: $CD4^+$ ratio (Duringer et al., 2020; Roberts et al., 2021). Our studies demonstrated that combined subclinical doses of FB and DON negatively affected the proliferation of the $CD8^+$ and $CD4^+$ T cells. FB and DON target the cell with high protein turnover and inhibit protein synthesis. $CD8^+$ and $CD4^+$ cells are considered highly proliferative cells (Overgaard et al., 2015) and are likely highly sensitive to FB and DON (Taranu et al., 2010; Daenicke et al., 2011). Impaired $CD8^+$ and $CD4^+$ cell proliferation can be expected to compromise the immune response to NE. Changes in T-helper and cytotoxic T cell profiles, along with changes in inflammatory cytokines, suggest that the chicken immune system is altered by chronic exposure to *Fusarium* mycotoxins even at a subclinical dose in broiler chickens leading to impaired resistance to NE. Our results suggest that the $CD8^+$: $CD4^+$ ratio could be a potential biomarker of early *Fusarium* mycotoxin exposure.

Lactobacillus spp. and *Bifidobacterium* spp. are considered to be beneficial bacteria in the chicken gut. In this present study, the subclinical dose of FB and DON decreased the *Lactobacillus* spp. load in the ceca. Similar results were found when chickens were exposed to DON 5 mg/kg diet (Antonissen et al., 2015; Guo et al., 2021). Chronic exposure to subclinical doses of FB and DON increased the *C. perfringens* load and caused intestinal dysbiosis, and hence, this current study identified that FB and DON mycotoxins can be predisposing factors for *C. perfringens*-induced NE in chickens. Increased *C. perfringens* altered the balance between intestinal microbiota, with major changes observed in *Lactobacillus* spp. (Antonissen et al., 2016; Zhang et al., 2018; Hernandez-Patlan et al., 2019). The chronic exposure to FB + DON increased the cecal *C. perfringens* load but had no effect on *Bifidobacterium* spp. (Lucke et al., 2018). Therefore, it can be concluded that chronic exposure to subclinical doses of combined FB + DON affected the relative abundance of *Lactobacillus* spp. and exacerbated the NE by enhancing intestinal inflammation and shifting the gut microbiome towards pathogenic microorganisms (Yang et al., 2021).

The findings reported here have significant practical importance and reflect the real-world problem because of the common occurrence of *Fusarium* mycotoxins in poultry feeds and subclinical necrotic enteritis occurrence in the field. According to the FDA, the recommended level for FB and DON in the poultry finished diet is 50 mg/kg and 5 mg/kg (FDA, 2001; FDA, 2010). The level of FB and DON in the experimental diets of the current study was much lower than the FDA tolerance levels. The findings of this study represent the effects of chronic exposure to the subclinical levels of FB and DON in broiler chickens and their role in inducing subclinical necrotic enteritis. Our findings identified the mechanism through which FB and DON exhibited synergistic effects and predicted the specific thresholds of combined toxins and their adverse effects in chickens. Our data suggested that *Fusarium* mycotoxins not only directly affected the production performance but also influenced chicken health by inducing NE and acerbated the severity of NE.

Our data demonstrated that chronic feeding of a combined dose of 3 mg/kg FB and 4 mg/kg DON in the poultry diet downregulates the tight junction proteins and increased the severity of NE in broiler chickens. Chicken diets with FB and DON contamination, even at subclinical levels, induced a negative impact on performance, altered small intestinal morphology, and significantly increased the incidence of NE. In conclusion, the presence of FB and DON decreased the BWG, increased the FCR, increased gut permeability, decreased jejunal tight junction protein, increased inflammatory cytokines in the cecal tonsil, decreased $CD8^+$:$CD4^+$ ratio in the cecal tonsil and spleen, increased *C. perfringens* load in the cecal content, and decreased *Lactobacillus* spp. loads in the cecal content and predisposed broiler birds to NE.

DATA AVAILABILITY STATEMENT

The original contributions presented in the study are included in the article/Supplementary Material; further inquiries can be directed to the corresponding author.

ETHICS STATEMENT

The animal study was reviewed and approved by the SPRG IACUC committee.

AUTHOR CONTRIBUTIONS

RS: conceptualization, investigation, methodology, data curation, and writing—original draft preparation. DA: methodology and writing—review and editing. SR: funding acquisition. RM: funding acquisition. TA: conceptualization and writing—review and editing. SC: methodology. AP-A: methodology and writing—review and editing. AG: resources and writing—review and editing.

FUNDING

This work was funded by USDA ARS award number 6040-42000-045-00D.

ACKNOWLEDGMENTS

The authors acknowledge D. Olson (USDA) for preparing and growing the fungal culture material producing FB and DON; T. Mitchell (USDA) and J. Hawkins (USDA) for quantifying FB and DON in culture materials; Romer Labs Inc. for independent quantification of mycotoxins in the poultry feed; L. Fuller (UGA) for providing *Eimeria maxima* sporulated oocysts, and C. McDonough (USDA), C. Miller (USDA), and H. Yeh (USDA) for their assistance in sampling. The authors thank M. Jones (Southern Poultry Research Group) for NE lesion scoring and C. Hofacre (SPRG) and other crew members at SPRG for assistance in animal trial.

REFERENCES

Alqaisi, O., Ndambi, O. A., and Williams, R. B. (2017). Time Series Livestock Diet Optimization: Cost-Effective Broiler Feed Substitution Using the Commodity Price Spread Approach. *Agric. Food Econ.* 5 (1), 1–19. doi:10.1186/s40100-017-0094-9

Altpeter, F., and Posselt, U. K. (1994). Production of High Quantities of 3-acetyldeoxynivalenol and Deoxynivalenol. *Appl. Microbiol. Biotechnol.* 41 (4), 384–387. doi:10.1007/bf01982524

Amit-Romach, E., Sklan, D., and Uni, Z. (2004). Microflora Ecology of the Chicken Intestine Using 16S Ribosomal DNA Primers. *Poult. Sci.* 83 (7), 1093–1098. doi:10.1093/ps/83.7.1093

Andrade, C. (2019). The P Value and Statistical Significance: Misunderstandings, Explanations, Challenges, and Alternatives. *Indian J. Psychol. Med.* 41 (3), 210–215. doi:10.4103/IJPSYM.IJPSYM_193_19

Antonissen, G., Croubels, S., Pasmans, F., Ducatelle, R., Eeckhaut, V., Devreese, M., et al. (2015). Fumonisins Affect the Intestinal Microbial Homeostasis in Broiler Chickens, Predisposing to Necrotic Enteritis. *Vet. Res.* 46, 98. doi:10.1186/s13567-015-0234-8

Antonissen, G., Eeckhaut, V., Van Driessche, K., Onrust, L., Haesebrouck, F., Ducatelle, R., et al. (2016). Microbial Shifts Associated with Necrotic Enteritis. *Avian Pathol.* 45 (3), 308–312. doi:10.1080/03079457.2016.1152625

Antonissen, G., Van Immerseel, F., Pasmans, F., Ducatelle, R., Haesebrouck, F., Timbermont, L., et al. (2014). The Mycotoxin Deoxynivalenol Predisposes for the Development of Clostridium Perfringens-Induced Necrotic Enteritis in Broiler Chickens. *PLoS One* 9 (9), e108775. doi:10.1371/journal.pone.0108775

Awad, W. A., Vahjen, W., Aschenbach, J. R., and Zentek, J. (2011). A Diet Naturally Contaminated with the Fusarium Mycotoxin Deoxynivalenol (DON) Downregulates Gene Expression of Glucose Transporters in the Intestine of Broiler Chickens. *Livest. Sci.* 140 (1-3), 72–79. doi:10.1016/j.livsci.2011.02.014

Azcona-Olivera, J. I., Ouyang, Y.-L., Warner, R. L., Linz, J. E., and Pestka, J. J. (1995). Effects of Vomitoxin (Deoxynivalenol) and Cycloheximide on IL-2, 4, 5 and 6 Secretion and mRNA Levels in Murine CD4+ Cells. *Food Chem. Toxicol.* 33 (6), 433–441. doi:10.1016/0278-6915(95)00012-q

Bhat, N., and Fitzgerald, K. A. (2014). Recognition of Cytosolic DNA by cGAS and Other STING-dependent Sensors. *Eur. J. Immunol.* 44 (3), 634–640. doi:10.1002/eji.201344127

Biomin (2021). World Mycotoxin Survey Impact 2021. [Online]. Available: https://www.biomin.net/science-hub/world-mycotoxin-survey-impact-2021 [Accessed].

Bouhet, S., Hourcade, E., Loiseau, N., Fikry, A., Martinez, S., Roselli, M., et al. (2004). The Mycotoxin Fumonisin B1 Alters the Proliferation and the Barrier Function of Porcine Intestinal Epithelial Cells. *Toxicol. Sci.* 77 (1), 165–171. doi:10.1093/toxsci/kfh006

Bracarense, A.-P. F. L., Lucioli, J., Grenier, B., Drociunas Pacheco, G., Moll, W.-D., Schatzmayr, G., et al. (2012). Chronic Ingestion of Deoxynivalenol and Fumonisin, Alone or in Interaction, Induces Morphological and Immunological Changes in the Intestine of Piglets. *Br. J. Nutr.* 107 (12), 1776–1786. doi:10.1017/s0007114511004946

Broom, L. J. (2017). Necrotic Enteritis; Current Knowledge and Diet-Related Mitigation. *World's Poult. Sci. J.* 73 (2), 281–292. doi:10.1017/s0043933917000058

Brown, T. P., Rottinghaus, G. E., and Williams, M. E. (1992). Fumonisin Mycotoxicosis in Broilers: Performance and Pathology. *Avian Dis.* 36, 450–454. doi:10.2307/1591528

Chen, Y. P., Cheng, Y. F., Li, X. H., Yang, W. L., Wen, C., Zhuang, S., et al. (2017). Effects of Threonine Supplementation on the Growth Performance, Immunity, Oxidative Status, Intestinal Integrity, and Barrier Function of Broilers at the Early Age. *Poult. Sci.* 96 (2), 405–413. doi:10.3382/ps/pew240

NRC (1994). *Nutrient Requirements of Poultry*Ninth Revised Edition. Washington, DC: National Academies Press, 19–34.

Daenicke, S., Keese, C., Goyarts, T., and Döll, S. (2011). Effects of Deoxynivalenol (DON) and Related Compounds on Bovine Peripheral Blood Mononuclear Cells (PBMC) *In Vitro* and *In Vivo*. *Mycotox Res.* 27 (1), 49–55. doi:10.1007/s12550-010-0074-3

Dänicke, S., Gareis, M., and Bauer, J. (2001). Orientation Values for Critical Concentrations of Deoxynivalenol and Zearalenone in Diets for Pigs, Ruminants and Gallinaceous Poultry. *Proc. Soc. Nutr. Physiol.*, 171–174.

Duringer, J. M., Roberts, H. L., Doupovec, B., Faas, J., Estill, C. T., Jiang, D., et al. (2020). Effects of Deoxynivalenol and Fumonisins Fed in Combination on Beef Cattle: Health and Performance Indices. *World Mycotoxin J.* 13 (4), 533–543. doi:10.3920/wmj2020.2567

Filazi, A., Yurdakok-Dikmen, B., Kuzukiran, O., and Sireli, U. T. (2017). "Mycotoxins in Poultry," in *Poultry Science*. Editor Dr. Milad Manafi (USA: InTech), 73–92.

Findley, M. K., and Koval, M. (2009). Regulation and Roles for Claudin-Family Tight Junction Proteins. *IUBMB life* 61 (4), 431–437. doi:10.1002/iub.175

Food and Administration (2010). *Advisory Levels for Deoxynivalenol (DON) in Finished Wheat Products for Human Consumption and Grains and Grain By-Products Used for Animal Feed*. Food and Drug Administration: Rockville, MD.

FDA (2001). *Guidance for Industry: Fumonisin Levels in Human Foods and Animal Feeds*. Washington DC: United States Food and Drug Administration.

Fujita, K., Katahira, J., Horiguchi, Y., Sonoda, N., Furuse, M., and Tsukita, S. (2000). Clostridium Perfringensenterotoxin Binds to the Second Extracellular Loop of Claudin-3, a Tight Junction Integral Membrane Protein. *FEBS Lett.* 476 (3), 258–261. doi:10.1016/s0014-5793(00)01744-0

Gao, Y., Li, S., Wang, J., Luo, C., Zhao, S., and Zheng, N. (2018). Modulation of Intestinal Epithelial Permeability in Differentiated Caco-2 Cells Exposed to Aflatoxin M1 and Ochratoxin A Individually or Collectively. *Toxins (Basel)* 10 (1), 13. doi:10.3390/toxins10010013

Girgis, G. N., Barta, J. R., Girish, C. K., Karrow, N. A., Boermans, H. J., and Smith, T. K. (2010). Effects of Feed-Borne Fusarium Mycotoxins and an Organic Mycotoxin Adsorbent on Immune Cell Dynamics in the Jejunum of Chickens Infected with Eimeria Maxima. *Veterinary Immunol. Immunopathol.* 138 (3), 218–223. doi:10.1016/j.vetimm.2010.07.018

Girgis, G. N., Sharif, S., Barta, J. R., Boermans, H. J., and Smith, T. K. (2008). Immunomodulatory Effects of Feed-Borne Fusarium Mycotoxins in Chickens Infected with Coccidia. *Exp. Biol. Med. (Maywood)* 233 (11), 1411–1420. doi:10.3181/0805-rm-173

Glenn, A. E. (2007). Mycotoxigenic Fusarium Species in Animal Feed. *Animal Feed Sci. Technol.* 137 (3), 213–240. doi:10.1016/j.anifeedsci.2007.06.003

Grenier, B., Dohnal, I., Shanmugasundaram, R., Eicher, S., Selvaraj, R., Schatzmayr, G., et al. (2016). Susceptibility of Broiler Chickens to Coccidiosis when Fed Subclinical Doses of Deoxynivalenol and Fumonisins-Special Emphasis on the Immunological Response and the Mycotoxin Interaction. *Toxins* 8 (8), 231. doi:10.3390/toxins8080231

Grenier, B., and Oswald, I. (2011). Mycotoxin Co-contamination of Food and Feed: Meta-Analysis of Publications Describing Toxicological Interactions. *World Mycotoxin J.* 4 (3), 285–313. doi:10.3920/wmj2011.1281

Guerre, P. (2016). Worldwide Mycotoxins Exposure in Pig and Poultry Feed Formulations. *Toxins* 8 (12), 350. doi:10.3390/toxins8120350

Guo, H., Chang, J., Wang, P., Yin, Q., Liu, C., Li, S., et al. (2021). Detoxification of Aflatoxin B1 in Broiler Chickens by a Triple-Action Feed Additive. *Food Addit. Contam. Part A* 38 (9), 1583–1593. doi:10.1080/19440049.2021.1957159

Hernandez-Patlan, D., Solis-Cruz, B., Pontin, K. P., Hernandez-Velasco, X., Merino-Guzman, R., Adhikari, B., et al. (2019). Impact of a Bacillus Direct-Fed Microbial on Growth Performance, Intestinal Barrier Integrity, Necrotic Enteritis Lesions, and Ileal Microbiota in Broiler Chickens Using a Laboratory Challenge Model. *Front. Vet. Sci.* 6, 108. doi:10.3389/fvets.2019.00108

Hirakawa, R., Nurjanah, S., Furukawa, K., Murai, A., Kikusato, M., Nochi, T., et al. (2020). Heat Stress Causes Immune Abnormalities via Massive Damage to Effect Proliferation and Differentiation of Lymphocytes in Broiler Chickens. *Front. Vet. Sci.* 7, 46. doi:10.3389/fvets.2020.00046

Hofacre, C. L., Froyman, R., Gautrias, B., George, B., Goodwin, M. A., and Brown, J. (1998). Use of Aviguard and Other Intestinal Bioproducts in Experimental Clostridium Perfringens-Associated Necrotizing Enteritis in Broiler Chickens. *Avian Dis.* 42, 579–584. doi:10.2307/1592685

Hofacre, C. L., Smith, J. A., and Mathis, G. F. (2018). An Optimist's View on Limiting Necrotic Enteritis and Maintaining Broiler Gut Health and Performance in Today's Marketing, Food Safety, and Regulatory Climate. *Poult. Sci.* 97 (6), 1929–1933. doi:10.3382/ps/pey082

Hopkins, A. M., Walsh, S. V., Verkade, P., Boquet, P., and Nusrat, A. (2003). Constitutive Activation of Rho Proteins by CNF-1 Influences Tight Junction Structure and Epithelial Barrier Function. *J. cell Sci.* 116 (4), 725–742. doi:10.1242/jcs.00300

Immerseel, F. V., Buck, J. D., Pasmans, F., Huyghebaert, G., Haesebrouck, F., and Ducatelle, R. (2004). Clostridium Perfringensin Poultry: an Emerging Threat for Animal and Public Health. *Avian Pathol.* 33 (6), 537–549. doi:10.1080/03079450400013162

Kuttappan, V. A., Berghman, L. R., Vicuña, E. A., Latorre, J. D., Menconi, A., Wolchok, J. D., et al. (2015). Poultry Enteric Inflammation Model with Dextran Sodium Sulfate Mediated Chemical Induction and Feed Restriction in Broilers. *Poult. Sci.* 94 (6), 1220–1226. doi:10.3382/ps/pev114

Langendijk, P. S., Schut, F., Jansen, G. J., Raangs, G. C., Kamphuis, G. R., Wilkinson, M. H., et al. (1995). Quantitative Fluorescence *In Situ* Hybridization of Bifidobacterium Spp. With Genus-specific 16S rRNA-Targeted Probes and its Application in Fecal Samples. *Appl. Environ. Microbiol.* 61 (8), 3069–3075. doi:10.1128/aem.61.8.3069-3075.1995

Li, Y., Zhang, H., Chen, Y. P., Yang, M. X., Zhang, L. L., Lu, Z. X., et al. (2015). Bacillus Amyloliquefaciens Supplementation Alleviates Immunological Stress and Intestinal Damage in Lipopolysaccharide-Challenged Broilers. *Animal Feed Sci. Technol.* 208, 119–131. doi:10.1016/j.anifeedsci.2015.07.001

Liu, J., Teng, P.-Y., Kim, W. K., and Applegate, T. J. (2021). Assay Considerations for Fluorescein Isothiocyanate-Dextran (FITC-D): An Indicator of Intestinal Permeability in Broiler Chickens. *Poult. Sci.* 100 (7), 101202. doi:10.1016/j.psj.2021.101202

Livak, K. J., and Schmittgen, T. D. (2001). Analysis of Relative Gene Expression Data Using Real-Time Quantitative PCR and the 2−ΔΔCT Method. *methods* 25 (4), 402–408. doi:10.1006/meth.2001.1262

Lucke, A., Böhm, J., Zebeli, Q., and Metzler-Zebeli, B. U. (2018). Dietary Deoxynivalenol and Oral Lipopolysaccharide Challenge Differently Affect Intestinal Innate Immune Response and Barrier Function in Broiler Chickens. *J. Anim. Sci.* 96 (12), 5134–5143. doi:10.1093/jas/sky379

Markazi, A. D., Luoma, A., Shanmugasundaram, R., Murugesan, R., Mohnl, M., and Selvaraj, R. (2019). Effect of Acidifier Product Supplementation in Laying Hens Challenged with Salmonella. *J. Appl. Poult. Res.* 28 (4), 919–929. doi:10.3382/japr/pfz053

Martin, S. J., Burton, D. R., Roitt, I. M., and Delves, P. J. (2016). *Roitt's Essential Immunology*. New Jersey: John Wiley & Sons.

McGlone, J. (2010). *Guide for the Care and Use of Agricultural Animals in Teaching and Research*. United States: American Dairy Science Association.

Mensikova, M., Stepanova, H., and Faldyna, M. (2013). Interleukin-17 in Veterinary Animal Species and its Role in Various Diseases: a Review. *Cytokine* 64 (1), 11–17. doi:10.1016/j.cyto.2013.06.002

Mora, Z. V.-d. l., Macías-Rodríguez, M. E., Arratia-Quijada, J., Gonzalez-Torres, Y. S., Nuño, K., and Villarruel-López, A. (2020). *Clostridium perfringens* as Foodborne Pathogen in Broiler Production: Pathophysiology and Potential Strategies for Controlling Necrotic Enteritis. *Animals* 10 (9), 1718. doi:10.3390/ani10091718

Novak, B., Vatzia, E., Springler, A., Pierron, A., Gerner, W., Reisinger, N., et al. (2018). Bovine Peripheral Blood Mononuclear Cells Are More Sensitive to Deoxynivalenol Than Those Derived from Poultry and Swine. *Toxins* 10 (4), 152. doi:10.3390/toxins10040152

Ogbuewu, I. (2011). Effects of Mycotoxins in Animal Nutrition: A Review. *Asian J. Anim. Sci.* 5, 19–33. doi:10.3923/ajas.2011.19.33

Overgaard, N. H., Jung, J.-W., Steptoe, R. J., and Wells, J. W. (2015). CD4+/CD8+double-positive T Cells: More Than Just a Developmental Stage? *J. Leukoc. Biol.* 97 (1), 31–38. doi:10.1189/jlb.1ru0814-382

Pinton, P., and Oswald, I. (2014). Effect of Deoxynivalenol and Other Type B Trichothecenes on the Intestine: A Review. *Toxins* 6 (5), 1615–1643. doi:10.3390/toxins6051615

Rauber, R. H., Oliveira, M. S., Mallmann, A. O., Dilkin, P., Mallmann, C. A., Giacomini, L. Z., et al. (2013). Effects of Fumonisin B1 on Selected Biological Responses and Performance of Broiler Chickens. *Pesq. Vet. Bras.* 33 (9), 1081–1086. doi:10.1590/s0100-736x2013000900006

Ren, Z., Wang, Y., Deng, H., Deng, Y., Deng, J., Zuo, Z., et al. (2015). Deoxynivalenol-induced Cytokines and Related Genes in Concanavalin A-Stimulated Primary Chicken Splenic Lymphocytes. *Toxicol. Vitro* 29 (3), 558–563. doi:10.1016/j.tiv.2014.12.006

Riley, R. T., Voss, K. A., Norred, W. P., Bacon, C. W., Meredith, F. I., and Sharma, R. P. (1999). Serine Palmitoyltransferase Inhibition Reverses Anti-proliferative Effects of Ceramide Synthase Inhibition in Cultured Renal Cells and Suppresses Free Sphingoid Base Accumulation in Kidney of BALBc Mice. *Environ. Toxicol. Pharmacol.* 7 (2), 109–118. doi:10.1016/s1382-6689(98)00047-7

Roberts, H. L., Bionaz, M., Jiang, D., Doupovec, B., Faas, J., Estill, C. T., et al. (2021). Effects of Deoxynivalenol and Fumonisins Fed in Combination to Beef Cattle: Immunotoxicity and Gene Expression. *Toxins* 13 (10), 714. doi:10.3390/toxins13100714

Roitt, I. (1992). Essential Immunology. *Rev. Inst. Med. Trop. S. Paulo* 34, 32. doi:10.1590/s0036-46651992000100014

Ruhnau, D., Hess, C., Grenier, B., Doupovec, B., Schatzmayr, D., Hess, M., et al. (2020). The Mycotoxin Deoxynivalenol (DON) Promotes Campylobacter Jejuni Multiplication in the Intestine of Broiler Chickens with Consequences on Bacterial Translocation and Gut Integrity. *Front. Veterinary Sci.* 1027, 573894. doi:10.3389/fvets.2020.573894

Šefcová, M., Larrea-Álvarez, M., Larrea-Álvarez, C., Revajová, V., Karaffová, V., Koščová, J., et al. (2020). Effects of Lactobacillus Fermentum Supplementation on Body Weight and Pro-inflammatory Cytokine Expression in Campylobacter Jejuni-Challenged Chickens. *Veterinary Sci.* 7 (3), 121. doi:10.3390/vetsci7030121

Shanmugasundaram, R., Acevedo, K., Mortada, M., Akerele, G., Applegate, T. J., Kogut, M. H., et al. (2021). Effects of *Salmonella enterica* Ser. Enteritidis and Heidelberg on Host CD4+CD25+ Regulatory T Cell Suppressive Immune Responses in Chickens. *Plos one* 16 (11), e0260280. doi:10.1371/journal.pone.0260280

Shanmugasundaram, R., Kogut, M. H., Arsenault, R. J., Swaggerty, C. L., Cole, K., Reddish, J. M., et al. (2015). Effect of Salmonella Infection on Cecal Tonsil Regulatory T Cell Properties in Chickens. *Poult. Sci.* 94 (8), 1828–1835. doi:10.3382/ps/pev161

Shanmugasundaram, R., Markazi, A., Mortada, M., Ng, T. T., Applegate, T. J., Bielke, L. R., et al. (2020). Research Note: Effect of Synbiotic Supplementation on Caecal *Clostridium perfringens* Load in Broiler Chickens with Different Necrotic Enteritis Challenge Models. *Poult. Sci.* 99 (5), 2452–2458. doi:10.1016/j.psj.2019.10.081

Shanmugasundaram, R., Mortada, M., Cosby, D. E., Singh, M., Applegate, T. J., Syed, B., et al. (2019a). Synbiotic Supplementation to Decrease Salmonella

Colonization in the Intestine and Carcass Contamination in Broiler Birds. *Plos one* 14 (10), e0223577. doi:10.1371/journal.pone.0223577

Shanmugasundaram, R., Mortada, M., Murugesan, G. R., and Selvaraj, R. K. (2019b). *In Vitro* characterization and Analysis of Probiotic Species in the Chicken Intestine by Real-Time Polymerase Chain Reaction. *Poult. Sci.* 98 (11), 5840–5846. doi:10.3382/ps/pez188

Shanmugasundaram, R., and Selvaraj, R. K. (2012). Effect of Killed Whole Yeast Cell Prebiotic Supplementation on Broiler Performance and Intestinal Immune Cell Parameters. *Poult. Sci.* 91 (1), 107–111. doi:10.3382/ps.2011-01732

Shanmugasundaram, R., Wick, M., and Lilburn, M. S. (2019c). Effect of a Post-hatch Lipopolysaccharide Challenge in Turkey Poults and Ducklings after a Primary Embryonic Heat Stress. *Dev. Comp. Immunol.* 101, 103436. doi:10.1016/j.dci.2019.103436

Shanmugasundaram, R., Wick, M., and Lilburn, M. S. (2018). Effect of Embryonic Thermal Manipulation on Heat Shock Protein 70 Expression and Immune System Development in Pekin Duck Embryos. *Poult. Sci.* 97 (12), 4200–4210. doi:10.3382/ps/pey298

Shimshoni, J. A., Cuneah, O., Sulyok, M., Krska, R., Galon, N., Sharir, B., et al. (2013). Mycotoxins in Corn and Wheat Silage in Israel. *Food Addit. Contam. Part A* 30 (9), 1614–1625. doi:10.1080/19440049.2013.802840

Smith, J. A. (2019). Broiler Production without Antibiotics: United States Field Perspectives. *Animal Feed Sci. Technol.* 250, 93–98. doi:10.1016/j.anifeedsci.2018.04.027

Taranu, I., Marin, D. E., Burlacu, R., Pinton, P., Damian, V., and Oswald, I. P. (2010). Comparative Aspects Ofin Vitroproliferation of Human and Porcine Lymphocytes Exposed to Mycotoxins. *Archives Animal Nutr.* 64 (5), 383–393. doi:10.1080/1745039x.2010.492140

Taranu, I., Marin, D. E., Pistol, G. C., Motiu, M., and Pelinescu, D. (2015). Induction of Pro-inflammatory Gene Expression by *Escherichia coli* and Mycotoxin Zearalenone Contamination and Protection by a Lactobacillus Mixture in Porcine IPEC-1 Cells. *Toxicon* 97, 53–63. doi:10.1016/j.toxicon.2015.01.016

Timbermont, L., Haesebrouck, F., Ducatelle, R., and Van Immerseel, F. (2011). Necrotic Enteritis in Broilers: an Updated Review on the Pathogenesis. *Avian Pathol.* 40 (4), 341–347. doi:10.1080/03079457.2011.590967

Tomaszewska, E., Rudyk, H., Dobrowolski, P., Donaldson, J., Świetlicka, I., Puzio, I., et al. (2021). Changes in the Intestinal Histomorphometry, the Expression of Intestinal Tight Junction Proteins, and the Bone Structure and Liver of Pre-laying Hens Following Oral Administration of Fumonisins for 21 Days. *Toxins* 13 (6), 375. doi:10.3390/toxins13060375

van der Most, P. J., de Jong, B., Parmentier, H. K., and Verhulst, S. (2011). Trade-off between Growth and Immune Function: a Meta-analysis of Selection Experiments. *Funct. Ecol.* 25 (1), 74–80. doi:10.1111/j.1365-2435.2010.01800.x

Van Nevel, C. J., Decuypere, J. A., Dierick, N. A., and Molly, K. (2005). Incorporation of Galactomannans in the Diet of Newly Weaned Piglets: Effect on Bacteriological and Some Morphological Characteristics of the Small Intestine. *Archives Animal Nutr.* 59 (2), 123–138. doi:10.1080/17450390512331387936

Wallach, D., Kang, T.-B., and Kovalenko, A. (2014). Concepts of Tissue Injury and Cell Death in Inflammation: a Historical Perspective. *Nat. Rev. Immunol.* 14 (1), 51–59. doi:10.1038/nri3561

Wang, E., Norred, W. P., Bacon, C. W., Riley, R. T., and Merrill, A. H., Jr (1991). Inhibition of Sphingolipid Biosynthesis by Fumonisins. Implications for Diseases Associated with Fusarium Moniliforme. *J. Biol. Chem.* 266 (22), 14486–14490. doi:10.1016/s0021-9258(18)98712-0

Wang, R. F., Cao, W. W., and Cerniglia, C. E. (1996). PCR Detection and Quantitation of Predominant Anaerobic Bacteria in Human and Animal Fecal Samples. *Appl. Environ. Microbiol.* 62 (4), 1242–1247. doi:10.1128/aem.62.4.1242-1247.1996

Wang, R. J., Fui, S. X., Miao, C. H., and Feng, D. Y. (2005). Effects of Different Mycotoxin Adsorbents on Performance, Meat Characteristics and Blood Profiles of Avian Broilers Fed Mold Contaminated Corn. *Asian Australas. J. Anim. Sci.* 19 (1), 72–79. doi:10.5713/ajas.2006.72

Yang, Q., Liu, J., Wang, X., Robinson, K., Whitmore, M. A., Stewart, S. N., et al. (2021). Identification of an Intestinal Microbiota Signature Associated with the Severity of Necrotic Enteritis. *Front. Microbiol.* 12, 703693. doi:10.3389/fmicb.2021.703693

Yu, S., Jia, B., Lin, H., Zhang, S., Yu, D., Liu, N., et al. (2022). Effects of Fumonisin B and Hydrolyzed Fumonisin B on Growth and Intestinal Microbiota in Broilers. *Toxins* 14 (3), 163. doi:10.3390/toxins14030163

Zhang, B., Lv, Z., Li, Z., Wang, W., Li, G., and Guo, Y. (2018). Dietary L-Arginine Supplementation Alleviates the Intestinal Injury and Modulates the Gut Microbiota in Broiler Chickens Challenged by *Clostridium perfringens*. *Front. Microbiol.* 9, 1716. doi:10.3389/fmicb.2018.01716

Zhang, C., Zhao, X. H., Yang, L., Chen, X. Y., Jiang, R. S., Jin, S. H., et al. (2017). Resveratrol Alleviates Heat Stress-Induced Impairment of Intestinal Morphology, Microflora, and Barrier Integrity in Broilers. *Poult. Sci.* 96 (12), 4325–4332. doi:10.3382/ps/pex266

Zhou, H.-R., Yan, D., and Pestka, J. J. (1997). Differential Cytokine mRNA Expression in Mice after Oral Exposure to the Trichothecene Vomitoxin (Deoxynivalenol): Dose Response and Time Course. *Toxicol. Appl. Pharmacol.* 144 (2), 294–305. doi:10.1006/taap.1997.8132

Conflict of Interest: SR and RM were employed by the company DSM Animal Nutrition and Health.

The remaining authors declare that the research was conducted in the absence of any commercial or financial relationships that could be construed as a potential conflict of interest.

Publisher's Note: All claims expressed in this article are solely those of the authors and do not necessarily represent those of their affiliated organizations, or those of the publisher, the editors, and the reviewers. Any product that may be evaluated in this article, or claim that may be made by its manufacturer, is not guaranteed or endorsed by the publisher.

frontiers | Frontiers in Physiology

TYPE Original Research
PUBLISHED 13 September 2022
DOI 10.3389/fphys.2022.1012212

OPEN ACCESS

EDITED BY
Sandra G. Velleman,
The Ohio State University, United States

REVIEWED BY
Gregoy Y. Bedecarrats,
University of Guelph, Canada
Alejandro Bielli,
University of the Republic, Uruguay

*CORRESPONDENCE
Joëlle Dupont,
joelle.dupont@inrae.fr

SPECIALTY SECTION
This article was submitted to Avian Physiology,
a section of the journal
Frontiers in Physiology

RECEIVED 05 August 2022
ACCEPTED 26 August 2022
PUBLISHED 13 September 2022

CITATION
Bernardi O, Reverchon M, Estienne A, Baumard Y, Ramé C, Brossaud A, Combarnous Y, Froment P and Dupont J (2022), Chicken white egg chemerin as a tool for genetic selection for egg weight and hen fertility. *Front. Physiol.* 13:1012212. doi: 10.3389/fphys.2022.1012212

Chicken white egg chemerin as a tool for genetic selection for egg weight and hen fertility

Ophélie Bernardi[1,2], Maxime Reverchon[2], Anthony Estienne[1], Yannick Baumard[3], Christelle Ramé[1], Adeline Brossaud[1], Yves Combarnous[1], Pascal Froment[1] and Joëlle Dupont[1]*

[1]Centre National de la Recherche Scientifique, Institut Français du Cheval et de l'Equitation, Institut National de Recherche pour l'Agriculture, l'Alimentation et l'Environnement (INRAE), Université de Tours, Physiologie de la Reproduction et des Comportements, UMR85, Paris, France, [2]SYSAAF-Syndicat des Sélectionneurs Avicoles et Aquacoles Français, Centre INRA Val de Loire, France, [3]INRAE—Unité Expérimentale Pôle D'expérimentation Avicole de Tours, France

Embryo mortality rate, which can reach up to 40% in avian species, is a major issue for breeding. It is therefore important to identify new embryo development biomarkers for genetic selection to improve reproductive performances. We have recently shown that chemerin is expressed in the oviductal hen magnum, accumulates in egg white, is correlated with embryo survival and could thus be used as a molecular marker of embryo development. Eggs from seven hen breeds (n = 70) were collected during five successive days at the end of the laying period. After weighing eggs, yolk and albumen, an egg white sample from each egg was collected and a blood sample was taken from each hen. Chemerin concentrations in albumen and blood samples were measured by a specific home made ELISA assay. Hen's plasma and egg's albumen chemerin levels were found to be correlated with reproductive parameters such as fecundity, fertility, embryo mortality, hatchability and laying rates. The inter-hen chemerin level variability in albumen was higher than intra-hen except for one breed (R+). We observed significantly different levels of chemerin in egg white between breeds. However, chemerin concentrations in egg white were not significantly associated to variations of hen plasma chemerin levels. Interestingly, we observed negative correlations between albumen chemerin concentrations and egg weight (r = −0.43, p = 0.001), between albumen weight (r = −0.40, p = 0.002), and between yolk weight (r = −0.28, p = 0.03). We also showed negative correlations between egg white chemerin concentrations and fecundity (r = −0.32, p = 0.011) and fertility (r = −0.27, p = 0.04) whereas no significant correlation was observed with the laying rate. Taken together, these results suggest that egg white chemerin concentration might be a good biomarker for genetic selection for egg weight and fertility in hens, provided these data are confirmed on a larger scale.

Abbreviations: BCA, bicinchoninic acid; BSA, Bovine Serum Albumin; CCRL2, C-C chemokine receptor-like 2; CMKLR1, Chemerin Chemokine-Like Receptor; IGF-1, Insulin-Like Growth Factor 1; ELISA, Enzyme-Linked ImmunoSorbent Assay; TIG2, Tazarotene-Induced Gene 2; EEM, Early Embryonic Mortality; GPR1, G protein receptor 1; LEM, Late Embryonic Mortality; RARRES2, Retinoic Acid Receptor Responder 2.

KEYWORDS
hen, egg white, chemerin, fertility, egg performance

Introduction

One of the breeding companies' goals is the production of viable and robust one day-old chicks to renew their reproductive flock. However, embryo and chick mortality rates during the first week of their life are major issues for profitability and competitiveness in poultry industry. This early mortality rate is an important and often used index to assess chick quality and it is also a welfare indicator (Tona et al., 2005). In addition to environmental factors, other parameters such as hen and egg production type, storage of eggs, albumen and egg quality affect the embryo development, hatchability and chick quality (Peebles et al., 2001; Schmidt et al., 2009; Nasri et al., 2020; Özlü et al., 2021). New tools are necessary to improve the quality of embryo development and the eggs hatchability. Indeed, the identification of new regulators/biomarkers of embryo development is a potential way to improve production performances at all steps of chicken breeding (laying, fertility and hatchability rates and the robustness of chicks). Nutrition and energy metabolism are well known to influence reproduction in all vertebrates. In broiler chicken, the rapid growth and the fattening are often associated with undesirable reproductive capacities such as a high sexual precocity, a loss of the follicular hierarchy, multiple ovulations and a decrease of egg production, fertility and hatchability (Chen et al., 2006; Briere et al., 2011; Zhang et al., 2018). Some variations in nutritional status could impact the reproductive system through changes in plasma metabolic protein secretions (Briere et al., 2011). Indeed, metabolic tissues synthesize and release protein and peptides hormones named adipokines that are involved in the regulation of various physiological functions including reproduction in mammals but also in birds (Ahima and Flier, 2000; Zhang et al., 2018; Estienne et al., 2020; Bernardi et al., 2021).

Chemerin was discovered in 1997 as a novel retinoid-responsive gene in human skin (Nagpal et al., 1997). Later, chemerin (18 kDa), also named TIG2 (tazarotene-induced gene 2) or RARRES2 (retinoic acid receptor responder 2), was identified as an adipokine mainly secreted by adipose tissue and liver. In mammals, chemerin is expressed in several other tissues such as pancreas, placenta, skin, kidneys, intestines and gonads (Mattern et al., 2014). After several successive cleavages, the active form of chemerin is able to bind three G-coupled receptors with seven transmembrane domains named CMKLR1 (Chemokine like receptor 1), GPR1 (G protein receptor 1) and CCRL2 (C-C chemokine receptor-like 2) (Yoshimura and Oppenheim, 2011). Chemerin is involved in many physiological processes such as the regulation of immune system and adipogenesis, angiogenesis, reproductive functions and metabolic disorders (Bernardi et al., 2021). Bozaoglu et al. showed plasma chemerin levels are positively associated with body fat, plasma glucose and triglyceride and lipid metabolism in humans (Bozaoglu et al., 2007). However, in contrary to mammals, plasma chemerin levels are negatively correlated with fattening in turkeys (Diot et al., 2015) and chickens (Mellouk et al., 2018d). Mellouk et al. studied the expression profiles of various adipokines in metabolic tissue during the chicken embryo development and they showed that the chemerin amount was specifically increased at hatching in various metabolic tissues, and this was associated with an increase in the weight of the embryo (Mellouk et al., 2018c). Concerning reproductive functions, many studies demonstrated the expression of chemerin and its receptors in ovary including granulosa and theca cells, corpus luteum and oocytes in different mammals including humans. These studies showed that chemerin inhibits Insulin-like Growth Factor 1 (IGF-1)-induced steroidogenesis in primary granulosa cells (Reverchon et al., 2012, 2014). Chemerin hormone and receptor are expressed by granulosa and theca cells in both broiler hens (Mellouk et al., 2018a) and turkeys (Diot et al., 2015) but at different levels. Moreover, proteomic analyzes have identified chemerin within the albumen and perivitelline membranes of chicken eggs (Mann, 2007, 2008). Our laboratory recently demonstrated that chemerin is highly present in the albumen compared to the yolk and plasma (Estienne et al., 2022). Moreover in the oviduct of hens, chemerin and its receptors are more expressed in the magnum, where the egg white is formed (Estienne et al., 2022). Also, a chemerin system is present in extraembryonic membranes such as allantoic and amniotic membranes and fluids suggesting a passage of chemerin from albumen to the extraembryonic membranes (Estienne et al., 2022). Mellouk et al. showed that plasma chemerin concentrations were negatively correlated with egg hatchability in chicken (Mellouk et al., 2018b). In addition, we also demonstrated an increase of embryo mortality after *in ovo* injections of anti-chemerin and anti-CMKLR1 antibodies in egg white (Estienne et al., 2022). Thus, our working hypothesis is that chemerin in egg white is involved in the embryo development in chicken and could be a new reproductive trait for genetic selection.

The aims of the present study were 1. To investigate the egg white and plasma concentrations of chemerin using a new home-made chicken chemerin ELISA, 2. To compare them in individual laying hens, and in successive eggs from the same hen to evaluate the intra and inter hen coefficient of variation and 3. To determine potential relationships between egg white chemerin concentration and hen egg performance and fertility parameters.

TABLE 1 Peculiarities and phenotypes of the breeds used for experimental design.

Breed	Pecularities	References
R-/R+ (Rhode Island Red)	Selected for low and high residual feed consumption and metabolism and reproduction performances	Tixier-Boichard et al. (1995)
FAYOUMI (Local breed)	Origin Egypt and resistance to disease in particular coccidiosis	(Hamet et al., 1982; Mérat et al., 1983)
OD (Leghorn)	Multiple ovulations	Lowry et al. (1979)
GAVORA (Leghorn)	Absence of endogenous viral genes	Gavora et al. (1989)
	High egg production	
CHEPTEL1 (Local breed)	Origin of variant Pea comb	Chang et al. (2007)
DwNa (INRAE breed)	DWARF gene for metabolism and laying performances	(Chen and Tixier-Boichard, 2003a; 2003b)

Material and methods

Ethical issues

All the zootechnical parameters (total egg laying, incubated eggs, unfertilized eggs, eggs mortality and hatched chicks) were routinely collected by the Experimental Unit "Pôle Expérimental Avicole de Tours" UEPEAT (INRAE, Nouzilly, France, doi: https://doi.org/10.15454/1.5572326250887292E12) for the monitoring of the breeding. Plasma and tissues were collected during meat processing as abattoir by-products by highly qualified and experienced laboratory staff. Thus, according to the ethical issues for the protection of animals, this project does not require the consent of the competent ethics committee for animal experiments. The UEPEAT experimental unit is registered by the Ministry of Agriculture with the license number D-37-175-1 for animal experimentation. All experiments were performed in accordance with the European Communities Council Directive 2010/63/UE. Human plasma was collected from patients (n = 3) undergoing bariatric surgery and included in the prospective monocentric METABOSE cohort (Nutrition Department, CHU Tours) following patient written consent and after local ethical committee agreement (CNIL n° 18254562). Mice plasma was collected from three control adult animals included in a protocol approved by an ethics committee (Comité d'Ethique en Expérimentation Animale Val de Loire, CEEA VdL, protocol reference number 2021032516245453.V2-30673).

Animals and samples collection

Seven breeds composed of 6–10 hens (54 weeks-old, end of laying) were reared at UEPEAT according to the conventional breeding conditions. The peculiarities of each breed are summarized in Table 1. The number of animals used for each breed is indicated in Table 2. During five successive days of laying, eggs were collected every day in order to weigh the egg, egg white (albumen) and yolk individually. For each egg, an albumen sample was collected and stored at −20°C until use. At the end of the protocol, all overnight fasted hens were euthanized by electrical stuning and bled out for blood sample collection, as recommended by the ethical committee. Blood samples were centrifuged (5000 g for 10 min at 4°C) and plasma samples stored at −20°C until use. The experimental design is summarized in Figure 1. Nine hens out of 70 were eliminated from the protocol because they laid less than three eggs that's why n = 6 to 10 hens dependent on the breed.

Reproductive parameters

The reproductive parameters of the animals (6-10 animals in each breed) were determined at 21 week-old during 20 successive weeks (Table 3). For each breed, the semen of several roosters was collected and pooled to form a single sample. The hens were artificially inseminated with 2×10^8 spermatozoa from the pool and eggs were collected and counted daily for two weeks following the artificial insemination and then artificially incubated. The number of unfertilized eggs, and early (EEM) and late (LEM) embryonic mortality were evaluated by breaking eggs and candling on the 7th (EEM) and 14th day of incubation (LEM).

For each hen, the different performances and reproductive parameters (laying, fecundity, fertility, EEM, LEM and hatchability percentage) were calculated using the following formulae:

$$\%\,\textbf{laying} = \frac{number\ of\ eggs\ laid}{number\ of\ laying\ days}\ x\ 100 \quad (1)$$

$$\%\,\textbf{fecundity} = \frac{(number\ of\ incubated\ eggs - unfertilized\ eggs)}{number\ of\ incubated\ eggs}\ x\ 100$$

$$\%\,\textbf{fertility} = \frac{\left(number\ of\ incubated\ eggs - unfertilized\ eggs - number\ of\ egg\ mortality\right)}{number\ of\ incubated\ eggs}\ x\ 100$$

TABLE 2 Egg performances of different breed. Data are shown as the mean ± SEM; n = 6–10 animals per breed. Groups showing different letters are significantly different ($p < 0.05$). The laying rate was determined during 20 successive weeks in 21 weeks-old animals from different breeds.

Breed		Laying (%)	Egg weight (g)	Albumen weight (g)	Yolk weight (g)	Ratio albumen/yolk	Ratio egg/albumen
R-	$n = 9$	85.39 ± 1.18^{ab}	54.65 ± 0.98^{bc}	30.80 ± 0.64^{b}	16.31 ± 0.33^{ab}	1.89 ± 0.05^{bc}	1.78 ± 0.02^{b}
R+	$n = 9$	90.12 ± 1.11^{b}	52.16 ± 1.21^{b}	28.53 ± 0.91^{ab}	16.48 ± 0.38^{ab}	1.73 ± 0.05^{ab}	1.83 ± 0.02^{ab}
FAYOUMI	$n = 10$	79.97 ± 1.76^{a}	43.89 ± 1.04^{a}	21.75 ± 0.63^{a}	14.80 ± 0.49^{a}	1.48 ± 0.05^{a}	2.02 ± 0.04^{a}
OD	$n = 7$	91.61 ± 4.02^{b}	60.68 ± 1.38^{c}	33.85 ± 0.93^{b}	18.04 ± 0.61^{b}	1.88 ± 0.05^{bc}	1.80 ± 0.02^{b}
GAVORA	$n = 10$	86.80 ± 2.23^{ab}	58.13 ± 0.93^{bc}	32.66 ± 0.52^{b}	16.80 ± 0.33^{ab}	1.95 ± 0.03^{c}	1.78 ± 0.01^{b}
CHEPTEL1	$n = 10$	83.36 ± 2.30^{ab}	54.55 ± 1.06^{bc}	29.66 ± 0.78^{b}	16.96 ± 0.33^{b}	1.75 ± 0.04 ^{abc}	1.84 ± 0.02^{ab}
DwNa	$n = 6$	89.61 ± 2.21^{ab}	55.32 ± 1.33^{bc}	29.69 ± 0.95^{ab}	17.39 ± 0.42^{b}	1.71 ± 0.03^{abc}	1.87 ± 0.02^{ab}
p value		0.004	<0.0001	<0.0001	0.002	<0.0001	<0.0001

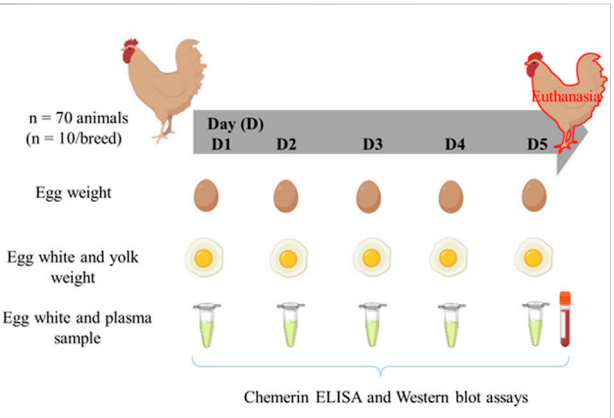

FIGURE 1
Experimental design. Seventy fasted hens (54 weeks-old, end of laying) from seven Rhode Island breeds (n = 10 hen per breed) were used. During five days of laying, eggs were successively collected in order to weigh the egg, egg white (albumen) and yolk individually. For each egg, an albumen sample was stored at −20°C until use. At the end of the protocol, all hens were euthanized by electrical stunning and bled out for blood sample collection.

$$\%\ \boldsymbol{EEM} = \frac{number\ of\ EEM}{(number\ of\ incubated\ eggs - unfertilized\ eggs)}\ x\ 100$$

$$\%\ \boldsymbol{LEM} = \frac{number\ of\ LEM}{(number\ of\ incubated\ eggs - unfertilized\ eggs + number\ of\ EEM)}\ x\ 100$$

$$\%\ \boldsymbol{hatchability} = \frac{number\ of\ hatched\ chicks}{number\ of\ fertile\ eggs\ after\ 14\ days\ of\ incubation}\ x\ 100$$

Production of recombinant chicken chemerin and monoclonal chicken chemerin antibody

The recombinant chicken chemerin protein (full length, rRARRES2) was obtained from the *Gallus gallus* sequence (NM_001277476.1), produced in *Escherichia coli* and purified by a chromatography column-based on His-Tag under denaturing conditions (Agro-Bio, La Ferté Saint

TABLE 3 Reproductive parameters of the different breed. Data are shown as the mean ± SEM; n = 6–10 animals per breed. Groups showing different letters are significantly different ($p < 0.05$).

Breed	Number of animals (n)	Fecundity (%)	Fertility (%)	EEM (%)	LEM (%)
R-	9	77.16 ± 10.63	68.94 ± 9.19	4.90 ± 2.01	3.89 ± 2.30
R+	9	74.73 ± 8.40	60.37 ± 10.82	16.88 ± 8.39b	3.46 ± 2.40
FAYOUMI	10	87.10 ± 4.90	85.43 ± 5.59	0a	2.22 ± 2.22
OD	7	88.78 ± 7.61	80.12 ± 8.02	5.77 ± 2.27	4.52 ± 3.54
GAVORA	10	92.33 ± 3.17	84.95 ± 4.15	4.81 ± 1.71	3.39 ± 1.95
CHEPTEL1	10	83.06 ± 5.91	78.45 ± 6.19	5.25 ± 2.34	0.77 ± 0.77
DwNa	6	85.48 ± 6.04	79.69 ± 5.20	3.75 ± 2.60	2.67 ± 1.69
p value		0.56	0.28	0.10	0.84

Aubin, France) (Estienne et al., 2020). Monoclonal chicken chemerin antibodies were produced by AgroBio (La Ferté Saint Aubin, France), and their specificity was tested as previously described (Mellouk et al., 2018a, 2018c; Estienne et al., 2020, 2021).

Detection and quantification of chemerin by western blot analysis

Egg whites were lysed using an Ultraturax (Invitrogen™ by Life Technologies™, Villebon sur Yvette, France) in lysis buffer 50% (vol/vol, Tris 1 M (pH 7.4), NaCl 0.15 M, EDTA 1.3 mM, EGTA 1 mM, VO43−23 mM, NaF 0.1 M, NH2PO41%, Triton 0.5%). The protein concentration of lysates was measured using the bicinchoninic acid (BCA) protein assay (Interchim, Montluçon, France). Egg white (80 µg) were mixed with Laemmli buffer 5 X and proteins were denatured for 5 min by heating at 95°C. Proteins were loaded on an electrophoresis sodium dodecyl sulfate-polyacrylamide gel (12% for high protein weight (110-20 kDa) or 15% for low protein weight (<20 kDa)) and then proteins were transferred to a nitrocellulose membrane. Membranes were blocked with Tris-Buffered Saline Tween buffer containing 0.05% of Tween 20 and 5% of milk for 30 min at room temperature. Membranes were incubated overnight at 4°C with the appropriate primary antibody (anti-chemerin antibody). Then, membranes were incubated 90 min at room temperature with a Horse Radish Peroxidase-conjugated anti-mouse IgG. Chemerin protein was detected by enhanced chemiluminescence (ECL, Western Lightning Plus-ECL, Perkin Elmer, Villebon-sur-Yvette, France) with a G-box SynGene (Ozyme, St Quentin en Yvelines, France) and the GeneSnap software (Ozyme, St Quentin en Yvelines, France). Then, protein amounts were quantified with GeneTools software. The results were expressed as the intensity signal in arbitrary units after normalization of chemerin protein signals with the total protein amount as evaluated by Ponceau-red staining. Albumen of eggs from different avian species such as Galliforms (chicken *Gallus gallus*, turkey *Meleagris gallopavo*, pheasant *Phasianus colchicus*, quail *Coturnix japonica*, guinea fowl *Numida meleagris* and red-legged partridge *Alectoris rufa*), Anseriforms (ducks *Cairina moschata* and *Anas platyrhynchos* and goose *Anser anser*) and Colombiform (pigeon *Columba livia*) species were tested. All these eggs were provided by different breeders from Région Centre Val de Loire (France).

Development of a sandwich ELISA for chicken chemerin

Microtiter plates (NUNC Maxisorb, ThermoFisher Scientific, Les Ulis, France) were coated with bovine serum albumin (100 mM NaHCO3 pH 9.6) at 4°C for 16 h. After blocking of free binding sites with 200 µL of assay buffer containing 0.2% BSA and 0.01% Tween 20 in PBS pH 7.3 at RT for 1 h, the plates were washed 3 times with PBS containing 0.01% Tween 20, filled with 200 µL of assay buffer. Then, serial 2-fold dilutions of the chicken recombinant chemerin (256–2 ng/ml) were prepared in the assay buffer to generate the calibration curve. For the assay, plates were decanted, and 100 µL of reference recombinant chicken chemerin or prediluted white egg in lysis buffer (Tris 1 M (pH 7.4), NaCl 0.15 M, EDTA 1.3 mM, EGTA 1 mM, VO43−23 mM, NaF 0.1 M, NH2PO41%, Triton 0.5%) (1/2) or pure plasma were pipetted in duplicate into the specified wells and then incubated for 3 h at room temperature. After 3 washings, one hundred microliters of the monoclonal chicken chemerin antibody (used at final concentration of 100 ng/ml) was added and the plate was incubated for 1 h at RT. After 3 washings, 100 µL of peroxidase-conjugated secondary antibody (1/2000; Sigma; A1949) was added and incubated for 1 h at RT. After 3 washings, the TMB substrate solution (100 µL) was added and incubated for 30 min at 25°C in the dark. The reaction was stopped with 50 µL of 1 M H2SO4, and optical density was determined at 450 nm with a microtiter plate reader (Tecan, Magellan, Männedorf, Switzerland). A standard curve was drawn for the determination of chemerin levels. The accuracy of the ELISA was determined by showing parallelism of serial dilutions of chicken serum and egg white samples and the standard curve. No cross-reactivity was shown for human, bovine, ovine and goat serum samples. The mean recovery of 4 different concentrations of recombinant chicken chemerin spiked into a serum and egg white sample determined in 4 different dilutions was 118 ± 9.2% and 116% ± 8.5, respectively. The intra-assay and interassay variation were determined by repeated measurement (n = 10) of 2 different serum and egg white samples at 2 different dilutions (n = 4) within one assay plate and across different assays (n = 8). The mean intra-assay CV was 6 and 8%, the inter-assay CV was 10 and 11% for blood plasma and egg white samples, respectively.

Alignment of nucleic and proteic RARRES 2 sequence of various avian species

The gene and protein sequences of *RARRES2* of different avian species were downloaded from the National Centre for Biotechnology Information (NCBI http://www.ncbi.nlm.nih.gov) under GenBank accession number. Multiple RARRES2 sequences of different avian species were aligned using Clustal Omega to check their percent homology and identity matrix for *RARRES2* gene and protein of avian species compared to *RARRES*2 chicken.

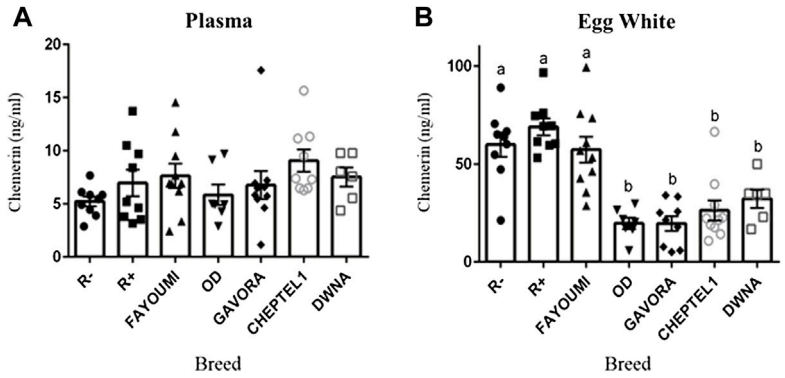

FIGURE 2
Concentration of chemerin in plasma **(A)** and egg white **(B)** in each breed of hen as determined by ELISA assay. Concentration of chemerin in plasma **(A)** and in egg white from eggs **(B)** was determined by ELISA assay in seventy 54-old hens from seven different breeds. Data are shown as the mean ± SEM; n = 6–10 animals per breed. Groups showing different letters are significantly different ($p < 0.05$).

Statistical analysis

The GraphPad Prism® software (version 6) was used for all analyses. All data are represented as means ± standard error of mean (SEM) with a level of significance less than 0.05 ($p < 0.05$). One-way ANOVA and multiple comparisons were used to compare reproductive parameters, chemerin concentration in albumen and blood among the different breeds. A Pearson test was used to analyse correlations. The correlation was noted "r" and the p value was considered significant if p value <0.05. Different letters indicate significant differences ($p < 0.05$).

Results

Laying performance and reproductive parameters of chicken breeds

As described in Table 2, we used seven breeds of hen ($n = 61$) that have significant difference on laying rate, egg weight and egg white and yolk weights. Overall, Fayoumi hens lay significantly fewer eggs than R+ and OD animals (Table 2). The egg weights were lower in Fayoumi hens compared to the other breeds (Table 2), whereas the reproductive parameters, i.e. the percentages of fecundity, fertility, EEM, LEM and hatchability were similar in the seven breeds under study (Table 3).

Chemerin in hen plasma and egg white

As shown in Figure 2A, hen plasma chemerin concentrations were similar ($p= 0.261$), whereas they were very different in egg whites from the seven breeds. In addition, as shown in Figure 2B, chemerin concentrations were up to 5 to 10 fold higher in egg white as compared to their mother's plasma. Chemerin concentration in egg white was about two-fold higher in R-, R+ and Fayoumi breeds than in OD, Gavora, Cheptel1 and DwNa breeds ($p < 0.0001$) (Figure 2B). The intra-hen variability coefficient was determined from chemerin concentrations in albumen of each egg laid during five successive days, whereas the inter-hen variability coefficient was calculated from chemerin concentrations in egg white for all hens of each breed. Data showed a lower intra-hen variability of chemerin concentration compared with the inter-hen variability except for R+ breed (Table 4). Most importantly, in the seven breeds of hen (n = 61 animals), no correlation was observed between chemerin concentrations in egg white and in their mother's plasma (Table 5).

Comparison of chemerin concentration in hen egg white measured by ELISA and western-blot analysis

Samples of the hens's albumen were analyzed by two methods: Western-blot and ELISA. As shown in Figure 3A, the amount of egg white chemerin as determined by western-blot analysis in 4 or 5 successive eggs showed a three-fold difference between two hens (C254 *vs.* C261 hen). This difference was similar between egg white chemerin concentrations measured by ELISA (Figure 3B). These data were confirmed for six hens. We also determined correlation between these two methods (ELISA *vs.* Western-blot) by using egg white samples from hens of seven breeds (n = 61 with only one value for each hen). In this case, the correlation analysis confirmed the comparability of the results from both methods ($p < 0.0001$); r was 0.51 when individual data (egg white from different hens) were used (Figure 3C).

TABLE 4 Concentration of chemerin in biological fluids (plasma and albumen) and their variability inter-hen and intra-hen. Data are shown as the mean ± SEM; n = 6–10 animals per breed. Groups showing different letters are significantly different ($p < 0.05$).

Breed	Number of animals (n)	Chemerin plasma (ng/ml)	Variability inter-hen (%)	Chemerin albumen (ng/ml)	Variability inter-hen (%)	Variability intra-hen (%)
R-	9	5.23 ± 0.46	26.50	59.86 ± 6.15[a]	30.81	29.06
R+	9	6.97 ± 1.25	53.79	68.96 ± 4.27[a]	18.56	29.20
FAYOUMI	10	7.62 ± 1.14	47.41	57.29 ± 6.68[a]	36.86	26.61
OD	7	5.83 ± 0.96	43.79	19.74 ± 2.92[b]	39.17	22.51
GAVORA	10	6.76 ± 1.32	61.74	19.63 ± 3.56[b]	57.30	28.31
CHEPTEL1	10	9.07 ± 1.00	34.90	26.39 ± 5.13[b]	61.44	27.95
DwNa	6	7.52 ± 0.90	29.31	32.32 ± 4.70[b]	35.61	27.04
p value		0.26		<0.0001		

TABLE 5 Pearson correlation coefficient (r) calculated between chemerin concentration in plasma and egg white with egg performances and reproductive parameters in 7 breeds of hen (n = 61). The correlation noted « r » and p-value was significant if $p < 0.05$. NS, indicated no difference significant.

r / *p value*	Egg weight	Albumen weight	Yolk weight	Laying	Fecundity	Fertility	EEM	LEM	Hatchability	Chemerin plasma	Chemerin albumen
Chemerin plasma	NS	NS	NS	NS	NS	NS	NS	NS	NS		NS
Chemerin albumen	−0.43	−0.39	−0.28	NS	−0.32	−0.27	NS	NS	NS	NS	
	0.001	0.002	0.03		0.01	0.03					

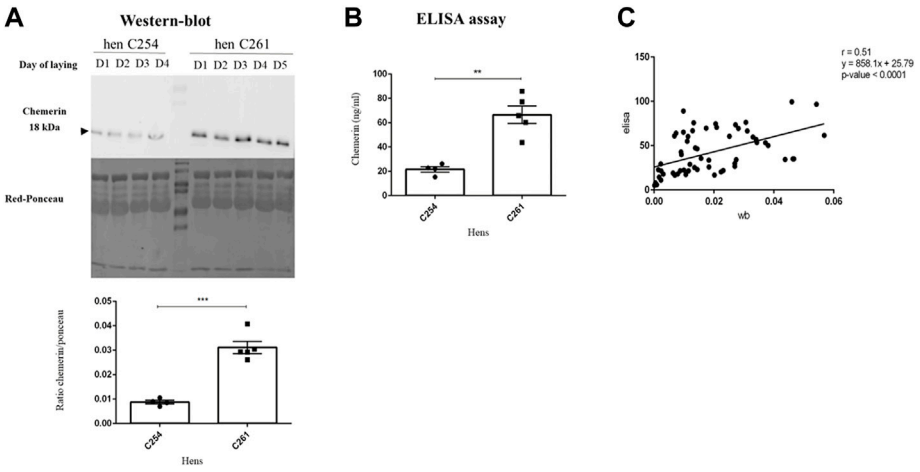

FIGURE 3
Concentration of chemerin in egg white by two methods of analysis. **(A)** Protein abundance of chemerin detected by western blotting within 3 or 4 or 5 egg whites laid successively in two hens named C254 and C261, respectively (n = 4–5). **(B)** Chemerin concentration determined by ELISA assay within the same egg whites samples as **(A)**. Data are shown as the mean ± SEM; n = 4 to 5 samples per animal. Significant differences are indicated by $p < 0.01$ ** and ***$p < 0.001$. **(C)** Sixty-one egg white samples from eggs laid by different hens were collected and analysed by both ELISA and Western-blot assays. Correlation between chemerin concentration within albumen obtained by western blotting and ELISA assay (n = 61) is shown.

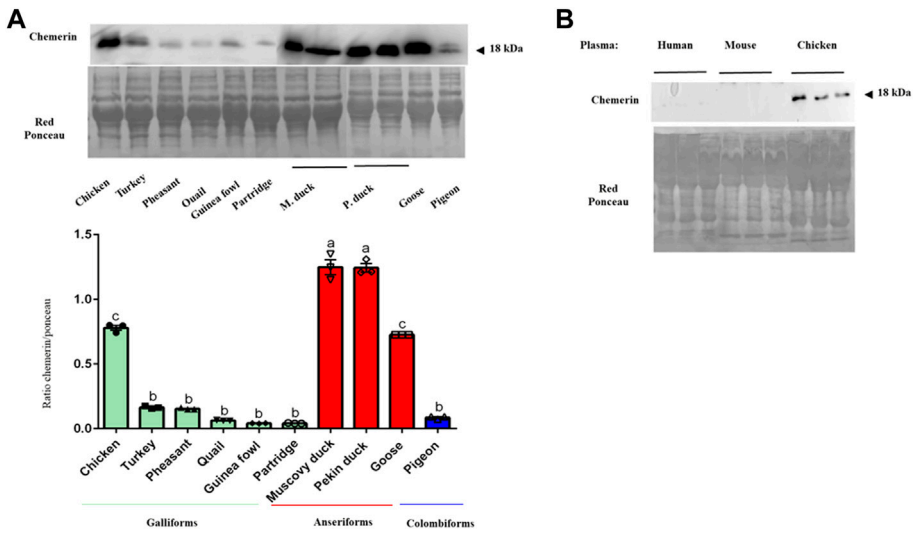

FIGURE 4
Abundance of chemerin in egg white of different avian species. **(A)** Protein amount of chemerin in egg white from egg of different avian species was detected by western blotting. Data are shown as the mean ± SEM; $n = 3$ egg white samples from different animals of various avian species. Groups showing different letters are significantly different ($p < 0.05$). **(B)** Chemerin protein expression in human, mouse and chicken blood plasma samples ($n = 3$ for each species). All plasma samples contained equal amounts of proteins, as confirmed by staining the nitrocellulose membrane with Red Ponceau.

Chemerin concentration in plasma and egg white associated with performance parameters

We next analyzed a potential link between chemerin concentrations in egg white and plasma with egg performance and reproductive parameters with Pearson correlations by using data from the seven breeds of hen ($n = 61$ animals). As shown in Table 5, chemerin concentration in egg white was negatively correlated with egg weight ($r = -0.43$, $p = 0.001$), albumen weight ($r = -0.39$, $p = 0.002$) and yolk weight ($r = -0.28$, $p = 0.029$). Concerning reproductive parameters, we also evidenced negative correlations between chemerin concentrations in egg white and hen fecundity ($r = -0.32$, $p = 0.01$) and fertility ($r = -0.27$, $p = 0.037$) (Table 5). However, no correlation was observed between plasma chemerin levels and egg performances or reproductive parameters (Table 5).

Chemerin presence in egg white from other avian species

Egg white samples from different avian species were analyzed by Western blot to detect chemerin by using our monoclonal chicken chemerin antibody. As shown in Figure 4, we found the presence of chemerin in egg white in Galliforms including inter alia chicken, turkey, quail, guinea fowl, red partridge and pheasant with a higher amount in chicken. Chemerin in egg white was also detected in Anseriforms such as muscovy duck, pekin duck and goose and one species of Colombiforms (pigeon). The chemerin abundance in egg white was significantly higher for the two species of duck compared to the other avian species tested even if the percentage of homology and identity sequence between duck RARRES2 gene and protein and these species was lower (Table 6). Probably because of phylogenetic distance, we were not able to detect the chemerin protein in human and mouse plasma or tissue (Figure 4) in agreement with the lack of chicken chemerin detection with anti-mammalian antibodies.

Discussion

In the present study, we investigated for the first time plasma and egg white chemerin concentrations in seven hen breeds by using a home-made chicken chemerin monoclonal antibody and a new ELISA assay. We showed that chemerin egg white concentration was not correlated with chemerin plasma concentration and laying rate, whereas it was negatively correlated with total, egg white, and egg yolk weights, and fecundity and fertility.

We observed that chemerin concentrations in egg white were significantly higher than in blood plasma and there was no correlation between these two parameters. These data are in good agreement with our previous study (Estienne et al., 2022) showing that chemerin was 10 times more concentrated in egg white than in plasma. In the present study, we developed a

TABLE 6 Sequence homology and identity (%) for *RARRES2* gene and protein between chicken and two mammals (human and mouse) and various avian species.

RARRES2	*Gallus gallus*	
	Chicken	
	Gene (% homology)	Protein (% identity)
Human (*Homo Sapiens*)	56	37
Mouse (*Mus musculus*)	54	36
Turkey (*Meleagris gallopavo*)	94	90
Ring-necked pheasant (*Phasianus colchicus*)	93	92
Japanese quail (*Coturnix japonica*)	92	90
Guinea fowl (*Numida meleagris*)	91	89
Pekin duck (*Anas platyrhynchos*)	76	70
Swan goose (*Anser cygnoides*)	76	62
Rock Pigeon (*Columba livia*)	74	72

specific chicken chemerin ELISA by using specific monoclonal chicken chemerin antibodies and recombinant chicken chemerin. The absence of link between plasma and egg white chemerin concentrations could originate from a local production of chemerin within the oviduct, more precisely at the magnum level, independently of chemerin in the blood circulation. Indeed, the oviduct's magnum is the main site of egg white protein synthesis (Jeong et al., 2012). Furthermore, several studies demonstrated that chemerin mRNA and protein are found in the magnum of hen reproductive tract (Bílková et al., 2018; Estienne et al., 2022). Interestingly, we observed in each breed studied here, some hens with high or low chemerin protein levels in their egg white. However, the chemerin concentration in egg white as determined by both ELISA and Western-blot assays was relatively stable for eggs laid successively for 3, 4 or 5 days. These data suggest that egg white chemerin concentration could be used as a potential trait for genetic selection if these differences are conserved by the offsprings. Indeed, it could be interesting to study descendants of these hens over several generations in order to determine if these variations of chemerin concentrations in egg white are heritable. In the present study, we also observed significant differences of egg white chemerin between the seven breeds studied. For example, Fayoumi was one of the breeds with the higher egg white chemerin concentration as compared to OD and GAVORA breeds. Our results are also in a good agreement with a study showing that egg white protein abundance may differ between hens and between breeds (Wang et al., 2012).

Concerning egg performances, we showed that laying rates could be significantly different between breeds as well as the total egg, the albumen and the yolk weights. For example, Fayoumi hens laid fewer and smaller eggs probably because of their smaller body size as previously described (Khawaja et al., 2012; Kebede, E. 2017). In addition, we also established a link between egg white chemerin concentration and the egg parameters. We showed, for the first time, that egg white chemerin concentrations were negatively correlated with total egg, egg white and egg yolk weights. Studies have shown that egg weight is an important factor that influences the composition and the proportion of basic morphological elements, i.e., albumen, yolk, and shell (Bleu et al., 2019). Ayeni et al., 2018 reported that the eggs with the highest albumen content and the lowest yolk content showed worse hatchability results. Hagger et al., 1986 also found that the embryos that died during the entire incubation process were found in the heaviest eggs. Farooq et al., 2001 also observed a negative correlation between egg weight and hatchability rate. In addition, the body weight of hatched chicks depend on the weight of the eggs; hence, the larger the eggs, the heavier the chicks (Ramaphala and Mbajiorgu, 2013). An important indicator of chick quality is its length, which is highly positively correlated with the chick weight without the yolk sac. Thus, egg weight presents different physical and chemical qualities that affect hatchability and chick quality (Zakaria et al., 2009). Consequently, it is important to find biomarkers to genetically select hen laying eggs with optimal sizes. Furthermore, egg white and yolk are important in the food industry (Mine, Y. 2015). For example, foaming, emulsifying and gelling are functional properties of albumen.

In the present study, we showed that chemerin concentrations in the egg white were negatively correlated with two of the reproductive parameters of their mothers: fecundity and fertility. We have already shown a negative effect of chemerin on egg fertilization three days after artificial insemination (AI) with sperm pre-incubated with recombinant chicken chemerin (Estienne et al., 2020). At variance with these negative effects of chemerin in egg development, we reported in

another previous study that *in-ovo* injections of anti-chemerin or anti-CMKLR1 antibodies to neutralize the chemerin system in egg white, increased embryo mortality (Estienne et al., 2022). In brief, too much chemerin appears deleterious but this hormone is indispensable for egg development probably because the chemerin system is involved in chicken embryo angiogenesis (Estienne et al., 2022). Taken together, data provide more evidence of a potential role of chemerin in egg performance and embryo development in chicken. However, in the present study, the hens' plasma chemerin levels were not correlated with their reproductive parameters. In a previous study, we found that plasma chemerin concentrations were negatively correlated with egg hatchability in broiler breed hen (Mellouk et al., 2018b). This discrepancy could be due to the age and/or the breed of animals.Indeed, Mellouk et al. studied 39 weeks-old broiler hens whereas in our study we analysed data from laying hens at the end of the laying period (Mellouk et al., 2018b). Thus, plasma and egg white chemerin concentrations in broiler and laying hen during all their egg-laying period must be compared. It must be pointed out in this respect that chemerin plasma levels decreased during the laying period in turkeys (Diot et al., 2015).

Conclusion

Taken together, our data show that chemerin concentration in egg white is negatively associated to egg weight and to hen fecundity and fertility parameters in chicken. Thus, chemerin could influence egg quality, chicken embryogenesis and chick quality. In consequence, determination of its level in egg white could be a potential trait for genetic selection. The improvement of reproductive rates and quality of chick would obviously have huge impacts for breeding companies thanks to the number of animals generated.Tixier-Boichard et al., 1994.

Data availability statement

The datasets presented in this study can be found in online repositories. The names of the repository/repositories and accession number(s) can be found in the article/ Supplementary material.

Ethics statement

The studies involving human participants were reviewed and approved by Human plasma was collected from patients (n = 3) undergoing bariatric surgery and included in the prospective monocentric METABOSE cohort (Nutrition Department, CHU Tours) following patient written consent and after local ethical committee agreement (CNIL n° 18254562). The patients/ participants provided their written informed consent to participate in this study. Ethical review and approval was not required for the animal study because Plasma and tissues were collected during meat processing as abattoir by-products by highly qualified and experienced laboratory staff. Thus, according to the ethical issues for the protection of animals, this project does not require the consent of the competent ethics committee for animal experiments.

Author contributions

OB, MR, AE, YC, PF, and JD contributed to the overall approach and design of experiments. OB, MR, and JD performed statistical data analysis. YB take care of animals and help for samples collection. AB and CR realized the analyses of chemerin protein expression in egg white from different avian species. YC helped to set up the chicken chemerin ELISA assay. OB and JD wrote the manuscript. All authors critically revised the manuscript and approved the final version.

Funding

The authors thank the SYSAAF for the financial support (Project number 3440, FERTILICHEM).

Acknowledgments

The authors are grateful to all the persons from the experimental unit (INRAE, PEAT, Centre Val de Loire DOI: 10.15454/1.5572326250887292E12) who take care of animals.

Conflict of interest

The authors declare that the research was conducted in the absence of any commercial or financial relationships that could be construed as a potential conflict of interest.

Publisher's note

References

Ahima, R. S., and Flier, J. S. (2000). Adipose tissue as an endocrine organ. *Trends Endocrinol. Metab.* 11, 327–332. doi:10.1016/S1043-2760(00)00301-5

Ayeni, A., Agbede, J. O., Francis, I., Onibi, G. E., and Muyiwa, A. (2018). Effect of egg sizes on egg qualities, hatchability and initial weight of the hatched-chicks. *Int. J. Environ. Agric. Biotechnol.* 3, 987–993. doi:10.22161/ijeab/3.3.35

Bernardi, O., Estienne, A., Reverchon, M., Bigot, Y., Froment, P., and Dupont, J. (2021). Adipokines in metabolic and reproductive functions in birds: An overview of current knowns and unknowns. *Mol. Cell. Endocrinol.* 534, 111370. doi:10.1016/j.mce.2021.111370

Bílková, B., Świderská, Z., Zita, L., Laloë, D., Charles, M., Beneš, V., et al. (2018). Domestic fowl breed variation in egg white protein expression: Application of proteomics and transcriptomics. *J. Agric. Food Chem.* 66, 11854–11863. doi:10.1021/acs.jafc.8b03099

Bleu, J., Agostini, S., Angelier, F., and Biard, C. (2019). Experimental increase in temperature affects eggshell thickness, and not egg mass, eggshell spottiness or egg composition in the great tit (*Parus major*). *Gen. Comp. Endocrinol.* 275, 73–81. doi:10.1016/j.ygcen.2019.02.004

Bozaoglu, K., Bolton, K., McMillan, J., Zimmet, P., Jowett, J., Collier, G., et al. (2007). Chemerin is a novel adipokine associated with obesity and metabolic syndrome. *Endocrinology* 148, 4687–4694. doi:10.1210/en.2007-0175

Briere, S., Brillard, J. P., Panheleux, M., and Froment, P. (2011). Alimentation, fertilité et bien-être des oiseaux reproducteurs domestiques : Des liens complexes. *INRAE Prod. Anim.* 24, 171–180. doi:10.20870/productions-animales.2011.24.2.3251

Chang, C. M., Furet, J. P., Coville, J. L., Coquerelle, G., Gourichon, D., and Tixier-Boichard, M. (2007). Quantitative effects of an intronic retroviral insertion on the transcription of the tyrosinase gene in recessive white chickens: Transcription of tyrosinase gene in recessive white chickens. *Anim. Genet.* 38, 162–167. doi:10.1111/j.1365-2052.2007.01581.x

Chen, C.-F., and Tixier-Boichard, M. (2003b). Estimation of genetic variability and selection response for clutch length in dwarf brown-egg layers carrying or not the naked neck gene. *Genet. Sel. Evol.* 35, 219. doi:10.1186/1297-9686-35-2-219

Chen, C., and Tixier-Boichard, M. (2003a). Correlated responses to long-term selection for clutch length in dwarf brown-egg layers carrying or not carrying the naked neck gene. *Poult. Sci.* 82, 709–720. doi:10.1093/ps/82.5.709

Chen, S. E., McMurtry, J. P., and Walzem, R. L. (2006). Overfeeding-induced ovarian dysfunction in broiler breeder hens is associated with lipotoxicity. *Poult. Sci.* 85, 70–81. doi:10.1093/ps/85.1.70

Diot, M., Reverchon, M., Rame, C., Froment, P., Brillard, J.-P., Brière, S., et al. (2015). Expression of adiponectin, chemerin and visfatin in plasma and different tissues during a laying season in turkeys. *Reprod. Biol. Endocrinol.* 13, 81. doi:10.1186/s12958-015-0081-5

Estienne, A., Brossaud, A., Ramé, C., Bernardi, O., Reverchon, M., Rat, C., et al. (2022). Chemerin is secreted by the chicken oviduct, accumulates in egg albumen and could promote embryo development. *Sci. Rep.* 12, 8989. doi:10.1038/s41598-022-12961-4

Estienne, A., Ramé, C., Ganier, P., Chahnamian, M., Barbe, A., Grandhaye, J., et al. (2021). Chemerin impairs food intake and body weight in chicken: Focus on hypothalamic neuropeptides gene expression and AMPK signaling pathway. *Gen. Comp. Endocrinol.* 304, 113721. doi:10.1016/j.ygcen.2021.113721

Estienne, A., Reverchon, M., Partyka, A., Bourdon, G., Grandhaye, J., Barbe, A., et al. (2020). Chemerin impairs *in vitro* testosterone production, sperm motility, and fertility in chicken: Possible involvement of its receptor CMKLR1. *Cells* 9, 1599. doi:10.3390/cells9071599

Farooq, M., Durrani, F. R., Aleem, M., Naila, C., and Muqaarp, A. K. (2001). Egg traits and hatching performance of desi, fayumi and Rhode Island red chicken. *Pak. J. Biol. Sci.* 4, 909–911. doi:10.3923/pjbs.2001.909.911

Gavora, J. S., Kuhnlein, U., and Spencer, J. L. (1989). Absence of endogenous viral genes in an inbred line of leghorn chickens selected for high egg production and Marek's disease resistance. *J. Anim. Breed. Genet.* 106, 217–224. doi:10.1111/j.1439-0388.1989.tb00232.x

Hagger, C., Steiger-Stafl, D., and Marguerat, C. (1986). Embryonic mortality in chicken eggs as influenced by egg weight and inbreeding. *Poult. Sci.* 65, 812–814. doi:10.3382/ps.0650812

Hamet, N., Mérat, P., Bertrand, F., and Coquerelle, G. (1982). Etude des particularités de la poule Fayoumi. II. – Résistance à la coccidiose (Eimeria tenella) des poussins Fayoumi, Rhode-Island et de leur croisement. *Genet. Sel. Evol.* 14, 453. doi:10.1186/1297-9686-14-4-453

Jeong, W., Lim, W., Kim, J., Ahn, S. E., Lee, H. C., Jeong, J.-W., et al. (2012). Cell-specific and temporal aspects of gene expression in the chicken oviduct at different stages of the laying Cycle1. *Biol. Reprod.* 86. doi:10.1095/biolreprod.111.098186

Kebede, E. (2017). Growth performance and rearing costs of Fayoumi and white leghorn chicken breeds. *East Afr. J. Sci.* 11, 37–42.

Khawaja, T., Khan, S. H., Mukhtar, N., Ali, M. A., Ahmed, T., and Ghafar, A. (2012). Comparative study of growth performance, egg production, egg characteristics and haemato-biochemical parameters of *Desi* , Fayoumi and Rhode Island Red chicken. *J. Appl. Anim. Res.* 40, 273–283. doi:10.1080/09712119.2012.672310

Lowry, D. C., Dobbs, J. C., and Abplanalp, H. (1979). Yolk deposition in eggs of a line selected for simultaneous multiple ovulations. *Poult. Sci.* 58, 498–501. doi:10.3382/ps.0580498

Mann, K. (2008). Proteomic analysis of the chicken egg vitelline membrane. *PROTEOMICS* 8, 2322–2332. doi:10.1002/pmic.200800032

Mann, K. (2007). The chicken egg white proteome. *PROTEOMICS* 7, 3558–3568. doi:10.1002/pmic.200700397

Mattern, A., Zellmann, T., and Beck-Sickinger, A. G. (2014). Processing, signaling, and physiological function of chemerin: Processing, signaling, and physiological function of chemerin. *IUBMB Life* 66, 19–26. doi:10.1002/iub.1242

Mellouk, N., Ramé, C., Barbe, A., Grandhaye, J., Froment, P., and Dupont, J. (2018a2018). Chicken is a useful model to investigate the role of adipokines in metabolic and reproductive diseases. *Int. J. Endocrinol.*, 1–19. doi:10.1155/2018/4579734

Mellouk, N., Ramé, C., Delaveau, J., Rat, C., Marchand, M., Mercerand, F., et al. (2018b). Food restriction but not fish oil increases fertility in hens: Role of RARRES2? *Reproduction* 155, 321–331. doi:10.1530/REP-17-0678

Mellouk, N., Ramé, C., Delaveau, J., Rat, C., Maurer, E., Froment, P., et al. (2018c). Adipokines expression profile in liver, adipose tissue and muscle during chicken embryo development. *Gen. Comp. Endocrinol.* 267, 146–156. doi:10.1016/j.ygcen.2018.06.016

Mellouk, N., Ramé, C., Marchand, M., Staub, C., Touzé, J.-L., Venturi, É., et al. (2018d). Effect of different levels of feed restriction and fish oil fatty acid supplementation on fat deposition by using different techniques, plasma levels and mRNA expression of several adipokines in broiler breeder hens. *PLOS ONE* 13. doi:10.1371/journal.pone.0191121e0191121

Mérat, P., Bordas, A., L'Hospitalier, R., Protais, J., Bougon, M., Coquerelle, G., et al. (1983). Etude des particularités de la poule Fayoumi. III. Ponte, caractéristiques des œufs, efficacité alimentaire et paramètres physiologiques de poules Fayoumi, Rhode-Island et F1 en batteries. *Genet. Sel. Evol.* 15, 147. doi:10.1186/1297-9686-15-1-147

Mine, Y. (2015). "Egg proteins," in *Applied food protein Chemistry*. Editor Z. Ustunol (Chichester, UK: John Wiley & Sons)), 459–490. doi:10.1002/9781118860588.ch17

Nagpal, S., Patel, S., Jacobe, H., DiSepio, D., Ghosn, C., Malhotra, M., et al. (1997). Tazarotene-induced gene 2 (TIG2), a novel retinoid-responsive gene in skin. *J. Invest. Dermatol.* 109, 91–95. doi:10.1111/1523-1747.ep12276660

Nasri, H., van den Brand, H., Najjar, T., and Bouzouaia, M. (2020). Egg storage and breeder age impact on egg quality and embryo development. *J. Anim. Physiol. Anim. Nutr.* 104, 257–268. doi:10.1111/jpn.13240

Özlü, S., Uçar, A., Erkuş, T., Yasun, S., Nicholson, A. D., and Elibol, O. (2021). Effects of flock age, storage temperature, and short period of incubation during egg storage, on the albumen quality, embryonic development and hatchability of long stored eggs. *Br. Poult. Sci.* 62, 611–619. doi:10.1080/00071668.2021.1887454

Peebles, E. D., Doyle, S. M., Zumwalt, C. D., Gerard, P. D., Latour, M. A., Boyle, C. R., et al. (2001). Breeder age influences embryogenesis in broiler hatching eggs. *Poult. Sci.* 80, 272–277. doi:10.1093/ps/80.3.272

Ramaphala, N. O., and Mbajiorgu, C. A. (2013). Effect of egg weight on hatchability and chick hatch-weight of COBB 500 broiler chickens. *Asian J. Anim. Vet. Adv.* 8, 885–892. doi:10.3923/ajava.2013.885.892

Reverchon, M., Bertoldo, M. J., Ramé, C., Froment, P., and Dupont, J. (2014). CHEMERIN (RARRES2) decreases *in vitro* granulosa cell steroidogenesis and blocks oocyte meiotic progression in bovine Species1. *Biol. Reprod.* 90. doi:10.1095/biolreprod.113.117044

Reverchon, M., Cornuau, M., Rame, C., Guerif, F., Royere, D., and Dupont, J. (2012). Chemerin inhibits IGF-1-induced progesterone and estradiol secretion in human granulosa cells. *Hum. Reprod.* 27, 1790–1800. doi:10.1093/humrep/des089

Schmidt, G., Figueiredo, E., Saatkamp, M., and Bomm, E. (2009). Effect of storage period and egg weight on embryo development and incubation results. *Rev. Bras. Ciênc. Avícola* 11, 1–5. doi:10.1590/S1516-635X2009000100001

Tixier-Boichard, M., Boichard, D., Groeneveld, E., and Bordas, A. (1995). Restricted maximum likelihood estimates of genetic parameters of adult male and female Rhode Island red chickens divergently selected for residual feed consumption. *Poult. Sci.* 74, 1245–1252. doi:10.3382/ps.0741245

Tixier-Boichard, M., Durand, L., Morisson, M., Ricard, F., and Coquerelle, G. (1994). Comparative analysis of avian leukosis virus-related endogenous viral genes in experimental strains of the domestic chicken, *Genetics Selection Evolution*. 15. doi:10.1186/1297-9686-26-S1-S53

Tona, K., Bruggeman, V., Onagbesan, O., Bamelis, F., Gbeassor, M., Mertens, K., et al. (2005). Day-old chick quality: Relationship to hatching egg quality, adequate incubation practice and prediction of broiler performance. *Avian Poult. Biol. Rev.* 16, 109–119. doi:10.3184/147020605783438787

Wang, J., Liang, Y., Omana, D. A., Kav, N. N. V., and Wu, J. (2012). Proteomics analysis of egg white proteins from different egg varieties. *J. Agric. Food Chem.* 60, 272–282. doi:10.1021/jf2033973

Yoshimura, T., and Oppenheim, J. J. (2011). Chemokine-like receptor 1 (CMKLR1) and chemokine (C–C motif) receptor-like 2 (CCRL2); Two multifunctional receptors with unusual properties. *Exp. Cell Res.* 317, 674–684. doi:10.1016/j.yexcr.2010.10.023

Zakaria, A. H., Plumstead, P. W., Romero-Sanchez, H., Leksrisompong, N., and Brake, J. (2009). The effects of oviposition time on egg weight loss during storage and incubation, fertility, and hatchability of broiler hatching eggs. *Poult. Sci.* 88, 2712–2717. doi:10.3382/ps.2009-00069

Zhang, X. Y., Wu, M. Q., Wang, S. Z., Zhang, H., Du, Z. Q., Li, Y. M., et al. (2018). Genetic selection on abdominal fat content alters the reproductive performance of broilers. *Animal* 12, 1232–1241. doi:10.1017/S1751731117002658

frontiers | Frontiers in Physiology

TYPE Perspective
PUBLISHED 25 October 2022
DOI 10.3389/fphys.2022.1011629

OPEN ACCESS

EDITED BY
Sandra G. Velleman,
The Ohio State University, United States

REVIEWED BY
Jennifer Merritt,
Columbia University, United States

*CORRESPONDENCE
Jasmine L. Loveland,
jasmine.loveland@univie.ac.at

SPECIALTY SECTION
This article was submitted to Avian Physiology,
a section of the journal
Frontiers in Physiology

RECEIVED 04 August 2022
ACCEPTED 07 October 2022
PUBLISHED 25 October 2022

CITATION
Loveland JL, Giraldo-Deck LM and Kelly AM (2022), How inversion variants can shape neural circuitry: Insights from the three-morph mating tactics of ruffs. *Front. Physiol.* 13:1011629.
doi: 10.3389/fphys.2022.1011629

How inversion variants can shape neural circuitry: Insights from the three-morph mating tactics of ruffs

Jasmine L. Loveland[1]*, Lina M. Giraldo-Deck[2] and Aubrey M. Kelly[3]

[1]Department of Cognitive and Behavioral Biology, University of Vienna, Vienna, Austria, [2]Behavioural Genetics and Evolutionary Ecology, Max Planck Institute for Biological Intelligence (in Foundation), Seewiesen, Germany, [3]Department of Psychology, Emory University, Atlanta, GA, United States

Behavior polymorphisms underlying alternative mating tactics can evolve due to genetic inversions, especially when inversions capture sets of genes involved in hormonal regulation. In the three-morph system of the ruff (*Calidris pugnax*), two alternative morphs (Satellites and Faeders) with distinct behaviors and low circulating testosterone are genetically determined by an inverted region on an autosomal chromosome. Here, we discuss recent findings on the ruff and present novel insights into how an inversion that poses drastic constraints on testosterone production might lead to morph-specific differences in brain areas that regulate social behavior. A gene responsible for converting testosterone to androstenedione (*HSD17B2*) is located inside the inverted region and is a promising candidate. We identify a single missense mutation in the *HSD17B2* gene of inverted alleles that is responsible for a 350–500% increase in testosterone to androstenedione conversion, when mutated in the human HSD17B2 protein. We discuss new evidence of morph differences in neural *HSD17B2* expression in embryos and circulating androgens in sexually-immature juveniles. We suggest processes that shape morph differences in behavior likely begin early in ontogeny. We propose that the organization of behaviorally relevant neuron cell types that are canonically sexually dimorphic, such as subpopulations of aromatase and vasotocin neurons, should be particularly affected due to the life-long condition of low circulating testosterone in inversion morphs. We further emphasize how HSD17B2 catalytic activity extends beyond androgens, and includes estradiol oxidation into estrone and progesterone synthesis. Lastly, we underscore dimerization of HSD17B2 as an additional layer of complexity that merits consideration.

KEYWORDS

HSD17B2, supergene, chromosome inversion, aromatase, vasotocin, alternative reproductive tactics, *Calidris pugnax*, testosterone

Introduction

The ruff: Behavior, hormones, and genetics

Ruffs (*Calidris pugnax*) have long fascinated ornithologists because of their ornamental breeding plumage and lekking behavior, though the genetic basis for their unique mating system was discovered only recently (Küpper et al., 2016; Lamichhaney et al., 2016). Their mating system consists of three genetically determined morphs called Independents, Satellites and Faeders, that have striking differences in behavioral repertoires, hormonal profiles, nuptial plumage and body size (Hogan-Warburg, 1966; van Rhijn, 1973; Küpper et al., 2016; Lamichhaney et al., 2016; Loveland et al., 2021a) (Figure 1A).

Independent males aggressively defend mating courts on leks, display courtship behaviors and have dark colored ruffs. The behavior of Independent males is so intense that in some languages the species name is simply "fighter" or "walking fighter" (*combatiente*, Spanish; *Kampfläufer*, German). In contrast, Satellite males are not aggressive, co-display courtship behaviors with Independent males and have mostly white colored ruffs. Faeder males do not display courtship or aggressive behaviors, lack ruff feathers and are the smallest of the three morphs (Figure 1A) (Jukema and Piersma, 2006; Lank et al., 2013). Given their cryptic appearance, Faeders pass as female mimics and rely on a strictly sneaker strategy to attain matings.

The genetic polymorphism underlying the alternative mating strategies in ruffs is controlled by a 4.5 Mb inversion, also called a supergene, that contains approximately 125 genes (Küpper et al., 2016; Lamichhaney et al., 2016). Independents are the ancestral morph, whereas Satellites and Faeders are both inversion carriers, however, of distinct inversion haplotypes. Inversion haplotypes are dominant, homozygous lethal and contain several genes associated with sex steroid metabolism (Küpper et al., 2016; Lamichhaney et al., 2016; Loveland et al., 2021b). The Faeder inversion appeared first, 3.8 million years ago and the Satellite inversion arose by the recombination of Independent and Faeder alleles 500,000 years ago (Küpper et al., 2016; Lamichhaney et al., 2016) (Figure 1A). For simplicity, we will use "inversion morphs" to collectively refer to Satellites and Faeders, even though their inversion haplotypes are not identical.

Hormonally, adult Satellite and Faeder males have low levels of testosterone, but high levels of androstenedione, compared to Independents (Küpper et al., 2016; Loveland et al., 2021a) (Figure 1A). While the overt behavioral differences among male morphs are likely heavily influenced by differences in their capacity to produce testosterone (Loveland et al., 2021a), when and how this feature shapes their morph-specific behavioral repertoires is unknown. Here we will highlight key findings and ongoing work that informs future research aimed at mechanistic explanations of how inversion haplotypes facilitate the display of male morph-specific behaviors in the ruff.

The *HSD17B2* gene

Since the discovery of the genetic basis for the alternative ruff morphs, the *HSD17B2* gene, located inside the inverted region, has been considered a key candidate to explain circulating androgenic differences between Independent and inversion morph males. *HSD17B2* encodes the hydroxysteroid 17-beta dehydrogenase two enzyme, which has been well characterized in humans and rodent models showing it converts with high affinity testosterone to androstenedione, estradiol to estrone, and with lower affinity 20-alpha-dihydroprogesterone to progesterone (Figure 1B) (Wu et al., 1993).

HSD17B2 enzyme function could have become different between Independents and inversion morphs through mutations in regulatory and/or coding regions. There are three major deletions surrounding the *HSD17B2* gene that could potentially lead to widespread or tissue-specific expression changes (Figure 1C) (Küpper et al., 2016; Lamichhaney et al., 2016). Both Satellites and Faeders have these deletions in their respective inversions. Ruff and human HSD17B2 share 54% and 67% sequence identity across the entire protein and 'HSD17beta type 2 classical SDR domain' sequences, respectively (Altschul et al., 1997). We confirmed that the ruff HSD17B2 possesses all functional domains described for the human HSD17B2 enzyme comprising 37 amino acid sites identified with the conserved domains search tool (Marchler-Bauer and Bryant, 2004; Lu et al., 2020) (Figure 2A).

While no crystal structure exists for any HSD17B2 enzyme in the Protein Database (Berman et al., 2000) recent *in silico* three-dimensional modeling, site-directed mutagenesis and *in vivo* functional validation experiments show that mutations to Lys275 in human HSD17B2 confer up to a 5-fold increase in the testosterone to androstenedione conversion rate, and approximately a 2-fold increase in the estradiol to estrone conversion rate (Sager et al., 2021). Based on the pairwise alignment of human and ruff HSD17B2 proteins, the corresponding position is mutated from Leu279Phe in both Satellite and Faeder alleles relative to the non-inverted allele (Figure 2A). We propose that this mutation could harbor profound explanatory power for the increased circulating androstenedione, and low testosterone, in inversion morphs. As such, it undoubtedly warrants further investigation to validate its role in modifying catalytic activity. This adds to our previous note on another missense mutation occurring near positions that form the 'NSYK' catalytic tetrad of this enzyme (Loveland et al., 2021b).

While we initially reported a lack of testicular *HSD17B2* mRNA expression differences among morphs (Loveland et al., 2021b), in our most recent work we show there are clear morph

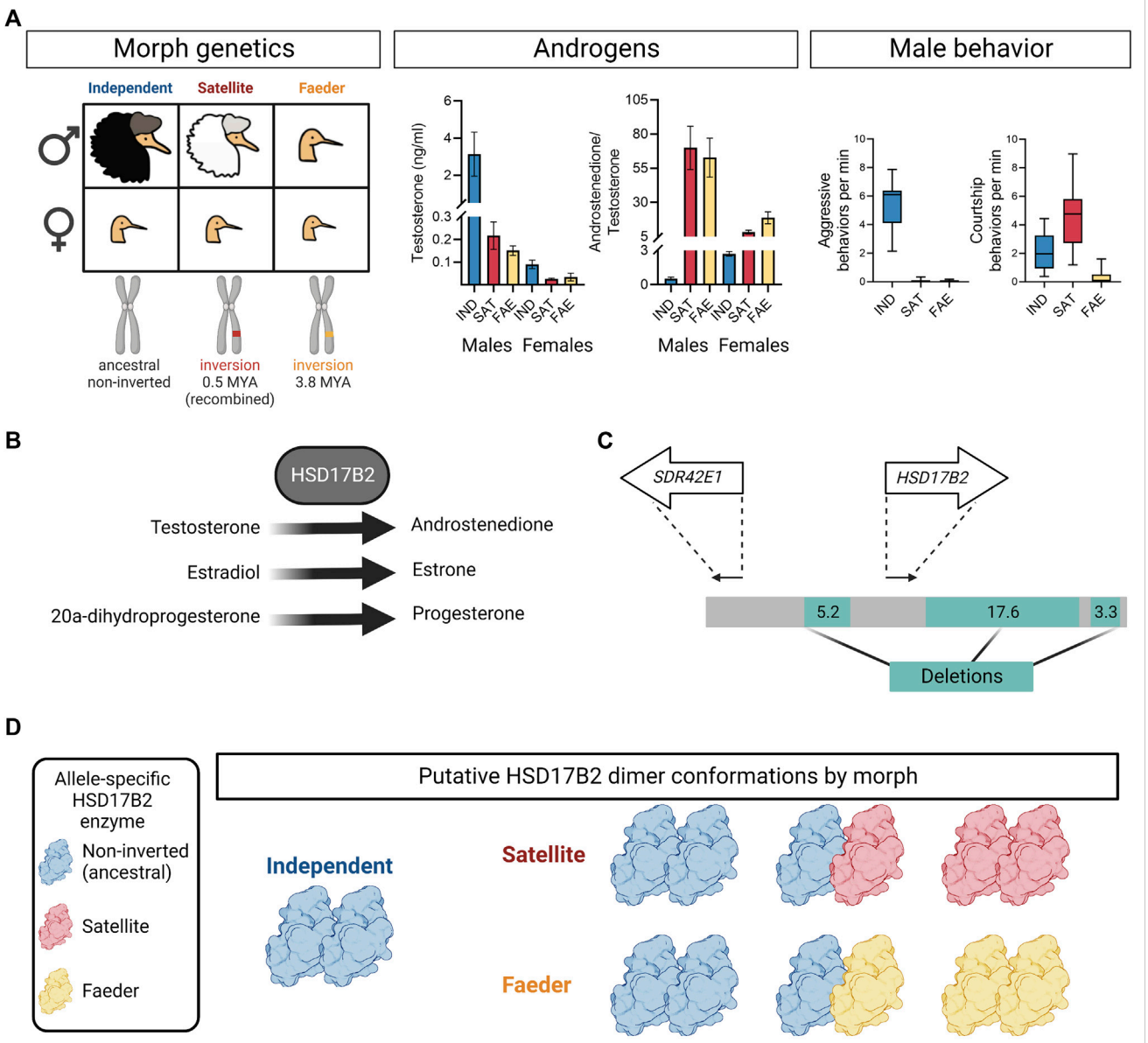

FIGURE 1
Overview of ruff morph genetics, testosterone, behavior and HSD17B2 features. **(A)** Illustration of morph profiles with corresponding genetics, circulating testosterone levels, androstenedione to testosterone ratio, and male behavior during the breeding season. In males, Independents and Satellites are ornamented, while Faeders are not. Satellites and Faeders are carriers of distinct inversion haplotypes on chromosome 11, thus present in both sexes. The Faeder inversion occurred 3.8 million years ago (MYA) and the Satellite inversion appeared ~0.5 MYA due to a recombination event between Independent and Faeder alleles. In both sexes, inversion morphs have lower circulating levels of testosterone and higher androstenedione to testosterone ratio, compared to Independent counterparts. Error bars are ± SEM. The *y*-axis breaks were introduced to provide informative detail. Boxplots show only Independent males aggressively defend territories and both Independents and Satellites actively court females, often with co-displays. Independent, IND; Satellite, SAT; Faeder, FAE. Plotted sample sizes in order Independent, Satellite, Faeder for testosterone in males: 17, 9, 9; females: 7, 5, 3; for androstenedione to testosterone ratio in males: 10, 7, 7; females: 5, 3, 3 [Data from (Loveland et al., 2021a) and females were processed in parallel]. **(B)** The HSD17B2 enzyme catalyzes with high affinity testosterone to androstenedione, estradiol to estrone and also with lower affinity, 20-alpha-dihydroprogesterone to progesterone. **(C)** Illustration of deletions (green) surrounding *HSD17B2* and *SDR42E1* genes inside inversion haplotypes. Both Faeder and Satellite haplotypes have these deletions. Arrows depict relative locations of *SDR42E1* and *HSD17B2* genes oriented in their direction of transcription. Numbers denote deletion sizes in kilobases. Redrawn based on (Lamichhaney et al., 2016). **(D)** Putative HSD17B2 dimer conformations by morph. As inversion heterozygotes, Satellites and Faeders are expected to express two HSD17B2 alleles: non-inverted (blue) and inversion (red, Satellite; yellow, Faeder) alleles. Therefore, if HSD17B2 acts in a dimer conformation, then Satellites and Faeders may have up to three possible dimer assemblies due to their heterozygosity, whereas Independents have only one possible homodimer. Solely for illustration purposes PDB ID: 6MNE was used in lieu of a crystal structure for HSD17B2

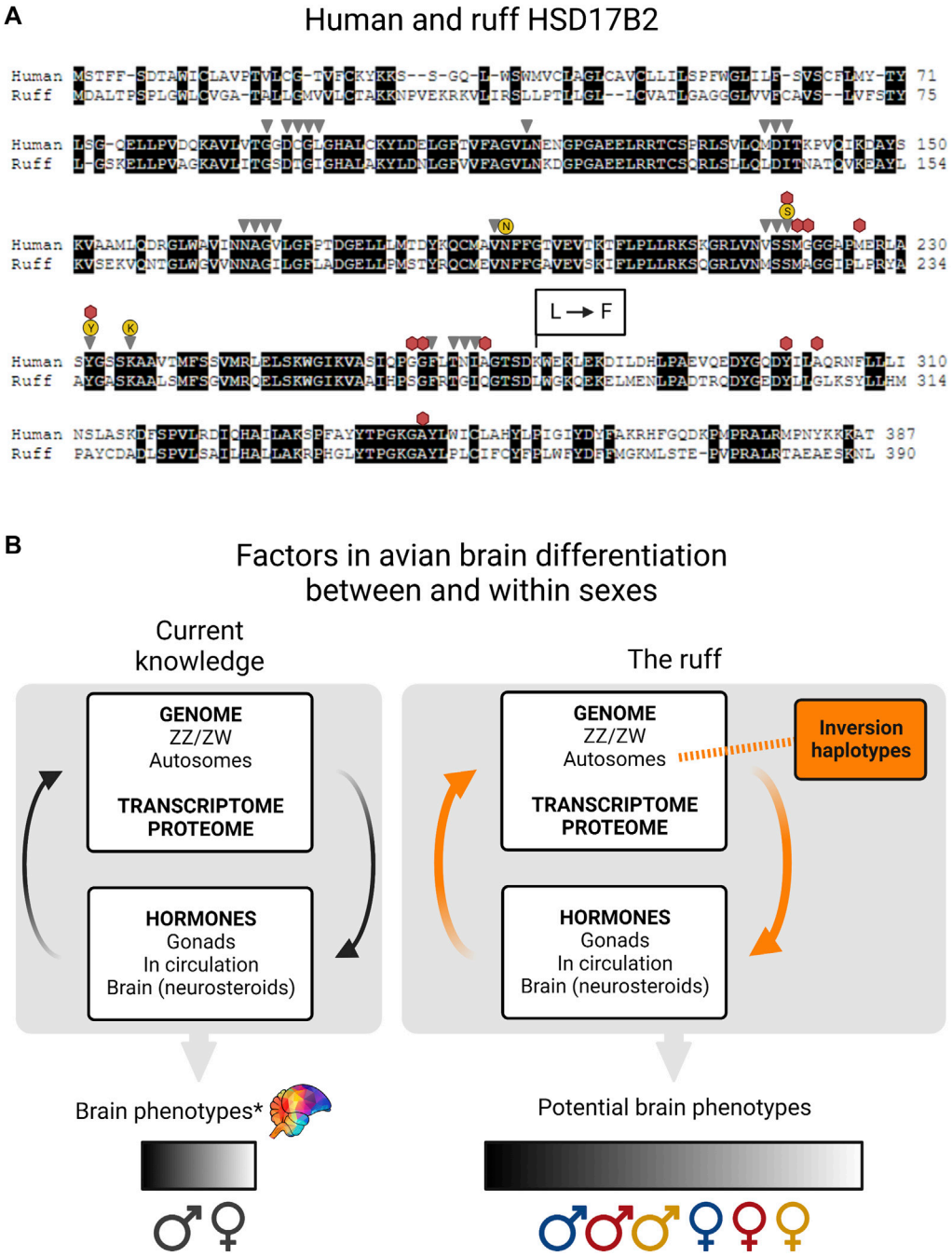

FIGURE 2
Missense mutation in ruff HSD17B2 and factors in avian brain differentiation. **(A)** Pairwise alignment of human and ruff HSD17B2 proteins (accession numbers NP_002144.1, XP_014797711.1) (BLOSUM45 matrix, internal gap penalty = -4) with identical residues in a black background). The 37 residues belonging to the HSD17beta type 2 conserved domain are indicated for NADP binding (gray triangles), steroid binding (red hexagons), catalytic tetrad (yellow circles). At ruff position 279, Satellite and Faeder alleles have the missense mutation that changes leucine to phenylalanine, indicated by L → F. Amino acid changes at this same position in the human protein increase catalytic activity for testosterone to androstenedione up to 5-fold compared to the non-mutated version (Sager et al., 2021). **(B)** The current knowledge of avian brain differentiation between and within the sexes relies on a series of complex interactions and here we show a simplified illustration of key factors: the genome, transcriptome, proteome and hormones. Sex chromosomes express specific genes that help determine gonadal sex, which in turn provides a hormonal environment from the synthesis of sex steroids from gonadal tissues. Sex hormones have a major effect on sexual differentiation. Once bound to receptors (i.e. androgen and estrogen receptors) these will then act as transcription factors and regulate the expression of target genes throughout the entire genome. Autosomes allow the expression of receptor genes to sense hormones and enzymes that can make hormones, including inside brain cells (neurosteroids). e.g. by aromatizing circulating testosterone into estradiol. All of these processes contribute to variation in
(*Continued*)

FIGURE 2 (Continued)
brain phenotypes within and between sexes. We acknowledge that for any sex difference in a brain trait there can be overlap between the sexes, denoted by the spectrum (*) Even so, this is oversimplified and does not fully take fully into account brain mosaicism [reviewed in (Joel, 2011, 2021)]. In ruffs, inversion haplotypes (orange box) form part of the genome and have a direct impact on genetic architecture. The expression of inversion allele(s) results in dramatically reduced testosterone levels (and perhaps also reduced estradiol levels). By producing a reduction in the amount of circulating sex hormones, the inversion modifies the typical influence of sex chromosomes on brain sexual differentiation (orange arrows). We predict that morph variation will add to variation between the sexes, but this will be constrained by interactions between hormones and gene expression of each morph + sex combination. Independents (blue), Satellites (red), Faeders (yellow).

differences in *HSD17B2* mRNA expression in the brains of embryos, as early as day 14 of incubation (Giraldo-Deck, 2022). Interestingly, these morph differences, with higher expression in inversion morphs compared to Independents, are present in both sexes and occur in areas containing nodes of the social behavior network (Newman, 1999; Goodson, 2005). The detection of *HSD17B2* expression differences at such an early stage strongly suggests that in addition to low circulating testosterone, the presence of the inversion can also lead to changes in brain estradiol levels. This is because inversion morphs must experience atypical levels of estradiol in the brain due to 1) less aromatizable testosterone and 2) greater conversion of estradiol into estrone by HSD17B2. As we move forward, it will be important to maintain an integrative interpretation of results, keeping in mind that inversion effects occur in both sexes and that even in females this could have effects on behaviorally relevant cell types.

A key issue that has yet to be acknowledged is that the ruff HSD17B2 likely catalyzes in a homodimer conformation adding an entire new layer of complexity to how we speculate HSD17B2 function might differ among morphs. The human HSD17B2 has been shown to function unequivocally as a homodimer in solution (Lu et al., 2002). As dimerization is a requirement for function, then that means that HSD17B2 dimers in Satellites and Faeders should always be composed of three possible combinations of HSD17B2 enzymes (given expression of variants from non-inverted and inverted alleles) (Figure 1D). Thus, the new dimer conformations may confer a different catalytic activity compared to the homodimer composed of only HSD17B2 expressed from the non-inverted allele.

Inversion haplotypes likely shape morph-specific neural organization

Foundational studies by Lank and others provided valuable insights and direction for inquiries into the neurobiological basis of behavioral differences in the ruff. In a key study, the authors reported that adult females implanted with testosterone displayed male behaviors and grew nuptial plumage that were typical to their corresponding male morph counterpart (Lank et al., 1999). This suggests that in the ruff, as is the case for several other bird species, broadly speaking, males are likely the "default" sex and females undergo a de-masculinization step by exposure to estrogens as embryos (Adkins-Regan, 1987). Considering the facts of differential *HSD17B2* gene expression in embryo brains and that morph differences in circulating androgens are detectable as early as the juvenile stage (Giraldo-Deck, 2022), we believe morph differences in neural organization may begin to take shape early in ontogeny. The behavioral effects of the inversion likely come from its ability to reduce not only circulating levels of testosterone, but perhaps even more so, from its ability to affect hormone synthesis in brain areas where the *de novo* synthesis of sex steroid hormones, especially estrogen from circulating testosterone, takes place.

Organizational and activational effects of testosterone and estradiol

Testosterone and estradiol play important roles in organizing and activating sex differences in neural circuits in vertebrates and several detailed studies have been conducted on this topic in rodent models [e.g. (Wu et al., 2009; Juntti et al., 2010; Gegenhuber et al., 2022)] and birds [e.g. (Adkins, 1979; Balthazart et al., 1986; Balthazart, 1991; Gahr, 2004; Court et al., 2020; Bentz et al., 2021)]. In the ruff we expect that the distinct morph-specific profiles of circulating androgens—and the amount of estradiol that can be synthesized from it—affects the development of neural circuitry that contains cell types that are otherwise typically sexually dimorphic.

As noted above, adult Satellite and Faeder males have low levels of testosterone (Figure 1A) but high levels of androstenedione, compared to Independent males (Küpper et al., 2016; Loveland et al., 2021a). These patterns in circulating androgens emerge already in both sexes as early at 10 days old, where variance in testosterone levels in Independents is three times greater than that of Satellites and Faeders, while the variance in androstenedione is greater in inversion morphs compared to Independents (Giraldo-Deck, 2022). Furthermore, we have also confirmed that it persists into adulthood for females as well, where even though circulating levels of testosterone are low, inversion morphs have even lower levels than Independent females (Figure 1A).

The activation of behavioral repertoires during the breeding season for many bird species is also testosterone

and estrogen dependent (Wingfield et al., 1987; Ball and Balthazart, 2004; Heimovics et al., 2018). We have demonstrated that the low levels of testosterone in inversion morph males remain virtually unperturbed even after stimulation with gonadotrophin releasing hormone (GnRH). In contrast, for Independent males who do not have the inversion, a GnRH injection induces a textbook-like robust and transient increase in testosterone (Loveland et al., 2021a). It is unclear still whether inversion morphs are only able to make limited amounts of testosterone or whether testosterone is always immediately back converted to androstenedione, such that we only ever detect the end of the reaction (i.e. high androstenedione). Regardless, this suggests potential morph differences in both organizational and activational effects of steroids on physiology and behavior.

Although estradiol has not been studied yet in the ruff, it is well known that many behavioral effects of testosterone can be abolished if administered along with aromatase inhibitors, demonstrating that aromatization of testosterone is necessary for eliciting aggressive and courtship behaviors (Wingfield et al., 1987; Foidart and Balthazart, 1995; Fusani et al., 2003; Balthazart et al., 2004). The ring dove is a species in which roles for testosterone and estradiol in activating specific behaviors in courtship has been studied extensively. In their courtship, chasing, bowing and nest-soliciting are activated by separate hormones. The first two behaviors are more aggressive and are regulated by testosterone, whereas nest-soliciting is specifically controlled by estradiol (Hutchison, 1970, 1971; Cheng and Lehrman, 1975; Adkins-Regan, 1981). Notably, its source is through the aromatization of circulating testosterone inside brain cells. Therefore, we speculate that something similar may occur in ruffs where the lack of aggression components in Satellite courtship displays is perhaps also due to low levels of circulating testosterone, and non-aggressive courtship behaviors (i.e. squats) are dependent on estradiol (from aromatized testosterone), rather than testosterone alone. Future studies could test this directly and see if aromatase inhibitors decrease the frequency of courtship displays.

At this point, we believe the androgenic differences documented thus far in ruffs are only a partial explanation leading to behavioral differences among morphs, and that estrogenic effects have yet to be explored and fully accounted for. We propose that the inversion affects not only circulating testosterone levels among morphs, but also the *de novo* synthesis of estradiol in the brain and that these two events combined, shape both the development and subsequent activation, of morph-specific behaviors in adulthood. Furthermore, increased *HSD17B2* mRNA expression in the brains of embryos suggests that estradiol may also be continually reduced to its less active form, estrone, adding yet another component that could influence morph-specific behavior.

Beyond typical sex differences in the brain

Elucidating the mechanisms by which chromosomal rearrangements allow for the evolution of intrasexual behavioral diversity will require a close study of brain areas containing behaviorally relevant neuron types. As examples, we briefly discuss the value in quantifying sex and morph differences in the distribution of aromatase and vasotocin (AVT) neurons in the ruff, as both are organized by, and sensitive to, circulating testosterone levels (Cornil et al., 2011). Profiling AVT neurons and how they relate to androgen levels has proven useful in the study of alternative mating tactics in fishes (reviewed in Mank, 2022). Thus, characterizing both aromatase and AVT systems in the ruff holds great potential for providing insight into the development of morph differences as well as behavioral plasticity in adulthood.

In our testicular expression study, we showed that in Independents and Satellites aromatase and the inversion gene *SDR42E1* have a positive co-expression relationship, whereas no such pattern is present in Faeders (Loveland et al., 2021b). If morph differences in brain aromatase are also present, this could profoundly affect neural organization. Mapping aromatase neurons in the ruff will help meet two goals: refining areas to investigate neuroanatomical differences among male morphs but also between the sexes. Knowing where aromatase neurons are located and identifying their projections has been proposed as an ideal focus for delineating brain areas that integrate sensory information and control motor output for behavioral differences between the sexes (Spool et al., 2022). Aromatase densities and distributions are sexually dimorphic in quail (Foidart et al., 1994; Foidart and Balthazart, 1995; Carere et al., 2007) and aromatase positive cells in the preoptic area that project to the periaqueductal gray are considered responsible for sex differences in testosterone-sensitivity and its ability to elicit copulatory behavior (Carere et al., 2007). Further, aromatase influences an array of behaviors. For example, aromatase neurons in the ventromedial hypothalamus (VMH) are involved in male-male agonistic behaviors in song-sparrows (Soma et al., 2003; Wacker et al., 2010) and estradiol implants in this same brain area induce copulation solicitation in female quail (Wild and Balthazart, 2013). Additionally, we envision that aromatase mapping will be crucial for being able to study hypothalamic nuclei with greater precision and provide a starting point to study female mate choice, which is fundamental to the evolution of sexually selected traits in the ruff.

The nonapeptide AVT is an evolutionarily conserved peptide that modulates a variety of social behaviors including affiliation, parental care, anxiety, aggression, courtship, and sexual behavior (Goodson, 2008). The AVT system consists of several populations of AVT-producing neurons throughout the basal forebrain and midbrain (De Vries and Panzica, 2006). AVT neuron size, cell density, and fiber innervations can be different between the sexes, though the extent can vary

depending on the cell group and species (De Vries and Panzica, 2006). Of particular interest is the AVT cell population of the medial bed nucleus of the stria terminalis (BSTm), which is sexually dimorphic in most species, with males having more cells and denser fiber projections than females (De Vries and Panzica, 2006). This cell group is also strongly regulated by sex steroids in seasonally breeding species (Goodson and Bass, 2001; De Vries and Panzica, 2006; Kelly et al., 2011). The BSTm AVT cell group modulates grouping behavior, affiliation, and aggression in a sex-specific manner in estrildid finches (Kelly et al., 2011), and courtship in chicken (Xie et al., 2011). Additionally, aromatase colocalizes with BSTm AVT neurons in zebra finches (Kabelik et al., 2010a), therefore highlighting the potential not only for sex steroids to shape the anatomy of this cell group (i.e., neuronal densities) but to also rapidly modulate behavior in a sex-specific manner (Kelly and Wilson, 2020). We hypothesize that BSTm AVT cell numbers will differ not only by sex, but also by morph in the ruff given the morph differences in sex steroid profiles. Further, it is feasible that testosterone may regulate BSTm AVT neural activity as has been observed in zebra finches (Kabelik et al., 2010b).

Conclusion and future directions

In the ruff, a genetic re-arrangement present in both sexes has led to the evolution of alternative mating tactics that showcase male phenotypes with distinct appearance, behavior and hormonal profiles. We offer novel insights on *HSD17B2*, a candidate gene expected to be a major explanatory variable for hormonal differences among morphs. We identified a missense mutation in the *HSD17B2* sequence of Satellite and Faeder inversions that has evidence in its human ortholog to be sufficient to produce a dramatic increase in catalytic activity (Sager et al., 2021). This possible enhancement of catalytic activity along with variety in dimer conformations could both contribute to the high androstenedione and low testosterone hormone profiles of inversion morphs. To add meaningful validation to the *HSD17B2* missense mutation findings, knowledge of functional differences that are actually conferred by inversion morph variants of this gene is crucial. For example, site-directed mutagenesis experiments could directly test the role of the leucine to phenylalanine mutation, all while accounting for dimerization combinations.

Neural circuits that underlie behavioral differences between the sexes and between morphs are influenced by the inversion. The presence of the inversion has a direct effect on genetic architecture and consequences proceed onto the transcriptome, proteome and hormone levels (Figure 2B). Ruff inversions produce a low testosterone phenotype in juveniles and adults of both sexes, compared to Independents (Küpper et al., 2016; Loveland et al., 2021a; Giraldo-Deck, 2022). If this pattern extends to embryos, then the inversion modifies the typical influence of sex chromosomes on brain development and organization likely producing even more complex variation between and within sexes. Variation in testosterone levels necessarily impacts the expression of genes that are testosterone-regulated (i.e. through androgen response elements in promoters). We expect estradiol-regulated genes to be similarly affected, though the degree is largely unknown because estradiol levels in circulation and in the brain have not been studied in detail. Nonetheless, low circulating testosterone could also lead to less available substrate for estradiol synthesis inside brain cells. In the white-throated sparrow, another species with inversion-based morphs, the expression of the estrogen receptor ESR1 in the nucleus taenia has been shown to be key in mediating aggression differences between morphs (Merritt et al., 2020). While in both species inversions affect sex hormone pathways in the ruff the variation among morphs in testosterone levels is far greater than that observed between the white-throated sparrow tan and white morphs (Maney and Küpper, 2022).

Inversion morph embryos express higher levels of *HSD17B2* in the brain (Giraldo-Deck, 2022) and future transcriptomic studies shall detail if this persists in adults. We aim to investigate how this could indirectly affect the neural organization of canonically sexually dimorphic neuron types such as aromatase- and vasotocin-producing neurons. We highlight the value of using the ruff to ask questions about the genetic and neural bases that facilitate the evolution of behavioral diversity, both within and between the sexes. We believe that mechanisms for morph-differentiation form an additional layer to those of sexual differentiation and we look forward to elucidating further mechanistic details in this fascinating species.

Data availability statement

Publicly available sequence datasets from (Küpper et al., 2016) were used to retrieve morph-specific HSD17B2 sequences. Hormone and behavior data is available in Edmond, the Open Research Data Repository of the Max Planck Society, at https://doi.org/10.17617/3.5z and in the Phaidra repository at https://phaidra.univie.ac.at/view/o:1604379.

Ethics statement

The animal study was reviewed and approved by Animal Care Committee of Simon Fraser University operating under guidelines from the Canadian Council on Animal Care.

Author contributions

JLL conceptualized the manuscript and wrote the first draft with input from AMK, JLL prepared figures with input from coauthors, all authors contributed to revisions.

Funding

This research was funded in part by the Austrian Science Fund (FWF) [M3302-B] to JLL, the Max Planck Society and the National Research Council of Canada.

Acknowledgments

We thank Wolfgang Goymann and Monika Trappschuh for hormone sample processing, and David B. Lank for assistance with sample collection. Figures were created with BioRender.com

Conflict of interest

The authors declare that the research was conducted in the absence of any commercial or financial relationships that could be construed as a potential conflict of interest.

Publisher's note

All claims expressed in this article are solely those of the authors and do not necessarily represent those of their affiliated organizations, or those of the publisher, the editors and the reviewers. Any product that may be evaluated in this article, or claim that may be made by its manufacturer, is not guaranteed or endorsed by the publisher.

References

Adkins, E. K. (1979). Effect of embryonic treatment with estradiol or testosterone on sexual differentiation of the quail brain. Critical period and dose-response relationships. *Neuroendocrinology* 29, 178–185. doi:10.1159/000122920

Adkins-Regan, E. (1981). Effect of sex steroids on the reproductive behavior of castrated male ring doves (Streptopelia sp.) *Physiol. Behav.* 26, 561–565. doi:10.1016/0031-9384(81)90125-6

Adkins-Regan, E. (1987). Sexual differentiation in birds. *Trends Neurosci.* 10, 517–522. doi:10.1016/0166-2236(87)90133-0

Altschul, S. F., Madden, T. L., Schäffer, A. A., Zhang, J., Zhang, Z., Miller, W., et al. (1997). Gapped BLAST and PSI-blast: A new generation of protein database search programs. *Nucleic Acids Res.* 25, 3389–3402. doi:10.1093/nar/25.17.3389

Ball, G. F., and Balthazart, J. (2004). Hormonal regulation of brain circuits mediating male sexual behavior in birds. *Physiol. Behav.* 83, 329–346. doi:10.1016/j.physbeh.2004.08.020

Balthazart, J., Baillien, M., Cornil, C. A., and Ball, G. F. (2004). Preoptic aromatase modulates male sexual behavior: Slow and fast mechanisms of action. *Physiol. Behav.* 83, 247–270. doi:10.1016/j.physbeh.2004.08.025

Balthazart, J., Schumacher, M., and Pröve, E. (1986). Brain testosterone metabolism during ontogeny in the zebra finch. *Brain Res.* 378, 240–250. doi:10.1016/0006-8993(86)90927-3

Balthazart, J. (1991). Testosterone metabolism in the avian hypothalamus. *J. Steroid Biochem. Mol. Biol.* 40, 557–570. doi:10.1016/0960-0760(91)90277-C

Bentz, A. B., Niederhuth, C. E., Carruth, L. L., and Navara, K. J. (2021). Prenatal testosterone triggers long-term behavioral changes in male zebra finches: Unravelling the neurogenomic mechanisms. *BMC Genomics* 22, 158. doi:10.1186/s12864-021-07466-9

Berman, H. M., Westbrook, J., Feng, Z., Gilliland, G., Bhat, T. N., Weissig, H., et al. (2000). The protein data bank. *Nucleic Acids Res.* 28, 235–242. doi:10.1093/nar/28.1.235

Carere, C., Ball, G. F., and Balthazart, J. (2007). Sex differences in projections from preoptic area aromatase cells to the periaqueductal gray in Japanese quail. *J. Comp. Neurol.* 500, 894–907. doi:10.1002/cne.21210

Cheng, M.-F., and Lehrman, D. (1975). Gonadal hormone specificity in the sexual behavior of ring doves. *Psychoneuroendocrinology* 1, 95–102. doi:10.1016/0306-4530(75)90026-8

Cornil, C. A., Ball, G. F., Balthazart, J., and Charlier, T. D. (2011). Organizing effects of sex steroids on brain aromatase activity in quail. *PLOS ONE* 6, e19196. doi:10.1371/journal.pone.0019196

Court, L., Vandries, L., Balthazart, J., and Cornil, C. A. (2020). Key role of estrogen receptor β in the organization of brain and behavior of the Japanese quail. *Horm. Behav.* 125, 104827. doi:10.1016/j.yhbeh.2020.104827

De Vries, G. J., and Panzica, G. C. (2006). Sexual differentiation of central vasopressin and vasotocin systems in vertebrates: Different mechanisms, similar endpoints. *Neuroscience* 138, 947–955. doi:10.1016/j.neuroscience.2005.07.050

Foidart, A., and Balthazart, J. (1995). Sexual differentiation of brain and behavior in quail and zebra finches: Studies with a new aromatase inhibitor, R76713. *J. Steroid Biochem. Mol. Biol.* 53, 267–275. doi:10.1016/0960-0760(95)00064-7

Foidart, A., de Clerck, A., Harada, N., Balthazart, J., and de Clerck, A. (1994). Aromatase-immunoreactive cells in the quail brain: Effects of testosterone and sex dimorphism. *Physiol. Behav.* 55, 453–464. doi:10.1016/0031-9384(94)90100-7

Fusani, L., Metzdorf, R., Hutchison, J. B., and Gahr, M. (2003). Aromatase inhibition affects testosterone-induced masculinization of song and the neural song system in female canaries. *J. Neurobiol.* 54, 370–379. doi:10.1002/neu.10141

Gahr, M. (2004). Hormone-dependent neural plasticity in the juvenile and adult song system: What makes a successful male? *Ann. N. Y. Acad. Sci.* 1016, 684–703. doi:10.1196/annals.1298.025

Gegenhuber, B., Wu, M. V., Bronstein, R., and Tollkuhn, J. (2022). Gene regulation by gonadal hormone receptors underlies brain sex differences. *Nature* 606, 153–159. doi:10.1038/s41586-022-04686-1

Giraldo-Deck, L. M. (2022). *Pleiotropic effects of a supergene underlying male alternative reproductive tactics*. Konstanz: Dissertation. University of Konstanz.

Goodson, J. L., and Bass, A. H. (2001). Social behavior functions and related anatomical characteristics of vasotocin/vasopressin systems in vertebrates. *Brain Res. Brain Res. Rev.* 35, 246–265. doi:10.1016/S0165-0173(01)00043-1

Goodson, J. L. (2008). Nonapeptides and the evolutionary patterning of sociality. *Prog. Brain Res.* 170, 3–15. doi:10.1016/S0079-6123(08)00401-9

Goodson, J. L. (2005). The vertebrate social behavior network: Evolutionary themes and variations. *Horm. Behav.* 48, 11–22. doi:10.1016/j.yhbeh.2005.02.003

Heimovics, S. A., Merritt, J. R., Jalabert, C., Ma, C., Maney, D. L., and Soma, K. K. (2018). Rapid effects of 17β-estradiol on aggressive behavior in songbirds: Environmental and genetic influences. *Horm. Behav.* 104, 41–51. doi:10.1016/j.yhbeh.2018.03.010

Hogan-Warburg, A. J. (1966). Social behavior of the ruff, Philomachus pugnax (L.) *Ardea* 55, 109–229. doi:10.5253/arde.v54.p109

Hutchison, J. B. (1970). Differential effects of testosterone and oestradiol on male courtship in barbary doves (Streptopelia risoria). *Anim. Behav.* 18, 41–51. doi:10.1016/0003-3472(70)90068-0

Hutchison, J. B. (1971). Effects of hypothalamic implants of gonadal steroids on courtship behaviour in Barbary doves (Streptopelia risoria). *J. Endocrinol.* 50, 97–113. doi:10.1677/joe.0.0500097

Joel, D. (2021). Beyond the binary: Rethinking sex and the brain. *Neurosci. Biobehav. Rev.* 122, 165–175. doi:10.1016/j.neubiorev.2020.11.018

Joel, D. (2011). Male or female? Brains are intersex. *Front. Integr. Neurosci.*, 5. doi:10.3389/fnint.2011.00057

Jukema, J., and Piersma, T. (2006). Permanent female mimics in a lekking shorebird. *Biol. Lett.* 2, 161–164. doi:10.1098/rsbl.2005.0416

Juntti, S. A., Tollkuhn, J., Wu, M. V., Fraser, E. J., Soderborg, T., Tan, S., et al. (2010). The androgen receptor governs the execution, but not programming, of male sexual and territorial behaviors. *Neuron* 66, 260–272. doi:10.1016/j.neuron.2010.03.024

Kabelik, D., Kelly, A. M., and Goodson, J. L. (2010a). Dopaminergic regulation of mate competition aggression and aromatase-Fos colocalization in vasotocin neurons. *Neuropharmacology* 58, 117–125. doi:10.1016/j.neuropharm.2009.06.009

Kabelik, D., Morrison, J. A., and Goodson, J. L. (2010b). Cryptic regulation of vasotocin neuronal activity but not anatomy by sex steroids and social stimuli in opportunistic desert finches. *Brain Behav. Evol.* 75, 71–84. doi:10.1159/000297522

Kelly, A. M., Kingsbury, M. A., Hoffbuhr, K., Schrock, S. E., Waxman, B., Kabelik, D., et al. (2011). Vasotocin neurons and septal V1a-like receptors potently modulate songbird flocking and responses to novelty. *Horm. Behav.* 60, 12–21. doi:10.1016/j.yhbeh.2011.01.012

Kelly, A. M., and Wilson, L. C. (2020). Aggression: Perspectives from social and systems neuroscience. *Horm. Behav.* 123, 104523. doi:10.1016/j.yhbeh.2019.04.010

Küpper, C., Stocks, M., Risse, J. E., dos Remedios, N., Farrell, L. L., McRae, S. B., et al. (2016). A supergene determines highly divergent male reproductive morphs in the ruff. *Nat. Genet.* 48, 79–83. doi:10.1038/ng.3443

Lamichhaney, S., Fan, G., Widemo, F., Gunnarsson, U., Thalmann, D. S., Hoeppner, M. P., et al. (2016). Structural genomic changes underlie alternative reproductive strategies in the ruff (Philomachus pugnax). *Nat. Genet.* 48, 84–88. doi:10.1038/ng.3430

Lank, D. B., Coupe, M., and Wynne-Edwards, K. E. (1999). Testosterone-induced male traits in female ruffs (Philomachus pugnax): Autosomal inheritance and gender differentiation. *Proc. R. Soc. Lond. B* 266, 2323–2330. doi:10.1098/rspb.1999.0926

Lank, D. B., Farrell, L. L., Burke, T., Piersma, T., and McRae, S. B. (2013). A dominant allele controls development into female mimic male and diminutive female ruffs. *Biol. Lett.* 9, 20130653. doi:10.1098/rsbl.2013.0653

Loveland, J. L., Giraldo-Deck, L. M., Lank, D. B., Goymann, W., Gahr, M., and Küpper, C. (2021a). Functional differences in the hypothalamic-pituitary-gonadal axis are associated with alternative reproductive tactics based on an inversion polymorphism. *Horm. Behav.* 127, 104877. doi:10.1016/j.yhbeh.2020.104877

Loveland, J. L., Lank, D. B., and Küpper, C. (2021b). Gene expression modification by an autosomal inversion associated with three male mating morphs. *Front. Genet.* 12, 641620. doi:10.3389/fgene.2021.641620

Lu, M.-L., Huang, Y.-W., and Lin, S.-X. (2002). Purification, reconstitution, and steady-state kinetics of the trans-membrane 17β-hydroxysteroid dehydrogenase 2. *J. Biol. Chem.* 277, 22123–22130. doi:10.1074/jbc.M111726200

Lu, S., Wang, J., Chitsaz, F., Derbyshire, M. K., Geer, R. C., Gonzales, N. R., et al. (2020). CDD/SPARCLE: The conserved domain database in 2020. *Nucleic Acids Res.* 48, D265–D268. doi:10.1093/nar/gkz991

Maney, D. L., and Küpper, C. (2022). Supergenes on steroids. *Philos. Trans. R. Soc. Lond. B Biol. Sci.* 377, 20200507. doi:10.1098/rstb.2020.0507

Mank, J. E. (2022). Sex-specific morphs: The genetics and evolution of intra-sexual variation. *Nat. Rev. Genet.*, 1–9. doi:10.1038/s41576-022-00524-2

Marchler-Bauer, A., and Bryant, S. H. (2004). CD-search: Protein domain annotations on the fly. *Nucleic Acids Res.* 32, W327–W331. doi:10.1093/nar/gkh454

Merritt, J. R., Grogan, K. E., Zinzow-Kramer, W. M., Sun, D., Ortlund, E. A., Yi, S. V., et al. (2020). A supergene-linked estrogen receptor drives alternative phenotypes in a polymorphic songbird. *Proc. Natl. Acad. Sci. U. S. A.* 117, 21673–21680. doi:10.1073/pnas.2011347117

Newman, S. W. (1999). The medial extended amygdala in male reproductive behavior A node in the mammalian social behavior network. *Ann. N. Y. Acad. Sci.* 877, 242–257. doi:10.1111/j.1749-6632.1999.tb09271.x

Sager, C. P., Weber, S., Negri, M., Banachowicz, P., Möller, G., Adamski, J., et al. (2021). Homology modeling meets site-directed mutagenesis: An ideal combination to elucidate the topology of 17β-HSD2. *J. Steroid Biochem. Mol. Biol.* 206, 105790. doi:10.1016/j.jsbmb.2020.105790

Soma, K. K., Schlinger, B. A., Wingfield, J. C., and Saldanha, C. J. (2003). Brain aromatase, 5α-reductase, and 5β-reductase change seasonally in wild male song sparrows: Relationship to aggressive and sexual behavior. *J. Neurobiol.* 56, 209–221. doi:10.1002/neu.10225

Spool, J. A., Bergan, J. F., and Remage-Healey, L. (2022). A neural circuit perspective on brain aromatase. *Front. Neuroendocrinol.* 65, 100973. doi:10.1016/j.yfrne.2021.100973

van Rhijn, J. (1973). Behavioural dimorphism in male ruffs, Philomachus pugnax (L.) *Behav.* 47, 153–227. doi:10.1163/156853973x00076

Wacker, D. W., Wingfield, J. C., Davis, J. E., and Meddle, S. L. (2010). Seasonal changes in aromatase and androgen receptor, but not estrogen receptor mRNA expression in the brain of the free-living male song sparrow, Melospiza melodia morphna. *J. Comp. Neurol.* 518, 3819–3835. doi:10.1002/cne.22426

Wild, J. M., and Balthazart, J. (2013). Neural pathways mediating control of reproductive behavior in male Japanese quail. *J. Comp. Neurol.* 521, 2067–2087. doi:10.1002/cne.23275

Wingfield, J. C., Ball, G. F., Dufty, A. M., Hegner, R. E., and Ramenofsky, M. (1987). Testosterone and aggression in birds. *Am. Sci.* 75, 602–608.

Wu, L., Einstein, M., Geissler, W. M., Chan, H. K., Elliston, K. O., and Andersson, S. (1993). Expression cloning and characterization of human 17 beta-hydroxysteroid dehydrogenase type 2, a microsomal enzyme possessing 20 alpha-hydroxysteroid dehydrogenase activity. *J. Biol. Chem.* 268, 12964–12969. doi:10.1016/s0021-9258(18)31480-7

Wu, M. V., Manoli, D. S., Fraser, E. J., Coats, J. K., Tollkuhn, J., Honda, S.-I., et al. (2009). Estrogen masculinizes neural pathways and sex-specific behaviors. *Cell* 139, 61–72. doi:10.1016/j.cell.2009.07.036

Xie, J., Kuenzel, W. J., Sharp, P. J., and Jurkevich, A. (2011). Appetitive and consummatory sexual and agonistic behaviour elicits FOS expression in aromatase and vasotocin neurones within the preoptic area and bed nucleus of the stria terminalis of male domestic chickens. *J. Neuroendocrinol.* 23, 232–243. doi:10.1111/j.1365-2826.2011.02108.x

Frontiers in Physiology

Understanding how an organism's components work together to maintain a healthy state

The second most-cited physiology journal, promoting a multidisciplinary approach to the physiology of living systems - from the subcellular and molecular domains to the intact organism and its interaction with the environment.

Discover the latest Research Topics

See more →

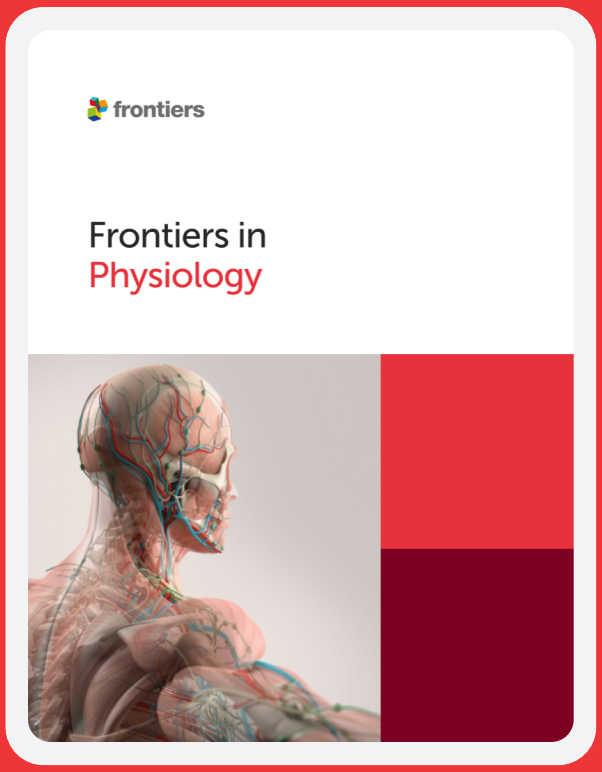

Frontiers

Avenue du Tribunal-Fédéral 34
1005 Lausanne, Switzerland
frontiersin.org

Contact us

+41 (0)21 510 17 00
frontiersin.org/about/contact